THE CELLULAR STRESS RESPONSE AND PHYSIOLOGICAL ADAPTATIONS OF CORALS SUBJECTED TO ENVIRONMENTAL STRESSORS AND POLLUTANTS

EDITED BY: Davide Seveso, Craig Downs and Ranjeet Bhagooli
PUBLISHED IN: Frontiers in Marine Science, Frontiers in Physiology and Frontiers in Genetics

frontiers Research Topics

frontiers

ISSN 1664-8714
ISBN 978-2-88976-584-3
DOI 10.3389/978-2-88976-584-3

About Frontiers

Frontiers is more than just an open-access publisher of scholarly articles: it is a pioneering approach to the world of academia, radically improving the way scholarly research is managed. The grand vision of Frontiers is a world where all people have an equal opportunity to seek, share and generate knowledge. Frontiers provides immediate and permanent online open access to all its publications, but this alone is not enough to realize our grand goals.

Frontiers Journal Series

The Frontiers Journal Series is a multi-tier and interdisciplinary set of open-access, online journals, promising a paradigm shift from the current review, selection and dissemination processes in academic publishing. All Frontiers journals are driven by researchers for researchers; therefore, they constitute a service to the scholarly community. At the same time, the Frontiers Journal Series operates on a revolutionary invention, the tiered publishing system, initially addressing specific communities of scholars, and gradually climbing up to broader public understanding, thus serving the interests of the lay society, too.

Dedication to Quality

Each Frontiers article is a landmark of the highest quality, thanks to genuinely collaborative interactions between authors and review editors, who include some of the world's best academicians. Research must be certified by peers before entering a stream of knowledge that may eventually reach the public - and shape society; therefore, Frontiers only applies the most rigorous and unbiased reviews.
Frontiers revolutionizes research publishing by freely delivering the most outstanding research, evaluated with no bias from both the academic and social point of view. By applying the most advanced information technologies, Frontiers is catapulting scholarly publishing into a new generation.

What are Frontiers Research Topics?

Frontiers Research Topics are very popular trademarks of the Frontiers Journals Series: they are collections of at least ten articles, all centered on a particular subject. With their unique mix of varied contributions from Original Research to Review Articles, Frontiers Research Topics unify the most influential researchers, the latest key findings and historical advances in a hot research area! Find out more on how to host your own Frontiers Research Topic or contribute to one as an author by contacting the Frontiers Editorial Office: frontiersin.org/about/contact

THE CELLULAR STRESS RESPONSE AND PHYSIOLOGICAL ADAPTATIONS OF CORALS SUBJECTED TO ENVIRONMENTAL STRESSORS AND POLLUTANTS

Topic Editors:
Davide Seveso, University of Milano-Bicocca, Italy
Craig Downs, Haereticus Environmental Laboratory, United States
Ranjeet Bhagooli, University of Mauritius, Mauritius

Citation: Seveso, D., Downs, C., Bhagooli, R., eds. (2022). The Cellular Stress Response and Physiological Adaptations of Corals Subjected to Environmental Stressors and Pollutants. Lausanne: Frontiers Media SA.
doi: 10.3389/978-2-88976-584-3

Table of Contents

frontiers in Marine Science

ORIGINAL RESEARCH
published: 13 May 2021
doi: 10.3389/fmars.2021.662220

Synergistic Effects of Thermal Stress and Estuarine Discharge on Transcriptomic Variation of *Montastraea cavernosa* Corals in Southeast Florida

Michael S. Studivan[1,2,3], Alycia Shatters[1], Danielle L. Dodge[1], Jeff L. Beal[4,5] and Joshua D. Voss[1]**

[1] Harbor Branch Oceanographic Institute, Florida Atlantic University, Fort Pierce, FL, United States, [2] Cooperative Institute for Marine and Atmospheric Studies, Rosenstiel School of Marine and Atmospheric Science, University of Miami, Miami, FL, United States, [3] Ocean Chemistry and Ecosystems Division, NOAA Atlantic Oceanographic and Meteorological Laboratory, Miami, FL, United States, [4] Florida Fish and Wildlife Conservation Commission, Tallahassee, FL, United States, [5] Ducks Unlimited, Memphis, TN, United States

OPEN ACCESS

Edited by:
Davide Seveso,
University of Milano-Bicocca, Italy

Reviewed by:
Mikhail V. Matz,
University of Texas at Austin, United States
Hannah Aichelman,
Boston University, United States

***Correspondence:**
Michael S. Studivan
studivanms@gmail.com
Joshua D. Voss
jvoss2@fau.edu

Specialty section:
This article was submitted to Aquatic Physiology, a section of the journal Frontiers in Marine Science

Received: 31 January 2021
Accepted: 06 April 2021
Published: 13 May 2021

Citation:
Studivan MS, Shatters A, Dodge DL, Beal JL and Voss JD (2021) Synergistic Effects of Thermal Stress and Estuarine Discharge on Transcriptomic Variation of Montastraea cavernosa Corals in Southeast Florida. Front. Mar. Sci. 8:662220. doi: 10.3389/fmars.2021.662220

Coral reefs at the northern extent of Florida's coral reef tract are exposed to many localized anthropogenic influences including controlled freshwater discharges, runoff, upwelling, and seasonal environmental variability. To better understand coral responses to sublethal stressors in nearshore environments, we conducted complementary experiments to assess the impacts of estuarine runoff and temperature stress on local populations of the scleractinian coral species, *Montastraea cavernosa*, using Tag-Seq global gene expression profiling. In an *in situ* time series experiment, fate-tracked colonies were sampled during periods of relatively low and high estuarine discharge over 4 years to investigate temporal trends in transcriptional patterns and to identify if coral stress indicators were regulated through time. There was significant transcriptomic variation through time, but patterns did not appear to be attributed to distance from nearby estuarine tidal flux. In an *ex situ* factorial experiment, clonal replicates of coral genotypes were exposed to temperature (25°C and 30°C) and water (offshore and estuarine discharge, representing typical oceanic conditions and episodic discharge conditions, respectively) treatments to quantify the potential individual and synergistic effects of sublethal stress on coral and algal gene expression. Comparative analyses suggested that corals and their algal symbionts were more responsive to thermal stress than to estuarine discharge, although there was evidence of a synergistic relationship between the two stressors. Strong genotype effects also demonstrated that transcriptomic responses to thermal stress were largely based on coral genotype, indicating the potential for stress resilience among certain members of coral populations from southeast Florida.

Keywords: Tag-Seq, marginal coral reefs, Florida's coral reef tract, Florida reef tract, freshwater runoff, sublethal stress, St. Lucie Reef, Symbiodiniaceae

INTRODUCTION

Increases in coastal development and changes to watershed use in recent decades have had profound implications for nearshore coral reefs. Coral reef habitats at the northern extent of Florida's coral reef tract are of particular concern, residing at their latitudinal environmental limits while also increasingly exposed to global and local anthropogenic stressors including land-based sources of pollution (e.g., freshwater runoff, sedimentation), annual temperature flux, and warming sea temperatures (Lirman and Fong, 2007; Gregg, 2013). Within this region, coral reefs inhabit an ecotone transition between subtropical and warm temperate climate zones (Lugo et al., 1999). Reefs in southeast Florida face high levels of both seasonal and episodic environmental variation that combine with anthropogenic impacts to impose multiple stressors on scleractinian corals. Land-based influences (e.g., controlled freshwater discharge and agricultural runoff), as well as natural environmental variability (e.g., seasonal rainfall and upwelling events), impact coastal habitats in the region (Yentsch et al., 2002; Beal et al., 2012; Gregg, 2013).

Two distinct climatological seasons dominate weather patterns along nearshore reefs in southeast Florida: (1) a wet season characterized by increased freshwater discharge and runoff, nutrient over-enrichment, and migration of dark, low-salinity water over coastal zones, and (2) a subsequent dry season during the winter with decreased rainfall and runoff (Beal et al., 2012). This pattern is also influenced by global environmental variations such as the El Niño Southern Oscillation and regional tropical storm intensity and duration (Lapointe et al., 2012). During periods of prolonged rainfall, coastal habitats including nearshore coral reefs are frequently subjected to discharge from a series of natural tributaries and artificial canals which are meant to contain stormwater runoff (Graves et al., 2004; Lapointe et al., 2012). This system controls water levels in Lake Okeechobee and manages a portion of flow from the surrounding watershed via periodic releases through control structures located on major canals (e.g., C-23, C-24, C-44; **Figure 1**). As a result, the majority of runoff water is drained from urban and agricultural lands into coastal zones, rather than into the Everglades to the south (Perry, 2004). Characteristics of discharge water during high levels of flow from the watershed have been documented to include increased levels of total suspended solids, water color (i.e., colored dissolved organic matter; CDOM), and nutrients such as nitrogen and phosphorous (Collier et al., 2008; Lapointe et al., 2017).

Restructuring and management of the Okeechobee and St. Lucie watersheds has drastically changed environmental stability through time, whereas water quality can rapidly fluctuate near St. Lucie Inlet at the southern terminus of the Indian River Lagoon (Pickering and Baker, 2015). This region also corresponds with the northernmost portion of Florida's coral reef tract, St. Lucie Reef (SLR), located within the St. Lucie Inlet Preserve State Park (**Figure 1** inset). This nearshore reef environment begins directly outside of the St. Lucie Inlet and continues approximately 7 km to the south (Walker and Gilliam, 2013). St. Lucie Reef is the northern known limit of at least eight scleractinian and octocoral species along the reef tract (Reed, 1982; Beal et al., 2012). Near the inlet, the reef is composed primarily of wormrock (*Phragmatopoma lapidosa*), with an increase in diversity and abundance of scleractinian corals toward the southern end of the park. The observed gradient of scleractinian diversity is hypothesized to be a result of increasing estuarine influence closer to the inlet (Beal et al., 2012; Shatters, 2017). Despite highly variable conditions, SLR supports a diverse community of 24 species of scleractinian corals, 100 other species of invertebrates, 23 algal species, four sea turtle species, and approximately 250 fish species (Beal et al., 2012). The two dominant scleractinian coral species found at SLR are *Pseudodiploria clivosa* and *Montastraea cavernosa*, with the former occurring throughout, and the latter absent from the northern third of the reef nearest the inlet (Walker and Gilliam, 2013). Their persistence on the reef despite highly variable water quality parameters may be in part due to their prolific ability to shed sediments through excessive mucus production and sloughing, heterotrophic feeding, and skeletal morphology characteristics (Bak and Elgershuizen, 1976; Lasker, 1980; Vargas-Ángel et al., 2006, 2007).

There have been ongoing efforts to monitor reef populations and seasonal environmental variability within the state park since 2006 (Beal et al., 2012; Walker and Gilliam, 2013; Gilliam et al., 2018). From 2010 to 2017, quarterly surveys have assessed survival of fate-tracked colonies of the dominant scleractinian species, *P. clivosa* and *M. cavernosa*, with occasional tissue sampling events to quantify coral health through physiological, histological, and population genetics approaches. These two species have shown relatively stable coral-algal assemblages over time, suggesting resilient Symbiodiniaceae associations despite environmental and seasonal changes (Klepac et al., 2015). Coral transcriptomic analyses using microarrays, however, have documented an increase in expression of stress response genes during the wet season (Beal et al., 2012). Histological analyses have indicated that these two coral species at SLR are not actively reproductive (Beal et al., 2012), despite evidence of historical population connectivity to other reefs ∼20–50 km to the south (Dodge et al., 2020). Coral skeletons appeared less dense in fate-tracked colonies relative to conspecifics elsewhere along Florida's coral reef tract, with additional tissue and skeletal loss due to the boring sponges *Cliona* spp. (Beal et al., 2012). In spite of these stressors, coral mortality was low at SLR from 2010 until Hurricane Irma in 2017 (Walker, 2018) and the recent outbreak of stony coral tissue loss disease (SCTLD) along Florida's coral reef tract starting in 2014 (reaching the northern regions in 2017) (Walton et al., 2018). Since 2017, monitoring efforts have increased both temporally and by individual fate-tracking to include all remaining scleractinian species on the reef (Voss and Combs, 2018; Walker, 2018). Prior to widespread coral mortality of the two dominant species at SLR due to SCTLD, colonies were remarkably persistent in the face of hypervariable conditions and stress.

This study builds on a decade of monitoring efforts to describe, at the molecular level, how corals at SLR respond to environmental variability. Using complementary temporal *in situ* and manipulative *ex situ* designs, we sought to quantify transcriptomic variation among individuals exposed to different

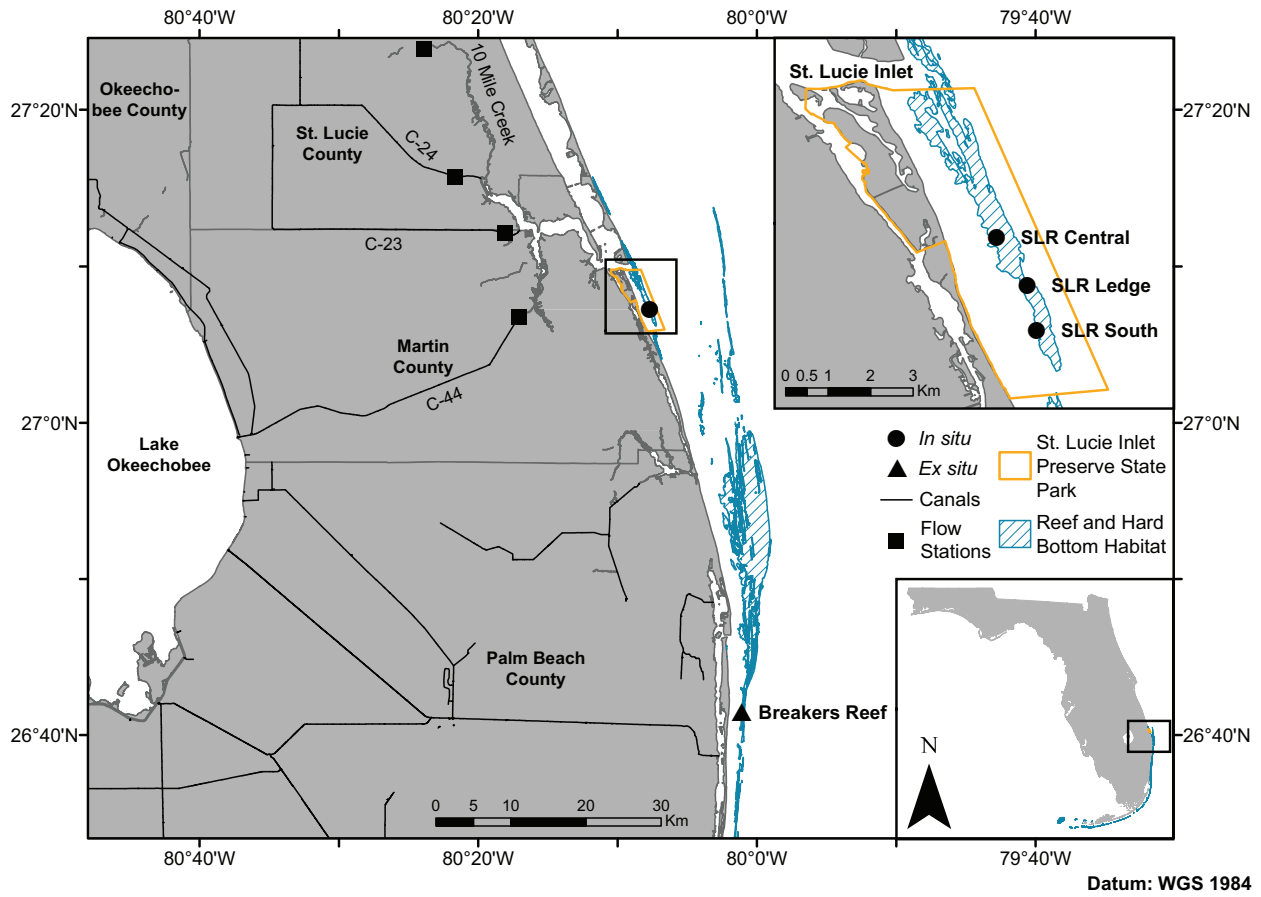

FIGURE 1 | Map of the northern extent of Florida's coral reef tract including the sampling sites in the *in situ* experiment (circles: SLR Central, SLR Ledge, and SLR South) and coral collection site for the *ex situ* experiment (triangle: Breakers Reef). Squares represent canal control structures where discharge flow rates and rainfall (C-44 only) data were obtained from the South Florida Water Management District's DBHYDRO database. State park shapefile sourced from the Florida Department of Environmental Protection's Division of Recreation and Parks, reef and hard bottom habitat shapefile sourced from the Florida Fish and Wildlife Conservation Commission-Fish and Wildlife Research Institute, canal shapefile sourced from the South Florida Water Management District.

levels of environmental stress. Recent advancements in RNA sequencing (RNA-seq) and analysis pipelines have enhanced assessments of coral health through whole-transcriptome gene expression profiling, especially in response to stressors (Kenkel et al., 2011, 2013b, 2014; Meyer et al., 2011; Wright et al., 2019). There is a growing body of literature examining transcriptomic responses to thermal stress in corals (Meyer et al., 2011; Kenkel et al., 2013b, 2014; Anderson et al., 2016; Davies et al., 2016; Dixon et al., 2020); though few studies to date have examined transcriptomic variability in corals exposed to estuarine and riverine runoff [Aguilar et al., 2017, 2019; Edge et al., 2013; Mayfield et al., 2013; see non-transcriptomic responses reviewed by Fabricius (2005)], or synergistic effects of multiple stressors therein (Wright et al., 2019). St. Lucie Reef provides an ecologically relevant scenario to investigate the potential synergistic impacts of thermal stress and estuarine discharge on coral health. Through comparative analyses between two experiments, we aimed to identify common responses to thermal and water quality stressors, in order to provide insight into the fundamental metabolic processes that may enhance stress tolerance and coral resilience in marginal reef environments.

MATERIALS AND METHODS

In situ Experiment

The scleractinian coral *Montastraea cavernosa* was chosen as the study species for both experiments as it is widely distributed throughout the study area, has annotated transcriptomic and genomic references (Kitchen et al., 2015)[1], and has temporally stable Symbiodiniaceae communities (*Cladocopium* spp.) documented for the fate-tracked colonies in the *in situ* experiment (Klepac et al., 2015). Fifteen *M. cavernosa* colonies were repeatedly sampled over nine time points spanning periods of relatively low and high estuarine discharge in 2013–2016, resulting in a total of 92 coral tissue fragments collected (**Table 1**). Variable water visibility and sea state conditions occasionally

[1]https://matzlab.weebly.com/data--code.html

TABLE 1 | Site coordinates and sampling information for the *in situ* experiment.

Site	Latitude	Longitude	Depth (m)	$n_{collected}$									$n_{in\ situ}$							
				2013	2014		2015			2016			2013	2014		2015			2016	
				October	June	September	March	June	October	March	July	November	October	September	June	October	March	July	November
SLR Central	27.1317	−80.1340	2.4	2	1	2	1	2	3	2	2	2	2	2	2	2	2	2	2	2
SLR Ledge	27.1214	−80.1275	9.7	6	6	5	3	7	6	4	6	5	3	3	3	3	3	3	3	3
SLR South	27.1119	−80.1255	3.0	3	2	3	3	2	4	3	3	4	2	2	2	2	2	2	2	2
			Total	11	9	10	7	11	13	9	11	11	7	7	7	7	7	7	7	7

Samples collected from fifteen fate-tracked M. cavernosa colonies at each time point denoted as $n_{collected}$, with samples used in statistical analyses denoted as $n_{in\ situ}$. Geographic coordinates given as decimal degrees (WGS 1984).

prevented collection of tissue samples from all colonies at each time point. Sampling occurred at three sites along St. Lucie Reef (SLR Central, SLR Ledge, SLR South; depths ranging from 2.4 to 9.7 m; **Table 1** and **Figure 1**) with increasing distance from the St. Lucie Inlet, which has been shown to approximate a gradient of decreasing exposure to estuarine discharge water (Beal et al., 2012; Shatters, 2017). Cumulative estuarine discharge flow rates measured at the canals C-44, C-23, C-24, and Ten Mile Creek (**Figure 1**) were obtained from the South Florida Water Management District's DBHYDRO database (**Supplementary Figure 1**), where daily flow rates were averaged for 2 weeks leading up to the corresponding sampling time points. Daily rainfall data were obtained from the same database at the C-44 canal control structure. Small tissue fragments (∼5 cm^2) were collected from the perimeter of each colony using a hammer and chisel, transported to the surface in separate zip-top bags containing ambient seawater, and preserved in TRIzol reagent within 30 min of collection. Preserved samples were then kept on ice until storage at −80°C prior to RNA extraction and library preparation.

Ex situ Experiment

Full details of the experimental apparatus used in the *ex situ* experiment are described in Shatters (2017). In summary, a two-factor (temperature and water) factorial apparatus was constructed using twelve 150-L glass aquaria across six open-top raceways. Three tank replicates per each of the four experimental treatments were randomly distributed among the raceways, with continuous monitoring of temperature, pH, and ORP with Neptune Systems Apex controllers, daily monitoring of salinity with a refractometer, and a 9-h photoperiod using Hydro Grow Sol LED lights set to comparable PAR levels (∼102 μmol m^{-2} s^{-1}) found at the coral collection site based on *in situ* data collection with Onset HOBO data loggers. Temperature treatment levels (control: 25°C; elevated: 30°C) were determined from mean temperatures recorded before and during discharge events, respectively, by Odyssey conductivity and temperature data loggers deployed from October 2013 to January 2015 at the St. Lucie Reef study sites (Shatters, 2017; **Figure 1** inset). Raceways were temperature-controlled using immersion heaters and in-line chillers to reflect the two temperature treatments, with three raceways per temperature treatment. Offshore water (∼32 psu) was collected via a subsurface pump from the Florida Oceanographic Society at high tide. The discharge water parameters were similarly determined from salinity data obtained before and during discharge events, where the mean salinity of the estuarine discharge plume during outgoing tides was ∼28 psu. Discharge water was collected via a pump at 0.5 m depth in the inlet during low slack tide, 5 days after flow rates through the canals from Lake Okeechobee reached a flow rate of 99.02 m^3 s^{-1} (Shatters, 2017). The resulting water (19 psu) was then adjusted with offshore water to achieve the treatment salinity of 28 psu, resulting in a ∼17/83% mix between discharge and offshore water, respectively. Both water types were initially filtered (50, 10, then 1 μm) and UV-sterilized, and stored in opaque holding tanks.

Due to state park regulations restricting whole-colony collection, eleven *Montastraea cavernosa* colonies of 150–175 cm^2 in size with no tissue loss, paling, or other visible signs of stress were collected south of SLR at Breakers Reef (26.6908 N, −80.0181 W) at depths of 13–17 m (**Figure 1**). Temperature data loggers deployed in June 2015 confirmed that ambient temperature was similar between sites (∼28°C) despite difference in depth. Following transport to the lab, colonies were cut with a tile saw into twelve 3 cm × 4 cm colony replicates [genotyped in Dodge et al. (2020)], and randomly positioned in each of the twelve treatment tanks (n = 33 per treatment, n = 132 total; **Table 2**). The *ex situ* experiment was conducted over 32 days, with a 7-day recovery/acclimatization period, 5-day ramp to experimental conditions (achieved with daily ∼15% water changes and <1°C temperature adjustments), and 20-day experimental treatment. Coral fragments were fed ∼10 g of brine shrimp per tank every 3–4 days over the course of the experiment. At the end of the treatment period, coral fragments were split into subsamples for gene expression and symbiont/chlorophyll analyses, and preserved in TRIzol/−80°C and dry/−20°C, respectively.

Symbiont and Chlorophyll Metrics

Symbiont and chlorophyll metrics, including Symbiodiniaceae density (cells cm^{-2}), areal chlorophylls *a* and c_2 (chl cm^{-2}), cellular chlorophylls *a* and c_2 (chl $cell^{-1}$), and chlorophyll a:c_2 ratio, were quantified from the frozen subsamples as described in Shatters (2017). All statistical analyses were conducted in the R statistical environment (R Core Team, 2019). Symbiont and chlorophyll metrics could not be normalized with data transformation, therefore non-parametric tests were used. Data were first assessed for homogeneity of variance among treatment groups using the *betadisper* function of the package *vegan* (Oksanen et al., 2015), utilizing Euclidean distance matrices and 9,999 permutations. Following identification of statistically equal variance (all $p > 0.05$), univariate PERMANOVAs were conducted using the *adonis* function in *vegan* to identify potential effects of experimental treatments (genotype, temperature, water) on symbiont and chlorophyll metrics. Pairwise comparisons were made among single-factor combinations of temperature and water treatments for each of the metrics using the *nctp* function of the package *nparcomp* (Konietschke et al., 2015). Multivariate effects were assessed using a three-factor PERMANOVA and pairwise colony tests using the packages *vegan* and *RVAideMemoire* (Hervé, 2019), respectively. Both multivariate tests used the same model parameters as indicated before, with FDR p value correction for the pairwise comparisons.

TABLE 2 | Sampling information for temperature and water treatment factors in the *ex situ* experiment.

Temperature	Water	Genotype		$n_{collected}$	$n_{ex\ situ}$
		n_{total}	n_{reps}		
Control	offshore	11	3	33	32
	discharge	11	3	33	33
Elevated	offshore	11	3	33	32
	discharge	11	3	33	33
			Total	132	130

Total number of coral genotypes denoted by n_{total}, with the number of genotypic replicates as n_{reps}. The total number of samples for each treatment group given as $n_{collected}$, with the number of samples used in statistical analyses as $n_{ex\ situ}$.

Library Preparation and Sequencing

For both experiments, RNA extractions and Tag-Seq library preparation protocols were followed as in Studivan and Voss (2020). In short, total RNA was extracted using a modified phenol-chloroform protocol (Chomczynski and Sacchi, 1987, 2006), DNase *I* treated using an Ambion kit, and purified using a LiCl precipitation. Only samples with at least 1 μg of total RNA were used for library preparation according to the Tag-Seq protocol first described in Meyer et al. (2011) and modified as in Studivan (2020b). In summary, cDNA libraries were amplified over 22 cycles, dual-barcoded with individual 5′ and 3′ Illumina indices, and equally combined using qPCR into three pools encompassing samples from both experiments. A total of 275 sample pools were generated (*in situ*: n = 111; *ex situ*: n = 164), including libraries that were removed for subsequent statistical analyses. Pools were then sequenced at the University of Wisconsin Biotechnology Center on an Illumina HiSeq 2500 with V4 chemistry and 15% *PhiX* spike-in, generating 1 × 50 bp single-end reads. For all samples across both experiments, 1.30 billion reads were produced, with a mean number of 4.73 ± 0.16 (mean ± SE) million reads per sample.

Differential Expression Analyses

Raw sequences were first processed separately for each experiment to obtain cleaned, mapped, and quantified reads using pipelines described in a GitHub repository associated with a previous study (Studivan, 2020b; Studivan and Voss, 2020). Cleaned reads were mapped to a concatenated reference transcriptome composed of the coral host *M. cavernosa* (Kitchen et al., 2015; updated genome-derived transcriptome from https://matzlab.weebly.com/data--code.html), and its dominant algal symbiont identified at SLR (Klepac et al., 2015; **Supplementary Data 1**), *Cladocopium* spp. (Davies et al., 2018). Creation and annotation of the combined coral host and algal symbiont reference transcriptome is described in a GitHub repository associated with a previous study (Studivan, 2020a; Studivan and Voss, 2020). Subset datasets were created to remove additional samples not part of the respective *in situ* and *ex situ* experimental designs. For the *in situ* experiment, 49 samples were retained (seven colonies with complete sampling coverage across seven time points) to achieve a balanced design with sufficient replication (**Table 1**). For the *ex situ* experiment, 130 samples were retained as part of the design (**Table 2**). Mapping efficiency to the sequenced samples from both experiments was 17.0 ± 0.3%, resulting in 24,182 isogroups for the *in situ* experiment (15,712 host and 8,470 symbiont), and 27,933 isogroups for the *ex situ* experiment (18,210 host and 9,723 symbiont). Low mapping efficiency has been previously shown to be an issue with the updated version of the *M. cavernosa* transcriptome (Studivan and Voss, 2020), however, improved

mapping with the original transcriptome was countered by relatively poor GO and KOG functional annotations. Statistical analyses were therefore conducted using counts generated from the updated coral transcriptome, following the separation of count data into host and symbiont datasets for separate statistical analyses of coral and algal gene expression for each experiment.

Datasets were pre-filtered to remove low-count genes (cumulative count <10 across all samples in a dataset) to decrease processing time, and then tested for outliers using the package *arrayQualityMetrics* (Kauffmann et al., 2009). Samples violating the distances between sample arrays (S_a) criterion for each of the respective datasets were removed, whereas three host and one symbiont samples were removed from the *in situ* experiment (**Supplementary Figure 2**), and three host and five symbiont samples from the *ex situ* experiment (**Supplementary Figure 3**). Count data were normalized using the variance stabilized transformation in the package *DESeq2* (Love et al., 2014) for data visualization and PERMANOVAs. PERMANOVAs were conducted using *vegan* with 9,999 permutations for both experiments to identify if model terms were significantly affecting gene expression patterns in either the coral host or algal symbionts. Multivariate differences among samples were visualized using PCoAs of Manhattan distance in *vegan* and heatmaps of individual gene expression patterns using the package *pheatmaps* (Kolde, 2019). Tests of differential expression for both experiments were conducted using *DESeq2* to identify differentially expressed genes (DEGs) associated with factors (model terms) and among factor levels (contrast statements) using the "reduced" flag on the respective main models. For the *in situ* experiment, a two-factor main model of time and site was used, with pairwise comparisons between sites and time points. For the *ex situ* experiment, a three-factor model of coral genotype, temperature, and water was used with interaction terms between the main model factors and a blocking factor (to assess whether tank location had an impact on gene expression patterns). Additionally, pairwise comparisons were made between single-factor levels of temperature and water treatments.

Gene Enrichment and Weighted Gene Co-expression Network Analyses

Differentially expressed genes were exported for each of the respective comparisons within experiments and analyzed for larger expression patterns across gene pathways using the package *GO-MWU* (Wright et al., 2015) for gene ontology (GO) databases, and the package *KOGMWU* (Dixon et al., 2015; Matz, 2016; Strader et al., 2016) for eukaryotic orthologous groups (KOGs). Both GO and KOG databases contain universal functional group annotations of individual genes based on biological and biochemical functions (Ashburner et al., 2000; Tatusov et al., 2000, 2003; The Gene Ontology Consortium, 2017). *GO-MWU* identifies GO categories that are significantly enriched by up-regulated or down-regulated genes using Mann–Whitney *U* tests. The resulting outputs identify significantly enriched GO categories and their relative levels of expression across the three GO divisions (Molecular Function, Biological Processes, and Cellular Components) according to an FDR-corrected *p* value cutoff of 0.05, or a fold change cutoff of 1. The *KOGMWU* analysis is similar, although enrichment of functional pathways is compared across universal KOG categories to produce a heatmap (Nordberg et al., 2014).

Prior to weighted gene co-expression network analysis (WGCNA) of the *ex situ* experiment, host and symbiont datasets were further filtered to remove genes with counts <10 across >90% of samples. Correlational networks were then created blind to experimental design based on gene expression patterns using the package *WGCNA* (Zhang and Horvath, 2005; Langfelder and Horvath, 2008). In short, groups of genes with similar expression patterns (modules) were first identified across samples, then correlated to experimental factors (coral genotypes, temperature/water treatments, symbiont, and chlorophyll metrics) based on strength of the module-trait associations. The protocol used to conduct WGCNA, as well as scripts for all other analyses described above, can be found in a GitHub repository associated with this study (Studivan, 2021). Soft thresholds were adjusted to fit each particular dataset (11 for host, 4 for symbiont) to achieve a suitable scale-free topology index, with no merging of original modules. Module-associated genes were then exported from the host dataset for GO enrichment analysis.

RESULTS

In situ Experiment

Differential Expression

Pre-filtering of raw counts produced datasets of 8,497 coral host and 1,652 symbiont transcripts across 46 and 48 samples, respectively. Analysis of gene expression patterns across *in situ* experiment factors (site, time) using PERMANOVA yielded that only time was a significant factor for both host and symbiont datasets (host: $R^2 = 0.24537$, $p < 0.0005$; symbiont: $R^2 = 0.27559$, $p < 0.0001$; **Table 3**). *DESeq2* identified 927 host and 50 symbiont differentially expressed genes (DEGs) associated with time, while only 60 host and 30 symbiont DEGs were identified for site, and zero DEGs for the interaction term (**Supplementary Table 1**). DEGs identified for each of the pairwise comparisons across sites and sampling time points can also be found in **Supplementary Table 1**. PCoAs and heatmaps of samples through time suggested that transcriptomic variation was primarily attributed to differences from the first two time points (October 2013 and September 2014) to all subsequent time points (**Figure 2**). There appeared to be limited overlap in the PCoAs between samples collected during periods of relatively high estuarine discharge and rainfall (indicated by cooler colors in **Figures 2A,C** and **Supplementary Figure 1**), however, similarities between sample dispersions from consecutive time points (e.g., October 2013 and September 2014) suggest that other environmental factors beyond discharge rates alone may have influenced gene expression patterns in both the coral host and their algal symbionts.

TABLE 3 | PERMANOVA model results for *in situ* and *ex situ* experiments, split into coral host (*M. cavernosa*) and symbiont (*Cladocopium* spp.) datasets.

Experiment	Transcriptome	Factor	df	*F*	R^2	*p*
In situ	*M. cavernosa*	time	6	1.97015	0.24537	0.0005
		site	2	1.08488	0.04504	ns
		time:site	12	0.76551	0.19067	ns
	Cladocopium spp.	time	6	2.55542	0.27559	0.0001
		site	2	1.33834	0.04811	ns
		time:site	12	0.88555	0.1910	ns
Ex situ	*M. cavernosa*	genotype	10	1.93917	0.14197	0.0001
		temp	1	1.50026	0.01098	0.0197
		water	1	1.34431	0.00984	0.0516‡
		genotype:temp	10	1.01897	0.07460	ns
		genotype:water	10	0.9474	0.06936	ns
		temp:water	1	1.38031	0.01011	0.0452
		tank:genotype	22	1.02122	0.16449	ns
		tank:temp	2	1.15954	0.01698	ns
		tank:water	2	1.00889	0.01477	ns
		genotype:temp:water	10	0.95034	0.06958	ns
	Cladocopium spp.	genotype	10	1.10535	0.08906	0.0871†
		temp	1	2.32889	0.01876	0.0013
		water	1	1.20874	0.00974	ns
		genotype:temp	10	0.97299	0.07839	ns
		genotype:water	10	0.84455	0.06805	ns
		temp:water	1	1.61407	0.0130	0.0208‡
		tank:genotype	22	0.97218	0.17232	ns
		tank:temp	2	1.05123	0.01694	ns
		tank:water	2	0.97611	0.01573	ns
		genotype:temp:water	10	0.92919	0.07487	ns

Insignificant p values are shown as ns, with marginal p values denoted with †, and ‡ identifies significant interaction terms despite one of the main factors being insignificant.

Gene Enrichment Analyses

Since site did not have a significant impact on gene expression, subsequent analyses were conducted among sampling time points, combining samples across sites. Analysis of gene ontology (GO) categories enriched for the coral host dataset over sampling time points identified two main groups of pairwise time comparisons. From the first two time points (October 2013 and September 2014) to subsequent time points, all but one GO category in the biological process (BP) division demonstrated reduced expression in the later versus earlier time point (**Supplementary Figure 4**). Of these, several categories were consistently represented in pairwise time comparisons, including: "RNA catabolic process," "nuclear-transcribed mRNA catabolic process, nonsense-mediated decay," "protein localization to endoplasmic reticulum," and "protein-containing complex disassembly." Between time points after October 2015, the majority of GO categories were instead over-expressed in later versus earlier time points, including several of the aforementioned categories (**Supplementary Figure 4**). This indicated a shift in expression of gene pathways through time, primarily occurring between 2013 and 2015–2016 time points, and between 2015 and 2016 time points. For the symbiont dataset, only one GO category in the BP division was significantly enriched in pairwise comparisons of time points ("negative regulation of metabolic process," comparing March 2016 versus June 2015).

Analysis of eukaryotic orthologous groups (KOGs) identified only one KOG class in the host dataset with relatively strong variation through time, where "nuclear structure" was negatively enriched between the first two time points and subsequent time points, and represented by higher-expressed genes between 2015 and 2016 time points (**Supplementary Figure 5**). Other KOG classes, including "cell motility," "nucleotide transport and metabolism," and "extracellular structures" demonstrated mild variation in expression through time. For the symbiont dataset, however, the majority of the KOG classes contained under-expressed genes in later versus earlier time points, with the exception of "extracellular structures" that showed variation through time. This KOG class was more highly-expressed in 2015–2016 versus 2013–2014 time points, but less-expressed in 2016 versus 2015 time points (**Supplementary Figure 5**).

Ex situ Experiment

Symbiont and Chlorophyll Metrics

Coral genotype and temperature treatments were significant factors affecting all symbiont and chlorophyll metrics, with the exception of cellular chlorophylls *a* and c_2 for temperature (**Supplementary Table 2**). Only areal chlorophyll *a* was marginally affected ($p < 0.0612$) by the water treatment; all other metrics were non-significant. Multivariate pairwise differences among coral genotypes are found in **Supplementary Table 3**. Significant pairwise *p* values between single-factor

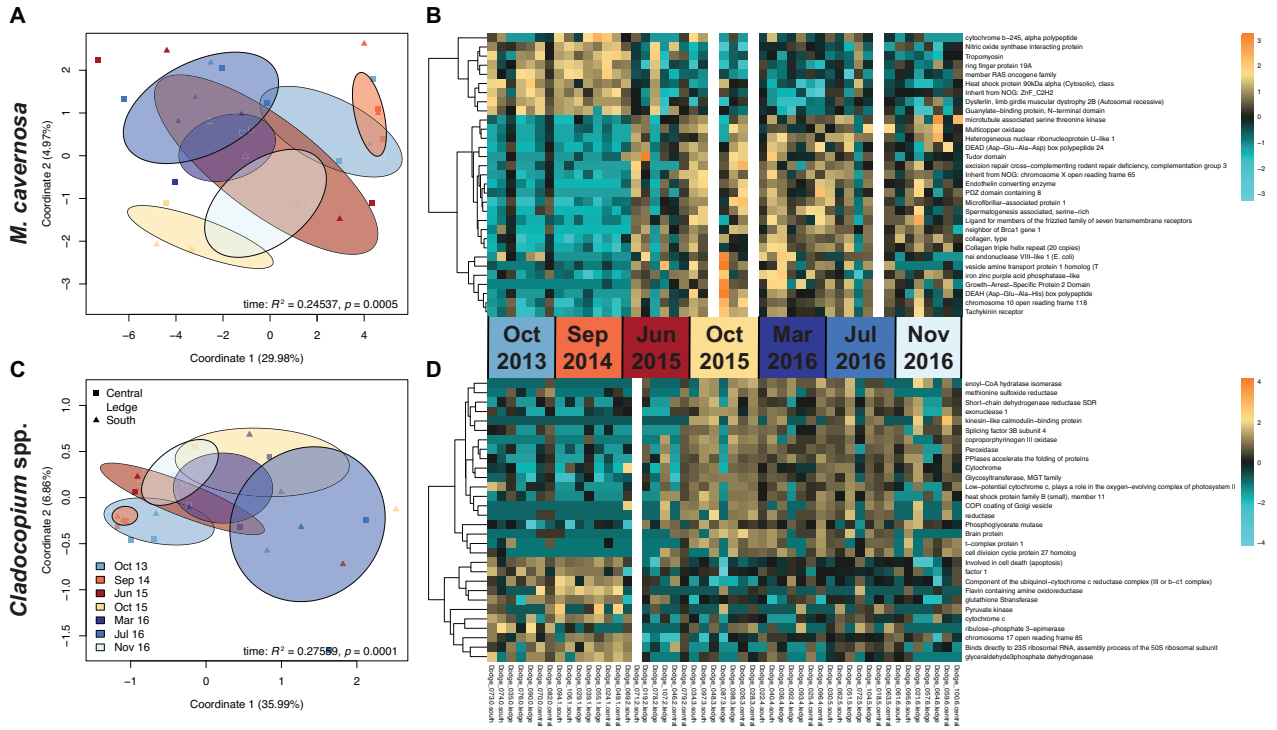

FIGURE 2 | (A,C) PCoAs of coral host and symbiont datasets depicting transcriptomic variation through time from the *in situ* experiment. Colors correspond to sampling time point, where warmer colors represent periods of relatively low estuarine discharge (South Florida Water Management District DBHYDRO; September 2014: 6.15 m^3 s^{-1}, June 2015: 3.08 m^3 s^{-1}, October 2015: 14.29 m^3 s^{-1}) and cooler colors represent periods of higher discharge (October 2013: 44.99 m^3 s^{-1}, March 2016: 70.52 m^3 s^{-1}, July 2016: 59.37 m^3 s^{-1}, November 2016: 33.31 m^3 s^{-1}). Ellipses denote the dispersion of each time point's samples, and sites are indicated by point shapes. Test statistics and p values were generated from PERMANOVAs in vegan. **(B,D)** Heatmaps of the most highly significant DEGs, organized by site within time points using a Benjamini-Hochberg-corrected p value cutoff of $1e^{-6}$ for host and 0.01 for symbiont datasets. Gaps represent outlier samples removed from each dataset. Increasing intensities of gold indicate higher expression of genes in samples, while increasing intensities of turquoise indicate lower expression.

combinations of temperature and water treatments were only found for comparisons between control and elevated temperature treatments for symbiont density and both areal chlorophyll metrics. Symbiont density and areal chlorophylls *a* and c_2 were significantly reduced in both elevated temperature treatments, with no significant pairwise differences between offshore and discharge water treatments, respectively (**Supplementary Figure 6**). The ratio of chlorophylls a:c_2 and cellular chlorophylls *a* and c_2 did not vary significantly among treatments.

Differential Expression

Pre-filtering of raw counts resulted in 11,248 coral host and 1,834 symbiont transcripts across 127 and 125 samples, respectively. PERMANOVA results for the *ex situ* experiment indicated that genotype and temperature were significant factors, while water was marginally significant for the host dataset, and there was a significant temperature:water interaction (genotype: R^2 = 0.14197, p < 0.0001; temperature: R^2 = 0.01098, p < 0.0197; water: R^2 = 0.00984, p < 0.0516; temperature:water: R^2 = 0.01011, p < 0.0452; **Table 3**). For the symbiont dataset, genotype was marginally significant while temperature significantly affected algal gene expression (genotype: R^2 = 0.08906, p < 0.0871; temperature: R^2 = 0.01876, p < 0.0013; **Table 3**). *DESeq2* identified 1,450 host and 18 symbiont differentially expressed genes (DEGs) associated with genotype, 1,575 [725 up, 850 down; (elevated/control)] host and 25 (8 up, 17 down) symbiont DEGs for temperature, while only 45 [13 up, 32 down; (discharge/offshore)] host and 0 symbiont DEGs for water, and 35 host and 0 symbiont DEGs for temperature:water (**Supplementary Table 1**). For both datasets, the highest number of DEGs were associated with pairwise treatment comparisons of elevated discharge over control offshore samples, with 269 (74 up, 195 down) host and 33 (6 up, 27 down) symbiont genes (**Figure 3**). Corals appeared to respond more strongly to estuarine discharge than did the symbionts across all treatments. DEGs associated with each of the remaining interaction terms and pairwise comparisons between treatments are found in **Supplementary Table 1**. PCoAs demonstrated that there was stronger genotypic variation in the coral host than in the symbiont dataset, as well as evidence of a synergistic effect of temperature and water treatments for both datasets (**Figure 4**). Each of the temperature and water treatments alone were relatively close to one another in the ordination space, with a somewhat distinct sample spread for the combined treatment (elevated discharge).

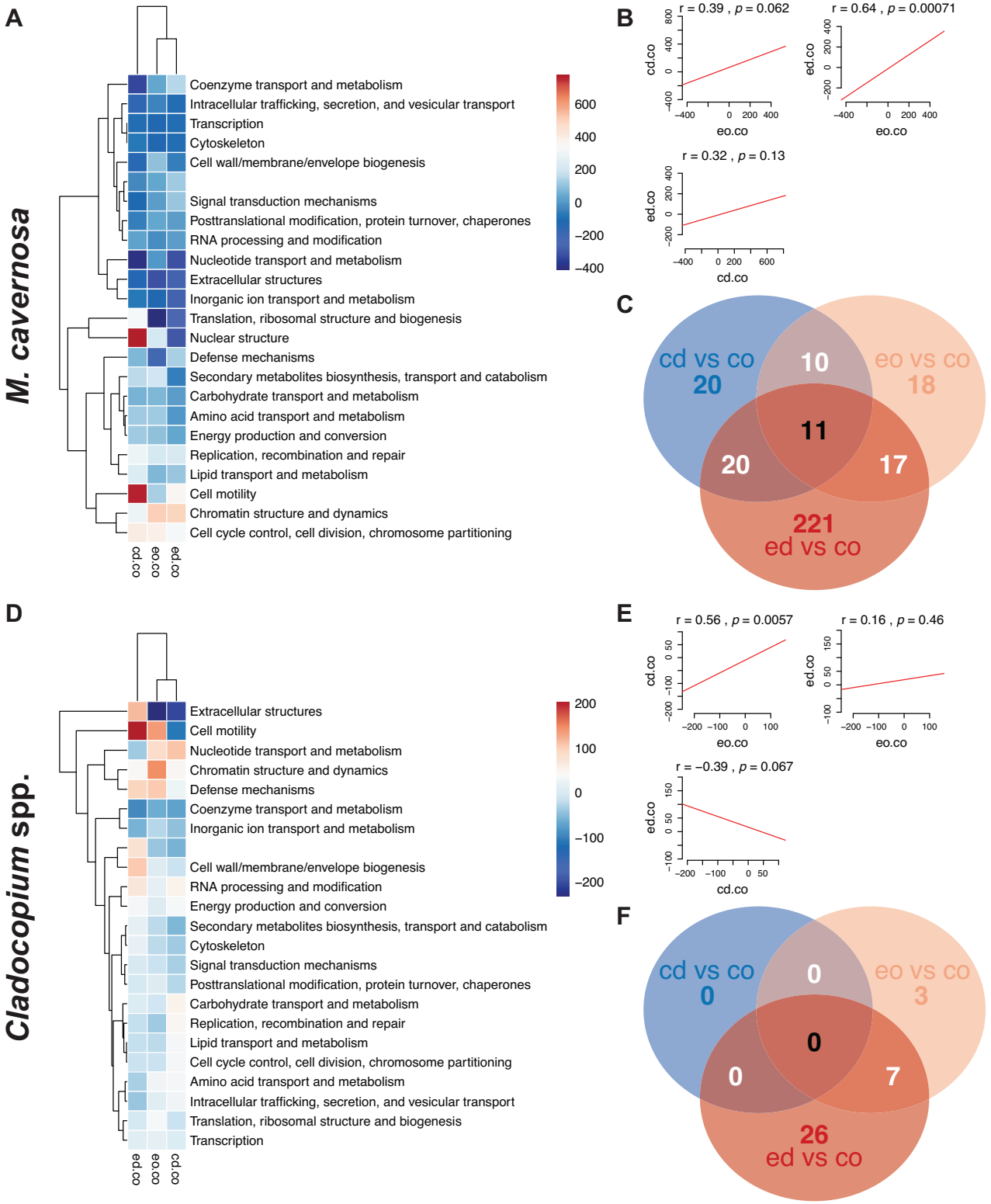

FIGURE 3 | (A,D) Heatmaps of eukaryotic orthologous groups (KOGs) among pairwise comparisons of water + temperature factors for the *ex situ* experiment, split into coral host (*M. cavernosa*) and symbiont (*Cladocopium* spp.) datasets. Increasing intensities of red/blue indicate enrichment of KOGs more-expressed/less-expressed in treatments (cd, control discharge; eo, elevated offshore; ed, elevated discharge) versus control offshore (co) samples. Color values represent ranks generated from Mann–Whitney *U* tests. Hierarchical networks on both axes display the similarities among pairwise comparisons (*x*-axis) and KOG classes (*y*-axis). **(B,E)** Panels of correlation analyses between pairwise comparison combinations. **(C,F)** Venn diagram displaying the number of DEGs associated with each pairwise treatment comparison.

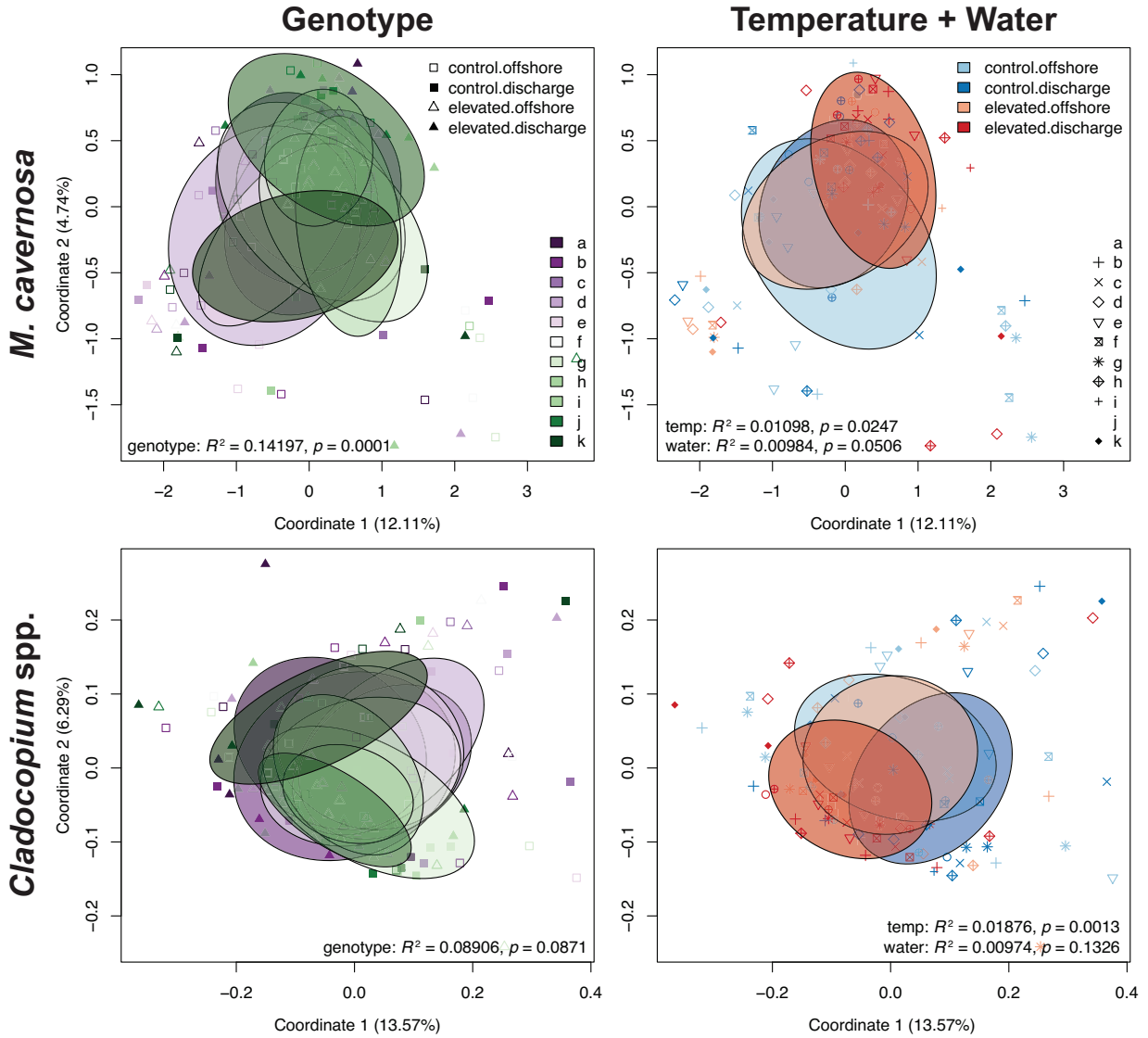

FIGURE 4 | PCoAs of coral host and symbiont datasets depicting transcriptomic variation for coral genotypes and temperature + water treatments from the *ex situ* experiment. Ellipses denote the dispersion of each factor's samples. Test statistics and *p* values generated from PERMANOVAs in *vegan*.

Gene Enrichment and Weighted Gene Co-expression Network Analyses

Gene ontology categories across all three divisions (molecular function, MF; biological process, BP; cellular component, CC) were largely positively-enriched in elevated versus control temperature and discharge versus offshore water, respectively (**Figure 5**). The overall number of significantly enriched GO terms, as well as the number of DEGs within those GO categories, were higher for the temperature treatment compared to the water treatment, although there were several similarities between the two. GO categories "structural constituent of ribosome" (MF), "translational initiation" (BP), "translational elongation" (BP), "RNA catabolic process" (BP), "cellular component disassembly" (BP), and several ribosomal pathways (CC) were elevated in both temperature and water treatments relative to their respective controls. Few GO categories, on the other hand, were under-expressed in treatments ["lysase" (MF), "transferase" (MF), "carboxylic acid catabolic process" (BP), "cell projection part" (CC), and "basolateral plasma membrane" (CC)], although none of these were represented across both temperature and water treatments.

Eukaryotic orthologous group analyses across main factors identified three main trends: (1) expression patterns for genotype and temperature factors were strongly correlated for both host and symbiont datasets, (2) some KOG classes had an inverse relationship between responses to temperature and water stress in both datasets, and (3) corals and symbionts responded differently to the same factors (**Supplementary Figure 7**). Indeed, correlation coefficients between genotype and temperature

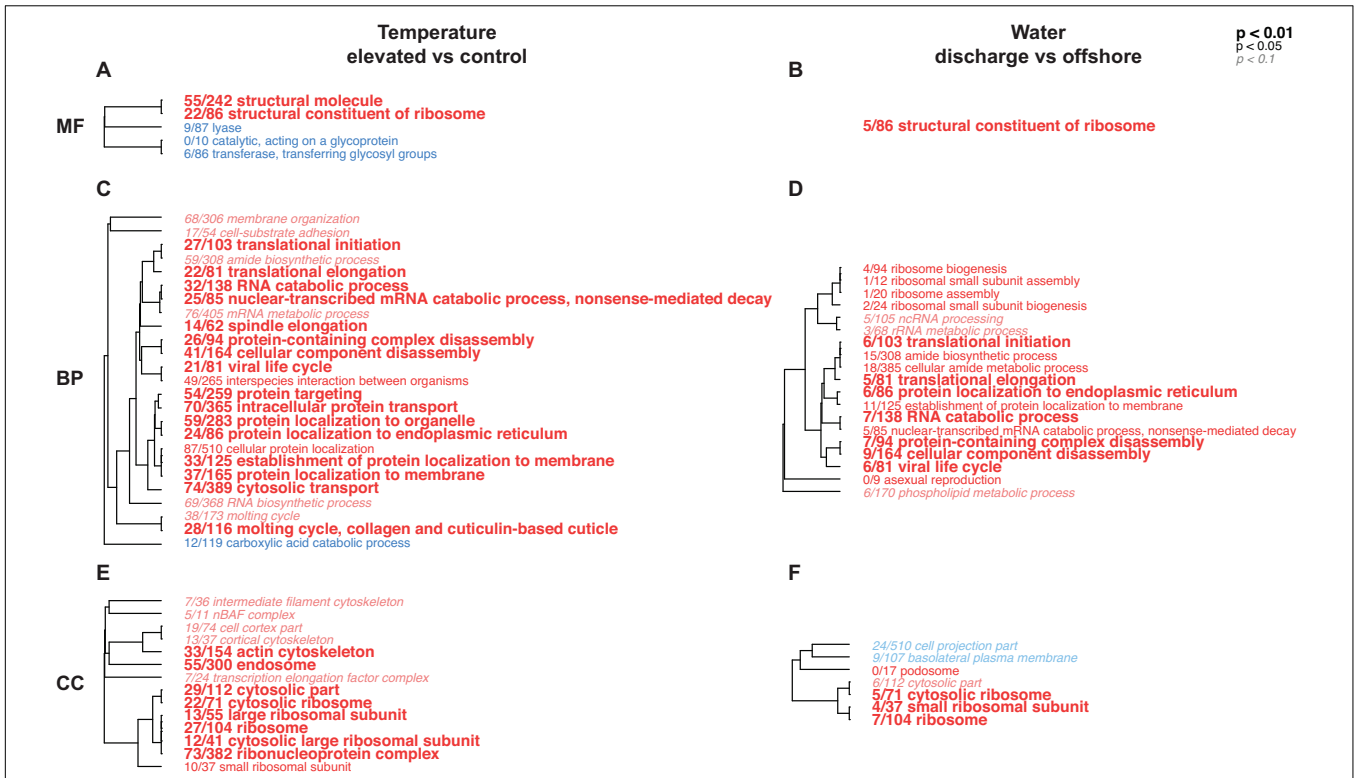

FIGURE 5 | Hierarchical trees representing significantly enriched gene ontology (GO) categories in pairwise comparisons between temperature and water treatments in the coral host dataset for the *ex situ* experiment. Blue terms represent under-expressed GO categories in (treatment/control), while red terms indicate over-expressed GO categories in (treatment/control). The size and typeface of the font correspond to the *p* value threshold, where larger, bolded GO terms are more significantly enriched compared to smaller, italicized GO terms, and the number fraction refers to the number of genes represented in each GO category. Annotations are presented for molecular function (MF; **A,B**), biological process (BP; **C,D**), and cellular component (CC; **E,F**) GO divisions.

responses were $r = 0.99$ with highly significant p values in both datasets, suggesting that variation in response to temperature stress was innately tied to coral genotype, and was largely captured by the latter term in statistical models. Several KOG classes, including "cytoskeleton," "extracellular structures," and "nuclear structure" were differentially expressed between water and temperature treatments for the coral host (**Supplementary Figure 7A**). For the symbiont dataset, "extracellular structures" and "coenzyme transport and metabolism" were differentially expressed between water and temperature treatments, while other KOG classes showed generally weaker enrichment in the water treatment compared to the temperature and genotype factors (**Supplementary Figure 7D**).

When examining pairwise combinations of treatments against the control (control offshore) for the host dataset, only two KOG classes ("nuclear structure" and "cell motility") were positively enriched in control discharge versus both elevated temperature treatments (**Figure 3A**). In the symbiont dataset, the same was true of "cell motility," while "extracellular structures" and "nucleotide transport and metabolism" classes were more-expressed in control discharge and elevated offshore treatments versus elevated discharge samples (**Figure 3D**). Both of these observations may imply that the coral host responded more strongly to elevated temperatures than estuarine discharge, while algal symbionts demonstrated a synergistic response to elevated temperatures and estuarine discharge combined.

Further filtering of raw gene counts for WGCNA resulted in a dataset of 967 host and 43 symbiont genes. WGCNA clustered genes into five modules for the host dataset and a single module for symbionts; therefore only host data are presented (**Supplementary Figure 8**; five host genes were unassigned). All of the modules demonstrated significant correlations to individual coral genotypes, while turquoise, yellow, green, and blue modules were also significantly correlated with experimental treatments, suggesting genotype-driven transcriptomic responses to stress. None of the symbiont or chlorophyll metrics were significantly correlated to any of the modules. Variation in module correlation directions between elevated offshore and elevated discharge treatments (turquoise, yellow, and green modules) corroborated a potential synergistic effect of temperature stress and water treatments on coral gene expression patterns. GO-MWU analysis of host modules identified significantly enriched GO categories within blue and brown modules only, with enriched ribosomal and cell division GO categories in the blue module, and immune/stress response and cell component GO terms enriched in the brown module (**Supplementary Figure 8**).

DISCUSSION

In situ Experiment

Temporal analyses of gene expression across three sites at St. Lucie Reef revealed that time was the only significant factor driving transcriptomic patterns for both the coral host and its symbiotic algae. This suggests that despite observations of rapid changes in water quality parameters following discharge events along a gradient with increasing distance from the St. Lucie Inlet (Beal et al., 2012; Pickering and Baker, 2015; Shatters, 2017), corals responded similarly at the transcriptomic level among sites. There did not appear to be a strong relationship between estuarine discharge rates at the time of sampling to either coral or symbiont expression profiles. Taken in the larger context of seasonal variation including rainfall and discharge rates, however, there were observed shifts in expression patterns from the first two time points to all subsequent time points (**Figure 2**). The wet and dry seasons in 2013–2014 followed the typical pattern described earlier (Beal et al., 2012; Klepac et al., 2015), but the 2015 "wet" season was unusually dry (Shatters, 2017), and was followed by an abnormally rainy 2015–2016 "dry" season (Stockley et al., 2018). Likewise, the number and magnitude of discharge events varied over the course of the study (**Supplementary Figure 1**). In 2013–2014, there were several larger pulses of discharge (>50 m^3 s^{-1}) during the wet season, with relatively low or no discharge events during the dry season. Beginning in 2015, conversely, there were lower (<40 m^3 s^{-1}), but consistent, discharges throughout the year, followed by approximately 9 months of discharge at rates in excess of 50 m^3 s^{-1}, and in excess of 150 m^3 s^{-1} in 2016 (**Supplementary Figure 1**; Stockley et al., 2018).

The apparent shifts in gene expression patterns at later versus earlier time points is perhaps the result of covarying environmental factors through time, namely compounding rainfall and discharge flow rates that introduce hyposalinity, nutrient, and elevated temperature stressors to the reef. In the coral host, this is best illustrated by relative expression through time of genes within the "nuclear structure" KOG class. Despite relatively low sequencing coverage associated with the algal symbionts, genes in the "extracellular structures" class were differentially expressed over time (**Supplementary Figure 5**). Many of the gene ontology (GO) categories that were under-expressed in comparisons between 2015–2016 and initial 2013–2014 time points were then over-expressed in 2016 versus 2015 time points, suggesting variable expression of the same gene pathways in response to different levels of estuarine discharge exposure and hyposalinity stress associated with increased rainfall. Few studies have examined transcriptomic responses to sublethal exposures of estuarine water in natural environments, where differentially expressed stress response genes were linked to increased precipitation and runoff events [Beal et al., 2012; Edge et al., 2013; but see also Wright et al. (2019)].

A recent metanalysis, however, has suggested that transcriptomic responses may be conserved across various stressors, with diverging responses dependent on stress intensity. Dixon et al. (2020) identified a type "A" response to high-intensity bleaching, heat, hyposalinity, or immune challenge stressors where cell death, immune response, and protein degradation pathways were generally up-regulated, and a type "B" response to lower-intensity stress exposures with an inverse relationship to type "A" expression levels. During the time period of our study, no phenotypic changes occurred in the fate-tracked colonies (i.e., bleaching or tissue mortality) to suggest that corals were exposed to high-intensity stress. Expression of gene pathways associated with cell growth [e.g., KOG terms "nuclear structure" in the coral host and "extracellular structures" in the symbionts (**Supplementary Figure 5**); GO terms "protein localization to endoplasmic reticulum" and several mitosis-related pathways in the coral host (**Supplementary Figure 4**)] were generally more expressed during later sampling time points when discharge rates and rainfall were higher, compared to earlier time points with less consistent freshwater inputs to the reef (**Supplementary Figure 1**). Immune GO pathways including "regulation of immune effector process" and "regulation of production of molecular mediator of immune response" were conversely down-regulated during the later sampling time points (**Supplementary Figure 4**). These patterns would therefore suggest that corals at St. Lucie Reef were exhibiting a more type "B" response following sublethal exposures to estuarine discharge and hyposaline stress.

While individual sublethal stressors may not cause significant disruptions to the coral-algal symbiosis, consecutive or concurrent stress events that are common in nearshore environments may form a "negative feedback loop" ultimately leading to colony mortality. In particular, exposure to salinity stress and/or sedimentation in estuarine discharge water has been shown to increase susceptibility of corals to diseases (Pollock et al., 2014; Shore-Maggio et al., 2018). While it was perhaps inevitable that SCTLD would reach coral populations in the northern extent of the reef tract, repeated exposure to estuarine discharge may have exacerbated individual corals' susceptibility to SCTLD infection and contributed to the spread of the disease across additional reefs. Testing this hypothesis requires further manipulative experiments applying multiple stressors experienced by nearshore reefs to observations of SCTLD transmission and progression. Transcriptomic approaches may also increase the ability to recognize early signs of infection following exposure to multiple sublethal stressors. Beyond synergistic effects on coral/symbiont physiology and health, estuarine discharge may have additional ramifications for the survival of coral populations in southeast Florida. For example, exposure to hyposalinity stress can severely limit coral fertilization success (Hédouin et al., 2015). The frequent hyposaline conditions (e.g., 27–28 psu commonly measured at St. Lucie Reef but as low as 19 psu for brief periods) in this region due to estuarine outflow, Lake Okeechobee discharges, and watershed runoff may contribute to the rare occurrence of reproduction in St. Lucie Reef corals (Beal et al., 2012).

Ex situ Experiment

In the *ex situ* factorial experiment, there was clear evidence of transcriptomic responses to thermal stress in both the coral host, and to a lesser extent, their algal symbionts (**Supplementary Table 1** and **Supplementary Figure 7**). It is possible that reduced representation of symbiont transcripts in part explains the limited variation among treatments and lack of significantly enriched GO pathways in the symbiont dataset. In the coral host, several gene pathways were elevated following exposure to the increased temperature treatments, including GO categories for metabolic and catabolic processes, protein translation and localization, and translational elongation, which are part of the metabolic and photosynthetic responses to thermal stress (Murata et al., 2007; Reyes-Bermudez et al., 2009; Seneca and Palumbi, 2015; Davies et al., 2016; Studivan and Voss, 2020). Ribosomal expression was also higher in elevated temperature corals, which is likely associated with an attempt by the corals to return to homeostasis following exposure to stress (Kültz, 2005; DeSalvo et al., 2008; Kenkel et al., 2013b). Several of the GO categories described above, including "protein localization to endoplasmic reticulum," "nuclear-transcribed mRNA catabolic process," and protein-containing complex and cellular component disassembly, were positively expressed in the final time points of the *in situ* experiment (**Supplementary Figure 4**). The KOG classes "nuclear structure" and "extracellular structures" were also differentially enriched for temperature and water treatments (**Supplementary Figure 7**), reinforcing the notion that *in situ* corals at St. Lucie Reef were likely responding to sublethal stress during 2015 and 2016 time points similarly to the artificial stress treatments applied in the *ex situ* experiment. These similarities also demonstrated that corals in the *ex situ* experiment were demonstrating a type "B" transcriptomic response to sublethal environmental stress (Dixon et al., 2020).

While exposure to estuarine discharge water alone did not significantly alter coral or symbiont gene expression patterns in the *ex situ* experiment, many of the same GO categories that were positively enriched with thermal stress were also enriched with exposure to discharge water (**Figure 5**). This observation concurs with the hypothesis of a conserved stress response among broad taxonomic groups including corals (Wang et al., 2009; Dixon et al., 2020), with variation of genes or expression levels within a general environmental stress response that may be stressor-specific. For example, hyposaline conditions can lead to differential expression of heat shock protein and oxidative stress genes, among others (Seveso et al., 2013; Aguilar et al., 2019). Our data suggest that responses were similar in terms of gene function, but that thermal stress caused stronger responses in both corals and their symbionts. There was also a synergistic effect between temperature and water treatments that could not be explained by elevated temperature or estuarine discharge alone (**Figures 3**, **4** and **Supplementary Figure 6**). Previous studies have observed synergistic effects of multiple stressors including temperature, salinity, and nutrient factors, with proteomic indicators of oxidative stress (Dias et al., 2019b), bleaching and reduced growth/condition (Coles and Jokiel, 1978), and reduced photosynthetic performance and/or mortality (Li et al., 2009; Faxneld et al., 2010; Dias et al., 2019a). Exposure to multiple stressors may cumulatively result in more severe impacts than with individual type "B" stressors alone, and can lead to a type "A" stress response (Dixon et al., 2020). In addition to direct effects of multiple stressors on coral health, thermal stress has been shown to impede several species' ability to cope with enhanced sedimentation (Bessell-Browne et al., 2017), and causes reductions of surface mucopolysaccharide layers (i.e., where mucus is produced) in *P. clivosa* (Pratte and Richardson, 2014). Such synergistic relationships could have important ramifications for the health of corals in Florida, as nearshore reef environments are often exposed to several stressors simultaneously with tidal fluctuations (Yentsch et al., 2002; Lirman and Fong, 2007; Beal et al., 2012; Gregg, 2013).

Synergistic effects of discharge water and thermal stress treatments were not apparent in the symbiont and chlorophyll metrics; significant differences among treatments were attributed only to elevated temperatures (**Supplementary Figure 6**). Previous studies examining physiological responses to hyposaline conditions identified reductions in symbiont densities and photosynthetic efficiency (Kerswell and Jones, 2003; Downs et al., 2009; Gardner et al., 2016), although this response may be dependent on the coral species. *Siderastrea radians*, a common shallow-water species found extensively in nearshore reef environments in Florida, was not affected by hyposalinity stress until its predicted lower tolerance limit of 10 psu (Chartrand et al., 2009; Lirman and Manzello, 2009). Such limits have not been established for *M. cavernosa*, but it has been hypothesized that salinity and light attenuation are major limiting factors in the distribution of nearshore coral populations (Yentsch et al., 2002; True, 2012), and that inshore environments experience seasonal stress and recovery phases (Haslun et al., 2016). While our *ex situ* experiment did not examine as many salinity treatments as the aforementioned studies, significant differences were observed between similar salinity levels as tested here. Also, areal chlorophyll metrics differed among treatments whereas cellular chlorophyll metrics did not, implying that decreases in areal chlorophylls *a* and c_2 were largely driven by reduced symbiont density in elevated temperature treatments, rather than a change in the number of symbiont cells within coral symbiosomes.

Variation in host responses to thermal stress was highly linked with coral genotype (**Figure 3** and **Supplementary Figure 6**), suggesting a strong genetic component to thermal stress susceptibility/resilience. A similar relationship has been identified with several coral species (Baums et al., 2013; Kenkel et al., 2013a; Bay and Palumbi, 2014), and host transcriptomic patterns may also be influenced by symbiont genotypes as well (DeSalvo et al., 2010; McGinley et al., 2012; Rocker et al., 2012; Cunning and Baker, 2020). In our study, it appears that *M. cavernosa* genotypes demonstrated variable susceptibility to thermal stress, as genotype explained an order of magnitude more transcriptomic variation in the coral dataset compared to temperature and water treatments (14.2% versus 1.1% and 1.0%, respectively; **Table 3**).

Additionally, there was a strong correlation of KOG expression between genotype and temperature factors (**Supplementary Figure 7**). Furthermore, in WGCNA, many of the significant correlations observed between experimental factors and modules of related genes were attributed to individual coral genotypes rather than to temperature or water treatments (**Supplementary Figure 8**).

In the symbiont dataset, there was also an influence of coral genotype on transcriptomic patterns, despite relatively homogeneous symbiont assemblages across all samples in the *ex situ* experiment (**Supplementary Data 1**). The marginally significant p value associated with the genotype factor was likely the direct result of a lack of variation in symbiont among coral genotypes. However, 8.9% of the transcriptomic variation was explained by coral genotype, versus 1.9% explained by the temperature treatment (**Table 3**). The strong links between coral genotypes and responses to thermal stress in both host and symbiont gene expression patterns may be indicative of resilience among some individuals in the sampled coral populations. Nearshore reef environments in southeast Florida (including Breakers Reef) experience seasonal and freshwater discharge-related environmental fluctuations, notably including changes in temperature at episodic and chronic temporal scales (Yentsch et al., 2002; Beal et al., 2012; Gregg, 2013). An interesting hypothesis is that these corals are particularly resilient to thermal stress given repeated exposure to temperature variation, resulting in a conserved transcriptomic response to sublethal stress events. Additional research is therefore warranted to further elucidate potential relationships between coral-algal genotypes and susceptibility to multiple stressors in this species across populations in Florida and beyond (Cunning and Baker, 2020; Smith et al., 2020).

Conclusion

Few studies to date have examined coral responses to multiple stressors (e.g., reduced salinity, higher nutrients, sedimentation, increased light attenuation) associated with estuarine discharge in coastal zones. Through complementary *ex situ* and *in situ* experiments, this study demonstrated that corals and their algal symbionts responded to thermal and estuarine discharge stressors, and that synergistic impacts from these stressors could influence their transcriptomic responses. Compared to a recent metanalysis of general environmental stress responses that generalized two characteristic transcriptomic patterns (Dixon et al., 2020), our results suggest that *M. cavernosa* displays a type "B" response following exposure to sublethal stress in both their natural environments and following manipulative treatments. Cell growth and protein production/modification pathways were observed to be up-regulated while immune pathways were down-regulated following temperature and hyposaline stress. Nearshore coral populations at the northern extent of Florida's coral reef tract are commonly exposed to multiple stressors in the form of variable temperature, salinity, and water quality (Yentsch et al., 2002; Lirman and Fong, 2007; Beal et al., 2012; Gregg, 2013) that may combine to negatively affect coral health. Continued examination of marginal populations found in this region may not only identify the molecular mechanisms responsible for coral resilience, but may also identify resilient genotypes for conservation and restoration initiatives. Given that modern coral reef ecosystems, especially those found in coastal environments, are more frequently exposed to multiple stressors, management actions are needed to mitigate potentially synergistic impacts of stressors on the health and resilience of coral reef organisms.

DATA AVAILABILITY STATEMENT

Raw Tag-Seq sequences are available in the National Center for Biotechnology Information (NCBI) Sequence Read Archive (SRA) under BioProject PRJNA698305, Accession numbers SAMN17712326 through SAMN17712600. Datasets generated from this study, including analysis scripts, are available in a GitHub repository (Studivan, 2021). Pipelines used for transcriptome annotation and bioinformatics followed protocols in previously-released GitHub repositories (Studivan, 2020a,b).

AUTHOR CONTRIBUTIONS

JV, JB, AS, and DD secured funding for this research, designed and performed the research, experiments, and initial data analyses, with field and lab assistance from MS. MS analyzed the data and wrote the manuscript, with significant contributions and revisions by all co-authors. All authors contributed to the article and approved the submitted version.

FUNDING

This study was supported by grants to JV and JB from Florida Sea Grant (R/LR-B-70), EPA (X700D66717), and NOAA Coral Reef Conservation Program (NA16NOS4820052), as well as a donation from the River Branch Foundation and from the Banbury Fund in memory of John and Andreija Robertson to establish the Robertson Coral Reef Research and Conservation Program at Harbor Branch Oceanographic Institute. Additional graduate fellowships and grants from the Women Divers Hall of Fame, PADI Foundation, and Indian River Lagoon Graduate Research Fellowship augmented this study.

ACKNOWLEDGMENTS

We thank Maureen Williams, Courtney Klepac, Amanda Alker, Jennifer Polinski, Patrick Gardner, Ashley Sproles, Miguel Martini, Lisa Cohen, and Sara Edge for assistance with field activities and sample collection. St. Lucie Inlet Preserve State Park, Martin County representatives, Florida Fish and Wildlife Conservation Commission, and the Florida Department of Environmental Protection, Coral Reef Conservation Program

provided critical feedback and support on the design of this study. Coral tissue samples were collected from the St. Lucie Inlet Preserve State Park under a permit from the Florida State Park Service (FL State Park permit number 06261715). Coral colonies were collected from Breakers Reef by permission of FWC. Paul Wills, Richard Baptiste, Peter Stock, Gary Luisi, Susan Laramore, and Jay Adams were integral in the development and construction of the *ex situ* experimental apparatus. Dennis Hanisak and Kristen Davis from the Indian River Lagoon Observatory at Florida Atlantic University's Harbor Branch Oceanographic Institute, and Brittany Biber from the Florida Oceanographic Society facilitated collection of estuarine discharge water and seawater. Sequencing services were provided by the University of Wisconsin Biotechnology Center, with exceptional sequencing support from Jeremy Niece and Joshua Hyman, and high-performance computing services were provided by Research Computing Services at Florida Atlantic University. This is contribution 2290 from Harbor Branch Oceanographic Institute at Florida Atlantic University.

SUPPLEMENTARY MATERIAL

The Supplementary Material for this article can be found online at: https://www.frontiersin.org/articles/10.3389/fmars.2021.662220/full#supplementary-material

REFERENCES

Aguilar, C., Raina, J. B., Fôret, S., Hayward, D. C., Lapeyre, B., Bourne, D. G., et al. (2019). Transcriptomic analysis reveals protein homeostasis breakdown in the coral *Acropora millepora* during hypo-saline stress. *BMC Genomics* 20:148. doi: 10.1186/s12864-019-5527-2

Aguilar, C., Raina, J. B., Motti, C. A., Fôret, S., Hayward, D. C., Lapeyre, B., et al. (2017). Transcriptomic analysis of the response of *Acropora millepora* to hypo-osmotic stress provides insights into DMSP biosynthesis by corals. *BMC Genomics* 18:612. doi: 10.1186/s12864-017-3959-0

Anderson, D. A., Walz, M. E., Weil, E., Tonellato, P., and Smith, M. C. (2016). RNA-Seq of the Caribbean reef-building coral *Orbicella faveolata* (Scleractinia–Merulinidae) under bleaching and disease stress expands models of coral innate immunity. *PeerJ* 4:e1616. doi: 10.7717/peerj.1616

Ashburner, M., Ball, C. A., Blake, J. A., Botstein, D., Butler, H., Cherry, J., et al. (2000). Gene Ontology: tool for the unification of biology. The Gene Ontology Consortium. *Nat. Genet.* 25, 25–29. doi: 10.1038/75556

Bak, R. P. M., and Elgershuizen, J. H. B. W. (1976). Patterns of oil-sediment rejection in corals. *Mar. Biol.* 37, 105–113. doi: 10.1007/BF00389121

Baums, I. B., Devlin-Durante, M. K., Polato, N. R., Xu, D., Giri, S., Altman, N. S., et al. (2013). Genotypic variation influences reproductive success and thermal stress tolerance in the reef building coral. Acropora palmata. *Coral Reefs* 32, 703–717. doi: 10.1007/s00338-013-1012-6

Bay, R. A., and Palumbi, S. R. (2014). Multilocus adaptation associated with heat resistance in reef-building corals. *Curr. Biol.* 24, 2952–2956. doi: 10.1016/j.cub.2014.10.044

Beal, J., Voss, J. D., Edge, S., and Cohen, L. (2012). *Assessment of Coral Stressors on St. Lucie Reef: Florida's Northernmost Coral Reef*. Washington, DC: US Fish and Wildlife Service, 1–54.

Bessell-Browne, P., Negri, A. P., Fisher, R., Clode, P. L., and Jones, R. (2017). Cumulative impacts: thermally bleached corals have reduced capacity to clear deposited sediment. *Sci. Rep.* 7:2716. doi: 10.1038/s41598-017-02810-0

Chartrand, K. M., Durako, M. J., and Blum, J. E. (2009). Effect of hyposalinity on the photophysiology of *Siderastrea radians*. *Mar. Biol.* 156, 1691–1702. doi: 10.1007/s00227-009-1204-3

Chomczynski, P., and Sacchi, N. (1987). Single-step method of RNA isolation by acid guanidinium thiocyanate-phenol-chloroform extraction. *Anal. Biochem.* 162, 156–159.

Chomczynski, P., and Sacchi, N. (2006). The single-step method of RNA isolation by acid guanidinium thiocyanate–phenol–chloroform extraction: twenty-something years on. *Nat. Protoc.* 1, 581–585. doi: 10.1038/nprot.2006.83

Coles, S. L., and Jokiel, P. L. (1978). Synergistic effects of temperature, salinity and light on the hermatypic coral *Montipora verrucosa*. *Mar. Biol.* 49, 187–195. doi: 10.1007/BF00391130

Collier, C., Ruzicka, R., Banks, K., Barbieri, L., Beal, J., Bingham, D., et al. (2008). "The state of coral reef ecosystems of Southeast Florida," in *The state of coral reef ecosystems of the United States and Pacific Freely Associated States: 2008*, eds J. Waddel and A. Clarke Silver Spring, MD, 131–160.

Cunning, R., and Baker, A. C. (2020). Thermotolerant coral symbionts modulate heat stress- responsive genes in their hosts. *Mol. Ecol.* 29, 2940–2950. doi: 10.1111/mec.15526

Davies, S. W., Marchetti, A., Ries, J. B., and Castillo, K. D. (2016). Thermal and *p*CO2 stress elicit divergent transcriptomic responses in a resilient coral. *Front. Mar. Sci.* 3:112. doi: 10.3389/fmars.2016.00112

Davies, S. W., Ries, J. B., Marchetti, A., and Castillo, K. D. (2018). *Symbiodinium* functional diversity in the coral *Siderastrea siderea* is influenced by thermal stress and reef environment, but not ocean acidification. *Front. Mar. Sci.* 5:150. doi: 10.3389/fmars.2018.00150

DeSalvo, M. K., Sunagawa, S., Fisher, P. L., Voolstra, C. R., Iglesias-Prieto, R., and Medina, M. (2010). Coral host transcriptomic states are correlated with *Symbiodinium* genotypes. *Mol. Ecol.* 19, 1174–1186. doi: 10.1111/j.1365-294X.2010.04534.x

DeSalvo, M. K., Voolstra, C. R., Sunagawa, S., Schwarz, J. A., Stillman, J. H., Coffroth, M. A., et al. (2008). Differential gene expression during thermal stress and bleaching in the Caribbean coral *Montastraea faveolata*. *Mol. Ecol.* 17, 3952–3971. doi: 10.1111/j.1365-294X.2008.03879.x

Dias, M., Ferreira, A., Gouveia, R., and Vinagre, C. (2019a). Synergistic effects of warming and lower salinity on the asexual reproduction of reef-forming corals. *Ecol. Ind.* 98, 334–348. doi: 10.1016/j.ecolind.2018.11.011

Dias, M., Madeira, C., Jogee, N., Ferreira, A., Gouveia, R., Cabral, H., et al. (2019b). Oxidative stress on scleractinian coral fragments following exposure to high temperature and low salinity. *Ecol. Ind.* 107:105586. doi: 10.1016/j.ecolind.2019.105586

Dixon, G., Abbott, E., and Matz, M. V. (2020). Meta-analysis of the general coral stress response: *Acropora* corals show opposing responses depending on stress intensity. *Mol. Ecol.* 29, 2855–2870. doi: 10.1111/mec.15535

Dixon, G. B., Davies, S. W., Aglyamova, G. A., Meyer, E., Bay, L. K., and Matz, M. V. (2015). Genomic determinants of coral heat tolerance across latitudes. *Science* 348, 1460–1462. doi: 10.1126/science.1261224

Dodge, D., Studivan, M. S., Eckert, R., Chei, E., Beal, J., and Voss, J. (2020). Population structure of the scleractinian coral. *Montastraea cavernosa*, in southeast Florida. *Bull. Mar. Sci.* 96, 767–782. doi: 10.5343/bms.2019.0074

Downs, C. A., Kramarsky-Winter, E., Woodley, C. M., Downs, A., Winters, G., Loya, Y., et al. (2009). Cellular pathology and histopathology of hypo-salinity exposure on the coral *Stylophora pistillata*. *Sci. Total Environ.* 407, 4838–4851. doi: 10.1016/j.scitotenv.2009.05.015

Edge, S. E., Shearer, T. L., Morgan, M. B., and Snell, T. W. (2013). Sub-lethal coral stress: detecting molecular responses of coral populations to environmental conditions over space and time. *Aquat. Toxicol.* 128–129, 135–146. doi: 10.1016/j.aquatox.2012.11.014

Fabricius, K. E. (2005). Effects of terrestrial runoff on the ecology of corals and coral reefs: review and synthesis. *Mar. Pollut. Bull,* 50, 125–146. doi: 10.1016/j.marpolbul.2004.11.028

Faxneld, S., Jörgensen, T. L., and Tedengren, M. (2010). Effects of elevated water temperature, reduced salinity and nutrient enrichment on the metabolism of the coral *Turbinaria mesenterina*. *Estuar. Coast. Shelf Sci.* 88, 482–487. doi: 10.1016/j.ecss.2010.05.008

Gardner, S. G., Nielsen, D. A., Laczka, O., Shimmon, R., Beltran, V. H., Ralph, P. J., et al. (2016). Dimethylsulfoniopropionate, superoxide dismutase and glutathione as stress response indicators in three corals under short-term hyposalinity stress. *Proc. R. Soc. B Biol. Sci.* 283, 1–9. doi: 10.1098/rspb.2015.2418

Gilliam, D. S., Hayes, N. K., Ruzicka, R. R., and Colella, M. (2018). *Southeast Florida Coral Reef Evaluation and Monitoring Project (SECREMP)*. Miami, FL: Florida DEP, 1–79.

Graves, G. A., Wan, Y., and Fike, D. L. (2004). Water quality characteristics of storm water from major land use in South Florida. *J. Am. Water Resour. Assoc.* 40, 1405–1419. doi: 10.1111/j.1752-1688.2004.tb01595.x

Gregg, K. L. (2013). *Literature Review and Synthesis of Land-Based Sources of Pollution Affecting Essential Fish Habitats in Southeast Florida*. West Palm Beach, FL: NOAA Fisheries Southeast Region , 1–55.

Haslun, J., Hauff, B., Strychar, K., and Cervino, J. (2016). Decoupled seasonal stress as an indication of chronic stress in *Montastraea cavernosa* and *Porites astreoides* inhabiting the Florida Reef Tract. *Int. J. Mar. Sci.* 6, 1–20. doi: 10.5376/ijms.2016.06.0021

Hédouin, L., Pilon, R., and Puisay, A. (2015). Hyposalinity stress compromises the fertilization of gametes more than the survival of coral larvae. *Mar. Environ. Res.* 104, 1–9. doi: 10.1016/j.marenvres.2014.12.001

Hervé, M. (2019). *RVAideMemoire: Testing and Plotting Procedures for Biostatistics. R Package Version 0.9-73*.

Kauffmann, A., Gentleman, R., and Huber, W. (2009). *arrayQualityMetrics* - a bioconductor package for quality assessment of microarray data. *Bioinformatics* 25, 415–416. doi: 10.1093/bioinformatics/btn647

Kenkel, C. D., Aglyamova, G., Alamaru, A., Bhagooli, R., Capper, R., Cunning, R., et al. (2011). Development of gene expression markers of acute heat-light stress in reef-building corals of the genus *Porites*. *PLoS One* 6:e26914. doi: 10.1371/journal.pone.0026914

Kenkel, C. D., Goodbody-Gringley, G., Caillaud, D., Davies, S. W., Bartels, E., and Matz, M. V. (2013a). Evidence for a host role in thermotolerance divergence between populations of the mustard hill coral (*Porites astreoides*) from different reef environments. *Mol. Ecol.* 22, 4335–4348. doi: 10.1111/mec.12391

Kenkel, C. D., Meyer, E., and Matz, M. V. (2013b). Gene expression under chronic heat stress in populations of the mustard hill coral (*Porites astreoides*) from different thermal environments. *Mol. Ecol.* 22, 4322–4334. doi: 10.1111/mec.12390

Kenkel, C. D., Sheridan, C., Leal, M. C., Bhagooli, R., Castillo, K. D., Kurata, N., et al. (2014). Diagnostic gene expression biomarkers of coral thermal stress. *Mol. Ecol. Resour.* 14, 667–678. doi: 10.1111/1755-0998.12218

Kerswell, A. A. P., and Jones, R. J. R. (2003). Effects of hypo-osmosis on the coral *Stylophora pistillata*: nature and cause of "low-salinity bleaching.". *Mar. Ecol. Prog. Ser.* 253, 145–154. doi: 10.3354/meps253145

Kitchen, S. A., Crowder, C. M., Poole, A. Z., Weis, V. M., and Meyer, E. (2015). *De novo* assembly and characterization of four anthozoan (Phylum Cnidaria) transcriptomes. *G3 Genes Genomes Genet.* 5, 2441–2452. doi: 10.1534/g3.115.020164

Klepac, C. N., Beal, J., Kenkel, C. D., Sproles, A., Polinski, J. M., Williams, M. A., et al. (2015). Seasonal stability of coral-*Symbiodinium* associations in the subtropical coral habitat of St. Lucie Reef, Florida. *Mar. Ecol. Prog. Ser.* 532, 137–151. doi: 10.3354/meps11369

Kolde, R. (2019). *pheatmap: Pretty Heatmaps. R Package Version 1.0.12*.

Konietschke, F., Placzek, M., Schaarschmidt, F., and Hothorn, L. A. (2015). *nparcomp*: an *R* software package for nonparametric multiple comparisons and simultaneous confidence intervals. *J. Stat. Softw.* 64, 1–17. doi: 10.18637/jss.v064.i09

Kültz, D. (2005). Molecular and evolutionary basis of the cellular stress response. *Annu. Rev. Physiol.* 67, 225–257. doi: 10.1146/annurev.physiol.67.040403.103635

Langfelder, P., and Horvath, S. (2008). *WGCNA*: an *R* package for weighted correlation network analysis. *BMC Bioinformatics* 9:559. doi: 10.1186/1471-2105-9-559

Lapointe, B. E., Herren, L. W., and Bedford, B. J. (2012). Effects of hurricanes, land use, and water management on nutrient and microbial pollution: St. Lucie Estuary, Southeast Florida. *J. Coast. Res.* 28, 1345–1361. doi: 10.2112/JCOASTRES-D-12-00070.1

Lapointe, B. E., Herren, L. W., and Paule, A. L. (2017). Septic systems contribute to nutrient pollution and harmful algal blooms in the St. Lucie Estuary, Southeast Florida, USA. *Harmful Algae* 70, 1–22. doi: 10.1016/j.hal.2017.09.005

Lasker, H. R. (1980). Sediment rejection by reef corals: the roles of behavior and morphology in *Montastrea cavernosa* (Linnaeus). *J. Exp. Mar. Biol. Ecol.* 47, 77–87. doi: 10.1016/0022-0981(80)90139-2

Li, X., Huang, H., Lian, J., Huang, L., and Dong, J. (2009). Effects of the multiple stressors high temperature and reduced salinity on the photosynthesis of the hermatypic coral *Galaxea fascicularis*. *Acta Ecol. Sin.* 29, 155–159. doi: 10.1016/j.chnaes.2009.07.002

Lirman, D., and Fong, P. (2007). Is proximity to land-based sources of coral stressors an appropriate measure of risk to coral reefs? An example from the Florida Reef Tract. *Mar. Pollut. Bull.* 54, 779–791. doi: 10.1016/j.marpolbul.2006.12.014

Lirman, D., and Manzello, D. P. (2009). Patterns of resistance and resilience of the stress-tolerant coral *Siderastrea radians* (Pallas) to sub-optimal salinity and sediment burial. *J. Exp. Mar. Biol. Ecol.* 369, 72–77. doi: 10.1016/j.jembe.2008.10.024

Love, M. I., Huber, W., and Anders, S. (2014). Moderated estimation of fold change and dispersion for RNA-seq data with *DESeq2*. *Genome Biol.* 15, 550–571. doi: 10.1186/s13059-014-0550-8

Lugo, A. E., Brown, S. B., Dodson, R., Smith, T. S., and Shugart, H. H. (1999). The Holdridge life zones of the conterminous United States in relation to ecosystem mapping. *J. Biogeogr.* 26, 1025–1038. doi: 10.1046/j.1365-2699.1999.00329.x

Matz, M. V. (2016). *KOGMWU: Functional Summary and Meta-Analysis of Gene Expression Data. R Package Version 1.1*.

Mayfield, A. B., Fan, T.-Y., and Chen, C.-S. (2013). Real-time PCR-based gene expression analysis in the model reef-building coral *Pocillopora damicornis*: insight from a salinity stress study. *Platax* 10, 1–29.

McGinley, M. P., Aschaffenburg, M. D., Pettay, D. T., Smith, R. T., LaJeunesse, T. C., and Warner, M. E. (2012). Transcriptional response of two core photosystem genes in *Symbiodinium* spp. exposed to thermal stress. *PLoS One* 7:e50439. doi: 10.1371/journal.pone.0050439

Meyer, E., Aglyamova, G. V., and Matz, M. V. (2011). Profiling gene expression responses of coral larvae (*Acropora millepora*) to elevated temperature and settlement inducers using a novel RNA-Seq procedure. *Mol. Ecol.* 20, 3599–3616. doi: 10.1111/j.1365-294X.2011.05205.x

Murata, N., Takahashi, S., Nishiyama, Y., and Allakhverdiev, S. I. (2007). Photoinhibition of photosystem *II* under environmental stress. *Biochim. Biophys. Acta Bioenerget.* 1767, 414–421. doi: 10.1016/j.bbabio.2006.11.019

Nordberg, H., Cantor, M., Dusheyko, S., Hua, S., Poliakov, A., Shabalov, I., et al. (2014). The genome portal of the department of energy joint genome institute: 2014 updates. *Nucleic Acids Res.* 42, D26–D31. doi: 10.1093/nar/gkt1069

Oksanen, J., Blanchet, F. G., Kindt, R., Legendre, P., Minchin, P. R., O'Hara, R., et al. (2015). *vegan: Community Ecology Package. R Package Version 2.0-10*.

Perry, W. (2004). Elements of South Florida's comprehensive everglades restoration plan. *Ecotoxicology* 13, 185–193. doi: 10.1023/B:ECTX.0000023564.10311.4a

Pickering, N., and Baker, E. S. (2015). *Watershed Scale Planning to Reduce Land-Based Sources of Pollution (LBSP) for the Protection of Coral Reefs in Southeast Florida*. West Palm Beach, FL: NOAA Fisheries Southeast Region, 1–121.

Pollock, F. J., Lamb, J. B., Field, S. N., Heron, S. F., Schaffelke, B., Shedrawi, G., et al. (2014). Sediment and turbidity associated with offshore dredging increase coral disease prevalence on nearby reefs. *PLoS One* 9:102498. doi: 10.1371/journal.pone.0102498

Pratte, Z. A., and Richardson, L. L. (2014). Impacts of temperature increase and acidification on thickness of the surface mucopolysaccharide layer of the Caribbean coral *Diploria* spp. *Coral Reefs* 33, 487–496. doi: 10.1007/s00338-013-1115-0

R Core Team (2019). *R: A Language and Environment for Statistical Computing*. Vienna: R Foundation for Statistical Computing.

Reed, J. K. (1982). *A Proposal for the Nearshore Reefs Adjacent to St. Lucie Inlet, Florida, as a part of an Atlantic Hardbottom Sanctuary*. Fort Pierce, FL: Harbor Branch Oceanographic Institute , 1–24.

Reyes-Bermudez, A., DeSalvo, M. K., Voolstra, C. R., Sunagawa, S., Szmant, A. M., Iglesias-Prieto, R., et al. (2009). Gene expression microarray analysis encompassing metamorphosis and the onset of calcification in the scleractinian coral *Montastraea faveolata*. *Mar. Genomics* 2, 149–159. doi: 10.1016/j.margen.2009.07.002

Rocker, M. M., Willis, B. L., and Bay, L. K. (2012). "Thermal stress-related gene expression in corals with different Symbiodinium types," in *Proceedings of the 12th International Coral Reef Symposium*, Vol. 9, Cairns, 1–5.

Seneca, F. O., and Palumbi, S. R. (2015). The role of transcriptome resilience in resistance of corals to bleaching. *Mol. Ecol.* 24, 1467–1484. doi: 10.1111/mec.13125

Seveso, D., Montano, S., Strona, G., Orlandi, I., Galli, P., and Vai, M. (2013). Exploring the effect of salinity changes on the levels of Hsp60 in the tropical coral *Seriatopora caliendrum*. *Mar. Environ. Res.* 90, 96–103. doi: 10.1016/j.marenvres.2013.06.002

Shatters, A. (2017). *Effects of St. Lucie Estuarine Discharge Water and Thermal Stress on the Coral Montastraea cavernosa*. MSc thesis. Boca Raton, FL: Biological Sciences Florida Atlantic University, 1–91.

Shore-Maggio, A., Aeby, G. S., and Callahan, S. M. (2018). Influence of salinity and sedimentation on *Vibrio* infection of the Hawaiian coral *Montipora capitata*. *Dis. Aquat. Organ.* 128, 63–71. doi: 10.3354/dao03213

Smith, E. G., Gurskaya, A., Hume, B. C. C., Voolstra, C. R., Todd, P. A., Bauman, A. G., et al. (2020). Low Symbiodiniaceae diversity in a turbid marginal reef environment. *Coral Reefs* 39, 545–553. doi: 10.1007/s00338-020-01956-0

Stockley, N., Sullivan, J. M., Hanisak, M. D., and McFarland, M. N. (2018). "Using observation networks to examine the impact of Lake Okeechobee discharges on the St. Lucie Estuary, Florida," in *Proceedings of SPIE, Ocean Sensing and Monitoring X* (Orlando, FL), 1063109. doi: 10.1117/12.2309797

Strader, M. E., Aglyamova, G. V., and Matz, M. V. (2016). Red fluorescence in coral larvae is associated with a diapause-like state. *Mol. Ecol.* 25, 559–569. doi: 10.1111/mec.13488

Studivan, M. S. (2020a). *mstudiva/Mcav-Cladocopium-Annotated-Transcriptome: Final Montastraea cavernosa/Cladocopium spp. transcriptome assembly (Version 2.0.0)*. Geneva: Zenodo, doi: 10.5281/zenodo.3728261

Studivan, M. S. (2020b). *mstudiva/Transcriptional-Plasticity-Mesophotic-Mcav: Final Tag-Seq Scripts for Analysis of Mesophotic Montastraea Cavernosa (Version 2.0.0)*. Geneva: Zenodo, doi: 10.5281/zenodo.3728281

Studivan, M. S. (2021). *mstudiva/Thermal-Stress-Estuarine-Discharge-Mcav: Thermal Stress and Estuarine Discharge Effects on Montastraea Cavernosa Gene Expression (Version 1.1.0)*. Geneva: Zenodo. doi: 10.5281/zenodo.4643062

Studivan, M. S., and Voss, J. D. (2020). Transcriptomic plasticity of mesophotic corals among natural populations and transplants of *Montastraea cavernosa* in the Gulf of Mexico and Belize. *Mol. Ecol.* 29, 2399–2415. doi: 10.1111/mec.15495

Tatusov, R. L., Fedorova, N. D., Jackson, J. D., Jacobs, A. R., Kiryutin, B., Koonin, E. V., et al. (2003). The COG database: an updated vesion includes eukaryotes. *BMC Bioinformatics* 4:41. doi: 10.1186/1471-2105-4-41

Tatusov, R. L., Galperin, M. Y., Natale, D. A., and Koonin, E. V. (2000). The COG database: a tool for genome-scale analysis of protein functions and evolution. *Nucleic Acids Res* 28, 33–36. doi: 10.1093/nar/28.1.33

The Gene Ontology Consortium (2017). Expansion of the gene ontology knowledgebase and resources. *Nucleic Acids Res.* 45, D331–D338. doi: 10.1093/nar/gkw1108

True, J. D. (2012). "Salinity as a structuring force for near shore coral communities," in *Proceedings of the 12th International Coral Reef Symposium*, Vol. 9, Cairns, e13.

Vargas-Ángel, B., Peters, E. C., Kramarsky-Winter, E., Gilliam, D. S., and Dodge, R. E. (2007). Cellular reactions to sedimentation and temperature stress in the Caribbean coral *Montastraea cavernosa*. *J. Invertebr. Pathol.* 95, 140–145. doi: 10.1016/j.jip.2007.01.003

Vargas-Ángel, B., Riegl, B., Gilliam, D. S., and Dodge, R. E. (2006). "An experimental histopathological rating scale of sedimentation stress in the Caribbean coral *Montastraea cavernosa*," in *Proceedings of the 10th International Coral Reef Symposium*, Okinawa, 1168–1173.

Voss, J. D., and Combs, I. (2018). *Fate Tracking, Molecular Investigation, and Amputation Assessment of Tissue Loss Disease on Corals in the Northern Florida Reef Tract*. Miami, FL: Florida DEP, 1–22.

Walker, B. K. (2018). *Southeast Florida Reef-Wide Post-Irma Coral Disease Surveys*. Miami, FL: Florida DEP, 1–37.

Walker, B. K., and Gilliam, D. S. (2013). Determining the extent and characterizing coral reef habitats of the northern latitudes of the Florida Reef Tract (Martin County). *PLoS One* 8:e80439. doi: 10.1371/journal.pone.0080439

Walton, C. J., Hayes, N. K., and Gilliam, D. S. (2018). Impacts of a regional, multi-year, multi-species coral disease outbreak in Southeast Florida. *Front. Mar. Sci.* 5:323. doi: 10.3389/fmars.2018.00323

Wang, P., Bouwman, F. G., and Mariman, E. C. M. (2009). Generally detected proteins in comparative proteomics - a matter of cellular stress response? *Proteomics* 9, 2955–2966. doi: 10.1002/pmic.200800826

Wright, R. M., Aglyamova, G. V., Meyer, E., and Matz, M. V. (2015). Gene expression associated with white syndromes in a reef building coral. *Acropora hyacinthus*. *BMC Genomics* 16:371. doi: 10.1186/s12864-015-1540-2

Wright, R. M., Correa, A. M. S., Quigley, L. A., Santiago-Vázquez, L. Z., Shamberger, K. E. F., and Davies, S. W. (2019). Gene expression of endangered coral (*Orbicella* spp.) in the Flower Garden Banks National Marine Sanctuary after Hurricane Harvey. *Front. Mar. Sci.* 6:672. doi: 10.3389/fmars.2019.00672

Yentsch, C. S., Yentsch, C. M., Cullen, J. J., Lapointe, B., Phinney, D. A., and Yentsch, S. W. (2002). Sunlight and water transparency: cornerstones in coral research. *J. Exp. Mar. Biol. Ecol.* 268, 171–183. doi: 10.1016/S0022-0981(01)00379-3

Zhang, B., and Horvath, S. (2005). A general framework for weighted gene co-expression network analysis. *Stat. Appl. Genet. Mol. Biol.* 4:17. doi: 10.2202/1544-6115.1128

Conflict of Interest: The authors declare that the research was conducted in the absence of any commercial or financial relationships that could be construed as a potential conflict of interest.

frontiers in Physiology

REVIEW
published: 07 June 2021
doi: 10.3389/fphys.2021.656562

Experimental Techniques to Assess Coral Physiology *in situ* Under Global and Local Stressors: Current Approaches and Novel Insights

*Walter Dellisanti[1,2], Jeffery T. H. Chung[1], Cher F. Y. Chow[1,3], Jiajun Wu[1], Mark L. Wells[4,5] and Leo L. Chan[1,2,6]**

[1]State Key Laboratory of Marine Pollution, City University of Hong Kong, Kowloon, China, [2]Department of Biomedical Sciences, City University of Hong Kong, Kowloon, China, [3]Centre for Biological Diversity, Scottish Oceans Institute, School of Biology, University of St Andrews, St Andrews, United Kingdom, [4]School of Marine Sciences, University of Maine, Orono, ME, United States, [5]State Key Laboratory of Satellite Ocean Environment Dynamics, Second Institute of Oceanography, Ministry of Natural Resources, Hangzhou, China, [6]Hong Kong Branch of Southern Marine Science and Engineering Guangdong Laboratory, Guangzhou, China

Coral reefs are declining worldwide due to global changes in the marine environment. The increasing frequency of massive bleaching events in the tropics is highlighting the need to better understand the stages of coral physiological responses to extreme conditions. Moreover, like many other coastal regions, coral reef ecosystems are facing additional localized anthropogenic stressors such as nutrient loading, increased turbidity, and coastal development. Different strategies have been developed to measure the health status of a damaged reef, ranging from the resolution of individual polyps to the entire coral community, but techniques for measuring coral physiology *in situ* are not yet widely implemented. For instance, while there are many studies of the coral holobiont response in single or limited-number multiple stressor experiments, they provide only partial insights into metabolic performance under more complex and temporally and spatially variable natural conditions. Here, we discuss the current status of coral reefs and their global and local stressors in the context of experimental techniques that measure core processes in coral metabolism (respiration, photosynthesis, and biocalcification) *in situ*, and their role in indicating the health status of colonies and communities. We highlight the need to improve the capability of *in situ* studies in order to better understand the resilience and stress response of corals under multiple global and local scale stressors.

Keywords: environmental monitoring, underwater respirometry, fluorometry, photobiology, coral metabolism

OPEN ACCESS

Edited by:
Davide Seveso, University of Milano-Bicocca, Italy

Reviewed by:
Tali Mass, University of Haifa, Israel
Fiorella Prada, University of Bologna, Italy

***Correspondence:**
Leo L. Chan
leochan@cityu.edu.hk

Specialty section:
This article was submitted to Aquatic Physiology, a section of the journal Frontiers in Physiology

Received: *21 January 2021*
Accepted: *09 April 2021*
Published: *07 June 2021*

Citation:
Dellisanti W, Chung JTH, Chow CFY, Wu J, Wells ML and Chan LL (2021) Experimental Techniques to Assess Coral Physiology in situ Under Global and Local Stressors: Current Approaches and Novel Insights. Front. Physiol. 12:656562. doi: 10.3389/fphys.2021.656562

INTRODUCTION

Coral reef ecosystems are hotspots of biodiversity and productivity in the ocean (Roberts et al., 2002) that exceed that of tropical rainforests (Ray, 1988). They provide crucial ecosystem functions and services such as providing goods for subsistence and economic fisheries, coastline protection from storms, and centers of the growing field of ecotourism (Cesar et al., 2003; Knowlton et al., 2010; Van Zanten et al., 2014). As a key habitat-forming taxa, corals are

critical to both reef systems and the coastal human populations that rely on them, and it is imperative to accelerate advances to ensure the longevity and survival of corals and coral reefs.

Coral reefs have drastically declined worldwide in the last 30 years because of recruitment failures, reduced growth rates, and acute and chronic mortalities (Hughes et al., 2011, 2019), with only a fraction expected to survive in their current form over the next three decades in the Indo-Pacific region (Bruno and Selig, 2007; Descombes et al., 2015). One of the most significant and widespread anthropogenic causes of this degradation is the change in climate drivers associated with the rise in atmospheric carbon dioxide (CO_2) and other greenhouse gases (Goulletquer et al., 2014; Hannah, 2016). Local stressors also go hand in hand with global stressors, such as coastline erosion or development, which threaten the resilience of corals through pollution and sedimentation (D'Angelo and Wiedenmann, 2014; Silbiger et al., 2018; Loiola et al., 2019; Jones et al., 2020).

Increased energy consumption since the Industrial Revolution has led to the highest CO_2 levels recorded in the atmosphere since human evolution (>410 ppm; Dlugokencky and Tans, 2020). Of the multiple greenhouse gases [such as N_2O, CH_4, or chlorofluorocarbons (CFCs)] affecting global biogeochemical cycles, biodiversity, and human health (Galloway et al., 2004; Bustamante et al., 2012), CO_2 has been the most relevant to marine ecology because of its dual role in marine heatwaves (Gruber, 2011) and ocean acidification (Ciais et al., 2013; **Figure 1**). Overall average seawater temperatures in tropical regions have increased by almost 1°C over the past 100 years and are projected to continue increasing at 1–2°C per century (Kuffner et al., 2015). Increased seawater temperatures are a major contributor to coral bleaching and are considered as the limiting factor for coral survival (Hughes et al., 2017b, 2019). Roughly half of the CO_2 emitted into the atmosphere dissolves into the surface ocean, reacting with water to form several dissolved inorganic components of the carbonate system (Zeebe and Wolf-Gladrow, 2001) and lowering seawater pH (Anthony et al., 2008). In comparison with pre-Industrial Revolution levels, seawater pH has decreased by approximately 0.1 (Caldeira and Wickett, 2003), which equates to roughly 30% increase in acidity and may decrease further by 0.06 to 0.32 based on emission scenarios (Ciais et al., 2013). This process of ocean acidification is particularly disruptive to marine organisms like reef-building hard corals that create calcium carbonate skeletons, increasing the energy requirements for growth and survival (Anthony et al., 2008; Cohen and Holcomb, 2009; Eyre et al., 2014). Thus, corals and coral reefs may be significantly more vulnerable than previously thought when considering the combined effects of ocean acidification and warming (Hoegh-Guldberg et al., 2007; Pandolfi et al., 2011).

Although climate drivers are widely recognized as dominating factors in coral loss and reef ecosystem shifts (Hughes et al., 2017b), localized stressors also are impacting coral health, where a survival-resilience pattern is observable in urban subtropical reefs subjected to several anthropogenic stressors (Heery et al., 2018). Here, there are indications that stress-tolerant hard coral species have been selected to foster more resistant though less diverse reefs (Darling et al., 2012). Impacts from eutrophication, increased turbidity, and lowered dissolved oxygen significantly affect coral metabolism, changing energy pathways and reef ecology (**Figure 1**). A coral as a holobiont includes diversity functional, genomic, and potential epigenetics traits that regulate its ecological plasticity under an environmental change. But not all coral species showed the same response patterns under anthropogenic threats.

Turbid water conditions commonly occur within inshore shallow coastal waters (Browne et al., 2014), owing to the collective interactions of river runoff and the natural re-suspension of sediments (e.g., tides or storms) as well as anthropogenic activities (e.g., ship wakes, coastline modification, and storm and other sewage discharge). The adaptive responses that corals require to survive these conditions are both stressful and energetically costly (Brown and Bythell, 2005), utilizing energy that otherwise would be put towards growth and reproduction. One consequence of increased turbidity is the reduction of the *in situ* irradiance and thereby photosynthesis, while high levels of settling sediments can hinder feeding or smother coral polyps (Fabricius, 2005). The resulting decreases in photosynthetic efficiency and increases in respiration lower the daily productivity of corals [measured as the ratio of photosynthesis to respiration (P/R)]. This decreased productivity, in turn, lowers the coral nutritional energy reserves (e.g., reduced lipids content and changes in lipids class composition), which can lead to mortality (Weber et al., 2012; Jones et al., 2020). Lower productivity also can increase coral susceptibility to infection and bleaching (Anthony et al., 2007), generating community- and ecosystem-level impacts. In contrast, corals associated with urban developments are frequently exposed to acute sedimentation but appear to escape tissue mortality by better acclimation to low light conditions (Dubinsky et al., 1984) and by increasing their feeding rates to offset energy deficits from photosynthesis (Anthony and Fabricius, 2000). However, any increased frequency or severity of acute sedimentation contributes additional stress to corals that can be functioning near the limits of their physiological tolerances (Bessell-Browne et al., 2017; Loiola et al., 2019; Jones et al., 2020).

Although increased planktonic production can enhance the food supply for corals, very high photosynthetic production rates can generate hyperoxic conditions in reef waters that can cause coral damage and photorespiration (Mass et al., 2010). At best, hyperoxic conditions may shift coral energy use into the production of antioxidants rather than calcification (Wijgerde et al., 2014). In contrast, low oxygen concentrations also challenges coral survival, stimulating metabolic acclimation through the expression of hypoxia-inducible factors in corals (Alderdice et al., 2021). There are few reports of hypoxic events and dead zones in the tropical coral reef environments, though episodic or seasonal hypoxia has been recently linked to bleaching and mortality in deeper water corals (Altieri et al., 2017).

The anthropogenically derived increased inputs of nutrients and organic matter in coastal regions have degraded many coral reefs, and this cultural eutrophication might exacerbate the effect of global warming on coral survival (Silbiger et al., 2018; DeCarlo et al., 2020). The nutrient gradient affects the nutritional

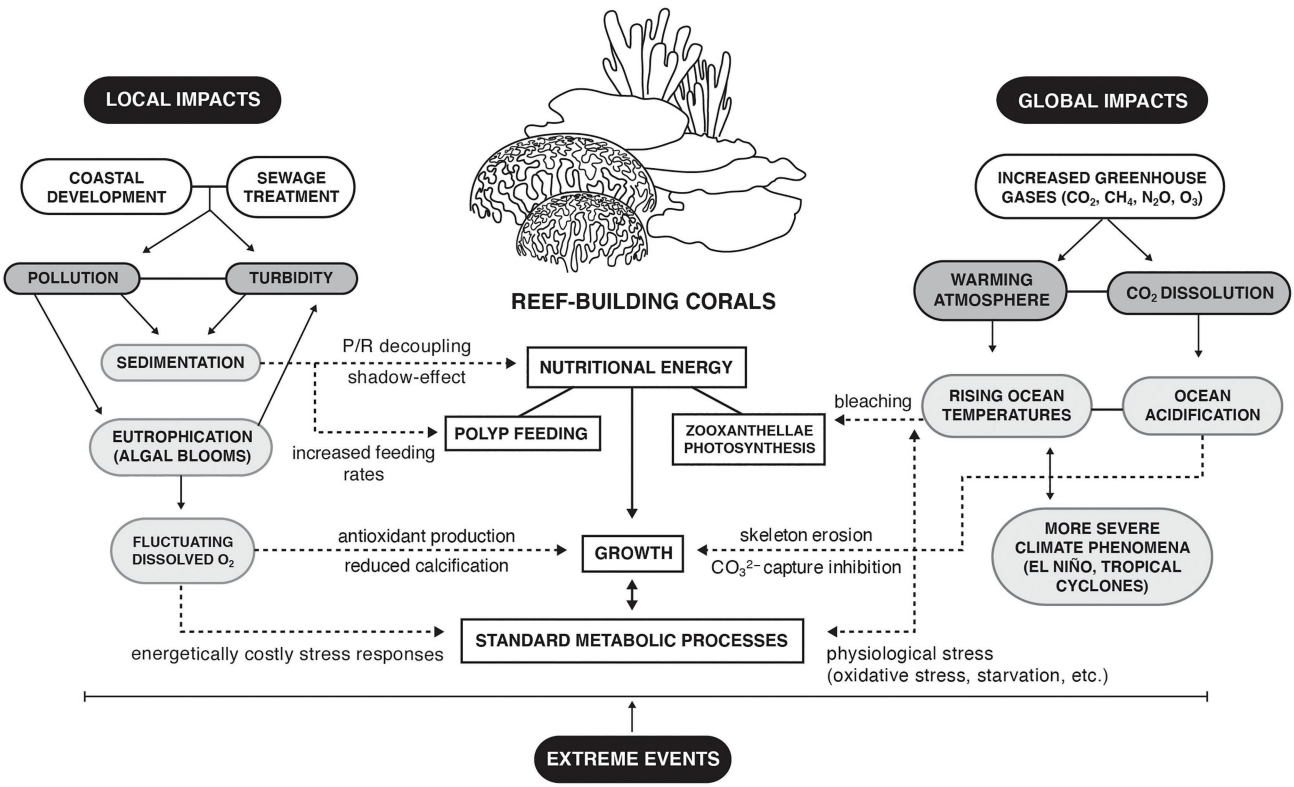

FIGURE 1 | Local and global impacts affecting the nutritional energy of reef-building corals. Full lines indicate direct interactions; dotted lines indicate indirect interactions.

status of corals, in particular when the calcification rate is reduced but heterotrophy enhanced under high nutrient loading (Sawall et al., 2011). Indeed, traces of nitrate pollution can be found in both hard and soft corals through the analysis of radioisotopes $\delta^{15}N$ in the tissue (Baker et al., 2011; Duprey et al., 2017) and $\delta^{13}C$ as an estimate of particulate organic matter ingestion (Baker et al., 2010; Conti-Jerpe et al., 2020). At the community level, a shift from net community calcification (NCC) to dissolution can occur under high nutrient conditions (Silbiger et al., 2018), due to combination of direct and indirect responses of corals. Indeed, nutrient enrichment might negatively affect the physiological performance of coral metabolism, increase the productivity of reef macroalgae, or both, inducing a cascade of change in the coral ecosystems (D'Angelo and Wiedenmann, 2014; Silbiger et al., 2018). Eutrophic conditions can increase the productivity of reef waters by increasing food availability (e.g., particulate matter; Fabricius, 2005), although macroalgae, turf, and bioeroders can inhibit competitively the coral recruitment (D'Angelo and Wiedenmann, 2014). However, several factors influencing the susceptibility to eutrophication have to be included, such as hydrodynamic connectivity and location (Fabricius, 2011). Even so, Sawall et al. (2011) found higher photosynthetic rates of coral endosymbionts nearshore along an anthropogenic driving inshore-offshore nutrient gradient, showing that eutrophication effects on coral may not always be negative.

Gaining knowledge of the stress responses of corals and their effects on reef ecology, along with the pathways to best minimize these impacts, depends on two related tasks: understanding coral health from polyp-endosymbiont symbiosis to the community level and achieving early detection of the onset of the stress responses. The first provides the foundation for studying and developing potential mitigation and managements strategies, and the second is crucial for implementing these strategies soon enough to help minimize impacts.

While most early studies of an environmental change on coral health focused on the effects of single drivers (e.g., temperature, ocean acidification, and turbidity), their interactive effects require addressing multiple stressor effects on physiological processes at the holobiont level if we are to comprehensively understand their impacts on coral communities. Some of these drivers have major effects (e.g., temperature and light), but there undoubtably are other interactions that can affect the resistance and recovery response of coral communities, factors critical for reef management and proactive preventative planning. However, our current understanding of coral stress responses is largely based on experimental manipulation studies in laboratory systems that are poor representations of their natural habitats. *In situ* studies, by either SCUBA or automated sensors, could provide a better understanding of local and global impacts, but only a few recent studies have undertaken the logistical

complexities of studying fine-scale physiological processes of corals *in situ* recently (Roth et al., 2019; Cyronak et al., 2020; Srednick et al., 2020). The primary objective of this review is to summarize the current strategies for quantifying aspects of coral metabolism to highlight the benefits of non-destructive methodologies. A list of recommendations is provided that would expand the efficacy of underwater studies for improving local knowledge and better understanding of how corals respond to stressors.

OVERVIEW OF THE CORAL METABOLISM

Metabolic Responses at Coral Polyp Level

The concept of the coral as a "holobiont" was introduced in the 2000s, whereby the coral comprises not only the animal polyps but also the associated symbiotic organisms, including photosynthetic endosymbionts, bacteria, viruses, fungi, and protists (Rohwer et al., 2002; Rosenberg et al., 2007). These have a fundamental role in nutrient and energy acquisition processes of coral polyps (Peixoto et al., 2017), genome evolution in the coral host and microbial partners, maintaining holobiont homeostasis, and the overall health of the holobiont (Thompson et al., 2015). The functional diversity of these microbes contributes to the stress response and acclimation to changing conditions, e.g., high seawater temperature and bleaching events (Jones et al., 2008; Hume et al., 2016).

The family Symbiodiniaceae includes several genera of dinoflagellates, which reside in the tissue of corals and other marine organisms (LaJeunesse et al., 2018). The coral-Symbiodiniaceae association is an obligate symbiosis for the coral, where the photosynthetic dinoflagellates provide the coral oxygen and energy in the form of glucose for aerobic respiration (Muscatine, 1998; Gardella and Edmunds, 1999). While most of the oxygen arising from photosynthesis is immediately utilized in coral respiration (Kuhl et al., 1995; Al-Horani et al., 2003a,b), the excess oxygen is released to the surrounding seawater throughout the day (Yonge et al., 1932; Finelli et al., 2006; Al-Horani et al., 2007; Mass et al., 2010), supporting the oxygen availability on the reef. Therefore, at night, corals must acquire oxygen from the surrounding environment to fuel the respiration process (Al-Horani et al., 2007). As a consequence, the energy acquisition follows a circadian pattern where endosymbiont-derived photosynthesis is dominant during the day while polyp-guided respiration is dominant at night.

This continuous loop is stable under normal conditions, but the symbiotic dynamics within the coral holobiont are changing rapidly in the Anthropocene (Hughes et al., 2017a). Temperature-induced stress damages a key protein (D1) in the dinoflagellate photosystem II within the dinoflagellate (PSII; Hill et al., 2011), inactivating the Rubisco center (Lilley et al., 2010), affecting the production of ATP (Franklin et al., 2004), and leading to the overproduction of reactive oxygen species that can induce damaging conditions for both the endosymbiont and coral host. The increased frequency and severity of temperature anomalies will lead to negative consequences for coral survival (Anthony et al., 2008; Randall and Szmant, 2009). Under warming and eutrophic conditions, coral host-endosymbiont relationship may shift from a mutualistic to parasitic strategy with respect to nutritional resource allocation (Lesser et al., 2013). This shift has important implications for the resilience of coral reefs under bleaching conditions, where decreases in net primary productivity of the holobiont mainly from increased respiration in the host, with little apparent metabolic cost to the endosymbiont (Douglas, 2008; Baker et al., 2018).

The coral symbioses also can be influenced by other types of stress related to environmental changes. The impact of high seawater pCO_2/low pH on corals is highly variable, where it can stimulate growth and photosynthetic efficiency in certain Symbiodiniaceae species (Brading et al., 2011). In other cases, increasing pCO_2 had no measurable effect on net photosynthesis (gross photosynthesis – respiration) but decreased biocalcification rates (Comeau et al., 2017). Similarly, elevated concentration of nitrates (NO_3^-) or phosphate (PO_4^{3-}) can stimulate both photosynthesis and respiration rates in corals, but not necessarily result in a concomitant increase in net biocalcification (Silbiger et al., 2018). Such imbalance between photosynthetic energy supply and biocalcification (as biologically induced formation of $CaCO_3$) may indicate increasing competition for dissolved inorganic carbon (DIC) between coral host and endosymbionts under conditions of high production. Adding further complexity to these responses, ammonia (NH_4^+) enrichment appears to support coral resistance to thermal stress, unlike enrichments of NO_3^-, which can lead to increased levels of reactive species and oxidative damage (Fernandes de Barros Marangoni et al., 2020).

Bleaching, where the endosymbionts may decrease their chlorophyll content or be ejected from the coral host, signals severe physiological consequences arising from oxidative stress and starvation, leading to reduced respiration rates and energy acquisition (Williams et al., 2017). Though the role of endosymbiont reactive oxygen species production is believed to be fundamental to this process, recent work shows that coral bleaching is more complex than previously thought (Rädecker et al., 2021). Although bleaching can be a reversible condition, it often leads to coral tissue death if sustained too long. However, endosymbionts have developed adaptive mechanisms to limit thermal stress by increasing electron flow in photosystem I as photoprotection (Hoogenboom et al., 2012), thereby limiting the extent of bleaching. Moreover, coral polyps may partially compensate for the lost photosynthetically derived energy during bleaching by enhanced feeding if sufficient prey are available (Anthony et al., 2007).

Responses of the Coral Community

When magnified across coral tissues, the polyp-level metabolic responses can affect reefs at the community level. Growth of coral colony, or NCC, is measured in terms of the deposition of its calcium carbonate ($CaCO_3$) foundation, which is determined largely by coral energy reserves and the need to maintain optimal chemical conditions in the calcifying fluid at the tissue/calcium carbonate interface. Hard corals build

their skeleton of $CaCO_3$ through the uptake of calcium and carbonate ions from seawater. The reaction occurs in the calicoblastic cells lining the surface where primary crystal secretion occurs (Cohen and Holcomb, 2009) and is facilitated at pH levels above that of seawater. However, ocean acidification reduces the seawater pH and the aragonite saturation state (a; Eyre et al., 2014), which can have a strong effect on NCC, along with the balance of organic matter production and respiration, or net community production (NCP; Albright et al., 2015). Moreover, the projected decreases in pH in the future ocean eventually will affect the stability of existing reef ecosystems, because the $CaCO_3$ formed by corals (aragonite) is more susceptible to dissolution than that formed by other biocalcifying organisms (Shaw et al., 2013). These effects overlay natural seasonal variations in the carbonate chemistry in reef systems, and the question remains of what extent does globally and locally derived ocean acidification have on the seasonal balance of NCP and NCC (Cyronak et al., 2018). However, these estimates remain imprecise, owing to the lack of information about seawater residence time and volume, which would modulate reef chemistry (Courtney et al., 2017). The relationship between host and endosymbionts is exacerbated under the combined effects of global drivers of stress (e.g., temperature, ocean acidification, and atmospheric conditions), leading to lower energy reserves for growth (Anthony et al., 2008; Hughes et al., 2011, 2018; Hoegh-Guldberg, 2014). These, in turn, are combined with local drivers in coastal regions (e.g., increased nutrient, turbidity, and freshwater inputs), causing reduced calcification and oxidative stress and eventually leading to bleaching events (Silbiger et al., 2018; Fernandes de Barros Marangoni et al., 2020).

Even with these impacts though, it is possible for coral communities to recover after destructive events. For example, the coral reef in Kaneʻohe Bay showed positive NCC and NCP about 1 year after the last drastic bleaching event in 2015 (Courtney et al., 2018), indicating the capacity of local rapid post-bleaching recovery. However, these estimates considered only the abiotic factors, such as carbonate chemistry and oceanographic patterns, without considering potential effects from the benthic community, which would contribute to the depletion or repletion of alkalinity in the coral reef (Page et al., 2017).

Defining the health of corals and coral communities is complex given the array of elements that contribute the status of reef ecosystems. The coral microenvironment comprises ecologically dependent niches (a network made up of bacteria, viruses, and fungi) that supports and regulate the general homeostasis and plasticity of the coral holobiont. But understanding these *in situ* responses to variable multistressor conditions cannot be adequately informed by just laboratory-based manipulation studies, so the adaptive resilience of coral species and their response thresholds remain only partially understood. It is difficult therefore to chart ways forward for pragmatic and effective steps towards protection and restoration. Overcoming these limitations will depend on applying new *in situ* observational techniques that can bridge from single organisms to ecosystems and on to regional global scales.

MATERIALS AND METHODS

We conducted a literature review based on case studies of *in situ* observations of coral metabolism from published peer-reviewed scientific literature. We included cases involved in original research on direct (e.g., using SCUBA divers, benthic chambers, and optical sensors) underwater measurements of metabolic rates on both coral individuals and coral communities. We excluded sample collections (e.g., coral fragmentation), laboratory experiments, and indirect measurements of metabolic fluxes (e.g., *ex situ* from sample incubations).

We used the advanced search on Google Scholar to identify studies with the keywords "coral *in situ* metabolism" and "underwater," excluding the keyword "collection," in articles published between 1991 and 2020. The search yield (n = 2,090) was scrutinized, and the literature was manually reviewed to fulfill our selection criteria described above. A final list of 55 studies was included for the analysis in this review (**Table 1**).

The literature screening was categorized in eight separate categories based on the methodology used (**Table 2**), including (1) SCUBA fast repetition rate (FRR) fluorometry; (2) SCUBA pulse amplitude modulated (PAM) fluorometry; (3) Clark-type O_2 sensors; (4) boundary layer; (5) SCUBA imaging; (6) benthic chambers; (7) submersible chambers; and (8) automated sensors. The database was further classified based on the system type (open, semi-closed, and enclosed); measured parameters [O_2, photosynthetic efficiency (Fv/Fm), electron transport rate (ETR), and calcification rate (CA)]; sampling frequency (minutes, hours, and days); sampling scale (symbionts, polyp, colony, and community); aim of the study (monitoring and experiment); and environmental stressor considered (light, temperature, turbidity, water quality, water flow, ocean acidification, and time). We ranked the database by publication year (**Table 3**) and identified the most commonly used techniques for studying *in situ* coral metabolism. We analyzed the objectives of the studies included in this review (**Figure 2**) in order to give an overview on the topics mostly studied between 1991 and 2020. Finally, we collated all 55 studies into a map to show the global distribution of experimental studies *in situ* discussed in this review (**Figure 3**).

RESULTS

Methodologies and Objectives for Coral *in situ* Metabolism

Several tools and instruments have been developed to noninvasively measure coral metabolic and physiological processes in both field and laboratory studies. These methods can be used to distinguish among healthy and stressed organisms, and the transitions between these states. We focus here on diver-portable technologies, designed to non-destructively estimate energy production and expenditure, such as respirometers and fluorometers. Although there is little consensus about the extent to which apparently healthy corals are adapting to the changing conditions (Baker et al., 2008), measures of

TABLE 1 | Reference studies discussed in this review, listed in chronological order of publication.

ID no.	Reference
1	Patterson et al., 1991
2	Gattuso et al., 1993
3	Beer et al., 1998
4	Ralph et al., 1999
5	Gorbunov et al., 2000
6	Lombardi et al., 2000
7	Lesser and Gorbunov, 2001
8	Banaszak et al., 2003
9	Winters et al., 2003
10	Yates and Halley, 2003
11	Levy et al., 2004
12	Okamoto et al., 2005
13	Wild et al., 2005
14	Levy et al., 2006
15	Carpenter and Patterson, 2007
16	Finelli et al., 2007
17	Nakamura and Nakamori, 2007
18	Weber et al., 2007
19	Frade et al., 2008
20	Piniak and Storlazzi, 2008
21	Nakamura and Nakamori, 2009
22	Schneider et al., 2009
23	Carpenter et al., 2010
24	Sawall et al., 2011
25	McGillis et al., 2011
26	Mass et al., 2011
27	Kline et al., 2012
28	Suggett et al., 2012
29	Wangpraseurt et al., 2012b
30	Haas et al., 2013
31	Ferrier-Pagès et al., 2013
32	Okazaki et al., 2013
33	Roder et al., 2013
34	Long et al., 2013
35	Wangpraseurt et al., 2014
36	Shaw et al., 2014
37	Treibitz et al., 2015
38	Rovelli et al., 2015
39	Camp et al., 2015
40	Takeshita et al., 2016
41	Chow et al., 2016
42	Biscéré et al., 2017
43	Albright et al., 2018
44	Takeshita et al., 2018
45	McMahon et al., 2018
46	Roth et al., 2019
47	Cyronak et al., 2020
48	Ramesh et al., 2019
49	de Froe et al., 2019
50	Doo et al., 2019
51	Pramneechote et al., 2020
52	Srednick et al., 2020
53	Oh et al., 2020
54	Roth et al., 2020
55	Dellisanti et al., 2020

metabolic proxies (e.g., variations in dissolved oxygen and pH) have been used at both individual coral and coral community scales to infer the metabolic state of benthic ecosystems (Bates et al., 2010). Quantitative links then are sought between these coral indicators and the wider status of the ecosystem physical and biogeochemical indicators.

Laboratory-based studies of coral metabolism in almost all cases involve the destructive sampling of individual colonies or fragments thereof. Although this framework provides crucial knowledge on isolated physiological responses, mechanisms, and pathways under well-controlled conditions, the study conditions cannot comprehensively reflect the stochasticity and cyclical fluctuations in environmental conditions on a reef, nor the cumulative effects of multiple chronic or acute stressors. In the last decades, experimental techniques to study the metabolic status of corals directly *in situ* have been developed, using specific tools engineered for automated analysis on coral surface and reef communities. Among these, microsensors and benthic chambers for respirometry and fluorometry techniques became the most popular for coral studies over a wide range of topics (**Table 2**).

The focus of instrumentation development for the *in situ* study of coral metabolism has shifted over the last three decades, from using fluorometric techniques to estimate endosymbiont photosynthetic efficiency to a more comprehensive investigation of the holobiont relationships in individuals and communities (**Table 3**). Indeed, through the use of benthic chambers, it is possible to run experimental manipulations of carbon or nutrient fluxes and monitor long-term ecosystem responses *via* automated sensors. With this shift, the linkages among biogeochemical and physiological processes in corals have greatly improved the understanding of coral ecosystems functioning to where modeling now has a realistic possibility to predict benthic conditions under future climate scenarios (Roth et al., 2019).

Among the objectives of coral physiology studies, 59% of the published works comprised investigations of the diel or seasonal changes in primary productivity, highlighting that quantification of natural variations in energetic fluxes is a central concern for the assessment of coral conditions (**Figure 2**). Moreover, coral primary productivity was the only objective of these studies being covered by all methodologies at different sampling scales, from polyp to community. Conversely, 25% of studies addressed coral physiology under stress, including bleaching responses, environmental changes, and bathymetric change conditions (transplantation). The assessment of recovery of health status was investigated by 9% of the studies. The remaining papers centered on issues of light limitation, including zonation (4%) and photo-inhibition (3%).

Underwater Fluorometry

The photochemical performance of coral endosymbionts is a key aspect influencing the health of scleractinian corals, so measures of holobiont photophysiology provide a valuable insight into coral metabolic status. Fluorometry can provide this insight in two broad ways: (i) by characterizing the abundance, character, and distribution of light-harvesting pigments (potential energy source) and fluorescent proteins (a sign of immune response and tissue repair) in corals and (ii) as an indicator of how efficiently these pigments are being used to generate energy for the coral, indicated by the photo-physiological status of the endosymbiont.

A fundamental measure of coral status is quantification of the light-harvesting pigments of the endosymbionts over time,

TABLE 2 | Experimental techniques available for *in situ* monitoring of coral physiological processes.

Method	System	Parameters	Sampling frequency	Sampling scale	Aim	Stressor	Reference ID no.
SCUBA FRR fluorometry	Open	ETR, Fv/Fm	Minutes	Symbionts	Monitoring	Light	5–7, 11, 14, 37
SCUBA PAM fluorometry	Semi-closed	ETR, Fv/Fm	Minutes	Symbionts	Monitoring	Light, temperature, water flow, water quality	3, 8, 9, 12, 15, 16, 19, 20, 24, 28, 33
Clark-type O_2 microsensor	Open	O_2	Hours	Symbionts, polyp	Experiment, monitoring	Water quality	18, 49
Diffusive boundary layer	Semi-closed	O_2, CA	Minutes	Symbionts, polyp	Monitoring	Light, water quality, time	10, 25, 34, 35, 38, 40
SCUBA imaging	Open	O_2	Hours	Symbionts, polyp, colony	Monitoring	Light, water quality	41, 48, 53
Benthic chamber	Enclosed	O_2, CA	Days	Colony	Experiment, monitoring	Light, water flow, water quality, ocean acidification	1, 2, 13, 21–23, 26, 30–32, 39, 42, 46, 52–55
Submersible chamber	Enclosed	O_2, CA	Hours	Colony, community	Experiment, monitoring	Light, water quality, ocean acidification	11, 14, 21, 22, 26, 39, 43, 50, 51
Automated sensors	Open	O_2, CA	Hours	Community	Monitoring	Water quality, ocean acidification	40, 43–45, 47

SCUBA FRR, SCUBA-based fast respiration rate fluorometer; SCUBA PAM fluorometry, SCUBA-based pulse amplitude modulation; O_2, dissolved oxygen; CA, calcification; ETR, electron transport rate; Fv/Fm, maximum quantum yield of photosystem II; Stressors, includes environmental stressors considered in the study; Reference, the identification number is referred to **Table 1.**

TABLE 3 | Time ranking of published peer-reviewed studies on coral *in situ* metabolism according to this study.

Year	Methodology	Objective	Sampling scale
B41991–2005	Fluorometry, benthic, and submersible chamber	Productivity, diel change	Polyp, colony
2006–2010	Fluorometry, benthic, chamber and automated sensors	Diel change, productivity, physiology under stress	Colony, community
2011–2015	Benthic and submersible chamber, diffusive boundary layer	Physiology under stress, productivity	Colony, polyp, community
2016–2020	Benthic and submersible chamber, automated sensors	Seasonal change, productivity, physiology under stress	Colony, community

whereby decreasing trends may provide early warning of the onset of bleaching events. The underwater fluorescence imaging has been adapted to conduct large-scale *in situ* assessments of coral reefs, through the detection of chlorophyll and green fluorescent proteins wide spatial scales (Treibitz et al., 2015; Oh et al., 2020). Chlorophyll concentrations are indicative of photo-acclimation, among other things, and green fluorescent proteins may, in addition to being a signal of tissue repair (D'Angelo et al., 2012), contribute to photoprotection in corals; and thus, quantifying these concentrations can provide crucial information on the bleaching susceptibility or resistance of corals (Salih et al., 2000; Kenkel et al., 2011; Roth and Deheyn, 2013). In addition, this imaging technique can also mark early signs of disease as well as help to detect coral juveniles thereby leading to more accurate assessment of coral reef health (Treibitz et al., 2015; Ramesh et al., 2019).

Early *in situ* studies on coral physiology estimated the rates of photosynthesis and respiration within recirculating chambers by measuring changes in oxygen concentrations (Patterson et al., 1991). While still a highly useful approach (see below), the introduction of variable fluorescence techniques has greatly increased the ability to assess the photophysiology of the endosymbionts and thus provide a sensitive indicator of their metabolic status. With variable fluorescence, very rapid pulses of light are used to probe the photosystems and inform on a number of photosynthetic parameters including the quantum yield of photosystem II (PSII), which is used as a metric for photosynthetic efficiency (Schreiber et al., 1986) and is a key indicator of the physiological status of the endosymbiont. Changes in photosynthetic efficiency provide an early signal of stress, some of which are natural responses to changes in irradiance but become more prolonged and severe when conditions of imminent bleaching occur.

The estimation of the potential quantum yield of PSII as a metric for photosynthetic rates was first applied to underwater organisms by Beer et al (Beer et al., 1998). PAM fluorometer uses light pulses of relatively long duration (300–1,200 ms, 3,000–10,000 mmol photons m^{-2} s^{-1}) to modify the fluorescence yields, generating multiple turnover for the reduction of PSII, allowing noninvasive chlorophyll fluorescence analysis, quantum yield, and ETR of coral endosymbionts. The introduction of an underwater version of this instrument (Diving-PAM, Walz) facilitated the direct observation of changes in coral health *in situ* conditions (Ralph et al., 1999). The introduction of *in situ* PAM fluorometry enabled the construction of photosynthesis-irradiance models for corals based on varying sun exposures in reefs (Beer et al., 1998; Ralph et al., 1999). For example, observations of decreased quantum yield during the day

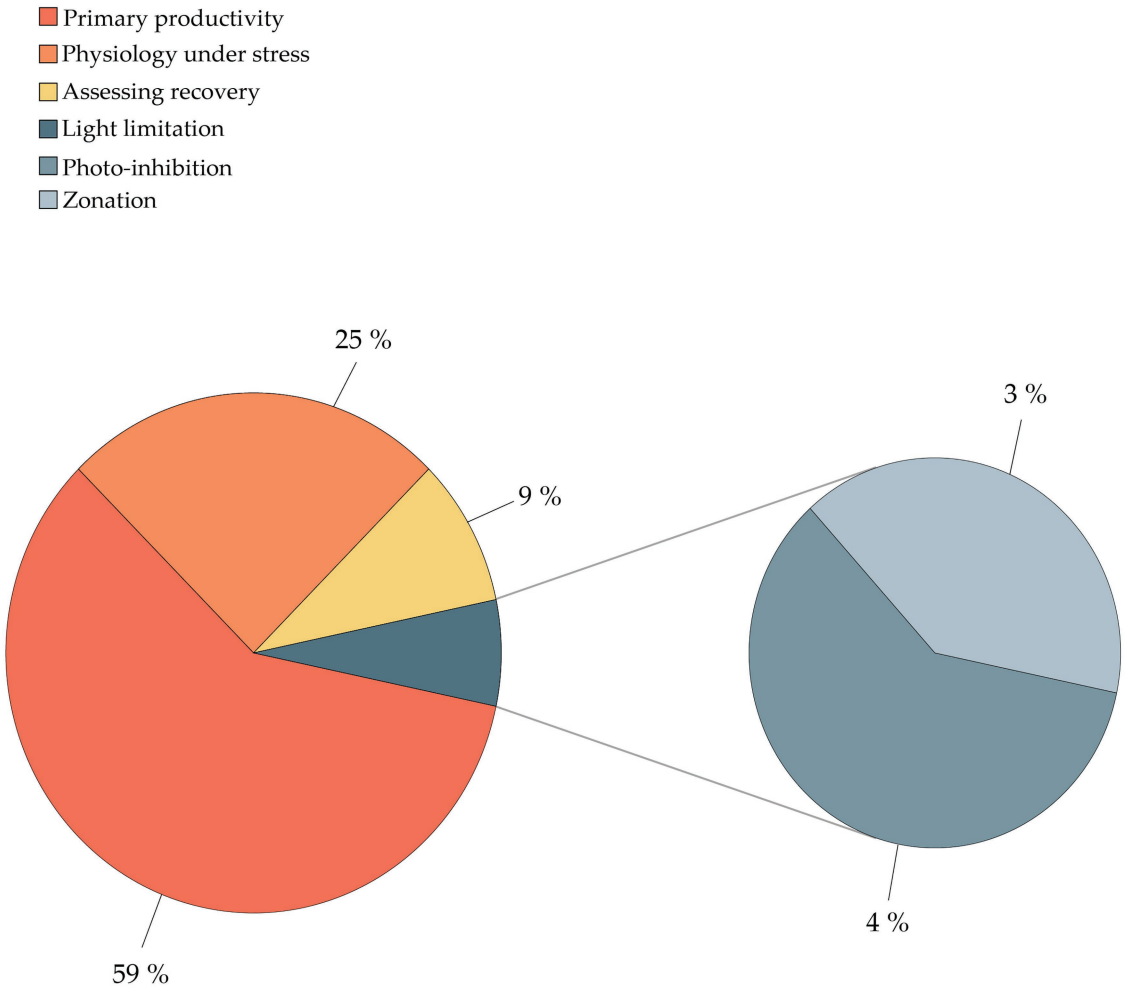

FIGURE 2 | Study objectives of *in situ* methodologies for the measurement of coral physiology.

reflected photoinhibition through loss of photosynthetic capacity, a response seen in shallow but not deeper water corals (Winters et al., 2003). Similar reduced photosynthetic efficiency has been observed in corals exposed to seasonal turbid conditions (Piniak and Storlazzi, 2008). The use of Diving-PAM continuous monitoring during bleaching events also showed that combined thermal and light stress generated greater reductions in photosynthetic efficiency and was a sensitive indicator of metabolic stress in impacted areas (Roder et al., 2013). Even so, variable responses in the coral community to these stresses suggested coral species-specific physiological responses (Banaszak et al., 2003; Okamoto et al., 2005; Frade et al., 2008; Suggett et al., 2012). Further development on PAM technology is the high-resolution imaging fluorometry used for analysis of heterogeneity within colonies, from coenosarc tissue to polyp tentacles, but so far, this methodology is not available for underwater studies (Ralph et al., 2005).

A second approach for measuring variable fluorescence is the FRR fluorometer, which uses a different approach to saturate the photochemistry during measurement. Here, shorter (150–400 ms, >20,000 mmol photons m^{-2} s^{-1}) but more intense light is used to generate a single turnover and reduction of the primary electron acceptor (Kromkamp and Forster, 2003; Suggett et al., 2003). The methodology is more sensitive than PAM fluorometry, which can be beneficial when endosymbiont abundance (or chlorophyll concentrations) is very low in corals. The SCUBA-based FRR fluorometry was developed by Gorbunov et al (Gorbunov et al., 2000) for measuring chlorophyll fluorescence from PSII reaction centers in corals, sea grasses, macroalgae, and algal turfs. FRR fluorometry has been also used to monitor coral physiology during bleaching events and their later recovery (Lombardi et al., 2000; Lesser and Gorbunov, 2001). Although nutrient availability (as nitrogen or iron) and sunlight irradiance were already recognized as the main factors directly affecting photosynthesis in the aquatic ecosystem (Falkowski and Kolber, 1995; Behrenfeld and Kolber, 1999), the use of FRR fluorometry enabled more direct measurements of nutrient limitation effects on photosynthetic efficiency of corals. Indeed, the FRR fluorometry predicted which corals

FIGURE 3 | Global map of scientific studies cited in this review. The reference identification numbers are listed in **Table 1.**

might be more susceptible to bleaching under stress conditions even when no signs of stress are visible, but photosynthetic quantum yield was reduced (Lesser and Gorbunov, 2001).

Submersible chambers have been used to study the evolution of diurnal hysteresis in coral photosynthesis *in situ*, enabling the comparison of respirometry and fluorometry-based techniques (see below; Levy et al., 2003, 2006). Marked discrepancies were observed, reflecting the importance of different scales of measurements. FRR and PAM fluorometry methods yield signals at the polyp-symbiont scale (Gorbunov et al., 2000), while changes in oxygen concentrations in chambers integrate the whole colony response (Schneider et al., 2009). The assumption here is that the chamber system designs and durations impart no added stress condition on the corals, which appears to be the case in many studies (Camp et al., 2015; Roth et al., 2019; Dellisanti et al., 2020). While it can be argued that chamber methods may be more informative in terms of the holobiont, the portability, ease of operation, and comparatively low cost of fluorescence instruments (Diving-PAM, FRR, and imaging systems) have greatly expanded their use for studying photosynthetic performance of coral symbionts and monitoring diel changes of coral productivity.

Benthic Chambers, Diffusive Flux Methods, and Flow Analysis

Early *in situ* studies on coral biology used the strategy of encapsulating single or multiple individuals within closed benthic systems (Patterson et al., 1991). These chamber methods enabled the non-destructive measurement of coral physiological rates through changes in water chemistry to better understand community level responses to perturbation (Patterson et al., 1991; Gattuso et al., 1993). For example, incubation chambers have been used to study *in situ* coral calcification and photosynthesis rates and showed that ocean acidification can lower the biocalcification rates (Okazaki et al., 2013). Larger incubation systems have enabled measurements of benthic community metabolism as well as conducting *in situ* experiments, providing a better insight into ecological responses in reefs than can be the focus of studies on host-symbiont relationships (Yates and Halley, 2003; Haas et al., 2013).

The common metrics to assess the health of corals are the levels of photosynthesis by the endosymbionts, respiration of the holobiont, and ideally the rates of biocalcification (or growth). Benthic chambers are well-suited to measure these essential parameters *in situ* (Wild et al., 2005; Nakamura and Nakamori, 2007; Ferrier-Pagès et al., 2013; Camp et al., 2015). For example, differences in coral metabolism were measured between shallow (reef flat) and deeper area (reef slope) at Ishigaki Island, Japan, with negative net calcification rates being attributed to nighttime decreases in pH due to benthic respiration (Nakamura and Nakamori, 2009). In another study, Sawall et al. (2011) used benthic chamber to study the coral nutritional status at elevated anthropogenic nutrient loading. The novel incorporation of a transparent 3-L urine bag into the "Flexi-Chamber" design led to an easily managed, low-cost device for use by any underwater scientists, where short incubations are able to detect changes in biological processes absent of any visual signs of coral stress or change in endosymbionts concentration (Camp et al., 2015). A similar benthic chamber design was used to show that abiotic conditions, including light intensity, were drivers of spatial-temporal patterns of reef metabolism, although some limitations on the use of these incubation chambers emerged when applied on large boulder colonies (Pramneechote et al., 2020). Here, the amount of light available for photosynthesis and the energetic budget can vary based on colony shape (micro niches) and the immediate surrounding environment (backscattering light; Wangpraseurt et al., 2014). However, newer designs of noninvasive

diver-portable *in situ* incubation chambers (~70 L, 0.2-m^2 area) have been developed to measure biogeochemical processes in both simple (sediments) and structurally complex (corals or rocky bottoms) reef communities, allowing the *in situ* study of diverse habitats, such as corals, sediments, and seagrass meadows (Roth et al., 2019). The introduction of benthic and submersible chambers has made it possible to link individual metabolic host-symbiont processes to community-wide reef responses, improving the generality and robustness of previous metabolic and physiology studies.

An ambitious program began in mid-1996 to adapt benthic chambers for use as flow respiratory systems to study the *in situ* responses of coral communities. Using a combination of *in situ* flow chambers and fluorometric techniques, Shepard et al. (1996) demonstrated how both water flow and temperature combined to influence coral physiology. Later, the "Submersible Habitat for Analyzing Reef Quality" was designed to maintain and measure a turbulent flow of water over benthic substrates for extended periods while measuring temperature, oxygen, salinity, pH, and irradiance (photosynthetically active radiation) and to monitor the daily variations in photosynthesis, respiration, and calcification (Yates and Halley, 2003). This system enabled some of the first studies of the direct influence of high CO_2 levels on coral communities in short-term experiments (Yates and Halley, 2003). But the real strength of this approach is the ability to study the ecology and biogeochemistry of coral/benthic communities and how they may acclimate to altered conditions over multiple days. A similar automated closed chamber was used to study coral responses over a variety of substrate types (Gevaert et al., 2011).

These flow systems have enabled new strategies for *in situ* investigation of the effects of environmental stressors on reef metabolism, ecology, and biogeochemistry. Flow systems have been used to demonstrate asymmetric patterns of photosynthetic yield across coral colonies (Carpenter et al., 2010), where the upper side has a reduced quantum yield (Carpenter and Patterson, 2007). Other experimental studies have used flow chambers to study coral physiology under chemical enrichment in a benthic chamber experiment (Biscéré et al., 2017), adding new findings on coral responses to high pCO_2 and the combined effect of chemical inputs and global warming. Haas et al. (2013) used large collapsible benthic isolation tents (cBITs) to study the integrated responses of corals, macroalgae, and microbes over diurnal cycles, and they showed how the release of algal exudates influenced microbial metabolism and energy transfer to higher trophic levels. Similarly, small benthic chambers enclosing ~70 L (Roth et al., 2019) were used to study complex benthic structures and to measure coral reef community budgets of primary production over coral-dominated or algae-dominated reef communities (Roth et al., 2020), adding new findings on the biogeochemical cycles of coral reef ecosystems. A common feature of these flow systems is that they commonly require constructing or placement of large or cumbersome structures on the reef, so replicating findings across and among reef systems is difficult. A new diver-portable respirometer [community *in situ* metabolism (CISME)] enables short-term (minutes) quantification of coral photosynthetic, respiration, and biocalcification rates combined with the ability to study the effects of flow and chemical manipulations (Dellisanti et al., 2020). Although its use has been limited to date, it offers many of the benefits of larger chamber devices but also the ability to assess individual coral colonies across and among reef environments with good accuracy and resolution.

Micro- and Automated Sensors

While benthic chambers provide a means for studying the community level responses, by design, these systems alter water flow dynamics around the study corals and restrict water exchange sufficiently to enable changes in water chemistry to accumulate (i.e., the measurement signals). It is unclear at what stage these changes in water flow and bulk chemical conditions may begin influencing coral responses. The use of micro- and automated sensors for unenclosed measurements has been developed to help avoid these potential artifacts. These approaches are broadly separated into community-scale and individual coral or polyp scales.

Unenclosed, diffusive boundary layer (DBL) approaches were developed to avoid these potential issues, whereby sensors placed well above the coral interface make unobstructed measurements of vertical gradients in velocity, temperature, and chemical constituents on the open reef to calculate the flux of momentum, heat, and O_2 in the boundary layer (McGillis et al., 2011). Use of these unenclosed strategies has revealed new insights into coral metabolism by showing the fluctuations in biologically mediated changes in chemical conditions under different natural regimes of dissolved oxygen, pH, and light intensity (Cyronak et al., 2018; McMahon et al., 2018; Takeshita et al., 2018).

The use of microsensors at coral tissue levels in turn has illustrated how these factors influence and are influenced by the coral-seawater interface (McGillis et al., 2011; Wangpraseurt et al., 2012a, 2014; Long et al., 2013; Takeshita et al., 2016). For example, the oxygen saturation at the coral-water interface fluctuates from supersaturated during daytime due to production by endosymbionts to hypoxic at night from respiration of the holobiont (Shashar et al., 1993; Kuhl et al., 1995; Gardella and Edmunds, 1999). However, despite these broad chemical changes, oxygen microsensors used in the microenvironment of coral-turf and coral-coralline algae showed that low oxygen concentrations were not generally found at the interface of *Porites* spp., turf algae, and crustose coralline algae (Wangpraseurt et al., 2012a), an observation that illustrated the value of combining microstructure measurements with benthic or flow chamber methods that can take into account multiple reef species.

More microenvironment studies are needed to better understand the metabolic regulation between corals and the surrounding environment (Wangpraseurt et al., 2014). Technological development of microsensors in a modified diver-operated system (Weber et al., 2007) allowed the quantification of irradiance at the coral surface and the measurement of the efficiency of photosynthetic system at polyp and coenosarc microscale (Wangpraseurt et al., 2012b), confirming the ability of corals to adapt to environmental changes, such as temperature

or irradiance (Brown et al., 2002). On a broader scale, micro- and automated sensors increasingly have been used in both closed (benthic chamber) and open (reef-scale) approaches to studying coral and reef ecologies. We consider now the subset of unconfined sensor-based studies of whole reef environments.

Reef Scale Experiments

The study of larger scale reef environments in open or unconfined natural systems was made possible by combining the sensors for measuring both water flow and relevant aspects of water chemistry. A common approach is the DBL method that relies on eddy correlation techniques (Berg et al., 2003), where noninvasive acoustic Doppler velocimeters measuring water flow are coupled with O_2 sensors to provide three-dimensional fields of oxygen distribution over benthic environments (Long et al., 2013). This method can examine *in situ* dynamics of O_2 production and consumption (i.e., respiration) in different habitats, including highly productive reef crests relative to reef slopes (Long et al., 2013) as well as cold-water (deep) coral reefs (Rovelli et al., 2015; de Froe et al., 2019). These ecosystem-scale measurements show how high oxygen fluxes are possible, even in nutrient-replete environments such as reef slopes and deep waters. The advantage of such techniques has been discussed by Takeshita et al. (2016) who introduced a new autonomous system (the benthic ecosystem and acidification measurement system) for simultaneous measurement of NCP and NCC from a coral reef through the autonomous use of O_2 and pH sensing technology. Using this strategy, Takeshita et al. (2018) showed how seawater carbonate chemistry is strongly driven by local benthic metabolism, and that these effects varied substantially over small-scale habitats, across the entire reef platform, and over seasonal timescales, an important perspective for better assessing the impacts of ocean acidification on these ecosystems.

A comparison between the enclosed and open system approaches showed good general agreement with respect to discrete measurements of oxygen from the gradient flux (GF) method at the DBL and a multiparametric probe in a benthic chamber (Yates and Halley, 2003), although other findings indicate that the GF method can offer more accurate measurements of these fluxes (McGillis et al., 2011). The low physical disruption with DBL methods means both less direct impacts on corals and more spatially integrative observation and interpretation of coral reef responses to changes in the natural environment at colony or community levels. Their smaller infrastructure requirements also make them an attractive strategy for investigations. Even so, these approaches can be complementary. For example, DBL studies show that water flow can be a factor affecting the light-limited photosynthesis in coral colonies (Finelli et al., 2006), and more spatially focused studies have used benthic chambers to show that increased water flow leads to increased calcification rates, carbonate deposition, protein concentration, and endosymbionts density (Mass et al., 2011).

Experiments at reef scale represent a key step forward in the *in situ* studies of coral responses in the natural environment (Kline et al., 2012; Albright et al., 2018; Doo et al., 2019; Srednick et al., 2020), but they also have provided the opportunity to quantify reef-scale responses to environmental perturbations. For example, manipulations to lower Ωa by ~20% led to a 34% decrease in NCC consistent with the effect of lower pH on biocalcification (Albright et al., 2016), although this finding may have been influenced by a high abundance of crustose coralline algae living in the reef community (Albright et al., 2018). Another free ocean CO_2 enrichment (FOCE) system was used to incubate coral reef communities at ambient pCO_2 (393 μatm) and high pCO_2 (949 μatm), and a decrease in daily NCC by 49% under high pCO_2 was observed over a 21-day experiment, corresponding to 26% reduction in NCC per unit of Ωa (Doo et al., 2019). These results were in line with previous studies on ecosystem-level responses of coral reef communities to ocean acidification level projected in the next century. Indeed, a modification of this experimental approach, the coral-proto free ocean carbon enrichment system, allowed the short-term *in situ* study of the induced ocean acidification on coral reef organisms and diel changes of the seawater carbonate system (Kline et al., 2012). Srednick et al. (2020) introduced another novel FOCE for spatial and temporal studies on shallow reefs, with the aim of studying a coral reef community *in situ* under controlled conditions of current and projected levels of pCO_2. They directly estimated the hysteresis of seawater carbonate chemistry along a reef transect, using high accuracy and precision measurements of seawater pH, pCO_2, and the biological responses of the reef community with high temporal resolution (Srednick et al., 2020). Other high-frequency sampling of coral reef carbonate dynamics and metabolic rates have used automated systems for measurements of alkalinity, pH, and pCO_2 at high-frequency sampling (McMahon et al., 2018; Cyronak et al., 2020). Through automated measurements with the slack water and flow respirometry approaches, it is now possible to characterize the net calcification and productivity of a reef system (either reef flats or crests), as well as reveal long-term changes driven by global changes (ocean acidification and global warming) or hysteresis under local changes (Albright et al., 2018; McMahon et al., 2018). However, dissimilarities in the methods used in community metabolism studies (Shaw et al., 2015) create potential uncertainties when applied to coral reefs, in terms of community calcification and seawater carbonate conditions. Limitations of metabolic studies at community level are related to lack of suitable controls, spatial heterogeneities, and thus replicability among sites, as well as confounding factors in open systems, such as the introduction of organisms and differing oceanographic settings in the surrounding reef environments.

DISCUSSION AND CONCLUSION

We have collated and summarized here the underwater methodologies from 55 studies on coral metabolism and physiology conducted since 1991 (**Table 1**). The current knowledge of combined effects of local and global stressors comes from a wide breadth of manipulation studies on coral responses under predicted future scenarios but limited in

representing complex abiotic factors in ecosystems. Interaction among environmental variables, including temporal changes in inorganic carbon chemistry, physical parameters, or nutrient loads, is an important factor affecting the biogeochemistry of coral health (Doo et al., 2019) and can play a key role in population dynamics. Though invaluable as a study tool, manipulation studies are limited in the ability to mimic important spatial-temporal patterns and interactions. On the other hand, comprehensive long-term *in situ* metabolic measurements still are lacking but nevertheless necessary to understand the energetics and trophodynamics of reef ecosystems.

Laboratory-based studies have provided a strong foundation for understanding coral metabolism and the responses to stress, and they will continue to serve as a primary means of research under controlled conditions. However, the expanding role of *in situ*-based studies of coral systems is essential for extrapolating and modulating these laboratory-based findings to the temporal and spatial complexity of natural reef and environmental conditions. The advantages of *in situ* experimental techniques described here relate to the ability for measuring metabolic and biogeochemical properties of different benthic habitats having both simple (sediments) and complex (corals or rocky bottom) structures. Standardization of methods and replication of experimental studies would allow the simultaneous measures of coral health in different locations with the ability to compare the ecosystem functions. However, there are limitations to *in situ* methodologies. In the case of benthic chambers, there are restrictions to which substrate surfaces are suitable for study, and they are not well suited, even with enhanced flow capabilities, for longer-term monitoring of coral health. These restricted systems also have limited spatial footprints and thus may not adequately account for all benthic of pelagic components (e.g., macroalgae and fish). In the case of DBL approaches, limitations include the needed maintenance and fragility of microsensors, which can limit deployments to shorter duration, or under more quiescent weather conditions.

Long-term continuous observations of coral biological process are critical to the assessment of responses to climate and other anthropogenic drivers and though so far lacking newly developed platforms for general oceanographic study offer this potential moving forward. In particular, autonomous platforms, such as gliders and surface vehicles, are incorporating biogeochemical sensors (i.e., pCO_2, dissolved oxygen, pH, and chlorophyll a), able to cover spatial, vertical, and temporal observations (Chai et al., 2020; Cryer et al., 2020). While these autonomous devices are not well suited for shallow reef environments, the advances in sensor development and operational constraints will be valuable in designing systems or autonomous robots that can provide reliable long-term assessments of the status of reef ecosystems. Indeed, autonomous measurements of light, dissolved oxygen, and alkalinity were used to estimate the NCP and NCC in order to evaluate the efficacy of coral restoration in supporting the net ecosystem metabolism (Platz et al., 2020). Autonomous sensors can be used also to measure the seasonal variability in carbonate chemistry and the relationship between carbonate chemistry and biological activity of benthic organisms identifying spatial differences according to different substrates, like corals, seagrasses, or mangroves (Meléndez et al., 2020). These systems are especially important in natural ocean acidification laboratories, such as hydrothermal vents, characterized by naturally high fluctuations of pH and temperature (Kerrison et al., 2011; Fabricius et al., 2015; Torres et al., 2021).

Co-deployment of multiple instrumentation approaches, from water chemistry and physics to coral physiology, will be needed to ensure both accuracy and logistic practicality in monitoring fluxes of O_2, changes of pH, and other aspects of the carbonate system in coral reefs. Even with these accounted for, most studies on coral metabolic rates rely on observation of changes in DIC and alkalinity in a specific (small) area to calculate the carbon fluxes for productivity and biocalcification estimates (Anthony et al., 2011); the movement of seawater flow and aspects of reef heterogeneity cannot be fully taken into account, leading to potentially biased findings that may not adequately reflect natural conditions. Moving forward then, it will be more informative by combining different scales of *in situ* techniques, such as the application of flow respirometry approaches to estimate carbon fluxes over a small spatial scales and different substrate type within a reef, coupled with reef-scale methods that provide an integrative assessment of the temporal variability in coral productivity and growth (McMahon et al., 2018).

AUTHOR CONTRIBUTIONS

WD and JC: conceptualization, methodology, formal analysis, and resources. WD: investigation, data curation, and writing – original draft preparation. WD, JC, CC, JW, MW, and LC: writing – review and editing. WD and CC: visualization. LC: supervision. JW and LC: project administration and funding acquisition. All authors contributed to the article and approved the submitted version.

FUNDING

This study was supported by the Hong Kong Branch of Southern Marine Science and Engineering Guangdong Laboratory (Guangzhou; SMSEGL20SC02); the Collaborative Research Fund (C7013-19G) of the Hong Kong Research Grants Council; the National Natural Science Foundation of China (41641047); the Internal Research Project of State Key Laboratory of Satellite Ocean Environment Dynamics, Second Institute of Oceanography, State Oceanic Administration (no. SOEDZZ1702); and the SKLMP Seed Collaborative Research Fund (SCRF/0027).

ACKNOWLEDGMENTS

The authors thank Florian Roth (University of Helsinki) for the constructive comments and John Hodgkiss for the proofreading.

REFERENCES

Albright, R., Benthuysen, J., Cantin, N., Caldeira, K., and Anthony, K. (2015). Coral reef metabolism and carbon chemistry dynamics of a coral reef flat. *Geophys. Res. Lett.* 42, 3980–3988. doi: 10.1002/2015GL063488

Albright, R., Caldeira, L., Hosfelt, J., Kwiatkowski, L., Maclaren, J. K., Mason, B. M., et al. (2016). Reversal of ocean acidification enhances net coral reef calcification. *Nature* 531, 362–365. doi: 10.1038/nature17155

Albright, R., Takeshita, Y., Koweek, D. A., Ninokawa, A., Wolfe, K., Rivlin, T., et al. (2018). Carbon dioxide addition to coral reef waters suppresses net community calcification. *Nature* 555, 516–519. doi: 10.1038/nature25968

Alderdice, R., Suggett, D. J., Cárdenas, A., Hughes, D. J., Kühl, M., Pernice, M., et al. (2021). Divergent expression of hypoxia response systems under deoxygenation in reef-forming corals aligns with bleaching susceptibility. *Glob. Chang. Biol.* 27, 312–326. doi: 10.1111/gcb.15436

Al-Horani, F. A., Al-Moghrabi, S. M., and De Beer, D. (2003a). Microsensor study of photosynthesis and calcification in the scleractinian coral, *Galaxea fascicularis*: active internal carbon cycle. *J. Exp. Mar. Biol. Ecol.* 288, 1–15. doi: 10.1016/S0022-0981(02)00578-6

Al-Horani, F. A., Al-Moghrabi, S. M., and De Beer, D. (2003b). The mechanism of calcification and its relation to photosynthesis and respiration in the scleractinian coral *Galaxea fascicularis*. *Mar. Biol.* 142, 419–426. doi: 10.1007/s00227-002-0981-8

Al-Horani, F. A., Tambutté, É., and Allemand, D. (2007). Dark calcification and the daily rhythm of calcification in the scleractinian coral, *Galaxea fascicularis*. *Coral Reefs* 26, 531–538. doi: 10.1007/s00338-007-0250-x

Altieri, A. H., Harrison, S. B., Seemann, J., Collin, R., Diaz, R. J., and Knowlton, N. (2017). Tropical dead zones and mass mortalities on coral reefs. *Proc. Natl. Acad. Sci.* 114, 3660–3665. doi: 10.1073/pnas.1621517114

Anthony, K. R. N., Connolly, S. R., and Hoegh-Guldberg, O. (2007). Bleaching, energetics, and coral mortality risk: effects of temperature, light, and sediment regime. *Limnol. Oceanogr.* 52, 716–726. doi: 10.4319/lo.2007.52.2.0716

Anthony, K. R. N., and Fabricius, K. E. (2000). Shifting roles of heterotrophy and autotrophy in coral energetics under varying turbidity. *J. Exp. Mar. Biol. Ecol.* 252, 221–253. doi: 10.1016/S0022-0981(00)00237-9

Anthony, K. R. N., Kleypas, J., and Gattuso, J. P. (2011). Coral reefs modify their seawater carbon chemistry - implications for impacts of ocean acidification. *Glob. Chang. Biol.* 17, 3655–3666. doi: 10.1111/j.1365-2486.2011.02510.x

Anthony, K. R. N., Kline, D. I., Diaz-Pulido, G., Dove, S., and Hoegh-Guldberg, O. (2008). Ocean acidification causes bleaching and productivity loss in coral reef builders. *Proc. Natl. Acad. Sci. U. S. A.* 105, 17442–17446. doi: 10.1073/pnas.0804478105

Baker, D. M., Freeman, C. J., Wong, J. C. Y. Y., Fogel, M. L., and Knowlton, N. (2018). Climate change promotes parasitism in a coral symbiosis. *ISME J.* 12, 921–930. doi: 10.1038/s41396-018-0046-8

Baker, A. C., Glynn, P. W., and Riegl, B. (2008). Climate change and coral reef bleaching: an ecological assessment of long-term impacts, recovery trends and future outlook. *Estuar. Coast. Shelf Sci.* 80, 435–471. doi: 10.1016/j.ecss.2008.09.003

Baker, D. M., Jordán-Dahlgren, E., Maldonado, M. A., and Harvell, C. D. (2010). Sea fan corals provide a stable isotope baseline for assessing sewage pollution in the Mexican Caribbean. *Limnol. Oceanogr.* 55, 2139–2149. doi: 10.4319/lo.2010.55.5.2139

Baker, D. M., Kim, K., Andras, J. P., and Sparks, J. P. (2011). Light-mediated 15N fractionation in Caribbean gorgonian octocorals: implications for pollution monitoring. *Coral Reefs* 30, 709–717. doi: 10.1007/s00338-011-0759-x

Banaszak, A. T., Ayala-Schiaffino, N., Rodriguez-Romàn, A., Enriquez, S., and Iglesisas-Prieto, R. (2003). Response of *Millepora alcicornis* (Milleporina: Milleporidae) to two bleaching events at Puerto Morelos Reef, Mexican Caribbean. *Rev. Biol. Trop.* 51, 57–66.

Bates, N. R., Amat, A., and Andersson, A. J. (2010). Feedbacks and responses of coral calcification on the Bermuda reef system to seasonal changes in biological processes and ocean acidification. *Biogeosciences* 7, 2509–2530. doi: 10.5194/bg-7-2509-2010

Beer, S., Ilan, M., Eshel, A., Weil, A., and Brickner, I. (1998). Use of pulse amplitude modulated (PAM) fluorometry for *in situ* measurements of photosynthesis in two Red Sea faviid corals. *Mar. Biol.* 131, 607–612. doi: 10.1007/s002270050352

Behrenfeld, M. J., and Kolber, Z. S. (1999). Widespread iron limitation of phytoplankton in the south pacific ocean. *Science* 283, 840–843. doi: 10.1126/science.283.5403.840

Berg, P., Røy, H., Janssen, F., Meyer, V., Jørgensen, B., Huettel, M., et al. (2003). Oxygen uptake by aquatic sediments measured with a novel non-invasive eddy-correlation technique. *Mar. Ecol. Prog. Ser.* 261, 75–83. doi: 10.3354/meps261075

Bessell-Browne, P., Negri, A. P., Fisher, R., Clode, P. L., Duckworth, A., and Jones, R. (2017). Impacts of turbidity on corals: the relative importance of light limitation and suspended sediments. *Mar. Pollut. Bull.* 117, 161–170. doi: 10.1016/j.marpolbul.2017.01.050

Biscéré, T., Lorrain, A., Rodolfo-Metalpa, R., Gilbert, A., Wright, A., Devissi, C., et al. (2017). Nickel and ocean warming affect scleractinian coral growth. *Mar. Pollut. Bull.* 120, 250–258. doi: 10.1016/j.marpolbul.2017.05.025

Brading, P., Warner, M. E., Davey, P., Smith, D. J., Achterberg, E. P., and Suggett, D. J. (2011). Differential effects of ocean acidification on growth and photosynthesis among phylotypes of *Symbiodinium* (Dinophyceae). *Limnol. Oceanogr.* 56, 927–938. doi: 10.4319/lo.2011.56.3.0927

Brown, B., and Bythell, J. (2005). Perspectives on mucus secretion in reef corals. *Mar. Ecol. Prog. Ser.* 296, 291–309. doi: 10.3354/meps296291

Brown, B. E., Dunne, R. P., Goodson, M. S., and Douglas, A. E. (2002). Experience shapes the susceptibility of a reef coral to bleaching. *Coral Reefs* 21, 119–126. doi: 10.1007/s00338-002-0215-z

Browne, N., Precht, E., Last, K., and Todd, P. (2014). Photo-physiological costs associated with acute sediment stress events in three near-shore turbid water corals. *Mar. Ecol. Prog. Ser.* 502, 129–143. doi: 10.3354/meps10714

Bruno, J. F., and Selig, E. R. (2007). Regional decline of coral cover in the Indo-Pacific: timing, extent, and subregional comparisons. *PLoS One* 2:e711. doi: 10.1371/journal.pone.0000711

Bustamante, M. M. C., Nardoto, G. B., Pinto, A.S., Resende, J. C. F., Takahashi, F. S. C., and Vieira, L. C. G. (2012). Potential impacts of climate change on biogeochemical functioning of Cerrado ecosystems. *Braz. J. Biol.* 72, 655–671. doi: 10.1590/S1519-69842012000400005

Caldeira, K., and Wickett, M. E. (2003). Anthropogenic carbon and ocean pH. *Nature* 425:365. doi: 10.1038/425365a

Camp, E. F., Krause, S. L., Santos, L. M. F., Naumann, M. S., Kikuchi, R. K. P., Smith, D. J., et al. (2015). The "Flexi-Chamber": A novel cost-effective *in situ* respirometry chamber for coral physiological measurements. *PLoS One* 10:e0138800. doi: 10.1371/journal.pone.0138800

Carpenter, L. W., and Patterson, M. R. (2007). Water flow influences the distribution of photosynthetic efficiency within colonies of the scleractinian coral Montastrea annularis (Ellis and Solander, 1786); implications for coral bleaching. *J. Exp. Mar. Biol. Ecol.* 351, 10–26. doi: 10.1016/j.jembe.2007.05.022

Carpenter, L. W., Patterson, M. R., and Bromage, E. S. (2010). Water flow influences the spatiotemporal distribution of heat shock protein 70 within colonies of the scleractinian coral Montastrea annularis (Ellis and Solander, 1786) following heat stress: implications for coral bleaching. *J. Exp. Mar. Biol. Ecol.* 387, 52–59. doi: 10.1016/j.jembe.2010.02.019

Cesar, H., Burke, L., and Pet-Soede, L. (2003). The economics of worldwide coral reef degradation. International Coral Reef Action Network Available at: https://agris.fao.org/agris-search/search.do?recordID=GB2013202743 (Accessed September 22, 2020).

Chai, F., Johnson, K. S., Claustre, H., Xing, X., Wang, Y., Boss, E., et al. (2020). Monitoring ocean biogeochemistry with autonomous platforms. *Nat. Rev. Earth Environ.* 1, 315–326. doi: 10.1038/s43017-020-0053-y

Chow, M. H., Tsang, R. H. L., Lam, K. Y., and Ang, P. Jr. (2016). Quantifying the degree of coral bleaching using digital photographic technique. *J. Exp. Mar. Biol. Ecol.* 479, 60–68. doi: 10.1016/j.jembe.2016.03.003

Ciais, P., Sabine, C., Bala, G., Bopp, L., Brovkin, V., and Canadell, J. (2013). "Carbon and other biogeochemical cycles," in *Climate Change 2013 the Physical Science Basis: Working Group I Contribution to the Fifth Assessment Report of the Intergovernmental Panel on Climate Change*. eds. T. F. Stocker, D. Qin, G.-K. Plattner, M. Tignor, S. K. Allen and J. Boschung et al. (Cambridge University Press), 465–570.

Cohen, A., and Holcomb, M. (2009). Why corals care about ocean acidification: uncovering the mechanism. *Oceanography* 22, 118–127. doi: 10.5670/oceanog.2009.102

Comeau, S., Edmunds, P. J., Lantz, C. A., and Carpenter, R. C. (2017). Daily variation in net primary production and net calcification in coral reef

communities exposed to elevated pCO_2. *Biogeosciences* 14, 3549–3560. doi: 10.5194/bg-14-3549-2017

Conti-Jerpe, I. E., Thompson, P. D., Wong, C. W. M., Oliveira, N. L., Duprey, N. N., Moynihan, M. A., et al. (2020). Trophic strategy and bleaching resistance in reef-building corals. *Sci. Adv.* 6, 5443–5453. doi: 10.1126/sciadv.aaz5443

Courtney, T. A., De Carlo, E. H., Page, H. N., Bahr, K. D., Barro, A., Howins, N., et al. (2018). Recovery of reef-scale calcification following a bleaching event in Kāneʻohe Bay, Hawai'i. *Limnol. Oceanogr. Lett.* 3, 1–9. doi: 10.1002/lol2.10056

Courtney, T. A., Lebrato, M., Bates, N. R., Collins, A., De Putron, S. J., Garley, R., et al. (2017). Environmental controls on modern scleractinian coral and reef-scale calcification. *Sci. Adv.* 3:e1701356. doi: 10.1126/sciadv.1701356

Cryer, S., Carvalho, F., Wood, T., Strong, J. A., Brown, P., Loucaides, S., et al. (2020). Evaluating the sensor-equipped autonomous surface vehicle C-worker 4 as a tool for identifying Coastal Ocean acidification and changes in carbonate chemistry. *J. Mar. Sci. Eng.* 8:939. doi: 10.3390/jmse8110939

Cyronak, T., Andersson, A. J., Langdon, C., Albright, R., Bates, N. R., Caldeira, K., et al. (2018). Taking the metabolic pulse of the world's coral reefs. *PLoS One* 13:e0190872. doi: 10.1371/journal.pone.0190872

Cyronak, T., Takeshita, Y., Courtney, T. A., DeCarlo, E. H., Eyre, B. D., Kline, D. I., et al. (2020). Diel temperature and pH variability scale with depth across diverse coral reef habitats. *Limnol. Oceanogr. Lett.* 5, 193–203. doi: 10.1002/lol2.10129

D'Angelo, C., Smith, E. G., Oswald, F., Burt, J., Tchernov, D., and Wiedenmann, J. (2012). Locally accelerated growth is part of the innate immune response and repair mechanisms in reef-building corals as detected by green fluorescent protein (GFP)-like pigments. *Coral Reefs* 31, 1045–1056. doi: 10.1007/s00338-012-0926-8

D'Angelo, C., and Wiedenmann, J. (2014). Impacts of nutrient enrichment on coral reefs: new perspectives and implications for coastal management and reef survival. *Curr. Opin. Environ. Sustain.* 7, 82–93. doi: 10.1016/j.cosust.2013.11.029

Darling, E. S., Alvarez-Filip, L., Oliver, T. A., Mcclanahan, T. R., and Côté, I. M. (2012). Evaluating life-history strategies of reef corals from species traits. *Ecol. Lett.* 15, 1378–1386. doi: 10.1111/j.1461-0248.2012.01861.x

DeCarlo, T. M., Gajdzik, L., Ellis, J., Coker, D. J., Roberts, M. B., Hammerman, N. M., et al. (2020). Nutrient-Supplying Ocean currents modulate coral bleaching susceptibility. *Sci. Adv.* 6:eabc5493. doi: 10.1126/sciadv.abc5493

de Froe, E., Rovelli, L., Glud, R. N., Maier, S. R., Duineveld, G., Mienis, F., et al. (2019). Benthic oxygen and nitrogen exchange on a cold-water coral reef in the north-East Atlantic Ocean. *Front. Mar. Sci.* 6:665. doi: 10.3389/fmars.2019.00665

Dellisanti, W., Tsang, R. H. L., Ang, P. Jr., Wu, J., Wells, M. L., and Chan, L. L. (2020). A diver-portable respirometry system for in-situ short-term measurements of coral metabolic health and rates of calcification. *Front. Mar. Sci.* 7:571451. doi: 10.3389/fmars.2020.571451

Descombes, P., Wisz, M. S., Leprieur, F., Parravicini, V., Heine, C., Olsen, S. M., et al. (2015). Forecasted coral reef decline in marine biodiversity hotspots under climate change. *Glob. Chang. Biol.* 21, 2479–2487. doi: 10.1111/gcb.12868

Dlugokencky, E., and Tans, P. (2020). Global Monitoring Laboratory - Carbon Cycle Greenhouse Gases. US Dep. Commer. NOAA, Glob. Monit. Lab. Available at: www.esrl.noaa.gov/gmd/ccgg/trends (Accessed July 6, 2020).

Doo, S. S., Edmunds, P. J., and Carpenter, R. C. (2019). Ocean acidification effects on *in situ* coral reef metabolism. *Sci. Rep.* 9, 1–8. doi: 10.1038/s41598-019-48407-7

Douglas, A. E. (2008). Conflict, cheats and the persistence of symbioses. *New Phytol.* 177, 849–858. doi: 10.1111/j.1469-8137.2007.02326.x

Dubinsky, Z., Falkowski, P. G., Porter, J. W., and Muscatine, L. (1984). Absorption and utilization of radiant energy by light- and shade-adapted colonies of the hermatypic coral *Stylophora pistillata*. *Proc. R. Soc. Lond. Ser. B Biol. Sci.* 222, 203–214. doi: 10.1098/rspb.1984.0059

Duprey, N. N., Wang, X. T., Thompson, P. D., Pleadwell, J. E., Raymundo, L. J., Kim, K., et al. (2017). Life and death of a sewage treatment plant recorded in a coral skeleton Δ15N record. *Mar. Pollut. Bull.* 120, 109–116. doi: 10.1016/j.marpolbul.2017.04.023

Eyre, B. D., Andersson, A. J., and Cyronak, T. (2014). Benthic coral reef calcium carbonate dissolution in an acidifying ocean. *Nat. Clim. Chang.* 4, 969–976. doi: 10.1038/nclimate2380

Fabricius, K. E. (2005). Effects of terrestrial runoff on the ecology of corals and coral reefs: review and synthesis. *Mar. Pollut. Bull.* 50, 125–146. doi: 10.1016/j.marpolbul.2004.11.028

Fabricius, K. E. (2011). "Factors determining the resilience of coral reefs to eutrophication: A review and conceptual model," in *Coral Reefs: An Ecosystem in Transition*. eds. Z. Dubinsky and N. Stambler (Netherlands: Springer), 493–505.

Fabricius, K. E., Kluibenschedl, A., Harrington, L., Noonan, S., and De'Ath, G. (2015). *In situ* changes of tropical crustose coralline algae along carbon dioxide gradients. *Sci. Rep.* 5, 1–7. doi: 10.1038/srep09537

Falkowski, P. G., and Kolber, Z. (1995). Variations in chlorophyll fluorescence yields in phytoplankton in the world oceans. *Aust. J. Plant Physiol.* 22, 341–355. doi: 10.1071/PP9950341

Fernandes de Barros Marangoni, L., Ferrier-Pagès, C., Rottier, C., Bianchini, A., and Grover, R. (2020). Unravelling the different causes of nitrate and ammonium effects on coral bleaching. *Sci. Rep.* 10:11975. doi: 10.1038/s41598-020-68916-0

Ferrier-Pagès, C., Gevaert, F., Reynaud, S., Beraud, E., Menu, D., Janquin, M.-A., et al. (2013). *In situ* assessment of the daily primary production of the temperate symbiotic coral *Cladocora caespitosa*. *Limnol. Oceanogr.* 58, 1409–1418. doi: 10.4319/lo.2013.58.4.1409

Finelli, C. M., Helmuth, B. S. T., Pentcheff, N. D., and Wethey, D. S. (2006). Water flow influences oxygen transport and photosynthetic efficiency in corals. *Coral Reefs* 25, 47–57. doi: 10.1007/s00338-005-0055-8

Finelli, C. M., Helmuth, B. S. T., Pentcheff, N. D., and Wethey, D. S. (2007). Intracolony variability in photosynthesis by corals is affected by water flow: role of oxygen flux. *Mar. Ecol. Prog. Ser.* 349, 103–110. doi: 10.3354/meps07101

Frade, P. R., Englebert, N., Faria, J., Visser, P. M., and Bak, R. P. M. (2008). Distribution and photobiology of *Symbiodinium* types in different light environments for three colour morphs of the coral *Madracis pharensis*: is there more to it than total irradiance? *Coral Reefs* 27, 913–925. doi: 10.1007/s00338-008-0406-3

Franklin, D., Hoegh-Guldberg, O., Jones, R., and Berges, J. (2004). Cell death and degeneration in the symbiotic dinoflagellates of the coral *Stylophora pistillata* during bleaching. *Mar. Ecol. Prog. Ser.* 272, 117–130. doi: 10.3354/meps272117

Galloway, J. N., Dentener, F. J., Capone, D. G., Boyer, E. W., Howarth, R. W., Seitzinger, S. P., et al. (2004). Nitrogen cycles: past, present, and future. *Biogeochemistry* 70, 153–226. doi: 10.1007/s10533-004-0370-0

Gardella, D. J., and Edmunds, P. J. (1999). The oxygen microenvironment adjacent to the tissue of the scleractinian Dichocoenia stokesii and its effects on symbiont metabolism. *Mar. Biol.* 135, 289–295. doi: 10.1007/s002270050626

Gattuso, J.-P., Yellowlees, D., and Lesser, M. (1993). Depth-and light-dependent variation of carbon partitioning and utilization in the zooxanthellate scleractinian coral *Stylophora pistillata*. *Mar. Ecol. Prog. Ser.* 92, 267–276. doi: 10.3354/meps092267

Gevaert, F., Delebecq, G., Menu, D., and Brutier, L. (2011). A fully automated system for measurements of photosynthetic oxygen exchange under immersed conditions: an example of its use in *Laminaria digitata* (Heterokontophyta: Phaeophyceae). *Limnol. Oceanogr. Methods* 9, 361–379. doi: 10.4319/lom.2011.9.361

Gorbunov, M. Y., Falkowski, P. G., and Kolber, Z. S. (2000). Measurement of photosynthetic parameters in benthic organisms *in situ* using a SCUBA-based fast repetition rate fluorometer. *Limnol. Oceanogr.* 45, 242–245. doi: 10.4319/lo.2000.45.1.0242

Goulletquer, P., Gros, P., Boeuf, G., and Weber, J. (2014). "Status and trends," in *Biodiversity in the Marine Environment*. Netherlands: Springer, 21–84.

Gruber, N. (2011). Warming up, turning sour, losing breath: ocean biogeochemistry under global change. *Philos. Trans. R. Soc. A Math. Phys. Eng. Sci.* 369, 1980–1996. doi: 10.1098/rsta.2011.0003

Haas, A. F., Nelson, C. E., Rohwer, F., Wegley-Kelly, L., Quistad, S. D., Carlson, C. A., et al. (2013). Influence of coral and algal exudates on microbially mediated reef metabolism. *PeerJ* 2013:e108. doi: 10.7717/peerj.108

Hannah, L. (2016). "Impacts of anthropogenic CO_2 and climate change on the biology of terrestrial and marine systems," in *Wildlife Toxicology: Emerging Contaminant and Biodiversity Issues*. eds. R. J. Kendall, T. E. Lacher, G. C. Cobb, S. B. Cox and T. E. Lacher (Boca Raton, Florida: CRC Press), 165–190.

Heery, E. C., Hoeksema, B. W., Browne, N. K., Reimer, J. D., Ang, P. O., Huang, D., et al. (2018). Urban coral reefs: degradation and resilience of

hard coral assemblages in coastal cities of east and Southeast Asia. *Mar. Pollut. Bull.* 135, 654–681. doi: 10.1016/j.marpolbul.2018.07.041

Hill, R., Brown, C. M., DeZeeuw, K., Campbell, D. A., and Ralph, P. J. (2011). Increased rate of D1 repair in coral symbionts during bleaching is insufficient to counter accelerated photo-inactivation. *Limnol. Oceanogr.* 56, 139–146. doi: 10.4319/lo.2011.56.1.0139

Hoegh-Guldberg, O. (2014). Coral reefs in the anthropocene: persistence or the end of the line? *Geol. Soc. Spec. Publ.* 395, 167–183. doi: 10.1144/SP395.17

Hoegh-Guldberg, O., Mumby, P. J., Hooten, A. J., Steneck, R. S., Greenfield, P., Gomez, E., et al. (2007). Coral reefs under rapid climate change and ocean acidification. *Science* 318, 1737–1742. doi: 10.1126/science.1152509

Hoogenboom, M. O., Campbell, D. A., Beraud, E., DeZeeuw, K., and Ferrier-Pagès, C. (2012). Effects of light, food availability and temperature stress on the function of photosystem II and photosystem I of coral symbionts. *PLoS One* 7:e30167. doi: 10.1371/journal.pone.0030167

Hughes, T. P., Anderson, K. D., Connolly, S. R., Heron, S. F., Kerry, J. T., Lough, J. M., et al. (2018). Spatial and temporal patterns of mass bleaching of corals in the Anthropocene. *Science* 359, 80–83. doi: 10.1126/science.aan8048

Hughes, T. P., Barnes, M. L., Bellwood, D. R., Cinner, J. E., Cumming, G. S., Jackson, J. B. C., et al. (2017a). Coral reefs in the Anthropocene. *Nature* 546, 82–90. doi: 10.1038/nature22901

Hughes, T. P., Bellwood, D. R., Baird, A. H., Brodie, J., Bruno, J. F., and Pandolfi, J. M. (2011). Shifting base-lines, declining coral cover, and the erosion of reef resilience: comment on Sweatman et al. (2011). *Coral Reefs* 30, 653–660. doi: 10.1007/s00338-011-0787-6

Hughes, T. P., Kerry, J. T., Álvarez-Noriega, M., Álvarez-Romero, J. G., Anderson, K. D., Baird, A. H., et al. (2017b). Global warming and recurrent mass bleaching of corals. *Nature* 543, 373–377. doi: 10.1038/nature21707

Hughes, T. P., Kerry, J. T., Baird, A. H., Connolly, S. R., Chase, T. J., Dietzel, A., et al. (2019). Global warming impairs stock–recruitment dynamics of corals. *Nature* 568, 387–390. doi: 10.1038/s41586-019-1081-y

Hume, B. C. C., Voolstra, C. R., Arif, C., D'Angelo, C., Burt, J. A., Eyal, G., et al. (2016). Ancestral genetic diversity associated with the rapid spread of stress-tolerant coral symbionts in response to holocene climate change. *Proc. Natl. Acad. Sci. U. S. A.* 113, 4416–4421. doi: 10.1073/pnas.1601910113

Jones, A., Berkelmans, R., van Oppen, M. J., Mieog, J., and Sinclair, W. (2008). A community change in the algal endosymbionts of a scleractinian coral following a natural bleaching event: field evidence of acclimatization. *Proc. R. Soc. B Biol. Sci.* 275, 1359–1365. doi: 10.1098/rspb.2008.0069

Jones, R., Giofre, N., Luter, H. M., Neoh, T. L., Fisher, R., and Duckworth, A. (2020). Responses of corals to chronic turbidity. *Sci. Rep.* 10:4762. doi: 10.1038/s41598-020-61712-w

Kenkel, C. D., Traylor, M. R., Wiedenmann, J., Salih, A., and Matz, M. V. (2011). Fluorescence of coral larvae predicts their settlement response to crustose coralline algae and reflects stress. *Proc. R. Soc. B Biol. Sci.* 278, 2691–2697. doi: 10.1098/rspb.2010.2344

Kerrison, P., Hall-Spencer, J. M., Suggett, D. J., Hepburn, L. J., and Steinke, M. (2011). Assessment of pH variability at a coastal CO_2 vent for ocean acidification studies. *Estuar. Coast. Shelf Sci.* 94, 129–137. doi: 10.1016/j.ecss.2011.05.025

Kline, D. I., Teneva, L., Schneider, K., Miard, T., Chai, A., Marker, M., et al. (2012). A short-term *in situ* CO_2 enrichment experiment on Heron Island (GBR). *Sci. Rep.* 2, 1–9. doi: 10.1038/srep00413

Knowlton, N., Brainard, R. E., Fisher, R., Moews, M., Plaisance, L., and Caley, M. J. (2010). "Coral reef biodiversity," in *Life in the World's Oceans*. ed. A. D. McIntyre (Oxford, UK: Wiley-Blackwell), 65–78.

Kromkamp, J. C., and Forster, R. M. (2003). The use of variable fluorescence measurements in aquatic ecosystems: differences between multiple and single turnover measuring protocols and suggested terminology. *Eur. J. Phycol.* 38, 103–112. doi: 10.1080/0967026031000094094

Kuffner, I. B., Lidz, B. H., Hudson, J. H., and Anderson, J. S. (2015). A century of ocean warming on Florida keys coral reefs: historic *in situ* observations. *Estuar. Coasts* 38, 1085–1096. doi: 10.1007/s12237-014-9875-5

Kuhl, M., Cohen, Y., Dalsgaard, T., Jorgensen, B. B., and Revsbech, N. P. (1995). Microenvironment and photosynthesis of zooxanthellae in scleractinian corals studied with microsensors for 02, pH and light. *Mar. Ecol. Prog. Ser.* 117, 159–172. doi: 10.3354/meps117159

LaJeunesse, T. C., Parkinson, J. E., Gabrielson, P. W., Jeong, H. J., Reimer, J. D., Voolstra, C. R., et al. (2018). Systematic revision of Symbiodiniaceae highlights the antiquity and diversity of coral endosymbionts. *Curr. Biol.* 28, 2570.e6–2580.e6. doi: 10.1016/j.cub.2018.07.008

Lesser, M., and Gorbunov, M. (2001). Diurnal and bathymetric changes in chlorophyll fluorescence yields of reef corals measured *in situ* with a fast repetition rate fluorometer. *Mar. Ecol. Prog. Ser.* 212, 69–77. doi: 10.3354/meps212069

Lesser, M. P., Stat, M., and Gates, R. D. (2013). The endosymbiotic dinoflagellates (*Symbiodinium* sp.) of corals are parasites and mutualists. *Coral Reefs* 32, 603–611. doi: 10.1007/s00338-013-1051-z

Levy, O., Achituv, Y., Yacobi, Y. Z., Dubinsky, Z., and Stambler, N. (2006). Diel "tuning" of coral metabolism: physiological responses to light cues. *J. Exp. Biol.* 209, 273–283. doi: 10.1242/jeb.01983

Levy, O., Dubinsky, Z., and Achituv, Y. (2003). Photobehavior of stony corals: responses to light spectra and intensity. *J. Exp. Biol.* 206, 4041–4049. doi: 10.1242/jeb.00622

Levy, O., Dubinsky, Z., Schneider, K., Achituv, Y., Zakai, D., and Gorbunov, M. Y. (2004). Diurnal hysteresis in coral photosynthesis. *Mar. Ecol. Prog. Ser.* 268, 105–117. doi: 10.3354/meps268105

Lilley, R. M., Ralph, P. J., and Larkum, A. W. D. (2010). The determination of activity of the enzyme Rubisco in cell extracts of the dinoflagellate alga *Symbiodinium* sp. by manganese chemiluminescence and its response to short-term thermal stress of the alga. *Plant Cell Environ.* 33, 995–1004. doi: 10.1111/j.1365-3040.2010.02121.x

Loiola, M., Cruz, I. C. S., Lisboa, D. S., Mariano-Neto, E., Leão, Z. M. A. N., Oliveira, M. D. M., et al. (2019). Structure of marginal coral reef assemblages under different turbidity regime. *Mar. Environ. Res.* 147, 138–148. doi: 10.1016/j.marenvres.2019.03.013

Lombardi, M. R., Lesser, M. P., and Gorbunov, M. Y. (2000). Fast repetition rate (FRR) fluorometry: variability of chlorophyll a fluorescence yields in colonies of the corals, *Montastraea faveolata* (w.) and *Diploria labyrinthiformes* (h.) recovering from bleaching. *J. Exp. Mar. Biol. Ecol.* 252, 75–84. doi: 10.1016/S0022-0981(00)00238-0

Long, M. H., Berg, P., de Beer, D., and Zieman, J. C. (2013). *In situ* coral reef oxygen metabolism: an Eddy correlation study. *PLoS One* 8:e58581. doi: 10.1371/journal.pone.0058581

Mass, T., Brickner, I., Hendy, E., and Genin, A. (2011). Enduring physiological and reproductive benefits of enhanced flow for a stony coral. *Limnol. Oceanogr.* 56, 2176–2188. doi: 10.4319/lo.2011.56.6.2176

Mass, T., Genin, A., Shavit, U., Grinstein, M., and Tchernov, D. (2010). Flow enhances photosynthesis in marine benthic autotrophs by increasing the efflux of oxygen from the organism to the water. *Proc. Natl. Acad. Sci. U. S. A.* 107, 2527–2531. doi: 10.1073/pnas.0912348107

McGillis, W. R., Langdon, C., Loose, B., Yates, K. K., and Corredor, J. (2011). Productivity of a coral reef using boundary layer and enclosure methods. *Geophys. Res. Lett.* 38, 1–15. doi: 10.1029/2010GL046179

McMahon, A., Santos, I. R., Schulz, K. G., Cyronak, T., and Maher, D. T. (2018). Determining coral reef calcification and primary production using automated alkalinity, pH and pCO_2 measurements at high temporal resolution. *Estuar. Coast. Shelf Sci.* 209, 80–88. doi: 10.1016/j.ecss.2018.04.041

Meléndez, M., Salisbury, J., Gledhill, D., Langdon, C., Morell, J. M., Manzello, D., et al. (2020). Seasonal variations of carbonate chemistry at two Western Atlantic coral reefs. *J. Geophys. Res. Ocean.* 125:e2020JC016108. doi: 10.1029/2020JC016108

Muscatine, L. (1998). "The role of symbiotic algae in carbon and energy flux in reef corals," in *Ecosystems of the World*. ed. Z. Dubinsky (Amsterdam: Elsevier), 75–87.

Nakamura, T., and Nakamori, T. (2007). A geochemical model for coral reef formation. *Coral Reefs* 26, 741–755. doi: 10.1007/s00338-007-0262-6

Nakamura, T., and Nakamori, T. (2009). Estimation of photosynthesis and calcification rates at a fringing reef by accounting for diurnal variations and the zonation of coral reef communities on reef flat and slope: a case study for the Shiraho reef, Ishigaki Island, Southwest Japan. *Coral Reefs* 28, 229–250. doi: 10.1007/s00338-008-0454-8

Oh, T., Sermsripong, J., and Hicks, B. W. (2020). Using scuba for *in situ* determination of chlorophyll distributions in corals by underwater near infrared fluorescence imaging. *J. Mar. Sci. Eng.* 8:53. doi: 10.3390/jmse8010053

Okamoto, M., Nojima, S., Furushima, Y., and Nojima, H. (2005). Evaluation of coral bleaching condition *in situ* using an underwater pulse amplitude modulated fluorometer. *Fish. Sci.* 71, 847–854. doi: 10.1111/j.1444-2906.2005.01036.x

Okazaki, R. R., Swart, P. K., and Langdon, C. (2013). Stress-tolerant corals of Florida Bay are vulnerable to ocean acidification. *Coral Reefs* 32, 671–683. doi: 10.1007/s00338-013-1015-3

Page, H. N., Courtney, T. A., Collins, A., De Carlo, E. H., and Andersson, A. J. (2017). Net community metabolism and seawater carbonate chemistry scale non-intuitively with coral cover. *Front. Mar. Sci.* 4:161. doi: 10.3389/fmars.2017.00161

Pandolfi, J. M., Connolly, S. R., Marshall, D. J., and Cohen, A. L. (2011). Projecting coral reef futures under global warming and ocean acidification. *Science* 333, 418–422. doi: 10.1126/science.1204794

Patterson, M. R., Sebens, K. P., and Olson, R. R. (1991). *In situ* measurements of flow effects on primary production and dark respiration in reef corals. *Limnol. Oceanogr.* 36, 936–948. doi: 10.4319/lo.1991.36.5.0936

Peixoto, R. S., Rosado, P. M., de Leite, D. C. A., Rosado, A. S., and Bourne, D. G. (2017). Beneficial microorganisms for corals (BMC): proposed mechanisms for coral health and resilience. *Front. Microbiol.* 8:341. doi: 10.3389/fmicb.2017.00341

Piniak, G. A., and Storlazzi, C. D. (2008). Diurnal variability in turbidity and coral fluorescence on a fringing reef flat: Southern Molokai, Hawaii. *Estuar. Coast. Shelf Sci.* 77, 56–64. doi: 10.1016/j.ecss.2007.08.023

Platz, M. C., Takeshita, Y., Bartels, E., and Arias, M. E. (2020). Evaluating the potential for autonomous measurements of net community production and calcification as a tool for monitoring coral restoration. *Ecol. Eng.* 158:106042. doi: 10.1016/j.ecoleng.2020.106042

Pramneechote, P., Sinutok, S., Wongkamhaeng, K., and Chotikarn, P. (2020). An assessment of the net ecosystem metabolism and respiration of a tropical coral reef. *Appl. Ecol. Env. Res.* 18, 1863–1881. doi: 10.15666/aeer/1801_18631881

Rädecker, N., Pogoreutz, C., Gegner, H. M., Cárdenas, A., and Roth, F. (2021). Heat stress destabilizes symbiotic nutrient cycling in corals. *Proc. Natl. Acad. Sci. U. S. A.* 118:e2022653118. doi: 10.1073/pnas.2022653118

Ralph, P., Gademann, R., Larkum, A., and Schreiber, U. (1999). *In situ* underwater measurements of photosynthetic activity of coral zooxanthellae and other reef-dwelling dinoflagellate endosymbionts. *Mar. Ecol. Prog. Ser.* 180, 139–147. doi: 10.3354/meps180139

Ralph, P. J., Schreiber, U., Gademann, R., Kühl, M., and Larkum, A. W. D. (2005). Coral photobiology studied with a new imaging pulse amplitude modulated fluorometer. *J. Phycol.* 41, 335–342. doi: 10.1111/j.1529-8817.2005.04034.x

Ramesh, C. H., Koushik, S., Shunmugaraj, T., and Ramana Murthy, M. V. (2019). A rapid *in situ* fluorescence census for coral reef monitoring. *Reg. Stud. Mar. Sci.* 28:100575. doi: 10.1016/j.rsma.2019.100575

Randall, C. J., and Szmant, A. M. (2009). Elevated temperature affects development, survivorship, and settlement of the Elkhorn coral, *Acropora palmata* (Lamarck 1816). *Biol. Bull.* 217, 269–282. doi: 10.1086/BBLv217n3p269

Ray, C. G. (1988). "Ecological diversity in coastal zones and oceans," in *Biodiversity*. eds. E. O. Wilson and F. M. Peter (Washington: National Academies Press (US)).

Roberts, C. M., McClean, C. J., Veron, J. E. N., Hawkins, J. P., Allen, G. R., McAllister, D. E., et al. (2002). Marine biodiversity hotspots and conservation priorities for tropical reefs. *Science* 295, 1280–1284. doi: 10.1126/science.1067728

Roder, C., Wu, Z., Richter, C., and Zhang, J. (2013). Coral reef degradation and metabolic performance of the scleractinian coral *Porites lutea* under anthropogenic impact along the NE coast of Hainan Island, South China Sea. *Cont. Shelf Res.* 57, 123–131. doi: 10.1016/j.csr.2012.11.017

Rohwer, F., Seguritan, V., Azam, F., and Knowlton, N. (2002). Diversity and distribution of coral-associated bacteria. *Mar. Ecol. Prog. Ser.* 243, 1–10. doi: 10.3354/meps243001

Rosenberg, E., Koren, O., Reshef, L., Efrony, R., and Zilber-Rosenberg, I. (2007). The role of microorganisms in coral health, disease and evolution. *Nat. Rev. Microbiol.* 5, 355–362. doi: 10.1038/nrmicro1635

Roth, M. S., and Deheyn, D. D. (2013). Effects of cold stress and heat stress on coral fluorescence in reef-building corals. *Sci. Rep.* 3, 1–8. doi: 10.1038/srep01421

Roth, F., Rädecker, N., Carvalho, S., Duarte, C. M., Saderne, V., Anton, A., et al. (2020). High summer temperatures amplify functional differences between coral- and algae-dominated reef communities. *Ecology* 102:e03226. doi: 10.1002/ecy.3226

Roth, F., Wild, C., Carvalho, S., Rädecker, N., Voolstra, C. R., Kürten, B., et al. (2019). An *in situ* approach for measuring biogeochemical fluxes in structurally complex benthic communities. *Methods Ecol. Evol.* 10, 712–725. doi: 10.1111/2041-210X.13151

Rovelli, L., Attard, K. M., Bryant, L. D., Flögel, S., Stahl, H., Roberts, J. M., et al. (2015). Benthic O_2 uptake of two cold-water coral communities estimated with the non-invasive eddy correlation technique. *Mar. Ecol. Prog. Ser.* 525, 97–104. doi: 10.3354/meps11211

Salih, A., Larkum, A., Cox, G., Kühl, M., and Hoegh-Guldberg, O. (2000). Fluorescent pigments in corals are photoprotective. *Nature* 408, 850–853. doi: 10.1038/35048564

Sawall, Y., Teichberg, M. C., Seemann, J., Litaay, M., Jompa, J., and Richter, C. (2011). Nutritional status and metabolism of the coral Stylophora subseriata along a eutrophication gradient in Spermonde Archipelago (Indonesia). *Coral Reefs* 30, 841–853. doi: 10.1007/s00338-011-0764-0

Schneider, K., Levy, O., Dubinsky, Z., and Erez, J. (2009). *In situ* diel cycles of photosynthesis and calcification in hermatypic corals. *Limnol. Oceanogr.* 54, 1995–2002. doi: 10.4319/lo.2009.54.6.1995

Schreiber, U., Schliwa, U., and Bilger, W. (1986). Continuous recording of photochemical and non-photochemical chlorophyll fluorescence quenching with a new type of modulation fluorometer. *Photosynth. Res.* 10, 51–62. doi: 10.1007/BF00024185

Shashar, N., Cohen, Y., and Loya, Y. (1993). Extreme diel fluctuations of oxygen in diffusive boundary layers surrounding stony corals. *Biol. Bull.* 185, 455–461. doi: 10.2307/1542485

Shaw, E. C., Mcneil, B. I., Tilbrook, B., Matear, R., and Bates, M. L. (2013). Anthropogenic changes to seawater buffer capacity combined with natural reef metabolism induce extreme future coral reef CO_2 conditions. *Glob. Chang. Biol.* 19, 1632–1641. doi: 10.1111/gcb.12154

Shaw, E. C., Phinn, S. R., Tilbrook, B., and Steven, A. (2014). Comparability of slack water and lagrangian flow respirometry methods for community metabolic measurements. *PLoS One* 9:e112161. doi: 10.1371/journal.pone.0112161

Shaw, E. C., Phinn, S. R., Tilbrook, B., and Steven, A. (2015). Natural *in situ* relationships suggest coral reef calcium carbonate production will decline with ocean acidification. *Limnol. Oceanogr.* 60, 777–788. doi: 10.1002/lno.10048

Shepard, A., Dinsmore, D., Miller, S., Cooper, C., and Wicklund, R. (1996). Aquarius undersea laboratory: the next generation. Available at: archive.rubicon-foundation.org/xmlui/handle/123456789/4703 (Accessed July 14, 2020).

Silbiger, N. J., Nelson, C. E., Remple, K., Sevilla, J. K., Quinlan, Z. A., Putnam, H. M., et al. (2018). Nutrient pollution disrupts key ecosystem functions on coral reefs. *Proc. R. Soc. B Biol. Sci.* 285, 2–10. doi: 10.1098/rspb.2017.2718

Srednick, G., Bergman, J. L., Doo, S. S., Hawthorn, M., Ferree, J., Rojas, R., et al. (2020). Shallow coral reef free ocean carbon enrichment: novel *in situ* flumes to manipulate pCO_2 on shallow tropical coral reef communities. *Limnol. Oceanogr. Methods* 18, 116–128. doi: 10.1002/lom3.10349

Suggett, D. J., Kikuchi, R. K. P., Oliveira, M. D. M., Spanó, S., Carvalho, R., and Smith, D. J. (2012). Photobiology of corals from Brazil's near-shore marginal reefs of Abrolhos. *Mar. Biol.* 159, 1461–1473. doi: 10.1007/s00227-012-1925-6

Suggett, D. J., Oxborough, K., Baker, N. R., MacIntyre, H. L., Kana, T. M., and Geider, R. J. (2003). Fast repetition rate and pulse amplitude modulation chlorophyll *a* fluorescence measurements for assessment of photosynthetic electron transport in marine phytoplankton. *Eur. J. Phycol.* 38, 371–384. doi: 10.1080/09670260310001612655

Takeshita, Y., Cyronak, T., Martz, T. R., Kindeberg, T., and Andersson, A. J. (2018). Coral reef carbonate chemistry variability at different functional scales. *Front. Mar. Sci.* 5:175. doi: 10.3389/fmars.2018.00175

Takeshita, Y., McGillis, W., Briggs, E. M., Carter, A. L., Donham, E. M., Martz, T. R., et al. (2016). Assessment of net community production and calcification of a coral reef using a boundary layer approach. *J. Geophys. Res. Ocean.* 121, 5655–5671. doi: 10.1002/2016JC011886

Thompson, J. R., Rivera, H. E., Closek, C. J., and Medina, M. (2015). Microbes in the coral holobiont: partners through evolution, development, and ecological interactions. *Front. Cell. Infect. Microbiol.* 4:176. doi: 10.3389/fcimb.2014.00176

Torres, O., Kwiatkowski, L., Sutton, A. J., Dorey, N., and Orr, J. C. (2021). Characterizing mean and extreme diurnal variability of ocean CO_2 system variables across marine environments. *Geophys. Res. Lett.* 48:e2020GL090228. doi: 10.1029/2020GL090228

Treibitz, T., Neal, B. P., Kline, D. I., Beijbom, O., Roberts, P. L. D., Mitchell, B. G., et al. (2015). Wide field-of-view fluorescence imaging of coral reefs. *Sci. Rep.* 5:7694. doi: 10.1038/srep07694

Van Zanten, B. T., Van Beukering, P. J. H., and Wagtendonk, A. J. (2014). Coastal protection by coral reefs: a framework for spatial assessment and economic valuation. *Ocean Coast. Manag.* 96, 94–103. doi: 10.1016/j.ocecoaman.2014.05.001

Wangpraseurt, D., Larkum, A. W. D., Ralph, P. J., and Kühl, M. (2012a). Light gradients and optical microniches in coral tissues. *Front. Microbiol.* 3:316. doi: 10.3389/fmicb.2012.00316

Wangpraseurt, D., Polerecky, L., Larkum, A. W. D., Ralph, P. J., Nielsen, D. A., Pernice, M., et al. (2014). The *in situ* light microenvironment of corals. *Limnol. Oceanogr.* 59, 917–926. doi: 10.4319/lo.2014.59.3.0917

Wangpraseurt, D., Weber, M., Røy, H., Polerecky, L., de Beer, D., Suharsono, et al. (2012b). *In situ* oxygen dynamics in coral-algal interactions. *PLoS One* 7:e31192. doi: 10.1371/journal.pone.0031192

Weber, M., De Beer, D., Lott, C., Polerecky, L., Kohls, K., Abed, R. M. M., et al. (2012). Mechanisms of damage to corals exposed to sedimentation. *Proc. Natl. Acad. Sci. U. S. A.* 109, E1558–E1567. doi: 10.1073/pnas.1100715109

Weber, M., Faerber, P., Meyer, V., Lott, C., Eickert, G., Fabricius, K. E., et al. (2007). *In situ* applications of a new diver-operated motorized microsensor profiler. *Environ. Sci. Technol.* 41, 6210–6215. doi: 10.1021/es070200b

Wijgerde, T., Silva, C. I. F., Scherders, V., Van Bleijswijk, J., and Osinga, R. (2014). Coral calcification under daily oxygen saturation and pH dynamics reveals the important role of oxygen. *Biol. Open* 3, 489–493. doi: 10.1242/bio.20147922

Wild, C., Rasheed, M., Jantzen, C., Cook, P., Struck, U., Huettel, M., et al. (2005). Benthic metabolism and degradation of natural particulate organic matter in carbonate and silicate reef sands of the northern Red Sea. *Mar. Ecol. Prog. Ser.* 298, 69–78. doi: 10.3354/meps298069

Williams, D. E., Miller, M. W., Bright, A. J., Pausch, R. E., and Valdivia, A. (2017). Thermal stress exposure, bleaching response, and mortality in the threatened coral *Acropora palmata*. *Mar. Pollut. Bull.* 124, 189–197. doi: 10.1016/j.marpolbul.2017.07.001

Winters, G., Loya, Y., Röttgers, R., and Beer, S. (2003). Photoinhibition in shallow-water colonies of the coral *Stylophora pistillata* as measured *in situ*. *Limnol. Oceanogr.* 48, 1388–1393. doi: 10.4319/lo.2003.48.4.1388

Yates, K. K., and Halley, R. B. (2003). Measuring coral reef community metabolism using new benthic chamber technology. *Coral Reefs* 22, 247–255. doi: 10.1007/s00338-003-0314-5

Yonge, S. C. M., Nicholls, A. G., and Yonge, M. J. (1932). The relationship between respiration in corals and the production of oxygen by their zooxanthellae. *Sci. Reports/Gt. Barrier Reef Exped.* 1, 213–251.

Zeebe, R. E., and Wolf-Gladrow, D. (2001). *CO2 in Seawater: Equilibrium, Kinetics, Isotopes. Vol. 65*. Amsterdam, Netherlands: Elsevier Oceanography, 360.

Conflict of Interest: The authors declare that the research was conducted in the absence of any commercial or financial relationships that could be construed as a potential conflict of interest.

frontiers in Physiology

ORIGINAL RESEARCH
published: 21 June 2021
doi: 10.3389/fphys.2021.695083

The Endosymbiotic Coral Algae Symbiodiniaceae Are Sensitive to a Sensory Pollutant: Artificial Light at Night, ALAN

Inbal Ayalon[1,2,3], Jennifer I. C. Benichou[1], Dror Avisar[3] and Oren Levy[1,2]**

[1] *Mina and Everard Goodman Faculty of Life Sciences, Bar-Ilan University, Ramat Gan, Israel,* [2] *Israel The H. Steinitz Marine Biology Laboratory, The Interuniversity Institute for Marine Sciences of Eilat, Eilat, Israel,* [3] *Faculty of Exact Sciences, Porter School of the Environment and Earth Sciences, Tel Aviv University, Tel Aviv, Israel*

Artificial Light at Night, ALAN, is a major emerging issue in biodiversity conservation, which can negatively impact both terrestrial and marine environments. Therefore, it should be taken into serious consideration in strategic planning for urban development. While the lion's share of research has dealt with terrestrial organisms, only a handful of studies have focused on the marine milieu. To determine if ALAN impacts the coral reef symbiotic algae, that are fundamental for sustainable coral reefs, we conducted a short experiment over a period of one-month by illuminating isolated Symbiodiniaceae cell cultures from the genera *Cladocopium* (formerly Clade C) and *Durusdinium* (formerly Clade D) with LED light. Cell cultures were exposed nightly to ALAN levels of 0.15 μmol quanta m^{-2} s^{-1} (~4–5 lux) with three light spectra: blue, yellow and white. Our findings showed that even in very low levels of light at night, the photo-physiology of the algae's Electron Transport Rate (ETR), Non-Photochemical Quenching, (NPQ), total chlorophyll, and meiotic index presented significantly lower values under ALAN, primarily, but not exclusively, in *Cladocopium* cell cultures. The findings also showed that diverse Symbiodiniaceae types have different photo-physiology and photosynthesis performances under ALAN. We believe that our results sound an alarm for the probable detrimental effects of an increasing sensory pollutant, ALAN, on the eco-physiology of symbiotic corals. The results of this study point to the potential effects of ALAN on other organisms in marine ecosystem such as fish, zooplankton, and phytoplankton in which their biorhythms is entrained by natural light and dark cycles.

Keywords: coral, light pollution, photosynthesis, Symbiodiniaceae, ALAN, light pollution

OPEN ACCESS

Edited by:
Davide Seveso, University of Milano-Bicocca, Italy

Reviewed by:
Carolina Arruda Freire, Federal University of Paraná, Brazil
Ming Li, Ningbo University, China

****Correspondence:***
Inbal Ayalon
inbalaya@gmail.com
Oren Levy
Oren.levy@biu.ac.il

Specialty section:
This article was submitted to Aquatic Physiology, a section of the journal Frontiers in Physiology

Received: *14 April 2021*
Accepted: *24 May 2021*
Published: *21 June 2021*

Citation:
Ayalon I, Benichou JIC, Avisar D and Levy O (2021) The Endosymbiotic Coral Algae Symbiodiniaceae Are Sensitive to a Sensory Pollutant: Artificial Light at Night, ALAN. Front. Physiol. 12:695083. doi: 10.3389/fphys.2021.695083

INTRODUCTION

The ever-increasing amount of nighttime light, known as Artificial Light at Night (ALAN), is an inherent consequence of population growth along ocean coastlines, and a major emerging sensory pollutant concern for coral reef ecosystems (Becker et al., 2013; Tamir et al., 2017; Ayalon et al., 2019, 2021). This is in addition to the other insults that these complex populations have been exposed to over the last few decades, either due to human actions (overfishing, chemical pollution), or natural stressors (storms, diseases, sedimentation, heatwaves), Baker et al. (2008),

Dubinsky and Stambler (2010), Caroselli et al. (2017), Tamir et al. (2017), Hughes et al. (2018), Ayalon et al. (2019, 2021). The three-dimensional habitats that comprise a coral reef are among the most diverse marine ecosystems on earth, supporting thousands of organisms that live in close association and dependency. It is possible that sensory pollution could affect this ecosystem by altering neural processing, behavioral patterns, and endocrine signaling (Cucurachi, 2014; Halfwerk and Slabbekoorn, 2015). For example, ALAN could disrupt ecological behavior such as feeding time, active time (Bolton et al., 2017), reproduction, and communication by masking the natural light of the moon and stars and increasing the apparent periodicity of daily light hours (Bourgeois et al., 2009; Kaniewska et al., 2015; Swaddle et al., 2015). The natural day-night cycle is a crucial factor for many processes in the marine ecosystem, including metabolism, photosynthesis, night recovery, and hormone secretion, among other physiological and metabolic responses.

Broadcast spawning, the main mode of coral reproduction, depends on very precise timing of gamete release into the water column to be successful (Shlesinger and Loya, 1985). This is achieved by synchronization of the corals with the lunar cycle (Babcock et al., 1986; Kaniewska et al., 2015; Ayalon et al., 2021). Corals possess an array of sensitive photoreceptors, including GPCRs rhodopsins and cryptochromes, which operate in the blue region of the light spectrum (Gorbunov and Falkowski, 2002; Levy et al., 2007), and are synchronized with the moon phase. However, exogenous environmental factors, such as water temperature, low tides, or time after sunset, can also cue spawning timing (Harriott, 1983; Hunter, 1988; Wyers et al., 1991; Guest et al., 2002).

The relationship with the intracellular symbiont dinoflagellates (family Symbiodiniaceae) (LaJeunesse et al., 2018) is essential for corals to thrive in low-nutrient tropical oceans and, consequently, for the entire coral reef system. As their contribution to this symbiotic relationship, the endosymbionts provide most of the coral host's metabolic energy requirements, enhancing calcification rates and coral growth (Muscatine and Porter, 1977). The role of symbiont diversity is key to coral survival under conditions that cause environmental bleaching or other stressors. Corals typically associate with Symbiodiniaceae from the genera *Symbiodinium* (formerly Clade A), *Breviolum* (formerly Clade B), *Cladocopium* (formerly Clade C), and *Durusdinium* (formerly Clade D), LaJeunesse et al. (2018), with each association being suitable for different environmental conditions such as irradiation, temperature, depth, and geographic location (Trench, 1993; Baker and Rowan, 1997; Rowan, 2004; Stat et al., 2008). The most common genera in symbiosis with corals are *Cladocopium* and *Symbiodinium*, while the association with *Durusdinium* is less common. Members of the latter genera display higher tolerance to thermal stress (Douglas, 1998; Hoegh-Guldberg, 1999).

The symbioses between corals and their endosymbiotic algae are strongly influenced by the surrounding environment (Douglas, 1998; Frade et al., 2008), and global or local multimodal pollutant stressors (Baker et al., 2008; Hughes et al., 2017) can impair the symbiotic relationship. The exponential rise in the anthropogenic stress of ALAN (Gaston et al., 2013; Davies et al., 2014; Tamir et al., 2017) resulting from population growth and the use of new electricity technology (Nicholls, 1995; Gaston et al., 2013; Davies et al., 2014) has prompted much research in this area in recent years (Davies et al., 2013; Tamir et al., 2017). We have previously described a strong impact of light at night on coral physiology, and the gametogenesis cycle and reproduction phylogeny (see Ayalon et al., 2019, 2021). Here we have extended these results by exploring the physiological and photosynthetic implications of light pollution by exposing two *Symbiodiniacea* cultures (*Cladocopium* and *Durusdinium*) to LED lights "cold white" (440–700 nm, 6,000–6,500 K) spectrum, and also to specific narrow light spectra (blue and yellow) that "mimic" the light spectrum and levels measured on shores close to coral reefs, in the Gulf of Eilat/Aqaba, which is an arm of the Red Sea (see Tamir et al., 2017). Our results clearly demonstrate that ALAN can influence *Symbiodiniacea* cultures, and that there are physiological differences in the responses of the two *Symbiodiniacea* alga types to light pollution.

MATERIALS AND METHODS

Experimental Setup

Symbiodiniacea cell cultures of *Cladocopium* (CCMP 2466) and *Durusdinium* (CCMP 2556) in stationary growth stage were used in this study. All cell cultures were grown in 2 L Fernbach flasks containing 1 L half-strength medium (f/2) without silica. Illumination was provided by lateral white LED bulbs (440–700 nm, 6,000–6,500 K) under a 12L:12D cycle. Irradiance was measured by a quantum spherical sensor (LI-COR, Lincoln, NE, United States) and was 100 μmol quanta m^{-2} s^{-1} (4,400 lux). The cell cultures were maintained at 25°C in a culture room with controlled temperature during experiments. After 3 weeks of growth, the cell cultures were subdivided (100 ml/flask) and triplicates of flasks with each algae type were allocated to one of three experimental light groups, with an extra group acting as control. The cultures were treated with one of three colors of LED lights as previously published by our group (Ayalon et al., 2019, 2021): blue (420–480 nm, 10,000 K); yellow (580–620 nm, 2,000 K); or white (440–700 nm, 6,000–6,500 K), with an intensity of 0.15 μmol quanta m^{-2} s^{-1} (∼4–5 lux). An Ocean optics JAZ spectrometer was used to make the spectral measurements. Cell cultures were illuminated every night from 19:00 until 7:00 in the morning using a photocell, and during the daytime, all groups were illuminated with a white LED lamp as described above (440–700 nm, 6,000–6,500 K). The control group did not experience any light pollution at night, as a black curtain was used between treatments to avoid light contamination between the experimental groups. The cell cultures were sampled after one-month of exposure to light pollution for physiological and fluorescence assessments.

Algae Density and Mitotic Index

The density of algae was measured on a 100-μl sample from each experimental treatment by counting cells on a Marienfeld hemacytometer. Cells were counted in five fields: all the corner squares plus the middle from each field, using a light

microscope (Nikon Eclipse TE 2000-E; Nikon) under ×100 magnification. The average of the counts in each field was multiplied by 10,000 to give the numbers of cells/ml (each field is 0.1 cm × 0.1 cm × 0.01 cm depth). The same squares were counted to evaluate the Mitotic Index (MI), which is the ratio between the numbers of cells undergoing mitosis and the total number of cells.

Algae Chlorophyll Measurements

In order to extract the chlorophyll from the symbiotic cells, 1 ml of each sample was centrifuged for 5 min at 2,000 *g* at 4°C. The pellet was then rinsed with 90% acetone and stored for 24 h at 4°C in the dark. The optical density (OD) at 630, 663, 750 nm was measured against a blank of 90% acetone using a Multiskan Spectrum Plate reader (Multiskan Spectrum; Thermo Scientific). The total concentration of chlorophyll (pg chlorophyll per cell) was calculated as described previously (Jeffrey and Humphrey, 1975).

Fluorescence Measurements

Photosynthetic efficiency was measured in triplicates of experimental cell cultures using the IMAGING-PAM fluorescence (Pulse Amplitude modulation, Maxi-PAM, Walz Gmbh). The results were analyzed with the Imaging Win software program (v2.00; Walz Gmbh). In order to estimate photosynthetic performances, fluorescence yield, rapid light curve (RLC), electron transfer rate (ETR), and non-photochemical quenching (NPQ) were calculated after increasing the illumination at 20 sec intervals (0, 10, 35, 55, 110, 185, 230, 280, and 335; μmol quanta m^{-2} s^{-1}). All samples were dark adapted for 40 min before measurements started.

Statistical Analysis

Effects of light treatments on the number of symbionts, the mitotic index, and the total amount of chlorophyll were evaluated using a one-way ANOVA, followed by Tukey's *post hoc* test. Homogeneity of variances and data normality were verified prior to the analysis by using Levene and Shapiro-Wilk tests, respectively. Results were expressed as mean ± standard error. Non–linear relationships between irradiance and ETR (or NPQ) under different light conditions were modeled with linear mixed-effects regressions. ETR (or NPQ) was defined as the outcome variable, and irradiance was defined as a continuous predictor. The light treatments were defined as a fixed factor, and the quantity of algae as a random effect. A third degree polynomial term for irradiance was included in the model, as well as an interaction between light treatments and irradiance, resulting in different curves for each light treatment. Several models were tested (with or without interactions, or with a lower polynomial degree) and the final models were selected based on the Akaike information criterion (AIC). Comparisons between light treatments were performed by pairwise comparisons of polynomial coefficients of the same degree. Statistical significance was assessed by testing linear contrasts and *p*-values were obtained by *Z*-tests and corrected for multiple comparisons using the FDR procedure (see **Supplementary Tables 1–4** for detailed results). Homoscedasticity and the normality of residuals were inspected visually with residual plots. Regression analyses were conducted using the R statistical environment (R Core Team, 2020). R: A language and environment for statistical computing. R Foundation for Statistical Computing, Vienna, Austria URL[1]. Linear mixed models were fitted using the LmerTest package (Kuznetsova et al., 2017). *Post hoc* analysis with linear contrasts was performed using the *glht* function from the *multcomp* package (Hothorn et al., 2008).

RESULTS

A number of parameters related to algae physiology were examined after one-month exposure to light pollution in order to evaluate the effect of ALAN on the symbiotic algae cell cultures. There was no significant effect of light conditions on the number of algae ($p > 0.05$) for either algal type, although the total number of cells per ml was higher for *Cladocopium* than *Durusdinium* cultures for all light treatments (**Figures 1A,B**). It should be noted that the starting concentrations were 1 million cells per ml for both types of algae. However, there was a significant reduction in the mitotic index of *Cladocopium* cultures after exposure to blue and yellow LED lights ($p < 0.05$) compared to the control, but no significant difference between control and exposure to white LED light ($p > 0.05$). In contrast the only significant difference in the mitotic index of *Durusdinium* cultures was between the control and the blue treatment ($p < 0.001$) with no difference observed with yellow or white light ($p > 0.05$, **Figures 1C,D**). Physiological analysis (**Figure 2**) revealed a significant reduction in total chlorophyll (pg total chl per ml) compared to the control in *Cladocopium* cultures after one-month exposure to ALAN (blue, yellow, and white LEDs, $p < 0.05$, **Figure 2A**). There were no such differences for *Durusdinium* cultures (**Figure 2B**).

The assay for maximal PSII Quantum Yield (F_v/F_m) performed after 40 min of darkness revealed significant differences between control and white treatments ($p < 0.01$) for the *Cladocopium* cells but no significant differences were induced by the other color lights (**Figure 3A**). In contrast, there were significant reductions in yield in the *Durusdinium* cell cultures after exposure to blue ($p < 0.001$), or yellow ($p < 0.05$) light, but not to white light ($p > 0.05$, see **Figure 3B**) compared to the relevant controls. As the next step, we modeled the non-linear relationship between ETR (and NPQ) and increasing irradiance levels under different light treatments with cubic polynomial linear mixed models (**Figures 3C,D** for *Cladocopium* and *Durusdinium,* respectively). The final models included interaction terms between irradiance and light treatment, resulting in a different regression model for each light treatment. For this reason, the models were compared by testing coefficients of same degree (see methods and supplementary material for results of pairwise comparisons of light treatments). The results revealed that all light treatments had a similar effect on NPQ in *Cladocopium* (the curves have a similar shape), although the distance between the curves slightly increases with rising irradiance levels, with the highest levels

[1]https://www.R-project.org/

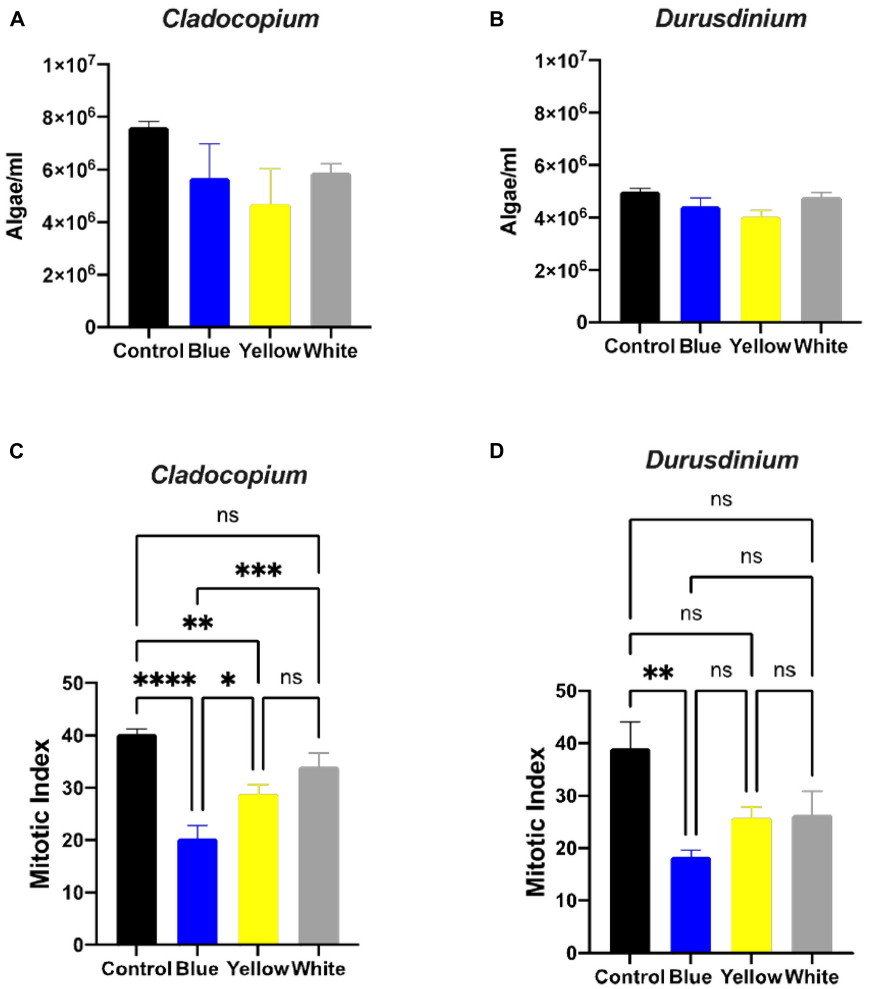

FIGURE 1 | Algae growth and mitotic index ration of the two algae cultures exposed to ALAN. No significant differences in algae density in *Cladocopium* and *Durusdinium* cell cultures **(A,B)** after one-month exposure to ALAN resulting from blue, yellow or white LEDs; irradiance level 0.15 μmol quanta m^{-2} s^{-1} (4–5 lux). Data are expressed as mean ± SEM ($n = 3$). One way-Anova ($p > 0.05$) between control and different light treatments **(A,B)**. In contrast there are significant differences in the Mitotic Index (MI) **(C,D)**, Data are expressed as mean ± SEM ($n = 3$), ANOVA was followed by *post hoc* Tukey's test, asterisks indicate significantly different mean values (*$p < 0.05$; **$p < 0.01$, ***$p < 0.001$, and ****$p < 0.0001$).

of NPQ in the control. The first-degree polynomial coefficients differed significantly between light treatments ($p < 0.0001$ for all comparisons), with the initial slope at an irradiance level of zero. In contrast, there were no differences between the control, blue, and yellow light for *Durusdinium* (most polynomial coefficients were not significantly different), while the white light treatment significantly reduced the NPQ compared to other light treatments (all polynomial coefficients were significantly different ($p < 0.01$), except for the third coefficient of the yellow light treatment). Regarding the effect of irradiance on ETR, the most significant effect of the light treatments was observed in *Cladocopium*, where the control ETR levels were significantly higher than all other light exposures (all polynomial coefficients, except the third degree, were significantly different, $p < 0.005$ for all comparisons).

All light treatments reduced ETR levels in *Durusdinium* but to a variable degree. Both blue and white light had the same effect on ETR (no significant differences between any coefficients). The control light treatment curve displays a similar shape to those of the blue and white lights, except an increased rate [first degree polynomial coefficient of the control was significantly different from those of the blue and white light ($p < 0.0001$)]. However, the yellow light treatment had a different effect; it generated a more gradual increase in ETR levels [3rd degree coefficients were significantly different between the yellow and other light treatments ($p < 0.05$ for all comparisons)].

DISCUSSION

In primary production chemical energy is converted into living biomass *via* photosynthesis, with light as the fundamental source. Since photosynthesis is usually closely linked to sunlight, the

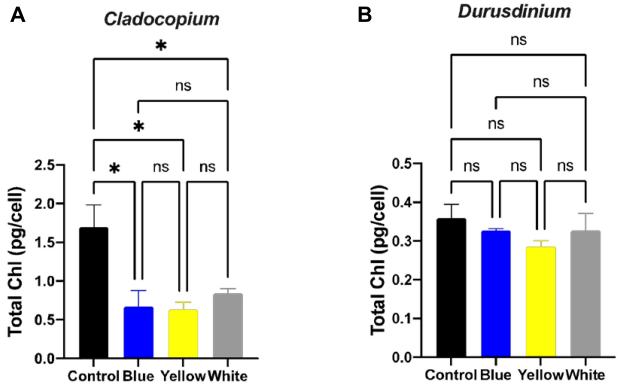

FIGURE 2 | Total chlorophyll concentrations under ALAN. *Cladocopium* **(A)** and *Durusdinium* **(B)** cell cultures (pg total chl per ml) after one-month exposure to ALAN resulting from blue, yellow or white LEDs; irradiance level 0.15 μmol quanta m^{-2} s^{-1} (4–5 lux). Data are expressed as mean ± SEM (n = 3), ANOVA was followed by *post hoc* Tukey's test, asterisks indicate significantly different mean values (*$p < 0.05$).

process is harmonically synchronized with daylight hours. While the photosynthesis machinery can theoretically function under irradiance levels slightly higher than moonlight (Raven and Cockell, 2006), and this may operate for algae adapted to long polar nights, the minimal thresholds for photosynthesis in nature have not been fully established (Grubisic, 2018). It is unclear whether light pollution can stimulate nocturnal photosynthesis, in this context, since the light typically supplied by street illumination is only 0.002% of daytime light levels (Grubisic, 2018). Light also serves as a universal cue in entraining the biological clock present in most living organisms on our planet to be harmonized with their environment. Therefore, altering the natural light regime by Artificial Light at Night, ALAN might impact the physiology of primary producers in complex and multiple ways, in addition to influencing photosynthesis.

Our results clearly show different responses of the algae cultures to light pollution which are genetically diverse. *Cladocopium* cell cultures were generally more sensitive to ALAN in comparison to *Durusdinium* cell cultures, This was observed as a significant decrease in the fluorescence yield under the white light exposer, a decrease in the mitotic index (MI) under blue and yellow light spectra, and a decrease in the total chlorophyll in all light treatments (**Figures 1C**, **2A**, **3A**). In the *Durusdinium* cell cultures there was a significant change in the MI decreasing only under the blue light spectra which was also more pronounced in the fluorescence yield values (**Figures 1D**, **3B**). Both cell cultures showed no significant difference in the total number of algae per ml, although *Durusdinium* cell cultures grow less. The difference response of the two cell cultures is also aligned with previous studies on the eco-physiology of *Cladocopium* and *Durusdinium*. Little et al. (2004) showed that *Acropora* coral juveniles grow faster when associated with *Cladocopium* compared to *Acropora* juveniles associated with *Durusdinium*. The authors related the juveniles' accelerated growth rate to a higher contribution of *Cladocopium* symbionts to the host nutrition related to faster rates of population growth inside the host (Little et al., 2004). Another observation resulted from our study was related to the performance of ETR of the two cell cultures. The control *Cladocopium* cell cultures showed higher ETR values when compared to *Durusdinium*, while both cell cultures had been affected with lower ETR values under ALAN. Nonetheless, this was far more evident and significant in *Cladocopium* cells (**Figure 3**). The decrease in photosynthetic capacities in our cell cultures is presumably due to oxidative stress as our previous research from our group examined corals exposed to ALAN showed a decrease in coral photosynthesis performances which was in line with oxidative stress (Ayalon et al., 2019; Levy et al., 2020) and even led to bleaching. The four coral species formerly tested under ALAN showed overproduction of reactive oxygen species (ROS) and an increase in oxidative damage to lipids in *Pocillopora damicornis*, *Acropora eurystoma,* and *Stylophora pistillata*, which experienced a more severe oxidative stress condition than the other species tested, *Turbinaria reniformis*. The question as to why *Durusdinium* cell cultures are less affected by ALAN may be related to lower phonesthetic capacity in the basal level as evident by the control ETR measurements, which probably lead to less ROS elevation and damage, or a more profound antioxidant scavenging system. This was shown in several types of *Symbiodiniacea* cultures. Among them, the most thermally sensitive was C*ladocopium,* which produced the highest amount of ROS at elevated temperatures, while *Durusdinium* cell cultures remain unaffected by elevated temperatures. This suggests that alternative mechanisms prevent ROS up-regulation in the first place, such as a more stable photosynthetic apparatus (McGinty et al., 2012).

Our study on *Symbiodiniacea* cultures is reported here for the first time. To the best of our knowledge, Poulin et al. (2014) was the first study to explore the effect of light pollution on diel changes in the photo-physiology of *Microcystis aeruginosa* (*freshwater cyanobacteria*). The researchers did this by mimicking the nearshore light conditions of a light−polluted area in the laboratory and investigating the effects on cyanobacteria cultures. They managed to show that nighttime irradiance levels comparable to nearshore light pollution in lakes can influence other aspects of the photo-physiology of *M. aeruginosa*. Thus, the study by Poulin et al. (2014) highlights the importance of looking specifically at the influence of artificial night lighting on phytoplankton. Their results revealed that while light with an irradiance level of six lux did not affect net photosynthesis or growth, it did influence photo−physiological parameters, such as photochemistry, functional absorption cross−section of photosystem II, and the RuBisCo number. Prolonged exposure to similar nocturnal illumination in the field was later reported by Hölker et al. (2015), who studied the influence of microbial communities in soft bottom sediments. In this case, artificial illumination changed the composition of the microbial community by increasing the numbers of primary producers, including diatoms and cyanobacteria (Hölker et al., 2015; Grubisic,

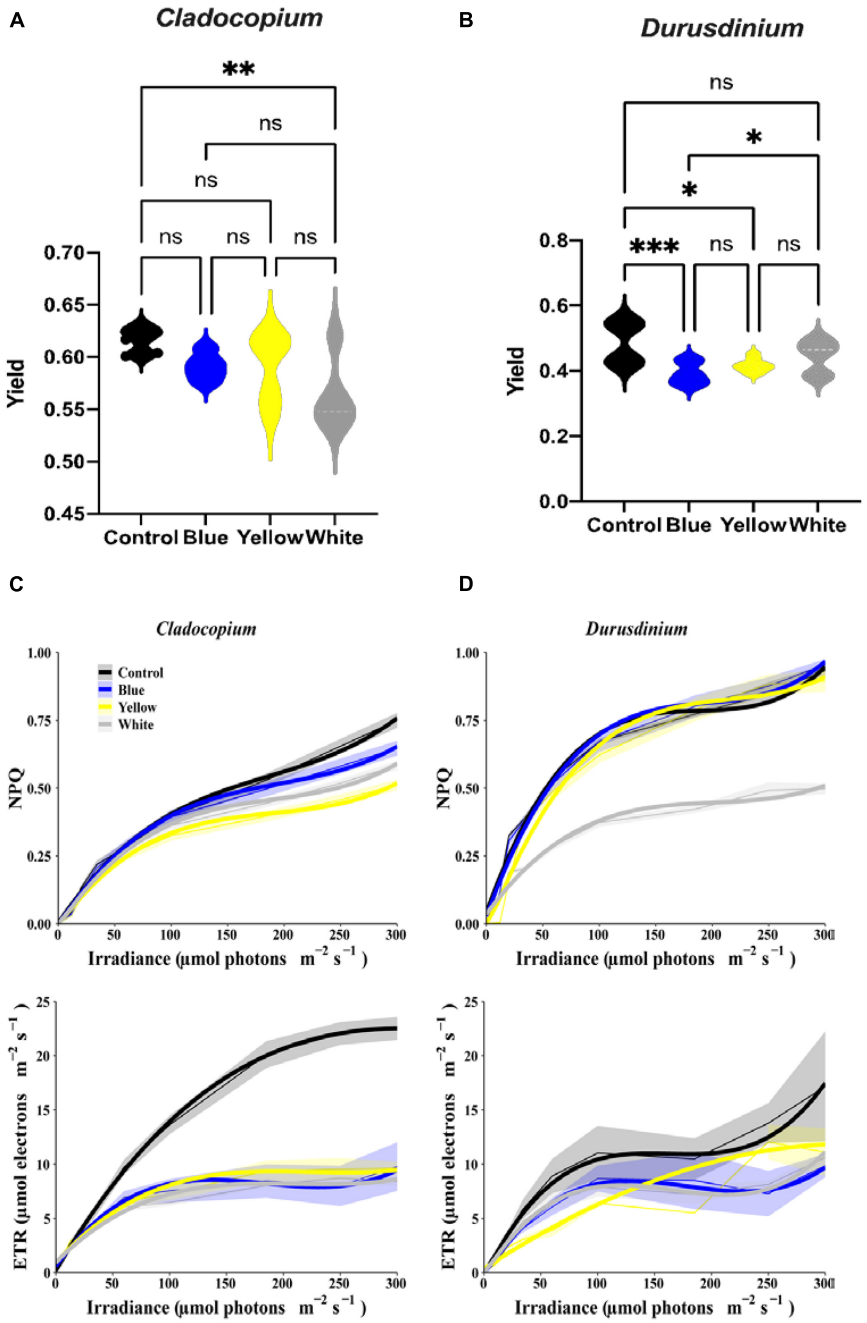

FIGURE 3 | Relationship between irradiance fluorescence measurements after one-month exposure to ALAN resulting from blue, yellow or white LEDs; irradiance level 0.15 µmol quanta m^{-2} s^{-1} (4–5 lux). Fluorescence yield **(A,B)**, presented by violin plots with $n = 12$ measurements for each light treatment. ANOVA was followed by *post hoc* Tukey's test, asterisks indicate significantly different mean values (*$p < 0.05$; **$p < 0.01$, and ***$p < 0.001$). Non-photochemical quenching NPQ (upper subplots) and ETR (lower subplots) for *Cladocopium* and *Durusdinium* **(C,D)**. Mean ETR (±SEM) for each irradiance level (left sub-plot). Thick lines represent the predicted fit obtained from 3rd degree polynomial linear mixed models. Thin lines represent mean NPQ (or ETR) ± SEM (represented by the ribbons).

2018). Their results also indicated that ALAN could stimulate nocturnal photosynthesis at higher light intensities in the lab. Another study examined the microbiome associated with the reef-building coral *Acropora digitifera*. It investigated the temporal effects of ALAN on the coral-associated microbial community, and showed that some of the microbial taxa were significantly enriched in corals subjected to ALAN (Baquiran et al., 2020).

Considering, that ALAN is a new evolving area of study in marine ecosystems, our combined results on symbiotic algae cell cultures demonstrate the potential deleterious impacts of ALAN on phytoplankton and symbiotic corals exposed to

increased light pollution, in particular blue and white light. As our worldwide-modeled light pollution atlas has shown, coral reefs in the Caribbean Sea, Red Sea, and places in the Pacific Ocean are under increasing light pollution (Ayalon et al., 2021). Therefore, we believe that ALAN can aggravate a decline in photosynthetic performance which will eventually led to deteriorated coral reefs. ALAN should now be considered as a chronic sensory pollutant which can lead to asynchronous in reproduction, decrease in growth rates and even bleaching. We hope that our results from this study can be used for urbane planning and mitigation of light pollution in coastal areas.

DATA AVAILABILITY STATEMENT

The original contributions presented in the study are included in the article/**Supplementary Material**, further inquiries can be directed to the corresponding author/s.

AUTHOR CONTRIBUTIONS

IA, OL, and DA: cell cultures growth, sampling processing, physiology analysis, photosynthesis measurements, manuscript writing, and data analyzing. JB, OL, and IA: statistical analysis. All authors contributed to the article and approved the submitted version.

FUNDING

OL acknowledges Israel Science Foundation (ISF), grant number 3928, and we further acknowledge the support from the Murray Foundation for IA.

ACKNOWLEDGMENTS

We would like to thank the staff at the Interuniversity Institute (IUI) for Marine Sciences in Eilat for their assistance, especially Moty Ohevia for helping with technical issues and Derya Akkaynak for measuring the light spectrum. We would also like to thank the Levy lab team members and Avisar team members. We also thank Hadas Marcus for her comments on the manuscript and English editing. This manuscript is in partial fulfillment of the requirements for a Ph.D. thesis for IA at Porter School of the Environment and Earth Sciences, Tel Aviv University, Israel.

SUPPLEMENTARY MATERIAL

The Supplementary Material for this article can be found online at: https://www.frontiersin.org/articles/10.3389/fphys.2021.695083/full#supplementary-material

Supplementary Table 1 | Summary of pairwise comparisons between different light treatments for each polynomial term obtained from cubic polynomial linear mixed modeling of non-linear relationship between NPQ and increasing irradiance levels, derived from **Figure 3C** for *Cladocopium*.

Supplementary Table 2 | Summary of pairwise comparisons between different light treatments for each polynomial term obtained from cubic polynomial linear mixed modeling of non-linear relationship between ETR and increasing irradiance levels, derived from **Figure 3C** for *Cladocopium*.

Supplementary Table 3 | Summary of pairwise comparisons between different light treatments for each polynomial term obtained from cubic polynomial linear mixed modeling of non-linear relationship between NPQ and increasing irradiance levels, derived from **Figure 3D** for *Durusdinium*.

Supplementary Table 4 | Summary of pairwise comparisons between different light treatments for each polynomial term obtained from cubic polynomial linear mixed modeling of non-linear relationship between ETR and increasing irradiance levels, derived from **Figure 3D** for *Durusdinium*.

REFERENCES

Ayalon, I., de Barros Marangoni, L. F., Benichou, J. I., Avisar, D., and Levy, O. (2019). Red sea corals under Artificial Light Pollution at Night (ALAN) undergo oxidative stress and photosynthetic impairment. *Global Change Biol.* 25, 4194–4207. doi: 10.1111/gcb.14795

Ayalon, I., Rosenberg, Y., Benichou, J. I., Campos, C. L. D., Sayco, S. L. G., Nada, M. A. L., et al. (2021). Coral gametogenesis collapse under artificial light pollution. *Curr. Biol.* 31, 413–419. doi: 10.1016/j.cub.2020.10.039

Babcock, R. C., Bull, G. D., Harrison, P. L., Heyward, A. J., Oliver, J. K., Wallace, C. C., et al. (1986). Synchronous spawnings of 105 scleractinian coral species on the Great Barrier Reef. *Mar. Biol.* 90, 379–394. doi: 10.1007/bf00428562

Baker, A. C., Glynn, P. W., and Riegl, B. (2008). Climate change and coral reef bleaching: An ecological assessment of long-term impacts, recovery trends and future outlook. *Estuarine Coastal Shelf Sci.* 80, 435–471. doi: 10.1016/j.ecss.2008.09.003

Baker, A. C., and Rowan, R. (1997). Diversity of symbiotic dinoflagellates (zooxanthellae) in scleractinian corals of the Caribbean and eastern Pacific. *Proc. 8th Int. Coral Reef Symp.* 2, 1301–1306.

Baquiran, J. I. P., Nada, M. A. L., Campos, C. L. D., Sayco, S. L. G., Cabaitan, P. C., Rosenberg, Y., et al. (2020). The Prokaryotic Microbiome of Acropora digitifera is stable under short-term artificial light pollution. *Microorganisms* 8:1566.

Becker, A., Whitfield, A. K., Cowley, P. D., Järnegren, J., and Næsje, T. F. (2013). Potential effects of artificial light associated with anthropogenic infrastructure on the abundance and foraging behaviour of estuary-associated fishes. *J. Appl. Ecol.* 50, 43–50. doi: 10.1111/1365-2664.12024

Bolton, D., Mayer-Pinto, M., Clark, G. F., Dafforn, K. A., Brassil, W. A., Becker, A., et al. (2017). Coastal urban lighting has ecological consequences for multiple trophic levels under the sea. *Sci. Total Environ.* 576, 1–9. doi: 10.1016/j.scitotenv.2016.10.037

Bourgeois, S., Gilot-Fromont, E., Viallefont, A., Boussamba, F., and Deem, S. L. (2009). Influence of artificial lights, logs and erosion on leatherback sea turtle hatchling orientation at Pongara National Park, Gabon. *Biol. Conserv.* 142, 85–93. doi: 10.1016/j.biocon.2008.09.028

Caroselli, E., Ricci, F., Brambilla, V., Marchini, C., Tortorelli, G., Airi, V., et al. (2017). Growth, population dynamics, and reproductive output model of the non-zooxanthellate temperate solitary coral *Caryophyllia* inornata (Scleractinia, Caryophylliidae): Coral growth, demography, and life table. *Limnol. Oceanogr.* 62, 1111–1121. doi: 10.1002/lno.10489

Cucurachi, S. (2014). *Impact assessment modelling of matter-less stressors in the context of Life Cycle Assessment*. PhD Thesis. Netherlands: Leiden University.

Davies, T. W., Bennie, J., Inger, R., de Ibarra, N. H., and Gaston, K. J. (2013). Artificial light pollution: are shifting spectral signatures changing the balance of species interactions? *Global Change Biol.* 19, 1417–1423. doi: 10.1111/gcb.12166

Davies, T. W., Duffy, J. P., Bennie, J., and Gaston, K. J. (2014). The nature, extent, and ecological implications of marine light pollution. *Front. Ecol. Environ.* 12:347–355. doi: 10.1890/130281

Douglas, A. E. (1998). Host benefit and the evolution of specialization in symbiosis. *Heredity* 81, 599–603. doi: 10.1046/j.1365-2540.1998.00455.x

Dubinsky, Z., and Stambler, N. (2010). *Coral Reefs: An Ecosystem in Transition*. Berlin: Springer Science & Business Media.

Frade, P. R., De Jongh, F., Vermeulen, F., Van Bleijswijk, J., and Bak, R. P. M. (2008). Variation in symbiont distribution between closely related coral species over large depth ranges. *Mol. Ecol.* 17, 691–703. doi: 10.1111/j.1365-294x.2007.03612.x

Gaston, K. J., Bennie, J., Davies, T. W., and Hopkins, J. (2013). The ecological impacts of nighttime light pollution: a mechanistic appraisal. *Biol. Rev.* 88, 912–927. doi: 10.1111/brv.12036

Gorbunov, M. Y., and Falkowski, P. G. (2002). Photoreceptors in the cnidarian hosts allow symbiotic corals to sense blue moonlight. *Limnol. Oceanogr.* 47, 309–315. doi: 10.4319/lo.2002.47.1.0309

Grubisic, M. (2018). Waters under artificial lights: does light pollution matter for aquatic primary producers? *Limnol. Oceanogr. Bull.* 27, 76–81. doi: 10.1002/lob.10254

Guest, J., Baird, A., Goh, B., and Chou, L. (2002). Multispecific, synchronous coral spawning in Singapore. *Coral Reefs* 21, 422–423. doi: 10.1007/s00338-002-0263-4

Halfwerk, W., and Slabbekoorn, H. (2015). Pollution going multimodal: the complex impact of the human-altered sensory environment on animal perception and performance. *Biol. Lett.* 11:20141051. doi: 10.1098/rsbl.2014.1051

Harriott, V. J. (1983). Reproductive seasonality, settlement, and post-settlement mortality of Pocillopora damicornis (Linnaeus), at lizard island, great barrier reef. *Coral Reefs* 2, 151–157. doi: 10.1007/bf00336721

Hoegh-Guldberg, O. (1999). Climate change, coral bleaching and the future of the world's coral reefs. *Mar. Freshwater Res.* 50, 839–866.

Hölker, F., Wurzbacher, C., Weißenborn, C., Monaghan, M. T., Holzhauer, S. I., and Premke, K. (2015). Microbial diversity and community respiration in freshwater sediments influenced by artificial light at night. *Philos. Trans. R. Soc.B Biol. Sci.* 370:20140130. doi: 10.1098/rstb.2014.0130

Hothorn, T., Bretz, F., and Westfall, P. (2008). Simultaneous inference in general parametric models. *Biom. J.* 50, 346–363. doi: 10.1002/bimj.200810425

Hughes, T. P., Anderson, K. D., Connolly, S. R., Heron, S. F., Kerry, J. T., Lough, J. M., et al. (2018). Spatial and temporal patterns of mass bleaching of corals in the Anthropocene. *Science* 359, 80–83. doi: 10.1126/science.aan8048

Hughes, T. P., Barnes, M. L., Bellwood, D. R., Cinner, J. E., Cumming, G. S., Jackson, J. B., et al. (2017). Coral reefs in the anthropocene. *Nature* 546, 82–90.

Hunter, C. L. (1988). Environmental cues controlling spawning in two Hawaiian corals, Montipora verrucosa and M. dilatata. *Proc. 6th Int. Coral Reef Symp.* 2, 727–732.

Jeffrey, S. W., and Humphrey, G. F. (1975). New spectrophotometric equations for determining chlorophylls a, b, c1 and c2 in higher plants, algae and natural phytoplankton. *Biochem. Und Physiol. Der Pflanzen* 167, 191–194. doi: 10.1016/s0015-3796(17)30778-3

Kaniewska, P., Alon, S., Karako-Lampert, S., Hoegh-Guldberg, O., and Levy, O. (2015). Signaling cascades and the importance of moonlight in coral broadcast mass spawning. *ELife* 4:e09991.

Kuznetsova, A., Brockhoff, P. B., and Christensen, R. H. (2017). lmerTest package: tests in linear mixed effects models. *J. Stat. Software* 82, 1–26.

LaJeunesse, T. C., Parkinson, J. E., Gabrielson, P. W., Jeong, H. J., Reimer, J. D., Voolstra, C. R., et al. (2018). Systematic Revision of symbiodiniaceae highlights the antiquity and diversity of coral endosymbionts. *Curr. Biol.* 28, 2570–2580. doi: 10.1016/j.cub.2018.07.008

Levy, O., Appelbaum, L., Leggat, W., Gothlif, Y., Hayward, D. C., Miller, D. J., et al. (2007). Light-responsive cryptochromes from a simple multicellular animal, the coral Acropora millepora. *Science* 318, 467–470. doi: 10.1126/science.1145432

Levy, O., de Barros Marangoni, L. F., Benichou, J. I., Rottier, C., Béraud, E., Grover, R., et al. (2020). Artificial light at night (ALAN) alters the physiology and biochemistry of symbiotic reef building corals. *Environ. Poll.* 266:114987. doi: 10.1016/j.envpol.2020.114987

Little, A. F., Van Oppen, M. J., and Willis, B. L. (2004). Flexibility in algal endosymbioses shapes growth in reef corals. *Science* 304, 1492–1494. doi: 10.1126/science.1095733

McGinty, E. S., Pieczonka, J., and Mydlarz, L. D. (2012). Variations in reactive oxygen release and antioxidant activity in multiple Symbiodinium types in response to elevated temperature. *Microb. Ecol.* 64, 1000–1007. doi: 10.1007/s00248-012-0085-z

Muscatine, L., and Porter, J. W. (1977). Reef corals: mutualistic symbioses adapted to nutrient-poor environments. *Bioscience* 27, 454–460. doi: 10.2307/1297526

Nicholls, R. J. (1995). Coastal megacities and climate change. *Geo. J.* 37, 369–379. doi: 10.1007/bf00814018

Poulin, C., Bruyant, F., Laprise, M.-H., Cockshutt, A. M., Marie-Rose Vandenhecke, J., and Huot, Y. (2014). The impact of light pollution on diel changes in the photophysiology of Microcystis aeruginosa. *J. Plankton Res.* 36, 286–291. doi: 10.1093/plankt/fbt088

Raven, J. A., and Cockell, C. S. (2006). Influence on photosynthesis of starlight, moonlight, planetlight, and light pollution (reflections on photosynthetically active radiation in the universe). *Astrobiology* 6, 668–675. doi: 10.1089/ast.2006.6.668

R Core Team (2020). *R: A language and environment for statistical computing*. Vienna, Austria: R Foundation for Statistical Computing.

Rowan, R. (2004). Thermal adaptation in reef coral symbionts. *Nature* 430:742. doi: 10.1038/430742a

Shlesinger, Y., and Loya, Y. (1985). Coral community reproductive patterns: red sea versus the great barrier reef. *Science* 228, 1333–1335. doi: 10.1126/science.228.4705.1333

Stat, M., Hoegh-Guldberg, O., Fitt, W. K., and Carter, D. (2008). Host symbiont acquisition strategy drives Symbiodinium diversity in the southern Great Barrier Reef. *Coral Reefs* 27, 763–772. doi: 10.1007/s00338-008-0412-5

Swaddle, J. P., Francis, C. D., Barber, J. R., Cooper, C. B., Kyba, C. C. M., Dominoni, D. M., et al. (2015). A framework to assess evolutionary responses to anthropogenic light and sound. *Trends Ecol. Evol.* 30, 550–560. doi: 10.1016/j.tree.2015.06.009

Tamir, R., Lerner, A., Haspel, C., Dubinsky, Z., and Iluz, D. (2017). The spectral and spatial distribution of light pollution in the waters of the northern gulf of aqaba (Eilat). *Sci. Rep.* 7:42329.

Trench, R. K. (1993). Microalgal-invertebrate symbiosis, a review. *Endocytobio. Cell Res.* 9, 135–175.

Wyers, S. C., Barnes, H. S., and Smith, S. R. (1991). *Spawning of hermatypic corals in Bermuda: a pilot study. In Coelenterate Biology: Recent Research on Cnidaria and Ctenophora*. Cham: Springer, 109–116.

Conflict of Interest: The authors declare that the research was conducted in the absence of any commercial or financial relationships that could be construed as a potential conflict of interest.

frontiers in Marine Science

ORIGINAL RESEARCH
published: 29 June 2021
doi: 10.3389/fmars.2021.681119

Manganese Benefits Heat-Stressed Corals at the Cellular Level

Enrico Montalbetti[1,2], Tom Biscéré[3], Christine Ferrier-Pagès[4], Fanny Houlbrèque[3], Ivan Orlandi[5], Matilde Forcella[5], Paolo Galli[1,2], Marina Vai[5] and Davide Seveso[1,2]**

[1] Department of Environmental and Earth Sciences (DISAT), University of Milano – Bicocca, Milan, Italy, [2] Marine Research and High Education Center (MaRHE Center), Magoodhoo, Maldives, [3] ENTROPIE, IRD, Université de la Réunion, CNRS, IFREMER, Université de Nouvelle-Calédonie, Nouméa, France, [4] Centre Scientifique de Monaco (CSM), Equipe Ecophysiologie Corallienne, Monaco, Monaco, [5] Department of Biotechnologies and Biosciences, University of Milano – Bicocca, Milan, Italy

The intensity and frequency of coral bleaching events have increased worldwide especially due to thermal stress and seawater pollution. Although it has been observed that metal concentration in seawater can affect the coral's ability to adopt cellular defensive mechanisms to counteract bleaching, more investigations are needed to better understand the role of metals in coral physiology. In this study, we analyzed the individual and combined effects of prolonged heat stress and manganese (Mn) and iron (Fe) enrichments at the cellular level on the coral *Stylophora pistillata*. Thermal stress caused an up-regulation in the expression of the host Heat shock proteins (Hsps) 60 and 70, which showed a parallel pattern of modulation in all treatments, as well as an increase of lipid peroxidation (LPO) in the holobiont. Fe enrichment did not induce any change in Hsp expression or in the oxidative status of the corals both at the ambient temperature of 26°C or at increased temperature, suggesting that Fe didn't seem to play a role in mitigating the cellular damages and the coral bleaching. Mn or MnFe enrichment at 26°C seemed to increase the oxidative stress in zooxanthellae, since high LPO and glutathione reductase (GR) levels were recorded, but it did not cause any effect on polyp Hsp expression, probably due to the antioxidant action of GR. With the temperature increase, Mn enrichments prevented any increase in Hsp levels and caused a significant decrease of LPO and GR activity, strengthening a previous hypothesis suggesting that Mn could mitigate the negative cellular effects produced by the thermal stress.

Keywords: metal enrichment, manganese, iron, thermal stress, *Stylophora pistillata*, coral bleaching, bleaching mitigation

OPEN ACCESS

Edited by:
Valerio Matozzo, University of Padua, Italy

Reviewed by:
Daniel Aagren Nielsen, University of Technology Sydney, Australia
Adília Pires, University of Aveiro, Portugal

****Correspondence:***
Marina Vai
marina.vai@unimib.it
Davide Seveso
davide.seveso@unimib.it

Specialty section:
This article was submitted to Aquatic Physiology, a section of the journal Frontiers in Marine Science

Received: *15 March 2021*
Accepted: *03 June 2021*
Published: *29 June 2021*

Citation:
Montalbetti E, Biscéré T, Ferrier-Pagès C, Houlbrèque F, Orlandi I, Forcella M, Galli P, Vai M and Seveso D (2021) Manganese Benefits Heat-Stressed Corals at the Cellular Level. Front. Mar. Sci. 8:681119. doi: 10.3389/fmars.2021.681119

INTRODUCTION

Over the last decades, coral bleaching events have become more frequent and severe, representing a persistent threat to reef health (Oliver et al., 2018; Eakin et al., 2019). During these events, the symbiotic relationship between corals and their photosynthetic algae is disrupted, causing hosts to lose their color and ultimately to die (Brown, 1997). Although bleaching can be caused by multiple stressors (Lesser, 2011), rising seawater temperature unequivocally represents the main bleaching-inducing factor (Hughes et al., 2017; Lough et al., 2018).

Thermal stress may elicit different types of damage within coral and symbiont cells (Hoegh-Guldberg, 1999; Weis, 2008). It may also disrupt the inter-partner molecular and cell signaling, causing the impairment of the cellular and physiological mechanisms that maintain the partnership homeostasis (Davy et al., 2012; Cleves et al., 2020; Rosset et al., 2020; Suggett and Smith, 2020; Williams et al., 2021). In this context, the production of reactive oxygen species (ROS) by heat-stressed algal chloroplasts as well as by host cells increases the oxidative stress of the coral holobiont and has been proposed to be an initiating cause of a series of events leading to symbiont loss (Downs et al., 2002; Weis, 2008; Oakley and Davy, 2018; Cziesielski et al., 2019). However, recent studies have found that ROS production by the symbiont does not seem to be the direct cause of bleaching, highlighting the need for further investigations (Nielsen et al., 2018; Rädecker et al., 2021).

In addition, local increases in the level of seawater pollutants, in particular that of metals, are another significant stress source for corals (Goh, 1991; van Dam et al., 2011; Ranjbar Jafarabadi et al., 2018; Patterson et al., 2020). Metals like iron, copper, and manganese are required at trace concentrations for many cellular processes, such as antioxidant defenses, and for the physiological functions, especially in photosynthetic organisms (Merchant, 2009; DalCorso et al., 2014; Reich et al., 2020). However, when metal concentrations reach or exceed the threshold level of tolerance, which is species and site-specific, processes such as coral growth and reproduction, larval development, photosynthetic efficiency and calcification can be compromised (Bielmyer-Fraser et al., 2010; Negri and Hoogenboom, 2011; Biscéré et al., 2015; Reichelt-Brushett and Hudspith, 2016; Gissi et al., 2017). At cellular level, exposure to metals can lead to oxidative stress and subsequent damages of both host and symbiont cells (Mitchelmore et al., 2007; Vijayavel et al., 2012; Siddiqui and Bielmyer-Fraser, 2015; Marangoni et al., 2017). In addition, metal pollution acts in synergy with thermal stress and further compromises different coral physiological pathways (Nyström et al., 2001; Shick et al., 2011; Kwok and Ang, 2013; Ferrier-Pagès et al., 2018; Reich et al., 2020). In this regard, an increased bleaching susceptibility of scleractinian corals has been observed when subjected to the combined effects of thermal stress and copper or nickel enrichment (Biscéré et al., 2017; Fonseca et al., 2017; Banc-Prandi and Fine, 2019). Also, iron enrichment has been shown to impair calcification and induce significant bleaching (Wells et al., 2011; Biscéré et al., 2018). On the contrary, manganese enrichment may alleviate the deleterious effect of heat stress on corals, by enhancing chlorophyll concentrations, photosynthetic efficiency, and gross photosynthetic rates at ambient and elevated temperature (Biscéré et al., 2018). All together, these studies suggest that the effects of metals on coral physiology are metal and concentration-dependent, and that interactions between metals also exist. Therefore, more investigations are needed to better understand the role of metals in coral physiology. In this context, since changes at cellular level are the first detectable response of an organism to an environmental perturbation (Bierkens, 2000; Kültz, 2005), the analysis of cellular stress biomarkers may represent a useful diagnostic tool, able to reflect changes in cellular integrity and pathways due to trace metals before larger scale physiological processes are affected (Downs, 2005; Seveso et al., 2017).

Heat shock proteins (Hsps) are molecular chaperones and are part of a cytoprotective mechanism able to mitigate the deleterious effects of stressors, and have consequently been frequently adopted as cellular stress biomarkers in corals (Downs et al., 2000, 2005; Chow et al., 2012; Kenkel et al., 2014; Louis et al., 2017; Seveso et al., 2018). Hsps maintain protein homeostasis by facilitating proper protein folding and translocation, deterring and/or reducing the aggregation of other proteins, and assisting in refolding or degrading stress-damaged proteins (Balchin et al., 2016). Hsp expression is usually up-regulated when organisms face conditions that may affect their cellular protein structure. Hsps are involved in the coral heat stress-induced bleaching response, while acting as a protection from ROS toxicity (Downs et al., 2002; DeSalvo et al., 2008; Seneca et al., 2010; Mayfield et al., 2011; Olsen et al., 2013; Seveso et al., 2016, 2020). However, to date very few studies have analyzed their expression in corals subjected to metal pollution (Venn et al., 2009). In addition, corals produce antioxidant enzymes in order to neutralize the harmful effects of ROS caused by metals and other stressors, and they also represent useful oxidative stress biomarkers (Lesser, 2006; Dias et al., 2019b, 2020; Marangoni et al., 2019b). Among these, superoxide dismutase (SOD) works as the first line of defense in the detoxification process, reducing the damaging potential of superoxide anion radicals ($O_2^{\bullet -}$) by catalyzing its dismutation to hydrogen peroxide (H_2O_2) (Lesser, 2006). Glutathione reductase (GR) catalyzes the NADPH-dependent reduction of glutathione disulfide (GSSG) to the sulfhydryl form glutathione (GSH), which is a critical molecule in counteracting oxidative stress and maintaining the reducing environment of the cell (Deponte, 2013). However, if ROS production is higher than the antioxidant system reductive potential, ROS may lead to cellular damage, including lipid peroxidation (LPO) (Gaschler and Stockwell, 2017).

A previous work dealing with the effect of manganese and/or iron enrichment in combination with thermal stress has shown interesting results on coral physiology, particularly with reference to the potential role of manganese in the reduction of heat stress impact, likely due to its involvement in the antioxidant system (Biscéré et al., 2018). Starting from these statements, we performed on the same coral samples an in-depth analysis of the cellular mechanisms underlying the response observed by Biscéré et al. (2018), in order to better understand the role of manganese and iron, which is poorly elucidated when compared to that of other metals (Schwarz et al., 2013; Biscéré et al., 2017; Bielmyer-Fraser et al., 2018; Zhou et al., 2018; Marangoni et al., 2019c). In particular, in this study we analyzed the individual and combined effects of prolonged heat stress and metal enrichment (Mn and Fe) at the cellular level on the coral *Stylophora pistillata*, by investigating changes in the host cellular protein homeostasis, and the holobiont oxidative status. In this regard, the expression of the cytoplasmic Hsp70 and the mitochondrial Hsp60 in the coral polyps, as well as the LPO levels and the SOD and GR enzymatic activity in the holobiont were measured. In the frame of the photophysiological

parameters determined by Biscéré et al. (2018) on the same samples, the data presented here support a possible role of Mn in mitigating the physiological impact of heat stress causing bleaching.

MATERIALS AND METHODS

Maintenance and Growth Condition of Corals

The experimental setup as well as the biological samples analyzed in this study corresponds to those reported in Biscéré et al. (2018). In particular, experiments were performed with small apexes (∼2 cm long) of the scleractinian species *S. pistillata,* obtained from several large mother colonies originally sampled in the Red Sea. Nubbins were kept in 25 l tanks for 3 weeks under controlled conditions in order to recover, as described in Biscéré et al. (2018). Briefly, tanks were supplied with seawater pumped from 40 m depth, with a 100% water turnover every 12 h. The photoperiod was generated by 400 W metal halide lamps (HPIT, Philips) at an irradiance of 200 ± 10 μmol photons m^{-2} s^{-1} switching from dark to light every 12 h. Light was controlled by a LI-COR data logger (LI-1000) connected to a spherical quantum sensor (LI-193) once a week. Temperature was set to an optimum of 26°C (±0.2°C) and was controlled along the experiment through heaters connected to the controllers (Elli-Well PC902/T). Corals were fed with nauplii of *Artemia salina* twice a week.

Experimental Design and Stress Exposure

After the recovery period, eight different experimental conditions were set up in duplicated aquaria by combining two seawater temperatures and two concentrations of Mn and Fe (Biscéré et al., 2018). Specifically, four different metal conditions were reproduced as follows: (1) Control, with Mn and Fe values of oligotrophic seawaters, respectively, 0.06 ± 0.05 μg/l Mn (Morley et al., 1997) and <0.22 μg/l Fe (Ferrier-Pagès et al., 2001); (2) Manganese enrichment (+Mn) to reach 4.1 ± 0.2 μg/l; (3) Iron enrichment (+Fe) to reach 3.0 ± 0.2 μg/l; (4) Manganese and iron enrichment (+MnFe) at the two respective concentrations indicated above. Mn and Fe enrichments were chosen based on the highest levels recorded for these metals in some fringing reefs along the coasts of New Caledonia (Moreton et al., 2009).

The metal enrichment was performed using two peristaltic pumps (ISMATEC), which continuously supplied the experimental tanks with 15 ml/h of a solution of stable Mn ($MnCl_2$, Humeau, France) or stable Fe ($FeCl_2$, Humeau, France). The divalent form was chosen for Fe and Mn, since Fe^{2+} and Mn^{2+} are considered the most soluble and bioavailable forms (Fairbrother et al., 2017). In addition, submersible pumps (Aquarium system, micro-jet MC 320, Mentor, OH, United States) were placed in each tank in order to avoid any metal concentration gradient and to ensure water circulation and oxygenation. To make sure that the metal concentrations in the tanks were the desired ones, seawater samples were collected and analyzed by sector field inductively coupled plasma-mass spectrometry (SF-ICP-MS) using a Thermo Element 2 instrument, as previously described (Biscéré et al., 2018).

Temperature was kept constant at 26°C in all tanks for the first 3 weeks of treatments, during which corals in the +Mn, +Fe, and +MnFe tanks were subject to metals enrichment as described above. After 3 weeks, temperature was gradually increased during 1 week to 32°C (1°C per day) in half of the tanks and maintained for an additional 2 week period without stopping metal enrichment (Biscéré et al., 2018). After 6 weeks from the beginning of the experiment, and thus after 3 weeks of thermal stress, five nubbins per condition were collected and immediately frozen to −80°C for further analyses.

Analysis of the Hsp Expression

Protein Extract Preparation and Western Analyses

To extract total proteins, frozen coral apexes were powdered with a pre-chilled mortar and pestle and homogenized in SDS-buffer (0.0625 M Tris–HCl, pH 6.8, 10% glycerol, 2.3% SDS, 5% 2-mercaptoethanol) containing 1 mM phenylmethylsulfonylfluoride (Sigma-Aldrich), and complete EDTA-free protease inhibitors cocktail (Roche Diagnostic). Samples were then processed following a previous method that allows removing, in addition to calcium carbonate debris, any Symbiodiniaceae contamination, obtaining extracts that contain only polyp proteins (Seveso et al., 2013, 2014). Extracts were stored at −80°C until further processing. Aliquots were used to determine total protein concentrations through Bio-Rad protein assay kit (Bio-Rad Laboratories). An equal amount of proteins for each sample was separated by SDS-PAGE on 8% polyacrylamide gels (Vai et al., 1986), then run in duplicates using a Mini-Protean Tetra Cell (Bio-Rad Laboratories). After the electrophoresis, a gel was stained with Coomassie Brilliant Blue to visualize total proteins, while the other was electroblotted onto nitrocellulose membrane (Amersham Protran 0,45 mm) for Western Blot analysis as previously described (Seveso et al., 2012). Filters were stained with Ponceau S Red (Sigma-Aldrich) to confirm correct protein transfer. The following primary antibodies were used: anti-Hsp70 monoclonal antibody (IgG2a mouse clone BB70, SPA-822, Enzo Life Sciences), anti-Hsp60 monoclonal antibody (IgGI1 mouse clone LK-2, SPA-807, Enzo Life Sciences) and anti-β-Actin monoclonal antibody (IgG1k mouse clone C4, MAB1501, Millipore). The primary antibodies were diluted 1:1,000 in TBS-0.1% Tween 20 and 5% skimmed milk, with the exception of β-Actin, diluted 1:3000. After being washed three times with fresh changes of TBS-0.1% Tween 20 (15 min each), filters were incubated with anti-mouse IgG polyclonal secondary antibodies conjugated with horseradish peroxidase (ADI-SAB-100, Enzo Life Sciences) diluted 1:1,000 for Hsp70 and 1:10,000 for Hsp60 and 1:15,000 for β–Actin in TBS-0,3% Tween 20 and 5% skimmed milk. Western blots were developed using Pierce ECL Western Blotting Substrate followed by exposition of filters to Amersham Hyperfilm ECL.

Densitometric Analysis

Densitometric analysis was performed as previously described (Seveso et al., 2013). Films were scanned on a Bio-Rad GS-800

calibrated imaging densitometer and the pixel density of the scanned bands were quantified with the ImageJ free software[1] of the NIH Image software package (National Institutes of Health, Bethesda, Md.). For each blot, the scanned intensity of the bands of each Hsp was normalized against the intensity of the β-Actin ones, which was used as an internal loading control since in all our experiments the β-Actin level did not display significant changes (**Supplementary Figure 1**). The densitometric data were expressed as relative levels (arbitrary units).

Analysis of the Antioxidant Enzymatic Activities

Protein Extraction

Coral fragments reduced into powder with pre-chilled mortar and pestle were transferred into tubes and homogenized in 750 μl lysis buffer (Tris–HCl 50 mM, pH 7.4, NaCl 150 mM, glycerol 10%, NP40 detergent 1%, EDTA 5 mM) containing 1 mM phenylmethylsulfonylfluoride (Sigma-Aldrich). After a first centrifugation step (5 min, 3,000 rpm) to remove skeletal components, cells were broken by sonication (6 × 10 s pulse on ice, amplitude 10 μm, Soniprep 150, Sanyo). Samples were then subjected to a second centrifugation step (15 min, 14,000 rpm, 4°C) and the supernatant was sampled and frozen immediately (−80°C) until subsequent assays. Total protein content of each sample was determined through the Bradford method using bovine serum albumin (BSA) as a calibration curve.

Superoxide Dismutase Activity Assay

Superoxide dismutase activity was assessed according to Vance et al. (1972). As SOD competes with ferricytochrome c for oxygen radicals, its activity was detected as the ability to inhibit the reduction of ferricytochrome c by O_2^- generated from the xanthine/xanthine oxidase system. For the reaction mix, the following reagents (purchased from Sigma-Aldrich), ferricytochrome c 0.01 mM, EDTA 0.1 mM, xanthine 0.01 mM, and xanthine oxidase 0.0061 U were used in a final volume of 1 ml. Different volumes of each sample were tested and added to the reaction mix to determine the 50% inhibition of the reaction rate. The rate of reduction of ferricytochrome c was followed spectrophotometrically at 550 nm, 25°C, through a Varian Cary 50 Scan Spectrophotometer (Agilent Technologies). Under the above conditions, one unit of SOD was defined as the amount of enzyme inhibiting the reduction of ferricytochrome c by 50%. Results are expressed as units (U) of enzyme per mg of proteins.

Glutathione Reductase Activity Assay

The enzymatic assay of GR was performed according to Wang et al. (2001). The activity of GR was evaluated through the spectrophotometric detection of the absorbance at 340 nm (Varian Cary 50 Scan spectrophotometer, Agilent Technologies) of NADPH oxidation to NADP + reaction, which occurs in conjunction with the glutathione reduction, and is proportional to the decrease in absorbance over time. In particular, NADPH reaction was initially detected in the reaction mix (containing 0.1 M potassium phosphate buffer pH 7.6, 0.16 mM NADPH, 1 mg ml^{-1} BSA, and 4.6 mM oxidized glutathione), and then adding different volumes of sample. GR activity was obtained from the difference of the two absorbance values. One unit of GR activity was defined as the oxidation of 1 nmol NADPH/min at 25°C. Results are expressed as units (U) of enzyme per mg of proteins.

Lipid Peroxidation

Lipid peroxidation levels were assessed *via* malondialdehyde (MDA) contents determined using a commercially available MDA assay kit (Bioxytech LPO-586, Oxis International, United States). The method is based on the reaction of a chromogenic reagent, *N*-methyl-2-phenylindole, with MDA at 45°C. Specifically, frozen coral apexes (approximately 1 g each) were reduced into powder with pre-chilled mortar and pestle and homogenized in 1 ml of 20 mM phosphate buffer, pH 7.4. To prevent sample oxidation, 10 μl 0.5 M butylated hydroxytoluene in acetonitrile was added to 1 ml of tissue homogenate. Following sample centrifugation (3,000 × *g* at 4°C for 10 min), an aliquot of supernatant was used for protein determination using the Bradford method. The subsequent assay procedure (hydrochloric acid solvent procedure) was performed according to the manufacturer's instructions. The blue product was quantified by measuring absorbance at 586 nm (Gérard-Monnier et al., 1998). Results are presented in μmol of MDA per μ g of proteins.

Data Analysis

Data normality was verified using the Shapiro–Wilk test and where assumptions were violated, the data were corrected by transformations. To evaluate significant differences in Hsp expression, enzymatic activity and LPO in corals subjected to metal stress at both ambient temperature (26°C) and following heat stress (32°C), separated one-way ANOVAs followed by Tukey's HSD *post hoc* tests were used. The same analysis was adopted in order to assess significant differences in the levels of each biomarker in coral colonies subjected to thermal stress within each metal treatment. All statistical analyses were performed using SPSS ver. 26 (IBM). Values were considered statistically significant at $p < 0.05$, and all data are presented as arithmetic means ± SE (n = 4, for each biomarker analyzed), unless stated otherwise.

A multivariate analysis was performed using the statistical package PRIMER-E v.7 (Clarke and Gorley, 2015) with the permutational multivariate analysis of variance (PERMANOVA) + add on (Anderson et al., 2008) to investigate together the modulation of all biomarkers in response to metal and thermal stresses. In particular, data related to the levels of all the biomarkers were normalized and square root transformed to calculate a matrix based on the Bray-Curtis similarity. To test for differences in biomarker levels among temperature and treatments and the combination of both, a non-parametric PERMANOVA was performed using 999 permutations with partial sum of squares and unrestricted permutation of raw data. Temperature and treatment were

[1] http://rsb.info.nih.gov/ij/

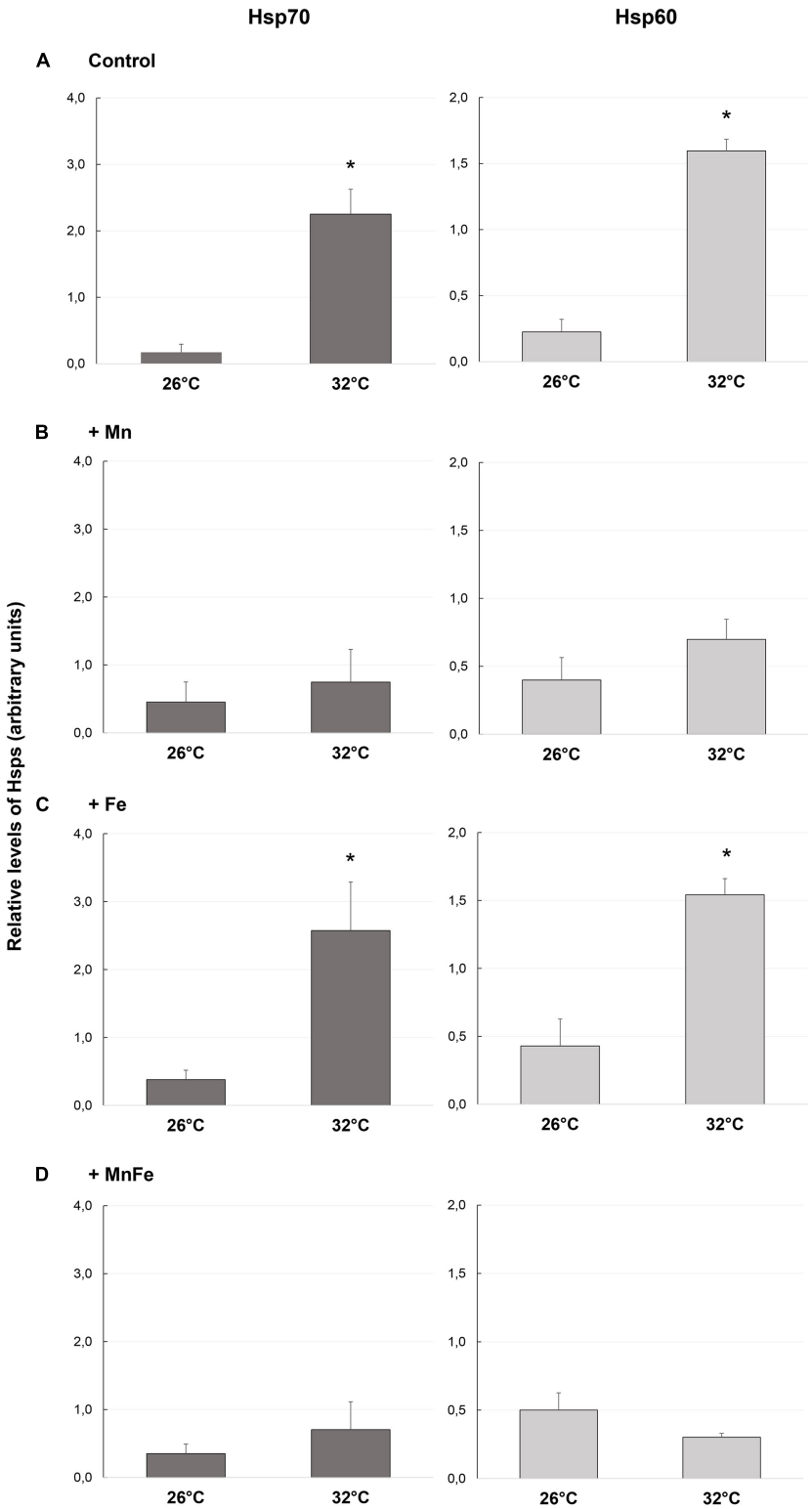

FIGURE 1 | Levels of Hsp70 and Hsp60 detected in samples of *S. pistillata* exposed to the different metal treatments (**A**: Control; **B**: +Mn; **C**: +Fe; **D**: +MnFe) after 6 weeks at 26°C or 3 weeks at 32°C. The values were determined by densitometric analysis as described under section "Materials and Methods." In the same section, the values related to the metal concentrations for each treatment are also shown. Data are expressed as arbitrary units and as mean ± SEM (n = 4, for both Hsp70 and Hsp60). For each biomarker, asterisks indicate significant differences between corals maintained at 26 and 32°C under different treatments and, within each treatment, between corals maintained at 26 and 32°C.

selected as fixed factors. Values were considered statistically significant at $p < 0.05$. Pairwise PERMANOVA tests were conducted to assess differences between treatments at 26 and 32°C and between temperatures within each metal treatment, as performed for the univariate analyses. Due to the restricted number of unique permutations in the pairwise tests, *p*-values were also obtained from Monte Carlo samplings (Anderson and Robinson, 2003). To visualize similarities among metal treatments and temperature responses, a non-metric multidimensional scaling plot (nMDS) was done using Bray-Curtis similarity.

RESULTS

Hsp Expression

The expression of Hsp70 and Hsp60 in the coral *S. pistillata* was investigated in different temperature conditions and Mn-Fe concentrations, applied alone and in combinations. Each monoclonal antibody (anti-Hsp70 and anti-Hsp60) produced in all samples a single specific band (**Supplementary Figure 1**), whose molecular weight corresponds to that expected based on the amino acid sequences (Seveso et al., 2020). Moreover, both Hsps showed common and comparable patterns of expression in each treatment, and thus responded in a similar way to single and combined stressors (**Figure 1**), further confirming that they work in tandem.

As expected, in the Control samples, starting from a low basal constitutive level, a significant up-regulation of the expression of both Hsp70 and Hsp60 was observed when the water temperature shifted from 26 to 32°C (**Figure 1A** and **Table 1**). On the contrary, no significant effect of metal addition was observed on Hsp expression at the ambient temperature of 26°C [one-way ANOVA, $F(3,12) = 0.39$, $p > 0.05$ for Hsp70; $F(3,12) = 0.59$, $p > 0.05$ for Hsp60; **Figure 1**].

At 32°C, the Hsp70 and Hsp60 levels detected in Mn and MnFe enriched samples were similar to those of corals maintained at 26°C and therefore no significant modulation of Hsps following heat stress was observed (**Figures 1B,D** and **Table 1**). In contrast, the combination of Fe enrichment and heat stress led to an expression of Hsp70 and Hsp60 similar to that observed in the Control tanks at 32°C (**Figure 1C** and **Table 1**). Consequently, significant differences in Hsp expression were observed among all conditions at 32°C [one-way ANOVA, $F(3,12) = 13.56$, $p = 0.04$ for Hsp70; $F(3,12) = 36.56$, $p = 0.001$ for Hsp60; **Figure 1**].

Antioxidant Activity

The antioxidant activity of two enzymes involved in ROS detoxification, namely SOD and GR, was assessed in the coral samples subjected to the different stressors.

No significant changes were observed in SOD antioxidant activity among different treatments both at 26°C or following the temperature shift at 32°C ($p > 0.05$; **Figure 2**).

As far as GR activity is concerned, significant differences were detected at 26°C [one-way ANOVA, $F(3,12) = 9.45$, $p = 0.005$]. In particular, a higher activity was recorded in +Mn and +MnFe treatments, compared to Control and +Fe samples (**Figure 2**). Moreover, at 32°C, GR activity significantly decreased in the treatment +Mn and +MnFe (**Figures 2B,D** and **Table 1**), while it did not change significantly in corals under Control conditions and in those subjected to Fe enrichment (**Figures 2A,C** and **Table 1**). As a result of these modulations, no significant differences were detected among all conditions at 32°C [one-way ANOVA, $F(3,12) = 0.89$, $p > 0.05$; **Figure 2**].

Lipid Peroxidation

Oxidative damage on *S. pistillata* was evaluated by analyzing the LPO levels through MDA production. Significant variations of the MDA levels were observed in corals maintained at 26°C and subjected to different metal enrichments [one-way ANOVA, $F(3,12) = 17.81$, $p = 0.001$]. Specifically, the enrichment of Mn and MnFe caused a significant increase of the MDA levels compared to Control and +Fe treatments (**Figure 3**).

However, heat stress produced a significant increase in MDA levels only in Control and in +Fe samples (**Figures 3A,C** and **Table 1**), while in coral subjected to Mn and MnFe enrichments a slight and not significant decrease of the MDA level was detected (**Figures 3B,D**). As a result, no significant differences were detected among all conditions at 32°C [one-way ANOVA, $F(3,12) = 3.26$, $p > 0.05$; **Figure 2**].

TABLE 1 | Summary of the one-way analysis of variance (ANOVA) for values of Hsp70, Hsp60, SOD, GR, and LPO in colonies maintained at 26°C vs. those subjected to thermal stress (32°C) at each metal treatment.

	26°C vs. 32°C											
	Control			**+Mn**			**+Fe**			**+MnFe**		
	MS	***F***	***P***	**MS**	***F***	***P***	**MS**	***F***	***P***	**MS**	***F***	***P***
Hsp70	6.478	27.017	**0.007**	0.130	0.262	ns	7.228	8.841	**0.040**	0.186	0.638	ns
Hsp60	3.757	111.781	**0.000**	0.180	1.820	ns	2.478	23.215	**0.003**	0.079	2.348	ns
SOD	0.100	0.001	ns	0.018	0.083	ns	0.065	1.106	Ns	0.113	0.530	ns
GR	0.100	2.278	ns	0.001	8.235	**0.040**	0.001	0.992	Ns	0.001	16.723	**0.015**
LPO	0.065	61.308	**0.001**	0.033	3.995	ns	0.116	12.745	**0.020**	0.016	5.832	ns

Significant values are in bold. Values not significant ($p \geq 0.05$) are indicated with ns.

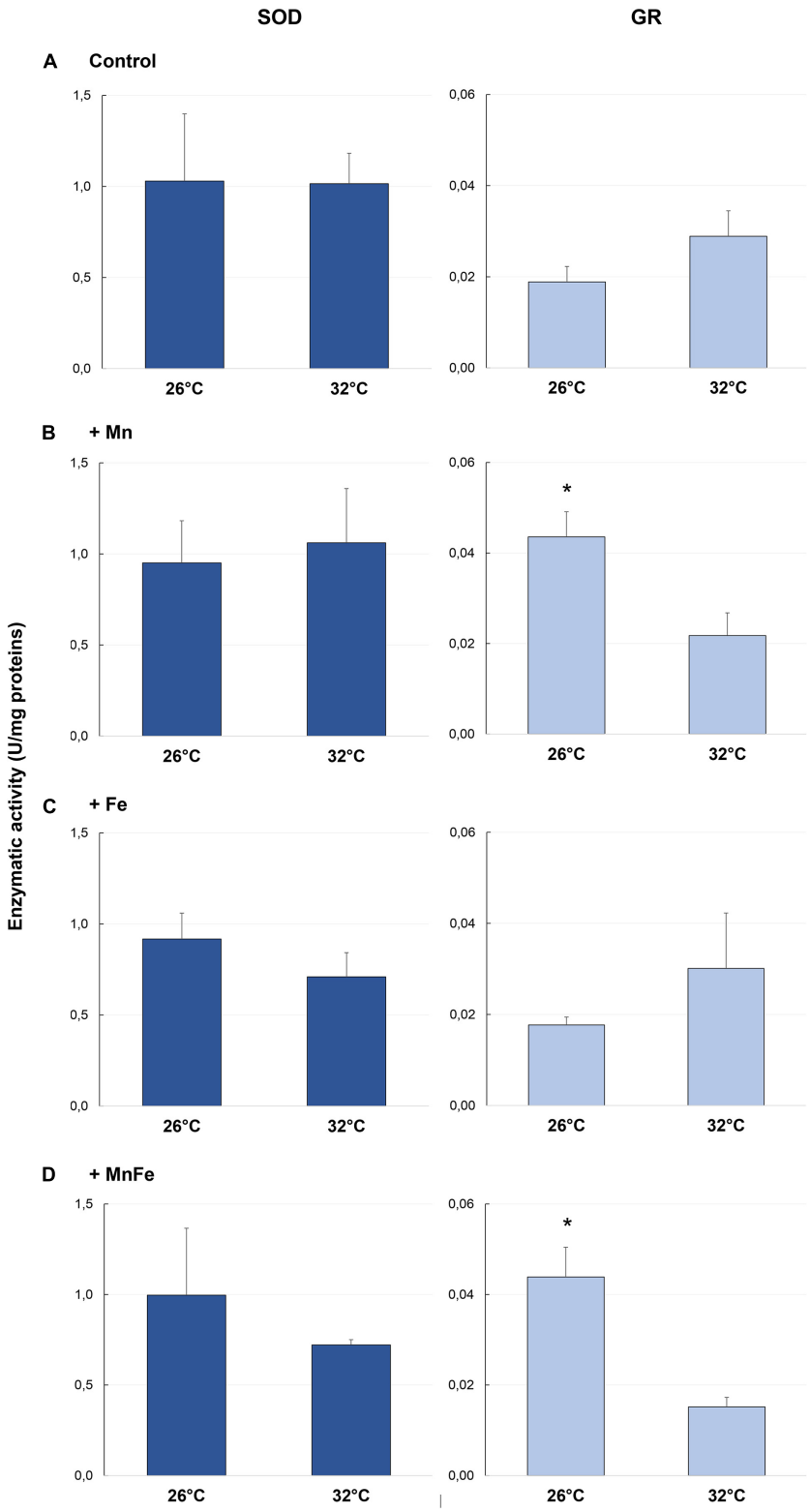

FIGURE 2 | Enzymatic activity of SOD and GR detected in samples of *S. pistillata* exposed to the different metal treatments (**A**: Control; **B**: +Mn; **C**: +Fe; **D**: +MnFe) after 6 weeks at 26°C or 3 weeks at 32°C. The values related to the metal concentrations for each treatment are reported in section "Materials and Methods." Data are expressed as units (U) of enzyme per mg of proteins and as mean ± SEM (n = 4, for both SOD and GR). For each biomarker, asterisks indicate significant differences between corals maintained at 26 and 32°C under different treatments and, within each treatment, between corals maintained at 26 and 32°C.

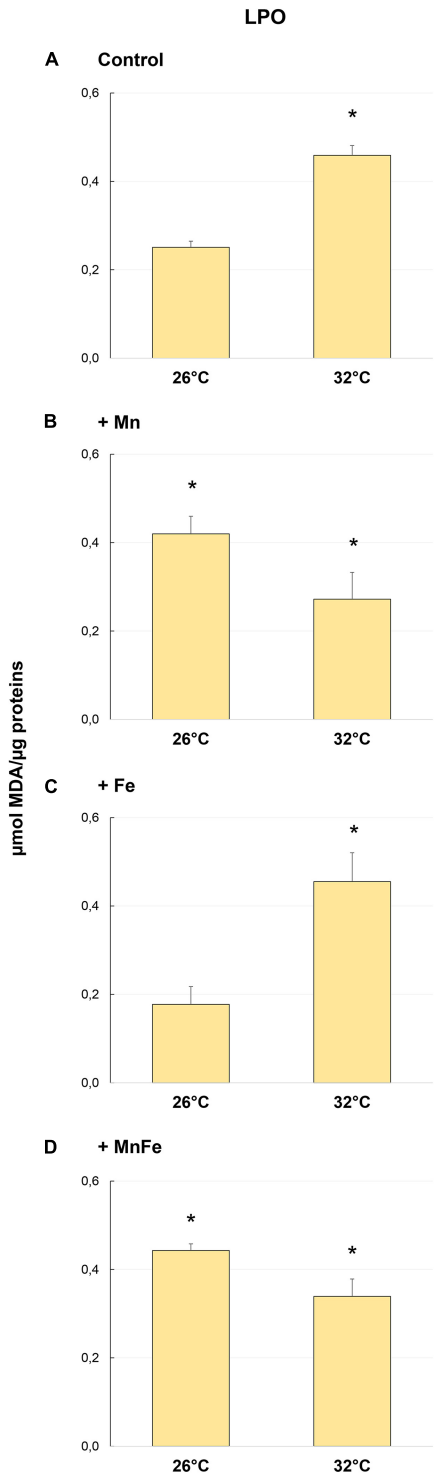

FIGURE 3 | Levels of lipid peroxidation (LPO) detected in samples of *S. pistillata* exposed to the different metal treatments (**A**: Control; **B**: +Mn; **C**: +Fe; **D**: +MnFe) after 6 weeks at 26°C or 3 weeks at 32°C. The values related to the metal concentrations for each treatment are reported in section "Materials and Methods." Data are expressed as µmol of MDA per µg of proteins and as mean ± SEM (n = 4). Asterisks indicate significant differences between corals maintained at 26 and 32°C under different treatments and, within each treatment, between corals maintained at 26 and 32°C.

Multivariate Analysis

In order to investigate together the modulation of Hsp expression, enzymatic activity and LPO in response to metal and thermal stresses, multivariate analyses were performed. The PERMANOVA revealed significant differences in biomarker levels among temperatures and treatments and the combination of both (**Table 2**). In particular, the biomarker levels in Mn and MnFe enriched corals appeared significantly different from that recorded in Control and +Fe treatments, especially when corals were subjected to temperature increase at 32°C (**Table 3**). In line with this, the nMDS analysis showed that Mn and MnFe enriched corals maintained at both ambient and increased temperatures, displayed a cellular response similar to corals kept in Control condition at 26°C, but different from that of Control and Fe enriched corals subjected to thermal stress (**Figure 4**).

DISCUSSION

The tolerance of corals to heat stress-induced bleaching can be influenced by metal concentrations in seawater. In this context, manganese and iron enrichments have previously been shown to exhibit contrasting effects on *S. pistillata* physiological parameters, such as cellular chlorophyll concentrations, photosynthetic efficiency, gross photosynthetic rates, and calcification (Biscéré et al., 2018). Going on with the characterization of the same coral samples, the results here obtained contribute to clarify the impact of these metals on the coral cellular homeostasis and their possible role in thermal stress-induced bleaching, suggesting that both temperature, metal enrichment and their interaction significantly affect the coral cellular response.

Hsp70 and Hsp60 showed similar patterns of expression in response to metal enrichment, temperature stress, and the combination of both stressors. Hsp70, as cytosolic chaperonin, is engaged in assembly of newly synthesized proteins and in the refolding of misfolded or aggregated proteins, contributing to the transfer of proteins to different cellular compartments or to the proteolytic machinery (Balchin et al., 2016). Hsp60 is a mitochondrial chaperonin that plays a crucial role in the synthesis and transportation of mitochondrial proteins and in the folding of newly imported or stress-denatured proteins (Arya et al., 2007). A parallel pattern of modulation of Hsp70 and Hsp60 in all treatments confirms that, despite their different cellular localization, these chaperones work in tandem and plays a synergic role in assisting the folding process, under both physiological and stressful conditions (Zhou et al., 1996; Feder and Hofmann, 1999; Papp et al., 2003; Chen et al., 2018; Rosenzweig et al., 2019). Moreover, both the Hsps displayed a low basal constitutive level in corals maintained at 26°C, as commonly observed in healthy corals (Fitt et al., 2009; Chow et al., 2012; Ross, 2014; Seveso et al., 2016, 2017, 2020).

We observed significant changes in the cellular response of *S. pistillata* to thermal stress. Elevated temperatures indeed resulted in a significant up-regulation of Hsp70 and Hsp60, as previously reported (Downs et al., 2002; Baird et al., 2009; Seveso et al., 2018, 2020; Louis et al., 2020), as well as in

TABLE 2 | Results of the PERMANOVA testing the effects of the temperature (26 and 32°C) and treatments (Control, +Mn, +Fe, and +MnFe) on the levels of Hsp70, Hsp60, SOD, GR, and LPO obtained by permutations (perm) for each group.

Source of variation	df	SS	MS	*F*	*P* (perms)	perms
Temperature	1	3357.3	3357.3	17.945	**0.001**	999
Treatment	3	2118.4	706.14	3.7744	**0.011**	999
Temperature × Treatment	3	5191.9	1730.6	9.2505	**0.001**	998
Error	24	4490.1	187.09			
Total	31	15158				

Significant p-values, P (perms), are in bold.

TABLE 3 | Results of the PERMANOVA pairwise comparisons between treatments at 26°C and 32°C (A), and between temperatures within each metal treatment (B) obtained by permutations (perm) for each group.

	Groups	*t*	*P* (perm)	perms	*P* (MC)
A					
26°C	Control vs. +Mn	1.883	0.06	35	0.061
	Control vs. +Fe	0.132	0.813	35	0.801
	Control vs. +MnFe	2.102	**0.028**	35	**0.042**
	+Mn vs. +Fe	1.854	0.078	35	0.099
	+Mn vs. +MnFe	0.624	0.707	35	0.699
	+Fe vs. +MnFe	2.164	**0.043**	35	0.051
32°C	Control vs. +Mn	3.205	**0.026**	35	**0.01**
	Control vs. +Fe	0.662	0.75	35	0.639
	Control vs. +MnFe	6.502	**0.034**	35	**0.003**
	+Mn vs. +Fe	2.892	**0.03**	35	**0.019**
	+Mn vs. +MnFe	1.424	0.173	35	0.215
	+Fe vs. +MnFe	4.561	**0.025**	35	**0.005**
B					
Control	26°C vs. 32°C	5.088	**0.028**	35	**0.001**
+Mn	26°C vs. 32°C	1.326	0.272	35	0.218
+Fe	26°C vs. 32°C	3.935	**0.021**	35	**0.007**
+MnFe	26°C vs. 32°C	2.385	0.065	35	0.073

Significant p-values, both P (perms) and Monte Carlo P (MC), are in bold.

the LPO levels. LPO reflects the structural integrity of the cell membranes and production of LPOs indicates that levels of ROS are overwhelming the antioxidant pathways, accumulating and damaging cellular membrane lipids, thus signaling an ongoing oxidative stress (Lesser, 2006; Weis, 2008). An increase of LPO in response to heat stress-inducing bleaching has been widely observed in corals (Downs et al., 2000; Flores-Ramírez and Liñán-Cabello, 2006; Dias et al., 2019a,b; Marangoni et al., 2019a). The increase of both Hsps and LPO in control samples following heat stress coincided with a significant decrease of symbiont density, chlorophyll concentration, and photosynthetic rate, measured previously on the same coral samples (Biscéré et al., 2018).

Iron enrichment did not induce any change in the cellular protein homeostasis and in the oxidative status of *S. pistillata* at the normal growth temperature of 26°C. This has to be linked to the lack of Fe effect on *S. pistillata* photophysiological parameters previously analyzed (Biscéré et al., 2018). However, when Fe was coupled to thermal stress, a strong rise in LPO and Hsp levels was observed, in conjunction with coral bleaching and reduced calcification reported by Biscéré et al. (2018). This indicates that Fe enrichment did not provide significant beneficial effects to the coral, although Fe is present in many molecules involved in photosynthesis such as chlorophyll, photosystem I and II, cytochrome b6f complex, and ferredoxin (Geider and La Roche, 1994; Shcolnick and Keren, 2006). This is surprising, as it has previously been reported that Fe limitation increased coral bleaching susceptibility (Shick et al., 2011), while a slight enrichment enhanced photosynthesis, but significantly decreased calcification (Ferrier-Pagès et al., 2001). Overall, these results suggest that Fe is essential to corals, as a complete lack of it impairs coral physiology, but it should remain in trace amounts to avoid becoming toxic. In addition, the high Fe level used in this study did not mitigate the thermal stress.

As far as Mn is concerned, it is a key element in photosynthetic organisms. It is directly involved in chlorophyll synthesis and is an essential component of the Oxygen Evolving Complex of photosystem II, one of the photosynthetic molecules of coral symbionts most affected by heat stress and responsible for ROS production (Hill and Ralph, 2008; Millaleo et al., 2010). In the same samples analyzed previously (Biscéré et al., 2018), Mn enrichment allowed corals to maintain high symbiont density and chlorophyll concentrations, maximal rates of photosynthesis, and to enhance host metabolism and calcification both at control temperature and during thermal stress, avoiding bleaching. While in this study there was no effect of Mn or MnFe on Hsps of *S. pistillata* at 26°C, we indeed observed beneficial effects of Mn or MnFe on the oxidative stress response of *S. pistillata* to thermal stress, as Mn is an essential metal involved in cell catalytic functions and antioxidant mechanisms (Papanikolaou and Pantopoulos, 2005; Santamaria, 2008). Mn and MnFe enrichments prevented any increase in Hsp levels following thermal stress, suggesting the absence of protein damage and strengthening the hypothesis that Mn could mitigate the negative cellular effects produced by the thermal stress (Biscéré et al., 2018). In addition to this, our data suggest that Mn could also be able to maintain the normal cellular protein homeostasis in the host facing heat shock, probably due to its key role in cellular adaptation to oxidative stress and ROS detoxification (Horsburgh et al., 2002; Aguirre and Culotta, 2012). There was also no change in LPO levels of Mn and MnFe-enriched corals between control and heat stress conditions. However, the lack of post-thermal change in LPO may be due to the pre-existing high LPO level detected in Mn-enriched corals kept at normal temperature, in

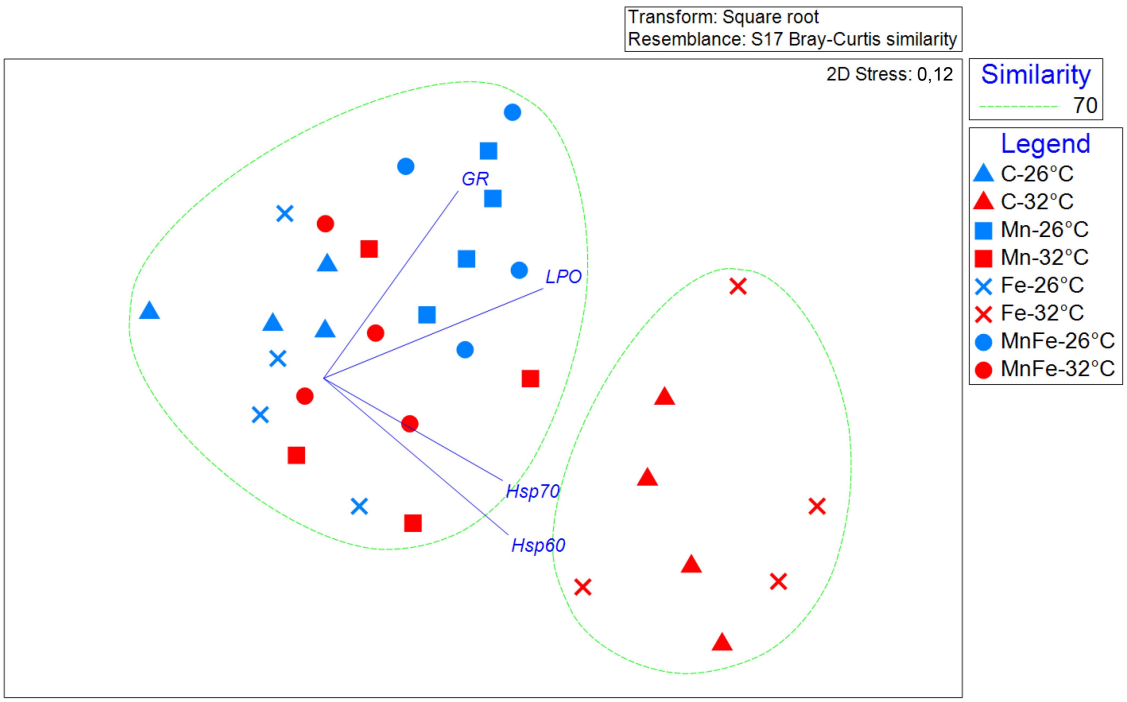

FIGURE 4 | Non-metric multidimensional scaling plot (nMDS) showing the response pattern of all the *S. pistillata* biomarkers analyzed by metal treatment and different temperatures, with vectors (Pearson's correlations ≥ 0.8) representing the variables (biomarkers) that drive significant similarities among experimental conditions.

which the Mn increase alone likely caused oxidative stress, as also indicated by the antioxidant activity of the GR. Indeed, our results showed that at 26°C the GR activity increased as well in corals under Mn enrichments (+Mn and +MnFe). In previous studies, an increased activity of the enzyme, together with LPO level, has been observed in larvae of *Pocillopora damicornis* after 7-days exposure to iron chloride [100 ppm] (Vijayavel et al., 2012), and after 96-h exposure to Cu (Bielmyer-Fraser et al., 2018). The enzyme GR is involved in maintaining and restoring the balance between oxidized and reduced forms of glutathione, a tripeptide able to react with different ROS forming a disulphide bond with another oxidized glutathione. This antioxidant action in coral bleaching response is well known (Lesser, 2006; Krueger et al., 2015). For this reason, it appears surprising that GR activity did not change with the temperature increase, although this trend has been already observed in corals (Liñán-Cabello et al., 2010; Nielsen et al., 2018). The same pattern was detected for corals exposed to Fe enrichment, while a significant decrease in the GR activity was observed after thermal stress in corals exposed to Mn enrichments.

The contrasting effect of Mn enrichments on the oxidative status of the holobiont and on the protein homeostasis of the host, revealed by LPO/GR and Hsps, respectively, needs to be explored. We speculate that Mn may initially be toxic to zooxanthellae, and the resulting oxidative damage could affect the polyp. Therefore, the high level of LPO and GR may be mostly associated with zooxanthellae, considering that Mn enhanced the coral's photosynthetic rate even at ambient temperature as measured in the same coral samples (Biscéré et al., 2018) and this increase may result in an overproduction of ROS in zooxanthellae (Roth, 2014; Foyer, 2018). In this context, high levels of GR in Mn enrichment conditions could detoxify the generated ROS, protecting the host proteins. This could possibly explain the low levels of Hsps measured here and the similar levels of symbiont density and bleaching status observed by Biscéré et al. (2018) in +Mn and Control conditions. In addition, the increased symbiont photosynthetic activity promoted by Mn could support the coral host for longer during heat stress, in line with recent findings indicating that altered symbiotic nutrient cycling may be the direct cause for symbiont expulsion (Rädecker et al., 2021).

Unexpectedly, the results of the SOD did not follow the same trend as those of the GR and LPO, as SOD activity did not show any significant variation at different temperatures and in the various treatments. SOD propels the disproportion of O_2^- ion into H_2O_2 and molecular oxygen (O_2) and can be found mainly in three forms, Cu/Zn SOD, MnSOD, and FeSOD, each one with a specific cellular location (Verma et al., 2019). Although our corals were treated with +Mn and +Fe, two fundamental cofactors for the enzyme functioning, SOD activity was not influenced by enhanced availability of these metals. In addition, the rise in temperature did not affect its activity, in line with previous reports (Yakovleva et al., 2004; Liñán-Cabello et al., 2010; Krueger et al., 2015).

Overall, our results, together with those obtained previously (Biscéré et al., 2018), provide a clear indication of how Mn enrichment causes a cellular and physiological response in

S. pistillata samples significantly different from the one recorded in Control and +Fe treatments. At the concentrations and exposure times considered here, Mn could increase the levels of oxidative stress by enhancing photosynthetic rates at 26°C (Biscéré et al., 2018), although this did not affect the cellular homeostasis of corals. In addition, Mn seems able to mitigate the negative cellular effects produced by thermal stress, increasing the coral's resistance to heat stress-induced bleaching, as previously hypothesized (Biscéré et al., 2018). On the contrary, the Fe enrichment does not appear to play any role, since it showed neither a mitigating effect of thermal stress nor a damaging effect at 26°C (Biscéré et al., 2018). Therefore, it appears evident that the underlying molecular mechanisms and pathways of host and symbiont response to metal and thermal stresses are more complex than expected. In this context, it becomes essential to better clarify the role of Mn, and in general that of metals, in preventing catastrophic outputs for coral reefs, such as coral bleaching.

DATA AVAILABILITY STATEMENT

The raw data supporting the conclusions of this article will be made available by the authors, without undue reservation.

AUTHOR CONTRIBUTIONS

EM and DS wrote the manuscript and analyzed the results. DS, TB, CF-P, and FH conceived and designed the research and the experiments. MV and CF-P provided significant contributions and revisions. PG secured funding for this research and for all reagents and materials. TB performed aquaria experiments. EM, IO, and MF performed and supervised the laboratory activities. All authors contributed to the article and approved the submitted version.

FUNDING

TB was beneficiary of a Ph.D. grant (CIFRE No. 2015/0301, France) supported by the Koniambo Nickel SAS and Ginger Soproner companies in New Caledonia. These funders were not involved in the study design, collection, analysis, interpretation of data, the writing of this article or the decision to submit it for publication. Part of this work was also funded by the CNRT Nickel (DYNAMINE project) to TB and FH.

ACKNOWLEDGMENTS

The authors would like to thank Simone Montano and Roberto Giacchini for the logistic support and technical assistance. The authors would also like to thank Elena Cotugno and Hayden Weiler for English revision.

SUPPLEMENTARY MATERIAL

The Supplementary Material for this article can be found online at: https://www.frontiersin.org/articles/10.3389/fmars.2021.681119/full#supplementary-material

REFERENCES

Aguirre, J. D., and Culotta, V. C. (2012). Battles with iron: manganese in oxidative stress protection. *J. Biol. Chem.* 287, 13541–13548. doi: 10.1074/jbc.R111.312181

Anderson, M., Gorley, R., and Clarke, K. (2008). *PERMANOVA+ for PRIMER: Guide to Software and Statistical Methods*. Plymouth: PRIMER-E.

Anderson, M. J., and Robinson, J. (2003). Generalized discriminant analysis based on distances. *Aust. N. Z. J. Stat.* 45, 301–318. doi: 10.1111/1467-842X.00285

Arya, R., Mallik, M., and Lakhotia, S. C. (2007). Heat shock genes - integrating cell survival and death. *J. Biosci.* 32, 595–610. doi: 10.1007/s12038-007-0059-3

Baird, A. H., Bhagooli, R., Ralph, P. J., and Takahashi, S. (2009). Coral bleaching: the role of the host. *Trends Ecol. Evol.* 24, 16–20. doi: 10.1016/j.tree.2008.09.005

Balchin, D., Hayer-Hartl, M., and Hartl, F. U. (2016). *In vivo* aspects of protein folding and quality control. *Science* 353:aac4354.

Banc-Prandi, G., and Fine, M. (2019). Copper enrichment reduces thermal tolerance of the highly resistant Red Sea coral *Stylophora pistillata*. *Coral Reefs* 38, 285–296. doi: 10.1007/s00338-019-01774-z

Bielmyer-Fraser, G. K., Grosell, M., Bhagooli, R., Baker, A. C., Langdon, C., Gillette, P., et al. (2010). Differential effects of copper on three species of scleractinian corals and their algal symbionts (*Symbiodinium* spp.). *Aquat. Toxicol.* 97, 125–133. doi: 10.1016/j.aquatox.2009.12.021

Bielmyer-Fraser, G. K., Patel, P., Capo, T., and Grosell, M. (2018). Physiological responses of corals to ocean acidification and copper exposure. *Mar. Pollut. Bull.* 133, 781–790.

Bierkens, J. (2000). Applications and pitfalls of stress-proteins in biomonitoring. *Toxicology* 153, 61–72.

Biscéré, T., Ferrier-Pagès, C., Gilbert, A., Pichler, T., and Houlbrèque, F. (2018). Evidence for mitigation of coral bleaching by manganese. *Sci. Rep.* 8:16789. doi: 10.1038/s41598-018-34994-4

Biscéré, T., Lorrain, A., Rodolfo-Metalpa, R., Gilbert, A., Wright, A., Devissi, C., et al. (2017). Nickel and ocean warming affect scleractinian coral growth. *Mar. Pollut. Bull.* 120, 250–258. doi: 10.1016/j.marpolbul.2017.05.025

Biscéré, T., Rodolfo-Metalpa, R., Lorrain, A., Chauvaud, L., Thébault, J., Clavier, J., et al. (2015). Responses of two scleractinian corals to cobalt pollution and ocean acidification. *PLoS One* 10:e0122898. doi: 10.1371/journal.pone.0122898

Brown, B. E. (1997). Coral bleaching: causes and consequences. *Coral Reefs* 16, 129–138.

Chen, B., Feder, M. E., and Kang, L. (2018). Evolution of heat-shock protein expression underlying adaptive responses to environmental stress. *Mol. Ecol.* 27, 3040–3054.

Chow, A. M., Beraud, E., Tang, D. W., Ferrier-Pagès, C., and Brown, I. R. (2012). Hsp60 protein pattern in coral is altered by environmental changes in light and temperature. *Comp. Biochem. Physiol. A Mol. Integr. Physiol.* 161, 349–353. doi: 10.1016/j.cbpa.2011.12.004

Clarke, K. R., and Gorley, R. N. (2015). *Getting started with PRIMER v7*. (Plymouth: PRIMER-E), 20.

Cleves, P. A., Krediet, C. J., Lehnert, E. M., Onishi, M., and Pringle, J. R. (2020). Insights into coral bleaching under heat stress from analysis of gene expression in a sea anemone model system. *Proc. Natl. Acad. Sci. U.S.A.* 117, 28906–28917. doi: 10.1073/pnas.2015737117

Cziesielski, M. J., Schmidt-Roach, S., and Aranda, M. (2019). The past, present, and future of coral heat stress studies. *Ecol. Evol.* 9, 10055–10066. doi: 10.1002/ece3.5576

DalCorso, G., Manara, A., Piasentin, S., and Furini, A. (2014). Nutrient metal elements in plants. *Metallomics* 6, 1770–1788. doi: 10.1039/c4mt00173g

Davy, S. K., Allemand, D., and Weis, V. M. (2012). Cell Biology of Cnidarian-Dinoflagellate Symbiosis. *Microbiol. Mol. Biol. Rev.* 76, 229–261. doi: 10.1128/MMBR.05014-11

Deponte, M. (2013). Glutathione catalysis and the reaction mechanisms of glutathione-dependent enzymes. *Biochim. Biophys. Acta* 830, 3217–3266. doi: 10.1016/j.bbagen.2012.09.018

DeSalvo, M. K., Voolstra, C. R., Sunagawa, S., Schwarz, J. A., Stillman, J. H., Coffroth, M. A., et al. (2008). Differential gene expression during thermal stress and bleaching in the Caribbean coral *Montastraea faveolata*. *Mol. Ecol.* 17, 3952–3971. doi: 10.1111/j.1365-294X.2008.03879.x

Dias, M., Ferreira, A., Gouveia, R., Madeira, C., Jogee, N., Cabral, H., et al. (2019a). Long-term exposure to increasing temperatures on scleractinian coral fragments reveals oxidative stress. *Mar. Environ. Res.* 150, 104758. doi: 10.1016/j.marenvres.2019.104758

Dias, M., Ferreira, A., Gouveia, R., and Vinagre, C. (2019b). Synergistic effects of warming and lower salinity on the asexual reproduction of reef-forming corals. *Ecol. Indic.* 98, 334–348. doi: 10.1016/j.ecolind.2018.11.011

Dias, M., Madeira, C., Jogee, N., Ferreira, A., Gouveia, R., Cabral, H., et al. (2020). Integrative indices for health assessment in reef corals under thermal stress. *Ecol. Indic.* 113:106230. doi: 10.1016/j.ecolind.2020.106230

Downs, C., Mueller, E., Phillips, S., Fauth, J. E., and Woodley, C. M. (2000). A molecular biomarker system for assessing the health of coral (*Montastraea faveolata*) during heat stress. *Mar. Biotechnol.* 2, 533–544. doi: 10.1007/s101260000038

Downs, C. A. (2005). "Cellular diagnostics and its application to aquatic and marine toxicology," in *Techniques in Aquatic Toxicology*, Vol. 2, ed. G. K. Ostrander (Boca Raton, FL: CRC Press), 181–208.

Downs, C. A., Fauth, J. E., Halas, J. C., Dustan, P., Bemiss, J., and Woodley, C. M. (2002). Oxidative stress and seasonal coral bleaching. *Free Radic. Biol. Med.* 33, 533–543. doi: 10.1016/S0891-5849(02)00907-3

Downs, C. A., Fauth, J. E., Robinson, C. E., Curry, R., Lanzendorf, B., Halas, J. C., et al. (2005). Cellular diagnostics and coral health: declining coral health in the Florida Keys. *Mar. Pollut. Bull.* 51, 558–569.

Eakin, C. M., Sweatman, H. P. A., and Brainard, R. E. (2019). The 2014–2017 global-scale coral bleaching event: insights and impacts. *Coral Reefs* 38, 539–545. doi: 10.1007/s00338-019-01844-2

Fairbrother, A., Wenstel, R., Sappington, K., and Wood, W. (2017). Framework for metals risk assessment. *Ecotoxicol. Environ. Saf.* 68, 145–227. doi: 10.1016/j.ecoenv.2007.03.015

Feder, M. E., and Hofmann, G. E. (1999). Heat-shock proteins, molecular chaperones, and the stress response: evolutionary and ecological physiology. *Annu. Rev. Physiol.* 61, 243–282.

Ferrier-Pagès, C., Sauzéat, L., and Balter, V. (2018). Coral bleaching is linked to the capacity of the animal host to supply essential metals to the symbionts. *Glob. Change Biol.* 24, 3145–3157. doi: 10.1111/gcb.14141

Ferrier-Pagès, C., Schoelzke, V., Jaubert, J., Muscatine, L., and Hoegh-Guldberg, O. (2001). Response of a scleractinian coral, *Stylophora pistillata*, to iron and nitrate enrichment. *J. Exp. Mar. Biol. Ecol.* 259, 249–261. doi: 10.1016/s0022-0981(01)00241-6

Fitt, W. K., Gates, R. D., Hoegh-Guldberg, O., Bythell, J. C., Jatkar, A., Grottoli, A. G., et al. (2009). Response of two species of Indo-Pacific corals, Porites cylindrica and *Stylophora pistillata*, to short-term thermal stress: the host does matter in determining the tolerance of corals to bleaching. *J. Exp. Mar. Biol. Ecol.* 373, 102–110.

Flores-Ramírez, L. A., and Liñán-Cabello, M. A. (2006). Relationships among thermal stress, bleaching and oxidative damage in the hermatypic coral, *Pocillopora capitata*. *Comp. Biochem. Physiol. C Toxicol. Pharmacol.* 146, 194–202. doi: 10.1016/j.cbpc.2006.09.008

Fonseca, J. S., Marangoni, L. F. B., Marques, J. A., and Bianchini, A. (2017). Effects of increasing temperature alone and combined with copper exposure on biochemical and physiological parameters in the zooxanthellate scleractinian coral, *Mussismilia harttii*. *Aquat. Toxicol.* 190, 121–132.

Foyer, C. H. (2018). Reactive oxygen species, oxidative signaling and the regulation of photosynthesis. *Environ. Exp. Bot.* 154, 134–142. doi: 10.1016/j.envexpbot.2018.05.003

Gaschler, M. M., and Stockwell, B. R. (2017). Lipid peroxidation in cell death. *Biochem. Biophys. Res. Commun.* 482, 419–425. doi: 10.1016/j.bbrc.2016.10.086

Geider, R. J., and La Roche, J. (1994). The role of iron in phytoplankton photosynthesis, and the potential for iron-limitation of primary productivity in the sea. *Photosynth. Res.* 39, 275–301. doi: 10.1007/BF00014588

Gérard-Monnier, D., Erdelmeier, I., Régnard, K., Moze-Henry, N., Yadan, J. C., and Chaudiere, J. (1998). Reactions of 1-methyl-2-phenylindole with malondialdehyde and 4-hydroxyalkenals. Analytical applications to a colorimetric assay of lipid peroxidation. *Chem. Res. Toxicol.* 11, 1176–1183.

Gissi, F., Stauber, J., Reichelt-Brushett, A., Harrison, P. L., and Jolley, D. F. (2017). Inhibition in fertilisation of coral gametes following exposure to nickel and copper. *Ecotoxicol. Environ. Saf.* 145, 32–41. doi: 10.1016/j.ecoenv.2017.07.009

Goh, B. P. (1991). Mortality and settlement success of *Pocillopora damicornis* planula larvae during recovery from low levels of nickel. *Pac. Sci.* 45, 276–286.

Hill, R., and Ralph, J. R. (2008). Dark-induced reduction of the plastoquinone pool in zooxanthellae of scleractinian corals and implications for measurements of chlorophyll a fluorescence. *Symbiosis* 46, 45–56.

Hoegh-Guldberg, O. (1999). Climate change, coral bleaching and the future of the world's coral reefs. *Mar. Freshw. Res.* 50, 839–866.

Horsburgh, M. J., Wharton, S. J., Karavolos, M., and Foster, S. J. (2002). Manganese: elemental defence for a life with oxygen. *Trends Microbiol.* 10, 496–501. doi: 10.1016/s0966-842x(02)02462-9

Hughes, T. P., Kerry, J., Álvarez-Noriega, M., Álvarez-Romero, J. G., Anderson, K. D., Baird, A. H., et al. (2017). Global warming and recurrent mass bleaching of corals. *Nature* 543, 373–377. doi: 10.1038/nature21707

Kenkel, C. D., Sheridan, C., Leal, M. C., Bhagooli, R., Castillo, K. D., Kurata, N., et al. (2014). Diagnostic gene expression biomarkers of coral thermal stress. *Mol. Ecol. Resour.* 14, 667–678. doi: 10.1111/1755-0998.12218

Krueger, T., Hawkins, T. D., Becker, S., Pontasch, S., Dove, S., Hoegh-Guldberg, O., et al. (2015). Differential coral bleaching contrasting the activity and response of enzymatic antioxidants in symbiotic partners under thermal stress. *Comp. Biochem. Physiol. A Mol. Integr. Physiol.* 190, 15–25. doi: 10.1016/j.cbpa.2015.08.012

Kültz, D. (2005). Molecular and evolutionary basis of the cellular stress response. *Annu. Rev. Physiol.* 67, 225–257. doi: 10.1146/annurev.physiol.67.040403.103635

Kwok, C. K., and Ang, P. O. Jr. (2013). Inhibition of larval swimming activity of the coral (*Platygyra acuta*) by interactive thermal and chemical stresses. *Mar. Pollut. Bull.* 74, 264–273. doi: 10.1016/j.marpolbul.2013.06.048

Lesser, M. P. (2006). Oxidative stress in marine environments: biochemistry and physiological ecology. *Annu. Rev. Physiol.* 68, 253–278. doi: 10.1146/annurev.physiol.68.040104.110001

Lesser, M. P. (2011). "Coral bleaching: causes and mechanisms," in *Coral Reefs: An Ecosystem in Transition*, eds Z. Dubinsky and N. Stambler (Dordrecht: Springer). doi: 10.1007/978-94-007-0114-4_23

Liñán-Cabello, M. A., Flores-Ramírez, L. A., Zenteno-Savin, T., Olguín-Monroy, N. O., Sosa-Avalos, R., Patiño-Barragan, M., et al. (2010). Seasonal changes of antioxidant and oxidative parameters in the coral *Pocillopora capitata* on the Pacific coast of Mexico. *Mar. Ecol.* 31, 407–417. doi: 10.1111/j.1439-0485.2009.00349.x

Lough, J. M., Anderson, K. D., and Hughes, T. P. (2018). Increasing thermal stress for tropical coral reefs: 1871–2017. *Sci. Rep.* 8:6079. doi: 10.1038/s41598-018-24530-9

Louis, Y. D., Bhagooli, R., Kenkel, C. D., Baker, A. C., and Dyall, S. D. (2017). Gene expression biomarkers of heat stress in scleractinian corals: promises and limitations. *Comp. Biochem. Physiol. C Toxicol. Pharmacol.* 191, 63–77. doi: 10.1016/j.cbpc.2016.08.007

Louis, Y. D., Bhagooli, R., Seveso, D., Maggioni, D., Galli, P., Vai, M., et al. (2020). Local acclimatisation-driven differential gene and protein expression patterns of Hsp70 in *Acropora muricata*: implications for coral tolerance to bleaching. *Mol. Ecol.* 29, 4382–4394. doi: 10.1111/mec.15642

Marangoni, L. F. B., Dalmolin, C., Marques, J. A., Klein, R. D., Abrantes, D. P., Pereira, C. M., et al. (2019a). Oxidative stress biomarkers as potential tools in reef degradation monitoring: a study case in a South Atlantic reef under influence of the 2015–2016 El Niño/Southern Oscillation (ENSO). *Ecol. Indic.* 106:105533. doi: 10.1016/j.ecolind.2019.105533

Marangoni, L. F. B., Marques, J. A., Duarte, G. A. S., Pereira, C. M., Calderon, E. N., Barreira, C., et al. (2017). Copper effects on biomarkers associated with photosynthesis, oxidative status and calcification in the Brazilian coral *Mussismilia harttii* (Scleractinia, Mussidae). *Mar. Environ. Res.* 130, 248–257. doi: 10.1016/j.marenvres.2017.08.002

Marangoni, L. F. B., Mies, M., Güth, A. Z., Banha, T. N. S., Inague, A., Fonseca, J. D. S., et al. (2019b). Peroxynitrite generation and increased heterotrophic capacity are linked to the disruption of the coral–dinoflagellate symbiosis in a scleractinian and hydrocoral species. *Microorganisms* 7:426.

Marangoni, L. F. B., Pinto, M. M. A. N., Marques, J. A., and Bianchini, A. (2019c). Copper exposure and seawater acidification interaction: antagonistic effects on biomarkers in the zooxanthellate scleractinian coral *Mussismilia harttii*. *Aquat. Toxicol.* 206, 123–133. doi: 10.1016/j.aquatox.2018.11.005

Mayfield, A. B., Wang, L. H., Tang, P. C., Fan, T. Y., Hsiao, Y. Y., Tsai, C. L., et al. (2011). Assessing the impacts of experimentally elevated temperature on the biological composition and molecular chaperone gene expression of a reef coral. *PLoS One* 6:e26529. doi: 10.1371/journal.pone.0026529

Merchant, S. S. (2009). His protects heme as it crosses the membrane. *Proc. Natl. Acad. Sci. U.S.A.* 106, 10069–10070. doi: 10.1073/pnas.0905189106

Millaleo, R., Reyes-Diaz, M., Ivanov, A. G., Mora, M. L., and Alberdi, M. (2010). Manganese as essential and toxic element for plants: transport, accumulation and resistance mechanisms. *J. Soil Sci. Plant Nutr.* 10, 470–481.

Mitchelmore, C. L., Alan Verde, E., and Weis, V. M. (2007). Uptake and partitioning of copper and cadmium in the coral *Pocillopora damicornis*. *Aquat. Toxicol.* 85, 48–56. doi: 10.1016/j.aquatox.2007.07.015

Moreton, B. M., Fernandez, J. M., and Dolbecq, M. B. (2009). Development of a field preconcentration/elution unit for routine determination of dissolved metal concentrations by ICP-OES in marine waters: application for monitoring of the New Caledonia lagoon. *Geostand. Geoanal. Res.* 33, 205–218. doi: 10.1111/j.1751-908X.2009.00899.x

Morley, N. H., Burton, J. D., Tankere, S. P. C., and Martin, J. M. (1997). Distribution and behaviour of some dissolved trace metals in the western Mediterranean Sea. *Deep Sea Res. Part II Top. Stud. Oceanogr.* 44, 675–691.

Negri, A. P., and Hoogenboom, M. O. (2011). Water contamination reduces the tolerance of coral larvae to thermal stress. *PLoS One* 6:e19703. doi: 10.1371/journal.pone.0019703

Nielsen, D. A., Petrou, K., and Gates, R. D. (2018). Coral bleaching from a single cell perspective. *ISME J.* 12, 1558–1567. doi: 10.1038/s41396-018-0080-6

Nyström, M., Nordemar, I., and Tedengren, M. (2001). Simultaneous and sequential stress from increased temperature and copper on the metabolism of the hermatypic coral *Porites cylindrica*. *Mar. Biol.* 138, 1225–1231. doi: 10.1007/s002270100549

Oakley, C. A., and Davy, S. K. (2018). "Cell biology of coral bleaching," in *Coral Bleaching. Ecological Studies (Analysis and Synthesis)*, Vol. 233, eds M. van Oppen and J. Lough (Cham: Springer). doi: 10.1007/978-3-319-75393-5_8

Oliver, J. K., Berkelmans, R., and Eakin, C. M. (2018). "Coral bleaching in space and time," in *Coral Bleaching. Ecological Studies (Analysis and Synthesis*, Vol. 233, eds M. van Oppen and J. Lough (Cham: Springer). doi: 10.1007/978-3-319-75393-5_3

Olsen, K., Ritson-Williams, R., Ochrietor, J. D., Paul, V. J., and Ross, C. (2013). Detecting hyperthermal stress in larvae of the hermatypic coral Porites astreoides: the suitability of using biomarkers of oxidative stress versus heat-shock protein transcriptional expression. *Mar. Biol.* 160, 2609–2618. doi: 10.1007/s00227-013-2255-z

Papanikolaou, G., and Pantopoulos, K. (2005). Iron metabolism and toxicity. *Toxic. Appl. Pharmacol.* 202, 199–211. doi: 10.1016/j.taap.2004.06.021

Papp, E., Nardai, G., Söti, C., and Csermely, P. (2003). Molecular chaperones, stress proteins and redox homeostasis. *Biofactors* 17, 249–257. doi: 10.1002/biof.5520170124

Patterson, J., Jeyasanta, K. I., Sathish, N., Edward, J. K. P., and Booth, A. M. (2020). Microplastic and heavy metal distributions in an Indian coral reef ecosystem. *Sci. Total Environ.* 744:140706. doi: 10.1016/j.scitotenv.2020.140706

Rädecker, N., Pogoreutz, C., Gegner, H. M., Cárdenas, A., Roth, F., Bougoure, J., et al. (2021). Heat stress destabilizes symbiotic nutrient cycling in corals. *Proc. Natl. Acad. Sci. U.S.A.* 118:e2022653118. doi: 10.1073/pnas.2022653118

Ranjbar Jafarabadi, A., Bakhtiari, A. R., Maisano, M., Pereira, P., and Cappello, T. (2018). First record of bioaccumulation and bioconcentration of metals in Scleractinian corals and their algal symbionts from Kharg and Lark coral reefs (Persian Gulf, Iran). *Sci. Total Environ.* 640-641, 1500–1511. doi: 10.1016/j.scitotenv.2018.06.029

Reich, H. G., Rodriguez, I. B., LaJeunesse, T. C., and Ho, T. Y. (2020). Endosymbiotic dinoflagellates pump iron: differences in iron and other trace metal needs among the Symbiodiniaceae. *Coral Reefs* 39, 915–927. doi: 10.1007/s00338-020-01911-z

Reichelt-Brushett, A., and Hudspith, M. (2016). The effects of metals of emerging concern on the fertilization success of gametes of the tropical scleractinian coral *Platygyra daedalea*. *Chemosphere* 150, 398–406. doi: 10.1016/j.chemosphere.2016.02.048

Rosenzweig, R., Nillegoda, N. B., Mayer, M. P., and Bukau, B. (2019). The Hsp70 chaperone network. *Nat. Rev. Mol. Cell Biol.* 20, 665–680.

Ross, C. (2014). Nitric oxide and heat shock protein 90 co-regulate temperature-induced bleaching in the soft coral *Eunicea fusca*. *Coral Reefs* 33, 513–522.

Rosset, S. L., Oakley, C. A., Ferrier-Pagès, C., Suggett, D. J., Weis, V. M., and Davy, S. K. (2020). The molecular language of the Cnidarian–Dinoflagellate symbiosis. *Trends Microbiol.* 29, 320–333. doi: 10.1016/j.tim.2020.08.005

Roth, M. S. (2014). The engine of the reef: photobiology of the coral-algal symbiosis. *Front. Microbiol.* 5:422. doi: 10.3389/fmicb.2014.00422

Santamaria, A. B. (2008). Manganese exposure, essentiality & toxicity. *Indian J. Med. Res.* 128, 484–500.

Schwarz, J. A., Mitchelmore, C. L., Jones, R., O'Dea, A., and Seymour, S. (2013). Exposure to copper induces oxidative and stress responses and DNA damage in the coral *Montastraea franksi*. *Comp. Biochem. Physiol. C Toxicol. Pharmacol.* 157, 272–279. doi: 10.1016/j.cbpc.2012.12.003

Seneca, F. O., Forêt, S., Ball, E. E., Smith-Keune, C., Miller, D. J., and van Oppen, M. J. (2010). Patterns of gene expression in a scleractinian coral undergoing natural bleaching. *Mar. Biotechnol.* 12, 594–604. doi: 10.1007/s10126-009-9247-5

Seveso, D., Arrigoni, R., Montano, S., Maggioni, D., Orlandi, I., Berumen, M. L., et al. (2020). Investigating the heat shock protein response involved in coral bleaching across scleractinian species in the central Red Sea. *Coral Reefs* 39, 85–98. doi: 10.1007/s00338-019-01878-6

Seveso, D., Montano, S., Maggioni, D., Pedretti, F., Orlandi, I., Galli, P., et al. (2018). Diel modulation of Hsp70 and Hsp60 in corals living in a shallow reef. *Coral Reefs* 37, 801–806. doi: 10.1007/s00338-018-1703-0

Seveso, D., Montano, S., Reggente, M. A. L., Maggioni, D., Orlandi, I., Galli, P., et al. (2017). The cellular stress response of the scleractinian coral *Goniopora columna* during the progression of the black band disease. *Cell Stress Chaperones* 22, 225–236. doi: 10.1007/s12192-016-0756

Seveso, D., Montano, S., Strona, G., Orlandi, I., Galli, P., and Vai, M. (2013). Exploring the effect of salinity changes on the levels of Hsp60 in the tropical coral *Seriatopora caliendrum*. *Mar. Environ. Res.* 90, 96–103. doi: 10.1016/j.marenvres.2013.06.002

Seveso, D., Montano, S., Strona, G., Orlandi, I., Galli, P., and Vai, M. (2014). The susceptibility of corals to thermal stress by analyzing Hsp60 expression. *Mar. Environ. Res.* 99, 69–75. doi: 10.1016/j.marenvres.2014.06.008

Seveso, D., Montano, S., Strona, G., Orlandi, I., Galli, P., and Vai, M. (2016). Hsp60 expression profiles in the reef-building coral *Seriatopora caliendrum* subjected to heat and cold shock regimes. *Mar. Environ. Res.* 119, 1–11.

Seveso, D., Montano, S., Strona, G., Orlandi, I., Vai, M., and Galli, P. (2012). Up-regulation of Hsp60 in response to skeleton eroding band disease but not by algal overgrowth in the scleractinian coral *Acropora muricata*. *Mar. Environ. Res.* 78, 34–39. doi: 10.1016/j.marenvres.2012.03.008

Shcolnick, S., and Keren, N. (2006). Metal homeostasis in cyanobacteria and chloroplasts. Balancing benefits and risks to the photosynthetic apparatus. *Plant Physiol.* 141, 805–810. doi: 10.1104/pp.106.079251

Shick, M. J., Iglic, K., Wells, M. L., Trick, C. G., Doyle, J., and Dunlap, W. C. (2011). Responses to iron limitation in two colonies of *Stylophora pistillata* exposed to high temperature: implications for coral bleaching. *Limnol. Oceanogr.* 56, 813–828. doi: 10.4319/lo.2011.56.3.0813

Siddiqui, S., and Bielmyer-Fraser, G. K. (2015). Responses of the sea anemone, *Exaiptasia pallida*, to ocean acidification conditions and copper exposure. *Aquat. Toxicol.* 167, 228–239. doi: 10.1016/j.aquatox.2015.08.012

Suggett, D. J., and Smith, D. J. (2020). Coral bleaching patterns are the outcome of complex biological and environmental networking. *Glob. Change Biol.* 26, 68–79. doi: 10.1111/gcb.14871

Vai, M., Popolo, L., and Alberghina, L. (1986). Immunological cross-reactivity of fungal and yeast plasma membrane H+-ATPase. *FEBS Lett.* 206, 135–141. doi: 10.1016/0014-5793(86)81355-2

van Dam, J. W., Negri, A. P., Uthicke, S., and Mueller, J. F. (2011). "Chemical pollution on Coral Reefs: exposure and ecological effects," in *Ecological Impact of Toxic Chemicals*, eds F. Sanchez-Bayo, P. J. van den Brink, and R. M. Mann (Sharjah: Bentham Science Publishers Ltd).

Vance, P. G., Keele, B. B. Jr., and Rajagopalan, K. V. (1972). Superoxide dismutase from *Streptococcus mutans*. Isolation and characterization of two forms of the enzyme. *J. Biol. Chem.* 247, 4782–4786.

Venn, A. A., Quinn, J., Jones, R., and Bodnar, A. (2009). P-glycoprotein (multi-xenobiotic resistance) and heat shock protein gene expression in the reef coral *Montastraea franksi* in response to environmental toxicants. *Aquat. Toxicol.* 93, 188–195.

Verma, M. K., Jaiswal, A., Sharma, P., Kumar, P., and Singh, A. N. (2019). Oxidative stress and biomarker of TNF-α, MDA and FRAP in hypertension. *J. Med. Life* 12, 253–259. doi: 10.25122/jml-2019-0031

Vijayavel, K., Downs, C., Ostrander, G., and Richmond, R. (2012). Oxidative DNA damage induced by iron chloride in the larvae of the lace coral *Pocillopora damicornis*. *Comp. Biochem. Physiol. C Toxicol. Pharmacol.* 155, 275–280. doi: 10.1016/j.cbpc.2011.09.007

Wang, Y., Oberley, L. W., and Murhammer, D. W. (2001). Antioxidant defense systems of two lipidopteran insect cell lines. *Free Radic. Biol. Med.* 30, 1254–1262. doi: 10.1016/s0891-5849(01)00520-2

Weis, V. M. (2008). Cellular mechanisms of Cnidarian bleaching: stress causes the collapse of symbiosis. *J. Exp. Biol.* 211, 3059–3066. doi: 10.1242/jeb.009597

Wells, M., Shick, J. M., and Long, P. (2011). *Effects of Trace Metal Limitation on Oxidative Stress in Zooxanthellae and Its Role in Coral Bleaching. University of Maine Office of Research and Sponsored Programs: Grant Reports Paper*. (Orono, ME: University of Maine), 291.

Williams, A., Chiles, E. N., Conetta, D., Pathmanathan, J. S., Cleves, P. A., Putnam, H. M., et al. (2021). Metabolomic shifts associated with heat stress in coral holobionts. *Sci. Adv.* 7:eabd4210.

Yakovleva, I., Bhagooli, R., Takemura, A., and Hidaka, M. (2004). Differential susceptibility to oxidative stress of two scleractinian corals: antioxidant functioning of mycosporine-glycine. *Comp. Biochem. Physiol. B Biochem. Mol. Biol.* 139, 721–730. doi: 10.1016/j.cbpc.2004.08.016

Zhou, J., Bruns, M. A., and Tiedje, J. M. (1996). DNA recovery from soils of diverse composition. *Appl. Environ. Microbiol.* 62, 316–322. doi: 10.1128/AEM.62.2.316-322.1996

Zhou, Z., Yu, X., Tang, J., Wu, Y., Wang, L., and Huang, B. (2018). Systemic response of the stony coral *Pocillopora damicornis* against acute cadmium stress. *Aquat. Toxicol.* 194, 132–139. doi: 10.1016/j.aquatox.2017.11.013

Conflict of Interest: The authors declare that the research was conducted in the absence of any commercial or financial relationships that could be construed as a potential conflict of interest.

frontiers in Marine Science

ORIGINAL RESEARCH
published: 19 July 2021
doi: 10.3389/fmars.2021.660153

Shotgun Proteomic Analysis of Thermally Challenged Reef Corals

Anderson B. Mayfield[1,2], Catalina Aguilar[1,2], Graham Kolodziej[1,2], Ian C. Enochs[2] and Derek P. Manzello[2,3]*

[1] Cooperative Institute for Marine and Atmospheric Studies, University of Miami, Miami, FL, United States, [2] Atlantic Oceanographic and Meteorological Laboratory, National Oceanic and Atmospheric Administration, Miami, FL, United States, [3] NOAA Coral Reef Watch, Center for Satellite Applications and Research, Satellite Oceanography & Climate Division, National Oceanic and Atmospheric Administration, College Park, MD, United States

Although coral reef ecosystems across the globe are in decline due to climate change and other anthropogenic stressors, certain inshore reefs of the Upper Florida Keys reef tract have persisted, with some even thriving, under marginalized conditions. To better understand the molecular basis of the thermotolerance displayed by these corals, a laboratory-based temperature challenge experiment that also featured conspecifics from a more stress-susceptible offshore reef was conducted with the common Caribbean reef-builder *Orbicella faveolata*, and the proteomes of both the coral hosts and their endosymbiotic dinoflagellate communities were profiled in (1) controls, (2) corals that succumbed to high-temperature stress and bleached, and (3) those that instead acclimated to high temperatures *ex situ*. Proteomic signatures varied most significantly across temperatures, host genotypes, and Symbiodiniaceae assemblages, and the two eukaryotic compartments of this mutualism exhibited distinct proteomic responses to high temperatures. Both partners maintained high levels of molecular chaperones and other canonical (eukaryotic) stress response (CSR) proteins in all treatments (including controls). Instead, proteins involved in lipid trafficking, metabolism, and photosynthesis played greater roles in the holobionts' high-temperature responses, and these energy mobilization processes may have sustained the elevated protein turnover rates associated with the constitutively active CSR.

Keywords: coral reefs, dinoflagellates, global climate change, proteomics, symbiosis

OPEN ACCESS

Edited by:
Davide Seveso, University of Milano-Bicocca, Italy

Reviewed by:
Brad Buckley, Portland State University, United States
Paul Yancey, Whitman College, United States

****Correspondence:***
Anderson B. Mayfield
abm64@miami.edu;
anderson.mayfield@noaa.gov

Specialty section:
This article was submitted to Aquatic Physiology, a section of the journal Frontiers in Marine Science

Received: *28 January 2021*
Accepted: *21 April 2021*
Published: *19 July 2021*

Citation:
Mayfield AB, Aguilar C, Kolodziej G, Enochs IC and Manzello DP (2021) Shotgun Proteomic Analysis of Thermally Challenged Reef Corals. Front. Mar. Sci. 8:660153. doi: 10.3389/fmars.2021.660153

INTRODUCTION

Corals reefs the world over are threatened by global climate change (GCC; Hoegh-Guldberg et al., 2017), and especially the rapidly increasing seawater temperatures associated with this phenomenon (Brown, 1997). South Florida's coral reefs, in particular, have deteriorated dramatically over the past decades (Manzello, 2015) as a result of land-based pollution, GCC, and disease, yet certain inshore reefs continue to persist (even thriving in certain cases; Gintert et al., 2018). These seemingly marginalized reefs are characterized by high summer seawater temperatures, high sediment loads, extreme high or low light levels (depending on season), high nutrient levels, and otherwise poor seawater quality conditions for coral survival (Manzello et al., 2015). Nevertheless, they feature a large number of massive coral colonies that do not regularly succumb to bleaching or disease [including the now-prevalent stony coral tissue loss disease (SCTLD)]. Only 1–2 km away, the offshore reefs have suffered to a greater extent (<5% live coral cover), and their resident corals appear to have lower resilience with respect to elevated

temperatures and disease (Manzello et al., 2019); this is despite the presumably more favorable seawater quality associated with these habitats.

To gain insight into the thermotolerance of massive corals of the Upper Florida Keys' inshore reef tract, we previously exposed *Orbicella faveolata* genotypes from sites of differing environmental tolerances to each of two high-temperature conditions: a 5-day (d) extreme high-temperature hold at 33°C and a 31-day exposure to 32°C (a temperature these corals encounter *in situ*, albeit not typically over multi-week durations; Manzello et al., 2019). As hypothesized, offshore corals were less thermotolerant than inshore genotypes, which failed to bleach at 33°C. Furthermore, some corals shuffled their endosymbiotic dinoflagellate (family Symbiodiniaceae) communities over the course of the study, though switching from *Breviolum*-dominated assemblages to those with higher proportions of the hypothetically more thermotolerant genus *Durusdinium* did not demonstrate improved survival at 32°C. Although the inshore-offshore gradient in thermotolerance was confirmed, even the most resilient inshore genotypes had at least begun to bleach slightly after 31 days at 32°C.

We sought to exploit this sample set to better understand the molecular basis of thermotolerance in this Caribbean reef-builder by specifically characterizing the cellular processes underlying (1) acclimation in corals found to be relatively more high-temperature resilient and (2) the stress response in those that were beginning to bleach. A mass spectrometry (MS)-based proteomics approach was taken because, although many works have attempted to characterize the cellular biology of thermotolerant corals based on mRNA profiling alone (e.g., Bellantuono et al., 2012; Pinzón et al., 2015), the lack of correlation between gene expression and concentration of the respective protein in both scleractinian corals and Symbiodiniaceae dinoflagellates (Mayfield et al., 2016, 2018a,b) signifies that those seeking to make inferences about the cellular biology of corals and their endosymbionts must instead profile proteins; unlike mRNAs, these macromolecules directly effect behavioral changes in cells.

MATERIALS AND METHODS

The Experiment

Key features of the experiment have been detailed in the **Supplementary Material**. Briefly, 20 *O. faveolata* colonies from each of three sites (**Table 1**; see Manzello et al., 2019 for maps and detailed site information.)-"Little Conch" (UKO2; offshore), "The Rocks" (UKI2; inshore), and "Cheeca Rocks" (UKI1; inshore)-were tagged, genotyped, and cored. After *in situ* recovery of the cores, they were moved to the laboratory, acclimated to aquarium conditions for several days, adhered to tile "pucks" (∼4 × 4 cm), again allowed to recover for several days, and then exposed to the treatments described above (33°C for 5 d or 32°C for 31 d, with a 7-d ramping period between the acclimation temperature of 30°C and the target temperature). The trailing two-week mean at the time of sampling (July 2017), 30°C, was used for the control treatment. Historical temperature data from Cheeca Rocks can be found at https://www.pmel.noaa.gov/co2/pco2data/cheeca/alldata/.

Extractions and MS

A subset of 16 samples was chosen for proteomic analyses (**Table 1**), and an "identical twin" design was employed in which the responses of fragments made from the same source genotype were tracked across all treatments. Genetic analyses (Manzello et al., 2019) revealed that all 20 offshore colonies from Little Conch are unique genotypes; one such clone of the black(a) genotype (2b-RAD nomenclature), colony C5, was randomly chosen for proteomics. In contrast, the inshore reef The Rocks lacks genetic diversity and is dominated by a single *O. faveolata* clone: skyblue (Manzello et al., 2019). One skyblue colony, A4, was chosen for proteomics. Randomly selected colonies from two genotypes of Cheeca Rocks, light-yellow (B5) and grey60 (D5), constituted the final two colonies whose fragments were analyzed in each of the four treatments. Four and two host coral and Symbiodiniaceae samples yielded few proteins upon MS (discussed below) and were omitted. This resulted in a total sample size of 12 and 14 for the host and endosymbionts, respectively (**Table 1**), with 3–4, 3, and 6–7 samples from Little Conch, The Rocks, and Cheeca Rocks, respectively (3–4 offshore and 9–10 inshore samples).

Coral pucks were flash-frozen in liquid nitrogen (LN_2) immediately upon sampling and quickly pulverized in additional LN_2 with a Baileigh Industrial hydraulic press (United States) into a wet, sand-like consistency prior to freezing (−80°C). Later, RNAs, DNAs, and proteins were extracted from ∼100 mg of partially ground tissue (including powdered skeleton) as described in the **Supplementary Material**. Briefly, coral and endosymbiont proteins were extracted with a modified TRIzol™ (Invitrogen, United States) protocol, and 15 μg were dissolved in ammonium bicarbonate (AB) supplemented with sodium dodecyl sulfate, quantified, electrophoresed [for protein quality control (QC)], repurified, resuspended in AB, denatured with urea, alkylated with iodoacetamide, digested overnight with trypsin, repurified, and resuspended in 20 μl of 2% acetonitrile with 0.1% formic acid (to aid in ionization) prior to nano-liquid chromatography (LC) on an Easy Nano LC™ 1000 [Thermo Fisher Scientific (TFS), United States] with a Nanospray Flex ion source (TFS) as described in Musada et al. (2020). Peptide eluates from a 2–98% acetonitrile gradient (84 min) were run on a Q Exactive Orbitrap MS (TFS) as in Musada et al. (2020). Details for all aforementioned steps can be found in the **Supplementary Material**.

MS Data Analysis

RAW data files from the MS were uploaded into Proteome Discoverer (ver. 2.2, TFS), and each of three fasta mRNA sequence libraries (conceptually translated to proteins) was queried: an *O. faveolata* transcriptome, a Symbiodiniaceae (*in hospite* with *O. faveolata*) transcriptome, and a *Pocillopora acuta*-Symbiodiniaceae transcriptome (Mayfield et al., 2014). All three sequence databases are described in detail in the **Supplementary Material**. The peak integration tolerance was 20 ppm, and the peak integration method was based on

TABLE 1 | *Orbicella faveolata* samples analyzed by shotgun proteomics.

Sample code	Temp. (°C) (level)	Time (days)	Temp. × time	Genotype (2b-RAD)	Shelf	Health status
A4-1	30 (control)	5	Control-short	Skyblue	Inshore	Healthy control
A4-5	32 (high)	31	High-long	Skyblue	Inshore	Stressed @ high temp.
A4-7	33 (very high)	5	High-short	Skyblue	Inshore	Healthy @ high temp.
A4-8*	30 (control)	31	Control-long	Skyblue	Inshore	Healthy control
B5-1	30 (control)	31	Control-long	Lightyellow	Inshore	Healthy control
B5-2*	32 (high)	31	High-long	Lightyellow	Inshore	Stressed @ high temp.
B5-4 bu	33 (very high)	5	High-short	Lightyellow	Inshore	Healthy @ high temp.
B5-7 bu	30 (control)	5	Control-short	Lightyellow	Inshore	Healthy control
C5-1	30 (control)	5	Control-short	Black(a)	Offshore	Healthy control
C5-2	32 (high)	31	High-long	Black(a)	Offshore	Stressed @ high temp.
C5-7	30 (control)	31	Control-long	black(a)	Offshore	Healthy control
C5-8[a,b]	33 (very high)	5	High-short	Black(a)	Offshore	Stressed @ high temp.
D5-2[a]	30 (control)	5	Control-short	Grey60	Inshore	Healthy control
D5-3	32 (high)	31	High-long	Grey60	Inshore	Stressed @ high temp.
D5-5	33 (very high)	5	High-short	Grey60	Inshore	Healthy @ high temp.
D5-8 bu[b]	30 (control)	31	Control-long	Grey60	Inshore	Healthy control

Underlined samples possessed Durusdinium *spp.-dominated Symbiodiniaceae (Sym) communities; all others were instead* Breviolum *spp.-dominated unless noted otherwise. In the "health status" column, designations were made from Coral Watch scores (Siebeck et al., 2006); those samples colored < E3 were considered to be potentially stressed. Samples denoted by asterisks (*) were omitted from analysis due to low host coral protein yield (<30 μg). "bu" = backup (i.e., original extraction attempt failed). temp. = temperature.*

[a]*Assessed Sym proteins only.* [b]*Mix of* Breviolum *spp. and* Durusdinium *spp. dinoflagellates.*

the most confident centroid. Precursor and fragment mass tolerances were 10 ppm and 0.02 Da, respectively, and up to two missed cleavages were permitted. Each of the 16 RAW files was queried separately against the three fasta libraries, and a false discovery rate (FDR)-adjusted *q*-value of 0.01 was set *a priori*. It should be noted that these stringent search parameters reduced the overall number of peptide "hits" (see "Results.") yet ensured confidence in assignment of the peptide to the correct compartment of origin (host coral vs. dinoflagellate endosymbiont). All proteomic data (RAW MS, MZML, and MZID files), as well as the fasta libraries against which the MZML files were queried, were submitted to "MassIVE" (University of California, San Diego; accession: MSV000086098), ProteomeXchange (Vizcaíno et al., 2014; accession PXD021349), and NOAA's Coral Reef Information System (CoRIS; accession 0227133). Finally, a tab-delineated **Online Supplementary Data File (OSDF)** accompanies this article and includes all data featured in analyses, figures, and tables.

Statistical Analysis-Overview

Sequenced proteins were manually checked by BLASTp (against NCBI nr) to determine if any represented duplicate hits found in both the (1) *O. faveolata* and *P. acuta* holobiont transcriptomes and (2) Symbiodiniaceae and *P. acuta* holobiont transcriptomes; duplicate data were concatenated and scored as presence (1) vs. absence (0) for each protein. Those host and endosymbiont proteins synthesized by only 1–2 samples were excluded from differentially concentrated protein (DCP) analyses, as were those sequenced from ≧11 and ≧12 samples, respectively ("housekeeping proteins"). This difference in criteria between compartments arises from the fact that two samples that were eliminated from the host analysis due to low number of peptide hits, C5-2 and D5-2, were *included* in the Symbiodiniaceae analysis (**Table 1**). When the host and endosymbiont proteins were combined for "total holobiont" analysis, these two samples were excluded ($n = 12$). DCP identification was therefore carried out with only the host and endosymbiont proteins found in 3–10 and 3–11 of the 12 and 14 samples, respectively (hereafter "variable proteins"). In contrast, multivariate statistical analyses (MSA) were conducted with all host coral, endosymbiont, and total holobiont proteins.

MSA

Multi-dimensional scaling (MDS) was undertaken to depict similarity among the 5-day, 31-day, and all 12–14 samples. To assess multivariate differences across eight experimental parameters (EP)- temperature (analyzed as 1: control vs. high and 2: 30, 32, or 33°C), (3) temperature × time, (4) genotype ($n = 4$), (5) site ($n = 3$), (6) shelf (inshore vs. offshore), (7) endosymbiont assemblage (*Breviolum*-dominated, *Durusdinium*-dominated, or mixed-lineage; **Table 1**), and (8) pigmentation (i.e., "health status;" **Table 1**)- PERMANOVA was carried out with PRIMER ver. 6 (United Kingdom) after ensuring that multivariate dispersion was similar across bins with PERMDISP (alpha = 0.05 for all MSA). PRIMER's "relate" algorithm was used to determine whether patterns in the proteomic dataset correlated with those in the experimental one after converting categorical EP data to integers (e.g., inshore = 1, offshore = 2). A Bray-Curtis (BC) similarity matrix was constructed from these recoded EP data and compared to the BC similarity matrix of the presence-absence proteomic data. These same two matrices were compared against one another with PRIMER's "BEST" algorithm to identify the EP that accounted for the greatest degree of variation in the proteomic dataset's similarity structure. As a

second, arguably more robust approach for selecting influential EP, PRIMER's distance-based linear modeling (DistLM) was used to generate backward selection models for which the Bayesian information criterion (BIC) was minimized.

DCPs

We sought to identify proteins sequenced in *all* samples of one treatment (or exclusively within one bin, e.g., genotype) and in *none* of the remaining. Since few fulfilled this criterion, five additional DCP identification methods were executed in JMP Pro® (United States; ver. 15): response screening (RSA; FDR-adjusted multiple comparisons), predictor screening (PSA; proteins accounting for the largest proportion of variation associated with each EP), stepwise discriminant analysis (SDA), stepwise regression (SRA), and generalized multivariate regression (GMR). Each approach is described in detail in the **Supplementary Material**.

RESULTS

Overview of Proteomic Data

Across all samples, 20,185 host and 3,470 Symbiodiniaceae peptides were sequenced (1,673,323 and 495,276 amino acids, respectively); these mapped to 3,824 and 1,116 proteins, respectively, in the coral and Symbiodiniaceae sequence databases queried (FDR-adjusted $q < 0.01$). It should be reiterated that this represents a subset of the total number of proteins sequenced given the high degree of stringency employed; had we been less concerned with correctly elucidating the compartment of origin, host or endosymbiont, a larger number would have been mapped and included in downstream analyses. Details on protein yield per sample, host/endosymbiont protein ratios, and protein coverage can be found in the **Supplementary Material** (notably **Supplementary Figure 1**). Of the 769 presumably unique anthozoan proteins, 300 were later found to be repeated in both the *O. faveolata* and *P. acuta* databases; MSA were carried out with the remaining 469 [of which all but 44 (9.4%) could be identified using alignment-based bioinformatics approaches]. Of the 1,116 endosymbiont proteins, 315 were unique and featured in such analyses [of which all but 74 (23%) could be identified]. Of these 469 host and 315 endosymbiont proteins, 96 and 15, respectively, were housekeeping proteins (**OSDF** and **Supplementary Figure 2**), and 160 and 212, respectively, were only identified in only 1–2 samples. Univariate DCP identification was carried out with the remaining 213 and 88 "variable" host and endosymbiont proteins, respectively.

Multivariate Effects

A number of multivariate effects (**Table 2**) were uncovered for the holobiont (**Figures 1A–C**), host coral (**Figures 1D–F** and **Supplementary Figure 2A**), and Symbiodiniaceae (**Figures 1G–I** and **Supplementary Figure 2B**) proteomes. Predominant findings of interest have been included below, with details found in the **Supplementary Material**. The holobiont proteome was affected by temperature (BEST and DistLM), site (BEST, DistLM, and PERMANOVA), and pigmentation (DistLM), though in the MDS plot (**Figure 1C**) some influence of Symbiodiniaceae assemblage is also evident. For the host proteome alone (**Figures 1D–F** and **Table 2**), site (BEST and PERMANOVA) and genotype (DistLM and PERMANOVA) best distinguished samples. Unlike the host, the PERMANOVA effect of temperature was marginally significant

TABLE 2 | Statistically significant multivariate effects on the *Orbicella faveolata*-Symbiodiniaceae (Sym) proteome.

Experimental parameter	df	Pseudo *F*	*p*	#Permutations	BEST model?	DistLM model?	PERMANOVA multiple comparisons
Holobiont (*n* = 784 proteins)*							
Correlation of BEST model = 0.401. DistLM BIC = 82.9 (R^2 = 0.334)							
Temp. (control vs. high)	1	1.079	0.306	406	Yes	Yes	
Site (*n* = 3)	2	1.543	**0.048**[a]	958	Yes	Yes	The Rocks≠Cheeca Rocks
Health status (*n* = 2)	1	1.216	0.245	216		Yes	
Host coral (*n* = 469 proteins)							
Correlation of BEST model = 0.261. DistLM BIC = 75.7 (R^2 = 0.158)							
Site	2	1.738	**0.030**	942	Yes		The Rocks≠Cheeca Rocks
Genotype	3	1.591	**0.045**[b]	973		Yes	No *post-hoc* differences
Endosymbiont (*n* = 315 proteins)*							
Correlation of BEST model = 0.366. DistLM BIC = 107 (R^2 = 0.130)							
Sym assemblage	2	1.53	**0.014**[c]	988		Yes	*Breviolum*-dominated≠*Durusdinium*-dominated
Health status	1	1.55	0.053	630	Yes		

*Experimental factors that either significantly affected the holobiont, host coral, or Symbiodiniaceae proteomes (PERMANOVA $p < 0.05$; bold font) or were included in PRIMER's BEST and/or DistLM models have been included in the table. For non-statistically significant model terms, please see **Supplementary Table 1**. Note that, although "health status" features three categories in **Table 1**, only two (healthy vs. bleached) were considered in the PERMANOVA. BIC = Bayesian information criterion. Temp. = temperature. *significant rho (Spearman rank-based) between experimental parameter data matrix and proteomic data matrix.*

[a] *See **Figures 1A,B**.* [b] *See **Figures 1D–F**.* [c] *See **Figures 1C,G–I**.*

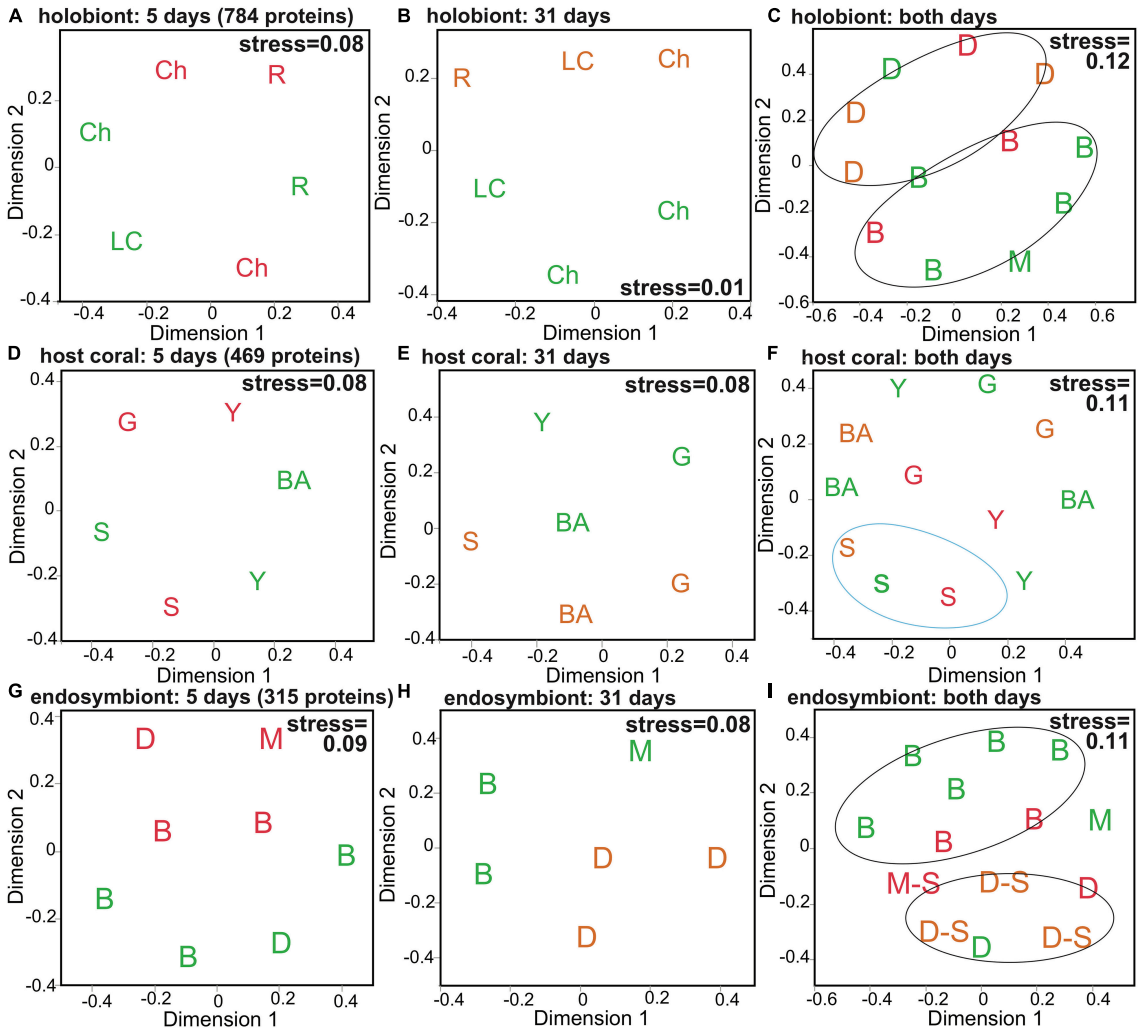

FIGURE 1 | Multivariate analysis of the *Orbicella faveolata*-Symbiodiniaceae (Sym) proteome. Multi-dimensional scaling (MDS) depicting similarity among samples at the 5-day **(A,D,G)**, 31-day **(B,E,H)**, and 5+31-day **(C,F,I)** sampling times for all 784 holobiont proteins **(A–C)**, the 469 host coral proteins **(D–F)**, and the 315 Sym proteins **(G–I)**. Icons have been coded to denote dominant PERMANOVA effects (**Table 2**). Site names **(A,B)** are abbreviated as "Ch" (Cheeca Rocks), "R" (The Rocks), and "LC" (Little Conch); Sym assemblages **(C,G–I)** as "B" (*Breviolum*-dominated), "D" (*Durusdinium*-dominated), and "M" (mixed-lineage; *Breviolum* and *Durusdinium*); and host genotypes **(D–F)** as "S" (skyblue), "G" (grey60), "Y" (lightyellow), and "BA" [black(a)]. In all panels, icons colored green, orange, and red correspond to control (30°C), high temperature (32°C), and very high temperature (33°C) samples, respectively, and samples that were **S**tressed at the time of sampling have been denoted by "–S" in **I**.

for the Symbiodiniaceae proteome (**Figures 1G–I** and **Table 2**), though Symbiodiniaceae assemblage most strongly affected the endosymbionts' proteomes (DistLM and PERMANOVA; i.e., the *Breviolum* and *Durusdinium* proteomes differed significantly from one another.).

DCP Overview

The five DCP identification approaches tended to yield the same suites of proteins as being responsive to each EP of interest (**Supplementary Figure 3** and **Supplementary Tables 2, 3**), and host genotype and temperature were the EP across which the largest number of proteins differed in abundance: 18/47 DCPs (38.3%) for each (**Supplementary Figure 4**). Host genotype also most strongly affected the host proteome at the multivariate scale (see above.), and temperature best accounted for the structure of the holobiont proteomic dataset (**Table 2**). In contrast, although site significantly affected both holobiont and host proteomes (**Table 2**), only three site-responsive DCPs were uncovered (**Supplementary Figure 4C**); this is because, with the exception of Cheeca Rocks (for which two genotypes were analyzed), only one genotype was analyzed at each of the remaining sites. For this reason, we generally discuss genotype and site effects in tandem hereafter. The functional breakdowns of the 27 coral (**Table 3**), 20 endosymbiont (**Table 4**), and 47 holobiont DCPs can be seen in **Figures 2A,B,** and **C**, respectively, and the most dominant cellular processes (gene ontology) of the coral hosts and endosymbiotic dinoflagellates were metabolism (**Figure 2A**) and photosynthesis (**Figure 2B**), respectively. When analyzing all

TABLE 3 | Host coral differentially concentrated proteins (DCPs).

Contig	Identity	Function	Trend(s)
Temperature-responsive proteins (*n* = 8; Figure 3)			
comp111800_c2_seq1	Ras-related protein rab11	Vesicle fusion and trafficking	High (32°C) > all others, stressed > healthy
contig8136	Large subunit ribosomal protein L18e	Translation	Control-temp. only, healthy > stressed
OFAVBQ_DN204682_c1_g1_i2	40S ribosomal protein S3	Translation	Control temp. only
OFAVBQ_DN211578_c1_g2_i4	Citrate synthase	Metabolism	Not expressed by stressed corals
OFAVBQ_DN212753_c2_g1_i4	Erlin-1	Cholesterol/lipid homeostasis	Control-5-day > all others
OFAVBQ_DN214053_c3_g2_i3	Calumenin	Protein folding and sorting	High > control temp., stressed > healthy
OFAVBQ_DN215575_c0_g1_i3	Glutamine synthetase-like	Metabolism	Control > high temp.
OFAVBQ_DN222739_c0_g1_i5	Unknown[a]	Unknown	High (32°C) > all others, stressed > healthy
Genotype-responsive proteins (including site effects; *n* = 14; Figure 4)			
OFAVBQ_DN221283_c3_g2	Collagen alpha-1(I) chain-like	Structural	Offshore only
OFAVBQ_DN218618_c3_g1_i10	Galaxin-like	Calcification	Not found in lightyellow
OFAVBQ_DN208448_c1_g1_i1	Protein DD3-3-like	Cell-cell interactions	Not found in lightyellow
OFAVBQ_DN224869_c0_g1_i2	Laccase-25-like isoform X1	Metabolism	Grey60 > other genotypes
OFAVBQ_DN218284_c7_g2_i4	Dermatopontin	Cell-cell interactions	Grey60 only
OFAVBQ_DN205148_c1_g2_i1	Rhamnose-binding lectin	Cell-cell interactions	Grey60 only
OFAVBQ_DN103730_c0_g1_i1	14-3-3 protein epsilon	Signaling	Grey60 > all other genotypes
OFAVBQ_DN210981_c4_g1_i3	Legumain-like	Protease	Not expressed by skyblue
OFAVBQ_DN213163_c3_g1_i11	Transaldolase	Metabolism	Cheeca genotypes > others
OFAVBQ_DN218286_c0_g1_i1[c]	Glycerol kinase	Metabolism	Cheeca genotypes > others
OFAVBQ_DN199317_c0_g3_i1	Collagen triple helix repeat-containing protein 1	Structural	Lightyellow only
OFAVBQ_DN197100_c0_g1_i1	Protein PRY1-like	Lipid secretion	Not found in offshore samples
OFAVBQ_DN203970_c3_g5_i1	Elongation factor 1-beta-like	Translation	Lightyellow > other genotypes
OFAVBQ_DN197154_c0_g3_i1	Galaxin-like	Calcification	Lightyellow only
Shelf-responsive proteins (*n* = 3; Supplementary Figure 5)			
OFAVBQ_DN217467_c0_g1_i3	40S ribosomal protein S4-like	Translation	Offshore > inshore
OFAVBQ_DN204853_c0_g1_i1	Nitrilase with biotinidase and vanin domains	Metabolism	Offshore > inshore
OFAVBQ_DN192542_c0_g1_i1	Nucleoside diphosphate kinase	Metabolism	Not found in offshore samples
Other effect types (*n* = 2; Supplementary Figure 5)			
OFAVBQ_DN198838_c3_g2_i3	40S ribosomal protein S20	Translation	*Breviolum* assemblages only
OFAVBQ_DN218234_c4_g1_i2[b]	MAC/perforin domain	Immunity	Stressed > healthy

For details on the analytical approach(es) used to identify the 27 DCPs, please see ***Supplementary Table 2****, and for a comparison with other studies, please see* ***Supplementary Table 4****. Sym = Symbiodiniaceae. temp. = temperature.*
[a]*also known as sushi, von Willebrand factor type A, EGF, and pentraxin domain-containing protein 1.* [b]Durusdinium-*dominated assemblages only.*

47 DCPs together (**Figure 2C**), these two processes accounted for nearly 40% of all DCPs, with translation being the third most affected process.

Host Coral DCPs

Of the 27 host DCPs (**Table 3** and **Supplementary Tables 2, 4**), 8 were significantly affected by temperature (**Figure 3**), and a PCA with these separated samples of the control, 32, and 33°C treatments (**Figure 3A**). Only one DCP, ras-related protein rab11 (**Figure 3B**), fulfilled our optimal criterion of being synthesized only by corals of a high-temperature treatment (32°C). Three additional DCPs (**Figure 3B**)- large subunit ribosomal protein L18e, 40S ribosomal protein S3, and glutamine synthetase- were instead *only* translated by controls. Metabolism and translation were the two cellular processes featuring the largest number of temperature-sensitive host coral proteins (**Figure 3C**). There was also a strong effect of host genotype on 14 of the 27 DCPs (**Figure 4**, **Table 3**, and **Supplementary Tables 2, 4**), and 5 of these were only found in one of the four genotypes (**Figure 4B**). For a detailed treatise of these 14 DCPs, please consult the **Supplementary Material**.

Symbiodiniaceae DCPs

Temperature and Symbiodiniaceae assemblage were the predictors that generated the greatest number of Symbiodiniaceae DCPs (**Supplementary Figure 4B**, **Table 4**, and **Supplementary Tables 3, 5**): 9 and 7, respectively (with 2 of these affected by both temperature and assemblage). These EP were also associated with the lowest PERMANOVA *p*-values (**Table 2**). The nine temperature-responsive DCPs led to separation among samples in a PCA (**Figure 5A**). Although none were maintained only in high-temperatures and not in controls, four were absent from high-temperature samples (**Figure 5B**): photosystem II chlorophyll-binding protein CP43, an unknown protein, a phosphoglycerate

TABLE 4 | Symbiodiniaceae (Sym) differentially concentrated proteins.

Contig	Identity	Function	Trend(s)
Temperature-responsive proteins (*n* = 9; Figure 5)			
SYMBOF_DN176524_c0_g1_i1.p1	Rab-related GTPase family rab5	Molecular trafficking	High-long > control long
SYMBOF_DN190166_c0_g1_i2.p1	ADP-ribosylation factor	Molecular trafficking	H33 < others
SYMBOF_DN201098_c1_g4_i1.p1	Photosystem II chlorophyll-binding protein CP43	Photosynthesis	Control temp. only
SYMBOF_DN192802_c0_g1_i2.p1	Unknown	Unknown	Control-short > all others
SYMBOF_DN196424_c4_g3_i3.p1	Phosphoglycerate kinase	Metabolism	Control > high temp.
SYMBOF_DN201284_c0_g2_i5.p1	Chaperone protein DNAJ (HSP40)	Stress response	Control > high temp., Healthy > stressed
SYMBOF_DN201349_c3_g4_i2.p1	Fucoxanthin-chlorophyll a-c binding protein B	Photosynthesis	Control > high temp., Healthy > stressed
SYMBOF_DN163023_c0_g2_i2.p1	60S ribosomal protein L3 (see also **Figure 6C**.)	Translation	Control > high temp., Mostly D < others
SYMBOF_DN218526_c0_g1_i5.p1	Chloroplast soluble PCP precursor-1 (see also **Figure 6C**.)	Photosynthesis	H32 < all others, Healthy > stressed, Mostly D < others
Sym assemblage-responsive proteins [*n* = 5 (excluding two that were also affected by temp. and instead found above); Figure 6]			
SYMBOF_DN191788_c0_g1_i1.p1	Peridinin chlorophyll a binding protein	Photosynthesis	Mostly B > all others, Lightyellow > others
SYMBOF_DN208331_c3_g1_i2.p1	Fucoxanthin-chlorophyll a-c binding protein F-1	Photosynthesis	Healthy > stressed, Mostly D < others
SYMBOF_DN211305_c3_g1_i1.p1	Chloroplast soluble PCP precursor-2	Photosynthesis	Mostly D only
SYMBOF_DN215694_c5_g7_i1.p1	Fucoxanthin-chlorophyll a-c binding protein F-2	Photosynthesis	Mostly B only
SYMBOF_DN217254_c0_g1_i1.p1	Heat shock protein 90 (HSP90)	Stress response	Not in mix of B and D
Other effects (*n* = 6; Supplementary Figure 5)			
SYMBOF_DN192258_c0_g6_i3.p1	Unknown	Unknown	Lightyellow > all others
SYMBOF_DN223629_c2_g4_i1.p2	Peridinin-chlorophyll A binding protein	Photosynthesis	Lightyellow < all others
SYMBOF_DN184263_c0_g2_i1.p1	Acyl-CoA-binding protein	Metabolism	Skyblue only
SYMBOF_DN181028_c0_g1_i1.p1	Luminal-binding protein 5 (BIP5)	Stress response	Grey60 only
SYMBOF_DN214774_c2_g1_i1.p1	Fucoxanthin-chlorophyll a-c binding protein F	Photosynthesis	Inshore > offshore, Healthy > stressed
SYMBOF_DN214550_c0_g1_i1.p1	Ubiquitin	Stress response	Cheeca Rocks < others

For details on the analytical approach(es) used to identify the 20 DCPs and a comparison with other published works, please see ***Supplementary Tables 3*** *and* ***5****, respectively. H32 and H33 = high-temperature (temp; 32°C) treatment and very high temp. (33°C) treatments, respectively. "mostly B," "mostly D," and "mix of B and D" correspond to* Breviolum*-dominated,* Durusdinium*-dominated, and mixed* Breviolum+Durusdinium *Sym assemblages, respectively. "Short" and "long" in the "Trend(s)" column correspond to the 5- and 31-day sampling times, respectively. PCP = peridinin chlorophyll-a binding protein. QC = quality control (protein trafficking and folding).*

kinase, and a DNAj chaperone protein (i.e., HSP40). Two additional proteins were not synthesized by any 32°C sample (**Figure 5B**): 60S ribosomal protein L3 and a chloroplast-soluble peridinin chlorophyll a-binding protein (PCP). One-third of the Symbiodiniaceae temperature-sensitive DCPs were involved in photosynthesis (**Figure 5C**). To gain greater insight into Symbiodiniaceae assemblage effects (**Figure 6**), the mRNA read breakdowns for the 14 samples were plotted (**Figure 6A**). For concentration trends and functional breakdowns of the seven Symbiodiniaceae assemblage-responsive DCPs (**Figures 6B,C**), please consult the **Supplementary Material** (particularly **Supplementary Figure 5**).

DISCUSSION

Herein we sought to uncover high-temperature effects on cellular biology of massive coral genotypes from distinct thermal habitats that varied in their capacity to acclimate to experimentally elevated temperatures. There were clear proteomic differences among the four host genotypes and three Symbiodiniaceae assemblages, and the Symbiodiniaceae proteomes were relatively more affected by high-temperature exposure at the multivariate scale than their hosts. Symbiodiniaceae dinoflagellates also demonstrate more pronounced mRNA-level responses to high temperatures than their cnidarian hosts (Mayfield et al., 2014), and their proteomic strategy for confronting environmental change is also different from that of other corals studied to date (Mayfield et al., 2016); the latter finding was corroborated herein. Proteins involved in metabolism and translation were most likely to be affected by high-temperature exposure in the cnidarian hosts, whereas the temperature-sensitive endosymbiont DCP pool was dominated by photosynthesis proteins; this substantiates findings dating back over 20 years (e.g., Jones et al., 1998). That being said, molecular trafficking proteins (e.g., rab) were affected by thermal stress in both compartments and are discussed in greater detail below.

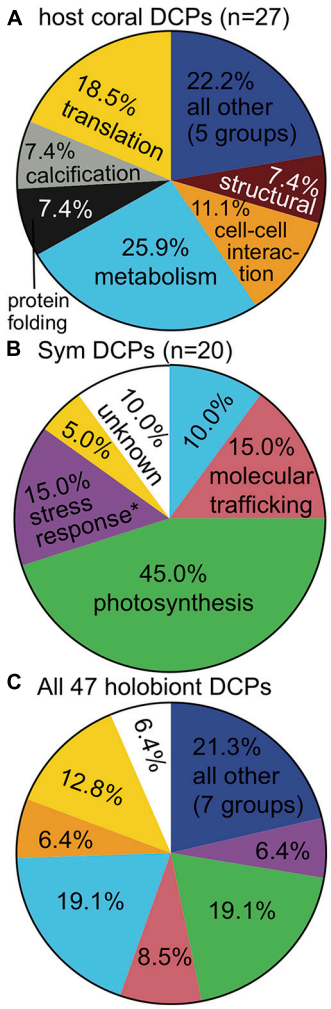

FIGURE 2 | Functional breakdown of differentially concentrated proteins (DCPs). The cellular process color codes are shown only the first time they are used (the exception being the "all other" category). When proteins involved in a cellular process (e.g., stress response) were documented at a significantly higher proportion in one compartment vs. the other (Fisher's exact test, $p < 0.01$), the process name in the compartment with the higher value has been denoted by an asterisk (*). Processes specific to anthozoan hosts **(A)** (i.e., calcification) and dinoflagellates **(B)** (i.e., photosynthesis) were excluded from this analysis.

Of the 784 proteins profiled, only 17 (2.2%) were significantly affected by temperature. This could be due to one of at least two reasons. First, there was high proteomic fidelity to host genotype. Even after several weeks of high-temperature exposure, the host proteomes clustered as much by genotype as by their temperature treatment. Such distinct differences in protein signatures (and the associated high inter-genotype variability) may have thwarted our ability to uncover temperature-sensitive host DCPs. Instead, those eight identified represent "core" proteins exploited by all four genotypes upon high-temperature exposure. Since the low number of universal high-temperature-sensitive proteins uncovered (including nine of endosymbiont origin) could have also been due to having pooled the data from samples that were bleaching with those that had instead potentially acclimated, a separate, genotype-to-genotype analysis has been provided in the **Supplementary Material**. Briefly, the four host genotypes manifested distinct stress responses, as well as dissimilar strategies for acclimating to high temperatures. For instance, of the 80 and 63 proteins found to be involved in high-temperature acclimation ($n = 3$ controls vs. $n = 3$ actively acclimating corals) and bleaching ($n = 3$ controls vs. $n = 3$ bleaching corals), respectively, only 4 (5%; **Supplementary Figure 6**) and 5 (8%; **Supplementary Figure 7**) were utilized in the acclimation and bleaching responses, respectively, of multiple genotypes. The fact that coral fragments sampled from colonies that were within even several meters of each other *in situ* utilized entirely different means of acclimating (or succumbing) to high temperatures is puzzling, unexpected, and is under active investigation by ourselves and others working in South Florida. Perhaps, the location on the colonies from which cores were made could accommodate some of the variation (despite efforts made to be consistent with respect to the relative positioning of the drill-bit); biopsies from more shaded areas might display differing means of thermo-acclimation on account of entrained light effects, even after acclimation in a common garden prior to experimentation. Given the low overlap in the acclimation and stress responses across genotypes/sites, as well as the current inability to rigorously account for such variation, we have instead focused the remainder of our discussion on the common elements uncovered.

Of the 17 temperature-sensitive DCPs, three differed in abundance between samples that were bleaching (C5-2) or beginning to bleach (A4-5 and D5-3) at the time of sampling vs. high-temperature samples that resisted bleaching: a host ras-related protein rab11 involved in vesicle trafficking and fusion [only synthesized by visibly stressed samples (color score < E3)], an unknown host coral protein with sushi, von Willebrand factor type A, EGF, and pentraxin domains (OFAVBQ_DN222739_c0_g1_i5; only synthesized by visibly stressed samples), and an endosymbiont fucoxanthin-chlorophyll a-c binding protein F (FCPE; chloroplastic; SYMBOF_DN208331_c3_g1_i2.p1-1) involved in photosynthesis (not translated by visibly stressed samples). Given the large number of FCPE proteins even within the endosymbiont DCP pool, it is unclear whether the absence of one isoform would have significant implications for photosynthetic function. In contrast, the two host proteins were distinct, and numerous rab proteins involved in vesicle and lipid trafficking were up-regulated at high temperatures in bleaching offshore samples in the genotype-by-genotype analysis (**Supplementary Figures 6, 7**). Furthermore, an endosymbiont rab5 protein was up-regulated in the three bleaching samples.

Prior works have also uncovered proteins involved in vesicle, lipid, and lipid body trafficking to be affected by high-temperature exposure in host corals and their endosymbionts (Mayfield et al., 2018a,b), and the role of lipid trafficking within the anthozoan-dinoflagellate endosymbiosis has been well-studied (Chen et al., 2012, 2015, 2017). Prior work on

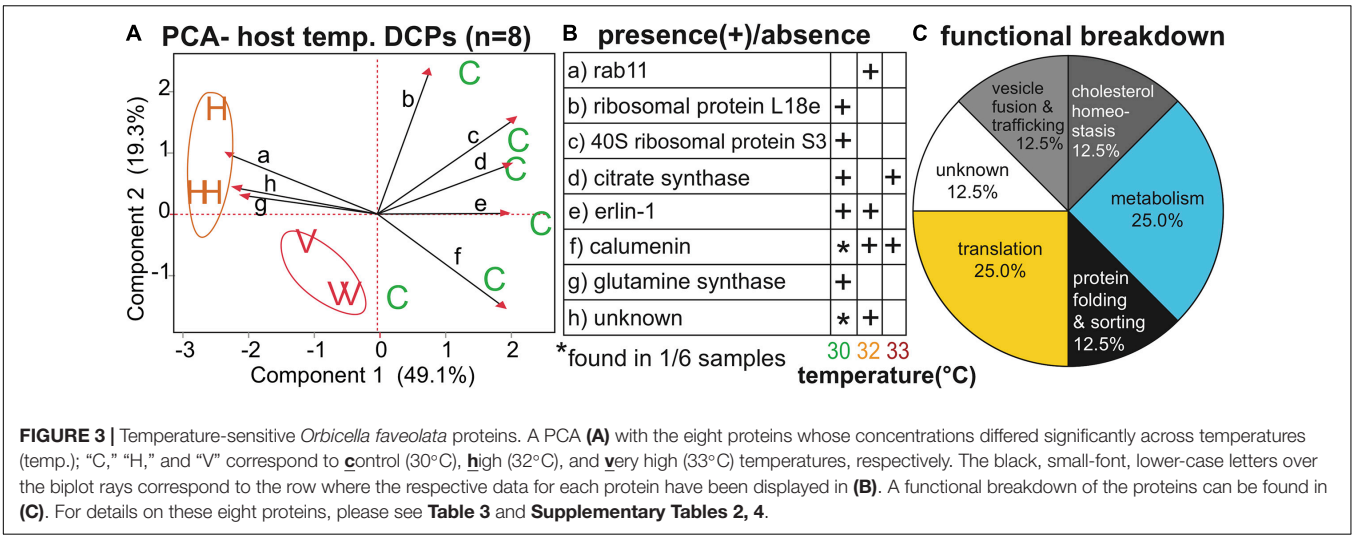

FIGURE 3 | Temperature-sensitive *Orbicella faveolata* proteins. A PCA **(A)** with the eight proteins whose concentrations differed significantly across temperatures (temp.); "C," "H," and "V" correspond to **c**ontrol (30°C), **h**igh (32°C), and **v**ery high (33°C) temperatures, respectively. The black, small-font, lower-case letters over the biplot rays correspond to the row where the respective data for each protein have been displayed in **(B)**. A functional breakdown of the proteins can be found in **(C)**. For details on these eight proteins, please see **Table 3** and **Supplementary Tables 2, 4**.

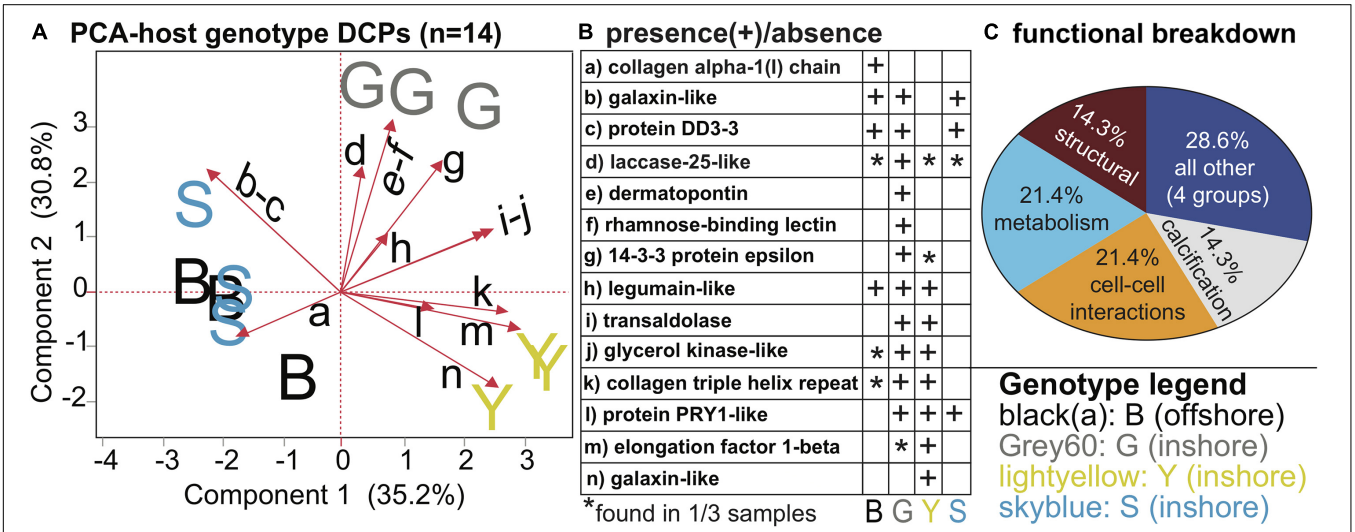

FIGURE 4 | Genotypic differences in *Orbicella faveolata* proteins. A PCA with the 14 proteins whose concentrations differed significantly across host genotypes **(A)**. Please note that the black, small-font, lower-case letters adjacent to the biplot rays correspond to the row where the respective data for each protein have been displayed in **(B)**, and the legend for the sample icons can be found in the bottom right corner. A functional breakdown of these proteins is depicted in **(C)**. For further details, please see **Table 3** and **Supplementary Tables 3, 5.**

rab11 in particular has implicated it in endocytic recycling (Lock and Stow, 2005), whereby membrane components internalized in endosomes are transported to (and then recycled at) the plasma membrane (Montealegre and van Endert, 2010). This protein has also been linked to the establishment and maintenance of the anemone-dinoflagellate endosymbiosis (Chen et al., 2003). Specifically, rab11 is normally kept away from the symbiosome, but high concentrations are documented around phagosomes containing dying endosymbionts at high temperatures (Chen et al., 2005a,b). Later, Downs et al. (2009) demonstrated that other rab proteins (e.g., rab7) are involved in symbiophagy, whereas Weston et al. (2015) took the large number of rab proteins uncovered in corals exposed to high temperatures for several hours to be indicative of dinoflagellate cell exocytosis. However, as was the case herein, their sampling regimen did not explicitly allow for the uncovering of proteins that *enact* bleaching, merely those *associated with* it. Whether up-regulation of rab11 and other rab proteins reflects the possibility of symbiophagy, dinoflagellate exocytosis, or simply an increased need to traffic membrane components to the plasma membrane during periods of elevated temperature remains to be determined. Furthermore, given that a many corals switched symbionts over the duration of the study (**Figure 6**), differential rab protein levels may simply be a testament to the need to resheath newly acquired dinoflagellate cells with symbiosome membranes.

Prior works on endosymbiotic anthozoans have yielded conflicting results with respect to the relative importance of canonical eukaryotic stress response (CSR) proteins

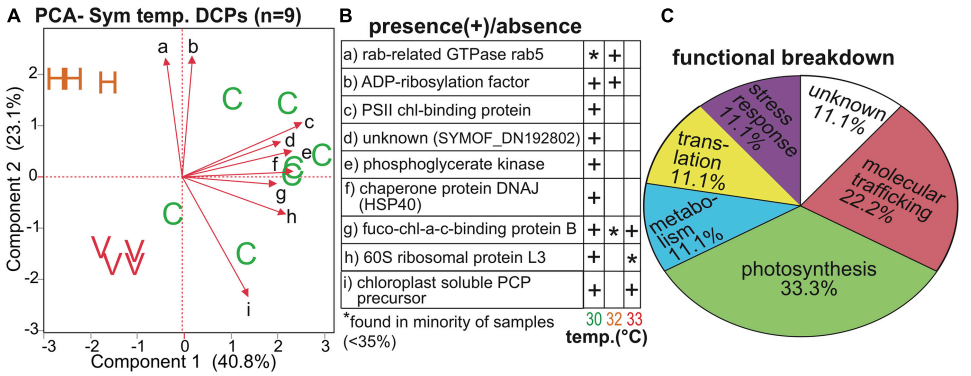

FIGURE 5 | Temperature-sensitive Symbiodiniaceae proteins. A PCA with the nine proteins whose concentrations differed significantly across temperatures **(A)** in which "C," "H," and "V" correspond to **c**ontrol (30°C), **h**igh (32°C), and **v**ery high (33°C) temperatures, respectively. The black, small-font, lower-case letters adjacent to the biplot rays correspond to the row where the respective data for each protein have been displayed in **(B)**. A functional breakdown of these proteins is depicted in **(C)**. chl = chlorophyll. Fuco-chl-a-c binding = fucoxanthin-chl-a-c binding protein B. PCP = peridinin chl-a-binding protein. PS = photosystem II. For details on these nine proteins, please see **Table 4** and **Supplementary Tables 3, 5**.

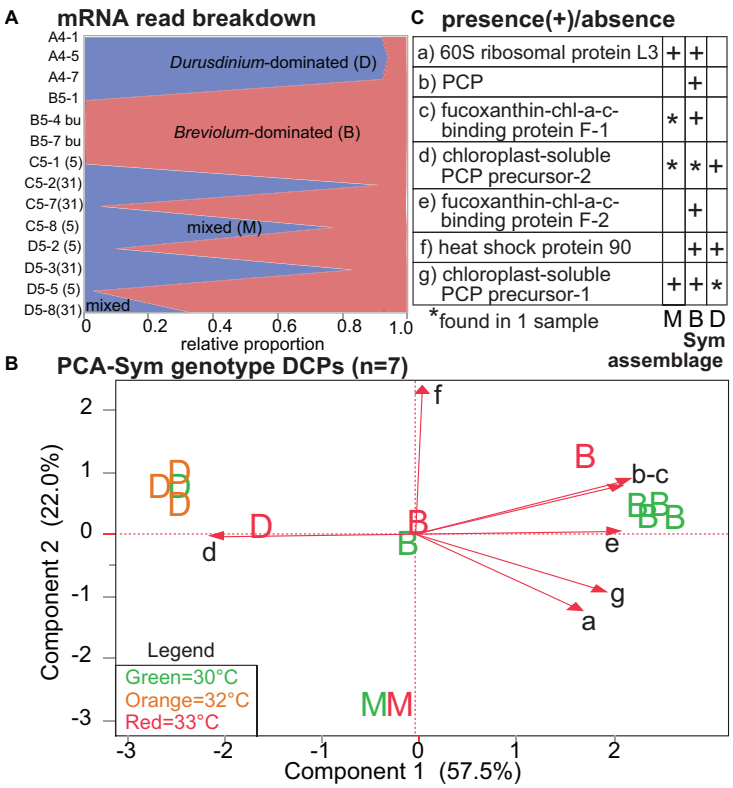

FIGURE 6 | Proteomic differences across Symbiodiniaceae (Sym) lineages. In the mRNA breakdown of the 14 samples analyzed by shotgun proteomics **(A)**, the blue and red shading reflect the proportions of *Durusdinium* spp. ("D") and *Breviolum* spp. ("B") dinoflagellates, respectively. Samples for which no genus comprised >80% of the mapped mRNA reads were deemed "mixed-lineage" ("M"). The numbers in parentheses following the sample codes for the two genotypes that underwent endosymbiont shuffling, C5 [black(a) from Little Conch (offshore)] and D5 [grey60 from Cheeca Rocks (inshore)], represent sampling days. A PCA with seven proteins whose concentrations differed significantly across Sym assemblages **(B)**; letters correspond to Sym assemblages, and the colors correspond to temperatures (see inset legend.) The black, small-font, lower-case letters adjacent to the biplot rays correspond to the row where the respective data for each protein have been displayed in **(C)**. Five, one, and one of these proteins were involved in photosynthesis (71.4%), the stress response (14.3%), and translation (14.3%), respectively. chl = chlorophyll. PCP = peridinin chl-a binding protein. For details on these nine proteins, please see **Table 4** and **Supplementary Tables 3, 5**.

TABLE 5 | Select stress response "housekeeping" proteins, stress-sensitive proteins involved in the canonical eukaryotic stress response (CSR), and anthozoan-dinoflagellate bleaching-associated proteins identified in prior works.

Accession	Compartment	Protein name	Prior mRNA/protein trend	mRNA/protein reference(s)	Prior trend corroborated?
HOUSEKEEPING CSR PROTEINS					
OFAVBQ_DN205531_c1_g1_i1	Coral host	78 kDa glucose-regulated protein (GRP78)	Stress-sensitive	Aranda et al. (2011) Lõhelaid et al. (2014)[a]	No No
OFAVBQ_DN217505_c2_g1_i3	Coral host	Endoplasmin-like isoform X1	Stress-sensitive	Ruiz-Jones and Palumbi (2017)	No
OFAVBQ_DN202907_c9_g3_i1	Coral host	Glutathione S-transferase	Constitutively maintained	**Whalen et al. (2010)[a]**	Yes
OFAVBQ_DN215553_c1_g3_i1	Coral host	Heat shock cognate 71 kDa protein	Constitutively maintained	**Oakley et al. (2017)[b]** Poli et al. (2017)	Yes Yes[c]
OFAVBQ_DN214823_c0_g2_i2	Coral host	HSP60	Stress-sensitive	**Chow et al. (2009)**	No
OFAVBQ_DN218952_c1_g1_i5	Coral host	HSP90-beta	Constitutively maintained	Nakamura et al. (2012)	Yes
OFAVBQ_DN225001_c3_g1_i2	Coral host	Peroxiredoxin-5	Stress-sensitive	Levy et al. (2016)	No
OFAVBQ_DN208085_c0_g2_i1	Coral host	Peroxiredoxin-6	Stress-sensitive	**Mayfield et al. (2018b)**	No
SYMBOF_DN199915_c1_g4_i1.p1	Endosymbiont	HSP70	Constitutively maintained	Putnam et al. (2013)	Yes
SYMBOF_DN200180_c0_g1_i1.p1	Endosymbiont	HSP70	Constitutively maintained	Mayfield et al. (2011)	Yes
SYMBOF_DN197301_c4_g6_i3.p1	Endosymbiont	HSP90[d]	Constitutively maintained	Mayfield et al. (2017a,b,c)	Yes No
SYMBOF_DN217254_c0_g1_i1.p1	Endosymbiont	HSP90	Stress-sensitive	Rosic et al. (2011)[e]	
SYMBOF_DN198813_c2_g3_i2.p1	Endosymbiont	HSP90	Stress-sensitive	Lin et al. (2019)	No
ANTHOZOAN-DINOFLAGELLATE STRESS RESPONSE AND BLEACHING-ASSOCIATED PROTEINS IDENTIFIED IN PRIOR WORKS					
OFAVBQ_DN172775_c0_g1_i1	Coral host	Beta-gamma crystallin	Stress-sensitive	Downs et al. (2002)	No
comp97680_c0_seq1	Coral host	Calmodulin	Stress-sensitive	Ricaurte et al. (2016)	No
SYMBOF_DN174588_c0_g1_i1.p1	Endosymbiont	Calmodulin	Stress-sensitive	Weston et al. (2015)	No
OFAVBQ_DN223119_c2_g2_i5.p1	Coral host	Carbonic anhydrase	Stress-sensitive	Weston et al. (2015)	No
OFAVBQ_DN214557_c1_g2_i5	Coral host	Caspase	Stress-sensitive	Tchernov et al. (2011)	No
SYMBOF_DN215553_c1_g1_i2.p1	Endosymbiont	Chaperone protein DNAK	Stress-sensitive	Weston et al. (2015)	No
SYMBOF_DN182054_c0_g1_i1.p1	Endosymbiont	E3 ubiquitin-protein ligase	Stress-sensitive	Mayfield et al. (2018b)	No
OFAVBQ_DN194262_c1_g1_i1	Coral host	HSP70	Stress-sensitive	Seveso et al. (2017)	No
SYMBOF_DN204865_c1_g2_i1.p1	Endosymbiont	HSP90	Stress-sensitive	Ross (2014)	No
SYMBOF_DN165260_c0_g1_i2.p1	Endosymbiont	Glutathione S-transferase	Stress-sensitive	Weston et al. (2015)	No
SYMBOF_DN239554_c0_g1_i1.p1	Endosymbiont	Peptidylprolyl isomerase D	Stress-sensitive	Mayfield et al. (2018b)	Yes
SYMBOF_DN228106_c0_g1_i1.p1	Endosymbiont	Peroxiredoxin-1	Stress-sensitive	Weston et al. (2015)	No
SYMBOF_DN205301_c4_g1_i1.p1	Endosymbiont	Peroxiredoxin-6[e]	Stress-sensitive	Mayfield et al. (2018b)	No
OFAVBQ_DN213774_c4_g1_i3	Coral host	Superoxide dismutase	Constitutively maintained	Coles and Brown (2003)	No
			Stress-sensitive	Oakley et al. (2017)	No
OFAVBQ_DN199726_c0_g2_i1	Coral host	Thioredoxin	Constitutively maintained	Cziesielski et al. (2018)	No
			Stress-sensitive	Ricaurte et al. (2016)	No
Contig14748	Coral host	(poly)ubiquitin-B	Stress-sensitive	Coles and Brown (2003)	No
SYMBOF_DN214550_c0_g1_i1.p1	Endosymbiont	Ubiquitin[f]	Stress-sensitive	Barshis et al. (2010)	No

*Please note that a more detailed version of this table featuring additional proteins can be found in the **Supplementary Material** (**Supplementary Table 6**). In the "Prior mRNA/protein trend" column, molecules have either been deemed "stress-sensitive" or "constitutively maintained" based on results of prior gene expression (reference in regular font) or protein-based (**bold font**) studies. In the second half of the table, we instead looked at CSR and bleaching-associated proteins identified in prior proteomic works of anthozoans to determine whether trends were congruent. Please note that this does not represent an exhaustive list of all proteins involved in the CSR (Kultz, 2005), and some heat shock proteins (HSPs) found previously at the mRNA level to be stress sensitive (e.g., hsp32 in Seveso et al., 2020) were not sequenced herein. One CSR protein uncovered herein, an endosymbiont HSP40 (SYMBOF_DN201284_c0_g2_i5.p1), was down-regulated in bleaching corals.*

*[a]Octocoral study. [b]Sea anemone study. [c]Subtle depth effects noted. [d]Note that one Symbiodiniaceae HSP90 differed in concentration across Symbiodiniaceae assemblages. [e]Affected by infection status in Sproles et al. (2019), with another isoform (peroxiredoxin-1) up-regulated at high temperatures in Weston et al. (2015). [f]See **Table 4**.*

in thermo-acclimation (**Table 5** and **Supplementary Tables 4–6**). Whereas both corals and Symbiodiniaceae from upwelling reefs constitutively express mRNAs encoding heat shock proteins (HSPs; Mayfield et al., 2011, 2012), others have observed a more traditional heat shock response at the gene (Rosic et al., 2011) and protein (Coles and Brown, 2003) levels in corals from stable temperature environments. Herein numerous CSR proteins in both the host and dinoflagellate compartments were among the most abundant housekeeping proteins found in all samples, including controls (**Table 5** and **OSDF**). Although one HSP90 was a DCP, it only differed in concentration across endosymbiont assemblages. Furthermore, an endosymbiont HSP40 (chaperone protein DNAj) was only sequenced from controls, and another endosymbiont molecular chaperone, DNAK, was only up-regulated at high temperatures in one host genotype (grey60; **Supplementary Figure 7** and **OSDF**). As an additional example, peroxiredoxins, which are important in the stress responses of both corals (Weston et al., 2015) and fish (Kultz et al., 2007), were instead constitutively maintained in the corals sampled herein (**Table 5**).

As a notable exception, one CSR protein, peptidylprolyl isomerase (Kim et al., 2017), was found only in stressed endosymbiont communities in Mayfield et al. (2018b), and, when profiling the bleaching response on a genotype-to-genotype basis herein (**Supplementary Material**), this antioxidant was also up-regulated at high temperatures in endosymbiont communities within two of the three inshore genotypes (skyblue and grey60). This remains, at present, the lone protein that both represents a CSR protein *and* has been found to be up-regulated at high temperature in more than one study (**Table 5**). The peptidylprolyl isomerase is also critical in the cellular response of sea squirts (Lopez et al., 2017), and even marine fish (Kultz et al., 2007), to environmental stress. With the exception of this molecule, our results obfuscate efforts to use CSR mRNA or protein concentration levels as biomarkers for coral health/resilience given their constitutively high abundance. Rab protein levels, as also recommended by Weston et al. (2015), appear to be better candidates for gauging levels of coral heat dosing.

Constitutive activation of the CSR is not a common strategy for most life forms (Hochachka and Somero, 2002) given the high metabolic burden it poses (Sokolova et al., 2012). Specifically, the energy associated with re-establishing homeostasis could detract from growth and reproduction. Perhaps the excess energy from endosymbiont photosynthesis permits sustained periods of engaged CSR. It is also possible that the constitutive maintenance of a large number of CSR and antioxidant proteins could simply be indicative of the high protein turnover and metabolic rate associated with these corals in summer; the low frequencies of oxidative stress and apoptosis markers (**Table 5** and **OSDF**) further signify that the control corals may not have actually been exhibiting a CSR. In the future, we will analyze the proteomes of field biopsies from these same coral colonies collected during different seasons to determine whether (1) the high control coral levels of certain CSR proteins documented herein reflect acclimation to a relatively high summer mean of 30°C or (2) they are presented year-round (*sensu* Mayfield et al., 2019). It will also be worthwhile repeating the experiment in winter (when ambient temperatures are only 21–22°C) to determine whether high-temperature-challenged corals acclimated to colder temperatures exhibit a more traditional CSR upon heating.

It was hypothesized over 20 years ago that protein turnover is the cellular process that ultimately dictates whether corals will effectively acclimatize (Gates and Edmunds, 1999), with highest turnover rates generally associated with the more thermotolerant massive corals like *O. faveolata*. If high concentrations of CSR and protein turnover-associated proteins are not necessarily indicative of stress, but instead high protein turnover rates, then the observation that the majority of the temperature-responsive proteins were involved in host coral lipid trafficking and metabolism and Symbiodiniaceae lipid trafficking and photosynthesis (see **Supplementary Material**.) could signify that these energy mobilization processes are modulated in a way that ensures that there is sufficient cellular ATP to maintain the high metabolic rate and turnover needed to continually break down proteins, refold denatured ones, and otherwise maintain proteostasis under elevated temperatures (beyond those already high protein turnover rates characteristic of controls). This could also explain the up-regulation of a key regulator of protein turnover, calumenin, in bleaching samples (herein and in Oakley et al., 2017); indeed, this protein is up-regulated upon chronic high-temperature exposure in other marine invertebrates (Sleight et al., 2018). Although signaling molecules went largely undetected by our proteomic approach, it is possible that lipid-signaling molecules generated by the lipid trafficking proteins uncovered served as the molecular "intermediaries" through which proteostasis and lipid metabolism were linked. Whether or not constitutively high protein turnover, or even an active CSR, is an energetically sustainable strategy over longer-term timescales remains to be determined, but, at the time of writing, the inshore corals continue to persist and reproduce annually, even as those around them succumb to bleaching and/or SCTLD.

DATA AVAILABILITY STATEMENT

The datasets presented in this study can be found in online repositories, as well as in the **Online Supplementary Data File**. The names of the repository/repositories and accession numbers can be found in the article and its **Supplementary Material**

ETHICS STATEMENT

Ethical review and approval was not required for the animal study because this study was carried out with reef corals (see **Supplementary Material** for permitting information).

AUTHOR CONTRIBUTIONS

AM, CA, and GK collected the samples, ran the experiments, and carried out the molecular benchwork. AM analyzed the data, created the figures, and wrote the manuscript. IE and DM secured funding and mobilized boat and laboratory support.

FUNDING

This project was funded by the NOAA 'OMICs Initiative (Project #NRDD18978 to DM and Kelly Goodwin).

ACKNOWLEDGMENTS

We thank members of the AOML Coral Program (OCED/AOML/NOAA) for field and experimental support.

SUPPLEMENTARY MATERIAL

The Supplementary Material for this article can be found online at: https://www.frontiersin.org/articles/10.3389/fmars.2021.660153/full#supplementary-material

REFERENCES

Aranda, M., Banaszak, A. T., Bayer, T., Luyten, J. R., Medina, M., and Voolstra, C. R. (2011). Differential sensitivity of coral larvae to natural levels of ultraviolet radiation during the onset of larval competence. *Mol. Ecol.* 20, 2955–2972. doi: 10.1111/j.1365-294x.2011.05153.x

Barshis, D. J., Stillman, J. H., Gates, R. D., Toonen, R. J., Smith, L. W., and Birkeland, C. (2010). Protein expression and genetic structure of the coral *Porites lobata* in an environmentally extreme Samoan back reef: does host genotype limit phenotypic plasticity? *Mol. Ecol.* 19, 1705–1720. doi: 10.1111/j.1365-294x.2010.04574.x

Bellantuono, A. J., Granados-Cifuentes, C., Miller, D. J., Hoegh-Guldberg, O., and Rodriguez-Lanetty, M. (2012). Coral thermal tolerance: tuning gene expression to resist thermal stress. *PLoS One* 7:e50685. doi: 10.1371/journal.pone.0050685

Brown, B. E. (1997). Coral bleaching: causes and consequences. *Coral Reefs* 16, 129–138.

Chen, H. K., Mayfield, A. B., Wang, L. H., and Chen, C. S. (2017). Coral lipid bodies as the relay center interconnecting diel-dependent lipidomic changes in different cellular compartments. *Sci. Rep.* 7:3244. doi: 10.1038/s41598-017-02722-z

Chen, H. K., Song, S. N., Wang, L. H., Mayfield, A. B., Chen, Y. J., Chen, W. N. U., et al. (2015). A compartmental comparison of major lipid species in a coral-*Symbiodinium* endosymbiosis: evidence that the coral host regulates lipogenesis of its cytosolic lipid bodies. *PLoS ONE* 10:e0132519. doi: 10.1371/journal.pone.0132519

Chen, M. C., Cheng, Y. M., Hong, M. C., and Fang, L. S. (2005a). Molecular cloning of Rab5 (ApRab5) in *Aiptasia pulchella* and its retention in phagosomes harboring live zooxanthellae. *Biochem. Biophys. Res. Commun.* 324, 1024–1033. doi: 10.1016/j.bbrc.2004.09.151

Chen, M. C., Cheng, Y. M., Sung, P. J., Kuo, C. E., and Fang, L. S. (2003). Molecular identification of Rab7 (ApRab7) in *Aiptasia pulchella* and its exclusion from phagosomes harboring zooxanthellae. *Biochem. Biophys. Res. Commun.* 308, 585–594.

Chen, M. C., Hong, M. C., Huang, Y. S., Liu, M. C., Cheng, Y. M., and Fang, L. S. (2005b). ApRab11, a cnidarian homologue of the recycling regulatory protein Rab11, is involved in the establishment and maintenance of the *Aiptasia-Symbiodinium* endosymbiosis. *Biochem. Biophys. Res. Commun.* 338, 1607–1616. doi: 10.1016/j.bbrc.2005.10.133

Chen, W. N. U., Kang, H. J., Weis, V. M., Mayfield, A. B., Fang, L. S., and Chen, C. S. (2012). Diel rhythmicity of lipid body formation in a coral-*Symbiodinium* endosymbiosis. *Coral Reefs* 31, 521–534. doi: 10.1007/s00338-011-0868-6

Chow, A. M., Ferrier-Pagès, C., Khalouei, S., Reynaud, S., and Brown, I. R. (2009). Increased light intensity induces heat shock protein Hsp60 in coral species. *Cell Stress Chaperones* 14, 469–476. doi: 10.1007/s12192-009-0100-6

Coles, S. L., and Brown, B. E. (2003). Coral bleaching-capacity for acclimatization and adaptation. *Adv. Mar. Biol.* 46, 183–223. doi: 10.1016/s0065-2881(03)46004-5

Cziesielski, M. J., Liew, Y. J., Cui, G., Schmidt-Roach, S., Campana, S., Marondedze, C., et al. (2018). Multi-omics analysis of thermal stress response in a Zooxanthellate cnidarian reveals the importance of associating with thermotolerant symbionts. *Proc. R. Soc. B.* 285, 20172654. doi: 10.1098/rspb.2017.2654

Downs, C. A., Fauth, J. E., Halas, J. C., Dustan, P., Bemiss, J., and Woodley, C. M. (2002). Oxidative stress and seasonal coral bleaching. *Free Radical Biol. Med.* 33, 533–543. doi: 10.1016/s0891-5849(02)00907-3

Downs, C. A., Kramarsky-Winter, E., Martinez, J., Kushmaro, A., Woodley, C. M., Loya, Y., et al. (2009). Symbiophagy as a cellular mechanism for coral bleaching. *Autophagy* 5, 211–216. doi: 10.4161/auto.5.2.7405

Gates, R. D., and Edmunds, P. J. (1999). The physiological mechanisms of acclimatization in tropical reef corals. *Am. Zool.* 39, 30–43. doi: 10.1093/icb/39.1.30

Gintert, B. E., Manzello, D. P., Enochs, I. C., Kolodziej, G., Carlton, R. D., Gleason, A. C. R., et al. (2018). Marked annual coral bleaching resilience of an inshore patch reef in the Florida Keys: a nugget of hope, aberrance, or last man standing? *Coral Reefs* 37, 533–547. doi: 10.1007/s00338-018-1678-x

Hochachka, P. W., and Somero, G. N. (2002). *Biochemical Adaptation*. Oxford: Oxford University Press.

Hoegh-Guldberg, O., Poloczanska, E. S., Skirving, W., and Dove, S. (2017). Coral reef ecosystems under climate change and ocean acidification. *Front. Mar. Sci.* 4:158. doi: 10.3389/fmars.2017.00158

Jones, R. J., Hoegh-Guldberg, O., Larkum, A. W. D., and Schreiber, U. (1998). Temperature-induced bleaching of corals begins with impairment of the CO2 fixation metabolism in Zooxanthellae. *Plant Cell Environ.* 21, 1219–1230. doi: 10.1046/j.1365-3040.1998.00345.x

Kim, E. Y., Choi, Y. H., Choi, C. G., and Nam, T. J. (2017). Effects of the cyclophilin-type peptidylprolyl cis-trans isomerase from *Pyropia* yezoensis against hydrogen peroxide-induced oxidative stress in HepG2 cells. *Mol. Med. Rep.* 15, 4132–4138. doi: 10.3892/mmr.2017.6517

Kultz, D. (2005). Molecular basis of the cellular stress response. *Annu. Rev. Physiol.* 67, 225–257. doi: 10.1146/annurev.physiol.67.040403.103635

Kultz, D., Fiol, D., Valkova, N., Gomez-Jimenez, S., Chan, S. Y., and Lee, J. (2007). Functional genomics and proteomics of the osmotic stress response in "non-model" organisms. *J. Exp. Biol* 210, 1593–1601. doi: 10.1242/jeb.000141

Levy, O., Karako-Lampert, S., Ben-Asher, H. W., Zoccola, D., Pages, G., and Ferrier-Pages, C. (2016). Molecular assessment of the effect of light and heterotrophy in the scleractinian coral *Stylophora pistillata*. *Proc. R. Soc. B.* 283, 20153025. doi: 10.1098/rspb.2015.3025

Lin, S., Yu, L., and Zhang, H. (2019). Transcriptomic responses to thermal stress and varied phosphorus conditions in Fugacium kawagutii. *Microorganisms* 7, 96. doi: 10.3390/microorganisms7040096

Lock, J. G., and Stow, J. L. (2005). Rab11 in recycling endosomes regulates the sorting and basolateral transport of e-cadherin. *Mol. Biol. Cell* 16, 1744–1755. doi: 10.1091/mbc.e04-10-0867

Lõhelaid, H., Teder, T., and Samel, N. (2014). Lipoxygenase-allene oxide synthase pathway in octocoral thermal stress response. *Coral Reefs* 34, 143–154. doi: 10.1007/s00338-014-1238-y

Lopez, C. E., Sheehan, H. C., Vierra, D. A., Azzinaro, P. A., Meedel, T. H., Howlett, N. G., et al. (2017). Proteomic responses to elevated ocean temperature in ovaries of the ascidian *Ciona* intestinalis. *Biol. Open* 6, 943–955. doi: 10.1242/bio.024786

Manzello, D. P. (2015). Rapid recent warming of coral reefs in the Florida Keys. *Sci. Rep.* 5, 16762. doi: 10.1038/srep16762

Manzello, D. P., Enochs, I. C., Kolodziej, G., and Carlton, R. (2015). Recent decade of growth and calcification of *Orbicella faveolata* in the Florida Keys: an

inshore—offshore comparison. *Mar. Ecol. Prog. Ser.* 521, 81–89. doi: 10.3354/meps11085

Manzello, D. P., Matz, M. V., Enochs, I. C., Valentino, L., Carlton, R. D., Kolodziej, G., et al. (2019). Role of host genetics and heat—tolerant algal symbionts in sustaining populations of the endangered coral *Orbicella faveolata* in the Florida Keys with ocean warming. *Glob. Change Biol.* 25, 1016–1031. doi: 10.1111/gcb.14545

Mayfield, A. B., Chan, P. H., Putnam, H. M., Chen, C. S., and Fan, T. Y. (2012). The effects of a variable temperature regime on the physiology of the reef-building coral Seriatopora hystrix: results from a laboratory-based reciprocal transplant. *J. Exp. Biol.* 215, 4183–4195. doi: 10.1242/jeb.071688

Mayfield, A. B., Chen, C. S., and Dempsey, A. C. (2017a). Biomarker profiling in reef corals of Tonga's Ha'apai and Vava'u Archipelagos. *PLoS One.* 12:e0185857. doi: 10.1371/journal.pone.0185857

Mayfield, A. B., Chen, C. S., and Dempsey, A. C. (2017b). Identifying corals displaying aberrant behavior in Fiji's Lau Archipelago. *PLoS One.* 12:e0177267. doi: 10.1371/journal.pone.0177267

Mayfield, A. B., Chen, C. S., and Dempsey, A. C. (2017c). The molecular ecophysiology of closely related pocilloporid corals of New Caledonia. *Platax* 14, 1–45.

Mayfield, A. B., Chen, C. S., and Dempsey, A. C. (2019). Modeling environmentally-mediated variation in reef coral physiology. *J. Sea Res.* 145, 44–54. doi: 10.1016/j.seares.2019.01.003

Mayfield, A. B., Chen, Y. J., Lu, C. Y., and Chen, C. S. (2018a). Exploring the environmental physiology of the Indo-Pacific reef coral *Seriatopora hystrix* using differential proteomics. *Open J. Mar. Sci.* 8, 223–252. doi: 10.4236/ojms.2018.82012

Mayfield, A. B., Chen, Y. J., Lu, C. Y., and Chen, C. S. (2018b). The proteomic response of the reef coral *Pocillopora* acuta to experimentally elevated temperature. *PLoS One* 13:e0192001. doi: 10.1371/journal.pone.0192001

Mayfield, A. B., Wang, L. H., Tang, P. C., Hsiao, Y. Y., Fan, T. Y., Tsai, C. L., et al. (2011). Assessing the impacts of experimentally elevated temperature on the biological composition and molecular chaperone gene expression of a reef coral. *PLoS One* 6:e26529. doi: 10.1371/journal.pone.0026529

Mayfield, A. B., Wang, Y. B., Chen, C. S., Chen, S. H., and Lin, C. Y. (2014). Compartment-specific transcriptomics in a reef-building coral exposed to elevated temperatures. *Mol. Ecol.* 23, 5816–5830. doi: 10.1111/mec.12982

Mayfield, A. B., Wang, Y. B., Chen, C. S., Chen, S. H., and Lin, C. Y. (2016). Dual-compartmental transcriptomic+ proteomic analysis of a marine endosymbiosis exposed to environmental change. *Mol. Ecol.* 25, 5944–5958. doi: 10.1111/mec.13896

Montealegre, S., and van Endert, P. M. (2010). Endocytic recycling of MHC class I molecules in non-professional antigen presenting and dendritic cells. *Front. Immunol.* 9:3098. doi: 10.3389/fimmu.2018.03098

Musada, G. R., Dvoriantchikova, G., Myer, C., Ivanov, D., Bhattacharya, S. K., and Hackam, A. S. (2020). The effect of extrinsic Wnt/β-catenin signaling in Muller glia on retinal ganglion cell neurite growth. *Dev. Neurobiol.* 80, 98–110. doi: 10.1002/dneu.22741

Nakamura, M., Morita, M., Kurihara, H., and Mitarai, S. (2012). Expression of hsp70, hsp90 and hsf1 in the reef coral *Acropora digitifera* under prospective acidified conditions over the next several decades. *Biol. Open* 1, 75–81. doi: 10.1242/bio.2011036

Oakley, C. A., Durand, E., Wilkinson, S. P., Peng, L., Weis, V. M., Grossman, A. R., et al. (2017). Thermal shock induces host proteostasis disruption and endoplasmic reticulum stress in the model symbiotic cnidarian *Aiptasia*. *J. Proteome Res.* 16, 2121–2134. doi: 10.1021/acs.jproteome.6b00797

Pinzón, J. H., Kamel, B., Burge, C. A., Harvell, C. D., Medina, M., Weil, E., et al. (2015). Whole transcriptome analysis reveals changes in expression of immune-related genes during and after bleaching in a reef-building coral. *R. Soc. Open Sci.* 2:140214. doi: 10.1098/rsos.140214

Poli, D., Fabbri, E., Goffredo, S., Airi, V., and Franzellitti, S. (2017). Physiological plasticity related to zonation affects hsp70 expression in the reef-building coral *Pocillopora verrucosa*. *PLoS One* 12:e0171456. doi: 10.1371/journal.pone.0171456

Putnam, H. M., Mayfield, A. B., Fan, T. Y., Chen, C. S., and Gates, R. D. (2013). The physiological and molecular responses of larvae from the reef-building coral *Pocillopora damicornis* exposed to near-future increases in temperature and pCO2. *Mar. Biol.* 160, 2157–2173. doi: 10.1007/s00227-012-2129-9

Ricaurte, M., Schizas, N. V., Ciborowski, P., and Boukli, N. M. (2016). Proteomic analysis of bleached and unbleached *Acropora palmata*, a threatened coral species of the Caribbean. *Mar. Pollut. Bull.* 107, 224–232. doi: 10.1016/j.marpolbul.2016.03.068

Rosic, N. N., Pernice, M., Dove, S., Dunn, S., and Hoegh-Guldberg, O. (2011). Gene expression profiles of cytosolic heat shock proteins Hsp70 and Hsp90 from symbiotic dinoflagellates in response to thermal stress: possible implications for coral bleaching. *Cell Stress Chaperones* 16, 69–80. doi: 10.1007/s12192-010-0222-x

Ross, C. (2014). Nitric oxide and heat shock protein 90 co-regulate temperature-induced bleaching in the soft coral *Eunicea fusca*. *Coral Reefs* 33, 513–522. doi: 10.1007/s00338-014-1142-5

Ruiz-Jones, L. J., and Palumbi, S. R. (2017). Tidal heat pulses on a reef trigger a fine-tuned transcriptional response in corals to maintain homeostasis. *Sci. Adv.* 3, e1601298. doi: 10.1126/sciadv.1601298

Seveso, D., Arrigoni, R., Montano, S., Maggioni, D., Orlandi, I., Berumen, M. L., et al. (2020). Investigating the heat shock protein response involved in coral bleaching across Scleractinian species in the central Red Sea. *Coral Reefs* 39, 85–98. doi: 10.1007/s00338-019-01878-6

Seveso, D., Montano, S., Reggente, M. A., Maggioni, D., Orlandi, I., Galli, P., et al. (2017). The cellular stress response of the scleractinian coral *Goniopora columna* during the progression of the black band disease. *Cell Stress Chaperones* 22, 225–236. doi: 10.1007/s12192-016-0756-7

Siebeck, U., Marshall, N., Klüter, A., and Hoegh-Guldberg, O. (2006). Monitoring coral bleaching using a colour reference card. *Coral Reefs* 25, 453–460. doi: 10.1007/s00338-006-0123-8

Sleight, V. A., Peck, L. S., Dyrynda, E. A., Smith, V. J., and Clark, M. S. (2018). Cellular stress responses to chronic heat shock and shell damage in temperate *Mya truncata*. *Cell Stress Chaperones* 23, 1003–1017. doi: 10.1007/s12192-018-0910-5

Sokolova, I. M., Frederich, M., Bagwe, R., Lannig, G., and Sukhotin, A. A. (2012). Energy homeostasis as an integrative tool for assessing limits of environmental stress tolerance in aquatic invertebrates. *Mar. Environ. Res.* 79, 1–15. doi: 10.1016/j.marenvres.2012.04.003

Sproles, A. E., Oakley, C. A., Matthews, J. L., Peng, L., Owen, J. G., Grossman, A. R., et al. (2019). Proteomics quantifies protein expression changes in a model cnidarian colonised (sp.) by a thermally tolerant but suboptimal symbiont. *ISME J.* 13, 2334–2345. doi: 10.1038/s41396-019-0437-5

Tchernov, D., Kvitt, H., Maramaty, L., Bibby, T. S., Gorbunov, M. Y., Rosenfield, H., et al. (2011). *Apoptosis* and the selective survival of host animals following thermal bleaching in Zooxanthellate corals. *Proc. Natl. Acad. Sci. U.S.A.* 108, 9905–9909. doi: 10.1073/pnas.1106924108

Vizcaíno, J., Deutsch, E., Wang, R., Csordas, A., Reisinger, F., Rios, D., et al. (2014). ProteomeXchange provides globally coordinated proteomics data submission and dissemination. *Nat. Biotechnol.* 32, 223–226. doi: 10.1038/nbt.2839

Weston, A. J., Dunlap, W. C., Beltran, V. H., Starcevic, A., Hranueli, D., Ward, M., et al. (2015). Proteomics links the redox state to calcium signaling during bleaching of the Scleractinian coral *Acropora microphthalma* on exposure to high solar irradiance and thermal stress. *Mol. Cell Proteomics* 14, 585–595. doi: 10.1074/mcp.m114.043125

Whalen, K. E., Lane, A. L., Kubanek, J., and Hahn, M. E. (2010). Biochemical warfare on the reef: the role of glutathione transferases in consumer tolerance of dietary prostaglandins. *PLoS One* 5:e8537. doi: 10.1371/journal.pone.0008537

Conflict of Interest: The authors declare that the research was conducted in the absence of any commercial or financial relationships that could be construed as a potential conflict of interest.

frontiers in Marine Science

ORIGINAL RESEARCH
published: 03 September 2021
doi: 10.3389/fmars.2021.715167

Physiological Response of Shallow-Water Hard Coral *Acropora digitifera* to Heat Stress *via* Fatty Acid Composition

Che Din Mohd Safuan[1], Muhammad Arif Samshuri[2], Siti Nurtahirah Jaafar[1,2], Chun Hong Tan[1,2] and Zainudin Bachok[1]*

[1] Institute of Oceanography and Environment, Universiti Malaysia Terengganu, Kuala Terengganu, Malaysia, [2] Faculty of Science and Marine Environment, Universiti Malaysia Terengganu, Kuala Terengganu, Malaysia

Heat stress disturbs the mutualistic relationship between the hard corals and the symbiotic algae, which cause coral bleaching. A wide array of biochemical parameters is used to demonstrate the phenomenon. This study exposed a shallow-water hard coral, *Acropora digitifera*, to a series of elevated temperatures over time while the interaction between Symbiodiniaceae (SD) density, antioxidants activities, fatty acid (FA) composition, and putative FA health indicators was evaluated. Heat stress caused a substantial loss in SD densities, consequently regulated the antioxidant activities and caused significant changes in FA composition. There was a lack of evidence showing *A. digitifera* experienced oxidative stress; nonetheless, a significant decrease of monounsaturated fatty acid as (MUFA) and polyunsaturated fatty acid (PUFA) during the thermally induced experiment demonstrated that corals utilize their unsaturated FA as a final barrier or as a repair system against oxidative damage once the antioxidant enzyme cannot cope with stress condition. The lower ratio of putative FA health indicators [i.e., n-3 LC:n-6 LC, eicosapentaenoic acid (EPA):arachidonic acid (ARA), and docosahexaenoic acid (DHA):ARA] characterized an unhealthy coral. The loss of SD density was significantly correlated with certain PUFA markers [i.e., linolenic acid (18:3n6), 20:5n3, and 22:6n3] and putative FA health indicator (i.e., n-3 LC:n-6 LC, EPA:ARA, and DHA:ARA). These notably imply that the FA linked with the symbiont can be a potential health indicator for assessing the effect of the environmental stressor on coral. This study also revealed the regulation of FAs during stress conditions, especially when heterotrophic feeding is limited. Future studies on FA profiles toward antagonistic or synergistic effects will offer a better understanding of the nature of this relationship under a harsh climate.

Keywords: stress response, heat-stress, Symbiodiniaceae, fatty acids, oxidative stress, coral bleaching

Abbreviations: SD, Symbiodiniaceae; MUFA, monounsaturated fatty acid; PUFA, polyunsaturated fatty acid; LC, linolenic acid; EPA, eicosapentaenoic acid; ARA, arachidonic acid; DHA, docosahexaenoic acid; SAFA, saturated fatty acid; CT, control tank; ET, exposure tank; ROS, reactive oxygen species; FA, fatty acid.

OPEN ACCESS

Edited by:
Davide Seveso, University of Milano-Bicocca, Italy

Reviewed by:
Carolina Arruda Freire, Federal University of Paraná, Brazil
Shiming Peng, East China Sea Fisheries Research Institute, Chinese Academy of Fishery Sciences, China

****Correspondence:***
Siti Nurtahirah Jaafar
tahirah@umt.edu.my

Specialty section:
This article was submitted to Aquatic Physiology, a section of the journal Frontiers in Marine Science

Received: *26 May 2021*
Accepted: *02 August 2021*
Published: *03 September 2021*

Citation:
Safuan CDM, Samshuri MA, Jaafar SNT, Tan CH and Bachok Z (2021) Physiological Response of Shallow-Water Hard Coral Acropora digitifera to Heat Stress via Fatty Acid Composition. Front. Mar. Sci. 8:715167. doi: 10.3389/fmars.2021.715167

INTRODUCTION

Coral reefs are declining worldwide subjected to natural and anthropogenic disturbances (Baker et al., 2008; De'ath et al., 2012; Cziesielski et al., 2019). During the stressful environmental condition, such as extremes in temperature, oxygen, salinity, and nutrient supply, the physiology of corals changes and leads to the disappearance of symbiotic algae or known as coral bleaching (Baird et al., 2008; Apprill, 2020). The cellular mechanism underlying the bleaching is tightly coupled with the accumulation of reactive oxygen species (ROS), which damages the D1 protein of photosystem II (PSII) in the thylakoid membrane of the symbiotic algae (Downs et al., 2002; Bhagooli and Hidaka, 2004; Lesser, 2006; Baird et al., 2008; Takahashi and Murata, 2008). Extended photooxidative damage and consequential photoinhibition of PSII should overwhelm the antioxidant system on both partners and should increase the cellular damage such as heat shock proteins and other danger-associated molecular patterns, which later suggesting the breakdown of symbiosis (Lesser, 1997; Downs et al., 2002; Takahashi and Murata, 2008; Weis, 2008; Palmer, 2018; Mansfield and Gilmore, 2019). Studies have shown that oxidative stress is primarily originated from the symbiotic algae and causes tissue damage to the host (Nesa and Hidaka, 2009; Yakovleva et al., 2009; Cunning and Baker, 2012). The production of ROS occurs in the chloroplast by the process linked with PSI- and PSII-catalyzed electron transfer, leading to the production of superoxide radical (O_2^-) and hydrogen peroxide (H_2O_2), which diffuses to the coral cytoplasm but it can be counterbalanced by enzymatic and non-enzymatic antioxidants from coral (Downs et al., 2002). The cellular antioxidant enzymes such as superoxide dismutases (SODs), peroxidases, catalases, and mycosporine-like amino acids function as scavengers to ROS and act as the primary defense against oxidative stress (Cook and Davy, 2001; Biel et al., 2007; Baird et al., 2008). However, under prolonged and severe stress, the antioxidant system might be unable to cope with the excessive production of ROS and cause oxidative damage to the cells (Baird et al., 2008). Due to this, the coral will regulate the secondary defense or repair system to fight against endogenous stress.

It is known that marine organisms regulate their fatty acid (FA) and sterol composition as a defense mechanism from the influence of changing temperature, pressure, or lipid peroxidation (Parrish, 2013). Field and experimental studies demonstrated that stress-related condition induces the FA composition, resulting in low FA composition (Bachok et al., 2006; Imbs et al., 2014; Rodríguez-Troncoso et al., 2016). Reduction in FA composition is directly coupled with their photosynthetic symbionts (Papina et al., 2003; Imbs et al., 2010b). The loss of the symbiotic algae during coral bleaching alters the FA composition in the coral, especially the polyunsaturated fatty acid (PUFA), contents (Bachok et al., 2006; Imbs and Yakovleva, 2012; Rodríguez-Troncoso et al., 2016). This is because some of the PUFAs were translocated from the symbiont to the host (Imbs and Yakovleva, 2012).

The PUFAs play an important role as a constituent of the phospholipids of all cell membranes (Calder, 2010). In general, some of the PUFAs mainly originated from primary producers and passed up to the animals *via* the food chain (Monroig et al., 2013). In a clinical test, the consumption of PUFA such as n-3 or known as omega-3 PUFAs is important for human health due to their capability of partly inhibiting many aspects of inflammation (Calder, 2010). In corals, the PUFAs of the n-3 series are mainly originated from symbiotic algae or external food sources *via* heterotrophy because the animal cannot produce these essential PUFAs (Papina et al., 2003; Imbs et al., 2010b). Experimental work by Imbs and Yakovleva (2012) found that PUFAs such as 18:3n6 and stearidonic acid (18:4n3) in *Montipora digitata* and *Acropora intermedia* were significantly reduced under thermal stress conditions. While the reduction of those PUFAs is associated with the loss of symbiotic algae, PUFA also plays an important role in the regulation of stress conditions (Betteridge, 2000). It is suggested that the depletion of PUFA composition after the loss of symbiont can be associated with oxidative stress (Imbs and Yakovleva, 2012; Rodríguez-Troncoso et al., 2016). When oxidative defenses are overwhelmed, the excess radicals will accumulate and react with the double bond in unsaturated FAs, especially in PUFAs that are susceptible to peroxidation (Catalá, 2010). In marine organisms, both n-3 and n-6 PUFAs such as eicosapentaenoic acid (EPA; 20:5n3), docosahexaenoic acid (DHA; 22:6n3), and arachidonic acid (ARA; 20:4n6) play an important role against oxidative stress (Okuyama et al., 2008; Parrish, 2013); hence, it has been used as coral health indicator (Rocker et al., 2019; Kim et al., 2021). Meanwhile, coral increased the production of saturated fatty acid (SAFA) to maintain the rigidity of their biological membrane (Imbs and Yakovleva, 2012) as the SAFAs are less reactive and more stable than unsaturated FAs (Ratnayake and Galli, 2009). The application of FAs (Bachok et al., 2006; Imbs and Yakovleva, 2012; Rodríguez-Troncoso et al., 2016) and antioxidant activities (Yakovleva et al., 2004; 2009; Teixeira et al., 2013) to evaluate the stress response in corals is well established. However, the interaction between these parameters during stress conditions is not well described and experimentally tested. For that reason, we examined the composition of FAs in the stress-induced experiment *via* heat stress to increase the understanding of the role of FAs during stress conditions. The aims of this study were (1) to investigate the changes in the composition of FAs, Symbiodiniaceae (SD) density, and antioxidant activities of coral species, *Acropora digitifera*, under elevated temperature and (2) to examine the relationship between the SD density with FA markers and health indicator. This study hypothesized that the environmental stressor such as heat stress significantly affects the SD density, antioxidant activities, and FA composition in hard corals consequently resulting in the potential role of specific FAs as bioindicators.

MATERIALS AND METHODS

Sample Collection

Colonies of shallow-water coral, *A. digitifera*, were collected in Pantai Pasir Tenggara (5°36′42.15″N, 103°3′32.44″E), Pulau Bidong, Terengganu, Malaysia (**Figure 1A**) where the species can

be found abundantly in the area (**Figure 1B**). The samples were collected using a hammer and chisel (**Figure 1C**). The range of *in situ* water temperature was from 26.5 to 28.0°C, with a salinity of 32.0 ± 0.5 ppt. The intensity of light penetrates the seawater was measured using a light meter (LI-COR LI-250A) with a measurement ranging from 150 to 200 μmol s^{-1} m^{-2}. The selection of healthy samples of *A. digitifera* was performed using Coral Color Reference Card developed by Siebeck et al. (2006) as a reference, and all samples were collected from a non-shaded area. A total of three different colonies were collected at a distance of at least 5 m to minimize the probability of genetic clones, and each colony was separated into four sub-colonies that consist of at least eight coral fragments. Relatively, the samples were taken at the same depth around 3–4 m during high tide. Samples were separately placed in a labeled transparent plastic bag filled with *in situ* seawater (**Figure 1D**) and kept in a container with ice and seawater before reaching land. Back on land, samples were washed to remove any unwanted organisms (**Figure 1E**) and transferred into the designated tanks.

Experimental Tank Preparation

The experiment was conducted in an indoor hatchery using two rectangular fiberglass tanks separated into control tank (CT) and exposure tank (ET). Each tank was equipped with a full-spectrum artificial light (Shark G90 195W LED Casing Lamp) to consistently illuminate both tanks. To provide continuous water flow inside the tank, wavemakers (SOBO aquarium super wavemaker WP-300M) were installed to provide vigorous aeration and kept the water well mixed throughout the experimental period. The temperature of treated seawater (32 ± 1.0 ppt) was acclimatized at 27 ± 1.0°C using an aquarium chiller (Hailea HX-90A 0.5 hp) for 30 days preceding sample collection day. A schematic diagram of the experimental design is shown in **Figure 2**.

Maintenance of Live *Acropora digitifera*

Three colonies of *A. digitifera* with 5- to 6-cm-long branches were broken into sub-colonies. Each sub-colony comprised 8–10 branches and was transferred into the tanks accordingly. Each of the sub-colonies was placed on a cylindrical polyvinyl chloride pipe to support the samples in an upright position. In total, each tank contained 12 sub-colonies. The coral colonies were acclimatized for 10 days without feeding. The temperature and salinity of the seawater were maintained at relatively similar to *in situ* measurements (temperature = 27 ± 1.0°C, salinity = 32 ± 1.0 ppm). Both tanks were illuminated with artificial light (±150 μmol photons m^{-2} s^{-1}) on a 12:12-h light/dark cycle. During the acclimatization, all samples exhibited active polyp extensions with no mucus suspension. Coral Color Reference Card (Siebeck et al., 2006) was used as a standard reference to indicate healthy coral samples.

Experimental Design

In CT, samples were treated similarly to the condition during acclimatization. Meanwhile, the heat-stress experiment was assigned in ET by gradually increased the seawater temperature

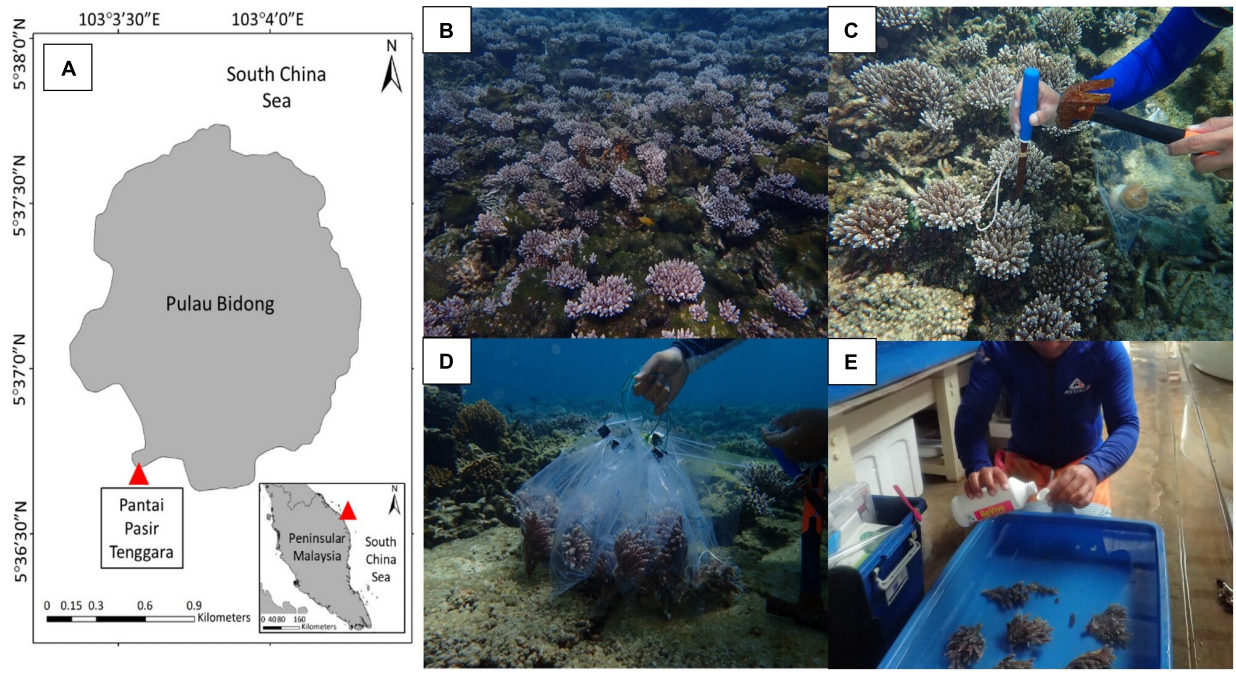

FIGURE 1 | Map shows the location of sampling sites in Pantai Pasir Tenggara, Pulau Bidong located in the east coast of Peninsular Malaysia **(A)**. Colonies of *Acropora digitifera* in Pantai Pasir Tenggara, Pulau Bidong can be found abundantly in the area **(B)**. A diver using a hammer and a chisel for collecting samples **(C)** and keeps them inside a transparent bag **(D)**. Back on land, samples were washed using ReVive Coral Cleaner solution and rinsed with clean seawater before placing the samples into the tanks **(E)**.

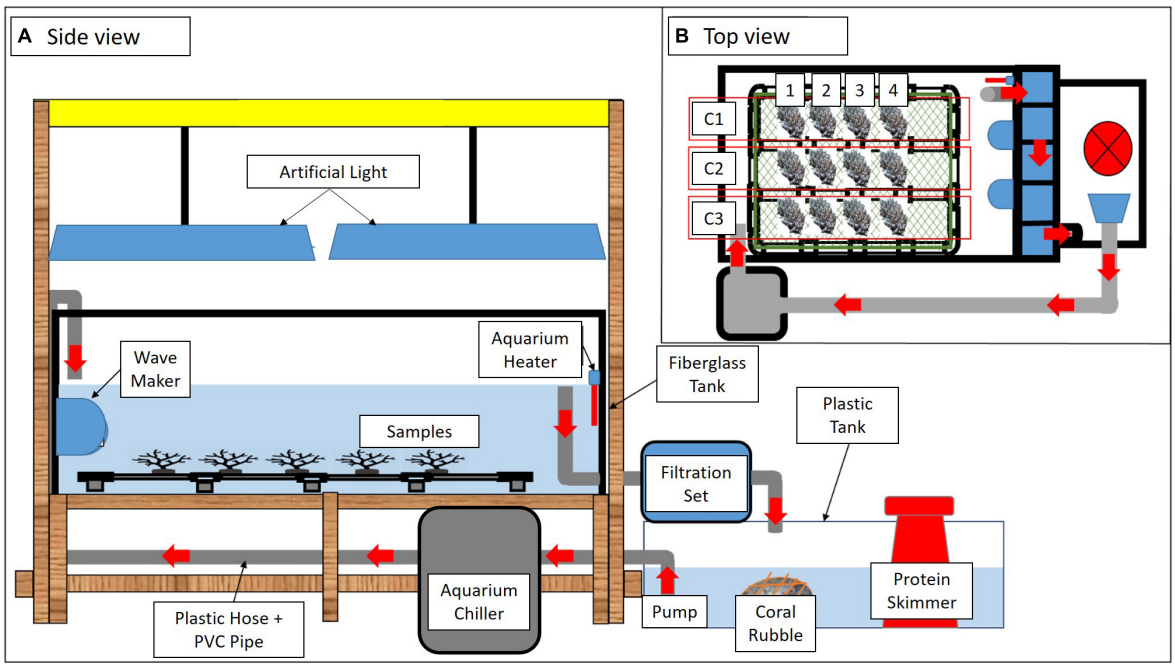

FIGURE 2 | A schematic diagram of the experimental tank set up in different views **(A,B)**. Red arrows indicate water flow. Three colonies of *A. digitifera* (C1, C2, and C3) separated into four sub-colonies (1–4) were arranged in each tank **(B)**.

at 0.5°C/12 h using an aquarium heater (SOBO aquarium heater 300W-HL) to obtain three temperature regimes (i.e., 27.0 ± 1.0, 29.0 ± 1.0, and 31 ± 1.0°C). The highest temperature (31 ± 1.0°C) was chosen following the natural bleaching event reported in Malaysia (Guest et al., 2012). The sample collection begins after 10 days of acclimatization by collecting the first sub-colonies in both tanks and represented as the samples on Day 1. Then, the seawater temperature in ET was gradually increased to 29.0 ± 1.0°C (0.5°C/12 h), and samples were collected after 24 h of exposure at 29.0 ± 1.0°C and labeled as Day 3. A similar procedure was applied for Day 5 when the temperature reached 31 ± 1.0°C.

The remaining samples were left for another 48 h of exposure at 31 ± 1.0°C before the final collection (Day 7). Samples in CT were collected following the sampling frequency in ET (Day 1, Day 3, Day 5, and Day 7). The summary of the experimental design is illustrated in **Figure 3**. In total, 144 fragments were collected from both tanks and directly kept in a −80°C freezer prior to the laboratory analysis. In the laboratory, the samples were divided accordingly for FA analysis, SD density, and enzymatic assays. For every sample collection (Day 1, Day 3, Day 5, and Day 7), three replicates of coral fragments were used for each of the analyses.

Preparation of Samples

Samples for FA analysis and SD density were prepared by removing the coral tissue from the skeleton using a jet of high-pressure air from an artist airbrush containing chilled distilled water (80 psi, approximately 1-cm distance from tip of airbrush to coral) into a thick, transparent polyethylene bag (Johannes and Wiebe, 1970). The tissue slurry was then poured into a 50-ml tube, and the plastic bag was rinsed using the airbrush to ensure full coverage of the remaining tissue on the plastic wall.

In contrast, samples for enzymatic assay were prepared by removing the coral tissue from the skeleton utilizing the jet of high-pressure air from an artist airbrush containing a phosphate-buffered saline solution. The slurry or homogenate that contained the tissue (host and symbiotic algae) was then transferred into 15-ml tubes and centrifuged (8,000 × *g*) at 4°C for 15 min. The tissue-free supernatant was removed and replaced with 1 ml of homogenized buffer [0.01 M Tris–Cl, 0.5 M sucrose, 0.001 M ethylenediaminetetraacetic acid (EDTA), 0.15 M KCl, and pH 7.4]. The pellet was then homogenized using an ultrasonic cell disruptor (Misonix Microson XL2000) for 20-s sonication and 50-s rest for 10 cycles on ice. The homogenate was then centrifuged (18,000 × *g*) for 20 min at 4°C. The coral protein extracts in the supernatant were harvested, the protein concentration was determined by the Bradford assay as previously described (Bradford, 1976), and the remaining coral protein extracts were transferred into a clean 1.5-ml tube and stored in a −80°C freezer before further analysis.

Symbiodiniaceae Cell Count

The density of SD was determined using an hemocytometer (Neubauer-Improved Tiefe Depth Profondeur, 0.100 mm). The resultant slurry was shaken vigorously, and the sub-sample was dropped onto the hemocytometer and viewed under Leica DME compound microscope at 40 × magnification. The number of algae cells was calculated from the replicate of the hemocytometer

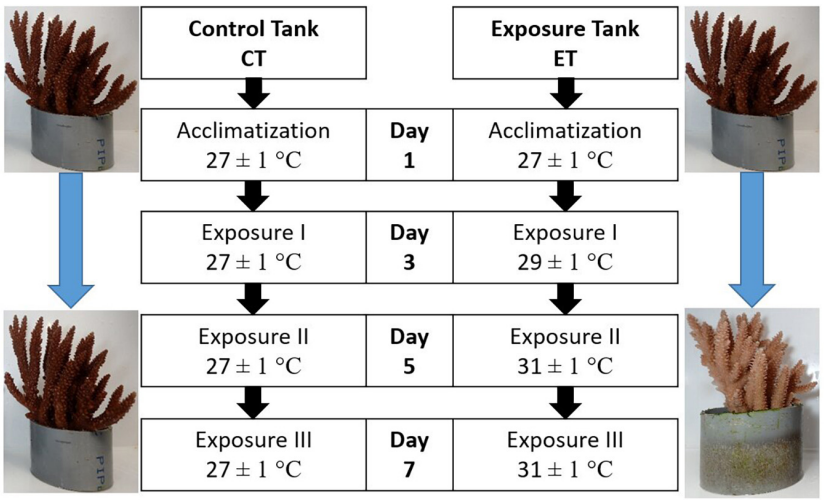

FIGURE 3 | Experimental design for control tank (CT) and exposure tank (ET). Samples were collected after 10 days of acclimatization and regarded as Day1, Day 3, Day 5, and Day 7. Both tanks were sampled at the same time.

count ($n = 8$). The SD density ($\times 10^6$ cell cm^{-2}) was determined by dividing the total number of SD cells with a surface area of the denuded skeleton.

Fatty Acid Analysis

The remaining slurry was then filtered using a known weight of blank filter paper (Sartorius, Glass-Microfiber Disks, MGC, Ø 47 mm, and retention rate of 1.2 μm). Samples were freeze-dried (Labconco FreeZone 4.5-L Benchtop Freeze Dry System) for 12 h at −40°C to remove the excess water and determine the dried coral tissue biomass. The dried samples were kept in the −20°C freezer prior to FA analysis.

Samples of dried coral tissue were used for FA analysis using the One-Step method as outlined by Abdulkadir and Tsuchiya (2008). Samples amounting to 200–300 mg were mixed with 4 ml of hexane and 1 ml of internal standard solution in a 50-ml centrifuge glass tube. A glass rod was used to ensure that the sample was soaked with the mixture of hexane and internal standard solution. Of note, 2 ml of 14% BF3 in methanol and a magnetic stirrer bar were added to the tube. Rapidly, the headspace of the tube was flushed with nitrogen gas before the tube was tightly closed with a Teflon-lined screw cap. The tube was then transferred into a glass beaker of boiling water heated using a hot plate at 100°C for 120 min under continuous stirring. Then, the tube was cooled at room temperature before adding 1 ml of hexane and 2 ml of distilled water. The tube was shaken vigorously and centrifuged at 2,500 rpm to obtain the fatty acid methyl ester (FAME) of the sample. Among the two layers formed, the upper layer was the hexane containing the FAME. Using a glass pipette, the layer of FAME was slowly transferred into a clean 5-ml sample vial, and the volume of the FAME collected was also recorded. All extracted FAMEs were then stored in a −20°C freezer prior to the gas chromatography (GC) analysis.

The component and composition of FAMEs were identified using Shimadzu 2010 GC-Flame Ionization Detector (GC-FID), Shimadzu, Japan, equipped with acapillary column (Shimadzu Rtx-2330 30 m × 0.25 mm internal diameter × 0.25 μm film thickness) and connected with a computer possessed of GC Solution (Shimadzu,Japan) software, autosampler, and splitless injection system, and connected with computer possessed GC Solution software. The injection volume was 1 μl, and the injector and detector temperatures were 300 and 270°C, respectively. The temperature program was set at 60°C held for 2 min, then from 60 to 160°C at 20 min, and held at 240°C for 10 min. Helium was used as a carrier gas and stream at a constant flow of 1.5 ml min^{-1}. Each component of FAMEs identified was compared with known external standards (FAME-37 Sigma–Aldrich, St. Louis, MO, United States, bacterial acid methyl esters (BAME), and Cod Liver Oil). The resulting peak was used to determine the FA composition.

Enzymatic Analysis

All of the chemicals used in the enzymatic analysis were obtained from Fisher Scientific, Loughborough, United Kingdom (Tris Base, Tris–Cl, sucrose, potassium dihydrogen phosphate, and KCl), Merck, Germany (NaOH, H_2O_2, and dipotassium hydrogen phosphate), Sigma–Aldrich, St. Louis, MO, United States [EDTA, 1-chloro-2,4-dinitrobenzene (CDNB), and reduced glutathione (GSH)], R&M Chemicals, United Kingdom (paraffin wax), and HmbG Chemicals, Hamburg, Germany (ethanol).

The enzymatic activity of catalase (CAT) was assessed by using a spectrophotometric method to measure the breakdown of H_2O_2 by CAT enzyme by following the study of Beers and Sizer (1952). Coral protein extracts were diluted with phosphate buffer (50 mM, pH 7.0) in a quartz cuvette and incubated to reach room temperature (±25°C). Immediately, 59 mM H_2O_2 was

added while blank was set with a similar condition without the presence of protein sample extracts. The decrease in absorbance was measured for 120 s by using UV-spectrometer (Shimadzu UV-1800 UV–Vis Spectrophotometer), and the enzyme activity was calculated based on the extinction coefficient of H_2O_2 at Δ240 nm (43.6 M^{-1} cm^{-1}). The unit of CAT activity is defined as decomposition of 1 μM H_2O_2 to O_2 and water per minute at pH 7.0 at 25°C and final substrate absorbance at 240-nm decay at a constant rate of 0.3–0.5.

The enzymatic assay for glutathione *S*-transferase (GST) activity was adapted from the study by Habig and Jakoby (1981) using the CDNB and GSH as substrates. Coral protein extracts were diluted with phosphate buffer (150 mM, pH 6.5) and 20 mM CDNB in a 96-well plate. The reaction was started by adding GSH, and immediately, the enzyme activity was determined spectrophotometrically at 340 nm using a microplate reader (Molecular Devices, SpectraMax® iD3 Multi-Mode Microplate Reader) at every 30 s for 5 min. The GST activity was calculated based on the absorbance increase per minute, using the CDNB extinction coefficient (340 nm = 9.6 mM^{-1} cm^{-1}). The unit of GST activity is defined as enzyme-conjugated 10 nmol of CDNB with the presence of GSH per minute in 1 mg of protein.

Superoxide dismutase activity was measured using the SOD Determination Kit (Sigma–Aldrich, St. Louis, MO, United States) following the instructions of the manufacturer. In brief, the reduction of oxygen to superoxide anion is detected by tetrazolium salt and produces formazan dye, which can be detected spectrophotometrically. In a 96-well plate containing coral protein extracts with and without superoxide-producing enzymes, absorbance at 450 nm was measured, compared, and standardized by the weight of protein used. Results were expressed in *U* per mg protein, where *U* is defined as the amount of enzyme necessary to produce 50% inhibition of the reduction rate of tetrazolium salt measured at 450 nm.

Statistical Analysis

Prior to statistical analysis, the normality of data sets comprised of SD density, antioxidant activities (CAT, GST, and SOD), and FA composition (FA classes, FA components, and putative FA health indicator) was tested by using the Shapiro–Wilk test and homogeneity test. However, most of the data sets were not normally distributed even after the arsine transformed; hence, the Kruskal–Wallis one-way ANOVA on ranks was used. The data were tested for differences among the samples collected from each tank (n = 9 per collection). Any data with a p-value less than 0.05 were considered significant and further analyzed using a pairwise multiple comparison test. To seek the relationship of SD densities with associated variables (CAT, GST, SOD, and FA composition), the Spearman's correlation was performed to the ET data sets to understand the changes during the experiment. All analyses were performed using the statistical software SPSS IBM.

RESULTS

Symbiodiniaceae Density

Symbiodiniaceae density in CT and ET during the experimental period changed over the experimental period (**Figure 4**). In CT, acclimatization temperature did not significantly affect the SD density (Kruskal–Wallis H = 4.345, p = 0.227). Daily observation showed no physical evidence of stress (polyp retraction, paleness or bleaching, and/or tissue rupture) among the samples. In contrast, samples in ET displayed a significant decline in mean SD densities (Kruskal–Wallis H = 25.887, $p < 0.001$) especially at 31 ± 1.0°C during Day 5 (1.19 ± 0.15 × 10^6 cells cm^{-2}) and continued to drop (0.71 ± 0.06 × 10^6 cells cm^{-2}) until the end of experiment. Even though the loss of SD densities occurred at Day 5, no physical evidence of stress (polyp retraction, paleness or bleaching, and/or tissue rupture) among the samples was observed within the period. No significant change was found

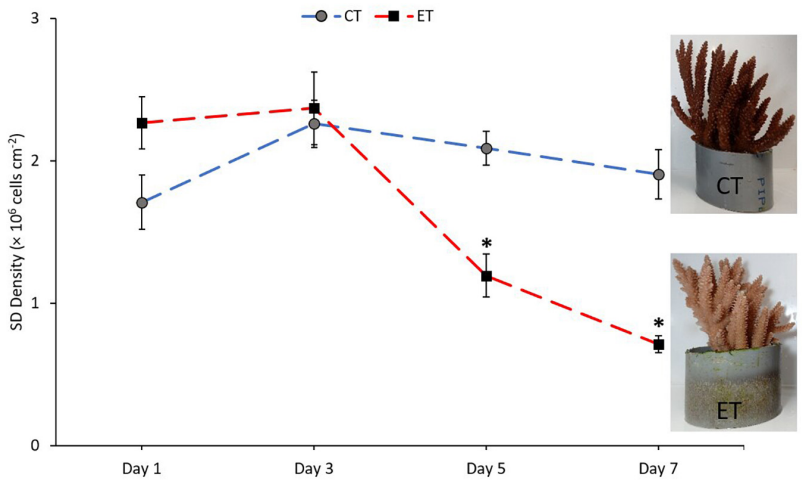

FIGURE 4 | Mean densities of Symbiodiniaceae in CT and ET throughout the experimental period with the images of samples taken from ET and CT during the end of experiment. All data points are mean ± SE (n = 9). Asterisk represent significant difference ($p < 0.05$).

during temperature changes at 27 ± 1.0 and 29 ± 1.0°C (Day 1 vs. Day 3, $p = 0.248$, adjusted significance = 1.000).

Antioxidant Enzyme Activities

In this study, antioxidant enzyme activities of CAT, GST, and SOD in the samples from both tanks were measured and shown in **Figure 5**. The activity of CAT in ET (Kruskal–Wallis $H = 14.651$, $p = 0.002$) and CT (Kruskal–Wallis $H = 13.116$, $p = 0.04$) was significantly different among the samples during the experimental period (**Figure 5A**). In both tanks, the activity of CAT increased significantly during Day 5 ($p < 0.05$) as revealed using the pairwise test. Even though the pattern of CAT activity in both tanks was relatively similar, the CAT activity in ET continued to decrease significantly as compared with CT during the end of experiment (Day 5 vs. Day 7; ET, $p = 0.001$, adjusted significance = 0.003, CT; $p = 0.235$, adjusted significance = 1.000).

No clear changes of GST activity were found in CT (Kruskal–Wallis $H = 3.068$, $p = 0.381$) as compared with ET (Kruskal–Wallis $H = 10.325$, $p = 0.016$; **Figure 5B**). In comparison with the samples in ET, samples taken during the end of experiment (Day 7) contained significantly lower GST activity than the samples from Day 1 ($p = 0.006$, adjusted significance = 0.038) and Day 3 ($p = 0.005$, adjusted significance = 0.029).

The activity of SOD in ET (Kruskal–Wallis $H = 16.924$, $p = 0.001$) and CT (Kruskal–Wallis $H = 23.603$, $p < 0.001$) was significantly different among the samples during the experimental period (**Figure 5C**). However, in ET, a gradual decrease of SOD activity can be observed on Day 7 as compared with Day 3 (Day 3 vs. Day 7; ET, $p = 0.001$, adjusted significance = 0.003).

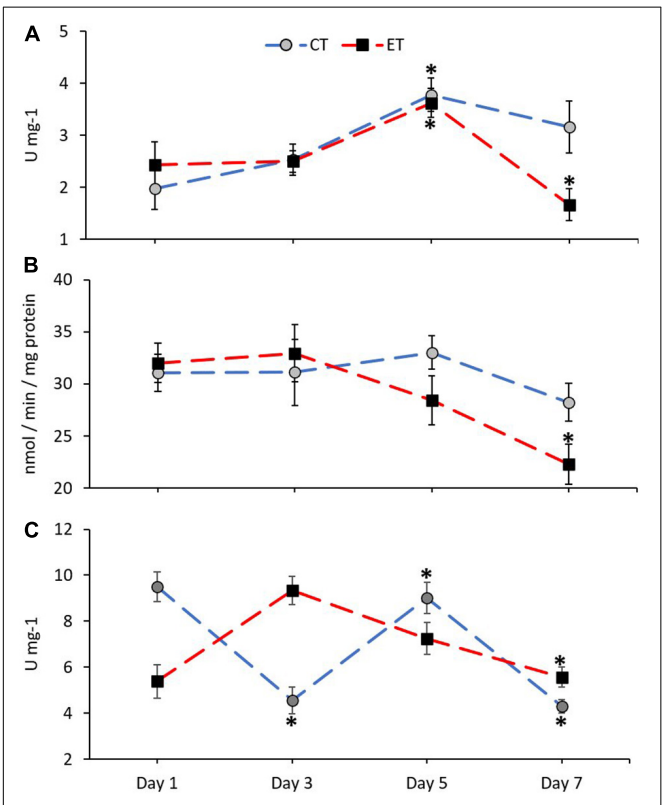

FIGURE 5 | Enzymatic activity of catalase, CAT **(A)**, glutathione *S*-transferases, GST **(B)**, and superoxide dismutase, SOD **(C)** in coral samples from CT and ET during the experimental period. All data points are mean ± SE ($n = 9$). Asterisk represents a significant difference ($p < 0.05$).

Fatty Acid Composition

Composition of SAFA, MUFA, and PUFA

The mean composition of SAFA (Kruskal–Wallis $H = 10.900$, $p = 0.012$), monounsaturated fatty acid (MUFA; Kruskal–Wallis $H = 10.063$, $p = 0.018$), and PUFA (Kruskal–Wallis $H = 8.187$, $p = 0.042$) was significantly changed between the samples in ET (**Figure 6**). In both tanks, the proportion of SAFA, MUFA, and PUFA remained stable from Day 1 to Day 5. In CT, PUFA composition significantly increased (Day 5 vs. Day 7; $p = 0.008$, adjusted significance = 0.047) during the end of experiment. Meanwhile, MUFA ($p = 0.003$, adjusted significance = 0.015) and PUFA ($p = 0.007$, adjusted significance = 0.044) drastically decreased, while SAFA composition increased significantly ($p = 0.003$, adjusted significance = 0.020) when the samples exposed to temperature of 31°C.

Polyunsaturated Fatty Acid Markers

In this study, the pattern of increase and decrease of FA markers (18:3n6, 18:4n3, 20:5n3, and 22:6n3) was observed in both tanks.

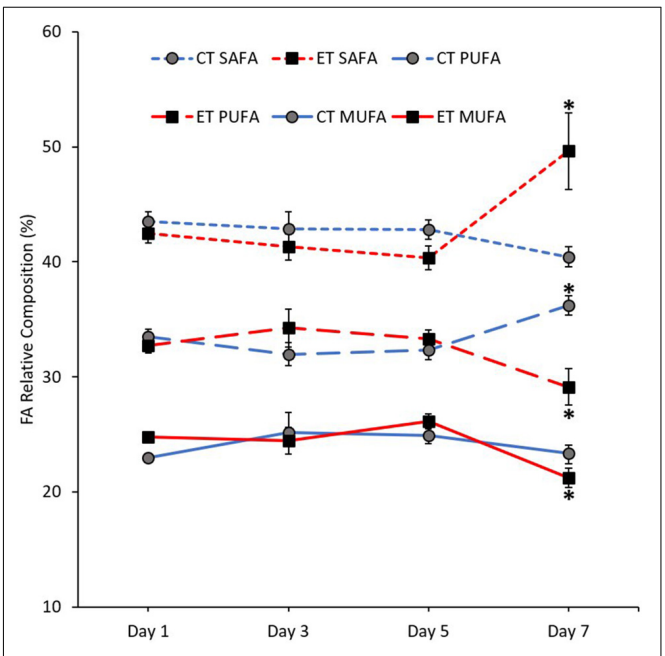

FIGURE 6 | Composition of fatty acid (FA) classes [saturated fatty acid (SAFA), monounsaturated fatty acid (MUFA), and polyunsaturated fatty acid (PUFA)] in coral samples from CT and ET during the experimental period. All data points are mean ± SE ($n = 9$). Asterisk represents a significant difference ($p < 0.05$).

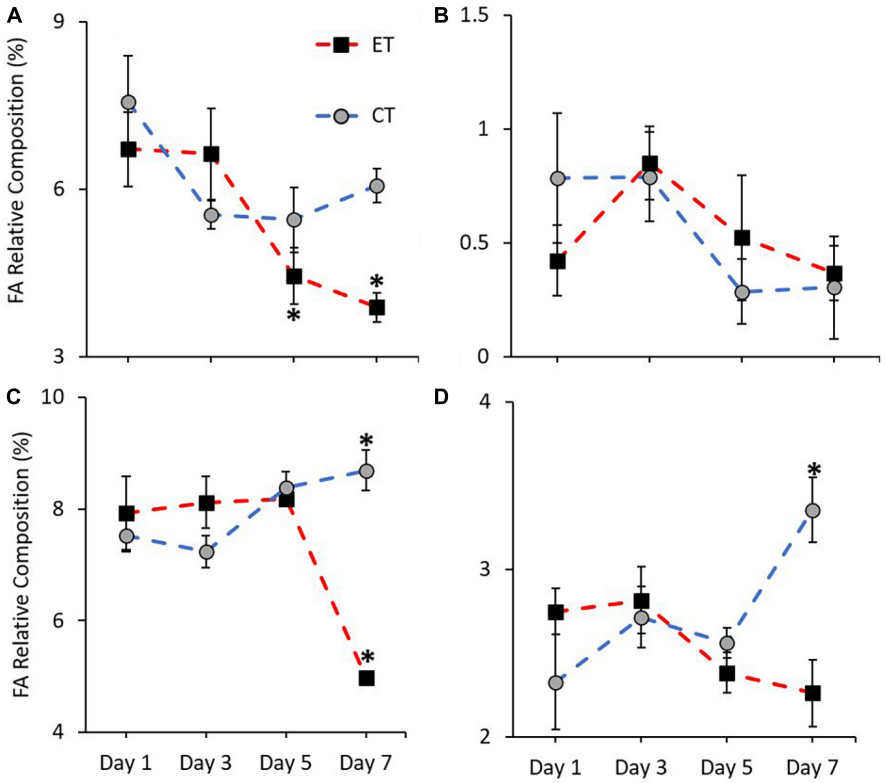

FIGURE 7 | Composition of most affected PUFA markers (**A** = 18:3n6, **B** = 18:4n3, **C** = 20:5n3, and **D** = 22:6n3) in coral samples from CT and ET during experimental period. All data points are mean ± SE (n = 9). Asterisk represents a significant difference ($p < 0.05$).

Except for 18:4n3 (CT; Kruskal–Wallis H = 4.187, p = 0.242, ET; Kruskal–Wallis H = 7.006, p = 0.072; **Figure 7B**), other markers show a significant change of FA composition during the experimental period. As shown in **Figure 7A**, no significant change of 18:3n6 composition was found in CT (Kruskal–Wallis H = 4.373, p = 0.224) but the composition decreased significantly in ET (Kruskal–Wallis H = 18.584, $p < 0.0.01$) especially when the samples were exposed from 29 ± 1.0 to 31 ± 1.0°C ($p < 0.001$, adjusted significance = 0.002). Meanwhile, the composition of 20:5n3 in CT increased significantly (Kruskal–Wallis H = 12.111, i = 0.007) from Day 3 to Day 7 (p = 0.003, adjusted significance = 0.019; **Figure 7C**). In contrast, the marker composition was significantly changed in ET (Kruskal–Wallis H = 19.649, $p < 0.001$), whereas the composition was decreased significantly during the end of experiment (Day 7 vs. Day 1, 3, and 5; $p < 0.05$, adjusted significance < 0.05). Slightly lower 22:6n3 composition in ET (Kruskal–Wallis H = 5.056, p = 0.168) was relatively observed as compared with CT (Kruskal–Wallis H = 12.842, p = 0.005), which showed a significant increase in the composition of these markers (**Figure 7D**).

Putative Fatty Acid Health Indicator

Figure 8 shows the ratio of FA health indicators examined in CT and ET. Samples in both tanks show a clear difference in n-3 LC:n-6 LC (CT; Kruskal–Wallis H = 14.892, p = 0.002, ET; Kruskal–Wallis H = 12.766, p = 0.005) and DHA:ARA (CT; Kruskal–Wallis H = 9.855, p = 0.020, ET; Kruskal–Wallis H = 16.770, p = 0.001) and also show relatively similar trend of increase and decrease (**Figures 8A,C**). However, the ratios were significantly lowered in ET as compared with CT, especially during the samples exposed to higher temperature from 29 ± 1.0 to 31 ± 1.0°C. Conversely, no clear difference was observed for EPA:ARA in CT (Kruskal–Wallis H = 2.471, p = 0.480) as compared with ET (Kruskal–Wallis H = 18.213, $p < 0.001$). In ET, the EPA:ARA drastically decreased when the samples were treated at 31 ± 1.0°C (**Figure 8B**).

Correlation With Symbiodiniaceae Density

In this study, a positive correlation was found between the enzymatic activity, FA markers, and health indicator ratio with the SD densities (**Table 1**). As the temperature increased, the SD density was positively correlated with GST activity, 18:3n6, 20:5n3, 22:6n3, and the ratio of n-3 LC:n-6 LC, EPA:ARA, and DHA:ARA.

DISCUSSION

Effect of Thermally Induced Stress

This study revealed the effect of heat stress on SD density, enzymatic activities, and FA composition in shallow-water

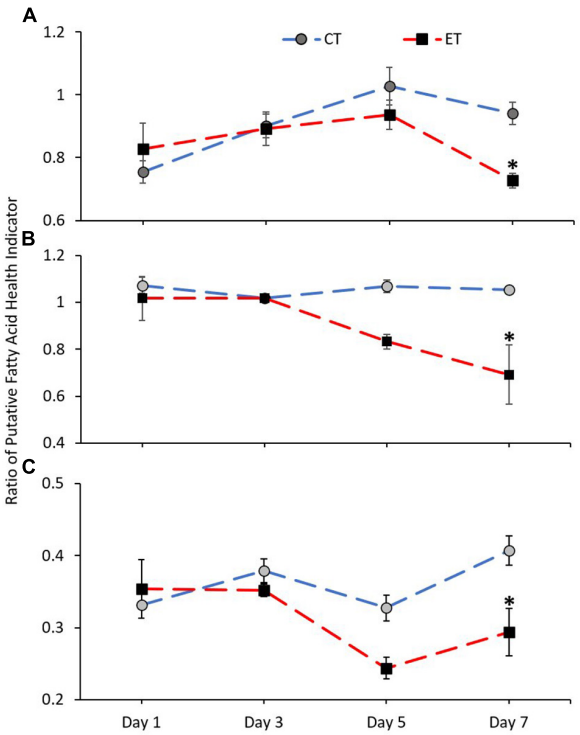

FIGURE 8 | Ratio of coral health indicators (**A** = n-3 LC:n-6 LC, **B** = EPA:ARA, and **C** = DHA:ARA) in coral samples from CT and ET during the experimental period. All data points are mean ± SE (n = 9). Asterisk represents a significant difference ($p < 0.05$).

TABLE 1 | Summary of significant correlation between SD density with enzymatic activity, fatty acid marker, and putative FA health indicator from data obtained in experimental tank data.

	rho	*P*
(a) Enzymatic activity		
GST	0.529**	< 0.001
(b) FA marker		
18:3n6	0.648**	< 0.001
20:5n3	0.499**	0.002
22:6n3	0.408*	0.014
(d) Putative FA health indicator		
n-3 LC: n-6 LC	0.338*	0.044
EPA: ARA	0.621**	< 0.001
DHA: ARA	0.493**	0.002

Non-significant relationships are not shown.
** Correlation is significant at the 0.05 level (2-tailed).*
*** Correlation is significant at the 0.01 level (2-tailed).*

coral, *A. digitifera*, *via* an experimental approach. The results clearly show that the bleaching response was obvious when the samples were exposed to 31 ± 1.0°C, which caused paleness or bleaching as a result of a significant loss of SD density from the corals. The symptom of bleaching was best explained by the expulsion of symbiotic algae from their host (Fitt et al., 2000; Imbs and Yakovleva, 2012; Rodríguez-Troncoso et al., 2016). In a prolonged heat exposure, the rate of symbiotic algae release is higher with the degraded forms of symbiotic algae among the expelled population increased in number. Fujise et al. (2014) also found that the proportion of degraded cells in hospice was low, whereas it was high in expelled populations. Therefore, heat stress can cause deterioration to the symbiotic algae, and the removal of symbiotic algae by the coral is an important mechanism to counterbalance the overproduction of ROS by symbiotic algae (Downs et al., 2002; Cunning and Baker, 2012).

Oxidative stress induced by elevated seawater temperature affected both corals and their symbiont that causes cellular damage, and the expulsion of the algae is due to the elimination or accumulation of toxic ROS (Lesser, 2006, Lesser, 2011; Baird et al., 2008; Weis, 2008). In normal conditions, the formation of radicals and the antioxidant system are well regulated to maintain the steady-state concentration of ROS at low levels involving antioxidant enzymes such as SOD, CAT, ascorbate peroxidase, GST, and glutathione peroxidase (Lesser, 2006; Rewitz et al., 2006; Lushchak, 2011). This can be observed in CT where our representative CAT, GST, and SOD antioxidant activities were normally high or well regulated during the steady-state of SD density as compared with the coral with reduced algae densities in ET. After 4 days of exposure at 31 ± 1.0°C, *A. digitifera* cannot recover their antioxidant defenses even the SD density has been at the lowest. During this condition, antioxidant enzyme activities can counterbalance with other oxidative damage products, but species that withstood longer thermal exposure could present low levels of antioxidant enzyme activities due to the exhaustion of enzyme production (Yakovleva et al., 2004; Dias et al., 2019). This is shown by the gradual decrease of enzymatic activity (GST and CAT) as demonstrated in this study. CAT activity in ET significantly decreases once corals lose their symbiont (Day 7) as compared with CT, indicating that the accumulation of H_2O_2 was significantly decreased. According to the theory of oxidative stress of coral bleaching, H_2O_2 generated by symbiotic algae can diffuse into coral cytoplasm, hence jeopardizing the antioxidant defenses of coral (Downs et al., 2002; Lesser, 2006). Prolonged exposure to high temperature can also damage ROS-sensitive enzymes, as observed by the decrease of CAT, GST, and SOD at the end of the experiment (Yakovleva et al., 2004; Dias et al., 2019). Therefore, we suggested that at high SD density, corals are vulnerable to oxidative stress, but prolonged exposure to heat can damage the enzymatic network and can be overwhelmed by ROS production. This is consistent with other studies that observed corals with high SD density are more susceptible to bleaching (Cunning and Baker, 2012; Xu et al., 2017) as the symbiotic algae produce harmful substances under high temperature stress, which cause tissue damage to their host (Nesa and Hidaka, 2009; Yakovleva et al., 2009). Therefore, it is suggested that the overproduction of harmful ROS induced by prolonged heat stress regulate the SD density and antioxidant activities in *A. digitifer*a.

During stress condition, corals significantly rely on their energy reserve, namely, FAs. The trend of increased SAFA and decreased PUFA composition during coral bleaching under heat stress has been well documented (Bachok et al., 2006; Imbs and Yakovleva, 2012). The reduction of unsaturated

FAs during stress condition is known to be related to lipid peroxidation (Okuyama et al., 2008; Ayala et al., 2014). Lipid peroxidation occurred when the primary defense by the antioxidant system overwhelms, causing oxidative damage to the lipid (Baird et al., 2008). During lipid peroxidation, the ROS attack lipid containing carbon–carbon double bond(s) such as MUFA and PUFA (Okuyama et al., 2008; Parrish, 2013; Ayala et al., 2014) because the double bond in unsaturated FA weakens the C–H bond on the carbon atom nearby to the double bond, which makes it more susceptible to oxidative stress (Catalá, 2010). The cell membrane consists of lipid that contains PUFA that is highly susceptible to toxic ROS. The hydrophobic characteristic of PUFA might prevent the entry of hydrophilic H_2O_2 molecules (Okuyama et al., 2008). Hence, PUFA composition can be the response of a coral to maintain membrane integrity and function during stress (Papina et al., 2007). At present, lower enzymatic activities during bleaching show that the antioxidant system is unable to tolerate the overproduction of toxic ROS, leading to oxidative damage that resulted in lower MUFA and PUFA composition. A significant decrease of FA composition in both classes during the thermally induced experiment shows that corals utilized their unsaturated FA as a final barrier or as a repair system toward oxidative damage (Baird et al., 2008). The membrane-shielding effect of PUFA, especially the long-chain n-3 series are likely to function as a primary protective barrier against the ROS (Okuyama et al., 2008). MUFA composition significantly decreased during the experiment. In contrast, the high composition of MUFA in bleached corals was observed due to the increase in bacteria colonization, which is proven by the presence of bacterial markers such as 16:1n7 and 18:1n7 (Bachok et al., 2006). However, in an experimentally control environment, the composition of these markers was found in trace amount. Meanwhile, the trend of increased SAFA in bleached corals is also related to the aforementioned lipid peroxidation (Parrish, 2013; Ayala et al., 2014) as well as to increase the rigidity of cellular membranes (Papina et al., 2007). Moreover, SAFA is the least reactive chemical and more stable than unsaturated FAs (Ratnayake and Galli, 2009).

Fatty Acid Markers

One of the particular interests in this study was the reduction in certain PUFA compositions such as 18:3n6, 18:4n3, EPA (20:5n3), and DHA (22:6n3). In this experiment, heat stress induced the reduction of 18:3n6 and 18:4n3 composition, which was similarly observed in other thermally induced experiments toward *A. intermedia* and *Montipora* sp. (Imbs and Yakovleva, 2012). Meanwhile, bleached corals such as *Pavona* sp., *Acropora* sp., and *Goniastrea* sp. contained significantly lower 18:4n3 and 22:6n3 than healthy corals, indicating that the loss of symbiotic algae from the host has influenced the FA composition (Bachok et al., 2006). The 18:3n6, 18:4n3, 20:5n3, and 22:6n3 were recognized as a possible FA characteristic in diatoms and dinoflagellates as well as recognized as symbiotic algae markers in hard and soft coral (Papina et al., 2003; Imbs and Dautova, 2008; Imbs et al., 2010b,c, 2014). It is suggested that the presence of specific markers to the symbiotic algae in the host tissue indicates that there is a translocation of specific PUFA markers from symbiotic algae to the host (Papina et al., 2003; Imbs et al., 2010b). Therefore, changes in SD densities during the experiment should be correlated with the FA markers. Among the PUFAs, the 18:3n6, 20:5n3, and 22:6n3 were positively correlated with the SD density, hence, a possible marker for symbiotic algae. No significant correlation was found in 18:4n3, and the composition was not significantly changed in both CT and ET, showing that the FA possibly represents the host marker. Several PUFAs can be synthesized by the host coral tissue *via de novo* synthesis (Monroig et al., 2013) and marked as the host markers (Treignier et al., 2008; Imbs et al., 2010a,b). To be clear, throughout the experimental period, the corals were not fed; thus, the effect of heterotrophy feeding is not significant, and this leaves the coral to rely on autotrophy for their daily energy requirement. Therefore, as the heterotrophy effect is limited, the 18:4n3 can be considered as the host marker.

Polyunsaturated fatty acids such as EPA and DHA are known to be involved in anti-inflammatory processes. PUFA from n-6 series such as 20:4n6 (ARA) is required for the synthesis of pro-inflammatory health hormones (Calder, 2017; Kumar et al., 2019). Inflammation is known as a defense mechanism that protects the host from stress (Calder, 2010). As shown in **Figures 7C,D**, the significant loss of EPA, DHA, and SD density in ET was observed after exposing the coral to the higher temperature. As the SD density is reduced, the coral loses the translocation of EPA and DHA from symbiotic algae, hence, increasing the possibility of excessive inflammation on the coral tissue under a prolonged bleaching condition (Innes and Calder, 2018).

Fatty Acid Health Indicator

Healthy corals can be indicated by a higher ratio of PUFA n-3 LC:n-6 LC (Dalsgaard et al., 2003). By the end of the experiment, all three PUFA ratios in the coral tissue of *A. digitifera* exposed to heat stress were significantly lower than the control condition. This is consistent with the field data showing that healthy corals contained a higher ratio of the PUFA n-3 LC:n-6 LC as compared with unhealthy corals (Rocker et al., 2019; Kim et al., 2021). Significant loss of the n-3 LC:n-6 LC in ET at the end of the experiment coincides with the significant loss of SD density, indicating some of these PUFAs, which were heavily transported to coral by their symbiotic algae, have been reduced. This is further proved by a positive correlation between the n-3 LC:n-6 LC with the SD density, showing that the n-3 LC PUFA is mainly obtained from the symbiotic algae. Under certain circumstances, n-3 LC:n-6 LC ratio may be preserved *via* heterotrophy and autotrophy feeding (Rocker et al., 2019). It is suggested that corals tend to modulate their feeding modes under certain conditions to provide an adaptive mechanism for sustaining their growth under stressful conditions (Grottoli et al., 2004; Teece et al., 2011). When the autotrophy mode is limited, corals sustain their metabolism by heterotrophy feeding (Treignier et al., 2008). For instance, bleached *Montipora capitata* extensively obtained their daily energy requirement *via* heterotrophic mode to assimilate lipid classes from zooplankton-derived carbon (Rodrigues et al., 2008). However, in our case, the corals in both tanks were not fed throughout the experiment; hence, the mechanism of switching

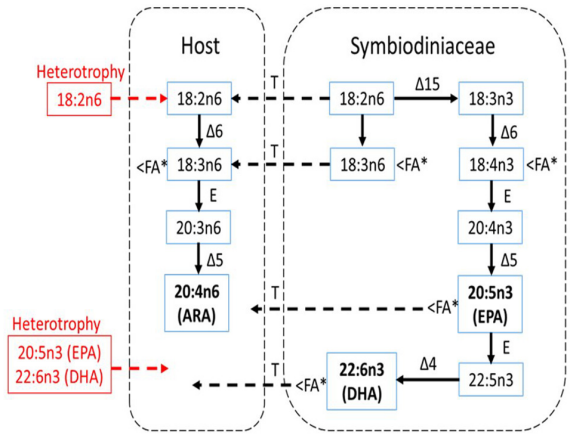

FIGURE 9 | The pathway of biosynthesis of n-3 and n-6 PUFA in shallow-water coral (*A. digitifera*) and a scheme for the possible transport of these FA between the host and symbiotic algae (Symbiodiniaceae) under experimental condition (modified from Imbs et al., 2010b). Essential FA components (ARA, EPA, and DHA) are bold while the red color shows the essential FAs that are not translocated from heterotrophy feeding. Δ4, Δ5, Δ6, and Δ15 are corresponding desaturase; E, elongase; T, transport. The < FA* indicates FA component that was significantly reduced during the thermally induced experiment.

the feeding mechanisms can be negligible. Naturally, the balance among this ratio is influenced by mixotrophic mechanisms, *via* autotrophy and heterotrophy feeding. Therefore, in this case, the balance is interrupted by limiting the heterotrophy feeding, and the corals extensively rely on their autotrophy mechanism.

The EPA and DHA were known as the FA characteristics for symbiotic algae and cannot be synthesized by the animals (**Figure 9**). At present, when heterotrophy feeding is reduced, coral heavily relies on symbiotic algae to obtain the EPA and DHA as shown in **Figure 9**. This is further proven by the positive correlation between EPA:ARA and DHA:ARA with the SD density. EPA and DHA are markers for symbiotic algae while ARA was suggested to be synthesized by the host (Treignier et al., 2008; Imbs et al., 2010a,b). Reduction in both ratios shows the loss of SD density affecting the EPA and DHA composition while the host preserved the ARA composition. The ARA can be synthesized by the host through the joint action of desaturase and elongase enzymes as follows: 18:3n6 → 20:3n6 → 20:4n6 (**Figure 9**). This is coincided with the decrement of 18:3n6 composition (**Figure 7A**), possibly indicating that the host maintained their ARA composition by synthesizing other PUFAs. The high composition of ARA is also related to heterotrophy feeding (Rocker et al., 2019), but limited heterotrophy feeding had required the corals to manipulate other FA to continue synthesizing the ARA.

CONCLUSION

At present, the heat stress has induced coral bleaching on shallow-water hard coral, *A. digitifera*, which causes significant changes in SD density, antioxidant enzyme activities, FA composition, and putative FA health indicator. Prolonged stress had caused the coral to expel their symbiont to counterbalance the stress condition. However, the significant decrease of CAT, GST, and SOD indicates that the antioxidant enzyme activities were overwhelmed by the overproduction of harmful ROS, and coral was unable to cope with the endogenous stress. As the first barrier against the stress collapsed, coral expels their symbiotic algae and regulates their energy reserved *via* FA to restore healthy homeostasis. A significant decrease in unsaturated FA (MUFA and PUFA) significantly correlated with the loss of SD density and was associated with their susceptibility to harmful ROS. An increase in SAFA composition shows that the FA remains stable against the stress condition as compared with unsaturated FA. Additionally, a significant decrease in certain PUFA markers (18:3n6, 20:5n3, and 22:6n3) and putative FA health indicators (n-3 LC:n-6 LC, EPA:ARA, and DHA:ARA) was associated with the loss of SD density. Perhaps, limited heterotrophy feeding during the experimental period makes the coral highly dependent on their symbiotic partners.

DATA AVAILABILITY STATEMENT

Written informed consent was obtained from the relevant individual(s) for the publication of any potentially identifiable images or data included in this article.

AUTHOR CONTRIBUTIONS

CS: conceptualization, methodology, formal analysis, investigation, writing—original draft, writing—review and editing, and visualization. MS: conceptualization, methodology, investigation, and writing—review and editing. SJ: writing—review and editing, supervision, and project administration. CT: writing—review and editing and supervision. ZB: writing—review and editing, supervision, project administration, and funding acquisition. All authors contributed to the article and approved the submitted version.

FUNDING

This study was supported by the Ministry of Higher Education Malaysia, Fundamental Research Grant (FRGS; Vot No. 59538), Collaborative grant IPC (International Petroleum Corp.; Vot No. 53392), and Higher Institution Center of Excellence (HICoE), the Institute of Oceanography and Environment (Vot No. 66928).

ACKNOWLEDGMENTS

The authors would like to express their gratitude to all the researchers and staff for their invaluable assistance during the study period especially Puteri Nurshazmimi Zaidi for helping us in the hatchery. All types of equipment were provided by the Institute of Oceanography and Environment. The experiment was conducted in the hatchery of the Institute of Tropical Aquaculture and Fisheries.

REFERENCES

Abdulkadir, S., and Tsuchiya, M. (2008). One-step method for quantitative and qualitative analysis of fatty acids in marine animal samples. *J. Exp. Mar. Biol. Ecol.* 354, 1–8. doi: 10.1016/j.jembe.2007.08.024

Apprill, A. (2020). The Role of Symbioses in the Adaptation and Stress Responses of Marine Organisms. *Annu. Rev. Mar. Sci.* 12, 291–314. doi: 10.1146/annurev-marine-010419-010641

Ayala, A., Muñoz, M. F., and Argüelles, S. (2014). Lipid peroxidation: production, metabolism, and signaling mechanisms of malondialdehyde and 4-hydroxy-2-nonenal. *Oxid. Med. Cell. Longev.* 2014:360438. doi: 10.1155/2014/360438

Bachok, Z., Mfilinge, P., and Tsuchiya, M. (2006). Characterization of fatty acid composition in healthy and bleached corals from Okinawa, Japan. *Coral Reefs* 25, 545–554. doi: 10.1007/s00338-006-0130-9

Baird, A. H., Bhagooli, R., Ralph, P. J., and Takahashi, S. (2008). Coral bleaching: the role of the host. *Trends Ecol. Evol.* 24, 16–20. doi: 10.1016/j.tree.2008.09.005

Baker, A. C., Glynn, P. W., and Riegl, B. (2008). Climate change and coral reef bleaching : An ecological assessment of long-term impacts, recovery trends and future outlook. *Estuar. Coast. Shelf Sci.* 80, 435–471. doi: 10.1016/j.ecss.2008.09.003

Beers, R. F., and Sizer, I. W. (1952). A spectrophotometric method for measuring the breakdown of hydrogen peroxide by catalase. *J. Biol. Chem.* 195, 133–140. doi: 10.1016/s0021-9258(19)50881-x

Betteridge, D. J. (2000). What is oxidative stress? *Metabolis* 49, 3–8.

Bhagooli, R., and Hidaka, M. (2004). Photoinhibition, bleaching susceptibility and mortality in two scleractinian corals, *Platygyra ryukyuensis* and *Stylophora pistillata*, in response to thermal and light stresses. *Comp. Biochem. Physiol. A* 137, 547–555. doi: 10.1016/j.cbpb.2003.11.008

Biel, K. Y., Gates, R. D., and Muscatine, L. (2007). Effects of free amino acids on the photosynthetic carbon metabolism of symbiotic dinoflagellates. *Russ. J. Plant Physiol.* 54, 171–83. doi: 10.1134/s1021443707020033

Bradford, M. M. (1976). A rapid and sensitive method for the quantitation of microgram quantities of protein utilizing the principle of protein-dye binding. *Anal. Biochem.* 72, 248–254. doi: 10.1016/0003-2697(76)90527-3

Calder, P. C. (2010). Omega-3 fatty acids and inflammatory processes. *Nutrients* 2, 355–374. doi: 10.3390/nu2030355

Calder, P. C. (2017). Omega-3 fatty acids and inflammatory processes: from molecules to man. *Biochem. Soc. Trans.* 45, 1105–1115. doi: 10.1042/BST20160474

Catalá, A. (2010). A synopsis of the process of lipid peroxidation since the discovery of the essential fatty acids. *Biochem. Bioph Res. Co.* 399, 318–323. doi: 10.1016/j.bbrc.2010.07.087

Cook, C. B., and Davy, S. K. (2001). Are free amino acids responsible for the 'host factor' effects on symbiotic zooxanthellae in extracts of host tissue? *Hydrobiologia* 461, 71–78. doi: 10.1023/A:1012785725378

Cunning, R., and Baker, A. C. (2012). Excess algal symbionts increase the susceptibility of reef corals to bleaching. *Nat. Clim. Chang.* 3, 259–262. doi: 10.1038/NCLIMATE1711

Cziesielski, M. J., Schmidt-Roach, S., and Aranda, M. (2019). The past, present, and future of coral heat stress studies. *Ecol. Evol.* 9, 10055–10066. doi: 10.1002/ece3.5576

Dalsgaard, J., John, M. S., Kattner, G., Müller-Navarra, D., and Hagen, W. (2003). Fatty acid trophic markers in the pelagic marine environment. *Adv. Mar. Biol.* 46, 227–318.

De'ath, G., Fabricius, K. E., Sweatman, H., and Puotinen, M. (2012). The 27 – year decline of coral cover on the Great Barrier Reef and its causes. *PNAS* 109:1208909109. doi: 10.1073/pnas.1208909109

Dias, M., Ferreira, A., Gouveia, R., Madeira, C., Jogee, N., Cabral, H., et al. (2019). Long-term exposure to increasing temperatures on scleractinian coral fragments reveals oxidative stress. *Mar. Environ. Res.* 150:104758. doi: 10.1016/j.marenvres.2019.104758

Downs, C. A., Fauth, J. E., Halas, J. C., Dustan, P., Bemiss, J., and Woodley, C. M. (2002). Oxidative stress and seasonal coral bleaching. *Free Radic. Biol. Med.* 33, 533–543. doi: 10.1016/s0891-5849(02)00907-3

Fitt, W. K., McFarland, F. K., Warner, M. E., and Chilcoat, G. C. (2000). Seasonal patterns of tissue biomass and densities of symbiotic dinoflagellates in reef corals and relation to coral bleaching. *Limnol. Oceanogr.* 45, 677–685. doi: 10.4319/lo.2000.45.3.0677

Fujise, L., Yamashita, H., Suzuki, G., Sasaki, K., Liao, L. M., and Koike, K. (2014). Moderate thermal stress causes active and immediate expulsion of photosynthetically damaged zooxanthellae (*Symbiodinium*) from corals. *PLoS One* 9:e114321. doi: 10.1371/journal.pone.0114321

Grottoli, A. G., Rodrigues, L. J., and Juarez, C. (2004). Lipids and stable carbon isotopes in two species of Hawaiian corals, *Porites compressa* and *Montipora verrucosa*, following a bleaching event. *Mar. Biol.* 145, 621–631. doi: 10.1007/s00227-004-1337-3

Guest, J. R., Baird, A. H., Maynard, J. A., Muttaqin, E., Edwards, A. J., Campbell, S. J., et al. (2012). Contrasting patterns of coral bleaching susceptibility in 2010 suggest an adaptive response to thermal stress. *PLoS One* 7:e33353.

Habig, W. H., and Jakoby, W. B. (1981). Assays for differentiation of glutathione S-Transferases. *Methods Enzymol.* 77, 398–405. doi: 10.1016/S0076-6879(81)77053-8

Imbs, A. B., and Dautova, T. N. (2008). Use of lipids for chemotaxonomy of octocorals (Cnidaria: Alcyonaria). *Russ. J. Mar. Biol.* 34, 174–178.

Imbs, A. B., and Yakovleva, I. M. (2012). Dynamics of lipid and fatty acid composition of shallow-water corals under thermal stress: an experimental approach. *Coral Reefs* 31, 41–53. doi: 10.1007/s00338-011-0817-4

Imbs, A. B., Latyshev, N. A., Dautova, T. N., and Latypov, Y. Y. (2010a). Distribution of lipids and fatty acids in corals by their taxonomic position and presence of zooxanthellae. *Mar. Ecol. Prog. Ser.* 409, 65–75. doi: 10.3354/meps08622

Imbs, A. B., Yakovleva, I. M., Dautova, T. N., Bui, L. H., and Jones, P. (2014). Diversity of fatty acid composition of symbiotic dinoflagellates in corals: Evidence for the transfer of host PUFAs to the symbionts. *Phytochemistry* 101, 76–82. doi: 10.1016/j.phytochem.2014.02.012

Imbs, A. B., Yakovleva, I. M., Latyshev, N. A., and Pham, L. Q. (2010b). Biosynthesis of polyunsaturated fatty acids in zooxanthellae and polyps of corals. *Russ. J. Mar. Biol.* 36, 452–457. doi: 10.1134/S1063074010060076

Imbs, A. B., Yakovleva, I. M., and Pham, Q. L. (2010c). Distribution of lipids and fatty acids in the zooxanthellae and host of the soft coral *Sinularia* sp. *Fish. Sci.* 76, 375–380. doi: 10.1007/s12562-009-0213-y

Innes, J. K., and Calder, P. C. (2018). Omega-6 fatty acids and inflammation. *Prostag Leukotr Essential Fatty Acids* 132, 41–48. doi: 10.1016/j.plefa.2018.03.004

Johannes, R. E., and Wiebe, W. J. (1970). Method for determination of coral tissue biomass and composition. *Limnol. Oceanogr.* 15, 822–824. doi: 10.4319/lo.1970.15.5.0822

Kim, T., Lee, J. C., Kang, D. H., Duprey, N. N., Leung, K. S., Archana, A., et al. (2021). Modification of fatty acid profile and biosynthetic pathway in symbiotic corals under eutrophication. *Sci. Total Environ.* 2021:145336. doi: 10.1016/j.scitotenv.2021.145336

Kumar, N. G., Contaifer, D., Madurantakam, P., Carbone, S., Price, E. T., Van Tassell, et al. (2019). Dietary bioactive fatty acids as modulators of immune function: implications on human health. *Nutrients* 11:2974. doi: 10.3390/nu11122974

Lesser, M. P. (1997). Oxidative stress causes coral bleaching during exposure to elevated temperatures. *Coral Reefs* 16, 187–192. doi: 10.1007/s003380050073

Lesser, M. P. (2006). Oxidative stress in marine environments: biochemistry and physiological ecology. *Annu. Rev. Physiol.* 68, 253–278. doi: 10.1146/annurev.physiol.68.040104.110001

Lesser, M. P. (2011). "Coral bleaching: causes and mechanisms," in *Coral Reefs: An Ecosystem in Transition*, eds Z. Dubinsky and N. Stambler (Dordrecht: Springer), 1–552. doi: 10.1007/978-94-007-0114-4_23

Lushchak, V. I. (2011). Environmentally induced oxidative stress in aquatic animals. *Aquat. Toxicol.* 101, 13–30. doi: 10.1016/j.aquatox.2010.10.006

Mansfield, K. M., and Gilmore, T. D. (2019). Innate immunity and cnidarian-Symbiodiniaceae mutualism. *Dev. Comp. Immunol.* 90, 199–209. doi: 10.1016/j.dci.2018.09.020

Monroig, Ó, Tocher, D. R., and Navarro, J. C. (2013). Biosynthesis of polyunsaturated fatty acids in marine invertebrates: recent advances in molecular mechanisms. *Mar. Drugs* 11, 3998–4018. doi: 10.3390/md11103998

Nesa, B., and Hidaka, M. (2009). High zooxanthella density shortens the survival time of coral cell aggregates under thermal stress. *J. Exp. Mar. Biol. Ecol.* 368, 81–87. doi: 10.1016/j.jembe.2008.10.018

Okuyama, H., Orikasa, Y., and Nishida, T. (2008). Significance of antioxidative functions of eicosapentaenoic and docosahexaenoic acids

in marine microorganisms. *Appl. Environ. Microbiol.* 74, 570–574. doi: 10.1128/AEM.02256-07

Palmer, C. V. (2018). Immunity and the coral crisis. *Commun. Biol.* 1, 1–7. doi: 10.1038/s42003-018-0097-4

Papina, M., Meziane, T., and Van Woesik, R. (2003). Symbiotic zooxanthellae provide the host-coral Montipora digitata with polyunsaturated fatty acids. *Comp. Biochem. Physiol. B Biochem. Mol. Biol.* 135, 533–537. doi: 10.1016/S1096-4959(03)00118-0

Papina, M., Meziane, T., and Van Woesik, R. (2007). Acclimation effect on fatty acids of the coral Montipora digitata and its symbiotic algae. *Comp. Biochem. Physiol. B Biochem. Mol. Biol.* 147, 583–589. doi: 10.1016/j.cbpb.2007.02.011

Parrish, C. C. (2013). Lipids in marine ecosystems. *Int. Sch. Res. Notices* 2013:604045. doi: 10.5402/2013/604045

Ratnayake, W. N., and Galli, C. (2009). Fat and fatty acid terminology, methods of analysis and fat digestion and metabolism. *Ann. Nutr. Metab.* 55, 8–43. doi: 10.1159/000228994

Rewitz, K. F., Styrishave, B., Løbner-Olesen, A., and Andersen, O. (2006). Marine invertebrate cytochrome P450: emerging insights from vertebrate and insect analogies. *Comp. Biochem. Physiol. C Toxicol. Pharmacol.* 143, 363–381. doi: 10.1016/j.cbpc.2006.04.001

Rocker, M. M., Francis, D. S., Fabricius, K. E., Willis, B. L., and Bay, L. K. (2019). Temporal and spatial variation in fatty acid composition in *Acropora tenuis* corals along water quality gradients on the Great Barrier Reef, Australia. *Coral Reefs* 38, 215–228. doi: 10.1007/s00338-019-01768-x

Rodrigues, L. J., Grottoli, A. G., and Pease, T. K. (2008). Lipid class composition of bleached and recovering *Porites compressa* Dana, 1846 and *Montipora capitata* Dana, 1846 corals from Hawaii. *J. Exp. Mar. Bio. Ecol.* 358, 136–143. doi: 10.1016/j.jembe.2008.02.004

Rodríguez-Troncoso, A. P., Carpizo-Ituarte, E., and Cupul-Magaña, A. L. (2016). Physiological response to high temperature in the Tropical Eastern Pacific coral *Pocillopora verrucosa*. *Mar. Ecol.* 37, 1168–1175. doi: 10.1111/maec.12392

Siebeck, U. E., Marshall, N. J., Klüter, A., and Hoegh-Guldberg, O. (2006). Monitoring coral bleaching using a colour reference card. *Coral Reefs* 25, 453–460. doi: 10.1007/s00338-006-0123-8

Takahashi, S., and Murata, N. (2008). How do environmental stresses accelerate photoinhibition? *Trends Plant Sci.* 13, 178–182. doi: 10.1016/j.tplants.2008.01.005

Teece, M. A., Estes, B., Gelsleichter, E., and Lirman, D. (2011). Heterotrophic and autotrophic assimilation of fatty acids by two scleractinian corals, *Montastraea faveolata* and *Porites astreoides*. *Limnol. Oceanogr.* 56, 1285–1296. doi: 10.4319/lo.2011.56.4.1285

Teixeira, T., Diniz, M., Calado, R., and Rosa, R. (2013). Coral physiological adaptations to air exposure: heat shock and oxidative stress responses in *Veretillum cynomorium*. *J. Exp. Mar. Biol. Ecol.* 439, 35–41. doi: 10.1016/j.jembe.2012.10.010

Treignier, C., Grover, R., Ferrier-Pages, C., and Tolosa, I. (2008). Effect of light and feeding on the fatty acid and sterol composition of zooxanthellae and host tissue isolated from the scleractinian coral *Turbinaria reniformis*. *Limnol. Oceanogr.* 53, 2702–2710. doi: 10.4319/lo.2008.53.6.2702

Weis, V. M. (2008). Cellular mechanisms of Cnidarian bleaching : stress causes the collapse of symbiosis. *J. Exp. Biol.* 211, 3059–3066. doi: 10.1242/jeb.009597

Xu, L., Yu, K., Li, S., Liu, G., Tao, S., Shi, Q., et al. (2017). Interseasonal and interspecies diversities of Symbiodinium density and effective photochemical efficiency in five dominant reef coral species from Luhuitou fringing reef, northern South China Sea. *Coral Reefs* 36, 477–487. doi: 10.1007/s00338-016-1532-y

Yakovleva, I. M., Baird, A. H., Yamamoto, H. H., Bhagooli, R., Nonaka, M., and Hidaka, M. (2009). Algal symbionts increase oxidative damage and death in coral larvae at high temperatures. *Mar. Ecol. Prog. Ser.* 378, 105–112. doi: 10.3354/meps07857

Yakovleva, I., Bhagooli, R., Takemura, A., and Hidaka, M. (2004). Differential susceptibility to oxidative stress of two scleractinian corals: antioxidant functioning of mycosporine-glycine. *Comp. Biochem. Physiol. B Biochem. Mol. Biol.* 139, 721–730. doi: 10.1016/j.cbpc.2004.08.016

Conflict of Interest: The authors declare that the research was conducted in the absence of any commercial or financial relationships that could be construed as a potential conflict of interest.

Publisher's Note: All claims expressed in this article are solely those of the authors and do not necessarily represent those of their affiliated organizations, or those of the publisher, the editors and the reviewers. Any product that may be evaluated in this article, or claim that may be made by its manufacturer, is not guaranteed or endorsed by the publisher.

frontiers in Marine Science

ORIGINAL RESEARCH
published: 08 October 2021
doi: 10.3389/fmars.2021.712214

Physiological Responses of *Pocillopora acuta* and *Porites lutea* Under Plastic and Fishing Net Stress

*Long Ying[1,2], Sutinee Sinutok[1,2], Pathompong Pramneechote[1,2], Pattara Aiyarak[3], Peter J. Ralph[4] and Ponlachart Chotikarn[1,2,5]**

[1] Faculty of Environmental Management, Prince of Songkla University, Hat Yai, Thailand, [2] Coastal Oceanography and Climate Change Research Center, Prince of Songkla University, Hat Yai, Thailand, [3] Faculty of Science, School of Computational Science, Prince of Songkla University, Hat Yai, Thailand, [4] Climate Change Cluster, University of Technology Sydney, Ultimo, NSW, Australia, [5] Faculty of Environmental Management, Marine and Coastal Resources Institute, Prince of Songkla University, Hat Yai, Thailand

Marine debris has become a global problem affecting coral health around the globe. However, the photophysiological responses of corals to marine debris stress remain unclear. Therefore, this study firstly investigated transparent and opaque plastic bag shading and fishing nets directly contacting the coral. Photosynthetic performance, pigment content, symbiont density, and calcification rate of a branching coral *Pocillopora acuta* and a massive coral *Porites lutea* were investigated after 4 weeks of exposure to marine debris. The results show that the maximum quantum yield of PSII significantly decreased in *P. lutea* with all treatments, while *P. acuta* showed no effect on the maximum quantum yield of PSII from any treatments. Transparent plastic bag shading does not affect *P. acuta*, but significantly affected the maximum photochemical efficiency of *P. lutea*. Photoacclimation of cellular pigment content was also observed under opaque plastic bag shading for both species at week 2. Fishing nets had the strongest effect and resulted in *P. acuta* bleaching and *P. lutea* partial mortality as well as a decline in zooxanthellae density. Calcification rate of *P. acuta* significantly decreased with treatments using opaque plastic bag and fishing net, but for *P. lutea* only the treatment with fishing net gave any observable effects. This study suggests that the sensitivities of corals to marine debris differ strongly by species and morphology of the coral.

Keywords: marine debris, plastic litter, fishing nets, ecophysiology, zooxanthellae, photoacclimation, corals

OPEN ACCESS

Edited by:
Ranjeet Bhagooli, University of Mauritius, Mauritius

Reviewed by:
Hiroya Yamano, National Institute for Environmental Studies (NIES), Japan
Suchana Chavanich, Chulalongkorn University, Thailand

***Correspondence:**
Ponlachart Chotikarn
ponlachart.c@psu.ac.th

Specialty section:
This article was submitted to Aquatic Physiology, a section of the journal Frontiers in Marine Science

Received: *20 May 2021*
Accepted: *30 August 2021*
Published: *08 October 2021*

Citation:
Ying L, Sinutok S, Pramneechote P, Aiyarak P, Ralph PJ and Chotikarn P (2021) Physiological Responses of Pocillopora acuta and Porites lutea Under Plastic and Fishing Net Stress. Front. Mar. Sci. 8:712214. doi: 10.3389/fmars.2021.712214

INTRODUCTION

Coral reefs are the most biologically diverse ecosystems in the world, and provide a variety of valuable ecosystem services to global communities (Moberg and Folke, 1999; Harrison and Booth, 2007). However, global warming, acidification of our oceans, and sea level rise can severely affect the survival of corals worldwide (Marshall and Baird, 2000; Orr et al., 2005; Anthony et al., 2008). Fishing gear found across shallow reefs can damage coral reef structure, destroying both benthic flora and fauna, as well as entangling macrofauna (Abu-Hilal and Al-Najjar, 2009). In addition, the anthropogenic activities over the last century have made marine debris a global problem (Ryan, 2015). It is estimated that about 4.8–12.7 MT of marine debris is discharged into the oceans every

year (Jambeck et al., 2015), with 5.25 trillion plastic particles weighing 268,940 tons floating in the oceans (Eriksen et al., 2014). Plastic waste, fishing gear and metals are the dominant three types of debris observed in the Red Sea (Abu-Hilal and Al-Najjar, 2009). Marine debris can be found in every marine habitat, from surface water down to the deep sea (Dameron et al., 2007; Barnes et al., 2009; Buhl-Mortensen and Buhl-Mortensen, 2017), and it affects hundreds of marine species worldwide (Schipper et al., 2008; Barnes et al., 2009; Todd et al., 2010) as well as disrupts whole reef ecological systems (de Carvalho-Souza et al., 2018) and causes loss of coral structural complexity and diversity (Figueroa-Pico et al., 2020). Marine debris has detrimental effects on coral and coral reef ecosystems both directly and indirectly (Donohue et al., 2001). Large debris items physically damage corals through abrasion, suffocation, or starvation (Richards and Beger, 2011). Lamb et al. (2018) found more than 11 billion plastic items entangled with coral reefs in the Asia-Pacific, and suggested that coral disease outbreaks increase when corals are entangled with plastic. Decreased light intensity from being covered by plastic debris has been documented to effect branching coral health and lead to coral bleaching (Muhammad et al., 2021). Field research in Kho Tao, Thailand, found that coral underneath a fishing net suffered the most damage (Valderrama Ballesteros et al., 2018). Massive and branching coral types are the most susceptible when compared with colonies of other morphologies (Putra et al., 2021). In addition, corals are particularly sensitive to abrasion (Tanner, 1995) and abrasion responses in corals are common with plastics. Marine debris has the potential to accumulate bacteria (Zhang et al., 2017), and coral health is controlled by the microbiome within the muco-polysaccharide layer (Kline et al., 2006). Rapid changes in environmental conditions alter coral microbiome, causing bleaching, and disease susceptibility (Bourne et al., 2016). Coral requires carbon both as an autotrophic and a heterotrophic nutrition source (Anthony and Fabricius, 2000; Richards and Beger, 2011). However, macro- and microplastics affect cold-water coral skeleton growth rate, as microplastics interfere with polyps capturing food particles (Chapron et al., 2018). Microplastics are found wrapped in mesenterial tissue within the coral gut cavity, and ingesting high concentrations of microplastics could potentially damage the health of corals (Hall et al., 2015). A number of studies have confirmed that there is abundant marine debris in the oceans, and that it devastates coral reefs. However, there are limited studies quantifying the damage from different types of debris on photosynthesis and productivity of corals and zooxanthellae. Therefore, this study aimed to investigate how *Pocillopora acuta* and *Porites lutea* coral species respond to different types of marine debris.

MATERIALS AND METHODS

Experimental Design

Six colonies each of the coral specie *P. acuta* and *P. lutea* were collected from Panwa Cape, Phuket Thailand (7°48′06.9″N 98°24′24.4″E) and transferred within 24 h to aquarium tanks at Prince of Songkla University, HatYai, Thailand, for acclimation. Temperature, salinity and light intensity from collection site were recorded. Every colony was acclimated in a holding tank for a week under 120 μmol photons m^{-2} s^{-1} light, 29°C, 33 psu salinity, and pH 8.20. After that, the coral colonies were cut into 192 nubbins (*P. acuta* with 3 cm length, *P. lutea* with size around 1.5 cm × 1.5 cm) and acclimated in holding tanks for another week, after which the nubbins were randomly placed to four sets (24 nubbins/specie/treatment) of experimental tanks and acclimated for 1 week. After acclimation, the tanks were subjected to four treatments. Control had no marine debris (Treatment 1); opaque plastic (High Density Polyethylene) bag-located 2 cm above nubbins (15% Light reduction, Treatment 2); transparent plastic (Low Density Polyethylene) bag-located 2 cm above nubbins (3% light reduction, Treatment 3); and Fishing net (13% light reduction and abrasion, Treatment 4). There were 6 replicate samples per treatment per species (**Figure 1**). The whole experiment was performed over 4 weeks to test the effects of marine debris on coral. We sampled nubbins for the zooxanthellae density and chlorophyll concentration analysis in week 2 and week 4. Heater chiller (JMC-02, JBA, China), COB light (TS-A600, Aquarium lamp, China), and LED light (A601, Chihiros, China) were, respectively, used to control water temperature and light intensity in the experimental tanks. Light intensity, temperature, salinity and pH in each experimental tank were set for 120 mmol photons m^{-2} s^{-1}, 29°C, 33 psu and pH 8.20, respectively. Light was turned on at 10:00 and turned off at 22:00 (12:12 hr light:dark period). Nitrate and phosphate concentrations were controlled below 0 mg L^{-1} and 2 mg L^{-1}, respectively. Aquariums were filled with natural seawater filtered with a nomex filter bag and treated with chlorine [50 mg chlorine L^{-1} (50 ppm)]. Thirty percent of the aquarium water was replaced every week, and all physical and chemical parameters were measured every 2 days. Photosynthetic performance of zooxanthellae and health of corals were monitored using chlorophyll *a* fluorescence, and this was randomly measured with the Diving-PAM at the top of nubbins. Pigment concentration and symbiotic cell density were investigated for supporting photosynthetic performance of zooxanthellae. Growth of corals was investigated using buoyant weight technique (Jokiel et al., 1978).

Chlorophyll *a* Fluorescence

Chlorophyll *a* fluorescence of *P. acuta* and *P. lutea* in each treatment was quantified every 2 days over the 4 weeks of experiment by using a Diving-PAM fluorometer (Walz GmbH, Germany) connected to a 6-mm diameter fiber-optic probe (6 replicates per species per treatment per time). Photochemical efficiency of PSII was described by maximum quantum yield (F_v/F_m) or active PSII centers (F_v/F_0) and measured at 08:00 (before light was turned on). Reduction of PSII reaction center number can provide photoinhibitory indication (Behrenfeld et al., 1998). Rapid light curves (RLCs) were measured at 13:00. Maximum relative electron transport rate ($rETR_{max}$), minimum saturating irradiance (E_k), and initial slope (alpha) were derived from curve fits (Platt et al., 1980; Ralph and Gademann, 2005).

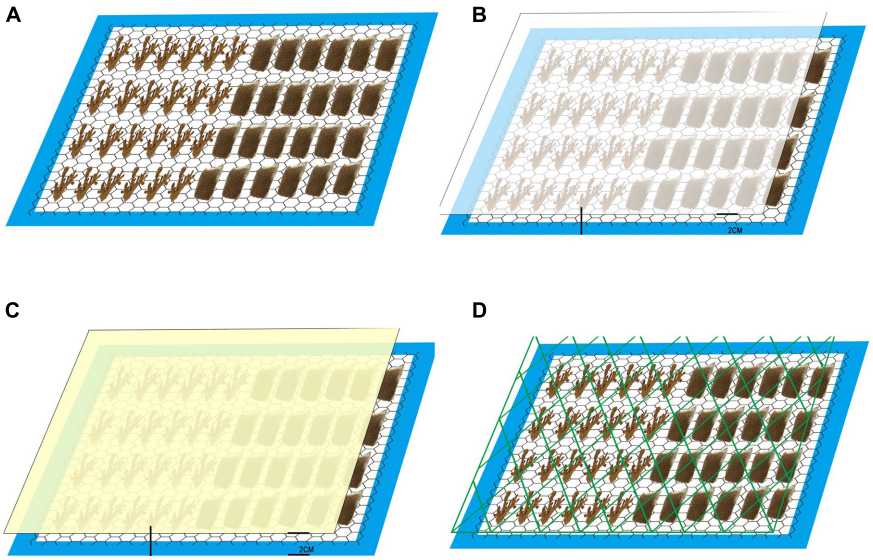

FIGURE 1 | Images of the experiment tank design. **(A)** Control, **(B)** Transparent bag, **(C)** Opaque bag, and **(D)** Fishing net.

Symbiotic Cell Density

Samples were collected every 2 weeks for zooxanthellae density analysis. The samples were water-picked into 50 mL of 0.2-μm-filtered seawater to remove the tissue from the skeleton. The slurry was centrifuged at 1,000 rpm for 10 min to produce a well-mixed sample (Hill and Ralph, 2007). Six replicates for each species and each experiment were counted using a haemocytometer under a light microscope. The cell density was determined per cm^2 following coral surface area determinations used the paraffin wax technique (Stimson and Kinzie, 1991).

Photosynthetic Pigment Concentration

The slurry from determination of symbiotic cell density was also used in pigment concentration determinations. For photosynthetic pigment [chlorophyll (Chl) *a* and c_2] analyses, the slurry was centrifuged for 5 min at 5,000 rpm. After that, the supernatant was discarded and algal pellets were re-suspended in 3 ml of 90% acetone and stored in darkness for 24 h at 4°C. After centrifugation, chlorophyll *a* and c_2 (μg cm^{-2}) concentrations were determined using the standard spectrophotometric method of Ritchie (2006) with absorbance measured at 630, 664, and 750 nm (Winters et al., 2009).

Calcification Rate

Buoyant weight technique was used for calculating calcification rate of the coral skeleton (Jokiel et al., 1978; Spencer Davies, 1989). In theory each sample is weighed in seawater of known density, and the dry weight of the sample in air is estimated by using Archimedes' principle (Sinutok et al., 2011). Each replicate coral nubbin was weighted at the start of the experiment and the end of experiment (week 4) using a 4-digit precision balance (OHAUS, United States). Skeleton bulk densities used for *P. lutea* and *P. acuta* were 1.19 and 2.01 g cm^{-3}, respectively (Tanzil et al., 2009; Ng et al., 2019). The temperature and salinity of seawater were measured first. Then the glass stopper was weighted both in air and in water for calculating the density of seawater (Spencer Davies, 1989). The skeleton growth rate was calculated from equation:

$$G = \sqrt[c]{\frac{a}{b}} - 1$$

in which G = growth, a = weight at the end of experiment, b = weight at the start of experiment, and c = number of days between measuring a and b.

Statistical Analysis

For zooxanthellae density, pigment contents and calcification rate, one-way ANOVA was used to test for significant differences between the marine debris treatments. For chlorophyll fluorescence parameters, mixed repeated ANOVA was used to determine statistical differences among times of sampling, treatments and species. All tests used 95% confidence level threshold. *Post hoc* LSD test was used to determine statistical differences among the distinct groups. If the data distribution was not normal (Kolmogorov–Smirnov test) or not equal in variances (Levene's test), the data were transformed with square-root or log10 before testing. If the transformed data did not meet the assumptions, non-parametric tests were used.

RESULTS

Visual Appearances and Physicochemical Properties of Seawater

In transparent plastic bag treatment, the plastic gradually turned opaque due to biofouling from algae. The light reduction increased from 3% at the start to 76% at the end of experiment. However, with the opaque plastic bag treatment, light reduction

increased from 15 to 89% during the same 4 weeks treatment. A few *P. acuta* fragments showed a slight color decrease during the experiment. Dissolved oxygen under opaque and transparent plastic covered area did not significantly decline when compared with the area above plastic, indicating no suffocation effects on the corals (**Table 1**). In the fishing net treatment, we observed the production of mucus. *P. acuta* showed significant bleaching after 2 weeks and death at the end of experiment (**Figure 2D**). *P. lutea* had partial tissue necrosis (**Figure 2H**) and swelling of the tissues as a result of the fishing net treatment (**Figure 2I**).

TABLE 1 | Statistical analysis of dissolved oxygen above and below marine debris in each treatment tank.

Treatments	Df	*F*	*P*-value
Control	1	0.072	0.791
Opaque plastic bag	1	1.419	0.245
Transparent plastic bag	1	0.039	0.845
Fishing net	1	0.487	0.493

Chlorophyll *a* Fluorescence

Mixed repeated ANOVA showed that F_v/F_m of *P. acuta* had stabilized and remained mostly constant over the 4-week experiment ($p = 0.115$; **Figure 3A**), and there were no significant differences among treatments ($p = 0.370$; **Figure 3A**). F_v/F_m of *P. lutea* was more sensitive to marine debris stress than *P. acuta* ($p < 0.05$). F_v/F_m of *P. lutea* that was exposed to opaque bag, transparent bag or net treatment significantly declined from T7 ($p < 0.05$; LSD's *post hoc* comparisons). At the end of the exposure period (week 4), F_v/F_m of *P. lutea* with opaque bag, transparent bag and net treatments were significantly lower than for the control ($p = 0.001$; **Figure 3B**). F_v/F_0 had similar trend as F_v/F_m in both of the two species. *P. lutea* responded more to marine debris than *P. acuta* in all three treatments ($p < 0.05$; **Figures 3C,D**). There was no significant difference

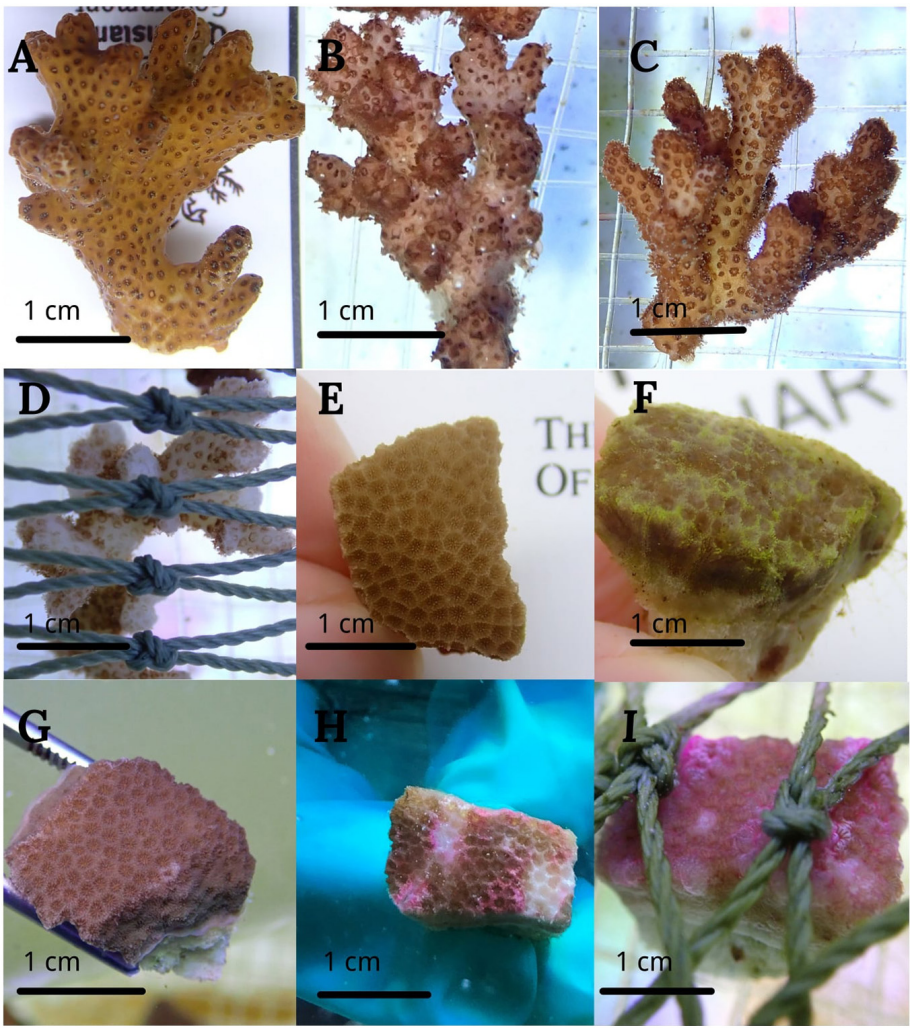

FIGURE 2 | Images of the different corals subjected to treatments for 4 weeks. *P. acuta* and *P. lutea* in control **(A,E)**, transparent bag **(B,F)**, opaque bag **(C,G)**, and fishing net treatments **(D,H,I)**.

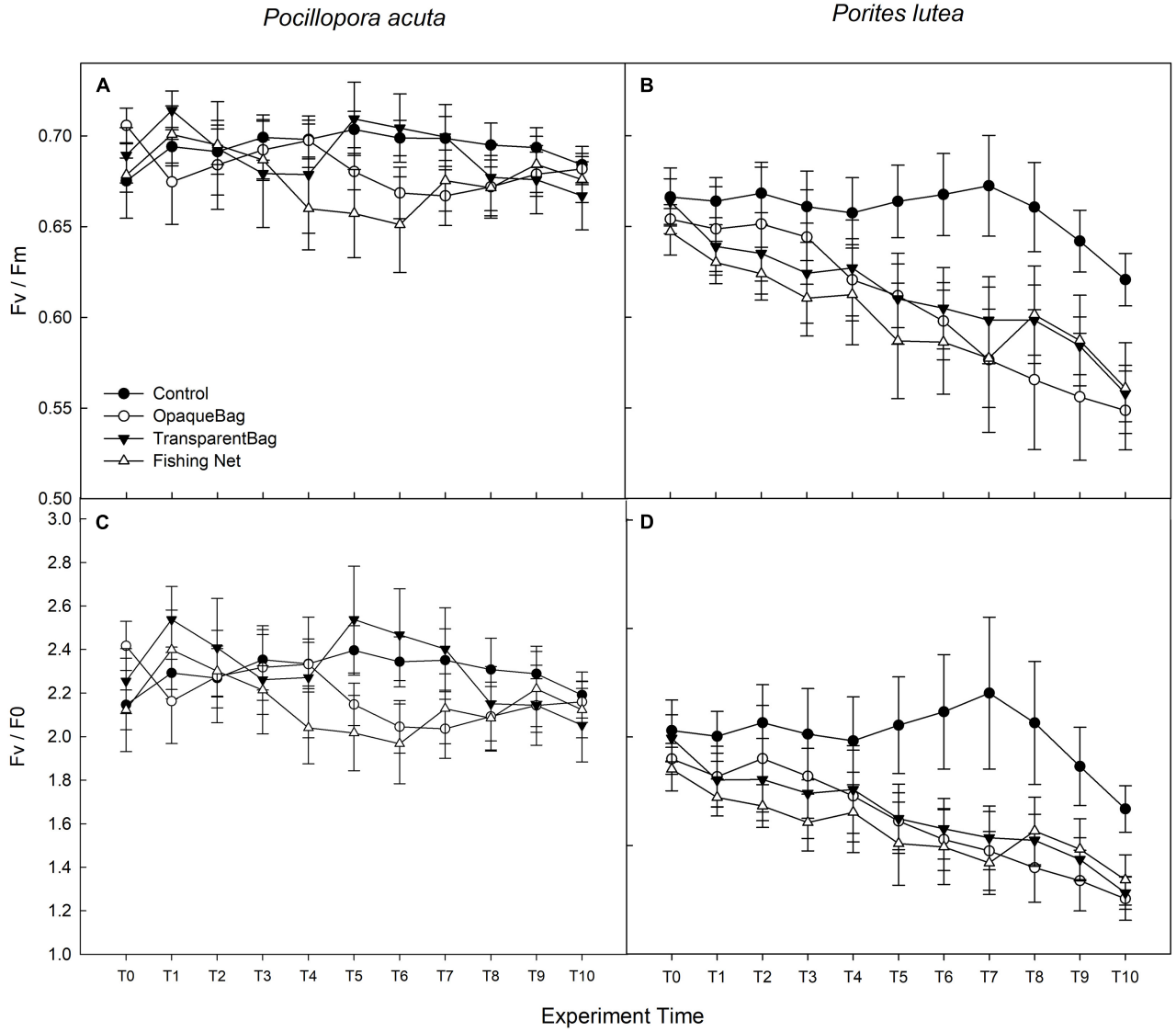

FIGURE 3 | Maximum quantum yield of PSII (F_v/F_m; **A,B**) and F_v/F_0 **(C,D)** in *P. acuta* (left column), and *P. lutea* (right column) from T0 to T10 (Graph treated with moving average, T1 in week 1, T4 in week 2, T7 in week 3, and T10 in week 4). Data are presented as Mean ± SE ($n = 6$).

among treatments in *P. acuta* ($p = 0.271$; **Figure 3C**), but F_v/F_0 in opaque bag, transparent bag and fishing net treatments were significantly lower than in control treatment of *P. lutea* ($p < 0.001$; **Figure 3D**) after 2 weeks (LSD *post hoc* comparisons) (**Table 2**).

Measurements of RLC were used to calculate alpha, $rETR_{max}$ and E_k. Alpha of *P. acuta* had slightly changed but without significant differences over time ($p = 0.672$; **Figure 4A**) or among treatments ($p = 0.927$; **Figure 4A**). In *P. lutea*, alpha significantly decreased over the exposure period ($p = 0.005$; **Figure 4B**), but had no significant differences amongst treatments ($p = 0.132$; **Figure 4B** and **Table 2**).

Regarding E_k and $rETR_{max}$ in *P. acuta* and *P. lutea*, the impact of marine debris was strong in the fishing net treatment. Both E_k and $rETR_{max}$ of *P. acuta* ($p < 0.001$ and $p < 0.001$, respectively; **Figures 4C,E**) and *P. lutea* ($p < 0.001$ and $p < 0.001$, respectively; **Figures 4D,F**) in fishing net treatments were significantly lower than in the control, opaque bag or transparent bag treatments (**Table 2**).

Chlorophyll Concentration

After 2 weeks, there were no significant differences in chlorophyll *a* and c_2 concentrations per surface area (μg cm^{-2}) in *P. acuta* ($p = 0.101$ and $p = 0.140$, respectively; **Figures 5A,C**) or in *P. lutea* ($p = 0.400$ and $p = 0.363$, respectively; **Figures 5B,D**) among the treatments. However, cellular chlorophyll *a* concentration (pg $cell^{-1}$) of *P. acuta* and *P. lutea* in opaque bag treatment were significantly higher than in control ($p = 0.001$ and $p = 0.002$, respectively; **Figures 5E,F**).

TABLE 2 | Statistical analysis of PAM between treatments (Mixed Two-way Repeated ANOVA).

	Pocillopora acuta			*Porites lutea*		
Parameter	**Df**	***F***	***P*-value**	**Df**	***F***	***P*-value**
F_v/F_m	3	1.106	0.370	3	8.772	0.001*
$rETR_{max}$	3	68.666	<0.001*	3	17.914	<0.001*
F_v/F_0	3	1.403	0.271	3	10.921	<0.001*
Alpha	3	0.153	0.927	3	2.100	0.132
E_k	3	26.911	<0.001*	3	15.003	<0.001*

*Significant difference.

When measured after 4 weeks, the cellular chlorophyll *a* concentration in both species had returned to the same level as the control ($p = 0.680$ and $p = 0.230$, respectively; **Figures 5E,F**).

After 2 weeks, there were no changes in chlorophyll *a* and c_2 concentrations in fishing net treated *P. acuta* ($p > 0.05$), but surface chlorophyll *a* and c_2 concentrations decreased from control in week 4 ($p = 0.021$ and $p = 0.021$, respectively; **Figures 5A,C,G**). In *P. lutea* chlorophyll *a* and c_2 concentrations per surface area declined in week 4 ($p = 0.026$ and $p = 0.013$, respectively; **Figures 5B,D**), but interestingly in week 2 chlorophyll *a* and c_2 concentrations per cell had increased ($p = 0.002$ and $p = 0.001$, respectively; **Figures 5F,H**). At the end of treatment, the chlorophyll *a* and c_2 concentrations per cell had the same levels as in control ($p = 0.230$ and $p = 0.244$, respectively; **Figures 5F,H** and **Table 3**).

Zooxanthellae Density

In *P. acuta*, there was no significant difference in symbiont density after 2 weeks of exposure to marine debris ($p = 0.201$; **Figure 6A**), while there was significantly lower symbiont density in the net treatment, compared to other treatments after 4 weeks of exposure ($p = 0.014$; **Figure 6A**). In *P. lutea*, significantly lower zooxanthellae densities in opaque bag and fishing net treatments were observed on weeks 2 and 4 of exposure ($p < 0.001$ and $p < 0.001$, respectively; **Figure 6B** and **Table 3**).

Calcification Rate

Average calcification rate (% day^{-1}) of both species in opaque bag, transparent bag and fishing net treatments was lower than in control treatment. Calcification rates of both species in fishing net treatment were significantly lower than in the other treatments ($p < 0.001$ and $p = 0.026$, respectively; **Figures 7A,B** and **Table 3**).

DISCUSSION

Opaque Plastic Bag and Transparent Plastic Bag

Plastic bag debris can cause coral shading and suffocation resulting in bleaching as well as physical damage by abrasion, necrosis and ultimately mortality (Ryan, 2015; Valderrama Ballesteros et al., 2018). Indeed, shading directly decreases light availability for photosynthesis used by zooxanthellae, and we measured that response with opaque plastic bag and transparent plastic bag which, respectively, reduced light by 15 and 3% at the start of treatment. Although corals in close contact with plastic bags can suffer suffocation from oxygen depletion and lack of metabolite exchange (Ryan, 2015; Mouchi et al., 2019), in our experiments the plastic bag was located 2 cm above the coral, and the dissolved oxygen level under plastic covered area did not significantly decline relative to the area above the plastic bag, and so no suffocation was observed (**Table 3**). After 4 weeks of experimental treatment, the shading had increased to 89 and 76% for opaque plastic bag and transparent plastic bag cases, which was caused by algae covering the plastic bags. *P. acuta* showed no significant change in any indicator of chlorophyll fluorescence from opaque or transparent plastic bag stress. In contrast, photochemical efficiency (F_v/F_m) of *P. lutea* significantly declined in transparent and opaque plastic bag treatments, while efficiency of photosynthesis (alpha), saturating irradiance (E_k), and maximum $rETR_{max}$ were not significantly different. This may indicate that *P. lutea* has less resilience to shading than *P. acuta*. Species-specific resilience to marine plastic debris has been found in scleractinian corals (Mouchi et al., 2019; Mueller and Schupp, 2020). A F_v/F_m decline can be caused by limited light availability, low density of symbionts and D1 protein degradation in PS II (Keren et al., 1997; Warner et al., 1999; Muller-Parker et al., 2015). As a result, the symbiont density decreased in the opaque plastic bag treatment in *P. lutea*, confirming the decline in maximum quantum yield. The study by Mueller and Schupp (2020) observed that *Porites rus* slightly paled in the first 21 days, then rapidly decreased when exposed to a transparent plastic bag, which might explain the fact that zooxanthellae density did not significantly decrease in our 4 weeks of experiment. Keshavmurthy et al. (2014) put forward the resistance mechanisms of hosts or the sustainable relationships with the clades or types of *Symbiodiniaceae* corals that can contend natural and anthropogenic stresses. Different coral species can associate with different symbiont compositions and the variety of components of *Symbiodiniaceae* provide unequal tolerances (Rouzé et al., 2016). Most of *P. acuta* in the sampling area associated with symbionts in *Durusdinium* spp. (D1) and *Durusdinium* sp. (D1-6; unpublicized report from Yucharoen, 2020), while *P. lutea* is commonly dominated by C15 (*Cladocopium* sp.; Chankong et al., 2018, 2020; Tan et al., 2020). However, there is no direct evidence to demonstrate that coral reactions to marine debris were affected by genus of

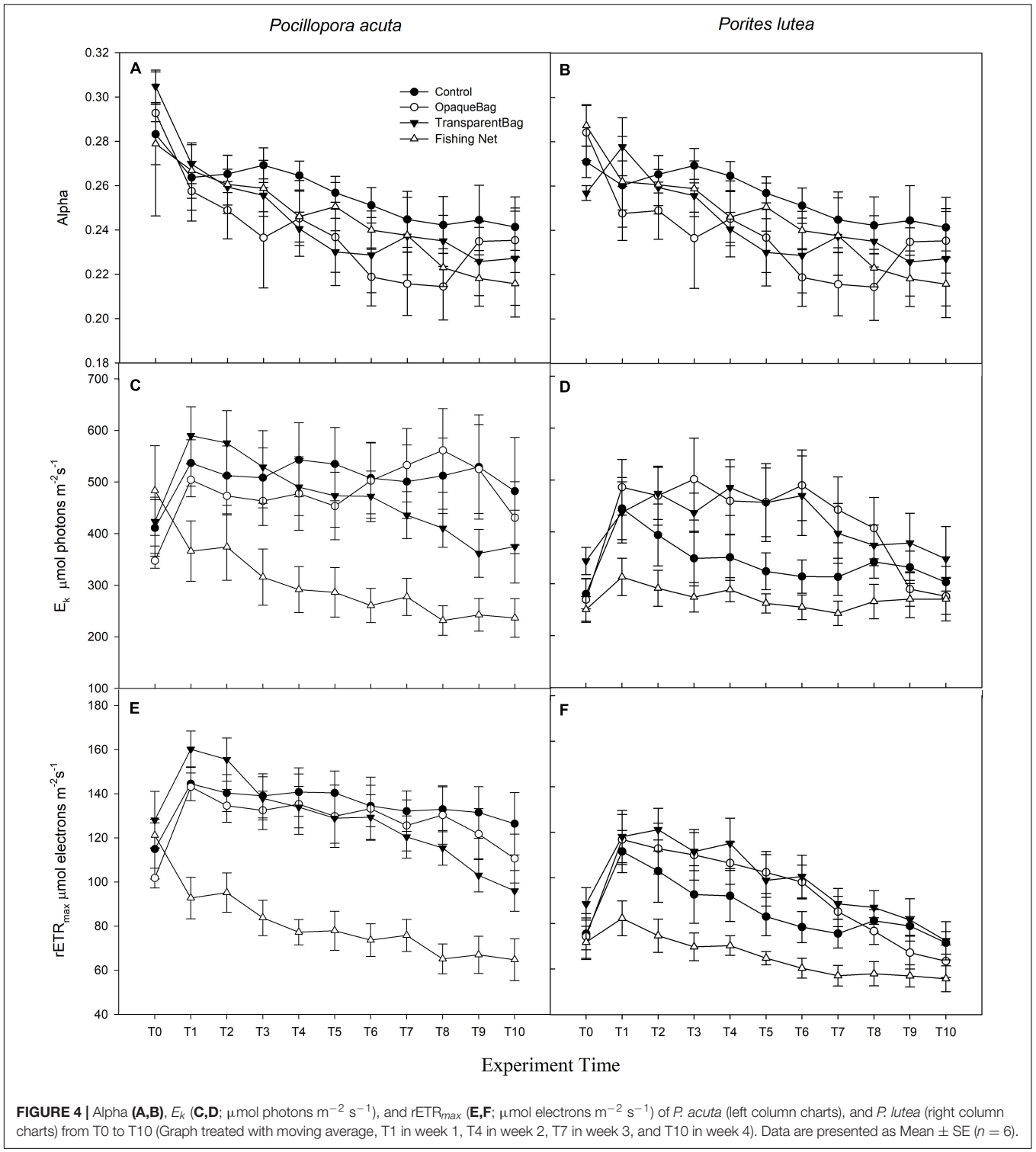

FIGURE 4 | Alpha **(A,B)**, E_k (**C,D**; µmol photons m^{-2} s^{-1}), and $rETR_{max}$ (**E,F**; µmol electrons m^{-2} s^{-1}) of *P. acuta* (left column charts), and *P. lutea* (right column charts) from T0 to T10 (Graph treated with moving average, T1 in week 1, T4 in week 2, T7 in week 3, and T10 in week 4). Data are presented as Mean ± SE ($n = 6$).

zooxanthellae, while from the changed environmental factors, we hypothesized that types of *Symbiodiniaceae* might drive the corals to perform differently under marine debris stress.

Physella acuta in the opaque plastic bag treatment had an effect on its calcification rate. The skeleton growth of scleractinian corals is mainly influenced by light and water flow (Scoffin et al., 1992; Houlbrèque et al., 2003; Schutter et al., 2011; Browne, 2012; Wijgerde et al., 2012). Light motivates coral tissue extension and skeleton growth (Mass et al., 2007; Schutter et al., 2011; Cohen and Dubinsky, 2015; Eyal et al., 2019). During the decreased light condition in opaque plastic bag treatment, we considered that calcification rate got affected by declined

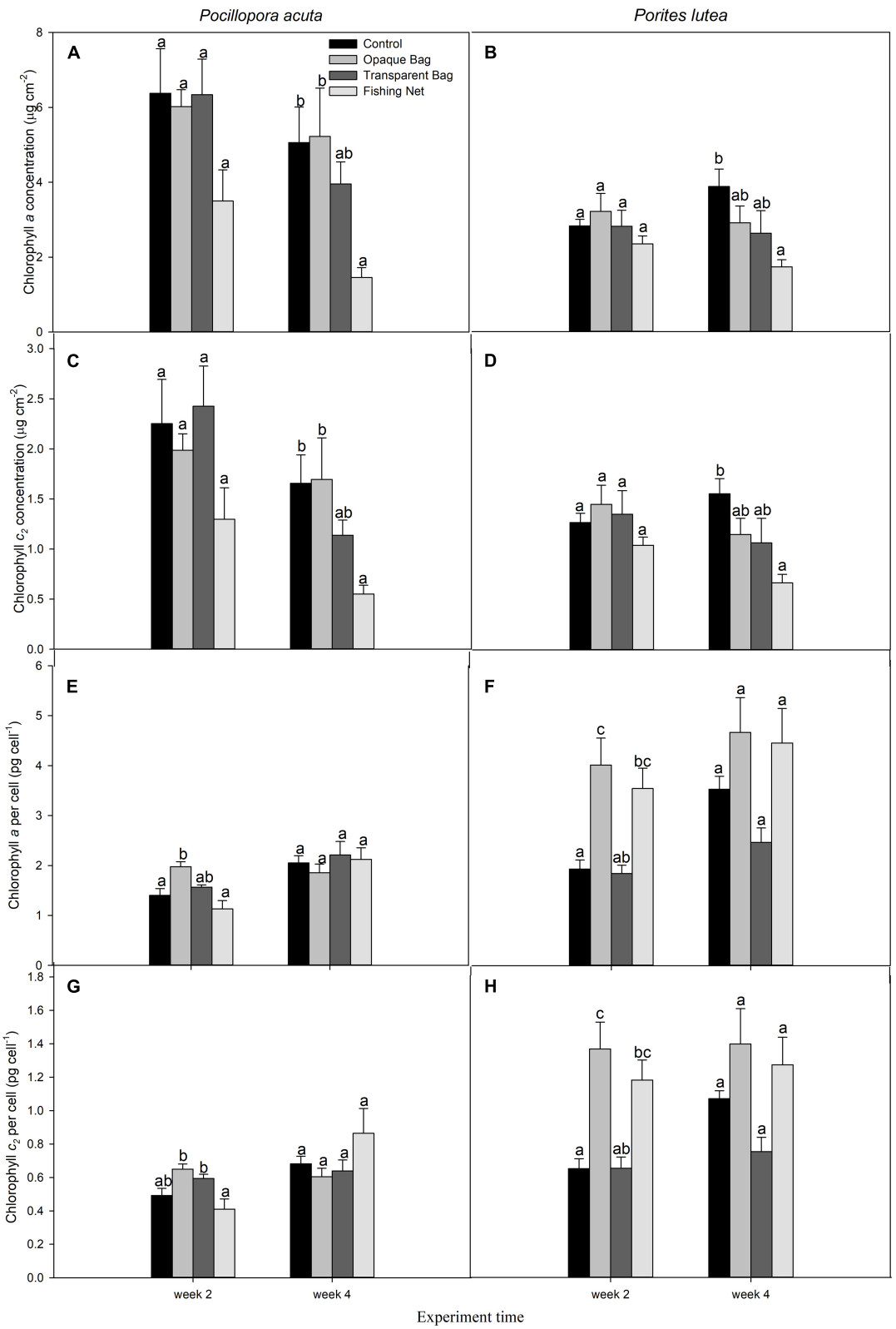

FIGURE 5 | Chlorophyll *a* concentration (μg cm^{-2}; **A,B**), chlorophyll c_2 concentration (μg cm^{-2}; **C,D**), cellular chlorophyll *a* concentration (pg $cell^{-1}$; **E, F)**, and cellular chlorophyll c_2 concentration (pg $cell^{-1}$; **G,H**) of *P. acuta* (left column chart) and *P. lutea* (right column chart) subjected to treatments, at week 2 and week 4. Data are presented as Mean ± SE ($n = 6$).). a, b, and c indicate significant difference.

advisability light. Furthermore, symbiotic zooxanthellae mainly affect hermatypic host calcification with photosynthesis, which supplies the inorganic carbon (Erez et al., 2011). Under lower light conditions, corals will reduce the growth rate due to less photosynthesis and calcification (Anthony and Hoegh-Guldberg, 2003b) Furthermore, decreased calcification may represent the photosynthetic performance of symbionts. In our study, the photosynthetic activity in *P. acuta* had no effect throughout, but the cellular chlorophyll *a* and c_2 concentrations temporarily increased in week 2, which confirms the photoacclimation mechanisms of endosymbiotic dinoflagellates that adapt to reduced light conditions (Falkowski and Dubinsky, 1981; Jones and Yellowlees, 1997; Anthony and Hoegh-Guldberg, 2003a; Stambler and Dubinsky, 2005; Jones et al., 2020). *P. lutea* also increased cellular chlorophyll *a* and c_2 concentrations in week 2, but continuous symbiont cell degradation was observed throughout. In some extreme low light conditions, decreased symbiont density also serves as photoacclimation of coral physiological responses to environmental conditions (Warner et al., 2002; Ulstrup et al., 2008).

In general, plastic shading affected more the response indicators for *P. lutea* than for *P. acuta*. This may be linked to the complex architecture of *P. acuta*, which provides light microhabitat diversification, thereby improving light utilization by the branching coral (Helmuth et al., 1997; Anthony and Hoegh-Guldberg, 2003b). Flow morphology like that of a massive coral has more work required for adaption to light-limited conditions, whereas species that have complex architectures, they are able to occupy extremely low or high-light regimes and consequently may have reduced competition in those habitats. Also, a greater physiological tolerance of light-habitat dynamics (e.g., after physical disturbances) will increase the physiological potential for colonization of newly formed light gaps.

The amount of biofouling by algae on plastic bags, which increased as the experiment proceeded, might also be a factor. Algal competition with coral has been proven, and it can affect corals via allelochemicals, abrasion, shading and overgrowth (McCook et al., 2001; Jompa and McCook, 2003; Rasher et al., 2011; Vieira et al., 2016). Swierts and Vermeij (2016) assumed that fast-growing corals (e.g., branching coral) suffer negative effects on growth from competition with epiphytic algae.

TABLE 3 | Statistical analysis of chlorophyll *a* and c_2, zooxanthellae density and calcification rate (One-way ANOVA).

Parameter	*Pocillopora acuta*			*Porites lutea*		
	Df	*F*	*P*-value	Df	*F*	*P*-value
Chl *a* (μg cm^{-2}) week 2	3	2.374	0.101	3	1.031	0.400
Chl c_2 (μg cm^{-2}) week 2	3	2.046	0.140	3	1.123	0.363
Chl *a* (pg cell^{-1}) week 2	3	8.621	0.001*	3	6.875	0.002*
Chl c_2 (pg cell^{-1}) week 2	3	6.356	0.003*	3	7.841	0.001*
Chl *a* (μg cm^{-2}) week 4	3	4.041	0.021*	3	3.802	0.026*
Chl c_2 (μg cm^{-2}) week 4	3	4.068	0.021*	3	4.594	0.013*
Chl *a* (pg cell^{-1}) week 4	3	0.510	0.680	3	1.559	0.230
Chl c_2 (pg cell^{-1}) week 4	3	1.710	0.197	3	1.502	0.244
Zooxanthellae ($\times 10^6$ cell cm^{-2}) week 2	3	1.693	0.201	3	10.057	0.001*
Zooxanthellae ($\times 10^6$ cell cm^{-2}) week 4	3	4.529	0.014*	3	11.319	0.001*
Calcification rate (% D^{-1})	3	9.749	0.001*	3	3.812	0.026*

**Significant difference.*

Fishing Net

In our experimental plan, the fishing net directly contacted coral fragments creating the potential for abrasion. Both species showed strong effects from fishing net stress, but different coral species respond to fishing nets differently. Heavy bleaching was observed in *P. acuta* after treatment with a fishing net for 2 weeks (**Figure 2D**). Bleaching is associated with coral health, because bleaching results from coral releasing symbiotic zooxanthellae (Douglas, 2003), making the coral more sensitive to diseases (Muller et al., 2008), and can negatively affect overall coral growth (Pratchett et al., 2015; McClanahan et al., 2018). Cell degradation occurred and surface chlorophyll concentration significantly declined after week 2, confirming this speculation. Tissue necrosis in *P. lutea* was observed under our treatments (**Figure 2H**), which can result in symbiont degradation and photosynthetic pigment decrease. Moreover, corals with small polyps have limited ability to physically clean up the foreign matter, leading to bleaching and tissue mortality (Philipp and Fabricius, 2003).

The significantly reduced $rETR_{max}$ indicates the maximum photosynthetic capacity and this might affect growth of symbionts (Gao and Zheng, 2010; Xu et al., 2020). From prior research, abrasion of coral tissue by marine debris can result in disease outbreaks (Lamb et al., 2018), leading to decreased chlorophyll pigments and zooxanthellae cell degradation (Cervino et al., 2004). Therefore, we hypothesize that after 4 weeks coverage with fishing net, the reduced symbiont density and lower chlorophyll are related to coral disease. Furthermore, physical connection of nets to the corals affected heterotrophic energy acquisition, and increased energy consumption to produce mucus (Philipp and Fabricius, 2003). Producing the mucus required 35% of energy from an endosymbiotic (Riegl and Branch, 1995). Mainly, this energy source is used for host calcification and reproduction via symbionts synthesizing surplus carbon (Castrillón-Cifuentes et al., 2017), but under sedimentation conditions, the respiration from mucus production reversed the dominance and took up 65% from symbionts. Long-term energy cost combined with limited photosynthetic energy gain severely affected coral calcification (Anthony and Fabricius, 2000).

Porites trematodiasis is the most common disease caused by trematode larvae and manifests as pink swollen nodules, which we observed when *P. lutea* tissue contacted fishing nets (**Figure 2I**). Both biotic

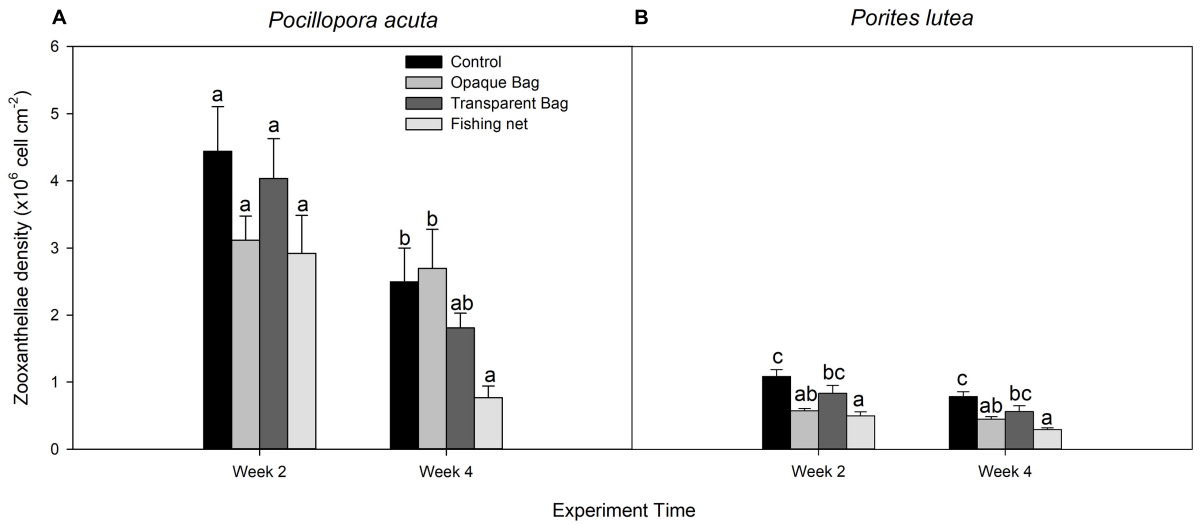

FIGURE 6 | Zooxanthellae density of *P. acuta* **(A)** and *P. lutea* **(B)** in control, opaque bag, transparent bag, and fishing net treatments at week 2 and week 4 of experiment. Data are presented as Mean ± SE ($n = 6$). a, b, and c indicate significant difference.

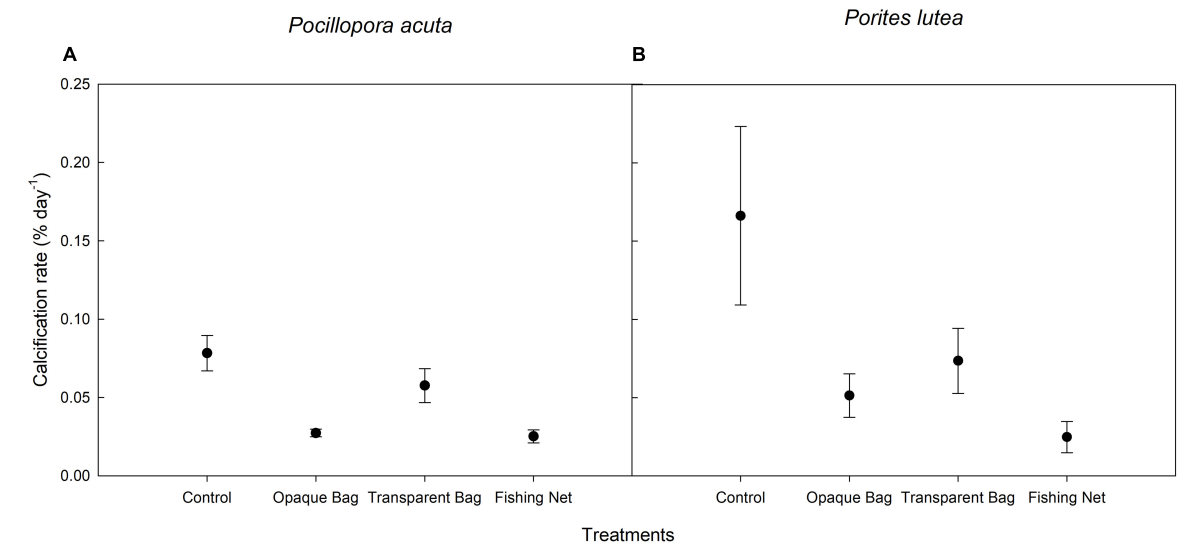

FIGURE 7 | Calcification rate of *P. acuta* **(A)** and *P. lutea* **(B)** in control, opaque bag, transparent bag, and fishing net treatments. Data are presented as Mean ± SE ($n = 6$).

and abiotic stresses can cause coral disease outbreaks, and changes in environmental conditions can promote physiological stresses that impair host immunity (Jackson and Tinsley, 2002; Lafferty and Holt, 2003). Similarly, the red algal *Corallophila huysmansii* overgrowth on *Porites cylindrica* caused severe stress and mortality (Jompa and McCook, 2003).

Fishing net not only severely affected maximum quantum yield of PSII, chlorophyll *a* and c_2 concentrations, symbiotic cell density and calcification rate, but also caused actual tissue necrosis in *P. lutea* under our laboratory conditions (**Figure 2H**). Instead, heavy bleaching was observed in *P. acuta* (**Figure 2D**). Corals with small polyps have limited ability to remove foreign matter and sediment particles, contributing to coral bleaching, and tissue mortality (Philipp and Fabricius, 2003). Significantly reduced $rETR_{max}$ as well as the maximum photosynthetic capacity indicated the poor growth status of symbionts (Gao and Zheng, 2010; Xu et al., 2020). From previous research, marine debris abrasion on coral tissue induces disease outbreaks (Lamb et al., 2018), and diseases have led to a decrease in chlorophyll pigment and to zooxanthellae cell degradation (Cervino et al., 2004). Therefore, we hypothesized that after 4 weeks of covering with fishing net, the reduced symbionts and decreased chlorophyll were related to coral

diseases. Interestingly, we also observed that cellular chlorophyll concentration increased in the second week, due to the photoacclimatization of living zooxanthellae that adapted to reduced light intensity and increased cellular chlorophyll to increase energy capture (Falkowski and Dubinsky, 1981; Jones and Yellowlees, 1997; Anthony and Hoegh-Guldberg, 2003a; Jones et al., 2020). Furthermore, exposure to fishing nets reduced energy acquired from photosynthesis and affected heterotrophic energy acquisition, increasing energy consumption to produce mucus (Philipp and Fabricius, 2003). Long-term negative energy costs combined with limited photosynthetic energy gains severely affected coral calcification (Anthony and Fabricius, 2000).

CONCLUSION

Different species of corals respond differently to various types of marine debris, differently. The responses may depend on the symbiont composition and density, coral morphology, and also on the resilience of the coral species. In this experiment, *P. acuta* showed less effects from each form of marine debris exposure than *P. lutea*, and a transparent plastic bag showed no effects on *P. acuta*. The different kinds of damage from different types of marine debris also make corals respond in different ways. Two types of plastic bag resulted in shading impacts on the corals in this experiment, whereas fishing net treatment affected corals with abrasion. The fishing net treatment had the strongest effects on both coral species tested. In conclusion, marine debris cover on coral causes stress responses in 2 weeks. We hope this work can help marine national parks and any related organizations to prioritize the clearing of marine debris. In aquarium experiments, we have separately assessed the shading and abrasion effects from marine debris, while in natural environment waves cause both shading and abrasion to happen simultaneously, which may accelerate the decline of coral health. The combined responses remain poorly understood and can be addressed in future work.

DATA AVAILABILITY STATEMENT

The raw data supporting the conclusions of this article will be made available by the authors, without undue reservation.

AUTHOR CONTRIBUTIONS

LY, SS, PA, PR, and PC contributed to conception and design of the study. LY, SS, PP, and PC processed the experiment. LY, SS, and PC organized the database, performed the statistical analysis, and wrote the first draft of the manuscript. All authors contributed to manuscript revision, read, and approved the submitted version.

FUNDING

This work is financially supported by The Institute for the Promotion of Teaching Science and Technology (IPST; DPST Graduate with First Placement; Grant Number: 006/2559), the Coastal Oceanography and Climate change Research Center, Prince of Songkla University (PSU), the Faculty of Environmental Management, PSU, and the Graduate School of PSU.

ACKNOWLEDGMENTS

We thank the Coastal Oceanography and Climate Change Research Center (COCC), the Marine and Coastal Resources Institute (MACORIN), and the Faculty of Environmental Management, Prince of Songkla University for research facilities. The authors thank Mathinee Yucharoen and Phatcharee Roekngandee for assistances in the laboratory. The authors thank Seppo Karrila and the Research and Development Office, PSU for assistance with proofing the English.

REFERENCES

Abu-Hilal, A., and Al-Najjar, T. (2009). Marine litter in coral reef areas along the Jordan Gulf of Aqaba, Red Sea. *J. Environ. Manag.* 90, 1043–1049. doi: 10.1016/j.jenvman.2008.03.014

Anthony, K. R. N., and Hoegh-Guldberg, O. (2003b). Variation in coral photosynthesis, respiration and growth characteristics in contrasting light microhabitats: an analogue to plants in forest gaps and understoreys? *Funct. Ecol.* 17, 246–259. doi: 10.1046/j.1365-2435.2003.00731.x

Anthony, K. R. N., and Hoegh-Guldberg, O. (2003a). Kinetics of photoacclimation in corals. *Oecologia* 134, 23–31. doi: 10.1007/s00442-002-1095-1

Anthony, K. R. N., and Fabricius, K. E. (2000). Shifting roles of heterotrophy and autotrophy in coral energetics under varying turbidity. *J. Exp. Mar. Biol. Ecol.* 252, 221–253. doi: 10.1016/S0022-0981(00)00237-9

Anthony, K. R. N., Kline, D. I., Diaz-Pulido, G., Dove, S., and Hoegh-Guldberg, O. (2008). Ocean acidification causes bleaching and productivity loss in coral reef builders. *Proc. Natl. Acad. Sci. U.S.A.* 105, 17442–17446. doi: 10.1073/pnas.0804478105

Barnes, D. K. A., Galgani, F., Thompson, R. C., and Barlaz, M. (2009). Accumulation and fragmentation of plastic debris in global environments. *Philos. Trans. R. Soc. B Biol. Sci.* 364, 1985–1998. doi: 10.1098/rstb.2008.0205

Behrenfeld, M. J., Prasil, O., Kolber, Z. S., Babin, M., and Falkowski, P. G. (1998). Compensatory changes in Photosystem II electron turnover rates protect photosynthesis from photoinhibition. *Photosynth. Res.* 58, 259–268. doi: 10.1023/A:1006138630573

Bourne, D. G., Morrow, K. M., and Webster, N. S. (2016). Insights into the coral microbiome: underpinning the health and resilience of reef ecosystems. *Annu. Rev. Microbiol.* 70, 317–340. doi: 10.1146/annurev-micro-102215-095440

Browne, N. K. (2012). Spatial and temporal variations in coral growth on an inshore turbid reef subjected to multiple disturbances. *Mar. Environ. Res.* 77, 71–83. doi: 10.1016/j.marenvres.2012.02.005

Buhl-Mortensen, L., and Buhl-Mortensen, P. (2017). Marine litter in the Nordic Seas: distribution composition and abundance. *Mar. Pollut. Bull.* 125, 260–270. doi: 10.1016/j.marpolbul.2017.08.048

Castrillón-Cifuentes, A. L., Lozano-Cortés, D. F., and Zapata, F. A. (2017). Effect of short-term subaerial exposure on the cauliflower coral, *Pocillopora damicornis*, during a simulated extreme low-tide event. *Coral Reefs* 36, 401–414. doi: 10.1007/s00338-017-1552-2

Cervino, J. M., Hayes, R., Goreau, T., and Smith, G. (2004). Zooxanthellae regulation in yellow blotch/band and other coral diseases contrasted with temperature related bleaching: in situ destruction vs expulsion. *Symbiosis* 37, 63–85.

Chankong, A., Kongjandtre, N., Senanan, W., and Manthachitra, V. (2018). Genetic diversity of symbiodiniaceae associated with *Porites lutea* and *Pocillopora damicornis* in the Gulf of Thailand Inferred from nucleotide sequences of internal transcribed spacer-2. *J. Fish. Environ.* 42, 66–79.

Chankong, A., Kongjandtre, N., Senanan, W., and Manthachitra, V. (2020). Community composition of Symbiodiniaceae among four scleractinian corals in the eastern Gulf of Thailand. *Reg. Stud. Mar. Sci.* 33:100918. doi: 10.1016/j.rsma.2019.100918

Chapron, L., Peru, E., Engler, A., Ghiglione, J. F., Meistertzheim, A. L., Pruski, A. M., et al. (2018). Macro- and microplastics affect cold-water corals growth, feeding and behaviour. *Sci. Rep.* 8:15299. doi: 10.1038/s41598-018-33683-6

Cohen, I., and Dubinsky, Z. (2015). Long term photoacclimation responses of the coral *Stylophora pistillata* to reciprocal deep to shallow transplantation: photosynthesis and calcification. *Front. Mar. Sci.* 2:45. doi: 10.3389/fmars.2015.00045

Dameron, O. J., Parke, M., Albins, M. A., and Brainard, R. (2007). Marine debris accumulation in the Northwestern Hawaiian Islands: an examination of rates and processes. *Mar. Pollut. Bull.* 54, 423–433. doi: 10.1016/j.marpolbul.2006.11.019

de Carvalho-Souza, G. F., Llope, M., Tinôco, M. S., Medeiros, D. V., Maia-Nogueira, R., and Sampaio, C. L. S. (2018). Marine litter disrupts ecological processes in reef systems. *Mar. Pollut. Bull.* 133, 464–471. doi: 10.1016/j.marpolbul.2018.05.049

Donohue, M. J., Boland, R. C., Sramek, C. M., and Antonelis, G. A. (2001). Derelict fishing gear in the Northwestern Hawaiian Islands: diving survey and debris removal in 1999 confirm threat to coral ecosystems. *Mar. Pollut. Bull.* 42, 1301–1312. doi: 10.1016/s0025-326x(01)00139-4

Douglas, A. E. (2003). Coral bleaching—how and why? *Mar. Pollut. Bull.* 46, 385–392. doi: 10.1016/S0025-326X(03)00037-7

Erez, J., Reynaud, S., Silverman, J., Schneider, K., and Allemand, D. (2011). "Coral calcification under ocean acidification and global change," in *Coral Reefs: An Ecosystem in Transition*, eds Z. Dubinsky and N. Stambler (Dordrecht: Springer), 151–176. doi: 10.1007/978-94-007-0114-4_10

Eriksen, M., Lebreton, L. C. M., Carson, H. S., Thiel, M., Moore, C. J., Borerro, J. C., et al. (2014). Plastic pollution in the world's oceans: more than 5 trillion plastic pieces weighing over 250,000 tons afloat at sea. *PLoS One* 9:e111913. doi: 10.1371/journal.pone.0111913

Eyal, G., Cohen, I., Eyal-Shaham, L., Ben-Zvi, O., Tikochinski, Y., and Loya, Y. (2019). Photoacclimation and induction of light-enhanced calcification in the mesophotic coral *Euphyllia paradivisa*. *R. Soc. Open Sci.* 6:180527. doi: 10.1098/rsos.180527

Falkowski, P. G., and Dubinsky, Z. (1981). Light-shade adaptation of *Stylophora pistillata*, a hermatypic coral from the Gulf of Eilat. *Nature* 289, 172–174. doi: 10.1038/289172a0

Figueroa-Pico, J., Tortosa, F. S., and Carpio, A. J. (2020). Coral fracture by derelict fishing gear affects the sustainability of the marginal reefs of Ecuador. *Coral Reefs* 39, 819–827. doi: 10.1007/s00338-020-01926-6

Gao, K., and Zheng, Y. (2010). Combined effects of ocean acidification and solar UV radiation on photosynthesis, growth, pigmentation and calcification of the coralline alga *Corallina sessilis* (Rhodophyta). *Glob. Chang. Biol.* 16, 2388–2398. doi: 10.1111/j.1365-2486.2009.02113.x

Hall, N. M., Berry, K. L. E., Rintoul, L., and Hoogenboom, M. O. (2015). Microplastic ingestion by scleractinian corals. *Mar. Biol.* 162, 725–732. doi: 10.1007/s00227-015-2619-7

Harrison, P. L., and Booth, D. J. (2007). Coral reefs: naturally dynamic and increasingly disturbed ecosystems. *Mar. Ecol.* 1, 316–377.

Helmuth, B. S. T., Timmerman, B. E. H., and Sebens, K. P. (1997). Interplay of host morphology and symbiont microhabitat in coral aggregations. *Mar. Biol.* 130, 1–10. doi: 10.1007/s002270050219

Hill, R., and Ralph, P. J. (2007). Post-bleaching viability of expelled zooxanthellae from the scleractinian coral *Pocillopora damicornis*. *Mar. Ecol. Prog. Ser.* 352, 137–144. doi: 10.3354/meps07159

Houlbrèque, F., Tambutté, E., and Ferrier-Pagès, C. (2003). Effect of zooplankton availability on the rates of photosynthesis, and tissue and skeletal growth in the scleractinian coral *Stylophora pistillata*. *J. Exp. Mar. Biol. Ecol.* 296, 145–166. doi: 10.1016/S0022-0981(03)00259-4

Jackson, J., and Tinsley, R. (2002). Effects of environmental temperature on the susceptibility of *Xenopus laevis* and *X. wittei* (Anura) to *Protopolystoma xenopodis* (Monogenea). *Parasitol. Res.* 88, 632–638. doi: 10.1007/s00436-002-0629-0

Jambeck, J. R., Geyer, R., Wilcox, C., Siegler, T. R., Perryman, M., Andrady, A., et al. (2015). Plastic waste inputs from land into the ocean. *Science* 347, 768–771. doi: 10.1126/science.1260352

Jokiel, P. L., Maragos, J. W., and Franzisket, L. (1978). "Coral growth buoyant weight technique," in *Coral Reefs: Research Methods*, eds D. R. Stoddart and R. E. Johannes (Paris: UNESCO), 529–542.

Jompa, J., and McCook, L. (2003). Coral-algal competition: macroalgae with different properties have different effects on corals. *Mar. Ecol. Prog. Ser.* 258, 87–95. doi: 10.3354/meps258087

Jones, R., Giofre, N., Luter, H. M., Neoh, T. L., Fisher, R., and Duckworth, A. (2020). Responses of corals to chronic turbidity. *Sci. Rep.* 10:4762. doi: 10.1038/s41598-020-61712-w

Jones, R. J., and Yellowlees, D. (1997). Regulation and control of intracellular algae (= zooxanthellae) in hard corals. *Philos. Trans. R. Soc. Lond. Ser. B Biol. Sci.* 352, 457–468. doi: 10.1098/rstb.1997.0033

Keren, N., Berg, A., van Kan, P. J. M., Levanon, H., and Ohad, I. (1997). Mechanism of photosystem II photoinactivation and D1 protein degradation at low light: the role of back electron flow. *Proc. Natl. Acad. Sci. U.S.A.* 94, 1579–1584. doi: 10.1073/pnas.94.4.1579

Keshavmurthy, S., Meng, P. J., Wang, J. T., Kuo, C. Y., Yang, S. Y., Hsu, C. M., et al. (2014). Can resistant coral-*Symbiodinium* associations enable coral communities to survive climate change? A study of a site exposed to long-term hot water input. *PeerJ* 2:e327. doi: 10.7717/peerj.327

Kline, D., Kuntz, N., Breitbart, M., Knowlton, N., and Rohwer, F. (2006). Role of elevated organic carbon levels and microbial activity in coral mortality. *Mar. Ecol. Prog. Ser.* 314, 119–125. doi: 10.3354/meps314119

Lafferty, K. D., and Holt, R. D. (2003). How should environmental stress affect the population dynamics of disease? *Ecol. Lett.* 6, 654–664. doi: 10.1046/j.1461-0248.2003.00480.x

Lamb, J. B., Willis, B. L., Fiorenza, E. A., Couch, C. S., Howard, R., Rader, D. N., et al. (2018). Plastic waste associated with disease on coral reefs. *Science* 359, 460–462. doi: 10.1126/science.aar3320

Marshall, P. A., and Baird, A. H. (2000). Bleaching of corals on the Great Barrier Reef: differential susceptibilities among taxa. *Coral Reefs* 19, 155–163. doi: 10.1007/s003380000086

Mass, T., Einbinder, S., Brokovich, E., Shashar, N., Vago, R., Erez, J., et al. (2007). Photoacclimation of *Stylophora pistillata* to light extremes: metabolism and calcification. *Mar. Ecol. Prog. Ser.* 334, 93–102. doi: 10.3354/meps334093

McClanahan, T. R., Weil, E., and Baird, A. H. (2018). "Consequences of coral bleaching for sessile reef organisms," in *Coral Bleaching: Patterns, Processes, Causes and Consequences*, eds M. J. H. van Oppen and J. M. Lough (Heidelberg: Springer International Publishing), 231–263. doi: 10.1007/978-3-319-75393-5_10

McCook, L., Jompa, J., and Diaz-Pulido, G. (2001). Competition between corals and algae on coral reefs: a review of evidence and mechanisms. *Coral Reefs* 19, 400–417. doi: 10.1007/s003380000129

Moberg, F., and Folke, C. (1999). Ecological goods and services of coral reef ecosystems. *Ecol. Econ.* 29, 215–233. doi: 10.1016/S0921-8009(99)00009-9

Mouchi, V., Chapron, L., Peru, E., Pruski, A. M., Meistertzheim, A. L., Vétion, G., et al. (2019). Long-term aquaria study suggests species-specific responses of two cold-water corals to macro-and microplastics exposure. *Environ. Pollut.* 253, 322–329. doi: 10.1016/j.envpol.2019.07.024

Mueller, J. S., and Schupp, P. J. (2020). Shading by marine litter impairs the health of the two Indo-Pacific scleractinian corals *Porites rus* and *Pavona cactus*. *Mar. Pollut. Bull.* 158:111429. doi: 10.1016/j.marpolbul.2020.111429

Muhammad, F., Zamani, N. P., and Ismet, M. S. (2021). The effect of plastic debris attachment to the health of branching corals in Kelapa Dua Island, Thousand Islands. *IOP Conf. Ser. Earth Environ. Sci.* 771:012017. doi: 10.1088/1755-1315/771/1/012017

Muller, E. M., Rogers, C. S., Spitzack, A. S., and van Woesik, R. (2008). Bleaching increases likelihood of disease on *Acropora palmata* (Lamarck) in Hawksnest Bay, St John, US Virgin Islands. *Coral Reefs* 27, 191–195. doi: 10.1007/s00338-007-0310-2

Muller-Parker, G., D'Elia, C. F., and Cook, C. B. (2015). "Interactions between corals and their symbiotic algae," in *Coral Reefs in the Anthropocene*, ed. C. Birkeland (Dordrecht: Springer Netherlands), 99–116. doi: 10.1007/978-94-017-7249-5_5

Ng, C. S. L., Lim, J., Sam, S. Q., Kikuzawa, Y., Toh, T. C., Wee, T., et al. (2019). Variability in skeletal bulk densities of common hard corals in Southeast Asia. *Coral Reefs* 38, 1133–1143. doi: 10.1007/s00338-019-01852-2

Orr, J. C., Fabry, V. J., Aumont, O., Bopp, L., Doney, S. C., Feely, R. A., et al. (2005). Anthropogenic ocean acidification over the twenty-first century and its impact on calcifying organisms. *Nature* 437, 681–686. doi: 10.1038/nature04095

Philipp, E., and Fabricius, K. (2003). Photophysiological stress in scleractinian corals in response to short-term sedimentation. *J. Exp. Mar. Biol. Ecol.* 287, 57–78. doi: 10.1016/S0022-0981(02)00495-1

Platt, T., Gallegos, C. L., and Harrison, W. G. (1980). Photoinhibition of photosynthesis in natural assemblages of marine phytoplankton. *J. Mar. Res.* 38, 687–701.

Pratchett, M., Anderson, K. D., Hoogenboom, M. O., Widman, E., Baird, A., Pandolfi, J., et al. (2015). Spatial, temporal and taxonomic variation in coral growth—implications for the structure and function of coral reef ecosystems. *Oceanogr. Mar. Biol.* 53, 215–295. doi: 10.1201/b18733-7

Putra, M. G. A., Zamani, N. P., Natih, N. M., and Harahap, S. A. (2021). Relationship between characteristics of marine debris and impact to coral reef. *J. Ilmiah Perikanan Dan Kelautan* 13, 11–19. doi: 10.20473/jipk.v13i1.18896

Ralph, P. J., and Gademann, R. (2005). Rapid light curves: a powerful tool to assess photosynthetic activity. *Aquat. Bot.* 82, 222–237. doi: 10.1016/j.aquabot.2005.02.006

Rasher, D., Stout, E., Engel, S., Kubanek, J., and Hay, M. (2011). Macroalgal terpenes function as allelopathic agents against reef corals. *Proc. Natl. Acad. Sci. U.S.A.* 108, 17726–17731. doi: 10.1073/pnas.1108628108

Richards, Z. T., and Beger, M. (2011). A quantification of the standing stock of macro-debris in Majuro lagoon and its effect on hard coral communities. *Mar. Pollut. Bull.* 62, 1693–1701. doi: 10.1016/j.marpolbul.2011.06.003

Riegl, B., and Branch, G. M. (1995). Effects of sediment on the energy budgets of four scleractinian (Bourne 1900) and five alcyonacean (Lamouroux 1816) corals. *J. Exp. Mar. Biol. Ecol.* 186, 259–275. doi: 10.1016/0022-0981(94)00164-9

Ritchie, R. J. (2006). Consistent sets of spectrophotometric chlorophyll equations for acetone, methanol and ethanol solvents. *Photosynth. Res.* 89, 27–41. doi: 10.1007/s11120-006-9065-9

Rouzé, H., Lecellier, G., Saulnier, D., and Berteaux-Lecellier, V. (2016). Symbiodinium clades A and D differentially predispose *Acropora cytherea* to disease and *Vibrio* spp. Colonization. *Ecol. Evol.* 6, 560–572.

Ryan, P. G. (2015). "A brief history of marine litter research," in *Marine Anthropogenic Litter*, eds M. Bergmann, L. Gutow, and M. Klages (Cham: Springer), 1–25. doi: 10.1007/978-3-319-16510-3_1

Schipper, J., Chanson, J. S., Chiozza, F., Cox, N. A., Hoffmann, M., Katariya, V., et al. (2008). The status of the world's land and marine mammals: diversity, threat, and knowledge. *Science* 322, 225–230. doi: 10.1126/science.1165115

Schutter, M., Kranenbarg, S., Wijffels, R. H., Verreth, J., and Osinga, R. (2011). Modification of light utilization for skeletal growth by water flow in the scleractinian coral *Galaxea fascicularis*. *Mar. Biol.* 158, 769–777. doi: 10.1007/s00227-010-1605-3

Scoffin, T. P., Tudhope, A. W., Brown, B. E., Chansang, H., and Cheeney, R. F. (1992). Patterns and possible environmental controls of skeletogenesis of Porites lutea, South Thailand. *Coral Reefs* 11, 1–11. doi: 10.1007/BF00291929

Sinutok, S., Hill, R., Doblin, M. A., Wuhrer, R., and Ralph, P. J. (2011). Warmer more acidic conditions cause decreased productivity and calcification in subtropical coral reef sediment-dwelling calcifiers. *Limnol. Oceanogr.* 56, 1200–1212. doi: 10.4319/lo.2011.56.4.1200

Spencer Davies, P. (1989). Short-term growth measurements of corals using an accurate buoyant weighing technique. *Mar. Biol.* 101, 389–395. doi: 10.1007/BF00428135

Stambler, N., and Dubinsky, Z. (2005). Corals as light collectors: an integrating sphere approach. *Coral Reefs* 24, 1–9. doi: 10.1007/s00338-004-0452-4

Stimson, J., and Kinzie, R. A. (1991). The temporal pattern and rate of release of zooxanthellae from the reef coral *Pocillopora damicornis* (Linnaeus) under nitrogen-enrichment and control conditions. *J. Exp. Mar. Biol. Ecol.* 153, 63–74. doi: 10.1016/S0022-0981(05)80006-1

Swierts, T., and Vermeij, M. J. (2016). Competitive interactions between corals and turf algae depend on coral colony form. *PeerJ* 4:e1984. doi: 10.7717/peerj.1984

Tan, Y. T. R., Wainwright, B. J., Afiq-Rosli, L., Ip, Y. C. A., Lee, J. N., Nguyen, N. T. H., et al. (2020). Endosymbiont diversity and community structure in *Porites lutea* from Southeast Asia are driven by a suite of environmental variables. *Symbiosis* 80, 269–277. doi: 10.1007/s13199-020-00671-2

Tanner, J. E. (1995). Competition between scleractinian corals and macroalgae an experimental investigation of coral growth, survival and reproduction. *J. Exp. Mar. Biol. Ecol.* 190, 151–168. doi: 10.1016/0022-0981(95)00027-O

Tanzil, J. T. I., Brown, B. E., Tudhope, A. W., and Dunne, R. P. (2009). Decline in skeletal growth of the coral *Porites lutea* from the Andaman Sea, South Thailand between 1984 and 2005. *Coral Reefs* 28, 519–528. doi: 10.1007/s00338-008-0457-5

Todd, P. A., Ong, X., and Chou, L. M. (2010). Impacts of pollution on marine life in Southeast Asia. *Biodivers. Conserv.* 19, 1063–1082. doi: 10.1007/s10531-010-9778-0

Ulstrup, K. E., Hill, R., van Oppen, M. J. H., Larkum, A. W. D., and Ralph, P. J. (2008). Seasonal variation in the photo-physiology of homogeneous and heterogeneous *Symbiodinium consortia* in two scleractinian corals. *Mar. Ecol. Prog. Ser.* 361, 139–150. doi: 10.3354/meps07360

Valderrama Ballesteros, L., Matthews, J. L., and Hoeksema, B. W. (2018). Pollution and coral damage caused by derelict fishing gear on coral reefs around Koh Tao, Gulf of Thailand. *Mar. Pollut. Bull.* 135, 1107–1116. doi: 10.1016/j.marpolbul.2018.08.033

Vieira, C., Thomas, O. P., Culioli, G., Genta-Jouve, G., Houlbreque, F., Gaubert, J., et al. (2016). Allelopathic interactions between the brown algal genus *Lobophora* (Dictyotales, Phaeophyceae) and scleractinian corals. *Sci. Rep.* 6:18637. doi: 10.1038/srep18637

Warner, M., Chilcoat, G., McFarland, F., and Fitt, W. (2002). Seasonal fluctuations in the photosynthetic capacity of photosystem II in symbiotic dinoflagellates in the Caribbean reef-building coral Montastraea. *Mar. Biol.* 141, 31–38. doi: 10.1007/s00227-002-0807-8

Warner, M. E., Fitt, W. K., and Schmidt, G. W. (1999). Damage to photosystem II in symbiotic dinoflagellates: a determinant of coral bleaching. *Proc. Natl. Acad. Sci. U.S.A.* 96, 8007–8012. doi: 10.1073/pnas.96.14.8007

Wijgerde, T., Jurriaans, S., Hoofd, M., Verreth, J. A. J., and Osinga, R. (2012). Oxygen and heterotrophy affect calcification of the scleractinian coral *Galaxea fascicularis*. *PLoS One* 7:e52702. doi: 10.1371/journal.pone.0052702

Winters, G., Holzman, R., Blekhman, A., Beer, S., and Loya, Y. (2009). Photographic assessment of coral chlorophyll contents: implications for ecophysiological studies and coral monitoring. *J. Exp. Mar. Biol. Ecol.* 380, 25–35. doi: 10.1016/j.jembe.2009.09.004

Xu, H., Feng, B., Xie, M., Ren, Y., Xia, J., Zhang, Y., et al. (2020). Physiological characteristics and environment adaptability of reef-building corals at the Wuzhizhou Island of South China Sea. *Front. Physiol.* 11:390. doi: 10.3389/fphys.2020.00390

Yucharoen, M. (2020). *Stress Indicator for Coral and Zooxanthellae at the Southern Reef of Phuket for Resistance to Coral Bleaching. NSTDA. P-17-52222 Report*. Thailand: National Science and Technology Development Agency.

Zhang, C., Chen, X., Wang, J., and Tan, L. (2017). Toxic effects of microplastic on marine microalgae *Skeletonema costatum*: interactions between microplastic and algae. *Environ. Pollut.* 220, 1282–1288. doi: 10.1016/j.envpol.2016.11.005

Conflict of Interest: The authors declare that the research was conducted in the absence of any commercial or financial relationships that could be construed as a potential conflict of interest.

Publisher's Note: All claims expressed in this article are solely those of the authors and do not necessarily represent those of their affiliated organizations, or those of the publisher, the editors and the reviewers. Any product that may be evaluated in this article, or claim that may be made by its manufacturer, is not guaranteed or endorsed by the publisher.

frontiers in Physiology

ORIGINAL RESEARCH
published: 23 December 2021
doi: 10.3389/fphys.2021.804678

Elevated Temperature and Exposure to Copper Leads to Changes in the Antioxidant Defense System of the Reef-Building Coral *Mussismilia harttii*

*Juliana da Silva Fonseca[1], Laura Fernandes de Barros Marangoni[2,3,4], Joseane Aparecida Marques[2,3] and Adalto Bianchini[3,5]**

[1]*Programa de Pós-Graduação em Ciências Fisiológicas, Instituto de Ciências Biológicas, Universidade Federal do Rio Grande, Rio Grande, Brazil,* [2]*Programa de Pós-Graduação em Oceanografia Biológica, Instituto de Oceanografia, Universidade Federal do Rio Grande, Rio Grande, Brazil,* [3]*Instituto Coral Vivo, Santa Cruz Cabrália, Brazil,* [4]*Smithsonian Tropical Research Institute, Ciudad de Panamá, Panama,* [5]*Instituto de Ciências Biológicas, Universidade Federal do Rio Grande, Rio Grande, Brazil*

OPEN ACCESS

Edited by:
Davide Seveso, University of Milano-Bicocca, Italy

Reviewed by:
Paula Mariela González, University of Buenos Aires, Argentina
Daniel Carneiro Moreira, University of Brasilia, Brazil

***Correspondence:**
Adalto Bianchini
adaltobianchini@furg.br

Specialty section:
This article was submitted to Aquatic Physiology, a section of the journal Frontiers in Physiology

Received: *29 October 2021*
Accepted: *01 December 2021*
Published: *23 December 2021*

Citation:
Fonseca JdS, Marangoni LFdB, Marques JA and Bianchini A (2021) Elevated Temperature and Exposure to Copper Leads to Changes in the Antioxidant Defense System of the Reef-Building Coral Mussismilia harttii. Front. Physiol. 12:804678. doi: 10.3389/fphys.2021.804678

The frequency and severity of coral bleaching events have increased in recent years. Global warming and contamination are primarily responsible for triggering these responses in corals. Thus, the objective of this study was to evaluate the isolated and combined effects of elevated temperature and exposure to copper (Cu) on responses of the antioxidant defense system of coral *Mussismilia harttii*. In a marine mesocosm, fragments of the coral were exposed to three temperatures (25.0, 26.6, and 27.3°C) and three concentrations of Cu (2.9, 5.4, and 8.6 μg/L) for up to 12 days. Levels of reduced glutathione (GSH) and the activity of enzymes, such as superoxide dismutase (SOD), catalase (CAT), glutathione S-transferase (GST), and glutamate cysteine ligase (GCL), were evaluated on the corals and symbionts. The short exposure to isolated and combined stressors caused a reduction in GSH levels and inhibition of the activity of antioxidant enzymes. After prolonged exposure, the combination of stressors continued to reduce GSH levels and SOD, CAT, and GCL activity in symbionts and GST activity in host corals. GCL activity was the parameter most affected by stressors, remaining inhibited after 12-days exposure. Interesting that long-term exposure to stressors stimulated antioxidant defense proteins in *M. harttii*, demonstrating a counteracting response that may beneficiate the oxidative state. These results, combined with other studies already published suggest that the antioxidant system should be further studied in order to understand the mechanisms of tolerance of South Atlantic reefs.

Keywords: coral bleaching, coral reefs, global warming, metal pollution, antioxidant enzymes, oxidative state

INTRODUCTION

Ocean warming is the main factor causing bleaching in coral reefs worldwide (Hoegh-Guldberg, 1999; McWilliams et al., 2005; Yuyama et al., 2012). Bleaching can be defined as the loss of color in the coral tissue, which can result from the expulsion of photosynthetic dinoflagellate endosymbionts from its tissues or degradation of photosynthetic pigments (Glynn, 1993; Downs et al., 2005). Under high stress conditions, reactive oxygen species (ROS) produced by symbionts can be passed to host coral tissues (Lesser, 1997, 2006; Weis, 2008; Yakovleva et al., 2009). In an attempt to avoid oxidative damage, corals eliminate an important source of ROS (their symbionts) what ultimately leads to the breakdown of the symbiotic relationship between the coral host and their photosynthetic symbionts (Downs et al., 2005; Howells et al., 2016). Due to the importance of such symbiosis, the bleaching is directly related to episodes of mass mortality on coral reefs, which contributes to the degradation of this important ecosystem (Glynn, 1993, 1996; Hoegh-Guldberg, 1999; Suggett and Smith, 2019).

The symbiosis between corals and photosynthetic algae produces chronic hyperoxic conditions during the light hours (Dykens, 1984; Kuhl et al., 1995; Schwarz et al., 2013). To protect themselves against potential damage induced by ROS, corals, and symbionts contain a variety of molecules with antioxidant properties (Lesser, 2006). The antioxidant defense system (ADS) includes enzymatic and non-enzymatic molecules, which reduce the amount of ROS and maintain the balance of the cellular oxidative state (Monteiro et al., 2006; Suggett and Smith, 2019). Antioxidant enzymes, such as superoxide dismutase (SOD), catalase (CAT), glutathione S-transferase (GST), and glutamate cysteine ligase (GCL), are responsible for acting in the neutralization of ROS. In fact, increased activity of such enzymes in corals is related to higher concentrations of ROS (Lesser et al., 1990; Higuchi et al., 2015). Reduced glutathione (GSH) has non-enzymatic antioxidant activity acting as substrate for the GST and glutathione peroxidase (GPx; Hermes-Lima, 2004). Due to the important role of these molecules in redox metabolism, they can be used as interesting parameters to assess an early warning response to coral bleaching in the face of multiple stressors (Weis, 2008; Higuchi et al., 2015).

Metal exposure is typically known to induce oxidative stress in many organisms through its participation in biochemical reactions that produce ROS, such as the superoxide anion ($O_2^{\bullet -}$), hydrogen peroxide (H_2O_2), and hydroxide radical ($^{\bullet}OH$; De Nadal et al., 2011; Schwarz et al., 2013). Copper (Cu) is a metal commonly found in the aquatic environment (Maria and Bebianno, 2011). This metal is considered an important micronutrient for the proper functioning of physiological systems, such as electron transport chain and antioxidant enzymes (Mercer and Llanos, 2003; Leary et al., 2009). However, elevated concentrations of Cu can be found in the aquatic environment due to run-off, mining, anti-fouling paints, and sewage (Jones, 1997). In fact, Cu contamination has been pointed out as a notable local threat to coral reefs (van Dam et al., 2011; Marques et al., 2019). When present in high concentrations, this metal can accumulate in organisms in concentrations above their capacity to excrete or detoxify (Rainbow, 2002). Toxic effects caused by Cu have been extensively reported in corals, including damage to the energy metabolism (Fonseca et al., 2019), reduction in the expression of antioxidant enzymes (Schwarz et al., 2013), DNA damage (Schwarz et al., 2013; Marangoni et al., 2017), reduced activity of enzymes related to the calcification process (Bielmyer et al., 2010; Marangoni et al., 2017), and bleaching (Jones, 2004; Gissi et al., 2019).

Thermal stress and exposure to heavy metals, such as Cu, can act in isolation and result in serious consequences. However, the impacts on the health of the organisms are more likely to be the result of a combination of stressors (Negri and Hoogenboom, 2011; Banc-Prandi and Fine, 2019). For example, the combination of these stressors presented a synergic effect in the coral *Mussismilia harttii* that led to reduced photosynthetic capacity (Fonseca et al., 2017), as well as decreased activity of enzymes involved in the energy metabolism (Fonseca et al., 2019). Cu is known to exhibit high affinity for thiol groups (−SH) present in antioxidants (Hultberg et al., 2001; Geracitano et al., 2002). Additionally, increased temperature can reduce the tolerance of organisms to exposure to metals (Portner, 2001, 2002). Therefore, it can be expected that the combination of thermal stress and Cu exposure could lead to increased deleterious effects in the oxidative metabolism of corals.

Most studies that evaluate the ADS of corals have been conducted with isolated stressors (Downs et al., 2000; Grant et al., 2003; Mitchelmore et al., 2007; Higuchi et al., 2009, 2012, 2015; Schwarz et al., 2013; Krueger et al., 2015). To date, only one study has evaluated the combined effect of increased temperature and exposure to copper on SOD activity in corals (Banc-Prandi and Fine, 2019). Considering the paucity of information on the combined effects of these stressors (temperature and Cu) in parameters associated with the ADS in corals, the present study aimed to contribute with a better understanding in this topic by evaluating in further details the ADS of an important scleractinian coral species of South Atlantic reefs, *M. harttii*, subjected to the combination of relevant stressors affecting coral reefs worldwide. For this purpose, we evaluated the levels of GSH and the activity of the antioxidant enzymes SOD, CAT, GST, and GCL in *M. harttii* exposed to different levels of thermal stress, Cu concentrations, and the combination of both. This species of coral is endemic and important in the construction of coral reefs in the South Atlantic. In addition, *M. harttii* has been subjected to Cu contamination associated with mining and sewage (Francini-Filho et al., 2019; Marques et al., 2019).

MATERIALS AND METHODS

Collection of Corals

Polyps from three colonies of the coral *M. harttii* were collected during July 2012 on the conservation area of the Municipal Natural Park of Recife de Fora (16°24′31"S; 038°58′39"W; Porto Seguro, Bahia, northeastern Brazil) and transported to the mesocosm facility of the Coral Vivo Project (Arraial d'Ajuda, Porto Seguro). Polyps were individualized, glued on ceramic

plates using cyanoacrylate, and acclimated to the experimental conditions for 20 days. Coral samples were collected under the permission of the Brazilian Environmental Agency (permit #85926584; IBAMA/SISBIO).

Coral Exposure in the Marine Mesocosm

Corals were kept in twenty seven 10 L tanks distributed according to three warming treatments [mean local temperature, and 1.5 and 2.5°C above the mean; that is, 25.0, 26.6, and 27.9°C, considering warming levels predicted to future climate scenarios issued by IPCC (2014)] and three Cu concentrations (0, 3, and 5 µg/L above the mean natural concentration, that is, 2.9, 5.4, and 8.6 µg/L). The concentrations of Cu used in the experiment are below or close the limits allowed by the international and Brazilian legislations for the protection of aquatic environments (CONAMA, 2005; EPA, 2005). All treatments were tested in triplicated tanks, where two *M. harttii* polyps, randomly distributed, were kept in each tank. After 4 and 12 days of exposure, polyps were sampled (between 5–6 pm/17–18 h) and immediately flash frozen for posterior laboratory analysis (see below).

In the mesocosm system, seawater is pumped through a continuous flow from the adjacent coral reef to four 5,000 L underground reservoirs to receive the desired temperature treatments before reaching the twenty seven 10 L tanks. Due to its direct connection to the reef environment, this system kept seawater conditions (e. g. natural daily variation of temperature, turbidity, salinity, pH, zooplankton availability) very similar to those in the natural environment. Temperature was monitored and controlled by an Arduino-based system (Reef Angel, Fremont) while two 15-kW submersible heaters maintained the temperature required for each treatment. Concomitantly, seawater captured from the reef environment was held in four pairs of 1,000- L underground sumps to receive stock solutions of Cu. Cu stock solutions were daily prepared (24 h before use) from a standard solution of $CuCl_2$ (1 g/L Cu). The seawater that received the Cu treatments was mixed with seawater coming from the primary treatment sumps using peristaltic pumps (flow rate of 0.17 L/min) before reaching the 10-L tanks. Seawater from the secondary system (Cu contamination) accounted for 10% of the total seawater flow reaching the 10-L aquariums, while heated water flow accounted for 90%. Before returning to the ocean, water was filtered and sterilized in an additional underground sump where ultraviolet filters and activated carbon cartridges were installed. Details on the functioning of this mesocosm system can be found in Duarte et al. (2015).

Seawater Collection and Analysis

Every 3 days seawater was collected from the test aquariums for monitoring concentrations of Cu and dissolved organic carbon (DOC) throughout the experiment. The concentrations of dissolved Cu were evaluated in filtered (0.45-mm mesh filter) water samples acidified with nitric acid (HNO_3, 1% final concentration; SupraPur, Merck®, Germany). For this purpose, water samples were desalted using the method proposed by Nadella et al. (2009) and the concentrations of Cu were determined through Atomic Absorption Spectrophotometry with Graphite Furnace (PerkinElmer®, Waltham, United States). DOC concentration was assessed by Total Organic Carbon analyzer (Shimadzu®, Japan). Pluviometry was obtained from the local weather station (Veracel Celulose, Brazil). Daily, random tanks from each treatment combination were assessed for temperature, pH (HI 9124, Hanna Instruments®, United States), and salinity (optical refractometer ITREF 10, Instrutemp®, São Paulo, Brazil). Temperature measurements were performed using loggers installed inside the tanks and at the reef environment to continuously monitor the seawater temperature every 30 min.

Sample Preparation

The antioxidant defense parameters were quantified in both coral host and endosymbiont microalgae fractions. Samples were prepared as described by Fonseca et al. (2021). Coral fragments were cut, homogenized on ice with a buffer for each analysis (1:1 w/v) using a sonicator (20 kHz, Sonaer Ultrasonics®, New York, United States). After homogenization, samples were centrifuged (2,530 *g*, 5 min, 4°C) to separate coral (supernatant) and symbiont (pellet) homogenates. Afterward, 200 µl of buffer was added to the pellet, which was sonicated (30 kHz) and used for analysis of the symbiotic microalgae. All results were normalized considering the protein concentration of the homogenates, which was quantified using a commercial kit based on the Bradford method.

Determination of Parameters of the Antioxidant Defense System

To determine the activity of the antioxidant enzymes CAT, SOD, and GST, the samples were homogenized in a buffer containing 20 mm Tris Base, 1 mm EDTA, 1 mm dithiothreitol, 500 mm sucrose, 150 mm KCl, and 0.1 mm PMSF. pH was adjusted to 7.6. For determination of the GCL activity and quantification of GSH content, the samples were homogenized in Tris-EDTA buffer containing 100 mm Tris-HCl, 2 mm EDTA, and 5 mm $MgCl_2{\cdot}6H_2O$. pH was adjusted to 7.75. All enzymatic assays were carried out at 25°C.

CAT activity was determined as described by Beutler (1975). The assay consists of the decomposition of H_2O_2 by CAT present in the sample in water (H_2O) and oxygen (O_2). The decomposition of H_2O_2 by CAT is monitored by the decrease of absorbance in 240 nm. The reaction was evaluated in quartz microplates containing the homogenate and reaction buffer (1 M tris base, 5 mm EDTA, and H_2O_2 (30%), pH 8.0). The results are expressed in units of CAT, which is defined as the amount of enzyme required to hydrolyze 1 µmol of H_2O_2 per min and per mg of protein.

SOD activity was assessed according to McCord and Fridovich (1969). This analysis reflects changes in superoxide anion ($O_2^{\bullet-}$) concentrations through the oxidation of cytochrome C by xanthine oxidase. The SOD assay was conducted using a buffer solution containing 50 mm KH_2PO_4 (pH 7.8). Absorbance readings were performed at 550 nm. SOD activity was expressed in enzyme units, where one unit is the amount of enzyme needed to inhibit 50% of cytochrome c reduction/min/mg protein.

Glutathione-S-transferase (GST) assay was performed as described by Habig and Jakoby (1981) using a phosphate buffer solution (100 mm, pH 7.0), following the conjugation of 1 mm GSH (Sigma-Aldrich, United States) with 0.77 mm 1-chloro-2,4- dinitrobenzene (CDNB; Sigma-Aldrich, United States). GST activity was measured as the increment in absorbance at 340 nm and was expressed in μmol CDNB/min/mg protein.

GCL activity and GSH concentration were analyzed according to White et al. (2003). The reaction is based on the measure of fluorescence emitted by the conjugation reaction of glutamylcysteine and GSH through fluorochrome NDA (naphthalene-2,3-dicarboxyaldehyde). The fluorescence measurement is evaluated by the wavelength of 472 nm (excitation) and 528 nm (emission). The activity of the GCL is expressed in ηmol of GSH per hour and per mg of protein and the GSH concentration in mg of GSH per mg of protein.

Statistical Analysis

The effects of elevated temperature and exposure to Cu on the activity of CAT, SOD, GST, GCL, and GSH content, on corals and symbionts, were evaluated using 2-way factorial ANOVA followed by the Fisher test for multiple comparisons. At each experimental time (4 and 12 days) we performed one ANOVA [fixed factors "temperature" (three levels, 25.0, 26.6 and 27.3°C), and "Cu" (three levels, 2.9, 5.4 and 8.6 μg/L)]. Data normality and homogeneity of variances were previously verified using the Shapiro-Wilk and Cochran C tests, respectively, and log-transformed when necessary. The confidence level adopted was 95% ($\alpha = 0.05$).

RESULTS

Seawater Physicochemical Parameters

The measured concentrations of dissolved Cu were 2.9 ± 0.7, 5.4 ± 0.9, 8.6 ± 0.3 μg/L, corresponding to the treatments of 0 (control), 3 and 5 μg/L above the mean natural concentration of 2.9 μg/L, respectively. Temperature levels were 25.0 ± 0.1 for control, 26.6 ± 0.1 and 27.3 ± 0.1°C, corresponding to the treatments of 1.5 and 2.5°C above ambient seawater temperature. The other physicochemical parameters analyzed in seawater are shown in **Supplementary Table S1**.

Parameters of the Antioxidant Defense System

CAT activity in the coral host fraction was inhibited after 4 days of exposure in the highest concentration of Cu tested (8.6 μg/L). In turn, after 12 days of exposure, an increased activity of CAT was observed in the temperature treatments of 26.6 and 27.3°C compared to the ones maintained at 25°C (**Figure 1**; **Table 1**).

No effects were observed in the CAT activity of symbionts after 4 days of exposure. However, effects of increased temperature, Cu, and the combination of both were observed after 12 days. Exposure to 5.4 μg/L Cu increased CAT activity on symbionts compared to 2.9 and 8.6 μg/L Cu. Exposure to 26.6°C reduced CAT activity compared to 25.0 and 27.3°C. In addition, the results of the combination of stressors showed an inhibition of CAT activity under 26.6°C and 8.6 μg/L compared to 2.9 μg/L at the same temperature. Exposure to 27.3°C and 5.4 μg/L increased CAT activity in symbionts compared to those maintained at 2.9 and 8.6 μg/L at the same temperature (**Figure 1**; **Table 1**).

SOD activity in the coral host increased after 4 days of exposure to the combination of stressors. An increased activity of the enzyme was observed under 27.3°C and 5.4ug/L Cu compared to 2.9 and 8.6ug/L Cu at the same temperature. After 12 days, exposure to 26.6°C led to an increased activity of SOD compared to 25.0°C (**Figure 2**; **Table 1**).

Effects of temperature and Cu applied in isolation were observed on SOD activity in symbionts after 4 days of exposure. Exposure to the concentration of 5.4 μg/L Cu increased SOD activity compared to 2.9 and 8.6 μg/L Cu. Exposure to 26.6°C inhibited SOD activity in symbionts compared to 25.0°C. In turn, exposure to 27.3°C increased SOD activity in symbionts compared to 25.0 and 26.6°C. After 12 days, the effect of exposure to isolated and combined stressors was observed on SOD activity in symbionts. A significant increase at 8.6 μg/L C compared to 2.9 μg/L Cu was observed. An increase was also observed under 26.6°C and 27.3°C compared to the control temperature (25.0°C). The combination of stressors led to an increase in SOD activity under 25.0 and 26.6°C combined with 8.6 μg/L Cu compared to 2.9 and 5.4 μg/L Cu at the same temperatures. Exposure to 27.3°C and 8.6 μg/L reduced SOD activity in symbionts compared to those maintained at 2.9 and 5.4 μg/L at the same temperature (**Figure 2**; **Table 1**).

No effects were observed in GST activity for any of the treatments tested on corals after 4 days. However, after 12 days, effects of temperature and the combination of stressors were observed on GST activity in the coral host. Exposure to 26.6°C increased GST activity compared to 25.0 and 27.3°C. In the combined exposure, an increase in GST activity was observed under 26.6°C and 8.6 μg/L compared to 2.9 μg/L Cu at the same temperature. However, corals maintained at 27.3°C and 8.6 μg/L Cu showed an inhibition of GST activity compared to those maintained at the same temperature at 2.9 μg/L Cu (**Figure 3**; **Table 1**).

Effects of Cu and temperature were observed on GST activity in symbionts after 4 days of exposure. Exposure to 5.4 μg/L Cu increased GST activity compared to 8.6 μg/L Cu. The opposite was observed for temperature. Exposure to 26.6°C inhibited GST activity compared to 25.0 and 27.3°C. No effects were observed in the symbiont GST activity after 12 days of exposure (**Figure 3**; **Table 1**).

GCL activity in the coral host was inhibited after 4 days of exposure to Cu and the combination of stressors. Exposure to 5.4 μg/L Cu inhibited GCL activity compared to 2.9 and 8.6 μg/L Cu. An inhibition was also observed under 26.6°C and 5.4 μg/L Cu compared to 2.9 μg/L Cu at the same temperature. Exposure to 27.3°C and 5.4 μg/L and 8.6 μg/L Cu also reduced GCL activity in corals compared to those maintained at 2.9 μg/L Cu at the same temperature. The isolated

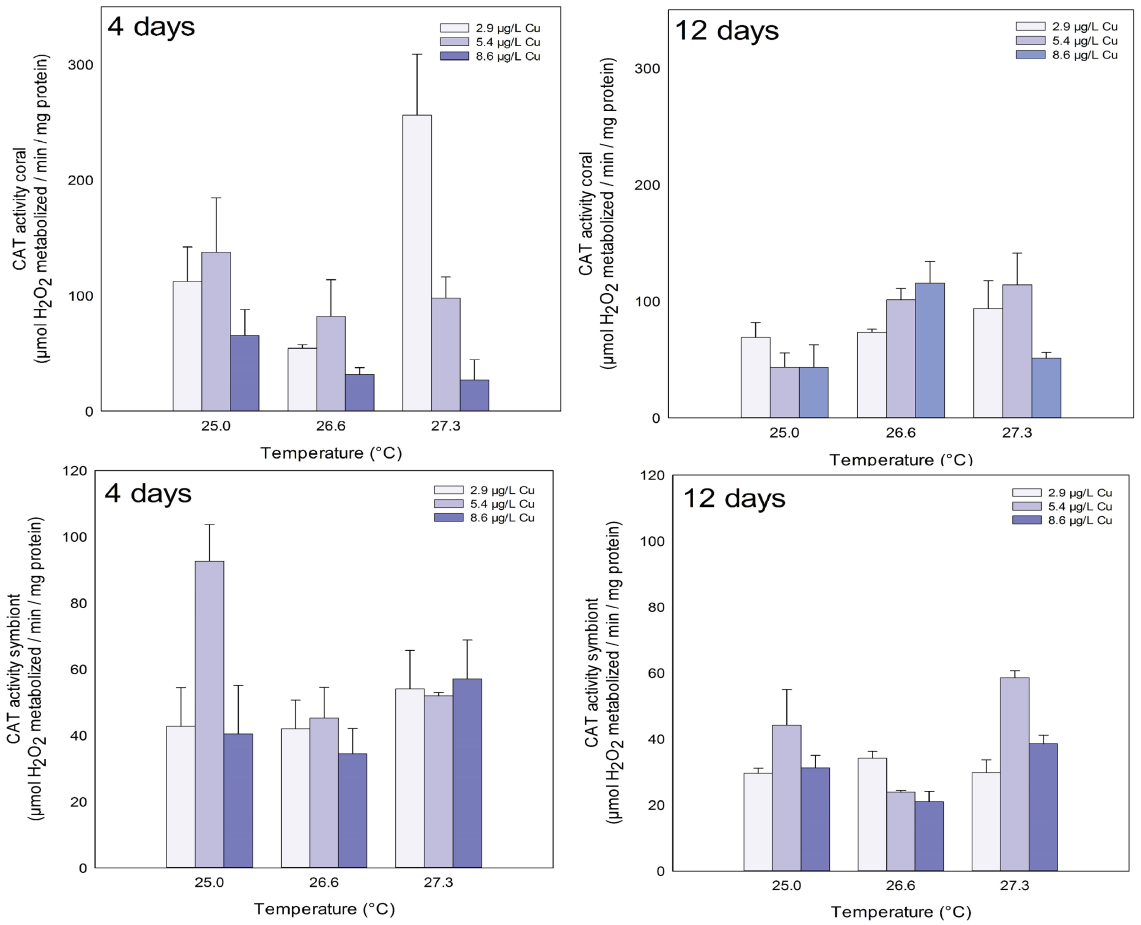

FIGURE 1 | CAT activity in the coral and for the symbiotic algae of coral *Mussismilia harttii* exposed to three different temperatures and three different copper (Cu) concentrations for 4 and 12 days.

effects of temperature and Cu exposure were observed on GCL activity in the coral host after 12 days. Exposure to 8.6 µg/L Cu inhibited GCL activity compared to 2.9 and 5.4 µg/L Cu. Similarly, exposure to 26.6°C inhibited GCL activity in corals compared to 25.0 and 27.3°C (**Figure 4**; **Table 1**).

The isolated effects of temperature were observed for GCL activity in symbionts after 4 days. Exposure to 26.6 and 27.3°C inhibited GCL activity in symbionts compared to 25.0°C. After 12 days, combined exposure to stressors inhibited GCL activity in symbionts. The results indicate a significant reduction after exposure to high concentration of Cu (8.6 µg/L) compared to 5.4 µg/L Cu. A reduction was also observed under 27.3°C and 5.4 µg/L Cu compared to 2.9 µg/L Cu at the same temperature (**Figure 4**; **Table 1**).

The levels of GSH in the coral host were reduced after 4 days of exposure to the combination of stressors. A significant reduction was observed after exposure to Cu at 5.4 µg/L compared to 2.9 and 8.6 µg/L. A reduction was also observed under 26.6°C and 8.6 µg/L Cu compared to 5.4 µg/L Cu at the same temperature. After 12 days, the isolated effects of temperature and Cu increased the levels of GSH in coral host. Exposure to 5.4 µg/L Cu increased the levels of GSH in the corals compared to those exposed to 2.9 µg/L Cu. Exposure to 27.3°C increased the levels of GSH in corals compared to those exposed 25.0 and 26.6°C (**Figure 5**; **Table 1**).

Effects of temperature, Cu, and the combination of both were observed on the GSH levels of the symbionts after 4 days of exposure. Exposure to 5.4 µg/L Cu reduced GSH levels in symbionts compared to 2.9 and 8.6 µg/L Cu treatments. In turn, exposure to 26.6°C increased GSH levels in symbionts compared to 25.0 and 27.3°C. The combined treatment of 26.6°C and 5.4 µg/L Cu reduced the levels of GSH in the symbionts compared to 2.9 µg/L Cu at the same temperature. After 12 days, the combination of stressors altered the levels of GSH in the symbionts. Specifically, a reduction after exposure to Cu alone at 8.6 µg/L was observed compared to the treatments of 2.9 and 5.4 µg/L Cu. In turn, an increase in GSH levels was observed under 26.6°C and 5.4 µg/L Cu compared to 2.9 µg/L Cu at the same temperature (**Figure 5**; **Table 1**).

TABLE 1 | Results for the 2-way factorial analysis of variance (ANOVA) conducted for *Mussismilia harttii* exposed to elevated temperature and Cu contamination for 4 and 12 days.

Variable	Treatment	4-days				12-days			
		df	*F*	*p*	Fisher	*df*	*F*	*p*	Fisher
CAT coral	Cu	2	11.94	0.00	*8.6 < 2.9, 5.4	2	0.56	0.58	
	Temperature	2	2.89	0.08		2	4.65	0.02	27.3, 26.6 > 25.0
	Cu × Temperature	4	2.14	0.11		4	2.07	0.13	
CAT symbiont	Cu	2	3.11	0.06		2	4.23	0.03	*5.4 > 2.9, 8.6
	Temperature	2	2.49	0.11		2	9.70	0.00	26.6 < 25.0, 27.3
	Cu × Temperature	4	2.68	0.06		4	4.51	0.01	26.6 (8.6 < 2.9)
									27.3 (5.4 > 2.9, 8.6)
SOD coral	Cu	2	0.80	0.46		2	0.60	0.55	
	Temperature	2	3.02	0.07		2	5.62	0.01	26.6 > 25.0
	Cu × Temperature	4	5.23	0.00	27.3 (5.4 > 2.9, 8.6)	4	0.93	0.46	
SOD symbiont	Cu	2	11.30	0.00	5.4 > 2.9, 8.6	2	6.90	0.00	*8.6 > 2.9
	Temperature	2	17.39	0.00	26.6 < 25.0 < 27.6	2	5.34	0.01	27.3, 26.6 > 25.0
	Cu × Temperature	4	1.65	0.20		4	13.00	0.00	25.0 (8.6 > 2.9, 5.4)
									26.6 (8.6 > 2.9, 5.4)
									27.3 (8.6 < 2.9, 5.4)
GST coral	Cu	2	2.33	0.12		2	0.53	0.59	
	Temperature	2	2.03	0.16		2	50.22	0.00	26.6 > 25.0, 27.3
	Cu × Temperature	4	1.10	0.38		4	3.10	0.04	26.6 (8.6 > 2.9)
									27.6 (8.6 < 2.9)
GST symbiont	Cu	2	6.21	0.00	5.4 > 8.6	2	1.36	0.28	
	Temperature	2	7.87	0.00	26.6 < 25.0, 27.3	2	2.75	0.09	
	Cu × Temperature	4	1.05	0.40		4	0.71	0.59	
GCL coral	Cu	2	11.47	0.00	5.4 < 2.9, 8.6	2	14.09	0.00	*8.6 < 2.9, 5.4
	Temperature	2	0.68	0.52		2	23.55	0.00	26.6 < 25.0, 27.3
	Cu × Temperature	4	4.29	0.02	26.6 (5.4 < 2.9)	4	2.53	0.09	
					27.3 (5.4, 8.6 < 2.9)				
GCL symbiont	Cu	2	3.10	0.07		2	2.38	0.13	
	Temperature	2	4.21	0.03	*27.6, 26.6 < 25.0	2	3.39	0.06	
	Cu × Temperature	4	1.93	0.16		4	3.40	0.04	*25.0 (8.6 < 5.4)
									27.0 (5.4 < 2.9)
GSH coral	Cu	2	1.61	0.22		2	4.09	0.03	5.4 > 2.9
	Temperature	2	1.67	0.21		2	8.38	0.00	27.3 > 26.6, 25.0
	Cu × Temperature	4	4.25	0.01	25.0 (5.4 < 2.9, 8.6)	4	2.40	0.09	
					26.6 (8.6 < 5.4)				
GSH symbiont	Cu	2	14.58	0.00	5.4 < 2.9, 8.6	2	1.89	0.31	
	Temperature	2	6.29	0.01	26.6 > 25.0, 27.3	2	1.26	0.18	
	Cu × Temperature	4	7.28	0.00	26.0 (5.4 < 2.9)	4	4.88	0.01	25.0 (8.6 < 2.9, 5.4)
									26.6 (5.4 > 2.9)

Significant values ($p < 0.05$) are in bold. The results marked in green represent an increase in the ADS, while the results marked in red represent the inhibitory effects on the ADS of M. harttii.

**indicates the data that has been log-transformed.*

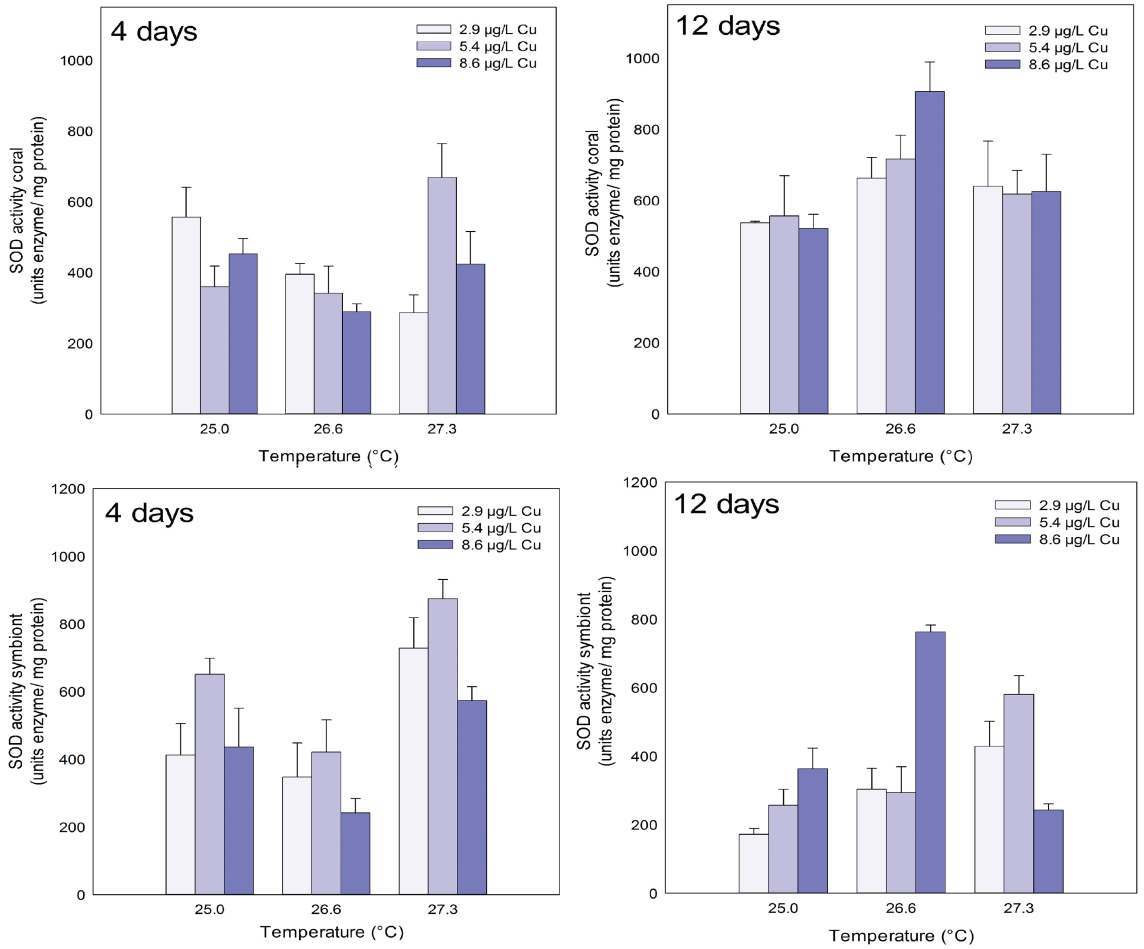

FIGURE 2 | SOD activity in the coral and for the symbiotic algae of coral *M. harttii* exposed to three different temperatures and three different copper (Cu) concentrations for 4 and 12 days.

DISCUSSION

Oxidative stress is defined as an imbalance in the pro-oxidant/antioxidant ratio, which favors increased pro-oxidants and results in oxidative damage (Downs et al., 2002; Halliwell and Gutteridge, 2007). Previous studies have shown that the elevated temperature and exposure to Cu are typically known to induce oxidative damage in *M. harttii* (Fonseca et al., 2017; Marangoni et al., 2017, 2019a,b; Fonseca et al., 2021), as well as in other coral species (Lesser, 1997; Schwarz et al., 2013; Dias et al., 2019). Given the clear connection between oxidative stress and coral bleaching (for a review see Suggett and Smith, 2019), it is paramount to evaluate changes in the activity of specific antioxidant molecules that are associated with this condition. In this context, the present study was carried out evaluating a higher number of parameters related to ADS (enzymatic and non-enzymatic) than previous studies conducted with reef-building corals. A larger picture of the oxidative profile of a coral species was obtained in the face of the combined exposure of global and local stressors.

Exposure to increased temperature and Cu generally caused an inhibition in the activity of antioxidant enzymes after short exposure (4 days). Interestingly, after prolonged exposure (12 days) many of these parameters recovered and an increase in the antioxidant defenses of the coral host and its symbionts was observed. Results suggest that prolonged exposure to stressors can increase ROS generation in *M. harttii*. However, the coral holobiont (coral host + microalgae symbionts) showed a counteracting response under such condition by increasing antioxidant defenses to prevent oxidative damage. In fact, Fonseca et al. (2017) showed a reduction in lipid damage (as lipid peroxidation) in *M. harttii* exposed for up to 12 days under the same experimental conditions. Later, an increase in total antioxidant capacity (TAC) in algae symbionts of *M. harttii* was observed after exposure to increasing temperature and Cu (Fonseca et al., 2021). Interestingly, South Atlantic corals have been suggested to be more tolerant to stressors compared to coral reefs in other parts of the world (Mies et al., 2020). The up-regulation shown by *M. harttii* ADS and results found for the same specie under a heat wave event (Marangoni et al., 2019a,b) suggest

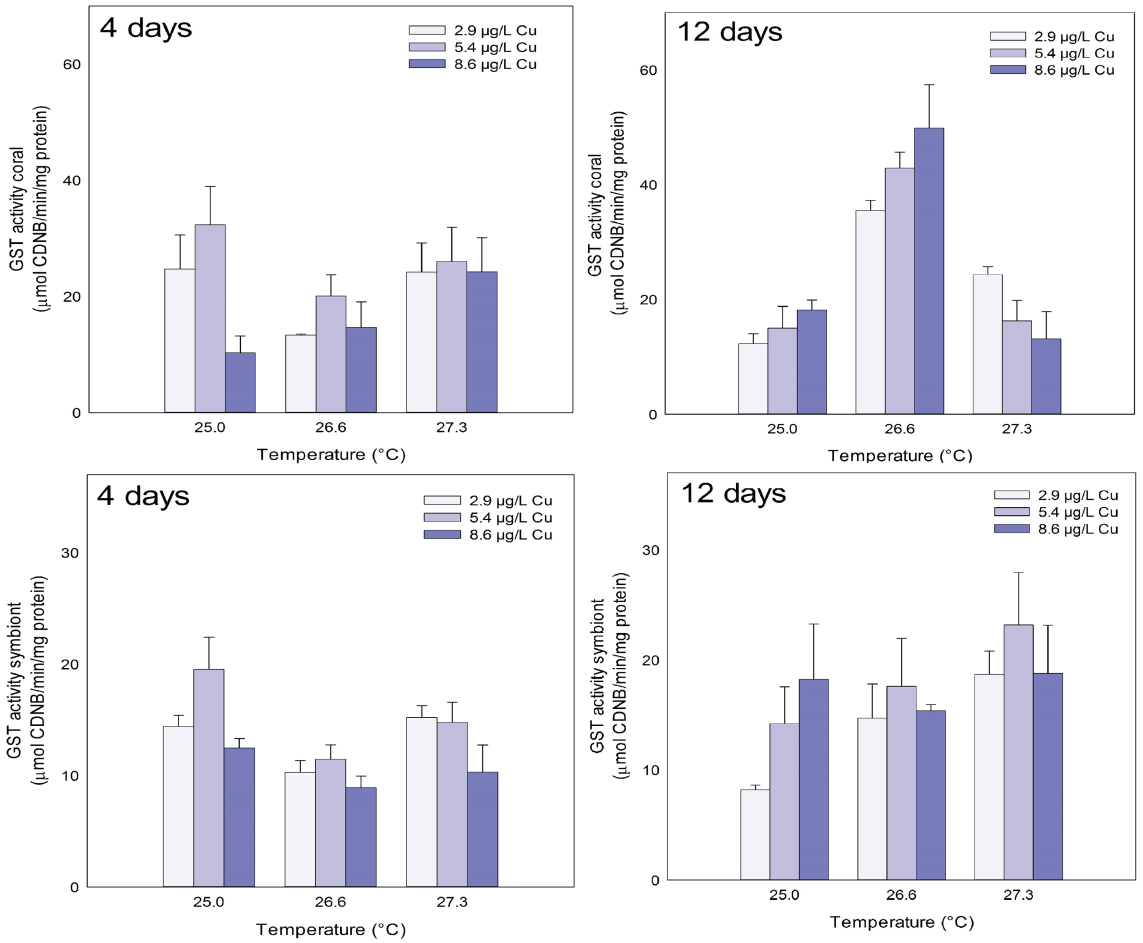

FIGURE 3 | GST activity in the coral and for the symbiotic algae of coral *M. harttii* exposed to three different temperatures and three different copper (Cu) concentrations for 4 and 12 days.

that the antioxidant response is an important mechanism potentially connected to the resilience of these corals and indicate that this process should be further studied in order to understand the traits that explain the tolerance of the South Atlantic corals.

SOD and CAT are enzymes involved with the neutralization of ROS and their performance have been related to coral bleaching (Higuchi et al., 2015). The high activity of SOD and CAT after prolonged exposure of the coral host to increasing temperature suggests an increased need for neutralization of superoxide anion ($O_2^{\bullet-}$), a radical with high potential of inducing oxidative damage. The dismutation of $O_2^{\bullet-}$ performed by SOD represents an important source of H_2O_2, a reactive species mainly reduced by CAT (Regoli and Giuliani, 2014). Therefore, a higher generation of $O_2^{\bullet-}$ would be expected after prolonged exposure of *M. harttii* to increasing temperature.

The symbiotic algae demonstrated an increase in SOD activity and a reduction in CAT after prolonged exposure to increasing temperature alone and combined with Cu. This can cause an accumulation of H_2O_2 in the symbiont cell. The excess of H_2O_2 can facilitate its reaction with transition metals, such as Fe and Cu, through the Fenton reactions facilitating the formation of hydroxyl radical ($^{\bullet}OH$; $H_2O_2 + Fe^{2+}/Cu^{+} \rightarrow Fe^{3+}/Cu^{2+} + {}^{\bullet}OH + OH^{-}$, see Hermes-Lima, 2004). In addition, high amounts of H_2O_2 can induce apoptosis and the formation of nitrite peroxide ($ONOO^{-}$; Perez and Weis, 2006; Weis, 2008; Hawkins et al., 2013; Hawkins and Davy, 2013), a highly reactive nitrogen species (RNS) that has been linked to the onset of coral bleaching (Marangoni et al., 2019b). RNS, such as $ONOO^{-}$, are generally responsible for causing damage to proteins and DNA, in addition to inhibiting key enzymes in energy metabolism (Wink and Mitchell, 1998; Brown and Borutaite, 2002). In accordance, the same stressors tested here caused drastic reductions in enzymes of the energy metabolism of *M. harttii* after prolonged exposure (Fonseca et al., 2019). Cu acts as a cofactor of SOD (Hermes-Lima, 2004), therefore, the higher concentrations of such metal may have acted as an important factor inducing SOD activity in symbionts. In accordance, the increase in SOD activity has already been reported in corals exposed to Cu (Banc-Prandi and Fine, 2019).

GST is an enzyme of the phase II of the detoxification processes responsible for conjugating GSH with many organic and inorganic compounds, including aldehydes produced during

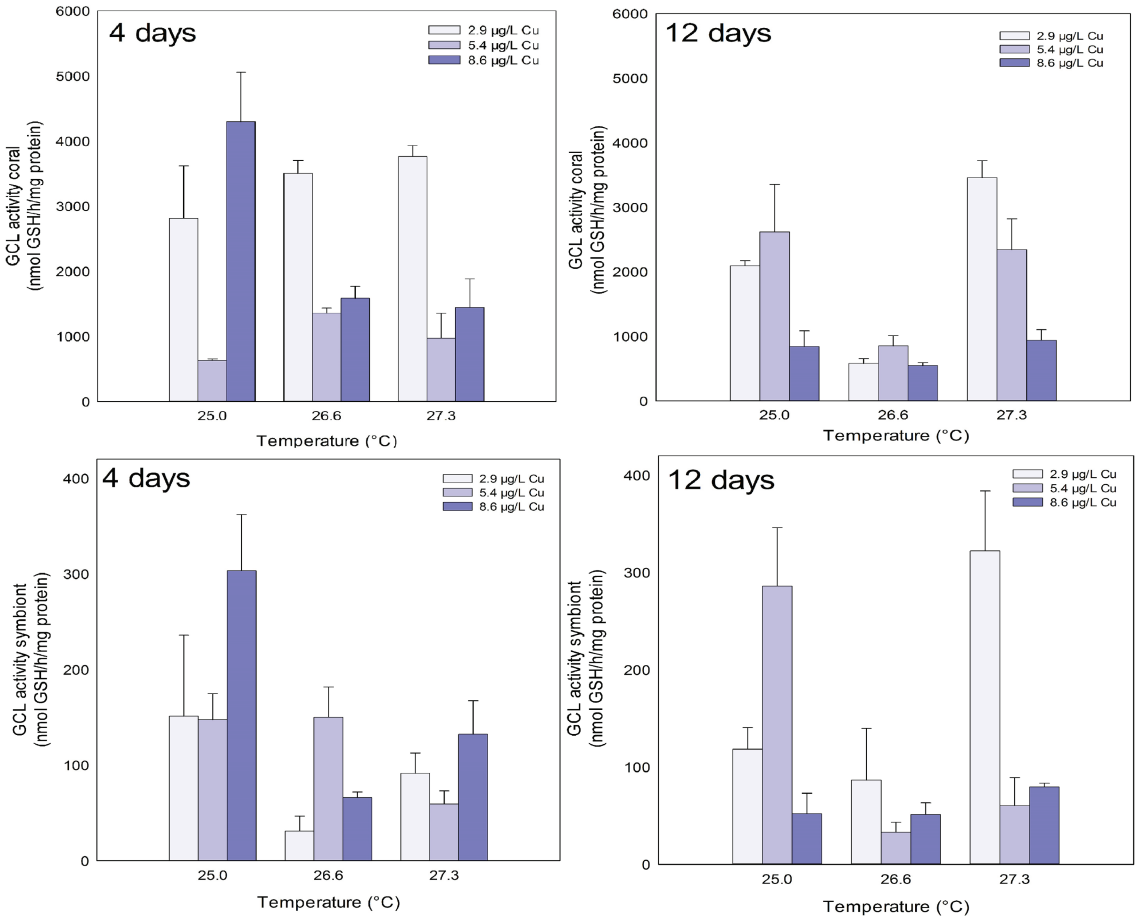

FIGURE 4 | GCL activity in the coral and for the symbiotic algae of coral *M. harttii* exposed to three different temperatures and three different copper (Cu) concentrations for 4 and 12 days.

lipid peroxidation (LPO; Higgins and Hayes, 2011). In fact, it has been shown that exposure to increased temperature alone induces LPO in host corals after prolonged exposure (Fonseca et al., 2021). This result was paralleled to increased GST activity and increased GSH levels in corals. Interestingly, increased temperature reduced the levels of LPO in the symbionts (Fonseca et al., 2021) and no changes were observed in the present study in GST activity and GSH levels. These results suggest a significant role of the glutathione system in the detoxification of LPO metabolites in corals and symbionts.

Considering the glutathione metabolism, GCL is the rate-limiting enzyme in GSH synthesis (White et al., 2003). The activity of this enzyme was inhibited in corals and symbionts throughout the experiment, which resulted in the reduction of GSH levels. Those parameters were the most affected by exposure to stressors, and similar results have already been observed in other studies (Downs et al., 2000; Pourahmad and O'Brien, 2000; Nagalakshmi and Prasad, 2001; Klein et al., 2017a; Maher, 2018). GCL is an ATP-dependent enzyme (Chen et al., 2005), and Cu and increased temperature have been previously shown to inhibit enzymes of energy metabolism in *M. harttii* (Fonseca et al., 2019). GSH plays an important role in numerous intracellular processes and provides protection for cells from damage caused by ROS and other stressors (Halliwell and Gutteridge, 2007). It contains a thiol group (−SH) with important reducing capacity, binding to electrophilic compounds by assisting its elimination or biotransformation (Townsend et al., 2003). Therefore, the reduction of GSH levels can compromise detoxification reactions of organic compounds, as well as the oxidative state of corals. Also, it is worth noting that exposure to isolated and combined stressors increased GSH levels in some treatments. Interestingly, the increase in GSH levels was parallel to the inhibition of GCL activity in host corals and their symbionts. In fact, it has already been observed that GCL activity can be inhibited by high levels of GSH (Maher, 2005; Klein et al., 2017b).

Reef-building corals need to have fine control in H_2O_2 neutralization to prevent bleaching (Lesser, 1997; Smith et al., 2005; Weis, 2008). The results of the present study showed a possible relationship between the activity of SOD and GST and the levels of GSH in corals and symbionts. Prolonged exposure to elevated temperature increased the activity of SOD in corals concomitantly with the increase in GST activity and levels of GSH. This relationship may be involved with the conjugation of GSH with LPO products produced by accumulation of H_2O_2,

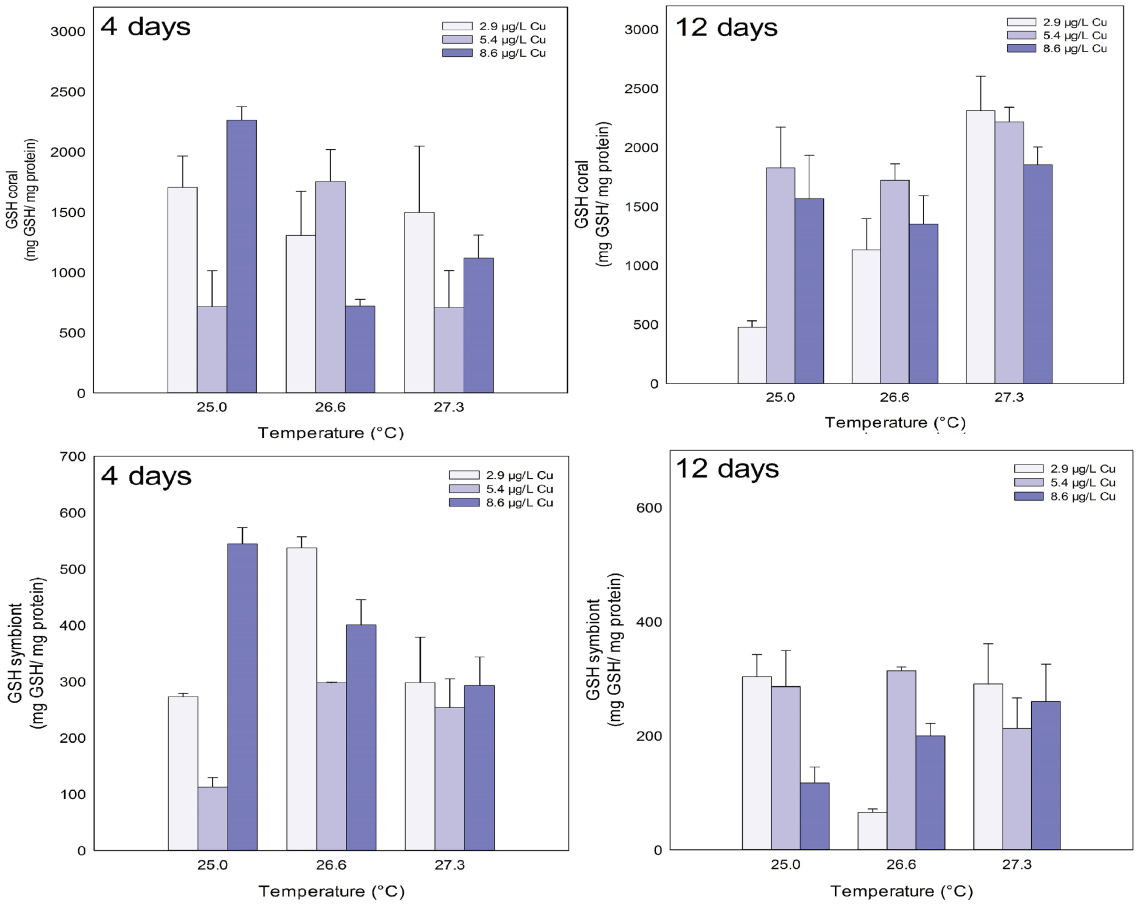

FIGURE 5 | GSH levels in the coral and for the symbiotic algae of coral *M. harttii* exposed to three different temperatures and three different copper (Cu) concentrations for 4 and 12 days.

which are catalyzed by GST. In fact, elevated temperature alone induced LPO in *M. harttii* (Fonseca et al., 2021). In addition, H_2O_2 can be decomposed by GPx oxidizing GSH in this process (Hermes-Lima, 2004), which could explain the increase in the production of this tripeptide. However, the symbiotic algae showed that the exposure to Cu alone induced SOD and GST activity after 4 days of exposure and this cause a depletion of GSH levels. In primary producers, the excess H_2O_2 generated in the presence of Cu is scavenged by peroxisomes. The detoxification pathway continues through the oxidation of GSH *via* the ascorbate-dehydroascorbate system (Nagalakshmi and Prasad, 2001). Thus, exposure to Cu can facilitate the accumulation of H_2O_2 in symbiotic algae and consequently trigger bleaching through this mechanism. In addition, GSH is known to be involved in metal scavenging (Hermes-Lima, 2004), so this can happen because GSH is facilitating the elimination of Cu in symbionts.

Symbiotic algae can be a major input of ROS to the coral host under stressful conditions, especially when it involves thermal stress and high light conditions (Suggett and Smith, 2019). Due to their photosynthetic nature, these organisms produce high amounts of ROS and therefore an efficient defense system to prevent oxidative damage can be expected. Indeed, exposure to stressors caused an increase in the parameters of the defense system of symbiotic algae. Increases in the TAC of low molecular weight scavengers have been observed in symbionts of *M. harttii* exposed to a combination of temperature and Cu (Fonseca et al., 2021). The up-regulation of antioxidant enzymes is an important component of the cellular response to stress of symbionts caused by exposure to stressors. This can provide the symbiotic algae a faster reduction of oxidative damage, prevent the process of apoptosis and consequently maintain the normal functioning of the photosynthetic process (Ralph et al., 2001). These results are interesting, as they reinforce that bleaching in *M. harttii* can be a response initiated by the symbiotic algae. Therefore, a response from the symbiotic algae defense system would be expected before any visual manifestation of bleaching. These results highlight the use of these parameters as potential tools of early warning response to corals bleaching.

Antioxidant enzyme analyzes are important and should be considered in future studies that evaluate the physiological responses of *M. harttii* coral under chronic exposure conditions. The evaluation of ADS parameters, preferentially combined with analysis of ROS and RNS, can improve our understanding about mechanisms of resilience in corals exposed to multiple stressors.

DATA AVAILABILITY STATEMENT

The original contributions presented in the study are included in the article/**Supplementary Material**, further inquiries can be directed to the corresponding author.

AUTHOR CONTRIBUTIONS

JF, LM, JM, and AB designed the work and collected and analyzed the data. All authors contributed to the writing of the manuscript.

FUNDING

We acknowledge the funding from "Coordenação de Aperfeiçoamento de Pessoal de Nível Superior" (CAPES; Programa Ciências do Mar, Brazil; grant #84/2010) and "Conselho Nacional de Desenvolvimento Científico e Tecnológico" (CNPq; Instituto Nacional de Ciência e Tecnologia de Toxicologia Aquática, Brazil; grant #573949/2008-5). Adalto Bianchini is research fellow of CNPq (Proc. #307647/2016-1) supported by "International Development Research Center" (IDRC; Ottawa, Canada). Juliana da Silva Fonseca was a graduate fellow from CAPES.

ACKNOWLEDGMENTS

We thank "Coral Vivo Project" and its sponsors Petrobras (Programa Petrobras Ambiental) and "Arraial d'Ajuda Eco Parque" for support in field research.

SUPPLEMENTARY MATERIAL

The Supplementary Material for this article can be found online at: https://www.frontiersin.org/articles/10.3389/fphys.2021.804678/full#supplementary-material

REFERENCES

Banc-Prandi, G., and Fine, M. (2019). Copper enrichment reduces thermal tolerance of the highly resistant Red Sea coral *Stylophora pistillata*. *Coral Reefs* 38, 285–296. doi: 10.1007/s00338-019-01774-z

Beutler, E. (1975). "The preparation of red cells for assay," in *Red Cell Metabolism: A Manual of Biochemical Methods* (New York, USA: Grune and Straton), 8–18.

Bielmyer, G. K., Grosell, M., Bhagooli, R., Baker, A. C., Langdon, C., Gillette, P., et al. (2010). Differential effects of copper on three species of scleractinian corals and their algal symbionts (*Symbiodinium spp.*). *Aquat. Toxicol.* 97, 125–133. doi: 10.1016/j.aquatox.2009.12.021

Brown, G. C., and Borutaite, V. (2002). Nitric oxide inhibition of mitochondrial respiration and its role in cell death. *Free Radic. Biol. Med.* 33, 1440–1450. doi: 10.1016/s0891-5849(02)01112-7

Chen, Y., Shertzer, H. G., Schneider, S. N., Nebert, D. W., and Dalton, T. P. (2005). Glutamate cysteine ligase catalysis: dependence on ATP and modifier subunit for regulation of tissue glutathione levels. *J. Biol. Chem.* 280, 33766–33774. doi: 10.1074/jbc.M504604200

CONAMA (2005). Conselho Nacional do Meio Ambiente. Resolução N° 357, de 17 de março de 2005. Brasília, Brazil. Available at: http://www.mma.gov.br/port/conama/res/res05/res35705.pdf (Accessed April, 2021).

De Nadal, E., Ammerer, G., and Posas, F. (2011). Controlling gene expression in response to stress. *Nat. Rev. Genet.* 12, 833–845. doi: 10.1038/nrg3055

Dias, M., Madeira, C., Jogee, N., Ferreira, A., Gouveia, R., Cabral, H., et al. (2019). Oxidative stress on scleractinian coral fragments following exposure to high temperature and low salinity. *Ecol. Indic.* 107:105586. doi: 10.1016/j.ecolind.2019.105586

Downs, C. A., Fouth, J. E., Halas, J. C., Dustan, P., Bemiss, J., and Woodley, C. M. (2002). Oxidative stress and seasonal coral bleaching. *Free Radic. Biol. Med.* 33, 533–543. doi: 10.1016/s0891-5849(02)00907-3

Downs, C. A., Fouth, J. E., Robinson, C. E., Curry, R., Lanzendorf, B., Halas, J., et al. (2005). Cellular diagnostics and coral health: declining coral health in the Florida keys. *Mar. Pollut. Bull.* 51, 558–569. doi: 10.1016/j.marpolbul.2005.04.017

Downs, C. A., Mueller, E., Phillips, S., Fauth, J. E., and Woodley, C. M. (2000). A molecular biomarker system for assessing the health of coral (*Montastraea faveolata*) During heat stress. *Mar. Biotechnol.* 2, 533–544. doi: 10.1007/s101260000038

Duarte, G., Calderon, E. N., Pereira, C. M., Marangoni, L. F. B., Santos, H. F., Peixoto, R. S., et al. (2015). A novel marine mesocosm facility to study global warming, water quality, and ocean acidification. *Ecol. Evol.* 5, 4555–4566. doi: 10.1002/ece3.1670

Dykens, J. A. (1984). Enzymic defenses against oxygen toxicity in marine cnidarians containing endosymbiotic algae. *Mar. Biol. Lett.* 5, 291–301.

EPA (2005). United States Environmental Protection Agency. Handbook for Developing Watershed Plans to Restore and Protect Our Waters. EPA 841-B-05-005: Washington. Available at: http://www.epa.gov/owow/nps/watershed_handbook/pdf/handbook.pdf (Accessed April 2021).

Fonseca, J. S., Marangoni, L. F., Marques, J. A., and Bianchini, A. (2017). Effects of increasing temperature alone and combined with copper exposure on biochemical and physiological parameters in the zooxanthellate scleractinian coral *Mussismilia harttii*. *Aquat. Toxicol.* 190, 121–132. doi: 10.1016/j.aquatox.2017.07.002

Fonseca, J. S., Marangoni, L. F. B., Marques, J. A., and Bianchini, A. (2019). Energy metabolism enzymes inhibition by the combined effects of increasing temperature and copper exposure in the coral M*ussismilia harttii*. *Chemosphere* 236:124420. doi: 10.1016/j.chemosphere.2019.124420

Fonseca, J. S., Mies, M., Paranhos, A., Taniguchi, S., Güth, A. Z., Bícego, M. C., et al. (2021). Isolated and combined effects of thermal stress and copper exposure on the trophic behavior and oxidative status of the reef-building coral *Mussismilia harttii*. *Environ. Pollut.* 268:115892. doi: 10.1016/j.envpol.2020.115892

Francini-Filho, R. B., Cordeiro, M. C., Omachi, C. Y., Rocha, A. M., Bahiense, L., Garcia, G. D., et al. (2019). Remote sensing, isotopic composition and metagenomics analyses revealed Doce River ore plume reached the southern Abrolhos Bank reefs. *Sci. Total Environ.* 697:134038. doi: 10.1016/j.scitotenv.2019.134038

Geracitano, L. A., Monserrat, J. M., and Bianchini, A. (2002). Physiological and antioxidant enzyme responses to acute and chronic exposure of *Laeonereis acuta* (Polychaeta: nereididae) to copper. *J. Exp. Mar. Biol. Ecol.* 277, 145–156. doi: 10.1016/S0022-0981(02)00306-4

Gissi, F., Reichelt-Brushett, A. J., Chariton, A. A., Stauber, J. L., Greenfield, P., Humphrey, C., et al. (2019). The effect of dissolved nickel and copper on the adult coral *Acropora muricata* and its microbiome. *Environ. Pollut.* 250, 792–806. doi: 10.1016/j.envpol.2019.04.030

Glynn, P. W. (1993). Coral reef bleaching: ecological perspectives. *Coral Reefs* 12, 1–17. doi: 10.1007/bf00303779

Glynn, P. W. (1996). Coral reef bleaching: facts, hypotheses and implications. *Glob. Chang. Biol.* 2, 495–509. doi: 10.1111/j.1365-2486.1996.tb00063.x

Grant, A. J., Graham, K., Frankland, S., and Hinde, R. (2003). Effect of copper on algal-host interactions in the symbiotic coral *Plesiastrea versipora*. *Plant Physiol. Biochem.* 41, 383–390. doi: 10.1016/S0981-9428(03)00034-2

Habig, W. H., and Jakoby, W. B. (1981). Assays for differentiation of glutathione-S-transferase. *Methods Enzymol.* 77, 398–405. doi: 10.1016/s0076-6879(81)77053-8

Halliwell, B., and Gutteridge, J. (2007). *Free Radicals in Biology and Medicine. 4th Edn*. New York: Oxford University Press.

Hawkins, T. D., Bradley, B. J., and Davy, S. K. (2013). Nitric oxide mediates coral bleaching through an apoptotic-like cell death pathway: evidence from a model sea anemone-dinoflagellate symbiosis. *FASEB J.* 27, 4790–4798. doi: 10.1096/fj.13-235051

Hawkins, T. D., and Davy, S. K. (2013). Nitric oxide and coral bleaching: is peroxynitrite generation required for symbiosis collapse? *J. Exp. Biol.* 216, 3185–3188. doi: 10.1242/jeb.087510

Hermes-Lima, M. (2004). "Oxygen in biology and biochemistry: role of free radicals," in *Functional Metabolism: Regulation and Adaptation*. *1st Edn*. ed. K. B. Storey. (New York: John Wiley & Sons), 319–368.

Higgins, L. G., and Hayes, J. D. (2011). Mechanisms of induction of cytosolic and microsomal glutathione transferase (GST) genes by xenobiotics and pro-inflammatory agents. *Drug Metab. Rev.* 43, 92–137. doi: 10.3109/03602532.2011.567391

Higuchi, T., Fujimura, H., Arakaki, T., and Oomori, T. (2009). "Activities of antioxidant enzymes (SOD and CAT) in the coral Galaxea fascicularis against increased hydrogen peroxide concentrations in seawater." In *Proceedings of the 11th International Coral Reef Symposium*. July 7-11, 2008. Lauderdale, Florida, 926–930.

Higuchi, T., Suzuki, Y., and Fujimura, H. (2012). "Multiple effects of hydrogen peroxide and temperature on antioxidants and bleaching." In *Proc 12th Intl Coral Reef Symp*. 9–13.

Higuchi, T., Yuyama, I., and Nakamura, T. (2015). The combined effects of nitrate with high temperature and high light intensity on coral bleaching and antioxidant enzyme activities. *Reg. Stud. Mar. Sci.* 2, 27–31. doi: 10.1016/j.rsma.2015.08.012

Hoegh-Guldberg, O. (1999). Climate change, coral bleaching and the future of the world's coral reefs. *Mar. Freshw. Res.* 50, 839–866. doi: 10.1071/mf99078

Howells, E. J., Abrego, D., Meyer, E., Kirk, N. L., and Burt, J. A. (2016). Host adaptation and unexpected symbiont partners enable reef-building corals to tolerate extreme temperatures. *Glob. Chang. Biol.* 22, 2702–2714. doi: 10.1111/gcb.13250

Hultberg, B., Andersson, A., and Isaksson, A. (2001). Interaction of metals and thiols in cell damage and glutathione distribution: potentiation of mercury toxicity by dithiothreitol. *Toxicology* 156, 93–100. doi: 10.1016/s0300-483x(00)00331-0

IPCC (2014). *The Fifth Assessment Report of the Intergovernmental Panel on Climate Change (IPCC)*. Cambridge, UK: Cambridge University Press.

Jones, R. J. (1997). Zooxanthellae loss as a bioassay for assessing stress in corals. *Mar. Ecol. Prog. Ser.* 149, 163–171. doi: 10.3354/meps149163

Jones, R. J. (2004). Testing the 'photoinhibition' model of coral bleaching using chemical inhibitors. *Mar. Ecol. Prog. Ser.* 284, 133–145. doi: 10.3354/meps284133

Klein, R. D., Borges, V. D., Rosa, C. E., Colares, E. P., Robaldo, R. B., Martinez, P. E., et al. (2017a). Effects of increasing temperature on antioxidant defense system and oxidative stress parameters in the Antarctic fish *Notothenia coriiceps* and *Notothenia rossii*. *J. Therm. Biol.* 68, 110–118. doi: 10.1016/j.jtherbio.2017.02.016

Klein, R. D., Rosa, C. E., Colares, E. P., Robaldo, R. B., Martinez, P. E., and Bianchini, A. (2017b). Antioxidant defense system and oxidative status in Antarctic fishes: the sluggish rockcod *Notothenia coriiceps* versus the active marbled notothen *Notothenia rossii*. *J. Therm. Biol.* 68, 119–127. doi: 10.1016/j.jtherbio.2017.02.013

Krueger, T., Hawkins, T. D., Becker, S., Pontasch, S., Dove, S., Hoegh-Guldberg, O., et al. (2015). Differential coral bleaching—contrasting the activity and response of enzymatic antioxidants in symbiotic partners under thermal stress. *Comp. Biochem. Phys.* 190, 15–25. doi: 10.1016/j.cbpa.2015.08.012

Kuhl, M., Cohen, Y., Dalsgaard, T., Jorgensen, B. B., and Revsbech, N. P. (1995). Microenvironment and photosynthesis of zooxanthellae in scleractinian corals studied with microsensors for O2, pH and light. *Mar. Ecol. Prog. Ser.* 117, 159–172. doi: 10.3354/meps117159

Leary, S. C., Winge, D. R., and Cobine, P. A. (2009). "Pulling the plug" on cellular copper: the role of mitochondria in copper export. *Biochim. Biophys. Acta* 1793, 146–153. doi: 10.1016/j.bbamcr.2008.05.002

Lesser, M. P. (1997). Oxidative stress causes coral bleaching during exposure to elevated temperatures. *Coral Reefs* 16, 187–192. doi: 10.1007/s003380050073

Lesser, M. P. (2006). Oxidative stress in marine environments: biochemistry and physiological ecology. *Annu. Rev. Physiol.* 68, 253–278. doi: 10.1146/annurev.physiol.68.040104.110001

Lesser, M. P., Stochaj, W. R., Tapley, D. W., and Shick, J. M. (1990). Bleaching in coral reef anthozoans: effects of irradiance, ultraviolet radiation, and temperature on the activities of protective enzymes against active oxygen. *Coral Reefs* 8, 225–232. doi: 10.1007/bf00265015

Maher, P. (2005). The effects of stress and aging on glutathione metabolism. *Ageing Res. Rev.* 4, 288–314. doi: 10.1016/j.arr.2005.02.005

Maher, P. (2018). Potentiation of glutathione loss and nerve cell death by the transition metals iron and copper: implications for age-related neurodegenerative diseases. *Free Radic. Biol. Med.* 115, 92–104. doi: 10.1016/j.freeradbiomed.2017.11.015

Marangoni, L. F. B., Dalmolin, C., Marques, J. A., Klein, R. D., Abrantes, D., Pereira, C. M., et al. (2019a). Oxidative stress biomarkers as potential tools in reef degradation monitoring: a study case in a South Atlantic reef under influence of the 2015-2016 El Niño/southern oscillation (ENSO). *Ecol. Indic.* 106:105533. doi: 10.1016/j.ecolind.2019.105533

Marangoni, L. F. B., Marques, J. A., Duarte, G. A. S., Pereira, C. M., Calderon, E. N., Castro, C. B., et al. (2017). Copper effects on biomarkers associated with photosynthesis, oxidative status and calcification in the Brazilian coral *Mussismilia harttii* (Scleractinia, Mussidae). *Mar. Environ. Res.* 130, 248–257. doi: 10.1016/j.marenvres.2017.08.002

Marangoni, L. F. B., Mies, M., Guth, A. Z., Banha, T. N. S., Inague, A., Fonseca, J. S., et al. (2019b). Peroxynitrite generation and increased heterotrophic capacity are linked to the disruption of the coral-Dinoflagellate symbiosis in a scleractinian and hydrocoral species. *Microorganisms* 7:426. doi: 10.3390/microorganisms7100426

Maria, V. L., and Bebianno, M. J. (2011). Antioxidant and lipid peroxidation responses in *Mytilusgallo provincialis* exposed to mixtures of benzo(a)pyrene and copper. *Comp. Biochem. Phys.* 154, 56–63. doi: 10.1016/j.cbpc.2011.02.004

Marques, J. A., Costa, P. G., Marangoni, L. F., Pereira, C. M., Abrantes, D. P., Calderon, E. N., et al. (2019). Environmental health in southwestern Atlantic coral reefs: geochemical, water quality and ecological indicators. *Sci. Total Environ.* 651, 261–270. doi: 10.1016/j.scitotenv.2018.09.154

McCord, J. M., and Fridovich, I. (1969). Superoxide dismutase: an enzymatic function for erythocuprein (hemocuprein). *J. Biol. Chem.* 244, 6049–6055. doi: 10.1016/S0021-9258(18)63504-5

McWilliams, J. P., Cote, I. M., Gill, J. A., Sutherland, W. J., and Watkinson, A. R. (2005). Acceler-ating impacts of temperature-induced coral bleaching in the Caribbean. *Ecology* 86, 2055–2060. doi: 10.1890/04-1657

Mercer, J. F., and Llanos, R. M. (2003). Molecular and cellular aspects of copper transport in developing mammals. *J. Nutr.* 133, 1481S–1484S. doi: 10.1093/jn/133.5.1481S

Mies, M., Francini-filho, R. B., Zilberberg, C., Garrido, A. G., Longo, G. O., Laurentino, E., et al. (2020). South Atlantic coral reefs are major global warming refugia and less susceptible to bleaching. *Front. Mar. Sci.* 7:514. doi: 10.3389/fmars.2020.00514

Mitchelmore, C. L., Verde, E. A., and Weis, V. M. (2007). Uptake and partitioning of copper and cadmium in the coral *Pocillopora damicornis*. *Aquat. Toxicol.* 85, 48–56. doi: 10.1016/j.aquatox.2007.07.015

Monteiro, D. A., Almeida, J. A., Rantin, F. T., and Kalinin, A. L. (2006). Oxidative stress biomarkers in the freshwater characid fish, *Brycon cephalus*, exposed to organophosphorus insecticide Folisuper 600 (methyl parathion). *Comp. Biochem. Phys.* 143, 141–149. doi: 10.1016/j.cbpc.2006.01.004

Nadella, S. D., Fitzpatrick, J. L., Franklin, N., Bucking, C., Smith, S., and Wood, C. M. (2009). Toxicity of dissolved cu, Zn, Ni and cd to developing embryos of the blue mussel (*Mytilus trossolus*) and the protective effect of dissolved organic carbon. *Comp. Biochem. Phys.* 149, 340–348. doi: 10.1016/j.cbpc.2008.09.001

Nagalakshmi, N., and Prasad, M. N. V. (2001). Responses of glutathione cycle enzymes and glutathione metabolism to copper stress in *Scenedesmus bijugatus*. *Plant Sci.* 160, 291–299. doi: 10.1016/s0168-9452(00)00392-7

Negri, A. P., and Hoogenboom, M. O. (2011). Water contamination reduces the tolerance of coral larvae to thermal stress. *PLoS One* 6:e19703. doi: 10.1371/journal.pone.0019703

Perez, S., and Weis, V. (2006). Nitric oxide and cnidarian bleaching: an eviction notice mediates breakdown of a symbiosis. *J. Exp. Biol.* 209, 2804–2810. doi: 10.1242/jeb.02309

Portner, H. O. (2001). Climate change and temperature dependent biogeography: oxygen limitation of thermal tolerance in animals. *Naturwissenschaften* 88, 137–146. doi: 10.1007/s001140100216

Portner, H. O. (2002). Climate variations and the physiological basis of temperature dependent biogeography: systemic to molecular hierarchy of thermal tolerance in animals. *Comp. Biochem. Phys.* 132, 739–761. doi: 10.1007/s001140100216

Pourahmad, J., and O'Brien, P. J. (2000). A comparison of hepatocyte cytotoxic mechanisms for Cu^{2+} and Cd^{2+}. *Toxicology* 143, 263–273. doi: 10.1016/s0300-483x(99)00178-x

Rainbow, P. S. (2002). Trace metal concentrations in aquatic invertebrates: why and so what? *Environ. Pollut.* 120, 497–507. doi: 10.1016/s0269-7491(02)00238-5

Ralph, P. J., Gademann, R., and Larkum, A. W. (2001). Zooxanthellae expelled from bleached corals at 33 °C are photosynthetically competent. *Mar. Ecol. Prog. Ser.* 220, 163–168. doi: 10.3354/MEPS220163

Regoli, F., and Giuliani, M. E. (2014). Oxidative pathways of chemical toxicity and oxidative stress biomarkers in marine organisms. *Mar. Environ. Res.* 93, 106–117. doi: 10.1016/j.marenvres.2013.07.006

Schwarz, J. A., Mitchelmore, C. L., Jones, R., O'dea, A., and Seymour, S. (2013). Exposure to copper induces oxidative and stress responses and DNA damage in the coral *Montastraea franksi*. *Comp. Biochem. Phys.* 157, 272–279. doi: 10.1016/j.cbpc.2012.12.003

Smith, D. J., Suggett, D. J., and Baker, N. R. (2005). Is photoinhibition of zooxanthellae photosynthesis the primary cause of thermal bleaching in corals? *Glob. Change Biol.* 11, 1–11. doi: 10.1111/j.1529-8817.2003.00895.x

Suggett, D. J., and Smith, D. J. (2019). Coral bleaching patterns are the outcome of complex biological and environmental networking. *Glob. Change Biol.* 26, 68–79. doi: 10.1111/gcb.14871

Townsend, D. M., Tew, K. D., and Tapiero, H. (2003). The importance of glutathione in human disease. *Biomed. Pharmacother.* 57, 145–155. doi: 10.1016/s0753-3322(03)00043-x

van Dam, J. W., Negri, A. P., Uthicke, S., and Mueller, J. F. (2011). "Chemical pollution on coral reefs: exposure and ecological effects," in *Ecological Impacts of Toxic Chemicals*. eds. F. Sánchez-Bayo, P. J. Brink and R. M. Mann (Amsterdam: Bentham Science Publishers).

Weis, V. M. (2008). Cellular mechanisms of cnidarian bleaching: stress causes the collapse of symbiosis. *J. Exp. Biol.* 211, 3059–3066. doi: 10.1242/jeb.009597

White, C. C., Viernes, H., Krejsa, C. M., Botta, D., and Kavanagh, T. J. (2003). Fluorescence based microtiter plate assay for glutamate-cysteine ligase activity. *Anal. Biochem.* 318, 175–180. doi: 10.1016/s0003-2697(03)00143-x

Wink, D. A., and Mitchell, J. B. (1998). Chemical biology of nitric oxide: insights into regulatory, cytotoxic, and cytoprotective mechanisms of nitric oxide. *Free Radic. Biol. Med.* 25, 434–456. doi: 10.1016/s0891-5849(98)00092-6

Yakovleva, I. M., Baird, A. H., Yamamoto, H. H., Bhagooli, R., Nonaka, M., and Hidaka, M. (2009). Algal symbionts increase oxidative damage and death in coral larvae at high temperatures. *Mar. Ecol. Prog. Ser.* 378, 105–112. doi: 10.3354/meps07857

Yuyama, I., Ito, Y., Watanabe, T., Hidaka, M., Suzuki, Y., and Nishida, M. (2012). Differential gene expression in juvenile polyps of the coral *Acropora tenuis* exposed to thermal and chemical stresses. *J. Exp. Mar. Biol. Ecol.* 430-431, 17–24. doi: 10.1016/j.jembe.2012.06.020

Conflict of Interest: The authors declare that the research was conducted in the absence of any commercial or financial relationships that could be construed as a potential conflict of interest.

frontiers in Marine Science

ORIGINAL RESEARCH
published: 24 December 2021
doi: 10.3389/fmars.2021.754808

Differential Affinities of a *Pocillopora damicornis* Galectin to Five Genera of Symbiodiniaceae at Different Temperatures

Xingjuan Wang[1,2], Zhongjie Wu[3], Yibo Wu[1,2], Mingxun An[1,2], Zhi Zhou[1,2]* and Senjie Lin[4]*

[1] State Key Laboratory of Marine Resource Utilization in South China Sea, Hainan Aquaculture Breeding Engineering Research Center, Hainan University, Haikou, China, [2] Hainan Provincial Key Laboratory for Tropical Hydrobiology and Biotechnology, Department of Marine Sciences, College of Marine Science, Hainan University, Haikou, China, [3] Hainan Academy of Ocean and Fisheries Sciences, Haikou, China, [4] Department of Marine Sciences, University of Connecticut, Groton, CT, United States

The symbiosis of coral-Symbiodiniaceae is the quintessential basis of the coral reef ecosystem, and its breakdown results in coral bleaching, one of the most severe ecological catastrophes in the ocean. Critical to the establishment of the symbiosis is the host's specific recognition of the symbionts through the binding of the coral host's pattern recognition receptors (PRRs) to the symbiont cell surface's glycoconjugates. However, the molecular basis for this recognition process is poorly understood. The present study investigated the binding affinities of the coral galectin PdGLT-1 to different symbiodiniacean species under different temperatures. At 25°C, the PdGLT-1 recombinant protein (rPdGLT-1) exhibited different binding affinities to different symbiodiniacean species from five genera, with a significantly higher binding affinity ($p < 0.05$) to *Fugacium kawagutii* (2.6-fold) and *Cladocopium goreaui* (1.9-fold) than *Symbiodinium microadriaticum*. The binding topology of rPdGLT-1 differed among the five symbiodiniacean species; for *S. microadriaticum*, *Breviolum minutum,* and *Durusdinium trenchii*, the binding was on some specific sites on the cell surface, whereas for *C. goreaui* and *F. kawagutii,* the binding signals were detected over the whole cell surface. Interestingly, PdGLT-1 binding induced agglutination of *F. kawagutii* cells but not of *C. goreaui*, explaining why *C. goreaui* was the most dominant symbiodiniacean symbionts in corals. Moreover, the affinity of rPdGLT-1 to Symbiodiniaceae was affected by temperature, and the highest binding affinities were observed at 30, 20, 30, 35, and 30°C for *S. microadriaticum*, *B. minutum*, *C. goreaui*, *D. trenchii*, and *F. kawagutii*, respectively. The optimal binding temperatures were consistent with the current understanding that *D. trenchii* was the most thermal resistant among these species. These results suggest that the binding affinity of the PRR PdGLT-1 may determine the specificity of host-symbiont pairing and explain why *Cladocopium* is the dominant symbionts of coral *P. damicornis* at normal temperature, and corals with *Durusdinium* symbionts may survive better at high temperature.

Keywords: scleractinian coral, symbiosis establishment, Symbiodiniaceae, heat stress, galectin

OPEN ACCESS

Edited by:
Ranjeet Bhagooli,
University of Mauritius, Mauritius

Reviewed by:
Beatriz Casareto,
Shizuoka University, Japan
Walter Dellisanti,
Hong Kong Polytechnic University,
Hong Kong SAR, China

****Correspondence:***
Zhongjie Wu
wuzj@hnhky.cn
Zhi Zhou
zhouzhi@hainanu.edu.cn

Specialty section:
This article was submitted to Aquatic Physiology, a section of the journal Frontiers in Marine Science

Received: *07 August 2021*
Accepted: *06 December 2021*
Published: *24 December 2021*

Citation:
Wang X, Wu Z, Wu Y, An M, Zhou Z and Lin S (2021) Differential Affinities of a Pocillopora damicornis Galectin to Five Genera of Symbiodiniaceae at Different Temperatures. Front. Mar. Sci. 8:754808. doi: 10.3389/fmars.2021.754808

INTRODUCTION

Due to the unrelentless global warming, coral reefs are facing the danger of massive bleaching predicted for the end of this century (Hoegh-Guldberg et al., 2007; Magel et al., 2019; Weis, 2019). Thus, there is an urgent need to preserve the remaining reefs and help restore the lost or degraded ones. The establishment and maintenance of coral-Symbiodiniaceae symbiosis are of vital importance for the coral holobiont functioning, which is initiated by the chemical recognition between the coral host and the Symbiodiniaceae (Berkelmans and van Oppen, 2006; Iguchi et al., 2011; Bellantuono et al., 2012; Kita et al., 2015). The cell surface of Symbiodiniaceae is populated with glycoconjugates, such as mannose-mannose and galactose-β(1-4)-N-acetylglucosamine (Markell et al., 1992; Tortorelli et al., 2021). These glycoconjugates, which form the microbe-associated molecular patterns (MAMPs), can be recognized by the pattern recognition receptors (PRRs) such as lectins on the surface of coral cells (Wood-Charlson et al., 2006; Weis et al., 2008). Such glycan-lectin interaction is critical for initiating the coral-Symbiodiniaceae symbiosis (Tortorelli et al., 2021). The adaptive evolution of the symbiont's glycan structure and the biochemical complementarity between the coral host and its symbionts are believed to determine the host specificity (Lin et al., 2015). For example, it has been shown that glycan ligands on the cell surface of *Cladocopium* C1f play a role in recognition during the initial contact at the onset of symbiosis with the coral *Fungia scutaria* larvae (Rodriguez-Lanetty et al., 2004; Wood-Charlson et al., 2006). Lectins in *Sinularia lochmodes* and *Acropora millepora* (Millectin) can recognize Symbiodiniaceae through the binding to their D-galactose and mannose (Kvennefors et al., 2008; Jimbo et al., 2013). Also, the recognition of coral host lectin induces the morphological transformation of *Symbiodinium* (Fransolet et al., 2012). Lectin in the coral *Ctenactis echinata* mediates the transformation of the flagellated motile form of Symbiodiniaceae into the non-motile coccoid form (Jimbo et al., 2010), a common form of coral symbionts. However, the molecular mechanisms and factors affecting the establishment and maintenance of the symbiosis between corals and Symbiodiniaceae are still poorly understood.

How lectins' binding affinity to symbiont's MAMPs differ among different species of Symbiodiniaceae is a fundamental question, and the answer can help address how the host corals selectively recruit symbionts from the surrounding environments. The symbiotic dinoflagellate algae in the family Symbiodiniaceae includes nine Clades named A-I (Pochon and Gates, 2010; LaJeunesse et al., 2018; Gonzalez-Pech et al., 2021). Out of the nine clades, *Symbiodinium* (Clade A) to *Durusdinium* (Clade D) are generally associated with the reef-building corals (Baker, 2003; Traylor-Knowles, 2021). Usually, there is one dominant species of Symbiodiniaceae in a host, which shapes the physiological performance of the corals under environmental stress (Silverstein et al., 2012). For instance, Clade D (*Durusdinium*) has been reported as a thermally tolerant symbionts. The thermal tolerance of coral *Acropora millepora* increases by 1–1.5°C when the dominant Clade C symbiont (*Cladocopium*) is replaced by Clade D (Berkelmans and van Oppen, 2006). Thus, to better protect or restore coral reefs under increasing seawater temperature, there is an urgent need to screen for the most heat-resistant coral-Symbiodiniaceae association, which requires a good understanding of the recognition process mediated by coral lectins.

Another critical issue is how environmental variables affect the establishment of the coral-Symbiodiniaceae symbiosis (Stat and Gates, 2011; Suggett and Smith, 2020). Seawater temperature, eutrophication, ocean acidification, and microplastic pollution are the most common factors affecting the health of corals (Hughes et al., 2003; Sully et al., 2019; Barott et al., 2021), among which heat stress is the most severe stressor. Recent studies have implicated lectins in the establishment of coral-Symbiodiniaceae symbiosis under heat stress. For instance, the C-type lectin from *P. damicornis* was found to be critical for the symbiont acquisition and sequestration under heat stress (Vidal-Dupiol et al., 2009). Furthermore, the galectin in *P. damicornis* (PdGLT-1) was shown to recognize both pathogenic bacteria and Symbiodiniaceae, and its binding activity was dramatically suppressed by high temperatures (>30°C) (Wu et al., 2019). However, how the binding activities of coral lectins to different genera of Symbiodiniaceae differ under heat stress has never been reported.

This study investigated the binding affinity of a previously identified coral lectin (PdGLT-1) (Wu et al., 2019) to five species from different major genera of the family Symbiodiniaceae. PdGLT-1 was a galectin from *P. damicornis*, a scleractinian coral belonging to Pocilloporidae, one of the most abundant and widespread corals (Schuttenberg and Hoegh-Guldberg, 2007). The five species of Symbiodiniaceae were *Symbiodinium microadriaticum* (Clade A), *Breviolum minutum* (Clade B), *Cladocopium goreaui* (Clade C), *Durusdinium trenchii* (Clade D), and *Fugacium kawagutii* (Clade F), which belong to the symbiont genera in *P. damicornis* (Cunning et al., 2018; Tang et al., 2018; Lin et al., 2019; Chankong et al., 2020; Li et al., 2021). The binding affinity of PdGLT-1 to these symbiodiniacean species was examined under a gradient of temperatures. Results in this study help us better understand the molecular mechanism underlying the initial establishment of the coral-Symbiodiniaceae symbiosis and lectins' potential roles in coral survival or recovery after a heat stress-induced bleaching event.

MATERIALS AND METHODS

Cultures of Symbiodiniacean Species

The five symbiodiniacean species, *S. microadriaticum* strain CCMP828, *B. minutum* strain CCMP830, *C. goreaui* strain CCMP2466, *D. trenchii* strain CCMP3428, and *F. kawagutii* strain CCMP2468, were provided by the National Center for Marine Algae and Microbiota (Bigelow Laboratory for Ocean Sciences, East Boothbay, Maine, United States). These strains were cultured in the L1 medium at 25°C in a light incubator (photon flux of 110 μmol photons m^{-2} s^{-1}) at 12 h/12 h light-dark cycle until logarithmic growth stage.

Preparation of PdGLT-1 Recombinant Protein and Determination of Binding Affinity of PdGLT-1 Recombinant Protein to Symbiodiniaceae

The expression and purification of the recombinant PdGLT-1 protein were carried out as previously reported (Wu et al., 2019). Briefly, the coding gene was isolated from *P. damicornis* and inserted in-frame into an expression plasmid to yield the recombinant construct PdGLT-1 (*pEASY*-E1-PdGLT-1), which was transformed into *E. coli* BL21 (DE3)-Transetta (TransGen, China). Positive transformants were screened using antibiotic resistance and sequencing, and one of them was selected and grown in the LB medium. The recombinant protein (designated rPdGLT-1) with 6 × His-tag was purified by a Ni^{2+} chelating Sepharose column (GE Healthcare).

In each binding affinity experiment, cells from the five symbiodiniacean species were harvested from 1 mL cultures by centrifugation at 5,000 *g* for 5 min at 4°C. The cell pellets were suspended in fresh medium and serially diluted to 10^5, 10^4, 10^3, 10^2, and 10 cells mL^{-1}. From each of these cell suspensions, 300 μL of cell suspension was transferred to a fresh 1.5 mL microfuge tube and co-incubated with 300 μL of 0.1 mg mL^{-1} rPdGLT-1 at 25°C for 1 h. For the negative control, bovine serum albumin (BSA) was used in place of rPdGLT-1 to be co-incubated with each symbiodiniacean species. After incubation, the algal cells were pelleted by centrifugation at 1,600 *g* for 6 min to eliminate the unbound proteins. After washing with PBST three times to remove the non-specifically binding rPdGLT-1, the cells were pelleted and resuspended in PBS.

In order to compare the binding affinity of rPdGLT-1 to different symbiodiniacean species, 300 μL of algal cells (10^4 cells) for each species were co-incubated with 300 μL of 0.2 mg mL^{-1} rPdGLT-1 at 25°C for 1 h. For the negative control, BSA was used in co-incubation with an even mixture of five symbiodiniacean species. The washing and resuspension were conducted as mentioned above.

The bound rPdGLT-1 on the symbiodiniacean cell surface was dissociated in 50 μL loading buffer by boiling and the resulting protein solution was loaded to a SDS-PAGE gel. A blank control was set up using the loading buffer. After electrophoretic separation, the target protein was transferred to the PVDF membrane at 200 mA for 1.5 h. After blocked for 2 h at 25°C, PVDF membrane was incubated with His-tag mouse monoclonal antibody (1:1,000 dilution, AH367, Beyotime, China) at 4°C overnight, and then incubated with AP-labeled goat-anti-mouse antibody (1:5,000 dilution, A0258, Beyotime, China) at 25°C for 2 h. After each combination, the membrane was washed three times with PBST on a concentrator for 10 min, and the membrane was subjected to processing with BCIP/NBT Alkaline Phosphatase Color Development Kit (C3206, Beyotime, China) at 25°C for 5–30 min until clear bands were observed. The reaction was terminated by adding distilled water to the PVDF membrane, and each band's optical density was measured using image processing software Image J (1.53c). In the comparison experiment of different symbiodiniacean species, incubation and western blotting were repeated three times ($N = 3$). The binding activity of rPdGLT-1 to a symbiodiniacean species was defined as the band intensity ratio of that species to *S. microadriaticum*.

Observation of Binding Site Topology of PdGLT-1 Recombinant Protein on Symbiodiniacean Cells

The binding area of rPdGLT-1 on the five symbiodiniacean species was observed using the immunofluorescence method. In brief, 10^5 algal cells from each species were resuspended in 200 μL of PBS. They were incubated with 200 μL of 0.1 mg mL^{-1} rPdGLT-1 at 25°C for 1 h. For negative and blank controls, BSA and PBS were used in place of rPdGLT-1, respectively. After incubation, the algae were washed by PBST three times and then centrifuged at 4,000 *g* for 5 min to eliminate the unbound protein. Twenty microliters of His-tag mouse monoclonal antibody (AH367, Beyotime, China) diluted at 1:200 was added to resuspend the algal cell pellets. After incubation at 25°C for 1 h and centrifugation at 1,600 *g* for 6 min, algal cells were washed three times with PBST. Next, algal cells were incubated with 20 μL of Alexa Fluor 488-labeled Goat Anti-Mouse IgG(H + L) diluted at 1:200 (A0428, Beyotime, China) in darkness at 25°C for 1 h. After triple washes with PBST, the algal cells were collected by centrifugation, resuspended in 20 μL of PBS, and observed under the IX71 Olympus fluorescence microscope.

Measurement of the Binding Activity of PdGLT-1 Recombinant Protein Under Different Temperatures

The binding activity of rPdGLT-1 to the five symbiodiniacean species was examined at the temperatures of 20, 25, 30, and 35°C. Briefly, each symbiodiniacean species from stock culture was split into 4 subsamples, and then 300 μL of 10^5 cells mL^{-1} of each symbiodiniacean species were incubated with 300 μL of 0.1 mg mL^{-1} rPdGLT-1 for 1 h at 20, 25, 30, and 35°C. For the negative control, BSA was used instead of rPdGLT-1. Each incubation was conducted in triplicate, and the subsequent SDS-PAGE and western blotting were performed as mentioned above. Loading buffer was used as the blank control. The band intensity of the incubation at a temperature was normalized to that of the incubation at 20°C.

Statistical Analysis

All data were expressed as mean ± standard deviation (SD). Before analysis, data were tested for normality using the Shapiro-Wilk test. When the variance was verified to be homogeneous, data were subjected to one-way analysis of variance (ANOVA) followed by multiple comparisons (S-N-K) to evaluate the significance of differences among different symbiodiniacean species or temperatures by using software IBM SPSS 20.0 (IBM, Inc.). Differences were considered significant at $p < 0.05$.

RESULTS

Comparison of Binding Affinity of PdGLT-1 Recombinant Protein Among Symbiodiniacean Species

A binding band was observed for each of the five symbiodiniacean species examined at 25°C, and the band intensity increased with increasing algal concentration from 10 to 10^5 cells mL^{-1}, especially for *B. minutum* and *D. trenchii* (**Figure 1**). The highest relative band intensity (2.6-fold) was observed in *F. kawagutii*, which exhibited a significantly higher binding affinity than other symbiodiniacean species (one-way ANOVA, $F = 22.841$, $p < 0.05$). *C. goreaui* exhibited the second highest band intensity, 1.9-fold higher than that of *S. microadriaticum*, and 1.4-fold higher than that of *D. trenchii* ($p < 0.05$ in both cases). No significant difference was found among *S. microadriaticum*, *B. minutum,* and *D. trenchii*. There were no detectable bands in the negative or blank control (**Figure 2**).

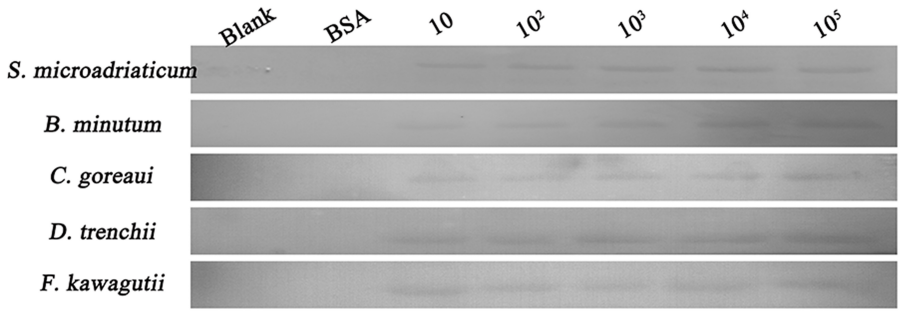

FIGURE 1 | Binding activity of PdGLT-1 recombinant protein to five symbiodiniacean species of different concentrations (10, 10^2, 10^3, 10^4, and 10^5 cells mL^{-1}) at 25°C, including *S. microadriaticum*, *B. minutum*, *C. goreaui*, *D. trenchii, and F. kawagutii.* BSA (bovine serum albumin) is employed as the negative control, while loading buffer is used as blank control.

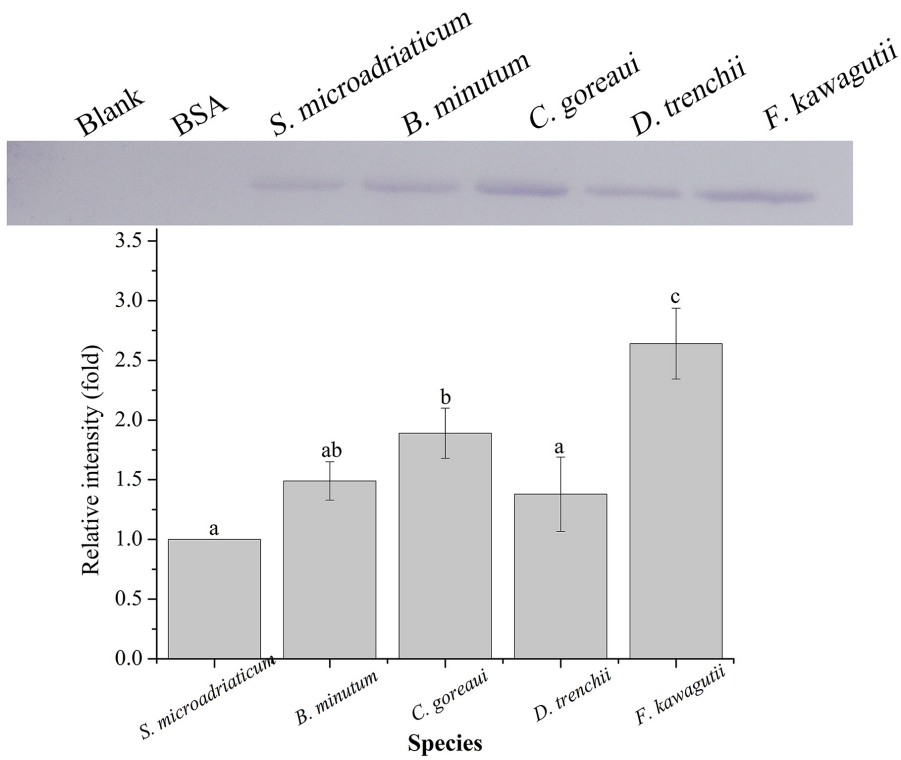

FIGURE 2 | Binding of PdGLT-1 recombinant protein to *S. microadriaticum*, *B. minutum*, *C. goreaui*, *D. trenchii,* and *F. kawagutii* at 25°C. The figure above shows the binding band obtained by western blotting, and the figure below shows the gray scale ratio. The gray scale of the binding band of *S. microadriaticum* is used as the basis to calculate the gray scale ratio. The column represents mean ± standard deviation ($N = 3$), and the column with different letters represents significant difference ($p < 0.05$).

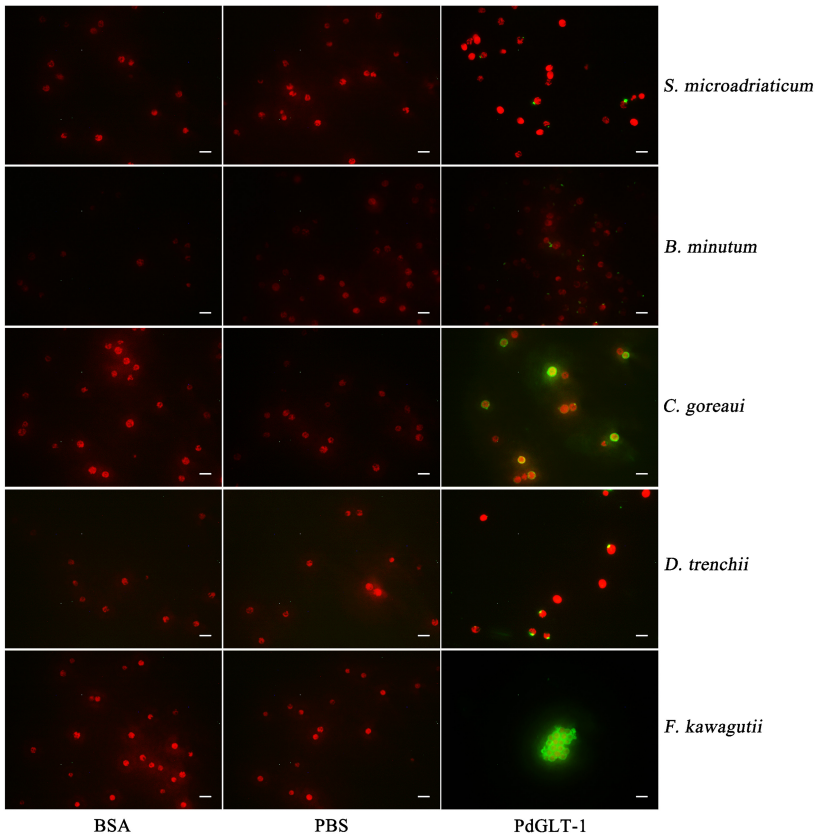

FIGURE 3 | The binding region of rPdGLT-1 to *S. microadriaticum*, *B. minutum*, *C. goreaui*, *D. trenchii,* and *F. kawagutii* at 25°C through immunofluorescence method. His-tag mouse monoclonal antibody and Alexa Fluor 488-labeled Goat Anti-Mouse IgG(H + L) are used as primary and second antibodies, respectively. BSA is employed as negative control and PBS as blank control. Scale-bars are 20 μm.

PdGLT-1 Recombinant Protein Binding Site Topology on Symbiodiniacean Cells

For *C. goreaui* and *F. kawagutii*, clear positive signals were widespread over the whole cell surface, and rPdGLT-1 bound *F. kawagutii* cells were agglutinated. In contrast, the positive signals were concentrated in smaller discrete regions on the cell surface of *S. microadriaticum*, *B. minutum,* and *D. trenchii*. No positive signals were observed in the negative (BSA) and blank (PBS) control (**Figure 3**).

Effects of Temperature on the Binding Affinity of PdGLT-1 Recombinant Protein

The relative band intensity of rPdGLT-1 bound to *D. trenchii* was highest at 35°C (1.5-fold), which was significantly higher than that at 30°C (1.4-fold; one-way ANOVA, $F = 38.712$, $p < 0.05$). The lowest intensities occurred at 20 and 25°C (1.0-fold, 1.0-fold, respectively), which were significantly lower ($p < 0.05$) than that at 30°C (**Figure 4**). The relative band intensity of rPdGLT-1 to *S. microadriaticum* was highest at 30°C (1.8-fold), slightly lower at 35°C (1.7-fold). The relative band intensities at 20 and 25°C were markedly lower, between which that at 25°C was significantly higher (1.4-fold; one-way ANOVA, $F = 44.272$, $p < 0.05$) than that at 20°C (**Figure 5**). Similar to *S. microadriaticum*, the highest band intensity of *C. goreaui*-bound rPdGLT-1 was detected at 30°C, which was 1.3-fold of that at 20°C, and significantly higher (one-way ANOVA, $F = 9.062$, $p < 0.05$) than those at 20, 25, and 35°C (1.1- and 1.0-fold; **Figure 6**). The highest relative band intensity of rPdGLT-1 bound to *F. kawagutii* also occurred at 30°C (1.5-fold), which was higher than that at 20°C (one-way ANOVA, $F = 5.183$, $p < 0.05$). The relative band intensities at 25 and 35°C (1.2- and 1.3-fold, respectively) were between that at 20 and 30°C, with no significant differences (**Figure 7**). In contrast, the highest relative band intensity of rPdGLT-1 bound to *B. minutum* was observed at 20°C, the lowest temperature among the five species examined. It was significantly higher than those at 25 and 35°C (one-way ANOVA, $F = 4.555$, $p < 0.05$). Furthermore, the band intensity at 30°C (0.8-fold) appeared to be higher than those at 25 and 35°C, but there were no significant differences among the three temperatures (**Figure 8**).

DISCUSSION

The establishment of the coral-Symbiodiniaceae symbiosis is essential to the prosperity of the coral reef ecosystem (Wood-Charlson et al., 2006). Recognition between corals and

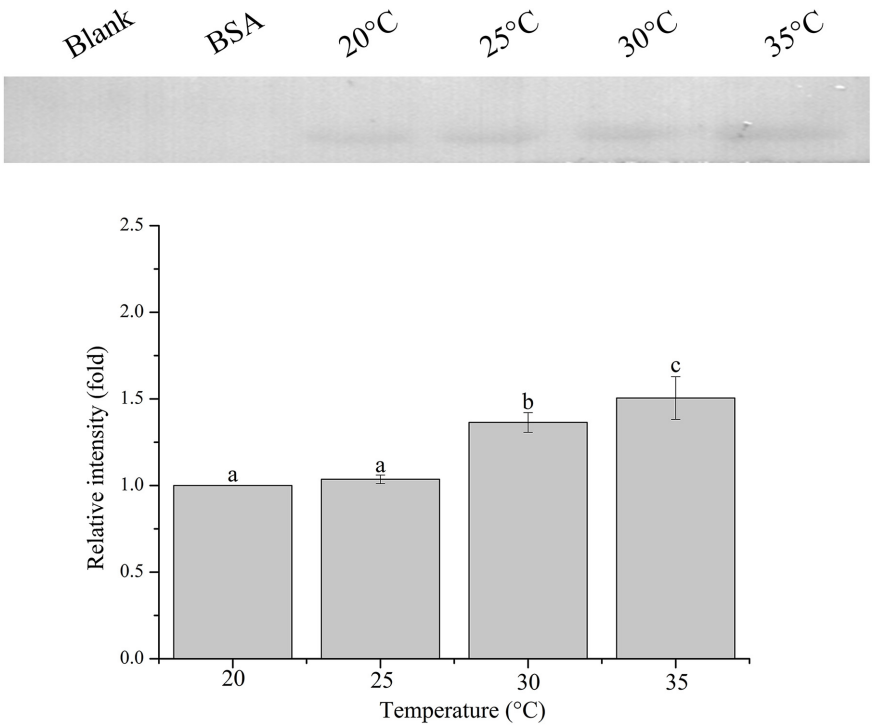

FIGURE 4 | Binding of PdGLT-1 recombinant protein to *D. trenchii* at different temperatures. The figure above shows the binding band obtained by western blotting, and the figure below shows the gray ratio. The gray scale of the binding band of 20°C is used as the basis to calculate the gray scale ratio. The column represents mean ± standard deviation ($N = 3$), and the column with different letters represents significant difference ($p < 0.05$).

Symbiodiniaceae is the very first and critical step, which requires the involvement of corals' lectins such as C-type lectins, galectins, rhamnose-binding lectins, and D-Galactose-binding lectins (Zhou et al., 2017, 2018; Weis, 2019; Wu et al., 2019). Besides, the binding of lectins to Symbiodiniaceae can be affected by temperature (Vidal-Dupiol et al., 2009; Bellantuono et al., 2012; Wu et al., 2019), and high temperature might decrease the binding affinity of coral lectins and further suppress their abilities to acquire and sequestrate the free Symbiodiniaceae to repopulate the bleached coral (Vidal-Dupiol et al., 2009). Therefore, information on the differential binding affinity of coral lectins to different genera of Symbiodiniaceae, and the differential effects of temperature on the binding capacity, is essential to understanding the underlying regulatory mechanism for the initial establishment of coral-Symbiodiniaceae symbiosis.

In the present study, a previously identified lectin (PdGLT-1) was expressed in *E. coli,* purified, and used to investigate the recognition of the coral *P. damicornis* to five species of Symbiodiniaceae. The results showed that rPdGLT-1 could bind to all five species of Symbiodiniaceae. Recognizable by PdGLT-1, these algae have the potential to establish symbiosis with *P. damicornis*. Consistent with this finding, high throughput sequencing studies on the symbiont communities of *P. damicornis* have indicated the presence of these five genera in this species of coral (Boulotte et al., 2016). Besides, the present study reported the differential binding affinities of PdGLT-1 to different symbiodiniacean species. A higher binding affinity was found to *C. goreaui* and *F. kawagutii* than *S. microadriaticum*, *B. minutum,* and *D. trenchii*. This result agrees with the mainstream academic view that clade C is the dominant Symbiodiniaceae in *P. damicornis* (Magalon et al., 2007).

To further explore the recognition characteristics between PdGLT-1 and Symbiodiniaceae, differences among five species of Symbiodiniaceae in the rPdGLT-1 binding pattern were carefully examined using immunofluorescence. Interestingly, rPdGLT-1 was generally bound to discrete loci on the surface of *S. microadriaticum*, *B. minutum,* and *D. trenchii*, while the binding sites of rPdGLT-1 to *C. goreaui* and *F. kawagutii* were widespread over the cell surface. These results were consistent with the higher binding affinity to *C. goreaui* and *F. kawagutii* measured by Western blotting. Intriguingly, rPdGLT-1 not only exhibited a higher binding affinity to *F. kawagutii* but also had an agglutinating effect (**Figure 2**). This finding suggests that PdGLT-1 is more likely to induce agglutination than endosymbiosis in *F. kawagutii*, which explains why *F. kawagutii* is not a dominant symbiont species in *P. damicornis* or other corals, and its role as an endosymbiont remains obscure. On the contrary, PdGLT-1 had high binding activity to *C. goreaui* but hardly with any agglutination effect. As such PdGLT-1 is more likely to induce symbiosis with *C. goreaui* than agglutination, consistent with the reports that *Cladopodium* spp. are dominant Symbiodiniaceae in *P. damicornis* (Magalon et al., 2007).

Furthermore, the establishment and maintenance of the coral-Symbiodiniaceae symbiosis are strongly influenced by

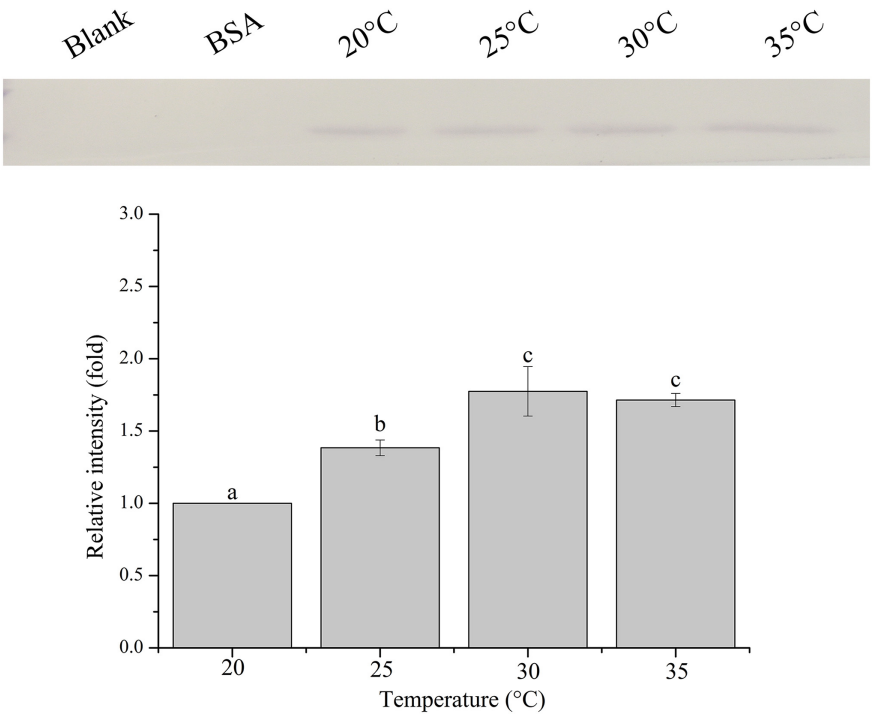

FIGURE 5 | Binding of PdGLT-1 recombinant protein to *S. microadriaticum* at different temperatures. The figure above shows the binding band obtained by western blotting, and the figure below shows the gray ratio. The gray scale of the binding band of 20°C is used as the basis to calculate the gray scale ratio. The column represents mean ± standard deviation ($N = 3$), and the column with different letters represents significant difference ($p < 0.05$).

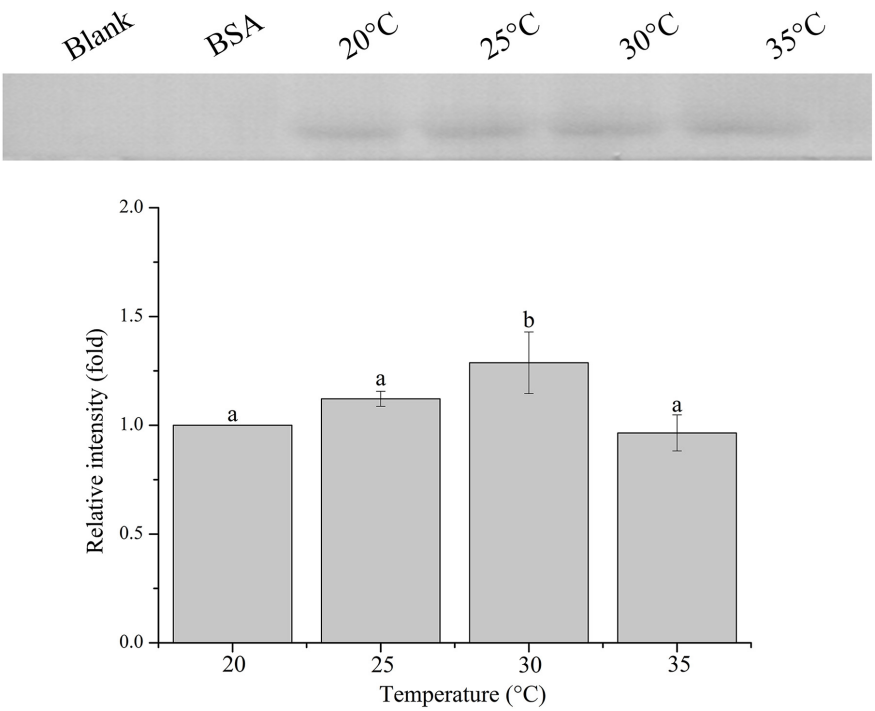

FIGURE 6 | Binding of PdGLT-1 recombinant protein to *C. goreaui* at different temperatures. The figure above shows the binding band obtained by western blotting, and the figure below shows the gray ratio. The gray scale of the binding band of 20°C is used as the basis to calculate the gray scale ratio. The column represents mean ± standard deviation ($N = 3$), and the column with different letters represents significant difference ($p < 0.05$).

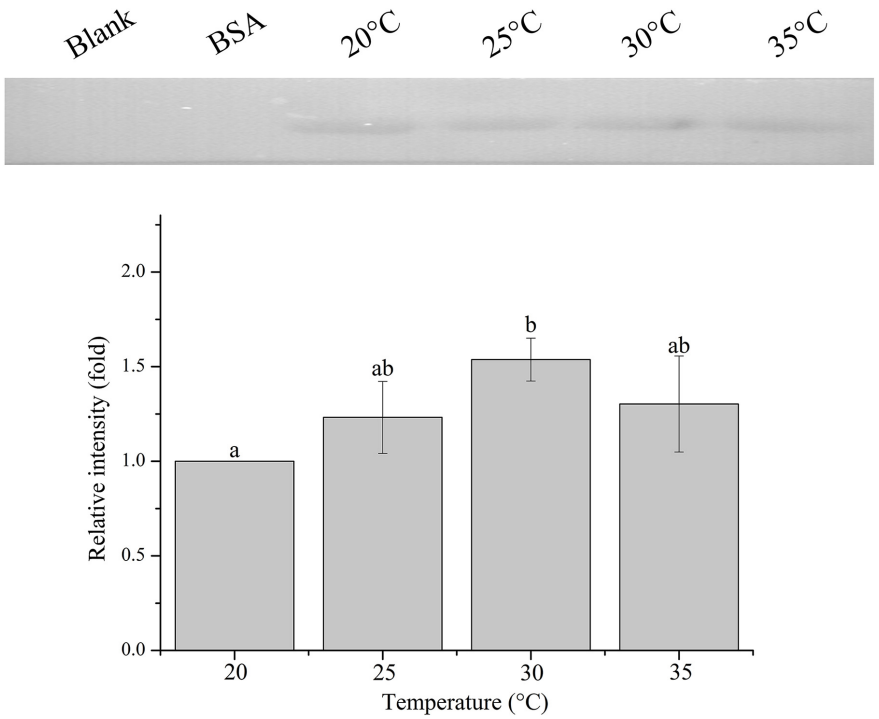

FIGURE 7 | Binding of PdGLT-1 recombinant protein to *F. kawagutii* at different temperatures. The figure above shows the binding band obtained by western blotting, and the figure below shows the gray ratio. The gray scale of the binding band of 20°C is used as the basis to calculate the gray scale ratio. The column represents mean ± standard deviation ($N = 3$), and the column with different letters represents significant difference ($p < 0.05$).

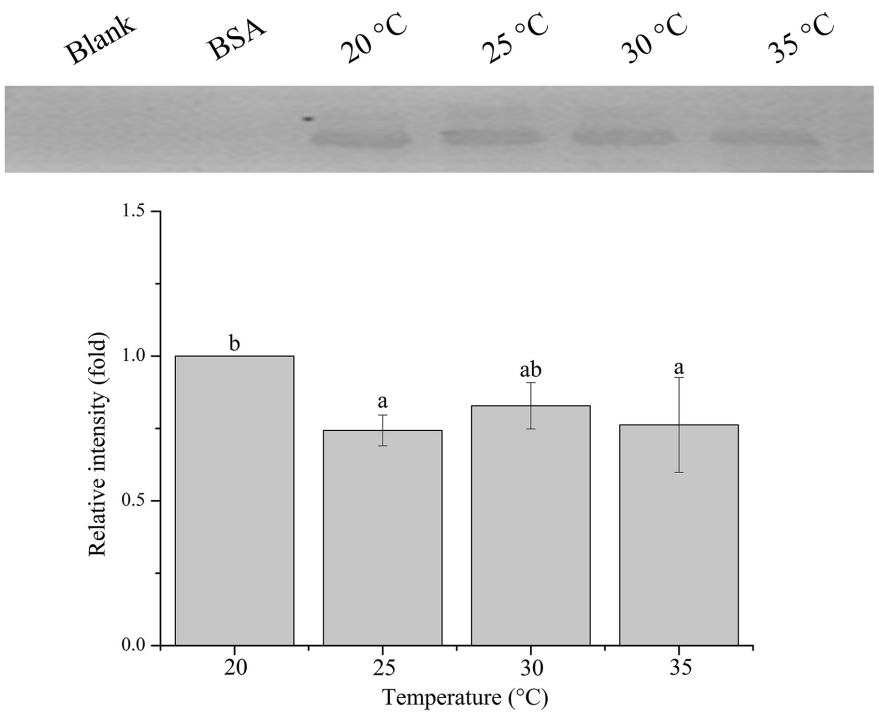

FIGURE 8 | Binding of PdGLT-1 recombinant protein to *B. minutum* at different temperatures. The figure above shows the binding band obtained by western blotting, and the figure below shows the gray ratio. The gray scale of the binding band of 20°C is used as the basis to calculate the gray scale ratio. The column represents mean ± standard deviation ($N = 3$), and the column with different letters represents significant difference ($p < 0.05$).

temperature, the severe coral bleaching in recent years have been attributed to heat stress (Sampayo et al., 2008; Stat and Gates, 2011; Klepac and Barshis, 2020). From the PdGLT-1 binding in five temperature (20, 25, 30, and 35°C) experiments, clear species-specific optimal PdGLT-1 binding temperature was noted. Interestingly, the highest optimal temperature (35°C) was found in *D. trenchii* (Clade D), the second highest (30°C) in *S. microadriaticum* (Clade A), *C. goreaui* (Clade C), and *F. kawagutii* (Clade F), and the lowest (20°C) was found in *B. minutum* (Clade B). These results suggest that coral lectins have variable potentials to acquire and sequestrate Symbiodiniaceae in a temperature-dependent manner. This might affect the differential repopulation of the symbionts in the bleached corals.

Accumulating evidence has indicated that a higher relative abundance of Clade D Symbiodiniaceae in corals contributes to the heat resistance of corals, and Clade D Symbiodiniaceae are regarded as the as most heat-tolerant clade among all Symbiodiniaceae clades (Abrego et al., 2009; Keshavmurthy et al., 2017; Thinesh et al., 2019). Moreover, symbionts type-switching from Clades A, B, C, or F to Clade D following a bleaching event is believed to be the strategy of corals to recover from bleaching (Thinesh et al., 2019). Results in the present study show that the binding affinity of PdGLT-1 to *D. trenchii* remains relatively high under thermal stress (35°C). This property may facilitate symbiosis establishment of *P. damicornis* with Clade D Symbiodiniaceae under high temperatures and the survival of the holobiont after thermal stress. This should be verified in the future using infection experiments.

In summary, the binding affinity of coral lectin PdGLT-1 to five genera of Symbiodiniaceae was investigated to shed light on the molecular recognition for symbiosis establishment. PdGLT-1 exhibits a greater binding affinity to *C. goreaui* and *F. kawagutii* than *B. minutum*, *D. trenchii,* and *S. microadriaticum*, implying a higher likelihood for those two species to be recruited by *P. damicornis* as symbionts. However, as PdGLT-1 binding induces cell agglutination in *F. kawagutii*, the potential of *F. kawagutii* to become symbionts is undermined. These findings explain why *C. goreaui* is the most dominant Symbiodiniaceae in *P. damicornis*. Furthermore, we find that the PdGLT-1's binding affinity to symbiodiniacean cells was affected by temperature, and the optimal binding temperature differed with species. The high binding affinity of PdGLT-1 to *D. trenchii* (thermal-tolerant Symbiodiniaceae) under heat stress (35°C) can explain why corals with *D. trenchii* as dominant symbionts are more heat-resistant.

DATA AVAILABILITY STATEMENT

The original contributions presented in the study are included in the article/supplementary material, further inquiries can be directed to the corresponding author/s.

AUTHOR CONTRIBUTIONS

XW and ZZ conceived, designed the experiments, and analyzed the data. XW, YW, and MA performed the experiments. ZW and ZZ contributed to the reagents, materials, and analysis tools. XW, ZZ, SL, and ZW contributed to the discussion and wrote the manuscript. All authors read and approved the final manuscript.

FUNDING

This research was supported by grants from the Hainan Provincial Natural Science Foundation of China (Grant Nos. 2019RC067 and 420CXTD432), the National Natural Science Foundation of China (Grant Nos. 31772460 and 42076145), and the Major Science and Technology Program of Hainan Province (Grant No. ZDKJ2019011).

ACKNOWLEDGMENTS

We were grateful to all of the laboratory members for their continuous technical advice and helpful discussions.

REFERENCES

Abrego, D., van Oppen, M. J. H., and Willis, B. L. (2009). Onset of algal endosymbiont specificity varies among closely related species of *Acropora* corals during early ontogeny. *Mol. Ecol.* 18, 3532–3543. doi: 10.1111/j.1365-294X.2009.04276.x

Baker, A. C. (2003). Flexibility and specificity in coral-algal symbiosis: diversity, ecology, and biogeography of *Symbiodinium*. *Annu. Rev. Ecol. Evol. Syst.* 34, 661–689.

Barott, K. L., Huffmyer, A. S., Davidson, J. M., Lenz, E. A., Matsuda, S. B., Hancock, J. R., et al. (2021). Coral bleaching response is unaltered following acclimatization to reefs with distinct environmental conditions. *Proc. Natl. Acad. Sci. U.S.A.* 118:e2025435118. doi: 10.1073/pnas.2025435118

Bellantuono, A. J., Granados-Cifuentes, C., Miller, D. J., Hoegh-Guldberg, O., and Rodriguez-Lanetty, M. (2012). Coral thermal tolerance: tuning gene expression to resist thermal stress. *PLoS One* 7:e50685. doi: 10.1371/journal.pone.0050685

Berkelmans, R., and van Oppen, M. J. (2006). The role of zooxanthellae in the thermal tolerance of corals: a 'nugget of hope' for coral reefs in an era of climate change. *Proc. Biol. Sci.* 273, 2305–2312. doi: 10.1098/rspb.2006.3567

Boulotte, N. M., Dalton, S. J., Carroll, A. G., Harrison, P. L., Putnam, H. M., Peplow, L. M., et al. (2016). Exploring the *Symbiodinium* rare biosphere provides evidence for symbiont switching in reef-building corals. *ISME J.* 10, 2693–2701. doi: 10.1038/ismej.2016.54

Chankong, A., Kongjandtre, N., Senanan, W., and Manthachitra, V. (2020). Community composition of Symbiodiniaceae among four scleractinian corals in the eastern Gulf of Thailand. *Reg. Stud. Mar. Sci.* 33:100918.

Cunning, R., Bay, R. A., Gillette, P., Baker, A. C., and Traylor-Knowles, N. (2018). Comparative analysis of the *Pocillopora damicornis* genome highlights role of immune system in coral evolution. *Sci. Rep.* 8:16134. doi: 10.1038/s41598-018-34459-8

Fransolet, D., Roberty, S., and Plumier, J.-C. (2012). Establishment of endosymbiosis: the case of cnidarians and *Symbiodinium*. *J. Exp. Mar. Biol.* 42, 1–7.

Gonzalez-Pech, R. A., Stephens, T. G., Chen, Y., Mohamed, A. R., Cheng, Y., Shah, S., et al. (2021). Comparison of 15 dinoflagellate genomes reveals extensive sequence and structural divergence in family Symbiodiniaceae and genus *Symbiodinium*. *BMC Biol.* 19:73. doi: 10.1186/s12915-021-00994-6

Hoegh-Guldberg, O., Mumby, P. J., Hooten, A. J., Steneck, R. S., Greenfield, P., Gomez, E., et al. (2007). Coral reefs under rapid climate change and ocean acidification. *Science* 318, 1737–1742. doi: 10.1126/science.1152509

Hughes, T. P., Baird, A. H., Bellwood, D. R., Card, M., Connolly, S. R., Folke, C., et al. (2003). Climate change, human impacts, and the resilience of coral reefs. *Science* 301, 929–933. doi: 10.1126/science.1085046

Iguchi, A., Shinzato, C., Foret, S., and Miller, D. J. (2011). Identification of fast-evolving genes in the scleractinian coral *Acropora* using comparative EST analysis. *PLoS One* 6:e20140. doi: 10.1371/journal.pone.0020140

Jimbo, M., Suda, Y., Koike, K., Nakamura-Tsuruta, S., Kominami, J., Kamei, M., et al. (2013). Possible involvement of glycolipids in lectin-mediated cellular transformation of symbiotic microalgae in corals. *J. Exp. Mar. Biol. Ecol.* 439, 129–135. doi: 10.1016/j.jembe.2012.10.022

Jimbo, M., Yamashita, H., Koike, K., Sakai, R., and Kamiya, H. (2010). Effects of lectin in the scleractinian coral *Ctenactis echinata* on symbiotic zooxanthellae. *Fish. Sci.* 76, 355–363. doi: 10.1007/s12562-009-0204-z

Keshavmurthy, S., Tang, K. H., Hsu, C. M., Gan, C. H., Kuo, C. Y., Soong, K., et al. (2017). *Symbiodinium* spp. associated with scleractinian corals from Dongsha Atoll (Pratas), Taiwan, in the South China Sea. *PeerJ* 5:e2871. doi: 10.7717/peerj.2871

Kita, A., Jimbo, M., Sakai, R., Morimoto, Y., and Miki, K. (2015). Crystal structure of a symbiosis-related lectin from octocoral. *Glycobiology* 25, 1016–1023. doi: 10.1093/glycob/cwv033

Klepac, C. N., and Barshis, D. J. (2020). Reduced thermal tolerance of massive coral species in a highly variable environment. *Proc. Biol. Sci.* 287:20201379. doi: 10.1098/rspb.2020.1379

Kvennefors, E. C., Leggat, W., Hoegh-Guldberg, O., Degnan, B. M., and Barnes, A. C. (2008). An ancient and variable mannose-binding lectin from the coral *Acropora millepora* binds both pathogens and symbionts. *Dev. Comp. Immunol.* 32, 1582–1592. doi: 10.1016/j.dci.2008.05.010

LaJeunesse, T. C., Parkinson, J. E., Gabrielson, P. W., Jeong, H. J., Reimer, J. D., Voolstra, C. R., et al. (2018). Systematic revision of Symbiodiniaceae highlights the antiquity and diversity of coral endosymbionts. *Curr. Biol.* 28, 2570–2580e2576. doi: 10.1016/j.cub.2018.07.008

Li, J., Long, L., Zou, Y., and Zhang, S. (2021). Microbial community and transcriptional responses to increased temperatures in coral *Pocillopora damicornis* holobiont. *Environ. Microbiol.* 23, 826–843. doi: 10.1111/1462-2920.15168

Lin, S., Cheng, S., Song, B., Zhong, X., Lin, X., Li, W., et al. (2015). The genome of *Symbiodinium kawagutii* illuminates dinoflagellate gene expression and coral symbiosis. *Science* 350, 691–694. doi: 10.1126/science.aad0408

Lin, S., Yu, L., and Zhang, H. (2019). Transcriptomic responses to thermal stress and varied phosphorus conditions in *Fugacium kawagutii*. *Microorganisms* 7:96. doi: 10.3390/microorganisms7040096

Magalon, H., Flot, J. F., and Baudry, E. (2007). Molecular identification of symbiotic dinoflagellates in Pacific corals in the genus *Pocillopora*. *Coral Reefs* 26, 551–558. doi: 10.1007/s00338-007-0215-0

Magel, J. M. T., Burns, J. H. R., Gates, R. D., and Baum, J. K. (2019). Effects of bleaching-associated mass coral mortality on reef structural complexity across a gradient of local disturbance. *Sci. Rep.* 9:2512. doi: 10.1038/s41598-018-37713-1

Markell, D. A., Trench, R. K., and Iglesias-Prieto, R. (1992). Macromolecules associated with the cell walls of symbiotic dinoflagellates. *Symbiosis* 12, 19–31.

Pochon, X., and Gates, R. D. (2010). A new *Symbiodinium* clade (Dinophyceae) from soritid foraminifera in Hawai'i. *Mol. Phylogenet. Evol.* 56, 492–497. doi: 10.1016/j.ympev.2010.03.040

Rodriguez-Lanetty, M., Krupp, D. A., and Weis, V. M. (2004). Distinct ITS types of *Symbiodinium* in Clade C correlate with cnidarian/dinoflagellate specificity during onset of symbiosis. *Mar. Ecol. Prog. Ser.* 275, 97–102.

Sampayo, E. M., Ridgway, T., Bongaerts, P., and Hoegh-Guldberg, O. (2008). Bleaching susceptibility and mortality of corals are determined by fine-scale differences in symbiont type. *Proc. Natl. Acad. Sci. U.S.A.* 105, 10444–10449. doi: 10.1073/pnas.0708049105

Schuttenberg, H., and Hoegh-Guldberg, O. (2007). A world with corals: what will it take? *Science* 318:42. doi: 10.1126/science.318.5847.42b

Silverstein, R. N., Correa, A. M., and Baker, A. C. (2012). Specificity is rarely absolute in coral-algal symbiosis: implications for coral response to climate change. *Proc. Biol. Sci.* 279, 2609–2618. doi: 10.1098/rspb.2012.0055

Stat, M., and Gates, R. D. (2011). Clade D *Symbiodinium* in scleractinian corals: a "Nugget" of hope, a selfish opportunist, an ominous sign, or all of the above? *J. Mar. Sci.* 2011:730715.

Suggett, D. J., and Smith, D. J. (2020). Coral bleaching patterns are the outcome of complex biological and environmental networking. *Glob. Change Biol.* 26, 68–79. doi: 10.1111/gcb.14871

Sully, S., Burkepile, D. E., Donovan, M. K., Hodgson, G., and van Woesik, R. (2019). A global analysis of coral bleaching over the past two decades. *Nat. Commun.* 10:1264. doi: 10.1038/s41467-019-09238-2

Tang, J., Ni, X., Zhou, Z., Wang, L., and Lin, S. (2018). Acute microplastic exposure raises stress response and suppresses detoxification and immune capacities in the scleractinian coral *Pocillopora damicornis*. *Environ. Pollut.* 243(Pt A), 66–74. doi: 10.1016/j.envpol.2018.08.045

Thinesh, T., Meenatchi, R., Jose, P. A., Kiran, G. S., and Selvin, J. (2019). Differential bleaching and recovery pattern of southeast Indian coral reef to 2016 global mass bleaching event: occurrence of stress-tolerant symbiont *Durusdinium* (Clade D) in corals of Palk Bay. *Mar. Pollut. Bull.* 145, 287–294. doi: 10.1016/j.marpolbul.2019.05.033

Tortorelli, G., Rautengarten, C., Bacic, A., Segal, G., Ebert, B., Davy, S. K., et al. (2021). Cell surface carbohydrates of symbiotic dinoflagellates and their role in the establishment of cnidarian-dinoflagellate symbiosis. *ISME J.* 1–10. doi: 10.1038/s41396-021-01059-w

Traylor-Knowles, N. (2021). Unlocking the single-cell mysteries of a reef-building coral. *Cell* 184, 2802–2804. doi: 10.1016/j.cell.2021.05.007

Vidal-Dupiol, J., Adjeroud, M., Roger, E., Foure, L., Duval, D., Mone, Y., et al. (2009). Coral bleaching under thermal stress: putative involvement of host/symbiont recognition mechanisms. *BMC Physiol.* 9:14. doi: 10.1186/1472-6793-9-14

Weis, V. M. (2019). Cell biology of coral symbiosis: foundational study can inform solutions to the coral reef crisis. *Integr. Comp. Biol.* 59, 845–855. doi: 10.1093/icb/icz067

Weis, V. M., Davy, S. K., Hoegh-Guldberg, O., Rodriguez-Lanetty, M., and Pringle, J. R. (2008). Cell biology in model systems as the key to understanding corals. *Trends Ecol. Evol.* 23, 369–376. doi: 10.1016/j.tree.2008.03.004

Wood-Charlson, E. M., Hollingsworth, L. L., Krupp, D. A., and Weis, V. M. (2006). Lectin/glycan interactions play a role in recognition in a coral/dinoflagellate symbiosis. *Cell. Microbiol.* 8, 1985–1993. doi: 10.1111/j.1462-5822.2006.00765.x

Wu, Y., Zhou, Z., Wang, J., Luo, J., Wang, L., and Zhang, Y. (2019). Temperature regulates the recognition activities of a galectin to pathogen and symbiont in the scleractinian coral *Pocillopora damicornis*. *Dev. Comp. Immunol.* 96, 103–110. doi: 10.1016/j.dci.2019.03.003

Zhou, Z., Yu, X., Tang, J., Zhu, Y., Chen, G., Guo, L., et al. (2017). Dual recognition activity of a rhamnose-binding lectin to pathogenic bacteria and zooxanthellae in stony coral *Pocillopora damicornis*. *Dev. Comp. Immunol.* 70, 88–93. doi: 10.1016/j.dci.2017.01.009

Zhou, Z., Zhao, S., Ni, J., Su, Y., Wang, L., and Xu, Y. (2018). Effects of environmental factors on C-type lectin recognition to zooxanthellae in the stony coral *Pocillopora damicornis*. *Fish Shellfish Immunol.* 79, 228–233. doi: 10.1016/j.fsi.2018.05.026

Conflict of Interest: The authors declare that the research was conducted in the absence of any commercial or financial relationships that could be construed as a potential conflict of interest.

Publisher's Note: All claims expressed in this article are solely those of the authors and do not necessarily represent those of their affiliated organizations, or those of the publisher, the editors and the reviewers. Any product that may be evaluated in this article, or claim that may be made by its manufacturer, is not guaranteed or endorsed by the publisher.

frontiers in Genetics

ORIGINAL RESEARCH
published: 11 January 2022
doi: 10.3389/fgene.2021.793306

Sea Anemones Responding to Sex Hormones, Oxybenzone, and Benzyl Butyl Phthalate: Transcriptional Profiling and *in Silico* Modelling Provide Clues to Decipher Endocrine Disruption in Cnidarians

Michael B. Morgan[1,2]*, *James Ross*[1,2,3], *Joseph Ellwanger*[1], *Rebecca Martin Phrommala*[1], *Hannah Youngblood*[1,2,4], *Dominic Qualley*[2] *and Jacob Williams*[1]

[1]Department of Biology, Berry College, Mount Berry, GA, United States, [2]Department of Chemistry and Biochemistry, Berry College, Mount Berry, GA, United States, [3]Department of Microbiology and Immunology, Emory Vaccine Center, Emory University School of Medicine, Atlanta, GA, United States, [4]Department of Cellular Biology and Anatomy, Augusta University, Augusta, GA, United States

OPEN ACCESS

Edited by:
Douglas Mark Ruden, Wayne State University, United States

Reviewed by:
Qing-Ping Xie, Zhejiang Academy of Agricultural Sciences, China
Bohu Pan, National Center for Toxicological Research (FDA), United States

***Correspondence:**
Michael B. Morgan
mbmorgan@berry.edu

Specialty section:
This article was submitted to Toxicogenomics, a section of the journal Frontiers in Genetics

Received: *25 October 2021*
Accepted: *24 December 2021*
Published: *11 January 2022*

Citation:
Morgan MB, Ross J, Ellwanger J, Phrommala RM, Youngblood H, Qualley D and Williams J (2022) Sea Anemones Responding to Sex Hormones, Oxybenzone, and Benzyl Butyl Phthalate: Transcriptional Profiling and in Silico *Modelling Provide Clues to Decipher Endocrine Disruption in Cnidarians. Front. Genet. 12:793306. doi: 10.3389/fgene.2021.793306*

Endocrine disruption is suspected in cnidarians, but questions remain how occurs. Steroid sex hormones are detected in corals and sea anemones even though these animals do not have estrogen receptors and their repertoire of steroidogenic enzymes appears to be incomplete. Pathways associated with sex hormone biosynthesis and sterol signaling are an understudied area in cnidarian biology. The objective of this study was to identify a suite of genes that can be linked to exposure of endocrine disruptors. *Exaiptasia diaphana* were exposed to nominal 20ppb concentrations of estradiol (E2), testosterone (T), cholesterol, oxybenzone (BP-3), or benzyl butyl phthalate (BBP) for 4 h. Eleven genes of interest (GOIs) were chosen from a previously generated EST library. The GOIs are *17β-hydroxysteroid dehydrogenases type 14* (*17β HSD14*) and *type 12* (*17β HSD12*), *Niemann-Pick C type 2* (*NPC2*), *Equistatin* (*EI*), *Complement component C3* (*C3*), *Cathepsin L* (*CTSL*), *Patched domain-containing protein 3* (*PTCH3*), *Smoothened* (*SMO*), *Desert Hedgehog* (*DHH*), *Zinc finger protein GLI2* (*GLI2*), and *Vitellogenin* (*VTG*). These GOIs were selected because of functional associations with steroid hormone biosynthesis; cholesterol binding/transport; immunity; phagocytosis; or Hedgehog signaling. Quantitative Real-Time PCR quantified expression of GOIs. *In silico* modelling utilized protein structures from Protein Data Bank as well as creating protein structures with SWISS-MODEL. Results show transcription of steroidogenic enzymes, and cholesterol binding/transport proteins have similar transcription profiles for E2, T, and cholesterol treatments, but different profiles when BP-3 or BBP is present. *C3* expression can differentiate between exposures to BP-3 versus BBP as well as exposure to cholesterol versus sex hormones. *In silico* modelling revealed all ligands (E2, T, cholesterol, BBP, and BP-3) have favorable binding affinities with 17β HSD14, 17β HSD12, NPC2, SMO, and PTCH proteins. *VTG* expression was down-regulated in the sterol treatments but up-regulated in BP-3 and BBP treatments. In summary, these eleven GOIs collectively generate unique transcriptional profiles capable of

discriminating between the five chemical exposures used in this investigation. This suite of GOIs are candidate biomarkers for detecting transcriptional changes in steroidogenesis, gametogenesis, sterol transport, and Hedgehog signaling. Detection of disruptions in these pathways offers new insight into endocrine disruption in cnidarians.

Keywords: endocrine disruption chemicals, cnidaria, in silico modelling and docking, biomarkers, sex hormones, xenobiotics, transcriptional profiling, hedgehog signaling

INTRODUCTION

In the past quarter century, public awareness of the dramatic declines in coral reefs has become increasingly evident. Extensive research has characterized how coral reefs are shifting in structure and biodiversity due to climate change, over-fishing, coastal development, and pollution (Gardner et al., 2003; Hughes et al., 2003; Pandolfi et al., 2003; Jones et al., 2004; Bruno and Selig, 2007). Understanding the impact of land-based pollution onto reefs is further complicated by pulses of anthropogenic activity, variations in tides, variations in seasonal precipitation, and sediments which can act as carriers for a variety of organic compounds (Dachs et al., 1999; Gavio et al., 2010; Singh et al., 2010; Burns and Brinkman, 2011; Edge et al., 2013). Both land-based pollution and sewage discharge produce terrestrial runoff which culminates in diminished water quality in coastal marine environments (McKenna et al., 2001; Fabricius, 2005; Gavio et al., 2010; Singh et al., 2010; Vidal-Dorsch et al., 2012; Bahr et al., 2015; French et al., 2015; Wear and Thurber, 2015; Yoshioka et al., 2016; Al-Jandal et al., 2018). The composition of sewage is a complex mixture of freshwater, heavy metals, inorganic nutrients, microplastics, pathogens, pesticides, pharmaceuticals, plasticizers, sediments, suspended solids, and toxins (Jones et al., 2003; Kerswell and Jones, 2003; Flood et al., 2005; Jones, 2010; Singh et al., 2010; Sutherland et al., 2010; Tijani et al., 2013; French et al., 2015; Mahon et al., 2017). Many components of sewage are recognized as endocrine disrupting chemicals (EDCs) whose impact on marine invertebrates needs to be characterized (Tan et al., 2007; Singh et al., 2010; Wear and Thurber, 2015).

One form of pollution in the marine environment that is ubiquitous even in sewage is plastic (Law, 2017; Mahon et al., 2017; Lebreton et al., 2018). Plastics are known to accumulate and persist longer in sediments than on land (Worm et al., 2017). With the global explosion of plastic pollution, there is evidence cnidarians are capable of ingesting microplastics which are known to release phthalates (Hall et al., 2015; Axworthy and Padilla-Gamiño, 2019; Rotjan et al., 2019; Deng et al., 2020). As a leachable compound from plastics, phthalates are one of the most frequently detected persistent organic pollutants in the environment (Gao and Wen, 2016). In addition to plastics, oxybenzone is becoming an increasingly significant environmental concern for coral reefs because it has been detected in coastal surface waters and sediments, and has been shown to influence larval development (Downs et al., 2016; Mitchelmore et al., 2019). Steroid sex hormones, phthalates, and oxybenzone are all recognized as EDCs and all have been detected in sewage effluent and coastal marine environments where anthropogenic activity is prevalent (Atkinson et al., 2003; Thibaut and Porte, 2004; Singh et al., 2010; Bargar et al., 2013; Tsui et al., 2014; French et al., 2015; Thorn et al., 2015; Al-Jandal et al., 2018; LaPlante et al., 2018; Matouskova et al., 2020). Sterols represent the second highest proportion of lipids (14–17%) found in cnidarians (Revel et al., 2016). Because steroid hormones, phthalates, and oxybenzone all have lipophilic characteristics, the lipid-rich tissues of cnidarians are likely targets for EDCs. It has been proposed that lipophilic compounds will easily diffuse into cnidarian tissues and bioaccumulate (Peters et al., 1997; Imbs, 2013; Ko et al., 2014). Using a variety of mass-spectrometry assays, steroid hormones (and/or their conjugates), phthalates, and oxybenzone have been detected in coral tissues (from <10 ng up to 650 ng g^{-1} dry weight) and/or the environment (from <10 ng L^{-1} to >100 μg L^{-1}), (Solbakken et al., 1985; Tarrant et al., 2003; Twan et al., 2003; Twan et al., 2006; Downs et al., 2016; Mitchelmore et al., 2019). Cnidarians have demonstrated the ability to uptake estrogens in the water column at concentrations as low as 300 pg/L (Tarrant et al., 2001).

Steroid sex hormones are known to be important in cnidarian development and reproduction (Atkinson and Atkinson, 1992; Gassman and Kennedy, 1992; Slattery et al., 1999; Tarrant et al., 1999; Twan et al., 2003; Twan et al., 2006; Armoza-Zvuloni et al., 2014). Exogenous estrogen is known to impact asexual reproduction (Thorn et al., 2015). A conundrum exists because anthozoans do not have nuclear estrogen receptors even though the hormone is detectable in tissues and functions in their reproductive biology (Reitzel et al., 2008; Reitzel and Tarrant, 2009). Nuclear receptors capable of binding estrogen have been identified in other cnidarians (medusozoans) (Khalturin et al., 2018), and although not yet well-characterized, a membrane-bound G-protein coupled estrogen receptor 1-like transcript (GPER1) genomic locus (LOC114576065) has been identified for *E. diaphana* (NCBI Nucleotide). GPER1 has recently been identified in humans in addition to the two traditional nuclear estrogen receptors ERα and ERβ (Fuentes and Silveyra, 2019). Perhaps GPER1 is also involved in physiologic estrogen-signaling in anthozoans and may be a target of EDCs, leading to downstream transcriptional changes.

Another conundrum exists because cnidarians are known to synthesize a diverse set of sterols (Tarrant et al., 2009; Revel et al., 2016), but their repertoire of steroidogenic enzymes appears to be incomplete. There is no genomic evidence that cnidarians produce aromatase, and yet aromatase activity has been detected (Tarrant et al., 2003; Twan et al., 2003; Twan et al., 2006). It is also possible that steroid sex hormones may play other significant roles (e.g., possibly chemical communication) which have yet to be fully elucidated (Tarrant et al., 2003; Blomquist

et al., 2006; Lafont and Mathieu, 2007; Shikina et al., 2016). Since cnidarians use steroid hormones as signaling molecules but they do not have an endocrine system, Tarrant (2007) asked a fundamental question: Can endocrine disruption occur in cnidarians? Previous investigations have identified steroid hormone-like signaling molecules but there are still significant gaps in understanding which metabolic pathways are impacted.

One approach of ecotoxicological investigations is to identify changes in gene transcription in aquatic organisms exposed to an exogenous substance (Snell et al., 2003; Snape et al., 2004). Calls have been made to develop a comprehensive assessment of steroid hormones, phthalates, and personal care products impacting marine environments (Singh et al., 2010; Tijani et al., 2013; Archer et al., 2017; DiNardo and Downs 2018). More detailed information regarding the impact of EDCs on specific pathways involved in both synthesis and metabolism of sex hormones would be highly desirable. Developing biomarkers for anthropogenic stressors can be useful tools for monitoring health on coral reefs (Kenkel et al., 2014). Validated mechanistic biomarkers for aquatic invertebrates which can identify responses to a particular class of chemical stressor a have been theorized (Snell et al., 2003; Hutchinson, 2007), but difficult to produce. Presently, biomarkers for cnidarians exposed to EDCs have not been developed and validated. This study seeks to identify a suite of genes that characterize exogenous EDC exposures. Such a suite of genes could help elucidate the cellular pathways leading to cnidarian endocrine disruption.

MATERIALS AND METHODS

Toxicant Exposure

Sea anemones (*Exaiptasia diaphana* previously known as *Aiptasia pallida*) were purchased from a supplier (Wards Natural Science, Rochester, NY, United States) and acclimated to laboratory conditions (45 L recirculating artificial seawater at 22°C and 36 ppt salinity) for 1 week. Anemones (100 individuals) were randomly subdivided into a control group or 20 ppb treatments of 17β-estradiol (E2), testosterone [T], cholesterol, benzyl butyl phthalate (BBP), or oxybenzone (BP-3). Toxicant purity was pharmaceutical secondary standard grade for E2, T, cholesterol, and BP-3 while BBP was analytical standard grade (Sigma-Aldrich, St. Louis, MO, United States). Acetone (150 µg/L) was used to solubilized toxicants were prior to dilution in seawater. Acetone has previously been used as a wetting agent (Morgan et al., 2001; Morgan et al., 2012). The 20 ppb concentration was chosen to induce responses and does not necessarily reflect environmental conditions even though BP-3 has been detected at concentrations >20 ppb (Downs et al., 2016) and cholesterol at 11ppb (French et al., 2015). All treatments were nominal concentrations for 4 h in 1L artificial seawater under ambient laboratory lighting during the early spring season. The 4-h exposure was chosen to detect responses at an early stage of exposure.

Selecting Candidate Genes of Interest

Complementary DNA sequences previously generated by Representational Difference Analysis (RDA) (Edman et al., 1997; Hubank and Schatz, 1999; Pastorian et al., 2000) were screened for candidate ESTs to be used in this investigation. Candidate ESTs were selected based on sequence homology (BLASTX analysis) to genes of interest (GOI) with known functions involving sex hormone synthesis, sterol binding, lipid transport, and/or indirect sterol interactions. Subsets of these ESTs have previously been used to characterize cnidarian stress responses (Morgan et al., 2012; Morgan et al., 2015).

Reverse Transcription Reactions

Anemones from each treatment were pooled and total RNA was isolated using Trizol (Invitrogen, United States). Two milliliter phase-lock gels (5′Prime, United States) aided in the recovery of the aqueous phase. Total RNA was DNase I digested and purified (New England BioLabs, United States). Messenger RNA (mRNA) was isolated (Oligotex, Qiagen, United States) from 100 µg of DNase I treated total RNA. First stand synthesis used SuperScript IV (Invitrogen, United States) along with random hexamers and oligo-dT primers to reverse transcribe 1 µg of poly-A enriched mRNA. The RT reaction conditions were 1 h at 37°C, followed by 1 min at each temperature between 42 and 50°C.

Quantitative Real-Time PCR

A QuantStudio 7 Flex Real-Time PCR system (Applied Biosystems Waltham, MA, United States) used a SYBR Green-based assay to perform qPCR. A 1/100 dilution of first-strand synthesis reactions were used as templates for all qPCR reactions. Primers for each GOI were created using Primer3 (https://primer3.org) (**Table 1**). Components for each 20 µl qPCR reaction included: 10 µl Luna® Universal qPCR Mix (New England BioLabs, United States), 2.5 µl Forward primer (10 µM), 2.5 µl Reverse primer (10 µM), 2.5 µl dH_2O, 2.5 µl sample. Thermocycling conditions were 1 cycle at 95°C for 1 min; 40 cycles of 95°C for 15 s and then 60°C for 30 s; and concluding with 1 cycle of melt curve analysis. Four replicate reactions were used for analyzing the relative expression of each GOI. Ribosomal protein L11 (*RPL11*) was used as qPCR reference gene (Kenkel et al., 2011). Melt-curve analysis, primer efficiencies, and gel electrophoresis confirmed specificity of priming. Replicate Cq values were averaged to determine ΔCq and ΔΔCq for each treatment and GOI. All ΔCq and ΔΔCq values are based on the consistent expression of *RPL11* across all treatments. The ΔΔCq method was used to determine the differences between targeted GOIs and a single reference gene (Bustin et al., 2009). Univariate ANOVA was performed on ΔΔCq data to identify significant expression of individual GOIs across treatments. Similarities in variance between treatments were determined by Levene's Test of Equality of Error Variances. If the variance between treatments was similar, then the Student-Neuman-Keuls (SNK) posthoc test was performed to determine which treatment(s) were significantly different from the rest. If variance between treatments was different, then Tamhane's T2 posthoc test was applied since Univariate ANOVA is generally insensitive to heteroscedasticity.

In silico Molecular Modelling

Human protein homologs have previously been used as substitutes for cnidarian proteins in molecular modelling (Khalturin et al., 2018). Some cnidarian proteins have such

TABLE 1 | BLAST results for RDA probes. Searches performed at NCBI using BLASTX algorithm and the non-redundant database (nr) with default search parameters.

Gene ID	Putative Gene Homolog	BLASTX E-value	Organism ID	Homolog Accession #
17βHSD14	17β-hydroxysteroid dehydrogenase type 14	5e-155	Exaiptasia diaphana	KXJ20962
17βHSD12	17β-hydroxysteroid dehydrogenase type 12	1e-61	Exaiptasia diaphana	KXJ12187
C3	Complement component C3	3e-57	Exaiptasia diaphana	KXJ11955
CTSL	Cathepsin L	6e-95	Exaiptasia diaphana	KXJ27439
NPC2	Niemann-Pick C type 2	1e-84	Exaiptasia diaphana	KXJ29862
EI	Equistatin	7e-57	Exaiptasia diaphana	KXJ18222
PTCH3	Patched domain-containing protein 3	3e-79	Exaiptasia diaphana	KXJ20037
DHH	Desert hedgehog protein A	3e-47	Exaiptasia diaphana	KXJ11164
SMO	Smoothened-like	1e-87	Exaiptasia diaphana	KXJ11374
GLI2	zinc finger protein GLi2	4e-146	Exaiptasia diaphana	XP_020898684
VTG	Vitellogenin 2	7e-38	Exaiptasia diaphana	KXJ14544

TABLE 2 | Binding affinities (in kcal/mol) of ligands to proteins, estimated by docking simulations. Values represent the lowest energy binding mode for each docking experiment. Cnid: cnidarian; CS: crystal structure. Total number of amino acids and the total number of physical contacts represent binding pocket interactions. * indicates no direct homolog for PTCH3 so PTCH1 PDB file (6OEU) was used.

Gene ID	Ligand	Binding energy (kcal/mol)		Binding pocket	
				Total # of aa/total # contacts	
		Cnid	CS	Cnidarian (accession #)	Crystal structure (PDB file)
17βHSD14	Estradiol	−8.8	−8.4	16aa/238 (KXJ20962)	17aa/243 (5HS6)
	Testosterone	−8	−8.5		
	Cholesterol	−7.5	−6.4		
	BBP	−7.8	−7.2		
	BP-3	−7.4	−7.4		
17βHSD12	Cholesterol	−6.9	−7.4	17aa/217 (KXJ12187)	22aa/202 (2ET6)
	Estradiol	−6.4	−7.5		
	Testosterone	−6.4	−7.3		
	BBP	−5.2	−6.1		
	BP-3	−5.8	−5.7		
PTCH3*	Cholesterol	−9.4	−7.3	25aa/281KXJ20037	14aa/2136OEU
	Estradiol	−7.9	−7.8		
	Testosterone	−8.5	−8.1		
	BBP	−6.9	−6.2		
	BP-3	−6.6	−7.0		
NPC2	Cholesterol	−9.5	−12.1	18aa/177KXJ29862	19aa/2375KWY
	Estradiol	−8.5	−10.6		
	Testosterone	−8.7	−10.3		
	BBP	−6.9	−8.5		
	BP-3	−6.6	−8.0		
SMO	Cholesterol	−8.4	−9.9	12aa/190KXJ11374	20aa/2106XBM
	Estradiol	−7.6	−9.0		
	Testosterone	−8.2	−9.2		
	BBP	−6.6	−7.9		
	BP-3	−6.5	−7.5		

significant homology to human proteins that they are even capable of stimulating human responses (Dunn et al., 2006; Wood-Charlson and Weis, 2009; Duffy and Frank, 2011; Dani et al., 2014; Brennan et al., 2017; Mansfield et al., 2017). The most similar vertebrate structures (according to BLASTX E-value) were used for selecting which Protein Databank (PDB) files should be used for initial docking experiments. Sequence alignments of cnidarian and relevant homologs determined which relevant protein sequences (i.e., PDB files) were to be used as representatives of corresponding cnidarian proteins. Protein coordinates (PDB files) for homologous constructs were downloaded from the PDB, and any existing ligands or small molecules (e.g., water or salt ions) were removed. Cnidarian protein structures were created with the SWISS-MODEL web server (https://swissmodel.expasy.org) using the homologs as templates. Ligands were created in Avogadro (Hanwell et al.,

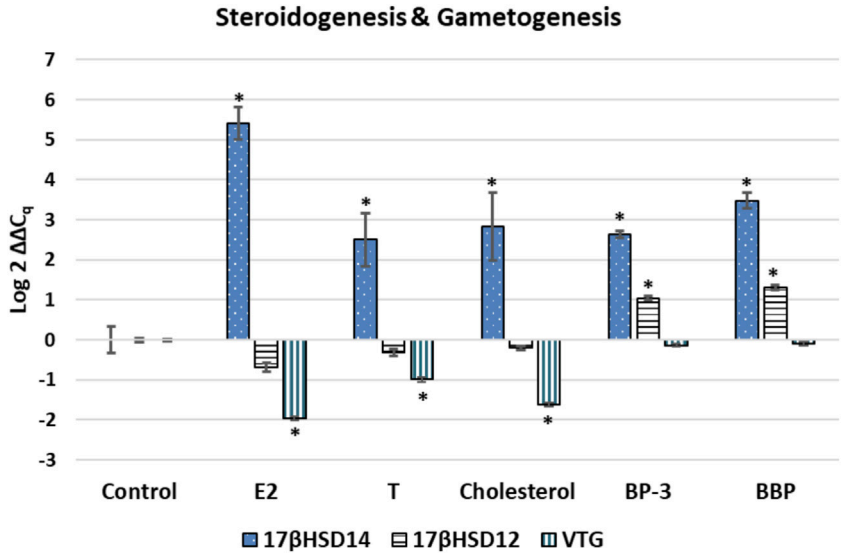

FIGURE 1 | Expression profile for transcripts associated with sex hormone steroidogenesis or gametogenesis. The ΔΔCq values represent transformed expression of a GOI relative to RPL11 expression. An * represents a treatment that was significantly different ($p < 0.01$) relative to the control condition. Error bars represent ± SE. E2: estradiol; T: testosterone; BP-3: oxybenzone; BBP: benzyl butyl phthalate; I7§HSD14: 17a-hydroxysteroid dehydrogenase type 14; 17bHSD12: 17b-hydroxysteroid dehydrogenase type 12: VTG: Vitellogenin 2

2012) and energy-minimized prior to docking. Docking was performed using AutoDock Vina (Trott and Olson, 2010); the search space was restricted to the known ligand binding site. After docking, the results were analyzed in UCSF Chimera (Pettersen et al., 2004) with the Find Clashes/Contacts function which was set to detect any atoms within 0.4 Å of the ligand with the best docking score.

RESULTS

Genes of Interest

BLASTX analysis of ESTs identified eleven candidate GOIs with of functions associated with steroidogenesis, gametogenesis, cholesterol transport, immunity, phagocytosis, or the Hedgehog signaling pathway (**Table 2**). These GOIs were: 17β-hydroxysteroid dehydrogenase type 14 (*17βHSD14*), 17β-hydroxysteroid dehydrogenase type 12 (*17βHSD12*), Niemann-Pick C type 2 (*NPC2*), Equistatin (*EI*), Complement component C3 (*C3*), Cathepsin L (*CTSL*), Patched domain-containing protein 3 (*PTCH3*), Smoothened (*SMO*), Desert Hedgehog protein A (*DHH*), zinc finger protein Gli2 (*GLI2*), and Vitellogenin (*VTG*). Two GOIs (*17βHSD14*; *17βHSD12*) are associated with steroidogenesis. *17βHSD14* converts E2 into E1 and T into androstenedione (A4), while *17βHSD12* performs the reverse reactions, E1 into E2, and A4 into T (Tarrant et al., 2003; Luu-The et al., 2006; Shikina et al., 2016; Salah et al., 2019). Three GOIs (*CTSL, EI, NPC2*) are associated with lysosome/endosomes and/or symbiosome/phagosome (Dani et al., 2014; Mohamed et al., 2016; Dani et al., 2017; Hambleton et al., 2019). One GOI (C3) is associated with innate immunity (Miller et al., 2007; Kvennefors et al., 2010; Palmer and Traylor-Knowles, 2012; Ocampo et al., 2015). Four GOIs (*PTCH3, SMO, DHH, GLI2*) are representative of Hedgehog (HH) signaling which is highly conserved within vertebrate mammals (Sinkovics, 2015). One GOI (*VTG*) is the precursor of the egg yolk protein vitellin (Matozzo et al., 2008; Shikina et al., 2013; Lotan et al., 2014).

Transcriptional Responses of Genes of Interests

For the GOIs associated with steroidogenesis, *17βHSD14* expression was significantly up-regulated ($p < 0.01$) in each exogenous chemical treatment compared to the control, whereas *17βHSD12* expression was significantly up-regulated ($p < 0.01$) only in the BP-3 and BBP treatments (**Figure 1**). *VTG* exhibited significant down-regulated expression ($p < 0.01$) in E2, T, and cholesterol treatments (see **Figure 1**).

GOIs associated with phagocytosis had significant differences in expression in various treatments when compared to the control condition (**Figure 2**). Cathepsin (*CTSL*) expression was significantly up-regulated in the BP-3 and BBP treatments ($p < 0.01$). Equistatin (*EI*) was significantly up-regulated in E2, BP-3, and BBP treatments ($p < 0.01$) and significantly down-regulated in the T and cholesterol treatments ($p < 0.01$) (see **Figure 2**). *NPC2* was significantly down-regulated in cholesterol ($p < 0.01$) and significantly up-regulated ($p < 0.01$) in BP-3 and BBP treatments (see **Figure 2**). Lastly, *C3* was significantly up-regulated in E2, T, and BP-3 treatments (see **Figure 2**).

For the GOIs associated with HH signaling, *PTCH3* was significantly down-regulated ($p < 0.01$) in response to all three sterols, but significantly up-regulated ($p < 0.01$) in BP-3 and BBP treatments (**Figure 3**). *SMO* was significantly down-regulated

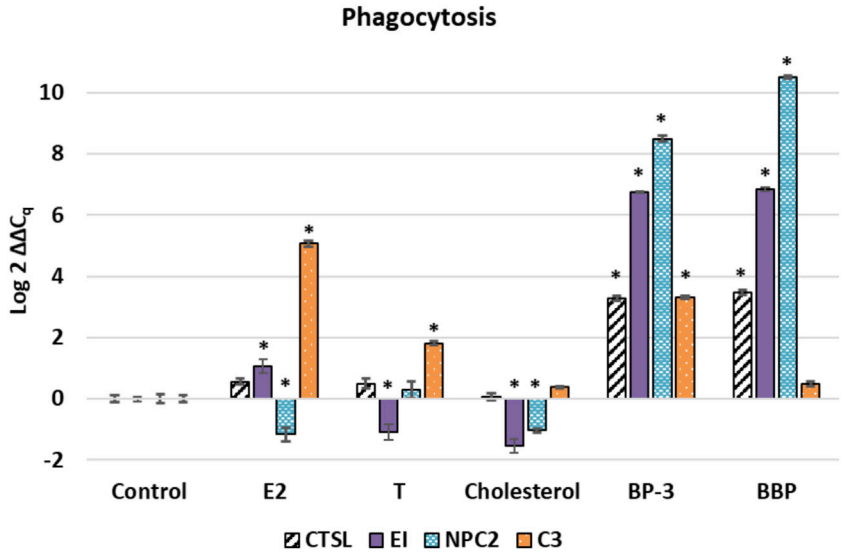

FIGURE 2 | Expression profile of transcripts associated with phagocytosis and cellular structures such as symbiosome, lysosome, or endosome. The ΔΔCq values represent transformed expression of a GOI relative to RPL11 expression. An * represents a treatment that was significantly different ($p < 0.01$) relative to the control condition. Error bars represent ± SE. E2: estradiol; T: testosterone; BP-3: oxybenzone; BBP: benzyl butyl phthalate. CSTL: cathepsin L; EI: equistatin; NPC2: Niemann-Pick C type 2; C3: complement component C3.

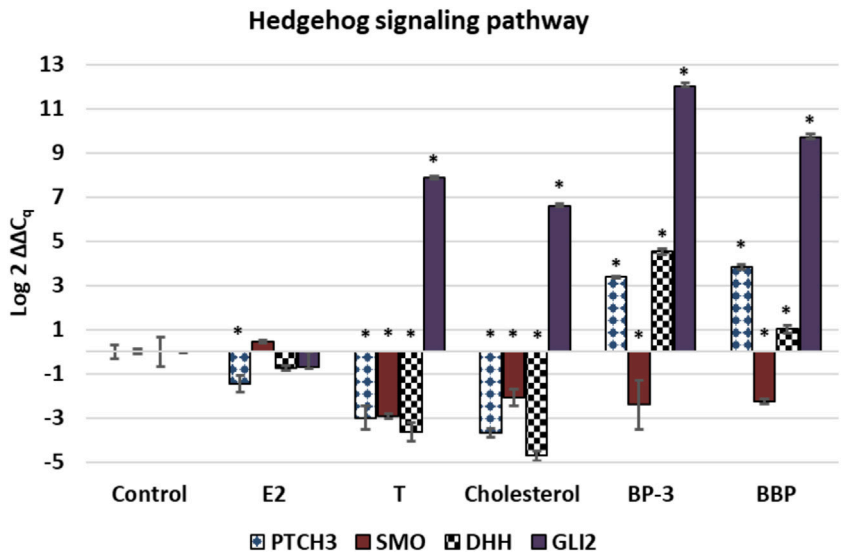

FIGURE 3 | Expression profiles of transcripts associated with Hedgehog signaling pathway. The ΔΔCq values represent transformed expression of GOI relative to RPL11 expression. An * represents a treatment that was significantly different ($p < 0.01$) relative to the control condition. Error bars represent ± SE. E2: estradiol; T: testosterone; BP-3: oxybenzone; BBP: benzyl butyl phthalate. PTCH3: patched domain-containing protein 3; SMO: smoothened-like; DHH: Desert hedgehog protein A; GLI2: zinc finger protein GLi2.

($p < 0.01$) in all treatments except E2 (see **Figure 3**). *DHH* was significantly down-regulated ($p < 0.01$) in T and cholesterol treatments, but significantly up-regulated ($p < 0.01$) in BP-3 and up-regulated in BBP treatments ($p < 0.05$) (see **Figure 3**). *GLI2* was significantly up-regulated ($p < 0.01$) in all treatments except E2 (see **Figure 3**).

Univariate ANOVA reveals all sterol treatments were significantly different from each other as well as the xenobiotics ($p < 0.01$). While the BP-3 and BBP treatments were significantly different from all the sterols ($p < 0.01$), they were not significantly different from each other (**Figure 4**).

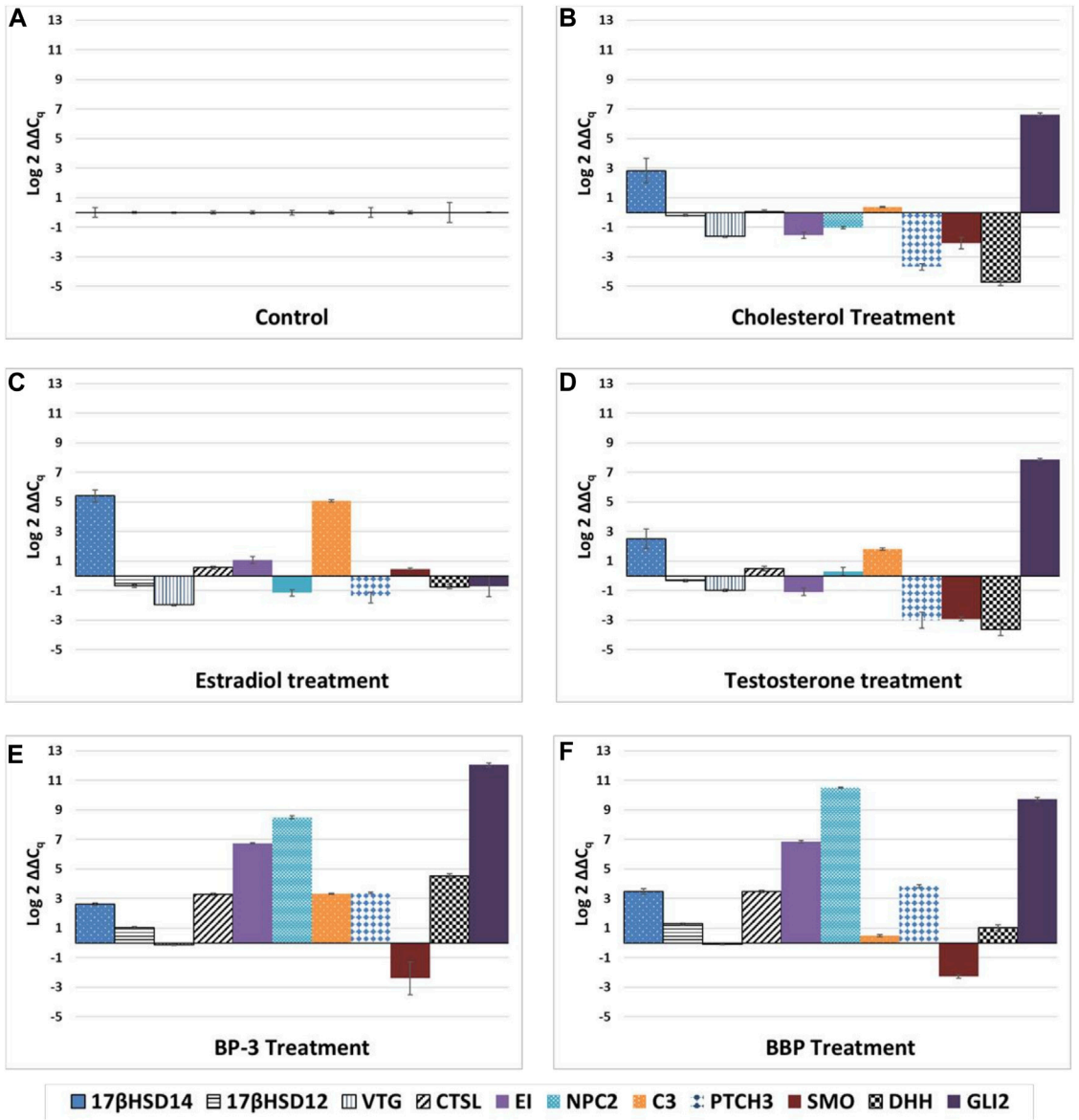

FIGURE 4 | Unique expression profiles for each treatment. **(A)** control, **(B)** cholesterol, **(C)** estradiol, **(D)** testosterone, **(E)** oxybenzone, **(F)** benzyl butyl phthalate. The ΔΔCq values represent transformed expression of GOI relative to RPL11 expression. Error bars represent ± SE.

Docking Simulations

In order to better understand how sterols and xenobiotics are able to interact with targeted proteins, *in silico* modelling was used to predict the most energetically favorable ligand/protein binding interactions. The binding affinities of each ligand to the proteins of interest were estimated using docking simulations. Comparative genomic analyses indicate that cnidarian genomes show important similarities to vertebrates in gene content, genomic structure, and organization (Putnam et al., 2007). However, the cnidarian proteome is not as well characterized as the human proteome. Therefore, macromolecular structures needed for the *in silico* modelling were generated in one of two ways. The first model was the structure in the Protein Databank with the highest degree of homology to the GOI. These PDB files were: 6oeu (PTCHD3), 5kwy (NPC2), 6xbm (SMO), 5hs6 (17βHSD14), and 2et6 (17βHSD12). The best PDB structures corresponded to the human sequences in all cases except for 17βHSD12, where the protein with the closest homology was from *Candida tropicalis*. The second model was generated using SWISS-MODEL, with the *Exaiptasia* sequence as input and the closest PDB structure as a template. Each ligand was docked to both protein models. The docking algorithm used flexible fitting with an energy-minimized ligand to determine possible binding conformations and relative binding affinities. All ligands bind to each protein, although the strength of the interactions varied. The binding free energy of the

TABLE 3 | Genes of Interest and their corresponding primers used in qPCR reaction. Annealing temperature for all primers was 60°C.

Gene ID	Primers	Amplicon length
17βHSD14	F: TGCACCCTTTGTTGTGACAT R: GATGGCATCCTCCAGAAAGA	209bp
17βHSD12	F: AGTCCAGATTTTCTTGCAACCA R: TAGACTTCAGTGGTGGGCAG	226bp
VTG	F: GCTGTAGTGGTTTTGGTCGG R: TGGTGCTTCTTGGCTTGTTC	198bp
CTSL	F: CATTGCCATTGCATTGATTC R: CTGCAAATGCCTACAAGCAA	215bp
EI	F: AGTTGCCCTGGTTTCAAAGA R: CCGTCGTCTGTACATTGTGG	200bp
NPC2	F: TCTTGCAGTTGCCACTTGAC R: AATGTTACCGATGCCGAGTC	204bp
C3	F: TTATCATGGTCCTGGGTGCT R: GCGTCAAACTCGAACGTTTT	208bp
PTCH3	F: TGGATGATTGAGGCTGTGGT R: CCTACGCAGCCATTTCCATC	180bp
SMO	F: GAACAGGGTTGGTTGCTCAG R: ATTGAAGGCGCTGCTGTTAG	174bp
DHH	F: CGCGTCCTCTCCCTAAACTA R: CCCACTCCAACATTCTCCCT	161bp
GLI2	F: GTGTGTGAAATGCAGCCTCA R: GCATCACCTGTCAAGTCCAC	191bp

best docking pose for each ligand/receptor combination is shown in **Table 3**.

Since a crystal structure of 17βHSD14 with a similar ligand (estrone) is available on the PDB (5HS6), it is possible to compare the binding site of an experimentally-determined protein-ligand structure with our docked models (Laskowski and Swindells, 2011). **Figure 5** shows a comparison between human 17βHSD14 with bound estrone, human 17βHSD14 with docked estradiol, and *Exaiptasia* 17βHSD14 with docked estradiol. The search space was confined to the binding pocket for each protein-ligand interaction, and the orientation of the ligand within the pocket was fairly well-conserved (see **Figure 5**). Additionally, the residues that interact with each ligand were well-conserved between cnidarian and homologous models. For example, estrone and estradiol formed hydrophobic contacts with His93, Gln148, Trp192, and Leu195 in both crystal structure and the docked model of human 17βHSD14. In the cnidarian protein, these residues correspond to His102, Gln157, Trp201, and Leu204, and are predicted to interact the estradiol ligand in the docked model as well (see **Figure 5**).

DISCUSSION

Attempts at detecting endocrine disruption in cnidarians has been enigmatic. Genomic studies indicate that cnidarians lack *CYP19a1a* (aka: aromatase) that vertebrates use for sex hormone steroidogenesis (Goldstone, 2008), and yet some cnidarians have demonstrated aromatase activity (Twan et al., 2003). This study sought to identify a suite of GOIs that exhibit differential transcriptional expression in anemones exposed to chemicals known to be endocrine disruptors. The EDCs used in this investigation are lipophilic and detected in the marine environment including sediments and sewage effluent in ng/L to μg/L concentrations (Atkinson et al., 2003; Singh et al., 2010; French et al., 2015; Wear and Thurber, 2015; Al-Jandal et al., 2018; Mitchelmore et al., 2019). Furthermore, all GOIs in this investigation have direct interactions or indirect associations with sterols. Using cholesterol in this investigation was critical as a positive control for evaluating GOIs binding of, and/or interactions with, cholesterol. Transcriptional activities and binding affinities of 17βHSDs in the presence of E2 and T are positive controls since these steroidal hormones are the natural ligands for 17βHSDs.

Links to Steroidogenesis

Endocrine disruption involves chemicals that alter steroidogenesis which interfere with the hormonal signaling leading to down-stream physiological abnormalities in reproduction, development, increased risk of disease, and/or interference with immune and nervous system functions (Heindel et al., 2012). The 17β-hydroxysteroid dehydrogenases (17βHSDs) are involved with steroidogenesis of both estrogens and androgens. 17βHSDs have been detected in cnidarians (Tarrant et al., 2003; Blomquist et al., 2006; Shikina et al., 2016). *17βHSD12* and *17βHSD14* represent the last step in the steroidogenesis pathway prior to the aromatization of T into E2.

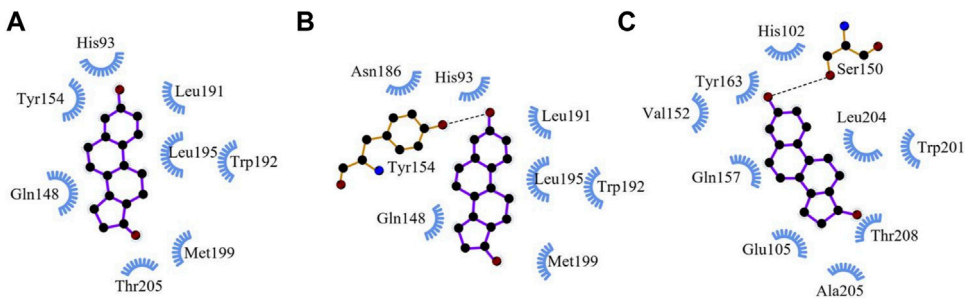

FIGURE 5 | Comparison of the docking poses of 17§HSD14 with similar ligands generated using LigPlot$^+$ v1.4 software (Laskowski and Swindells 2011). Circled residues indicate side chains that are involved in docking for at least two of the three models. **(A)** crystal structure of estrone bound to human 17§HSD14 (5HS6). **(B)** crystal structure of human 17bHSD14 docked to estradiol. **(C)** crystal structure of *Exaiptasia* I7§HSD14 docked to estradiol.

17βHSD12 reduces estrone (E1) into E2 as well as androstenedione (A4) into T, while *17βHSD14* performs the opposite reaction by oxidizing E2 into E1, and T into A4 (Luu-The et al., 2006; Caldwell et al., 2012; Sivik et al., 2012; Thomas and Potter, 2013; Shikina et al., 2016; Salah et al., 2019). Concentrations of competing sterols may drive which sterol gets converted by a specific 17βHSD (Lathe and Kotelevtsev, 2014). E2 concentration is known to regulate transcription of 17βHSDs (Rotinen et al., 2009). Transcriptional profiles herein demonstrate the organism (regardless of sex) responds to the environmental "overload" of E2 or T by modulating the transcription of the enzyme in order to transform both sex hormones into less potent sterols. These profiles also reveal that cholesterol and xenobiotics (BBP and BP-3) interfere with steroidogenesis by altering normal transcriptional demands for 17βHSDs (see **Figure 1**).

Links to Sterol Binding and Transport

Cnidarians get cholesterol and other sterols by either dietary intake and/or from their endosymbiont (Revel et al., 2016; Hambleton et al., 2019). Cholesterol transport and metabolism is tightly regulated (Maxfield et al., 2016). Due to lipid-rich tissues, it has been proposed that lipophilic compounds will easily diffuse into cnidarian tissues (Peters et al., 1997). Sterols are most concentrated in cnidarian epidermis and some sterols are known to increase in concentration after exposure to environmental pollutants (Revel et al., 2016; Stien et al., 2020). The lack of significant expression of *C3* in the cholesterol treatment is consistent with the fact that it is a natural constituent of animal membranes.

Five GOIs (*C3, PTCH3, CTSL, EI, NPC2*) have functional associations with the endocytic processes whereas a sixth GOI (*DHH*) is a secreted morphogen associated with exocytosis/secretion. *C3* is associated with phagocytosis of foreign particles into cnidarians (Palmer and Traylor-Knowles, 2012), while PTCH regulates functions of: receptor-mediated endocytosis of sterol-protein ligands; down-stream morphogens; and the removal of oxysterols (Incardona et al., 2000; Strutt et al., 2001; Corcoran and Scott, 2006; Zhong et al., 2014). Three GOIs (*CTSL, EI, NPC2*) are associated with lysosomes and phagocytosis. Cathepsins are lysosomal proteases and *EI* is the cnidarian homolog of an inhibitor of cathepsins (Lenarčič et al., 1997; Štrukelj et al., 2000). Lysosomes contribute to the termination of hormone effects by degrading proteins interacting with the hormone (Qualmann et al., 2000; Totta et al., 2014). NPC2 functions as a key regulator of sterol transport between *Symbiodinium* and cnidarian hosts which is representative of stable symbioses in a structure known as the symbiosome (Infante et al., 2008; Vance, 2010; Ganot et al., 2011; Dani et al., 2014; Bucher et al., 2016; Revel et al., 2016; Hambleton et al., 2019; Lu et al., 2020). Seven GOIs (*NPC2, 17βHSD14, C3, PTCH3, SMO, DHH, VTG*) have known linkages to endoderm. (Kvennefors et al., 2010; Shikina et al., 2013; Sanders et al., 2014; Shikina et al., 2016).

Five GOIs (*17βHSD14, 17βHSD12, NPC2, PTCH3, SMO*) that have sterol binding pockets were used in *silico* modelling. *In silico* modelling has previously demonstrated phthalates and steroids without an aromatic A-ring are capable of binding to sterol-binding proteins (Sheikh and Beg, 2017; Khalturin et al., 2018). Patched genes have multiple functionally redundant homologs that cannot discriminate between ligands (Carpenter et al., 1998; Zhulyn et al., 2015; Hu and Song, 2019). Justification for model docking is based on the fact that cnidarian genomes have representative vertebrate homologs of relevant proteins (Miller et al., 2007; Putnam et al., 2007; Kvennefors et al., 2010). *In silico* modelling demonstrates the lowest energy docking poses for the crystal structures of the homologous proteins and the models of the *Exaiptasia* proteins correlate well with each other (see **Table 3**). The binding scores for the *Exaiptasia* protein models generally follow the same trends as the homologs from the PDB. In both cases, the steroid ligands (cholesterol, E2, and T) bound more strongly than BP-3 or BBP, although the differences in binding energy seem to be smaller for the 17βHSD12 and 17βHSD14 proteins. This result was expected, since BBP and BP-3 are considerably smaller and as such, would make less contact with binding pocket residues (see **Table 3**). Although there are a few minor differences between homologs, such as hydrogen bonding patterns, the orientation of the ligand in the 17βHSD14 binding pocket and the side chains involved in binding are strikingly similar (see **Figure 5**). All sterols have similarities in orientations, binding affinities, and expression profiles (see **Table 3** and **Figure 5**). 17βHSDs are known to exhibit variability in substrate binding (Blomquist et al., 2006; Lathe and Kotelevtsev, 2014).

Data herein provides new information about the diversity of ligands, including xenobiotics that bind to NPC2, PTCH3, SMO, and the 17βHSDs. The differential expression of these sterol-binding proteins suggests that these proteins handle natural sterols and xenobiotics differently. Laboratory-induced exposure to cholesterol, E2, and T requires modulating transcript copy numbers to handle the environmental flux of natural ligands. However, laboratory-induced exposures of BBP and BP-3 appear to require transcriptional replacement for proteins after binding xenobiotics. All GOIs except *SMO* exhibit up-regulated expression in the BP-3 and BBP treatments (see **Figures 4E,F**).

Links to Development

Hedgehog (HH) signaling is a highly conserved developmental pathway that relies on cholesterol interacting with specific sterol-binding proteins. Endocrine disruption is known to interfere with HH signaling (Johansson and Svingen, 2020). Developmentally-regulated signaling pathways involving apoptosis, embryogenesis, cell proliferation, and development of diseases present in higher animals are also found in cnidarians including *Exaiptasia* (Technau et al., 2005; Matus et al., 2008; Sinkovics, 2015; Bucher et al., 2016). Four GOIs (*PTCH3, SMO, DHH, GLI2*) can be linked to HH signaling. E2 acts as a direct HH pathway antagonist (Lipinski and Bushman, 2010) and the E2 expression profile in **Figure 3** reaffirms this inhibitory effect. Recognized inhibitors of HH signaling also include the well-characterized steroidal alkaloid cyclopamine (Chen 2002). The down-regulated expression profiles of *PTCH3* in the E2, T, and cholesterol treatments and the down-regulated expression of *SMO* in the T and cholesterol treatments suggests all three sterols exhibit

similar inhibitory effects (see **Figure 3**). The HH pathway is also responsive to xenobiotics as well as sterols (Johansson and Svingen, 2020). Phthalates are known to impact DHH and PTCH expression, and BP-3 is considered estrogenic (Thibaut and Porte, 2004; Borch et al., 2006; Downs et al., 2016; Hong et al., 2016; LaPlante et al., 2018; Matouskova et al., 2020). Although PCTH3 and DHH were down-regulated in response to sterols, *PTCH3*, *DHH*, and *GLI2* were up-regulated in response to BP-3 and BBP (see **Figure 3**), suggesting opposing effects of sterols and xenobiotics on HH signaling, presumably with sterols exerting antagonists effects and xenobiotics exerting agonist effects. Regardless, the expression profiles in **Figure 3** highlight the inherent vulnerability of the HH pathway to diverse chemical signals.

Links to Gametogenesis

Gametogenesis is associated with HH signaling. HH signaling molecules are considered stem-cell factors (Zhang and Kalderon, 2001). Evidence exists in other metazoans that secreted molecules in the HH signaling pathway are one of the primary regulators of stem cells which are necessary precursors of oogenesis (Zhang and Kalderon, 2001). Shikina and Chang (2016) identifies cnidarian germline stem cells as originating in endodermal mesentery. HH signaling GOIs (*PTCH3, SMO, DHH*) are known to be restricted to the endoderm of male and female gonophores (Sanders et al., 2014). Germline stem cells are the essential cells responsible for this process in various metazoans. In *Drosophila*, somatic cells in the ovary of cannot proliferate normally in the absence of Smoothened activity (Zhang and Kalderon, 2000), and excessive HH signaling can result from aberrant expansion of stem cell pools (Zhang and Kalderon, 2001). Results show all exogenous treatments (except E2) caused down-regulation of *SMO* (see **Figure 4**). With the exception of *PTCH3*, results also show that HH signaling GOIs in the E2 treatment are not significantly expressed (see **Figure 3**).

Exaiptasia reproductive strategies include both sexual and asexual reproduction (Clayton, 1985; Grawunder et al., 2015). Subsets of anemones used for each treatment were taken from the same population as the control anemones. Although not confirmed, it is highly likely that all anemones used in this investigation were clonal. Detecting the presence of sex-specific tissues enhances the ability to interpret anemone responses to the EDCs. Although the sex of the colony was not known, expression profiles of the GOIs could provide clues about the sex of these animals. Vitellogenin is a female-specific protein commonly found across the animal kingdom and is the most abundant protein associated with oocyte development in cnidarians (Shikina et al., 2013; Levitan et al., 2015). Hormonal and/or environmental cues are known to stimulate release of oocytes (Levitan et al., 2015). Exogenous E2 is known to influence pedal laceration and egg bundle formation in cnidarians (Tarrant et al., 2004; Thorn et al., 2015). Blue-light cues have also been used to induce *Aiptasia sp* gametogenesis in a laboratory setting (Grawunder et al., 2015).

This investigation also did not attempt to identify the sex of the anemones nor their reproductive status, per se. Hermaphroditism and even Trioecy has been observed in closely related species (Schlesinger et al., 2010; Armoza-Zvuloni et al., 2014). A small amount of data from a previous study suggests male tissues from hermaphroditic corals also express *VTG* (Hayakawa et al., 2005). Results reveal *VTG* expression in the control treatment suggesting anemones are female and already transcribing *VTG* (see **Figure 1**). Decreases in vitellogenin in females can be useful for identifying EDCs (Ankley et al., 2002). If these anemones were male, then up-regulation of vitellogenin would have been expected. Up-regulation of vitellogenin in males is widely recognized as the prominent estrogenic effect in many aquatic animals exposed to exogenous E2 (Denslow et al., 1999; Matozzo et al., 2008). These results cannot confirm nor reject the possibility that male reproductive tissues were also present.

A second piece of evidence suggest that these anemones were female was the expression of *17βHSD14* in E2 which was significantly up-regulated ($p < 0.0001$) compared to the T, cholesterol, BBP, and BP-3 treatments. Female anemones perform oogenesis which is stimulated by the presence of E2 so when exogenous E2 is introduced, additional *17βHSD14* is required to reduce E2 potency by transformation into E1. In this investigation, *VTG* expression was crucial for differentiating E2 exposure from other EDC exposures. The expression profiles of *17βHSD14* and *17βHSD12* can be indirect measures of cellular demands for sex hormones. When exposed to exogenous sex hormones, transcription of *17βHSD14* is up-regulated while *17βHSD12* is not significantly different from the control. These results suggest these anemones were females responding to the EDCs in this investigation. Future investigations using these GOIs, coupled with lab-controlled methodologies to induce gametogenesis in recognized clonal lines of anemones should provide greater resolution in how these organisms respond to EDCs.

CONCLUSION

This data demonstrates that endocrine disrupting exogenous sterols (E2, T, cholesterol) and xenobiotics (BP-3, BBP) alter transcription of genes associated with steroidogenesis, sterol transport, oogenesis, and the Hedgehog signaling pathway (**Figures 1**–**4**). *In silico* modelling demonstrates that EDC's bind favorably into pockets of proteins involved with steroidogenesis, cholesterol transport, and HH signaling. Because these GOIs were expressed at basal levels in the control treatment (i.e. unstressed conditions) and significantly differentially expressed when exposed to EDCs (**Figure 4**), they may serve as transcriptional biomarkers. Biomarkers have the potential to link field and laboratory studies by acting as "mechanistic signposts" of exposure to anthropogenic chemicals (Hutchinson, 2007; Traylor-Knowles and Palumbi, 2014). The most validated biomarker of estrogenic exposure is *VTG*, an estrogen-dependent glycolipophosphoprotein naturally expressed only in oviparous females during the reproductive season (Verderame and Scudiero, 2017). The biomarkers used in this investigation offer new insight into BBP and BP-3

exposures. Understanding mechanisms of action for xenobiotics can be advanced by utilizing known biochemical pathways involving cholesterol and sex hormones.

Collectively, the expression profiles of this suite of GOIs are capable of discriminating seven distinct outcomes. 1) It is possible to discern differences between control vs exposure to exogenous chemicals (i.e. unstressed vs stressed) (see **Figures 1–4**). 2) Expression profiles of GOIs involved with HH signaling can differentiate E2 exposure from other sterols (see **Figure 3**). 3) Cholesterol exposure can be discriminated from sex hormones by expression of *C3* (see **Figures 4B–D**). 4) *C3* expression can also differentiate BP-3 versus BBP exposure (see **Figure 2**). 5) It is possible to differentiate natural sterols from xenobiotic exposure (see **Figure 4**). 6) Expression profiles of *VTG* and *17βHSD 12/14* provide a mechanism for discerning the responses of female reproductive tissues in E2 exposure compared to T or cholesterol exposures (see **Figure 1**). 7) Expression of *17βHSD14* and *17βHSD12* were critical for discerning BBP and BP-3 treatments compared to exogenous sterols (see **Figure 1**). Coupled with expression profiling, *in silico* results reveal proteins that bind cholesterol or modify sex hormones are vulnerable to endocrine disruption in the presence of either xenobiotics or exogenous sterols.

Future ecotoxicological investigations using more sensitive analytical measurements of chemical concentrations should enable identifying minimal concentrations necessary to alter expression of these GOIs. A primary goal of this investigation was to identify GOIs that are responsive to these EDCs. Moving forward, future work can focus on measuring GOI responses over recognized acute toxicity timeframes such as 24–96 hrs. Lastly, it will also be important to establish the baseline temporal variance in GOI expression before, during, and after the peak reproductive season.

In summary, this investigation provides new insight into anemone responsiveness to a small set of chemicals recognized as endocrine disruptors. Individually, each GOI provides a clue about a specific biochemical pathway, cellular process, and/or developmental pathway. Collectively, these GOIs offer greater resolution into understanding how anemones respond to different EDCs. More than a decade ago, Tarrant (2007) questioned if sex hormones are disrupting or even impacting cnidarians and the enigma of aromatase remains. However, the data herein offers new information towards deciphering endocrine disruption in cnidarians.

DATA AVAILABILITY STATEMENT

The original contributions presented in the study are included in the article/Supplementary Material, further inquiries can be directed to the corresponding author.

AUTHOR CONTRIBUTIONS

MM, JR, and JW conceived the investigation. JR, HY, JW, JE, RP, MM, DQ provided resources and financial support. JR, HY, JW, JE, MM, RP, DQ performed data collection and computational analysis. JW, HY, MM, DQ performed bioinformatics. MM wrote the manuscript with contributions from DQ, JR, JW, and HY. All authors approved the final manuscript.

FUNDING

Financial support was provided by Berry College for three Richards Scholarships (JR; JW; HY), and two Richards Undergraduate Support Grants (RP; JE).

REFERENCES

Al-Jandal, N., Saeed, T., Azad, I., Al-Subiai, S., Al-Zekri, W., Hussain, S., et al. (2018). Impact of Endocrine Disrupting Compounds in Sewage Impacted Coastal Area on Seabream. *Ecotoxicology Environ. Saf.* 150, 280–288. doi:10.1016/j.ecoenv.2017.12.035

Ankley, G. T., Kahl, M. D., Jensen, K. M., Hornung, M. W., Korte, J. J., Makynen, E. A., et al. (2002). Evaluation of the Aromatase Inhibitor Fadrozole in a Short-Term Reproduction Assay with the Fathead Minnow (*Pimephales promelas*). *Toxicol. Sci.* 67 (1), 121–130. doi:10.1093/toxsci/67.1.121

Archer, E., Petrie, B., Kasprzyk-Hordern, B., and Wolfaardt, G. M. (2017). The Fate of Pharmaceuticals and Personal Care Products (PPCPs), Endocrine Disrupting Contaminants (EDCs), Metabolites and Illicit Drugs in a WWTW and Environmental Waters. *Chemosphere* 174, 437–446. doi:10.1016/j.chemosphere.2017.01.101

Armoza-Zvuloni, R., Kramarsky-Winter, E., Loya, Y., Schlesinger, A., and Rosenfeld, H. (2014). Trioecy, a Unique Breeding Strategy in the Sea Anemone Aiptasia Diaphana and its Association with Sex Steroids1. *Biol. Repro* 90 (6), 1–8. doi:10.1095/biolreprod.113.114116

Atkinson, S., and Atkinson, M. J. (1992). Detection of Estradiol-17? during a Mass Coral Spawn. *Coral Reefs* 11 (1), 33–35. doi:10.1007/bf00291932

Atkinson, S., Atkinson, M. J., and Tarrant, A. M. (2003). Estrogens from Sewage in Coastal Marine Environments. *Environ. Health Perspect.* 111 (4), 531–535. doi:10.1289/ehp.5233

Axworthy, J. B., and Padilla-Gamiño, J. L. (2019). Microplastics Ingestion and Heterotrophy in Thermally Stressed Corals. *Sci. Rep.* 9 (1), 18193. doi:10.1038/s41598-019-54698-7

Bahr, K. D., Jokiel, P. L., and Toonen, R. J. (2015). The Unnatural History of Kāne'ohe Bay: Coral Reef Resilience in the Face of Centuries of Anthropogenic Impacts. *PeerJ* 3, e950. doi:10.7717/peerj.950

Bargar, T. A., Garrison, V. H., Alvarez, D. A., and Echols, K. R. (2013). Contaminants Assessment in the Coral Reefs of Virgin Islands National Park and Virgin Islands Coral Reef National Monument. *Mar. Pollut. Bull.* 70 (1-2), 281–288. doi:10.1016/j.marpolbul.2013.03.001

Blomquist, C. H., Lima, P. H., Tarrant, A. M., Atkinson, M. J., and Atkinson, S. (2006). 17β-Hydroxysteroid Dehydrogenase (17β-HSD) in Scleractinian Corals and Zooxanthellae. *Comp. Biochem. Physiol. B: Biochem. Mol. Biol.* 143 (4), 397–403. doi:10.1016/j.cbpb.2005.12.017

Borch, J., Metzdorff, S. B., Vinggaard, A. M., Brokken, L., and Dalgaard, M. (2006). Mechanisms Underlying the Anti-androgenic Effects of Diethylhexyl Phthalate in Fetal Rat Testis. *Toxicology* 223 (1-2), 144–155. doi:10.1016/j.tox.2006.03.015

Brennan, J. J., Messerschmidt, J. L., Williams, L. M., Matthews, B. J., Reynoso, M., and Gilmore, T. D. (2017). Sea Anemone Model Has a Single Toll-like Receptor that Can Function in Pathogen Detection, NF-Kb Signal Transduction, and Development. *Proc. Natl. Acad. Sci. USA* 114 (47), E10122–E10131. doi:10.1073/pnas.1711530114

Bruno, J. F., and Selig, E. R. (2007). Regional Decline of Coral Cover in the Indo-Pacific: Timing, Extent, and Subregional Comparisons. *PLoS One* 2 (8), e711. doi:10.1371/journal.pone.0000711

Bucher, M., Wolfowicz, I., Voss, P. A., Hambleton, E. A., and Guse, A. (2016). Development and Symbiosis Establishment in the Cnidarian Endosymbiosis Model Aiptasia Sp. *Sci. Rep.* 6 (1), 19867. doi:10.1038/srep19867

Burns, K., and Brinkman, D. (2011). Organic Biomarkers to Describe the Major Carbon Inputs and Cycling of Organic Matter in the central Great Barrier Reef Region. *Estuarine, Coastal Shelf Sci.* 93 (2), 132–141. doi:10.1016/j.ecss.2011.04.001

Bustin, S. A., Benes, V., Garson, J. A., Hellemans, J., Huggett, J., Kubista, M., et al. (2009). The MIQE Guidelines: Minimum Information for Publication of Quantitative Real-Time PCR Experiments. *Clin. Chem.* 55 (4), 611–622. doi:10.1373/clinchem.2008.112797

Caldwell, D. J., Mastrocco, F., Anderson, P. D., Länge, R., and Sumpter, J. P. (2012). Predicted-no-effect Concentrations for the Steroid Estrogens Estrone, 17β-Estradiol, Estriol, and 17α-Ethinylestradiol. *Environ. Toxicol. Chem.* 31 (6), 1396–1406. doi:10.1002/etc.1825

Carpenter, D., Stone, D. M., Brush, J., Ryan, A., Armanini, M., Frantz, G., et al. (1998). Characterization of Two Patched Receptors for the Vertebrate Hedgehog Protein Family. *Proc. Natl. Acad. Sci.* 95 (23), 13630–13634. doi:10.1073/pnas.95.23.13630

Chen, J. K., Taipale, J., Cooper, M. K., and Beachy, P. A. (2002). Inhibition of Hedgehog Signaling by Direct Binding of Cyclopamine to Smoothened. *Genes Dev.* 16 (21), 2743–2748. doi:10.1101/gad.1025302

Clayton, W. (1985). Pedal Laceration by the Anemone Aiptasia Pallida. *Mar. Ecol. Prog. Ser.* 21 (1-2), 75–80. doi:10.3354/meps021075

Corcoran, R. B., and Scott, M. P. (2006). Oxysterols Stimulate Sonic Hedgehog Signal Transduction and Proliferation of Medulloblastoma Cells. *Proc. Natl. Acad. Sci.* 103 (22), 8408–8413. doi:10.1073/pnas.0602852103

Dachs, J., Bayona, J. M., Ittekkot, V., and Albaigés, J. (1999). Monsoon-Driven Vertical Fluxes of Organic Pollutants in the Western Arabian Sea. *Environ. Sci. Technol.* 33 (22), 3949–3956. doi:10.1021/es990200e

Dani, V., Ganot, P., Priouzeau, F., Furla, P., and Sabourault, C. (2014). Are Niemann-Pick Type C Proteins Key Players in Cnidarian-Dinoflagellate Endosymbioses? *Mol. Ecol.* 23 (18), 4527–4540. doi:10.1111/mec.12876

Dani, V., Priouzeau, F., Mertz, M., Mondin, M., Pagnotta, S., Lacas-Gervais, S., et al. (2017). Expression Patterns of Sterol Transporters NPC1 and NPC2 in the Cnidarian-Dinoflagellate Symbiosis. *Cell Microbiol.* 19 (10), e12753. doi:10.1111/cmi.12753

Deng, Y., Yan, Z., Shen, R., Wang, M., Huang, Y., Ren, H., et al. (2020). Microplastics Release Phthalate Esters and Cause Aggravated Adverse Effects in the Mouse Gut. *Environ. Int.* 143, 105916. doi:10.1016/j.envint.2020.105916

Denslow, N. D., Bowman, C. J., Robinson, G., Lee, H. S., Ferguson, R. J., Hemmer, M. J., et al. (1999). "Biomarkers of Endocrine Disruption at the mRNA Level," in *Environmental Toxicology and Risk Assessment: Standardization of Biomarkers of Endocrine Disruption and Environmental Assessment*. Editors D. S. Henshel, M. C. Black, and M. C. Harrass (West Conshohocken: American Society for Testing Materials), 8, 24–35.

DiNardo, J. C., and Downs, C. A. (2018). Dermatological and Environmental Toxicological Impact of the Sunscreen Ingredient Oxybenzone/benzophenone-3. *J. Cosmet. Dermatol.* 17 (1), 15–19. doi:10.1111/jocd.12449

Downs, C. A., Kramarsky-Winter, E., Segal, R., Fauth, J., Knutson, S., Bronstein, O., et al. (2016). Toxicopathological Effects of the Sunscreen UV Filter, Oxybenzone (Benzophenone-3), on Coral Planulae and Cultured Primary Cells and its Environmental Contamination in Hawaii and the U.S. Virgin Islands. *Arch. Environ. Contam. Toxicol.* 70 (2), 265–288. doi:10.1007/s00244-015-0227-7

Duffy, D. J., and Frank, U. (2011). Modulation of COUP-TF Expression in a Cnidarian by Ectopic Wnt Signalling and Allorecognition. *PLoS One* 6 (4), e19443. doi:10.1371/journal.pone.0019443

Dunn, S. R., Phillips, W. S., Spatafora, J. W., Green, D. R., and Weis, V. M. (2006). Highly Conserved Caspase and Bcl-2 Homologues from the Sea Anemone *Aiptasia Pallida*: Lower Metazoans as Models for the Study of Apoptosis Evolution. *J. Mol. Evol.* 63 (1), 95–107. doi:10.1007/s00239-005-0236-7

Edge, S. E., Shearer, T. L., Morgan, M. B., and Snell, T. W. (2013). Sub-lethal Coral Stress: Detecting Molecular Responses of Coral Populations to Environmental Conditions over Space and Time. *Aquat. Toxicol.* 128-129, 135–146. doi:10.1016/j.aquatox.2012.11.014

Edman, C. F., Prigent, S. A., Schipper, A., and Feramisco, J. R. (1997). Identification of ErbB3-Stimulated Genes Using Modified Representational Difference Analysis. *Biochem. J* 323, 113–118. doi:10.1042/bj3230113

Fabricius, K. E. (2005). Effects of Terrestrial Runoff on the Ecology of Corals and Coral Reefs: Review and Synthesis. *Mar. Pollut. Bull.* 50 (2), 125–146. doi:10.1016/j.marpolbul.2004.11.028

Flood, V. S., Pitt, J. M., and Smith, S. R. (2005). Coral Communities on Patch Reefs in Castle Harbour Bermuda after More Than a century of Perturbations. *Mar. Poll Bull.* 51 (5-7), 545–557. doi:10.1016/j.marpolbul.2005.07.010

French, V. A., Codi King, S., Kumar, A., Northcott, G., McGuinness, K., and Parry, D. (2015). Characterisation of Microcontaminants in Darwin Harbour, a Tropical Estuary of Northern Australia Undergoing Rapid Development. *Sci. Total Environ.* 536, 639–647. doi:10.1016/j.scitotenv.2015.07.114

Fuentes, N., and Silveyra, P. (2019). Estrogen Receptor Signaling Mechanisms. *Adv. Protein Chem. Str* 116, 135–170. doi:10.1016/bs.apcsb.2019.01.001

Ganot, P., Moya, A., Magnone, V., Allemand, D., Furla, P., and Sabourault, C. (2011). Adaptations to Endosymbiosis in a Cnidarian-Dinoflagellate Association: Differential Gene Expression and Specific Gene Duplications. *Plos Genet.* 7 (7), e1002187. doi:10.1371/journal.pgen.1002187

Gao, D.-W., and Wen, Z.-D. (2016). Phthalate Esters in the Environment: A Critical Review of Their Occurrence, Biodegradation, and Removal during Wastewater Treatment Processes. *Sci. Total Environ.* 541, 986–1001. doi:10.1016/j.scitotenv.2015.09.148

Gardner, T. A., Côte´, I. M., Gill, J. A., Grant, A., and Watkinson, A. R. (2003). Long-Term Region-wide Declines in Caribbean Corals. *Science* 301 (5635), 958–960. doi:10.1126/science.1086050

Gassman, N., and Kennedy, C. (1992). Cytochrome P-450 Content and Xenobiotic Metabolizing Enzyme Activities in the Scleractinian Coral, *Favia fragum* (Esper). *Bull. Mar. Sci.* 50 (2), 320–330.

Gavio, B., Palmer-Cantillo, S., and Mancera, J. E. (2010). Historical Analysis (2000-2005) of the Coastal Water Quality in San Andrés Island, SeaFlower Biosphere Reserve, Caribbean Colombia. *Mar. Pollut. Bull.* 60 (7), 1018–1030. doi:10.1016/j.marpolbul.2010.01.025

Goldstone, J. V. (2008). Environmental Sensing and Response Genes in Cnidaria: the Chemical Defensome in the Sea Anemone *Nematostella vectensis*. *Cell Biol Toxicol* 24 (6), 483–502. doi:10.1007/s10565-008-9107-5

Grawunder, D., Hambleton, E. A., Bucher, M., Wolfowicz, I., Bechtoldt, N., and Guse, A. (2015). Induction of Gametogenesis in the Cnidarian Endosymbiosis Model Aiptasia Sp. *Sci. Rep.* 5 (1), 15677. doi:10.1038/srep15677

Hall, N. M., Berry, K. L. E., Rintoul, L., and Hoogenboom, M. O. (2015). Microplastic Ingestion by Scleractinian Corals. *Mar. Biol.* 162 (3), 725–732. doi:10.1007/s00227-015-2619-7

Hambleton, E. A., Jones, V. A. S., Maegele, I., Kvaskoff, D., Sachsenheimer, T., and Guse, A. (2019). Sterol Transfer by Atypical Cholesterol-Binding NPC2 Proteins in Coral-Algal Symbiosis. *eLife* 8, e43923. doi:10.7554/eLife.43923

Hanwell, M. D., Curtis, D. E., Lonie, D. C., Vandermeersch, T., Zurek, E., and Hutchison, G. R. (2012). Avogadro: an Advanced Semantic Chemical Editor, Visualization, and Analysis Platform. *J. Cheminform* 4 (1), 17. doi:10.1186/1758-2946-4-17

Hayakawa, H., Nakano, Y., Andoh, T., and Watanabe, T. (2005). Sex-dependent Expression of mRNA Encoding a Major Egg Protein in the Gonochoric Coral Galaxea Fascicularis. *Coral Reefs* 24 (3), 488–494. doi:10.1007/s00338-005-0485-3

Heindel, J. J., Zoeller, R. T., Jobling, S., Iguchi, T., Vandenberg, L., and Woodruff, T. J. (2012). "What Is Endocrine Disruption All about," in *State of the Science of Endocrine Disrupting Chemicals - 2012*. Editors Å. Bergman, J. J. Heindel, S. Jobling, K. A. Kidd, and R. T. Zoeller (Geneva, Switzerland: World Health Organization), 289.

Hong, H., Rua, D., Sakkiah, S., Selvaraj, C., Ge, W., and Tong, W. (2016). Consensus Modeling for Prediction of Estrogenic Activity of Ingredients Commonly Used in Sunscreen Products. *Ijerph* 13 (10), 958. doi:10.3390/ijerph13100958

Hu, A., and Song, B.-L. (2019). The Interplay of Patched, Smoothened and Cholesterol in Hedgehog Signaling. *Curr. Opin. Cel Biol.* 61, 31–38. doi:10.1016/j.ceb.2019.06.008

Hubank, M., and Schatz, D. G. (1999). "cDNA Representational Difference Analysis: A Sensitive and Flexible Method for Identification of Differentially Expressed Genes," in *Methods in Enzymology; cDNA Preparation and*

Characterization. Editor S. M. Weissman (San Diego, California, USA: Academic Press), 303, 325–349. doi:10.1016/s0076-6879(99)03021-9

Hughes, T. P., Baird, A. H., Bellwood, D. R., Card, M., Connolly, S. R., Folke, C., et al. (2003). Climate Change, Human Impacts, and the Resilience of Coral Reefs. *Science* 301 (5635), 929–933. doi:10.1126/science.1085046

Hutchinson, T. H. (2007). Small Is Useful in Endocrine Disrupter Assessment-Four Key Recommendations for Aquatic Invertebrate Research. *Ecotoxicology* 16 (1), 231–238. doi:10.1007/s10646-006-0107-z

Imbs, A. B. (2013). Fatty Acids and Other Lipids of Corals: Composition, Distribution, and Biosynthesis. *Russ. J. Mar. Biol.* 39 (3), 153–168. doi:10.1134/s1063074013030061

Incardona, J. P., Lee, J. H., Robertson, C. P., Enga, K., Kapur, R. P., and Roelink, H. (2000). Receptor-mediated Endocytosis of Soluble and Membrane-Tethered Sonic Hedgehog by Patched-1. *Proc. Natl. Acad. Sci. U S A.* 97 (22), 12044–12049. doi:10.1073/pnas.220251997

Infante, R. E., Wang, M. L., Radhakrishnan, A., Kwon, H. J., Brown, M. S., and Goldstein, J. L. (2008). NPC2 Facilitates Bidirectional Transfer of Cholesterol between NPC1 and Lipid Bilayers, a Step in Cholesterol Egress from Lysosomes. *Proc. Natl. Acad. Sci. U S A.* 105 (40), 15287–15292. doi:10.1073/pnas.0807328105

Johansson, H. K. L., and Svingen, T. (2020). Hedgehog Signal Disruption, Gonadal Dysgenesis and Reproductive Disorders: Is There a Link to Endocrine Disrupting Chemicals? *Curr. Res. Toxicol.* 1, 116–123. doi:10.1016/j.crtox.2020.10.001

Jones, G. P., McCormick, M. I., Srinivasan, M., and Eagle, J. V. (2004). Coral Decline Threatens Fish Biodiversity in marine Reserves. *Proc. Natl. Acad. Sci.* 101 (21), 8251–8253. doi:10.1073/pnas.0401277101

Jones, R. (2010). Environmental Contamination Associated with a marine Landfill ('seafill') beside a Coral Reef. *Mar. Pollut. Bull.* 60 (11), 1993–2006. doi:10.1016/j.marpolbul.2010.07.028

Jones, R., Muller, J., Haynes, D., and Schreiber, U. (2003). Effects of Herbicides Diuron and Atrazine on Corals of the Great Barrier Reef, Australia. *Mar. Ecol. Prog. Ser.* 251, 153–167. doi:10.3354/meps251153

Kenkel, C. D., Aglyamova, G., Alamaru, A., Bhagooli, R., Capper, R., Cunning, R., et al. (2011). Development of Gene Expression Markers of Acute Heat-Light Stress in Reef-Building Corals of the Genus *Porites*. *PLoS One* 6 (10), e26914. doi:10.1371/journal.pone.0026914

Kenkel, C. D., Sheridan, C., Leal, M. C., Bhagooli, R., Castillo, K. D., Kurata, N., et al. (2014). Diagnostic Gene Expression Biomarkers of Coral thermal Stress. *Mol. Ecol. Resour.* 14 (4), 667–678. doi:10.1111/1755-0998.12218

Kerswell, A., and Jones, R. (2003). Effects of Hypo-Osmosis on the Coral Stylophora Pistillata: Nature and Cause of 'low-Salinity Bleaching'. *Mar. Ecol. Prog. Ser.* 253, 145–154. doi:10.3354/meps253145

Khalturin, K., Billas, I. M. L., Chebaro, Y., Reitzel, A. M., Tarrant, A. M., Laudet, V., et al. (2018). NR3E Receptors in Cnidarians: A New Family of Steroid Receptor Relatives Extends the Possible Mechanisms for Ligand Binding. *J. Steroid Biochem. Mol. Biol.* 184, 11–19. doi:10.1016/j.jsbmb.2018.06.014

Ko, F.-C., Chang, C.-W., and Cheng, J.-O. (2014). Comparative Study of Polycyclic Aromatic Hydrocarbons in Coral Tissues and the Ambient Sediments from Kenting National Park, Taiwan. *Environ. Pollut.* 185, 35–43. doi:10.1016/j.envpol.2013.10.025

Kvennefors, E. C. E., Leggat, W., Kerr, C. C., Ainsworth, T. D., Hoegh-Guldberg, O., and Barnes, A. C. (2010). Analysis of Evolutionarily Conserved Innate Immune Components in Coral Links Immunity and Symbiosis. *Dev. Comp. Immunol.* 34 (11), 1219–1229. doi:10.1016/j.dci.2010.06.016

Lafont, R., and Mathieu, M. (2007). Steroids in Aquatic Invertebrates. *Ecotoxicology* 16 (1), 109–130. doi:10.1007/s10646-006-0113-1

LaPlante, C. D., Bansal, R., Dunphy, K. A., Jerry, D. J., and Vandenberg, L. N. (2018). Oxybenzone Alters Mammary Gland Morphology in Mice Exposed during Pregnancy and Lactation. *J. Endocr. Soc.* 2 (8), 903–921. doi:10.1210/js.2018-00024

Laskowski, R. A., and Swindells, M. B. (2011). LigPlot+: Multiple Ligand-Protein Interaction Diagrams for Drug Discovery. *J. Chem. Inf. Model.* 51 (10), 2778–2786. doi:10.1021/ci200227u

Lathe, R., and Kotelevtsev, Y. (2014). Steroid Signaling: Ligand-Binding Promiscuity, Molecular Symmetry, and the Need for Gating. *Steroids* 82, 14–22. doi:10.1016/j.steroids.2014.01.002

Law, K. L. (2017). Plastics in the Marine Environment. *Annu. Rev. Mar. Sci.* 9 (1), 205–229. doi:10.1146/annurev-marine-010816-060409

Lebreton, L., Slat, B., Ferrari, F., Sainte-Rose, B., Aitken, J., Marthouse, R., et al. (2018). Evidence that the Great Pacific Garbage Patch Is Rapidly Accumulating Plastic. *Sci. Rep.* 8 (1), 4666. doi:10.1038/s41598-018-22939-w

Lenarčič, B., Ritonja, A., Štrukelj, B., and Turk, V. (1997). Equistatin, a New Inhibitor of Cysteine Proteinases fromActinia Equina, Is Structurally Related to Thyroglobulin Type-1 Domain. *J. Biol. Chem.* 272 (21), 13899–13903. doi:10.1074/jbc.272.21.13899

Levitan, S., Sher, N., Brekhman, V., Ziv, T., Lubzens, E., and Lotan, T. (2015). The Making of an Embryo in a Basal Metazoan: Proteomic Analysis in the Sea anemoneNematostella Vectensis. *Proteomics* 15 (23-24), 4096–4104. doi:10.1002/pmic.201500255

Lipinski, R. J., and Bushman, W. (2010). Identification of Hedgehog Signaling Inhibitors with Relevant Human Exposure by Small Molecule Screening. *Toxicol. Vitro* 24 (5), 1404–1409. doi:10.1016/j.tiv.2010.04.011

Lotan, T., Chalifa-Caspi, V., Ziv, T., Brekhman, V., Gordon, M. M., Admon, A., et al. (2014). Evolutionary Conservation of the Mature Oocyte Proteome. *EuPA Open Proteomics* 3, 27–36. doi:10.1016/j.euprot.2014.01.003

Lu, Y., Jiang, J., Zhao, H., Han, X., Xiang, Y., and Zhou, W. (2020). Clade-Specific Sterol Metabolites in Dinoflagellate Endosymbionts Are Associated with Coral Bleaching in Response to Environmental Cues. *mSystems* 5 (5), e00765. doi:10.1128/msystems.00765-20

Luu-The, V., Tremblay, P., and Labrie, F. (2006). Characterization of Type 12 17β-Hydroxysteroid Dehydrogenase, an Isoform of Type 3 17β-Hydroxysteroid Dehydrogenase Responsible for Estradiol Formation in Women. *Mol. Endocrinol.* 20 (2), 437–443. doi:10.1210/me.2005-0058

Mahon, A. M., O'Connell, B., Healy, M. G., O'Connor, I., Officer, R., Nash, R., et al. (2017). Microplastics in Sewage Sludge: Effects of Treatment. *Environ. Sci. Technol.* 51 (2), 810–818. doi:10.1021/acs.est.6b04048

Mansfield, K. M., Carter, N. M., Nguyen, L., Cleves, P. A., Alshanbayeva, A., Williams, L. M., et al. (2017). Transcription Factor NF-Kb Is Modulated by Symbiotic Status in a Sea Anemone Model of Cnidarian Bleaching. *Sci. Rep.* 7 (1), 16025. doi:10.1038/s41598-017-16168-w

Matouskova, K., Jerry, D. J., and Vandenberg, L. N. (2020). Exposure to Low Doses of Oxybenzone during Perinatal Development Alters Mammary Gland Morphology in Male and Female Mice. *Reprod. Toxicol.* 92, 66–77. doi:10.1016/j.reprotox.2019.08.002

Matozzo, V., Gagné, F., Marin, M. G., Ricciardi, F., and Blaise, C. (2008). Vitellogenin as a Biomarker of Exposure to Estrogenic Compounds in Aquatic Invertebrates: A Review. *Environ. Int.* 34 (4), 531–545. doi:10.1016/j.envint.2007.09.008

Matus, D. Q., Magie, C. R., Pang, K., Martindale, M. Q., and Thomsen, G. H. (2008). The Hedgehog Gene Family of the Cnidarian, *Nematostella vectensis*, and Implications for Understanding Metazoan Hedgehog Pathway Evolution. *Dev. Biol.* 313 (2), 501–518. doi:10.1016/j.ydbio.2007.09.032

Maxfield, F. R., Iaea, D. B., and Pipalia, N. H. (2016). Role of STARD4 and NPC1 in Intracellular Sterol Transport. *Biochem. Cel Biol.* 94 (6), 499–506. doi:10.1139/bcb-2015-0154

McKenna, S. A., Richmond, R. H., and Roos, G. (2001). Assessing the Effects of Sewage on Coral Reefs: Developing Techniques to Detect Stress before Coral Mortality. *Bull. Mar. Sci.* 69 (2), 517–523.

Miller, D. J., Hemmrich, G., Ball, E. E., Hayward, D. C., Khalturin, K., Funayama, N., et al. (2007). The Innate Immune Repertoire in Cnidaria - Ancestral Complexity and Stochastic Gene Loss. *Genome Biol.* 8 (4), R59. doi:10.1186/gb-2007-8-4-r59

Mitchelmore, C. L., He, K., Gonsior, M., Hain, E., Heyes, A., Clark, C., et al. (2019). Occurrence and Distribution of UV-Filters and Other Anthropogenic Contaminants in Coastal Surface Water, Sediment, and Coral Tissue from Hawaii. *Sci. Total Environ.* 670, 398–410. doi:10.1016/j.scitotenv.2019.03.034

Mohamed, A. R., Cumbo, V., Harii, S., Shinzato, C., Chan, C. X., Ragan, M. A., et al. (2016). The Transcriptomic Response of the Coral Acropora Digitifera to a Competent Symbiodinium Strain: the Symbiosome as an Arrested Early Phagosome. *Mol. Ecol.* 25 (13), 3127–3141. doi:10.1111/mec.13659

Morgan, M. B., Parker, C. C., Robinson, J. W., and Pierce, E. M. (2012). Using Representational Difference Analysis to Detect Changes in Transcript Expression of *Aiptasia* Genes after Laboratory Exposure to Lindane. *Aquat. Toxicol.* 110-111, 66–73. doi:10.1016/j.aquatox.2012.01.001

Morgan, M. B., Vogelien, D. L., and Snell, T. W. (2001). Assessing Coral Stress Responses Using Molecular Biomarkers of Gene Transcription. *Environ. Toxicol. Chem.* 20 (3), 5372–5543. doi:10.1897/1551-5028(2001)020<0537:acsrum>2.0.co10.1002/etc.5620200312

Morgan, M., Goodner, K., Ross, J., Poole, A. Z., Stepp, E., Stuart, C. H., et al. (2015). Development and Application of Molecular Biomarkers for Characterizing Caribbean Yellow Band Disease inOrbicella Faveolata. *PeerJ* 3, e1371. doi:10.7717/peerj.1371

Ocampo, I. D., Zárate-Potes, A., Pizarro, V., Rojas, C. A., Vera, N. E., and Cadavid, L. F. (2015). The Immunotranscriptome of the Caribbean Reef-Building Coral Pseudodiploria Strigosa. *Immunogenetics* 67 (9), 515–530. doi:10.1007/s00251-015-0854-1

Palmer, C. V., and Traylor-Knowles, N. (2012). Towards an Integrated Network of Coral Immune Mechanisms. *Proc. R. Soc. B.* 279 (1745), 4106–4114. doi:10.1098/rspb.2012.1477

Pandolfi, J. M., Bradbury, R. H., Sala, E., Hughes, T. P., Bjorndal, K. A., Cooke, R. G., et al. (2003). Global Trajectories of the Long-Term Decline of Coral Reef Ecosystems. *Science* 301 (5635), 955–958. doi:10.1126/science.1085706

Pastorian, K., Hawel, L., and Byus, C. V. (2000). Optimization of cDNA Representational Difference Analysis for the Identification of Differentially Expressed mRNAs. *Anal. Biochem.* 283 (1), 89–98. doi:10.1006/abio.2000.4622

Peters, E. C., Gassman, N. J., Firman, J. C., Richmond, R. H., and Power, E. A. (1997). Ecotoxicology of Tropical Marine Ecosystems. *Environ. Toxicol. Chem.* 16 (1), 12–40. doi:10.1002/etc.5620160103

Pettersen, E. F., Goddard, T. D., Huang, C. C., Couch, G. S., Greenblatt, D. M., Meng, E. C., et al. (2004). UCSF Chimera?A Visualization System for Exploratory Research and Analysis. *J. Comput. Chem.* 25 (13), 1605–1612. doi:10.1002/jcc.20084

Putnam, N. H., Srivastava, M., Hellsten, U., Dirks, B., Chapman, J., Salamov, A., et al. (2007). Sea Anemone Genome Reveals Ancestral Eumetazoan Gene Repertoire and Genomic Organization. *Science* 317 (5834), 86–94. doi:10.1126/science.1139158

Qualmann, B., Kessels, M. M., Thole, H. H., and Sierralta, W. D. (2000). A Hormone Pulse Induces Transient Changes in the Subcellular Distribution and Leads to a Lysosomal Accumulation of the Estradiol Receptor α in Target Tissues. *Eur. J. Cel Biol.* 79 (6), 383–393. doi:10.1078/0171-9335-00061

Reitzel, A. M., Sullivan, J. C., Traylor-Knowles, N., and Finnerty, J. R. (2008). Genomic Survey of Candidate Stress-Response Genes in the Estuarine AnemoneNematostella Vectensis. *Biol. Bull.* 214 (3), 233–254. doi:10.2307/25470666

Reitzel, A. M., and Tarrant, A. M. (2009). Nuclear Receptor Complement of the Cnidarian *Nematostella vectensis*: Phylogenetic Relationships and Developmental Expression Patterns. *BMC Evol. Biol.* 9, 230. doi:10.1186/1471-2148-9-230

Revel, J., Massi, L., Mehiri, M., Boutoute, M., Mayzaud, P., Capron, L., et al. (2016). Differential Distribution of Lipids in Epidermis, Gastrodermis and Hosted Symbiodinium in the Sea Anemone Anemonia Viridis. *Comp. Biochem. Physiol. A: Mol. Integr. Physiol.* 191, 140–151. doi:10.1016/j.cbpa.2015.10.017

Rotinen, M., Celay, J., Alonso, M. M., Arrazola, A., Encio, I., and Villar, J. (2009). Estradiol Induces Type 8 17β-Hydroxysteroid Dehydrogenase Expression: Crosstalk between Estrogen Receptor α and C/EBPβ. *J. Endrocrinol* 200 (1), 85–92. doi:10.1677/JOE-08-0134

Rotjan, R. D., Sharp, K. H., Gauthier, A. E., Yelton, R., Lopez, E. M. B., Carilli, J., et al. (2019). Patterns, Dynamics and Consequences of Microplastic Ingestion by the Temperate Coral, Astrangia Poculata. *Proc. R. Soc. B.* 286, 20190726. doi:10.1098/rspb.2019.0726

Salah, M., Abdelsamie, A. S., and Frotscher, M. (2019). Inhibitors of 17β-Hydroxysteroid Dehydrogenase Type 1, 2 and 14: Structures, Biological Activities and Future Challenges. *Mol. Cell Endocrinol.* 489, 66–81. doi:10.1016/j.mce.2018.10.001

Sanders, S. M., Shcheglovitova, M., and Cartwright, P. (2014). Differential Gene Expression between Functionally Specialized Polyps of the Colonial Hydrozoan Hydractinia Symbiolongicarpus (Phylum Cnidaria). *BMC Genomics* 15 (1), 406. doi:10.1186/1471-2164-15-406

Schlesinger, A., Kramarsky-Winter, E., Rosenfeld, H., Armoza-Zvoloni, R., and Loya, Y. (2010). Sexual Plasticity and Self-Fertilization in the Sea Anemone Aiptasia Diaphana. *PLoS One* 5 (7), e11874. doi:10.1371/journal.pone.0011874

Sheikh, I. A., and Beg, M. A. (2017). Endocrine Disruption: In Silico Interactions between Phthalate Plasticizers and Corticosteroid Binding Globulin. *J. Appl. Toxicol.* 37 (12), 1471–1480. doi:10.1002/jat.3497

Shikina, S., and Chang, C.-F. (2016). "Sexual Reproduction in Stony Corals and Insight into the Evolution of Oogenesis in Cnidaria," in *The Cnidaria, Past, Present and Future* (Switzerland: Springer), 249–268. doi:10.1007/978-3-319-31305-4_16

Shikina, S., Chen, C.-J., Chung, Y.-J., Shao, Z.-F., Liou, J.-Y., Tseng, H.-P., et al. (2013). Yolk Formation in a Stony Coral Euphyllia Ancora (Cnidaria, Anthozoa): Insight into the Evolution of Vitellogenesis in Nonbilaterian Animals. *Endocrinology* 154 (9), 3447–3459. doi:10.1210/en.2013-1086

Shikina, S., Chung, Y.-J., Chiu, Y.-L., Huang, Y.-J., Lee, Y.-H., and Chang, C.-F. (2016). Molecular Cloning and Characterization of a Steroidogenic Enzyme, 17β-Hydroxysteroid Dehydrogenase Type 14, from the Stony Coral Euphyllia Ancora (Cnidaria, Anthozoa). *Gen. Comp. Endocrinol.* 228, 95–104. doi:10.1016/j.ygcen.2016.02.006

Singh, S. P., Azua, A., Chaudhary, A., Khan, S., Willett, K. L., and Gardinali, P. R. (2010). Occurrence and Distribution of Steroids, Hormones and Selected Pharmaceuticals in South Florida Coastal Environments. *Ecotoxicology* 19 (2), 338–350. doi:10.1007/s10646-009-0416-0

Sinkovics, J. (2015). The Cnidarian Origin of the Proto-Oncogenes NF-Kb/STAT and WNT-like Oncogenic Pathway Drives the Ctenophores (Review). *Int. J. Oncol.* 47 (4), 1211–1229. doi:10.3892/ijo.2015.3102

Sivik, T., Vikingsson, S., Gréen, H., and Jansson, A. (2012). Expression Patterns of 17β-Hydroxysteroid Dehydrogenase 14 in Human Tissues. *Horm. Metab. Res.* 44 (13), 949–956. doi:10.1055/s-0032-1321815

Slattery, M., Hines, G. A., Starmer, J., and Paul, V. J. (1999). Chemical Signals in Gametogenesis, Spawning, and Larval Settlement and Defense of the Soft Coral *Sinularia Polydactyla*. *Coral Reefs* 18 (1), 75–84. doi:10.1007/s003380050158

Snape, J. R., Maund, S. J., Pickford, D. B., and Hutchinson, T. H. (2004). Ecotoxicogenomics: the challenge of Integrating Genomics into Aquatic and Terrestrial Ecotoxicology. *Aquat. Toxicol.* 67 (2), 143–154. doi:10.1016/j.aquatox.2003.11.011

Snell, T. W., Brogdon, S. E., and Morgan, M. B. (2003). Gene Expression Profiling in Ecotoxicology. *Ecotoxicology* 12 (6), 475–483. doi:10.1023/B:ECTX.0000003033.09923.a8

Solbakken, J. E., Knap, A. H., and Orr, P. L. (1985). Uptake and Elimination of Lindane and a Phthalate Ester in Tropical Corals and Mussels. *Mar. Environ. Res.* 16, 103–113. doi:10.1016/0141-1136(85)90012-1

Stien, D., Suzuki, M., Rodrigues, A. M. S., Yvin, M., Clergeaud, F., Thorel, E., et al. (2020). A Unique Approach to Monitor Stress in Coral Exposed to Emerging Pollutants. *Sci. Rep.* 10 (1), 9601. doi:10.1038/s41598-020-66117-3

Štrukelj, B., Lenarčič, B., Gruden, K., Pungerčar, J., Rogelj, B., Turk, V., et al. (2000). Equistatin, a Protease Inhibitor from the Sea Anemone *Actinia equina*, Is Composed of Three Structural and Functional Domains. *Biochem. Biophysical Res. Commun.* 269 (3), 732–736. doi:10.1006/bbrc.2000.2356

Strutt, H., Thomas, C., Nakano, Y., Stark, D., Neave, B., Taylor, A. M., et al. (2001). Mutations in the Sterol-Sensing Domain of Patched Suggest a Role for Vesicular Trafficking in Smoothened Regulation. *Curr. Biol.* 11 (8), 608–613. doi:10.1016/S0960-9822(01)00179-8

Sutherland, K. P., Porter, J. W., Turner, J. W., Thomas, B. J., Looney, E. E., Luna, T. P., et al. (2010). Human Sewage Identified as Likely Source of white Pox Disease of the Threatened Caribbean elkhorn Coral, Acropora Palmata. *Environ. Microbiol.* 12 (5), 1122–1131. doi:10.1111/j.1462-2920.2010.02152.x

Tan, B. L. L., Hawker, D. W., Müller, J. F., Leusch, F. D. L., Tremblay, L. A., and Chapman, H. F. (2007). Comprehensive Study of Endocrine Disrupting Compounds Using Grab and Passive Sampling at Selected Wastewater Treatment Plants in South East Queensland, Australia. *Environ. Int.* 33 (5), 654–669. doi:10.1016/j.envint.2007.01.008

Tarrant, A., Atkinson, M., and Atkinson, S. (2001). Uptake of Estrone from the Water Column by a Coral Community. *Mar. Biol.* 139 (2), 321–325. doi:10.1007/s002270100556

Tarrant, A., Atkinson, M., and Atkinson, S. (2004). Effects of Steroidal Estrogens on Coral Growth and Reproduction. *Mar. Ecol. Prog. Ser.* 269, 121–129. doi:10.3354/meps269121

Tarrant, A. M., Atkinson, S., and Atkinson, M. J. (1999). Estrone and Estradiol-17β Concentration in Tissue of the Scleractinian Coral, Montipora Verrucosa.

Comp. Biochem. Physiol. Part A: Mol. Integr. Physiol. 122 (1), 85–92. doi:10.1016/s1095-6433(98)10155-1

Tarrant, A. M., Blomquist, C. H., Lima, P. H., Atkinson, M. J., and Atkinson, S. (2003). Metabolism of Estrogens and Androgens by Scleractinian Corals. *Comp. Biochem. Physiol. Part B: Biochem. Mol. Biol.* 136 (3), 473–485. doi:10.1016/s1096-4959(03)00253-7

Tarrant, A. M. (2007). Hormonal Signaling in Cnidarians: Do We Understand the Pathways Well Enough to Know whether They Are Being Disrupted? *Ecotoxicology* 16 (1), 5–13. doi:10.1007/s10646-006-0121-1

Tarrant, A. M., Reitzel, A. M., Blomquist, C. H., Haller, F., Tokarz, J., and Adamski, J. (2009). Steroid Metabolism in Cnidarians: Insights from *Nematostella vectensis*. *Mol. Cell Endocrinol.* 301 (1-2), 27–36. doi:10.1016/j.mce.2008.09.037

Technau, U., Rudd, S., Maxwell, P., Gordon, P. M. K., Saina, M., Grasso, L. C., et al. (2005). Maintenance of Ancestral Complexity and Non-metazoan Genes in Two Basal Cnidarians. *Trends Genet.* 21 (12), 633–639. doi:10.1016/j.tig.2005.09.007

Thibaut, R., and Porte, C. (2004). Effects of Endocrine Disrupters on Sex Steroid Synthesis and Metabolism Pathways in Fish. *J. Steroid Biochem. Mol. Biol.* 92 (5), 485–494. doi:10.1016/j.jsbmb.2004.10.008

Thomas, M. P., and Potter, B. V. L. (2013). The Structural Biology of Oestrogen Metabolism. *J. Steroid Biochem. Mol. Biol.* 137, 27–49. doi:10.1016/j.jsbmb.2012.12.014

Thorn, H. A., Quinn, J. E., and Roark, A. M. (2015). Reproductive and Developmental Effects of Tributyltin, Bisphenol A, and 17 β-estradiol in Pale Anemones (Aiptasia Pallida). *Endocr. Disruptors* 3 (1), e1030062. doi:10.1080/23273747.2015.1030062

Tijani, J. O., Fatoba, O. O., and Petrik, L. F. (2013). A Review of Pharmaceuticals and Endocrine-Disrupting Compounds: Sources, Effects, Removal, and Detections. *Water Air Soil Pollut.* 224 (11), 1–29. doi:10.1007/s11270-013-1770-3

Totta, P., Pesiri, V., Marino, M., Acconcia, F., and Migliaccio, A. (2014). Lysosomal Function Is Involved in 17β-Estradiol-Induced Estrogen Receptor α Degradation and Cell Proliferation. *PLoS One* 9 (4), e94880. doi:10.1371/journal.pone.0094880

Traylor-Knowles, N., and Palumbi, S. R. (2014). Translational Environmental Biology: Cell Biology Informing Conservation. *Trends Cel Biol.* 24 (5), 265–267. doi:10.1016/j.tcb.2014.03.001

Trott, O., and Olson, A. J. (2010). AutoDock Vina: Improving the Speed and Accuracy of Docking with a New Scoring Function, Efficient Optimization, and Multithreading. *J. Comput. Chem.* 31 (2), 455–461. doi:10.1002/jcc.21334

Tsui, M. M. P., Leung, H. W., Lam, P. K. S., and Murphy, M. B. (2014). Seasonal Occurrence, Removal Efficiencies and Preliminary Risk Assessment of Multiple Classes of Organic UV Filters in Wastewater Treatment Plants. *Water Res.* 53, 58–67. doi:10.1016/j.watres.2014.01.014

Twan, W.-H., Hwang, J.-S., and Chang, C.-F. (2003). Sex Steroids in Scleractinian Coral, Euphyllia Ancora: Implication in Mass Spawning1. *Biol. Repro* 68 (6), 2255–2260. doi:10.1095/biolreprod.102.012450

Twan, W.-H., Hwang, J.-S., Lee, Y.-H., Wu, H.-F., Tung, Y.-H., and Chang, C.-F. (2006). Hormones and Reproduction in Scleractinian Corals. *Comp. Biochem. Physiol. Part A: Mol. Integr. Physiol.* 144 (3), 247–253. doi:10.1016/j.cbpa.2006.01.011

Vance, J. E. (2010). Transfer of Cholesterol by the NPC Team. *Cell Metab* 12 (2), 105–106. doi:10.1016/j.cmet.2010.07.004

Verderame, M., and Scudiero, R. (2017). Estrogen-dependent, Extrahepatic Synthesis of Vitellogenin in Male Vertebrates: A Mini-Review. *C R. Biol.* 340 (3), 139–144. doi:10.1016/j.crvi.2017.01.005

Vidal-Dorsch, D. E., Bay, S. M., Maruya, K., Snyder, S. A., Trenholm, R. A., and Vanderford, B. J. (2012). Contaminants of Emerging Concern in Municipal Wastewater Effluents and marine Receiving Water. *Environ. Tox. Chem.* 31 (12), 2674–2682. doi:10.1002/etc.2004

Wear, S. L., and Thurber, R. V. (2015). Sewage Pollution: Mitigation Is Key for Coral Reef Stewardship. *Ann. N. Y Acad. Sci.* 1355 (1), 15–30. doi:10.1111/nyas.12785

Wood-Charlson, E. M., and Weis, V. M. (2009). The Diversity of C-type Lectins in the Genome of a Basal Metazoan, *Nematostella vectensis*. *Dev. Comp. Immunol.* 33 (8), 881–889. doi:10.1016/j.dci.2009.01.008

Worm, B., Lotze, H. K., Jubinville, I., Wilcox, C., and Jeambeck, J. (2017). Plastic as a Persistent marine Pollutant. *Ann. Rev. Environ. Resour.* 42, 1–26. doi:10.1146/annurev-environ-102016-060700

Yoshioka, R. M., Kim, C. J., Tracy, A. M., Most, R., and Harvell, C. D. (2016). Linking Sewage Pollution and Water Quality to Spatial Patterns of Porites Lobata Growth Anomalies in Puako, Hawaii. *Mar. Pollut. Bull.* 104 (1-2), 313–321. doi:10.1016/j.marpolbul.2016.01.002

Zhang, Y., and Kalderon, D. (2000). Regulation of Cell Proliferation and Patterning in Drosophila Oogenesis by Hedgehog Signaling. *Development* 127 (10), 2165–2176. doi:10.1242/dev.127.10.2165

Zhang, Y., and Kalderon, D. (2001). Hedgehog Acts as a Somatic Stem Cell Factor in the Drosophila Ovary. *Nature* 410 (6828), 599–604. doi:10.1038/35069099

Zhong, Y., Gu, L. J., Sun, X. G., Yang, S. H., and Zhang, X. H. (2014). Comprehensive Analysis of Patched Domain-Containing Genes Reveals a Unique Evolutionary Pattern. *Genet. Mol. Res.* 13 (3), 7318–7331. doi:10.4238/2014.February.13.11

Zhulyn, O., Nieuwenhuis, E., Liu, Y. C., Angers, S., and Hui, C.-C. (2015). Ptch2 Shares Overlapping Functions with Ptch1 in Smo Regulation and Limb Development. *Dev. Biol.* 397 (2), 191–202. doi:10.1016/j.ydbio.2014.10.023

Conflict of Interest: The authors declare that the research was conducted in the absence of any commercial or financial relationships that could be construed as a potential conflict of interest.

Publisher's Note: All claims expressed in this article are solely those of the authors and do not necessarily represent those of their affiliated organizations, or those of the publisher, the editors, and the reviewers. Any product that may be evaluated in this article, or claim that may be made by its manufacturer, is not guaranteed or endorsed by the publisher.

frontiers in Marine Science

ORIGINAL RESEARCH
published: 28 January 2022
doi: 10.3389/fmars.2021.805202

Microbiome Structuring Within a Coral Colony and Along a Sedimentation Gradient

James E. Fifer[1], Vy Bui[1], Justin T. Berg[2], Nicola Kriefall[1], Courtney Klepac[3], Bastian Bentlage[2] and Sarah W. Davies[1]*

[1] Department of Biology, Boston University, Boston, MA, United States, [2] Marine Laboratory, University of Guam, Mangilao, GU, United States, [3] Mote Marine Laboratory, Summerland Key, FL, United States

Reef-building corals form complex relationships with a wide range of microbial partners, including symbiotic algae in the family Symbiodiniaceae and various bacteria. These coral-associated communities can be shaped to varying degrees by environmental context. Sedimentation can structure a coral's microbial community by altering light availability for symbiotic algae, triggering the coral's stress response, or serving as a reservoir for both pathogenic and essential bacterial and algal symbionts. To examine the influence of sedimentation on a coral's microbiome, we used 16S rDNA and ITS-2 amplicon sequencing to characterize the bacterial and algal communities associated with the massive scleractinian coral *Porites lobata* across pairs of sites along a naturally occurring sedimentation gradient in Fouha Bay, southern Guam. Additionally, we investigate the influence of proximity to sediment on the coral colony scale, by sampling from the edge and center of colonies as well as the nearby sediment. The *P. lobata* colonies associated with several different genotypes of *Cladocopium* C15 algal symbionts and often harbored different genotypes within a single colony. However, the different *Cladocopium* genotypes showed no structuring according to colony position or location along the sedimentation gradient. Bacterial communities were largely consistent across the sedimentation gradient, however, some rarer taxa were differentially abundant across sites. *Planococcaceae* shows higher abundance closer to the river mouth in coral colonies in both the edge and center of colonies. *Peredibacter* also shows high abundance near the river mouth but only in sediment and the edges of the colony. We find sediment plays a larger role structuring bacterial communities at the colony scale compared to a coral's position along the sedimentation gradient. Edge communities look more similar to the sediment compared to the center communities and are also enriched in similar pathways such as those involved in nitrogen fixation. We also find center samples to be dominated by *Endozoicomonas* compared to the edge, supporting a role for this taxon in structuring bacterial communities and limiting bacterial diversity in coral colonies. Together these results show the differential impact sedimentation can have between sections of the coral colony microhabitat.

Keywords: coral, bacteria, intra-colony, sediment, Symbiodiniaceae

OPEN ACCESS

Edited by:
Ranjeet Bhagooli, University of Mauritius, Mauritius

Reviewed by:
Esti Kramarsky-Winter, Ben-Gurion University of the Negev, Israel
Annette Koenders, Edith Cowan University, Australia

****Correspondence:***
James E. Fifer
James.e.fifer@gmail.com

Specialty section:
This article was submitted to Aquatic Physiology, a section of the journal Frontiers in Marine Science

Received: *30 October 2021*
Accepted: *21 December 2021*
Published: *28 January 2022*

Citation:
Fifer JE, Bui V, Berg JT, Kriefall N, Klepac C, Bentlage B and Davies SW (2022) Microbiome Structuring Within a Coral Colony and Along a Sedimentation Gradient. Front. Mar. Sci. 8:805202. doi: 10.3389/fmars.2021.805202

INTRODUCTION

Reef-building corals form complex relationships with a wide range of microbial partners, including symbiotic algae in the family Symbiodiniaceae and a consortium of bacteria. These relationships can be established vertically (transmission from maternal colonies through egg provisioning), horizontally (acquisition from the local environment) or a combination of both (Byler et al., 2013). These transmission methods can lead to different strategies for responding to changing environmental conditions. For example, some horizontal transmitters replace their dominant algal symbiont with another compatible symbiont species that is more tolerant to a particular stressor (Huang et al., 2020). Once the stressful event is over, the coral host usually recovers its original symbiont species (Sampayo et al., 2016). In comparison, vertical transmitters are limited to either changing the relative abundances of their algal symbionts to alter their community composition (Gates, 1990; Warner et al., 2002; Berkelmans and van Oppen, 2006) or not changing at all (Goulet, 2006, 2007).

While transmission of the bacterial component of the coral microbiome receives comparatively less attention than their algal counterparts, bacterial transmission research has gained recent traction following the revelation of the importance of these partners. Bacteria can provide the coral with a variety of benefits [reviewed in Bourne et al. (2016)] including antibacterial compounds to protect against pathogens (Ritchie, 2006), ultraviolet light–absorbing pigments to reduce the impact of high light conditions (Ravindran et al., 2013) and provisioning important nutrients (Wild et al., 2004). Vertical transmission of bacteria, likely through the mucus layer that coats egg-sperm bundles (Damjanovic et al., 2020b) has been observed for several coral species (Leite et al., 2017; Bernasconi et al., 2019; Damjanovic et al., 2020b). Bacteria can also be transmitted horizontally to the coral from a variety of sources including sediment and the water column but also more charismatic sources such as fireworms (Aeby and Santavy, 2006), echinoderms (Chong-Seng et al., 2011), gastropods (Raymundo et al., 2010; Nicolet et al., 2018), and bites from butterflyfish (Aeby and Santavy, 2006; Raymundo et al., 2010; Chong-Seng et al., 2011; Martin et al., 2018; Nicolet et al., 2018) and parrotfish (Ezzat et al., 2020). While the main source of bacteria in the early life history stages of corals is thought to be the water column (Patten et al., 2008; Apprill et al., 2009, 2012), sediment bacterial communities are among the most taxonomically diverse within coral reef habitats (Schöttner et al., 2012) and bacterial taxa in the coral mucus layer show higher similarity with sediment than with surrounding seawater (Carlos et al., 2013). The plethora of bacterial sources that potentially interact with coral life stages makes understanding bacterial establishment in corals complex, with the exact role of reef sediment in these relationships remaining largely underexplored.

High sediment loads in environments such as reefs near river mouths can dramatically impact the health of a coral, directly affecting coral host physiology and changes in the microbial community. Sedimentation can contribute to compromised coral health (Weber et al., 2012; Sheridan et al., 2014; Pollock et al., 2016) coral species community structure can shift dramatically with proximity to river mouths (West and Van Woesik, 2001). Sediment can negatively impact the coral host directly by removing sperm from seawater surface during reproduction events (Ricardo et al., 2015) and forcing the coral to incur energetic costs through sediment shedding, as the coral would otherwise be smothered (Fabricius and Sea, 2005). Suspended sediments can reduce light availability as silt and clay particles block sunlight, thereby reducing photosynthesis in symbiotic corals (Cortes and Risk, 1985; Fabricius and Wolanski, 2000; Fabricius et al., 2003). Sedimentation further promotes low oxygen environments (Li et al., 2014) and increases the availability of organic material and nutrients on reefs (Haapkylä et al., 2011). These environmental impacts can alter the coral microbiome by changing abiotic conditions, some of which facilitate the growth of harmful bacteria (Erftemeijer et al., 2012). Sediment can also directly deliver harmful bacteria to the coral host, as may be the case with most instances of stony coral tissue loss disease (Rosales et al., 2020). Sediment thus can have a multifold impact on the coral organism including via restructuring of its microbial members.

Given the potential role of sediment as a major force in structuring coral microbial communities, it is possible that within a single colony, a coral polyp's distance from the boundary between the coral colony edge and the sediment substrate might determine its microbial composition. Corals can exhibit spatial intra-colony variation in their Symbiodiniaceae communities (Rowan et al., 1997; Reimer et al., 2006) and differences between sides of colonies (Garren et al., 2006) can directly correspond to light exposure (van Oppen et al., 2001; Ulstrup and Van Oppen, 2003; Kemp et al., 2015). These spatial differences in Symbiodiniaceae communities can result in within colony variation in bleaching during heat stress events (Kemp et al., 2014). While relatively understudied compared to Symbiodiniaceae, there is also evidence for intra-colony variation in coral bacterial communities. Corals can host discrete bacterial communities between compartments within a polyp (Engelen et al., 2018), between the mucus, tissue and skeleton of a coral (Sweet et al., 2011; Pollock et al., 2018), between different parts of the colony within both the tissue and/or mucus (Rohwer et al., 2002; Hansson et al., 2009; Daniels et al., 2011; Damjanovic et al., 2020a) as well as the skeleton (Marcelino et al., 2018). The ability for a single coral colony to harbor diverse microbial communities suggests that differences in sediment exposure across an individual colony may lead to intra-colony variation in the microbiome and its associated functions.

Here, we tested whether shifts in coral-associated microbial communities depend on proximity to sediment within a coral colony, as well as between sites along an established sedimentation gradient. We tested this hypothesis in Fouha Bay, Guam using the ubiquitous massive scleractinian coral, *Porites lobata*. In the absence of human activities, natural levels of suspended sediments on reefs are usually less than 5 mg/l (Larcombe et al., 1995; Kleypas, 1996), but on reefs adjacent to degraded watersheds, suspended sediments can reach 1,000 mg/l during periods of heavy rains, as is the case for Fouha Bay

(Wolanski et al., 2003; Rongo, 2004). During 1988 a coastal road was constructed within the watershed, which resulted in high sediment loads into the bay and buried and killed many corals from 1988 to 1990 (Richmond, 1993). Since then, roughly 10 major floods annually contribute to large sediment loads which are largely retained within the bay; flushing occurs only about 2–5 times per year by storm-driven swells (Wolanski et al., 2003). There is an established gradient of sediment load in the bay (**Figure 1**) with sediment loads decreasing with distance from the river mouth (Rongo, 2004). Coral richness declines exponentially with increasing sedimentation rate along this channel (Minton, 2015). However, *P. lobata* exists at almost all sites along this gradient. We sampled algal and bacterial communities from individual *P. lobata* colonies across this gradient to assess the role of sediment proximity in structuring the coral microbiome between sites and within coral colonies. We show that coral-associated microbial community composition depends on proximity to sediment within a coral colony. In addition, distance to the river mouth (site) has an effect on coral microbiome community composition, but this is largely limited to the rarer taxa living on the edge of the coral colony.

MATERIALS AND METHODS

Coral Colony and Environmental Data Collection

Eight to ten *P. lobata* colonies were sampled at each of the six locations in Fouha Bay, Guam (**Figure 1**) via hammer and chisel in April 2019. These locations were further clustered into sites (2–4) that reflect position along the sedimentation gradient as described by Rongo (2004; **Figure 1**). Site 1 was excluded from this study as it is virtually devoid of coral, with only a few colonies of *Leptastrea purpurea* remaining. The site closest to the river mouth (site 2) not only experiences higher sedimentation but also lower average light and more frequent decreases in salinity compared to the other two sites. All three sites experience similar temperatures (**Supplementary Figure 1**). The La Sa Fua River discharges into Fouha Bay through a small canyon cut through the reef flat. This canyon is about 20–30 m wide with depth varying between 0.5 m at the shore and about 7 m at the reef edge. Corals grow along the walls of the canyon with some additional coral outcrops scattered throughout the bay. All specimens collected for this study were growing on the edges of the canyon. All colonies (N = 52) were sampled in the center of the colony, half (N = 23) were also sampled at the edge and sediment (N = 18) was collected adjacent (<0.25 m) to the coral colony. Samples were placed in collection bags and flash frozen in liquid nitrogen upon collection and transferred to −80°C until DNA isolation.

Environmental data were sampled at 30 min intervals over 8 months (April 19, 2018–January 19, 2019) that spanned both dry and wet seasons. Temperature and conductivity were sampled using a HOBO U24-002-C (Onset Computer Corporation, Bourne, MA, United States) saltwater temperature/conductivity logger; conductivity was converted to salinity following calibration using a refractometer. Illuminance was recorded using HOBO UA-002-08 pendant temperature/light data logger.

To supplement the center versus edge intra-colony symbiont structure hypothesis addressed herein, contributions from fifteen *P. lobata* colonies collected during Klepac and Barshis (2020) were also included. *P. lobata* is a dominant species of the backreef lagoon pools on Ofu Island in American Samoa. Although these colonies are not influenced by sedimentation, three well-studied pools experience contrasting environmental regimes (high variability, moderate variability, and low variability), which could contribute to site-wide differences in Symbiodiniaceae

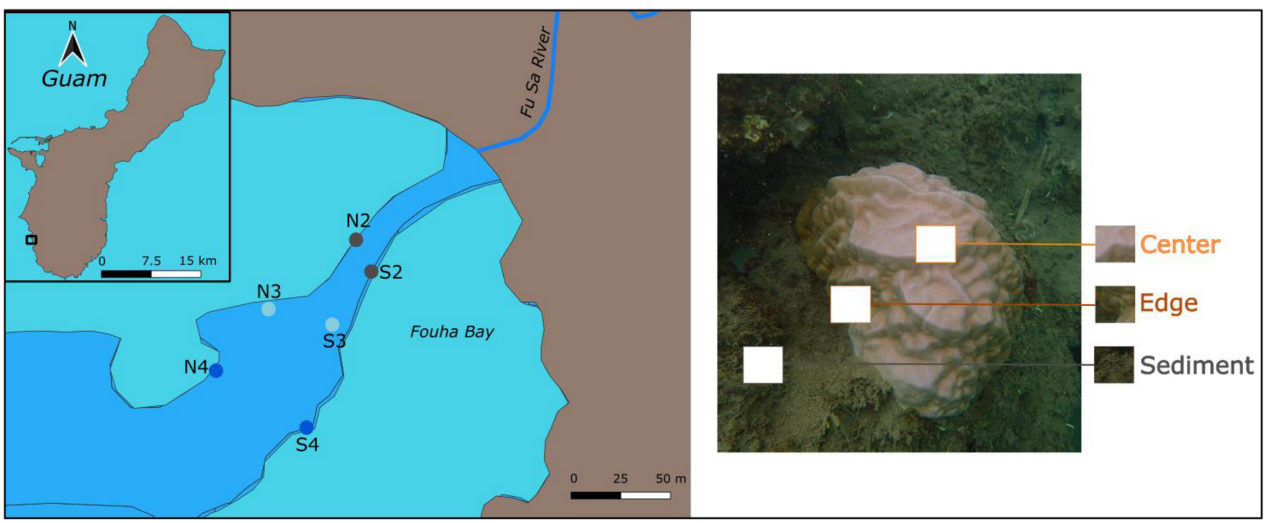

FIGURE 1 | Left panel: Map of *Porites lobata* coral collection locations (N = 6) in Fouha Bay on the island of Guam (inset). These locations are labeled based on their northern (N) or southern (S) location within the bay and distance from river mouth (2 = closest to mouth, 4 = furthest from mouth), which is a proxy for sedimentation (2 = highest sedimentation, 4 = lowest sedimentation). **Right panel**: Picture of a *P. lobata* colony showing the three sampled positions for each coral colony.

composition. Five large colonies (6–10 m^2) per site were sampled using a core punch (1.27 cm) and rock hammer. From each colony a core was taken from the top centroid and ∼0.5–1 m down (depending on the size of the colony; $N = 30$ samples) from the top sampling location to determine intra-colony differences in Symbiodiniaceae.

ITS2 and 16S Metabarcoding

DNA was extracted using the DNeasy PowerSoil (Qiagen, Hilden, Germany) kit at the University of Guam Marine Laboratory. Tissue samples were first placed in a bead beater for 30 s (with C1 solution), followed by centrifugation and transfer of the resulting supernatant to a fresh 1.5 ml tube. DNA was purified using a QIAcube automated liquid handler (Qiagen, Hilden, Germany). Bacterial 16S (for center, edge, and sediment samples) and algal ITS2 libraries (for center and edge only) were prepared at Boston University. 16S preps also included a negative control prepped with nuclease-free water. ITS2 libraries were generated following Baumann et al. (2017) and 16S libraries were generated by amplifying the V4/V5 region using modified 515f (Parada et al., 2016) and modified 806r (Apprill et al., 2015). These two library sets were then pooled in 1:2 ITS2:16S and sequenced on an Illumina MiSeqV2 (paired-end 250 bp) at Tufts University Core Facility (TUCF). All samples were prepared for 16S but sediment samples were excluded from ITS2 analysis as *P. lobata* transmits symbionts vertically (Richmond and Hunter, 1990). Colonies from Ofu Island were prepped for ITS2 as described in Klepac and Barshis (2020).

Symbiodiniaceae Community Analyses

Raw paired-end sequences for each sample were processed using SymPortal (Hume et al., 2019) with default parameters. ITS2 type profiles (representative of putative Symbiodiniaceae genotypes) were predicted and characterized by specific sets of defining intragenomic ITS2 sequence variants (DIVs). Pearson's Chi-Squared test was performed to compare differences in dominant ITS2 type profiles between sites and intra-colony positions. *T*-tests were used to compare bacterial beta diversity between dominant ITS2 type profiles that were different between center and edge versus colonies that showed the same profile.

Bacterial Community Analyses

16S Data were pre-processed in bbmap (Chaisson and Tesler, 2012) and cutadapt (Martin, 2013) removed primer sequences. DADA2 (Callahan et al., 2016) truncated reads, calculated error rates, de-duplicated reads, inferred sequence variants, merged paired reads, and removed chimeras (98% not chimeras). In total, 8,663 non-bimeric amplicon sequence variants (ASVs) were assigned taxonomy using the Silva v132 dataset (Glöckner et al., 2017) with a minimum bootstrap confidence of 50. Using phyloseq (McMurdie and Holmes, 2013), ASVs assigning to family "Mitochondria," order "Chloroplast," and any with taxonomic designations defined as "Eukaryota" were removed. Using the R package decontam (Davis et al., 2017), ASVs that were determined to be contaminants through the use of the negative control were also removed. ASVs were then mapped against NCBI's NT database using BLASTN (-*e* value 1e-5 -max_target_seqs 10) and all ASVs belonging to Eukaryota were removed. The resulting ASV table was rarefied to 5,000 reads (**Supplementary Figure 2**) using vegan (Oksanen et al., 2020). MCMC.OTU (Matz, 2016) trimmed ASVs representing <0.1% of counts or only present in less than 2% of samples, which retained 1,548 out of 7,654 ASVs. MCMC.OTU also identified putative outlier samples (defined as total counts falling below z-score cutoff of -2.5) and four samples were removed from all downstream 16S analyses (**Supplementary Data**).

To estimate bacterial diversity, Phyloseq (McMurdie and Holmes, 2013) calculated three alpha diversity metrics on an untrimmed, rarefied dataset: observed ASV richness, Shannon index, and inverse Simpson's index. Shapiro and Levene's tests were used to assess normality and heteroskedasticity, respectively. ANOVA, Kruskal-Wallis, or Welch's t-tests measured significance across intra-colony positions and sites. Beta diversities were compared using Bray-Curtis distances on trimmed datasets transformed to relative abundances. A PERMANOVA using the Adonis function in the vegan package (Oksanen et al., 2020) was run with 1,000 permutations to compare Bray-Curtis distances between intra-colony positions and sites. *Post hoc* pairwise PERMANOVAs were run as needed.

Bacterial Indicator Species and Overrepresented Pathways

The R package IndicSpecies with the command "multipatt" (De Cáceres and Jansen, 2016) was used to identify bacterial genera whose abundance was significantly associated with particular intra-colony position and site along the sedimentation gradient (p-value threshold = 0.05). PICRUSTV2 (Caicedo et al., 2020) was used to look for overrepresented pathways along the sedimentation gradient and across the coral colony. Copy numbers of gene families were predicted using the EC number database, which were then weighted by the relative abundance of ASVs. MetaCyc pathway abundances were inferred based on weighted EC number abundances and a generalized linear model (GLM) was used to compare pathway enrichment between intra-colony position and sites along the sedimentation gradient via the R package aldex (Gloor et al., 2020).

RESULTS

Algal Communities Associated With *Porites lobata*

ITS2 Metabarcoding data showed that samples were dominated by *Cladocopium* C15, but several distinct ITS2 profiles (commonly referred to as types; LaJeunesse, 2002) exist in this population (**Figure 2**). Individual coral colonies can harbor distinct C15 types between intra-colony positions, although intra-colony position does not predict the Symbiodiniaceae type (X-squared = 26.682, df = 22, p-value = 0.2235). Similarly, colonies from Ofu Island also showed distinct profiles within colonies but intra-colony position did not predict Symbiodiniaceae type (X-squared = 5.5824, df = 6,

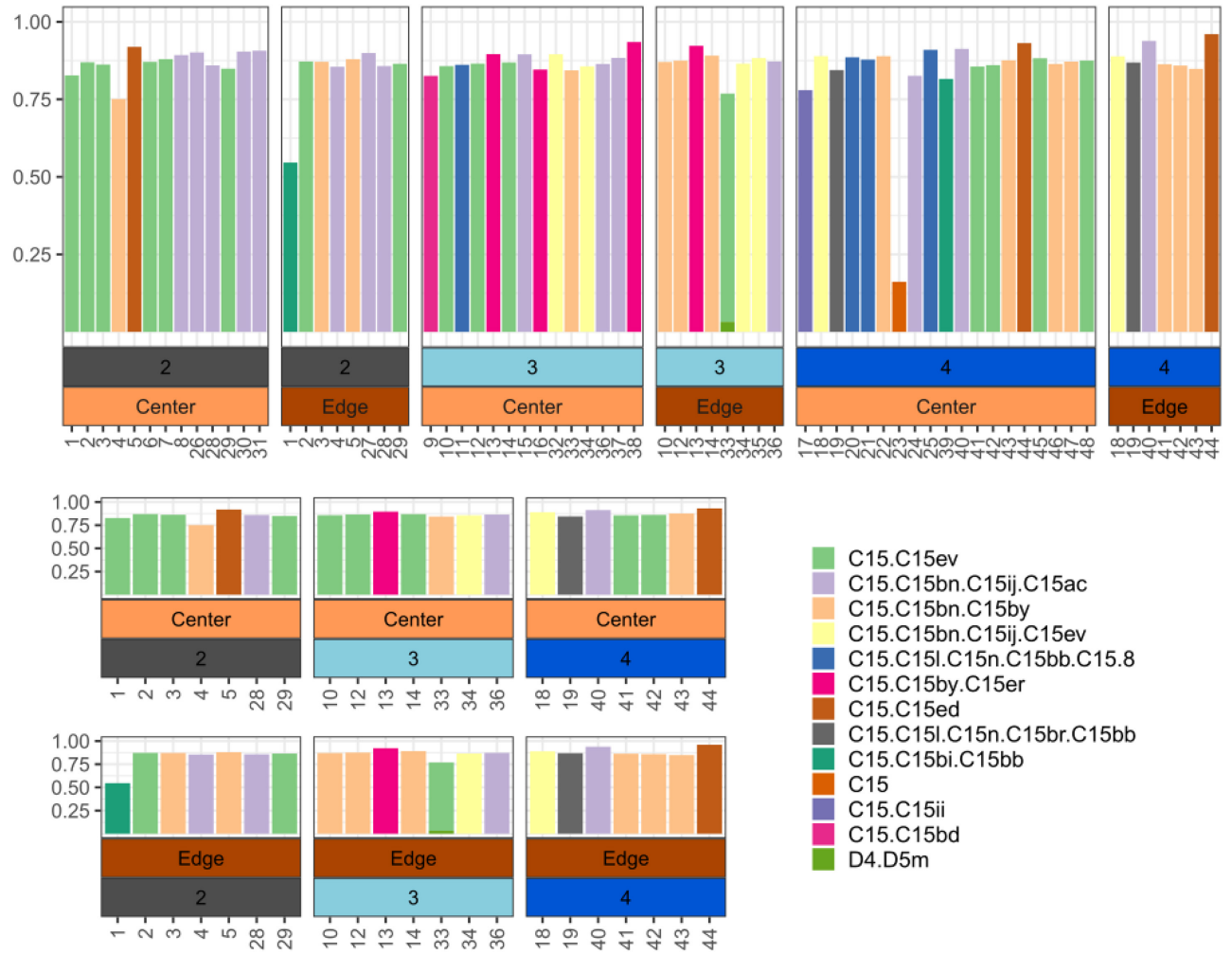

FIGURE 2 | Top: Relative abundance of dominant ITS2 profiles across all *Porites lobata* colonies along the sedimentation gradient (2: site closest to river mouth - 4: site furthest away from river mouth). **Bottom:** Relative abundance of dominant ITS2 type profiles across only *P. lobata* colonies where both edge and center were sampled. Numbers on X-axis correspond to unique coral colonies sampled.

p-value = 0.4716; **Supplementary Figure 3**). Within Fouha Bay, site did not predict Symbiodiniaceae type within both center (X-squared = 26.682, df = 22, *p*-value = 0.2235) and edge samples (X-squared = 15.754, df = 16, *p*-value = 0.4703). Comparisons of 16S beta diversity between a center-edge pair for a colony that showed intra-colony position-specific differences in dominant ITS2 profiles were no different from the pairwise beta diversity of a center-edge pair for colonies that maintained the same ITS2 profile ($t = -1.2871$, df = 36, *p*-value = 0.2063; **Supplementary Figure 4**).

Bacterial Communities Associated With *Porites lobata*

16S Alpha diversity and beta diversity comparisons for both center and edge communities revealed no significant differences along the sedimentation gradient (**Figures 3A,B** and **Supplementary Figure 5**). Alpha diversity for sediment communities was also not significantly different across sites (**Supplementary Figure 5**). However, beta diversity was significantly different between site 2 (the site with the highest sedimentation) and sites 3 and 4 (**Figure 3C**). Comparisons of diversity between intra-colony positions revealed striking differences, with edge, center and sediment communities all exhibiting significant differences in both alpha and beta diversity (**Figure 4**). Sediment bacterial communities were more similar to edge communities than they were to center communities (**Supplementary Figure 6**). Dominant bacterial families from center samples included Endozoicomonadaceae (mean 42.2% relative abundance), Xenococcaceae (6.3%) and Amoebophilaceae (5%) (**Supplementary Figure 7**). Dominant bacterial families from edge samples included Endozoicomonadaceae (11.7%) and Amoebophilaceae (6.1%) (**Supplementary Figure 8**). Dominant bacterial families from sediment samples included Cyclobacteriaceae (5.4%) and Rhodobacteraceae (5.3%) (**Supplementary Figure 9**).

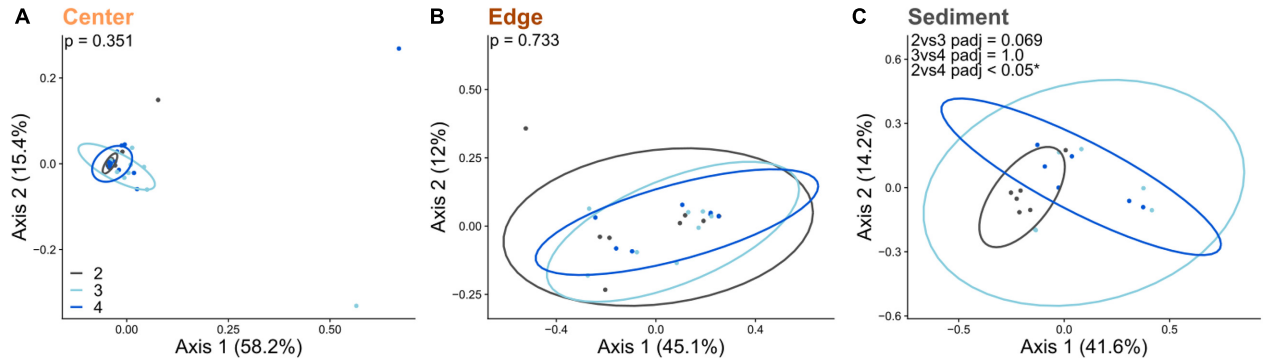

FIGURE 3 | Principal coordinates analysis (PCoA) based on Bray-Curtis dissimilarities of 16S bacterial communities across sites along a sedimentation gradient (2 = high, 3 = moderate, 4 = low sediment load) for **(A)** center of coral colonies, **(B)** edge of coral colonies, and **(C)** in the reef sediment. Percentages on each axis indicate the amount of variation explained by each axis. P-values indicate significant results of PERMANOVA tests for panels **(A,B)** and pairwise PERMANOVA for panel **(C)**.

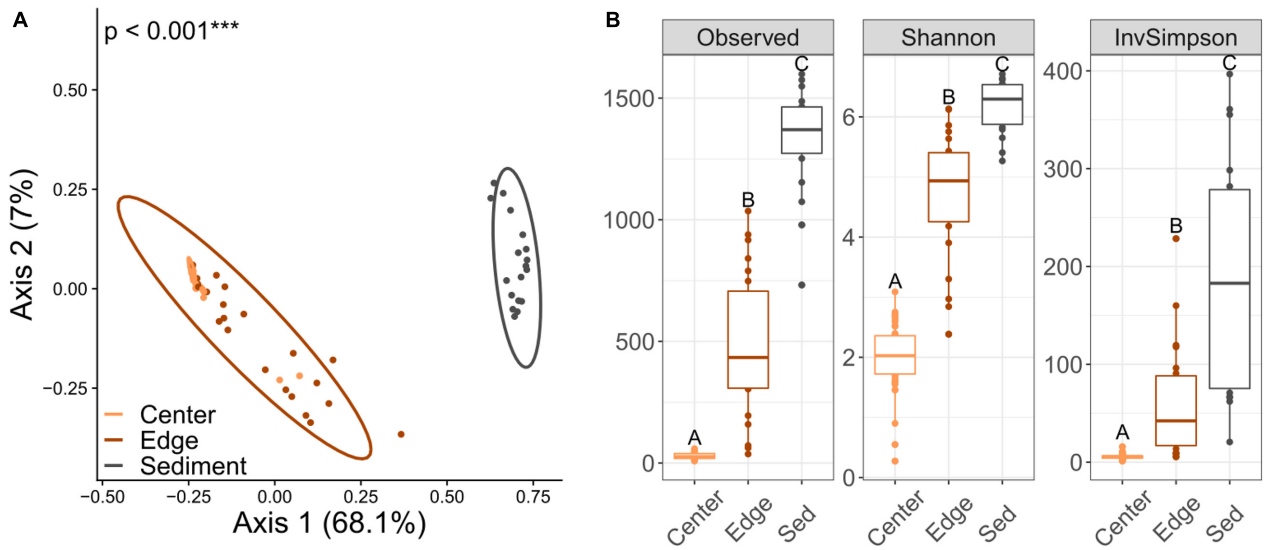

FIGURE 4 | (A) Principal coordinates analysis based on Bray-Curtis dissimilarities of 16S bacterial communities across intra-colony positions regardless of site location. Percentages on each axis indicate the amount of variation explained by each axis. p-values indicate significant results of the PERMANOVA test. **(B)** Alpha diversity metrics for bacterial communities across intra-colony positions. The box represents the interquartile range (IQR) between the upper and lower quartile. The whiskers maximally extend 1 time beyond the IQR. Letters denote significant ($p < 0.001$) differences between groups based on Tukey's *post hoc* tests of honest significant difference.

Indicator Species Between Bacterial Communities

For edge samples, several ASVs were more abundant at site 2 (the site with the highest sedimentation) or more abundant at sites 2 and 3 compared to site 4 (least sedimentation). These included ASVs belonging to genera *Catenococcus*, *Cohaesibacter*, *Filomicrobium*, *Halioglobus*, *Peredibacter*, *Pirellula*, *Rhodopirellula*, *Woeseia*, and *Kiloniellaceae* (**Supplementary Figure 10**). For samples collected from the center of the coral colony, several ASVs belonging to the genus *Endozoicomonas* were more abundant at sites 3 or 4 compared to 2 (i.e., associated with lower sedimentation). One ASV, of the genus *Burkholderiaceae*, was more abundant at sites 2 and 3 compared to 4 (**Supplementary Figure 10**). Only one ASV, which belonged to the genus *Planococcaceae*, was an indicator species for both edge and center colonies across sites. This ASV was most abundant for both intra-colony positions at site 2 (**Figure 5A**). Additionally, only 1 ASV, belonging to *Peredibacter*, was an indicator species for both coral (edge only) and sediment across sites. This ASV was also the most abundant for both sample types at site 2 (**Figure 5B**).

Enrichment of Functional Pathways in Bacterial Communities

Functional pathways significantly differentially enriched when comparing colony edge and center, but not between

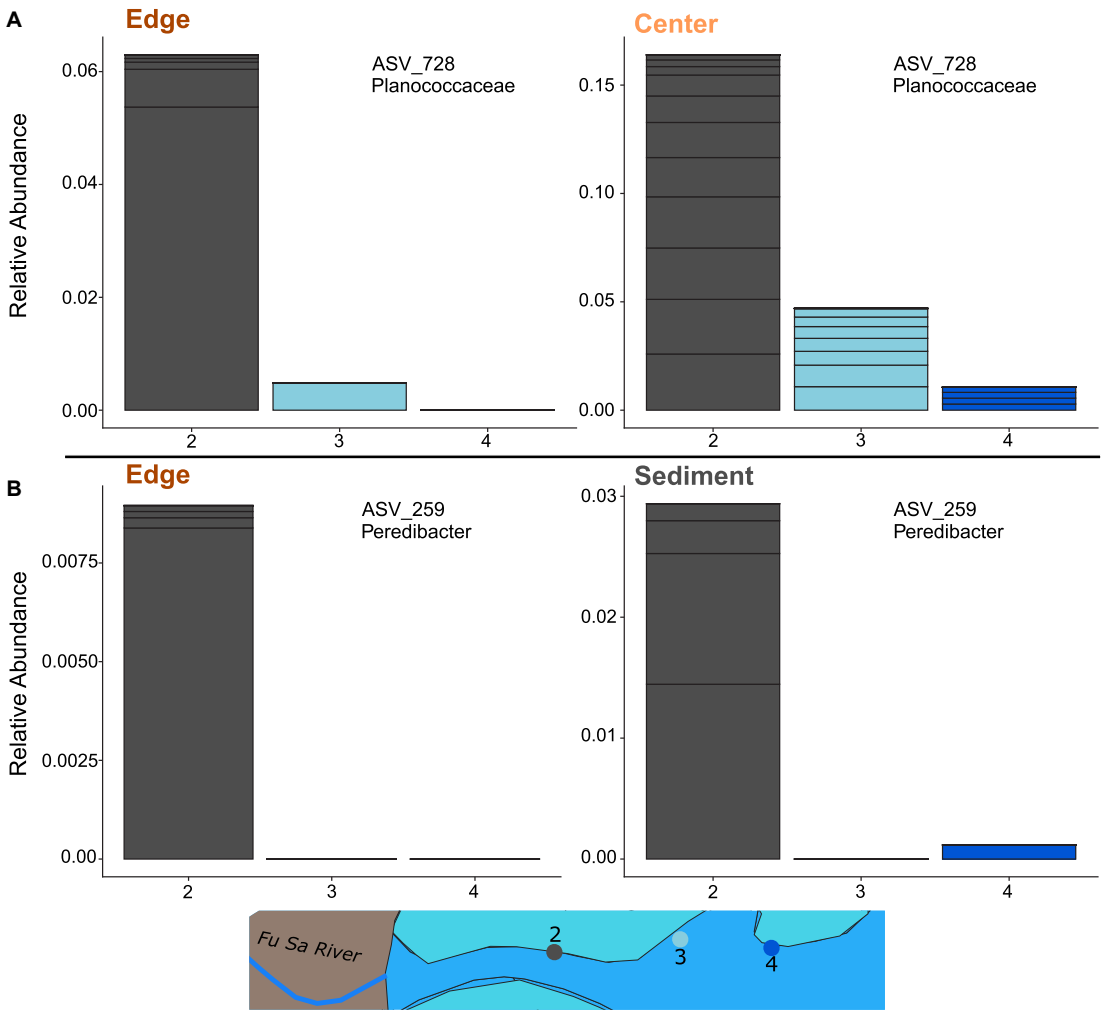

FIGURE 5 | Relative abundance of overlapping indicator species ASVs for **(A)** overlap of *P. lobata* colony edge and center and **(B)** overlap of coral colony edge and reef sediment. Stacked bins represent different ASVs from the same family/genera of bacteria. Bar colors correspond to sampling sites along the sedimentation gradient.

colony edge and reef sediment, were examined to investigate differences between the center and edge of colonies that were likely mediated by bacteria available in nearby sediment. All pathways that were overrepresented at the edge and sediment compared to the center are involved in cobalamin and amino acid synthesis (**Supplementary Figure 11**).

Pathways that were significantly enriched when comparing both coral colony edge and center as well as colony edge and reef sediment communities were then examined to investigate differences between the center and the edge of the colony that were not necessarily due to uptake at the edge from local sediment communities. There were many more pathways enriched in this group compared to those that had no differences between edge and sediment. This comparison was further split into three groups. Pathways that were most highly represented in the center, then the edge, and then the sediment included carbohydrate and amino acid degradation and TCA cycle pathways (**Supplementary Figure 12**). Pathways that were most highly represented in the sediment, then the edge, and then the center involved denitrification and methanogenesis (**Supplementary Figure 13**). Finally, pathways that were most highly represented in the edge, then sediment, and then center consisted of amino acid metabolism pathways (**Supplementary Figure 14**).

DISCUSSION

Porites lobata Harbors Distinct *Cladocopium* C15 Genotypes Within Individual Colonies

We sampled a total of 52 *P. lobata* corals along a steep sedimentation gradient in Fouha Bay, Guam, and characterized

their Symbiodiniaceae algae (ITS2) and bacterial (16S) microbiome communities across the center and edge of coral colonies (ITS2, 16S) and immediately adjacent to sediment (16S only). We observed that *P. lobata* in Fouha Bay almost exclusively associated with algae in the genus *Cladocopium* and harbors different putative C15 genotypes even within a single colony. Colonies of *P. lobata* from Ofu Island also harbored different genotypes of *Cladocopium* C15 genotypes within a single colony. Massive *Porites* corals were historically considered to have fixed and non-mixed Symbiodiniaceae associations (Fay and Weber, 2012) with most populations of this coral being associated with a single *Cladocopium* species, commonly referred to as the C15 lineage (Lajeunesse et al., 2004; Thornhill et al., 2006). These strict associations with a single algal lineage were previously thought to be a result of the vertical transmission during reproduction (Fay and Weber, 2012). However, it has since been discovered that massive *Porites* corals can harbor mixed *Cladocopium* and *Durusdinium* communities (Terraneo et al., 2019; Tan et al., 2020) and application of the within-sample informative intragenomic sequences used by SymPortal (Hume et al., 2019) revealed different colonies within a population of *P. lobata* can harbor different genotypes of *Cladocopium* (Gardner et al., 2019; Ziegler et al., 2019; Camp et al., 2020). This study adds to the literature providing evidence against the fixed and non-mixed infection theories by demonstrating intra-colony variation of dominant *Cladocopium* C15 genotypes within a single colony of *P. lobata* across small (Fouha Bay) and large (Guam and American Samoa) geographic locations. There are two possible scenarios for explaining mixed genotypes here and they are not mutually exclusive: (1) multiple genotypes are inherited vertically and symbionts "shuffle" (Baker et al., 2004; Berkelmans and van Oppen, 2006); (2) cryptic horizontal transmission of Symbiodiniaceae (Quigley et al., 2018). Further work sequencing ITS2 profiles of the water column, nearby sediment, and *P. lobata* larvae is needed in order to test these hypotheses.

There was neither a clear pattern of ITS2 profile structuring according to intra-colony position nor a discernable pattern of ITS2 profiles along the sedimentation gradient, suggesting that the ITS2 community composition in *P. lobata* is not directly driven by sedimentation. Massive *Porites* can harbor different dominant ITS2 profiles across latitudinal gradients (Terraneo et al., 2019), seasons (Ziegler et al., 2015), and habitats [e.g., higher diversity of ITS2 profiles among colonies in the open ocean compared to those in mangrove habitats; (Camp et al., 2019)]. These previous studies suggest that ITS2 profile structuring for this genus of corals is determined by the local environment. However, we do not observe such structuring here, implying either differences in profiles are random or due to differences in the microenvironment not captured by this study. It is possible resampling following the flooding events might reveal shifts in dominant profile-types. Interestingly, there was a trend where 7/10 colonies that showed differing profiles between the colony center and the colony edge hosted C15.C15bn.C15 on the edge. Furthermore, of these seven, six hosted C15.C15ev at the center. This suggests colonies hosting certain Symbiodiniaceae taxa might be more likely to host divergent populations between the center and edge. However, a greater sample size will be needed to properly investigate this pattern.

Porites lobata-Associated Bacterial Communities Are Dominated by *Endozoicomonas*

For *P. lobata*-associated bacterial communities, we observed largely homogenous bacterial communities along the sedimentation gradient. The majority of coral tissue samples from the center of the colony show high homogeneity and were dominated by ASVs belonging to the bacterial genus *Endozoicomonas* (Proteobacteria: Oceanospirillales). The ecological role of E*ndozoicomonas* in the coral microbiome remains unknown, albeit there are numerous theories, most of which reflect a positive role in coral health [reviewed in Neave et al. (2016)]. Previous work found that *Endozoicomonas* increased in abundance across several species of coral in response to heat stress and persisted 10 months after heat stress events (Maher et al., 2020). It is therefore possible that the dominance of *Endozoicomonas* observed here may be a result of the sediment-induced stress associated with the riverine environment of Fouha Bay. As *Endozoicomonas* abundance did not change across sites within the bay, we theorize that "stress events"–in this case acute large-scale flooding and associated sedimentation events that occur several times a year affecting the entire bay (Rongo, 2004)–play a stronger structuring role than the chronic sedimentation gradient observed for most of the year.

Our results are particularly interesting in light of those reported in Sweet et al. (2019), which found low abundance of *Endozoicomonas* in massive *P. lobata* less than 30 km from Fouha Bay. Given that the Guam site from Sweet et al. (2019) experiences little to no sedimentation, it is tempting to speculate that severely sedimented environments are associated with the dominance of *Endozoicomonas*. Alternatively, given massive *Porites* is a cryptic species complex (Forsman et al., 2009, 2020), these differences might reflect microbial associations correlating with discrete host lineages. The Fouha Bay *P. lobata* population might show an absence of community changes along the sedimentation gradient because it belongs to a lineage with an inflexible bacterial microbiome, for which there is also precedent in *Endozoicomonas* coral dominated colonies (Pogoreutz et al., 2018). Regardless, future work investigating host genetic structure as well as common garden experiments exposing corals to different sediment loads would be the next steps to understanding the forces that structure these microbial communities.

Rarer Taxa Show Differential Abundances in *Porites lobata*-Associated Bacterial Communities Along a Sedimentation Gradient

Only the rarer bacterial taxa demonstrated abundance patterning according to the site along the sedimentation gradient. The

single ASV that was differentially abundant across sites for both center and edge samples belongs to the family Planococcaceae and was most abundant closest to the river mouth, regardless of where on the colony we sampled. This family contains many genera that exhibit diverse functions (Shivaji et al., 2014) making it difficult to disentangle the potential role these microbes are playing. However, this family is well represented in coral samples worldwide (Rodríguez-Gómez et al., 2021) and has also previously been reported to change abundance based on proximity to different pollution sources (Qin et al., 2020). Another ASV which belongs to the genus *Peredibacter* was differentially abundant across the sedimentation gradient for both edge and sediment samples. This ASV was also more abundant closest to the river mouth and is part of a genus classified as a predatory, Gram-negative, bacteriovorus group ubiquitous in soil and sewage (Davidov and Jurkevitch, 2004) that has previously been found in association with *Pocillopora* coral hosts (Doering et al., 2021). In edge samples, two other bacteriovorus ASVs–*Pirellula* and *Rhodopirellula*–were also in their greatest abundance at sites by the river mouth. The presence of these three bacteriovores in greater abundance near the river mouth at the edge of colonies might be significant as micropredators can drive microbiome changes in corals even at low abundances (Doering et al., 2021).

Two pathogenic bacteria, *Catenococcus* and *Cohaesibacter* were also present in highest abundances at the edge of coral colonies closer to the river mouth. *Catenococcus* is a member of the Vibrionaceae family and has been described as a pathogen in the seaweed *Kappaphycus alvarezii* in which infection by *Catenococcus thiocyli* causes bleaching (Zheng et al., 2016), and showed toxic activity in both sponges (Yoghiapiscessa et al., 2016) and clams (Guibert et al., 2020), suggesting that edges of coral colonies may be more susceptible to infection closer to the river mouth. *Cohaesibacter* has been shown to be enriched in corals exhibiting stony coral tissue loss disease (Rosales et al., 2020; Becker et al., 2021) as well as in white plague-affected corals (Sunagawa et al., 2009; Roder et al., 2014), providing further evidence that colonies at the high sedimentation site might be more at risk for coral disease. Two ASVs from putative denitrifiers *Filomicrobium* (Asakura et al., 2014) and *Kiloniellaceae* (Wiese et al., 2020) were also abundant closest to the river mouth. These findings suggest the functions of the bacterial communities are largely the same across sites, consistent with the observed lack of pathway enrichment, but differences in some of the rarer bacteria reflects the potential for differential functional capabilities. Additionally, these site differences in rare bacteria are only seen in edge samples suggesting the edges of coral colonies are more vulnerable to infection by potentially harmful bacteria compared to the center of the coral colony.

We acknowledge that there are limitations with this study in regard to the association between abundance of these rare ASVs and sediment stress. There are other environmental variables that we are unable to decouple across the sediment gradient. For one, we note that the site closest to the river experiences more extreme drops in salinity throughout the year compared to the other two sites, likely due to the freshwater influx during the rainy season. Previous research on the impact of reduced salinity on coral microbiomes is limited, but short-term salinity stress has been shown to increase Vibrio infection of the coral *Montipora capitata* (Shore-Maggio et al., 2018), suggesting hyposalinity can restructure bacterial communities. The site closest to the river also experiences lower light. While this is likely due to the presence of sediment in the water column, it demonstrates the difficulty of disentangling the exact mechanisms by which higher sedimentation might be impacting microbial communities. Finally, we acknowledge the possibility that the overlap between sediment and coral bacterial communities for these few rare taxa could be a result of coral expulsion of these taxa into the sediment instead of pickup from the sediment into the coral microbiome. Future work should include sampling along a sediment gradient in areas without coral colonies as well as *ex situ* experiments designed to parse apart the relative impacts of sediment and salinity on the structuring of coral bacterial communities.

Bacterial Communities of *Porites lobata* Show Greater Structuring According to Intra-colony Position Than Location Along the Sedimentation Gradient

Contrary to the minimal differences in coral-associated bacterial communities observed across the sites along the sedimentation gradient, we find significant differences in bacterial diversity between samples collected from the center and edge of colonies. Similar variation in bacterial communities has previously been shown for massive *Porites* across the skeleton (Marcelino et al., 2018), but we describe discrete bacterial communities based on intra-colony position within the tissue of massive *Porites*. High diversity differences between positions of the colony are likely due to proximity of the edge samples to surrounding sediments. This is reflected in the greater similarity between edge and sediment communities versus center and sediment communities. Additionally, many ASVs that were observed in greater abundance at the edge compared to the center were not differentially abundant between the edge and the sediment. One might have also expected to observe higher overlap between edge and sediment communities at sites with greater sedimentation, but this was not a pattern observed in our dataset. However, this study only sampled a single time point during the dry season, making it possible that edge communities exhibit increased similarity with sediment communities during large scale sedimentation events during the rainy season. Additionally, we found that colonies that hosted different *Cladocopium* genotypes between intra-colony positions did not show any greater differences in their bacterial communities, suggesting the forces structuring microbial communities are different between the algal and bacterial partners.

These differences in bacterial composition between colony edge and center samples also corresponded to substantial differences in functional profiles of the bacterial communities.

Edge and sediment communities both showed functional enrichment of pathways relating to cobalamin and amino acid synthesis compared to center communities. Both Symbiodiniaceae and coral cells lack the ability to synthesize certain vitamins, including vitamin B12 (cobalamin), which is important for nucleic acid biosynthesis (Wagle et al., 1958) and is provided to them by bacterial symbionts (Hopkinson and Morel, 2009; Agostini et al., 2012). Greater availability of these important compounds at the edge might sustain increased coral tissue growth rates at the leading edge compared to the center of a coral colony. Edge communities were also enriched for methanogenesis and denitrification pathways compared to the center. As high sedimentation can produce low oxygen environments (Li et al., 2014), enrichment of methanogenesis at the edge might compensate for carbon buildup by providing alternative mechanisms for carbohydrate breakdown at the colony edge that do not require oxygen. Higher denitrification at the edge might be a response to a disruption in the N to P ratio as bacteria that mediate N availability through denitrifying processes can strengthen host tolerance to nutrient replete conditions and help maintain a favorable N to P ratio (Tilstra et al., 2019). However, given Fouha Bay's proximity to a riverine environment, it seems unlikely that these corals are living under nitrogen limited conditions. Regardless, nitrogen availability impacts the coral-algal symbiont relationship as this association is largely maintained through provision and limitation of N from host to symbiont (Falkowski et al., 1993; Beraud et al., 2013; Tilstra et al., 2019). Intra-colony spatial differences in nitrogen availability suggest possible differences in the stability of this relationship across the colony. At the center, bacterial communities showed greater enrichment in functions relating to carbohydrate metabolism. This same pattern is exhibited by bacterial communities in coral colonies that are more resilient to heat stress (Ziegler et al., 2017). As heat stress can modulate the relative abundance of different sugar compounds in coral mucus (Lee et al., 2016), it is possible sediment stress is acting similarly, resulting in niche differentiation between the edge and center and ultimately discrete bacterial communities that have different metabolic profiles. Further research should investigate the concentration of these relevant compounds across the colony and in coral tissue experiencing different levels of sediment exposure to corroborate these interpretations.

CONCLUSION

Our findings imply that thorough characterization of a coral's microbiome and its potential ecological roles requires sampling across a coral colony to capture the variability of its microbiome. More work is needed to elucidate if bacterial communities associated with coral colony edges have any significant bearing on the health of the rest of the colony. The notion that bacterial structuring in corals occurring within a colony can be much greater than structuring between colonies, even across a steep environmental gradient, suggests coral health and resilience at small spatial scales is challenging to predict. Additionally, this study adds to the literature describing *Endozoicomonas*-dominated coral colonies contributing to a seemingly fixed microbiome. *Endozoicomonas* species possess relatively large genomes, coding for diverse metabolites that may contribute to coral resilience (Neave et al., 2017). Characterizing the genome and metabolome of *Endozoicomonas* strains in Fouha Bay will be necessary to begin understanding their role in *Porites lobata* resilience to sedimentation.

DATA AVAILABILITY STATEMENT

All scripts for analyses and figures can be found at https://github.com/jamesfifer/Fouha. The datasets presented in this study can be found in online repositories. The names of the repository/repositories and accession number(s) can be found below: https://www.ncbi.nlm.nih.gov/, PRJNA774203.

AUTHOR CONTRIBUTIONS

JF, BB, and SD conceived the project. JB and BB collected the samples from the field and extracted DNA. JF and VB carried out library preparation work. JF analyzed the data with assistance from NK, created the figures, and drafted the manuscript. SD and BB contributed to the writing. SD, BB, NK, and CK provided critical revisions. All authors contributed to the article and approved the submitted version.

FUNDING

Funding for this project came from startup funds to SD from Boston University. BB and JB were supported by Guam NSF EPSCoR (OIA-1946352). VB was supported by Greater Boston Area Research Opportunities For Young Women (GROW).

ACKNOWLEDGMENTS

We thank Hanny Rivera, Dan Wuitchik, Colleen Bove, and Hannah Aichleman for comments on experimental design and figures, Boston University's SCC for facilitating computational work and Ben Hume for the SymPortal analysis. We wish to thank Melissa Gabriel for providing environmental data for characterization of our study site. We also thank Marine Laboratory captain Jason Miller for facilitating the field work for this study.

SUPPLEMENTARY MATERIAL

The Supplementary Material for this article can be found online at: https://www.frontiersin.org/articles/10.3389/fmars.2021.805202/full#supplementary-material

REFERENCES

Aeby, G. S., and Santavy, D. L. (2006). Factors affecting susceptibility of the coral. *Mar. Ecol. Progr. Ser.* 318, 103–110.

Agostini, S., Suzuki, Y., Higuchi, T., Casareto, B. E., Yoshinaga, K., Nakano, Y., et al. (2012). Biological and chemical characteristics of the coral gastric cavity. *Coral Reefs* 31, 147–156. doi: 10.1007/s00338-011-0831-6

Apprill, A., Marlow, H. Q., Martindale, M. Q., and Rappé, M. S. (2009). The onset of microbial associations in the coral Pocillopora meandrina. *ISME J.* 3, 685–699. doi: 10.1038/ismej.2009.3

Apprill, A., Marlow, H. Q., Martindale, M. Q., and Rappé, M. S. (2012). Specificity of associations between bacteria and the coral Pocillopora meandrina during early development. *Appl. Environ. Microbiol.* 78, 7467–7475. doi: 10.1128/AEM.01232-12

Apprill, A., Mcnally, S., Parsons, R., and Weber, L. (2015). Minor revision to V4 region SSU rRNA 806R gene primer greatly increases detection of SAR11 bacterioplankton. *Aquat. Microb. Ecol.* 75, 129–137. doi: 10.3354/ame01753

Asakura, T., Date, Y., and Kikuchi, J. (2014). Comparative analysis of chemical and microbial profiles in estuarine sediments sampled from kanto and tohoku regions in Japan. *Anal. Chem.* 86, 5425–5432. doi: 10.1021/ac5005037

Baker, A. C., Starger, C. J., McClanahan, T. R., and Glynn, P. W. (2004). Corals' adaptive response to climate change. *Nature* 430, 741–741. doi: 10.1038/430741a

Baumann, J., Davies, S., Aichelman, H., and Castillo, K. (2017). Coral *Symbiodinium community* composition across the Belize Mesoamerican Barrier Reef System is driven by host species and environmental variability. *bioRxiv* [Preprint]. doi: 10.1007/s00248-017-1096-6

Becker, C., Brandt, M., Miller, C., and Apprill, A. (2021). Stony coral tissue loss disease biomarker bacteria identified in corals and overlying waters using a rapid field-based sequencing approach. *bioRxiv* [Preprint]. doi: 10.1101/2021.02.17.431614

Beraud, E., Gevaert, F., Rottier, C., and Ferrier-Pages, C. (2013). The response of the scleractinian coral *Turbinaria reniformis* to thermal stress depends on the nitrogen status of the coral holobiont. *J. Exp. Biol.* 216, 2665–2674. doi: 10.1242/jeb.085183

Berkelmans, R., and van Oppen, M. J. H. (2006). The role of zooxanthellae in the thermal tolerance of corals: a "nugget of hope" for coral reefs in an era of climate change. *Proc. R. Soc. Lond. B Biol. Sci.* 273, 2305–2312. doi: 10.1098/rspb.2006.3567

Bernasconi, R., Stat, M., Koenders, A., Paparini, A., Bunce, M., and Huggett, M. J. (2019). Establishment of coral-bacteria symbioses reveal changes in the core bacterial community with host ontogeny. *Front. Microbiol.* 10:1529. doi: 10.3389/fmicb.2019.01529

Bourne, D. G., Morrow, K. M., and Webster, N. S. (2016). Insights into the coral microbiome: underpinning the health and resilience of reef ecosystems. *Annu. Rev. Microbiol.* 70, 317–340. doi: 10.1146/annurev-micro-102215-095440

Byler, K. A., Carmi-Veal, M., Fine, M., and Goulet, T. L. (2013). Multiple symbiont acquisition strategies as an adaptive mechanism in the coral *Stylophora pistillata*. *PLoS One* 8:e59596. doi: 10.1371/journal.pone.0059596

Caicedo, H. H., Hashimoto, D. A., Caicedo, J. C., Pentland, A., and Pisano, G. P. (2020). Overcoming barriers to early disease intervention. *Nat. Biotechnol.* 38, 669–673. doi: 10.1038/s41587-020-0550-z

Callahan, B. J., McMurdie, P. J., Rosen, M. J., Han, A. W., Johnson, A. J. A, and Holmes, S. P. (2016). DADA2: high-resolution sample inference from Illumina amplicon data. *Nat. methods*. 13, 581–583.

Camp, E. F., Edmondson, J., Doheny, A., Rumney, J., Grima, A. J., Huete, A., et al. (2019). Mangrove lagoons of the Great Barrier Reef support coral populations persisting under extreme environmental conditions. *Mar. Ecol. Progr. Ser.* 625, 1–14. doi: 10.3354/meps13073

Camp, E. F., Suggett, D. J., Pogoreutz, C., Nitschke, M. R., Houlbreque, F., Hume, B. C. C., et al. (2020). Corals exhibit distinct patterns of microbial reorganisation to thrive in an extreme inshore environment. *Coral Reefs* 39, 701–716. doi: 10.1007/s00338-019-01889-3

Carlos, C., Torres, T. T., and Ottoboni, L. M. M. (2013). Bacterial communities and species-specific associations with the mucus of Brazilian coral species. *Sci. Rep.* 3:1624. doi: 10.1038/srep01624

Chaisson, M. J., and Tesler, G. (2012). Mapping single molecule sequencing reads using basic local alignment with successive refinement (BLASR): application and theory. *BMC Bioinformatics* 13:238. doi: 10.1186/1471-2105-13-238

Chong-Seng, K. M., Cole, A. J., Pratchett, M. S., and Willis, B. L. (2011). Selective feeding by coral reef fishes on coral lesions associated with brown band and black band disease. *Coral Reefs* 30, 473–481. doi: 10.1007/s00338-010-0707-1

Cortes, J., and Risk, M. J. (1985). A reef under siltation stress: Cahuita, Costa Rica. *Bull. Mar. Sci.* 36, 339–356.

Damjanovic, K., Blackall, L. L., Peplow, L. M., and van Oppen, M. J. H. (2020a). Assessment of bacterial community composition within and among *Acropora loripes* colonies in the wild and in captivity. *Coral Reefs* 39, 1245–1255. doi: 10.1007/s00338-020-01958-y

Damjanovic, K., Menéndez, P., Blackall, L. L., and van Oppen, M. J. H. (2020b). Early life stages of a common broadcast spawning coral associate with specific bacterial communities despite lack of internalized bacteria. *Microb. Ecol.* 79, 706–719. doi: 10.1007/s00248-019-01428-1

Daniels, C. A., Zeifman, A., Heym, K., Ritchie, K. B., Watson, C. A., Berzins, I., et al. (2011). Spatial heterogeneity of bacterial communities in the mucus of *Montastraea annularis*. *Mar. Ecol. Progr. Ser.* 426, 29–40. doi: 10.3354/meps09024

Davidov, Y., and Jurkevitch, E. (2004). Diversity and evolution of *Bdellovibrio*-and-like organisms (BALOs), reclassification of *Bacteriovorax starrii* as *Peredibacter starrii* gen. nov., comb. nov., and description of the *Bacteriovorax-Peredibacter* clade as *Bacteriovoracaceae* fam. nov. *Int. J. Syst. Evol. Microbiol.* 54, 1439–1452. doi: 10.1099/ijs.0.02978-0

Davis, N. M., Proctor, D. M., Holmes, S. P., Relman, D. A., and Callahan, B. J. (2017). Simple statistical identification and removal of contaminant sequences in marker-gene and metagenomics data. *bioRxiv* [Preprint]. doi: 10.1101/221499

De Cáceres, M., and Jansen, F. (2016). *Package 'indicspecies' for R: Relationship Between Species and Groups of Sites. R Cran*. 1–31.

Doering, T., Wall, M., Putchim, L., Rattanawongwan, T., Schroeder, R., Hentschel, U., et al. (2021). Towards enhancing coral heat tolerance: a "microbiome transplantation" treatment using inoculations of homogenized coral tissues. *Microbiome* 9, 1–16. doi: 10.1186/s40168-021-01053-6

Engelen, A. H., Mota, C., Serrao, E. A., Coelho, M., and Marbà, N. (2018). Differentiation in fitness-related traits in response to elevated temperatures between leading and trailing edge populations of marine macrophytes. *PLoS One* 13:e0203666. doi: 10.1371/journal.pone.0203666

Erftemeijer, P. L. A., Riegl, B., Hoeksema, B. W., and Todd, P. A. (2012). Environmental impacts of dredging and other sediment disturbances on corals: a review. *Mar. Pollut. Bull.* 64, 1737–1765. doi: 10.1016/j.marpolbul.2012.05.008

Ezzat, L., Lamy, T., Maher, R. L., Munsterman, K. S., Landfield, K. M., Schmeltzer, E. R., et al. (2020). Parrotfish predation drives distinct microbial communities in reef-building corals. *Anim. Microbiome* 2:5. doi: 10.1186/s42523-020-0024-0

Fabricius, K. E., and Sea, R. (2005). Effects of terrestrial runoff on the ecology of corals and coral reefs: review and synthesis. *Mar. Pollut. Bull.* 50, 125–146. doi: 10.1016/j.marpolbul.2004.11.028

Fabricius, K. E., and Wolanski, E. (2000). Rapid smothering of coral reef organisms by muddy. *Estuar. Coast. Shelf Sci.* 50, 115–120.

Fabricius, K. E., Wild, C., Wolanski, E., and Abele, D. (2003). Effects of transparent exopolymer particles and muddy terrigenous sediments on the survival of hard coral recruits. *Estuar. Coast. Shelf Sci.* 57, 613–621. doi: 10.1016/S0272-7714(02)00400-6

Falkowski, P. G., Dubinsky, Z., Muscatine, L., and McCloskey, L. (1993). Population control in symbiotic corals – Ammonium ions and organic materials maintain the density of zooxanthellae. *BioScience* 43, 606–611. doi: 10.2307/1312147

Fay, S. A., and Weber, M. X. (2012). The occurrence of mixed infections of *Symbiodinium* (Dinoflagellata) within individual hosts. *J. Phycol.* 48, 1306–1316. doi: 10.1111/j.1529-8817.2012.01220.x

Forsman, Z. H., Barshis, D. J., Hunter, C. L., and Toonen, R. J. (2009). Shape-shifting corals: molecular markers show morphology is evolutionarily plastic in Porites. *BMC Evol. Biol.* 9:45. doi: 10.1186/1471-2148-9-45

Forsman, Z. H., Ritson-Williams, R., Tisthammer, K. H., Knapp, I. S. S., and Toonen, R. J. (2020). Host-symbiont coevolution, cryptic structure, and

bleaching susceptibility, in a coral species complex (Scleractinia; Poritidae). *Sci. Rep.* 10:16995. doi: 10.1038/s41598-020-73501-6

Gardner, S. G., Camp, E. F., Smith, D. J., Kahlke, T., Osman, E. O., Gendron, G., et al. (2019). Coral microbiome diversity reflects mass coral bleaching susceptibility during the 2016 El Niño heat wave. *Ecol. Evol.* 9, 938–956. doi: 10.1002/ece3.4662

Garren, M., Walsh, S. M., Caccone, A., and Knowlton, N. (2006). Patterns of association between *Symbiodinium* and members of the *Montastraea annularis* species complex on spatial scales ranging from within colonies to between geographic regions. *Coral Reefs* 25, 503–512. doi: 10.1007/s00338-006-0146-1

Gates, R. D. (1990). Seawater temerature and sublethal bealching in Jamaica. *Coral Reefs* 8, 193–197.

Glöckner, F. O., Yilmaz, P., Quast, C., Gerken, J., Beccati, A., Ciuprina, A., et al. (2017). 25 years of serving the community with ribosomal RNA gene reference databases and tools. *J. Biotechnol.* 261, 169–176. doi: 10.1016/j.jbiotec.2017.06.1198

Gloor, A. G., Fernandes, A., Macklaim, J., Albert, A., Links, M., Quinn, T., et al. (2020). *Package ' ALDEx2 .'*.

Goulet, T. L. (2006). Most corals may not change their symbionts. *Mar. Ecol. Progr. Ser.* 321, 1–7. doi: 10.3354/meps321001

Goulet, T. L. (2007). Most scleractinian corals and octocorals host a single symbiotic zooxanthella clade. *Mar. Ecol. Progr. Ser.* 335, 243–248. doi: 10.3354/meps335243

Guibert, I., Lecellier, G., Torda, G., Pochon, X., and Berteaux-Lecellier, V. (2020). Metabarcoding reveals distinct microbiotypes in the giant clam *Tridacna maxima*. *Microbiome* 8:57. doi: 10.1186/s40168-020-00835-8

Haapkylä, J., Unsworth, R. K. F., Flavell, M., Bourne, D. G., Schaffelke, B., and Willis, B. L. (2011). Seasonal rainfall and runoff promote coral disease on an inshore reef. *PLoS One* 6:e16893. doi: 10.1371/journal.pone.0016893

Hansson, L., Agis, M., Maier, C., and Weinbauer, M. G. (2009). Community composition of bacteria associated with cold-water coral *Madrepora oculata*: within and between colony variability. *Mar. Ecol. Progr. Ser.* 397, 89–102. doi: 10.3354/meps08429

Hopkinson, B. M., and Morel, F. M. M. (2009). The role of siderophores in iron acquisition by photosynthetic marine microorganisms. *BioMetals* 22, 659–669. doi: 10.1007/s10534-009-9235-2

Huang, Y. Y., Carballo-Bolaños, R., Kuo, C. Y., Keshavmurthy, S., and Chen, C. A. (2020). Leptoria phrygia in Southern Taiwan shuffles and switches symbionts to resist thermal-induced bleaching. *Sci. Rep.* 10:7808. doi: 10.1038/s41598-020-64749-z

Hume, B. C. C., Smith, E. G., Ziegler, M., Warrington, H. J. M., Burt, J. A., LaJeunesse, T. C., et al. (2019). SymPortal: a novel analytical framework and platform for coral algal symbiont next-generation sequencing ITS2 profiling. *Mol. Ecol. Resour.* 19, 1063–1080. doi: 10.1111/1755-0998.13004

Kemp, D. W., Hernandez-Pech, X., Iglesias-Prieto, R., Fitt, W. K., and Schmidt, G. W. (2014). Community dynamics and physiology of *Symbiodinium* spp. before, during, and after a coral bleaching event. *Limnol. Oceanogr.* 59, 788–797. doi: 10.4319/lo.2014.59.3.0788

Kemp, D. W., Thornhill, D. J., Rotjan, R. D., Iglesias-Prieto, R., Fitt, W. K., and Schmidt, G. W. (2015). Spatially distinct and regionally endemic *Symbiodinium* assemblages in the threatened Caribbean reef-building coral *Orbicella faveolata*. *Coral Reefs* 34, 535–547. doi: 10.1007/s00338-015-1277-z

Klepac, C. N., and Barshis, D. J. (2020). Reduced thermal tolerance of massive coral species in a highly variable environment: reduced heat tolerance of massive corals. *Proc. R. Soc. Lond. B Biol. Sci.* 287, 19–21. doi: 10.1098/rspb.2020.1379rspb20201379

Kleypas, J. A. (1996). Coral reef development under naturally turbid conditions: fringing reefs near Broad Sound, Australia. *Coral Reefs* 15, 153–167. doi: 10.1007/BF01145886

LaJeunesse, T. C. (2002). Diversity and community structure of symbiotic dinoflagellates from Caribbean coral reefs. *Mar. Biol.* 141, 387–400. doi: 10.1007/s00227-002-0829-2

Lajeunesse, T. C., Bhagooli, R., Hidaka, M., deVantier, L., Done, T., Schmidt, G., et al. (2004). Closely related *Symbiodinium* spp. differ in relative dominance in coral reef host communities across environmental, latitudinal and biogeographic gradients. *Mar. Ecol. Progr. Ser.* 284, 147–161.

Larcombe, P., Ridd, P. V., Prytz, A., and Wilson, B. (1995). Factors controlling suspended sediment on inner-shelf coral reefs, Townsville, Australia. *Coral Reefs* 14, 163–171. doi: 10.1007/BF00367235

Lee, S. T. M., Davy, S. K., Tang, S. L., and Kench, P. S. (2016). Mucus sugar content shapes the bacterial community structure in thermally stressed *Acropora muricata*. *Front. Microbiol.* 7:371. doi: 10.3389/fmicb.2016.00371

Leite, D. C. A., Leão, P., Garrido, A. G., Lins, U., Santos, H. F., Pires, D. O., et al. (2017). Broadcast spawning coral *Mussismilia hispida* can vertically transfer its associated bacterial core. *Front. Microbiol.* 8:176. doi: 10.3389/fmicb.2017.00176

Li, J., Chen, Q., Long, L. J., Dong, J. D., Yang, J., and Zhang, S. (2014). Bacterial dynamics within the mucus, tissue and skeleton of the coral *Porites lutea* during different seasons. *Sci. Rep.* 4:7320. doi: 10.1038/srep07320

Maher, R. L., Schmeltzer, E. R., Meiling, S., McMinds, R., Ezzat, L., Shantz, A. A., et al. (2020). Coral microbiomes demonstrate flexibility and resilience through a reduction in community diversity following a thermal stress event. *Front. Ecol. Evol.* 8:555698. doi: 10.3389/fevo.2020.555698

Marcelino, V. R., Van Oppen, M. J. H., and Verbruggen, H. (2018). Highly structured prokaryote communities exist within the skeleton of coral colonies. *ISME J.* 12, 300–303. doi: 10.1038/ismej.2017.164

Martin, M. (2013). Cutadapt removes adapter sequences from high-throughput sequencing reads. *EMBnet* 7, 2803–2809.

Martin, S. B., Sasal, P., Cutmore, S. C., Ward, S., Aeby, G. S., and Cribb, T. H. (2018). Intermediate host switches drive diversification among the largest trematode family: evidence from the Polypipapiliotrematinae n. subf. (Opecoelidae), parasites transmitted to butterflyfishes via predation of coral polyps. *Int. J. Parasitol.* 48, 1107–1126. doi: 10.1016/j.ijpara.2018.09.003

Matz, M. V. (2016). *MCMC.OTU: Bayesian Analysis of Multivariate counts Data. R Package*.

McMurdie, P. J., and Holmes, S. (2013). Phyloseq: an r package for reproducible interactive analysis and graphics of microbiome census data. *PLoS One* 8:e61217. doi: 10.1371/journal.pone.0061217

Minton, D. (2015). *Changes in Coral Reef Structure Along a Sediment Gradient in Fouha Bay. Final Report for National Oceanic and Atmospheric Administration Pacific Islands Regional Office*. Honolulu, HI: National Oceanic and Atmospheric Administration Pacific Islands Regional Office, 190.

Neave, M. J., Apprill, A., Ferrier-Pagès, C., and Voolstra, C. R. (2016). Diversity and function of prevalent symbiotic marine bacteria in the genus Endozoicomonas. *Appl. Microbiol. Biotechnol.* 100, 8315–8324. doi: 10.1007/s00253-016-7777-0

Neave, M. J., Rachmawati, R., Xun, L., Michell, C. T., Bourne, D. G., Apprill, A., et al. (2017). Differential specificity between closely related corals and abundant Endozoicomonas endosymbionts across global scales. *ISME J.* 11, 186–200. doi: 10.1038/ismej.2016.95

Nicolet, K. J., Chong-Seng, K. M., Pratchett, M. S., Willis, B. L., and Hoogenboom, M. O. (2018). Predation scars may influence host susceptibility to pathogens: evaluating the role of corallivores as vectors of coral disease. *Sci. Rep.* 8:5258. doi: 10.1038/s41598-018-23361-y

Oksanen, A. J., Blanchet, F. G., Friendly, M., Kindt, R., Legendre, P., Mcglinn, D., et al. (2020). *Package ' vegan .'*.

Parada, A. E., Needham, D. M., and Fuhrman, J. A. (2016). Every base matters: assessing small subunit rRNA primers for marine microbiomes with mock communities, time series and global field samples. *Environ. Microbiol.* 18, 1403–1414. doi: 10.1111/1462-2920.13023

Patten, N. L., Mitchell, J. G., Middelboe, M., Eyre, B. D., Seuront, L., Harrison, P. L., et al. (2008). Bacterial and viral dynamics during a mass coral spawning period on the Great Barrier Reef. *Aquat. Microb. Ecol.* 50, 209–220. doi: 10.3354/ame01179

Pogoreutz, C., Rädecker, N., Cárdenas, A., Gärdes, A., Wild, C., and Voolstra, C. R. (2018). Dominance of Endozoicomonas bacteria throughout coral bleaching and mortality suggests structural inflexibility of the *Pocillopora verrucosa* microbiome. *Ecol. Evol.* 8, 2240–2252. doi: 10.1002/ece3.3830

Pollock, F. J., Lamb, J. B., Field, S. N., Heron, S. F., Schaffelke, B., Shedrawi, G., et al. (2016). Correction: sediment and turbidity associated with offshore dredging increase coral disease prevalence on nearby reefs (PLoS ONE (2016) 9:7 (e102498) *PLoS One* 11:e0165541. doi: 10.1371/journal.pone.0165541

Pollock, F. J., McMinds, R., Smith, S., Bourne, D. G., Willis, B. L., Medina, M., et al. (2018). Coral-associated bacteria demonstrate phylosymbiosis

and cophylogeny. *Nat. Commun.* 9:4921. doi: 10.1038/s41467-018-07275-x

Qin, Z., Zhao, Z., Jiao, W., Han, Z., Xia, L., Fang, Y., et al. (2020). Coupled photocatalytic-bacterial degradation of pyrene: removal enhancement and bacterial community responses. *Environ. Res.* 183:109135. doi: 10.1016/j.envres.2020.109135

Quigley, K. M., Warner, P. A., Bay, L. K., and Willis, B. L. (2018). Unexpected mixed-mode transmission and moderate genetic regulation of *Symbiodinium* communities in a brooding coral. *Heredity* 121, 524–536. doi: 10.1038/s41437-018-0059-0

Ravindran, J., Kannapiran, E., Manikandan, B., Francis, K., Arora, S., Karunya, E., et al. (2013). UV-absorbing bacteria in coral mucus and their response to simulated temperature elevations. *Coral Reefs* 32, 1043–1050. doi: 10.1007/s00338-013-1053-x

Raymundo, L. J., Halford, A. R., Maypa, A. P., and Kerr, A. M. (2010). Functionally diverse reef-fish communities ameliorate coral disease (Proceedings of the National Academy Sciences of United States of America (2009) 106, 40 (17067-17070) *Proc. Natl. Acad. Sci. U.S.A.* 107:513. doi: 10.1073/pnas.0913173107 doi: 10.1073/pnas.0900365106

Reimer, J. D., Takishita, K., Ono, S., Maruyama, T., and Tsukahara, J. (2006). Latitudinal and intracolony ITS-rDNA sequence variation in the symbiotic dinoflagellate genus *Symbiodinium* (Dinophyceae) in *Zoanthus sansibaricus* (Anthozoa: Hexacorallia). *Phycol. Res.* 54, 122–132. doi: 10.1111/j.1440-1835.2006.00419.x

Ricardo, G. F., Jones, R. J., Clode, P. L., Humanes, A., and Negri, A. P. (2015). Suspended sediments limit coral sperm availability. *Sci. Rep.* 5:18084. doi: 10.1038/srep18084

Richmond, R. H. (1993). Coral reefs: Present problems and future concerns resulting from anthropogenic disturbance. *Integr. Comparat. Biol.* 33, 524–536. doi: 10.1093/icb/33.6.524

Richmond, R., and Hunter, C. (1990). Reproduction and recruitment of corals: comparisons among the Caribbean, the Tropical Pacific, and the Red Sea. *Mar. Ecol. Progr. Ser.* 60, 185–203. doi: 10.3354/meps060185

Ritchie, K. B. (2006). Regulation of microbial populations by coral surface mucus and mucus-associated bacteria. *Mar. Ecol. Progr. Ser.* 322, 1–14. doi: 10.3354/meps322001

Roder, C., Arif, C., Bayer, T., Aranda, M., Daniels, C., Shibl, A., et al. (2014). Bacterial profiling of white plague disease in a comparative coral species framework. *ISME J.* 8, 31–39. doi: 10.1038/ismej.2013.127

Rodríguez-Gómez, C., Durán-Riveroll, L. M., Okolodkov, Y. B., Oliart-Ros, R. M., García-Casillas, A. M., and Cembella, A. D. (2021). Diversity of bacterioplankton and bacteriobenthos from the veracruz reef system, southwestern gulf of Mexico. *Microorganisms* 9, 1–26. doi: 10.3390/microorganisms9030619

Rohwer, F. L., Seguritan, V., Azam, F., and Knowlton, N. (2002). Diversity and distribution of coral-associated bacteria. *Mar. Ecol. Progr. Ser.* 243, 1–10. doi: 10.3354/meps243001

Rongo, T. (2004). *Coral Community Change along a Sediment Gradient in Fouha Bay, Guam.* Master's thesis. Mangilao, GU: University of Guam Marine Laboratory.

Rosales, S. M., Clark, A. S., Huebner, L. K., Ruzicka, R. R., and Muller, E. M. (2020). Rhodobacterales and rhizobiales are associated with stony coral tissue loss disease and its suspected sources of transmission. *Front. Microbiol.* 11:681. doi: 10.3389/fmicb.2020.00681

Rowan, R., Knowlton, N., Baker, A., and Jara, J. (1997). Landscape ecology of algal symbionts creates variation in episodes of coral bleaching. *Nature* 388, 265–269. doi: 10.1038/40843

Sampayo, E. M., Ridgway, T., Franceschinis, L., Roff, G., Hoegh-Guldberg, O., and Dove, S. (2016). Coral symbioses under prolonged environmental change: living near tolerance range limits. *Sci. Rep.* 6:36271. doi: 10.1038/srep36271

Schöttner, S., Wild, C., Hoffmann, F., Boetius, A., and Ramette, A. (2012). Spatial scales of bacterial diversity in cold-water coral reef ecosystems. *PLoS One* 7:e32093. doi: 10.1371/journal.pone.0032093

Sheridan, C., Grosjean, P., Leblud, J., Palmer, C. V., Kushmaro, A., and Eeckhaut, I. (2014). Sedimentation rapidly induces an immune response and depletes energy stores in a hard coral. *Coral Reefs* 33, 1067–1076. doi: 10.1007/s00338-014-1202-x

Shivaji, S., Srinivas, T. N. R., and Reddy, G. S. N. (2014). "The family Planococcaceae," in *The Prokaryotes: Firmicutes and Tenericutes*, eds E. Rosenberg, E. F. DeLong, S. Lory, E. Stackebrandt, and F. Thompson (Berlin: Springer), doi: 10.1007/978-3-642-30120-9

Shore-Maggio, A., Aeby, G. S., and Callahan, S. M. (2018). Influence of salinity and sedimentation on Vibrio infection of the Hawaiian coral *Montipora capitata*. *Dis. Aquat. Organ.* 128, 63–71. doi: 10.3354/dao03213

Sunagawa, S., Desantis, T. Z., Piceno, Y. M., Brodie, E. L., Desalvo, M. K., Voolstra, C. R., et al. (2009). Bacterial diversity and white Plague disease-associated community changes in the caribbean coral montastraea faveolata. *ISME J.* 3, 512–521. doi: 10.1038/ismej.2008.131

Sweet, M. J., Croquer, A., and Bythell, J. C. (2011). Bacterial assemblages differ between compartments within the coral holobiont. *Coral Reefs* 30, 39–52. doi: 10.1007/s00338-010-0695-1

Sweet, M., Burian, A., Fifer, J., Bulling, M., Elliott, D., and Raymundo, L. (2019). Compositional homogeneity in the pathobiome of a new, slow-spreading coral disease. *Microbiome* 7:139. doi: 10.1186/s40168-019-0759-6

Tan, Y. T. R., Wainwright, B. J., Afiq-Rosli, L., Ip, Y. C. A., Lee, J. N., Nguyen, N. T. H., et al. (2020). Endosymbiont diversity and community structure in *Porites lutea* from Southeast Asia are driven by a suite of environmental variables. *Symbiosis* 80, 269–277. doi: 10.1007/s13199-020-00671-2

Terraneo, T. I., Fusi, M., Hume, B. C. C., Arrigoni, R., Voolstra, C. R., Benzoni, F., et al. (2019). Environmental latitudinal gradients and host-specificity shape Symbiodiniaceae distribution in Red Sea Porites corals. *J. Biogeogr.* 46, 2323–2335. doi: 10.1111/jbi.13672

Thornhill, D. J., Fitt, W. K., and Schmidt, G. W. (2006). Highly stable symbioses among western Atlantic brooding corals. *Coral Reefs* 25, 515–519. doi: 10.1007/s00338-006-0157-y

Tilstra, A., El-Khaled, Y. C., Roth, F., Rädecker, N., Pogoreutz, C., Voolstra, C. R., et al. (2019). Denitrification aligns with N2 fixation in Red Sea Corals. *Sci. Rep.* 9:19460. doi: 10.1038/s41598-019-55408-z

Ulstrup, K. E., and Van Oppen, M. J. H. (2003). Geographic and habitat partitioning of genetically distinct zooxanthellae (*Symbiodinium*) in *Acropora* corals on the Great Barrier Reef. *Mol. Ecol.* 12, 3477–3484. doi: 10.1046/j.1365-294X.2003.01988.x

van Oppen, M. J., Palstra, F. P., Piquet, A. M., and Miller, D. J. (2001). Patterns of coral-dinoflagellate associations in *Acropora*: significance of local availability and physiology of *Symbiodinium* strains and host-symbiont selectivity. *Proc. Biol. Sci.* 268, 1759–1767. doi: 10.1098/rspb.2001.1733

Wagle, S. R., Vaughan, D. A., Mistry, S. P., and Johnson, B. C. (1958). Vitamin B12 and nucleic acid biosynthesis. *J. Biol. Chem.* 239, 917–921.

Warner, M. E., Chilcoat, G. C., McFarland, F. K., and Fitt, W. K. (2002). Seasonal fluctuations in the photosynthetic capacity of photosystem II in symbiotic dinoflagellates in the Caribbean reef-building coral Montastraea. *Mar. Biol.* 141, 31–38. doi: 10.1007/s00227-002-0807-8

Weber, M., De Beer, D., Lott, C., Polerecky, L., Kohls, K., Abed, R. M. M., et al. (2012). Mechanisms of damage to corals exposed to sedimentation. *Proc. Natl. Acad. Sci. U.S.A.* 109, E1558–E1567. doi: 10.1073/pnas.1100715109

West, K., and Van Woesik, R. (2001). Spatial and temporal variance of river discharge on Okinawa (Japan): Inferring the temporal impact on adjacent coral reefs. *Mar. Pollut. Bull.* 42, 864–872. doi: 10.1016/S0025-326X(01)00040-6

Wiese, J., Imhoff, J. F., Horn, H., Borchert, E., Kyrpides, N. C., Göker, M., et al. (2020). Genome analysis of the marine bacterium *Kiloniella laminariae* and first insights into comparative genomics with related *Kiloniella* species. *Arch. Microbiol.* 202, 815–824. doi: 10.1007/s00203-019-01791-0

Wild, C., Huettel, M., Klueter, A., Kremb, S. G., Rasheed, M. Y. M., and Jørgensen, B. B. (2004). Coral mucus functions as an energy carrier and particle trap in the reef ecosystem. *Nature* 428, 66–70. doi: 10.1038/nature02344

Wolanski, E., Richmond, R. H., Davis, G., and Bonito, V. (2003). Water and fine sediment dynamics in transient river plumes in a small, reef-fringed bay, Guam. *Estuar. Coast. Shelf Sci.* 56, 1029–1040. doi: 10.1016/S0272-7714(02)00321-9

Yoghiapiscessa, D., Batubara, I., and Wahyudi, A. T. (2016). Antimicrobial and antioxidant activities of bacterial extracts from marine bacteria associated with

sponge Stylotella sp. *Am. J. Biochem. Biotechnol.* 12, 36–46. doi: 10.3844/ajbbsp.2016.36.46

Zheng, Y., Yu, M., Liu, Y., Su, Y., Xu, T., Yu, M., et al. (2016). Comparison of cultivable bacterial communities associated with Pacific white shrimp (*Litopenaeus vannamei*) larvae at different health statuses and growth stages. *Aquaculture* 451, 163–169. doi: 10.1016/j.aquaculture.2015.09.020

Ziegler, M., Grupstra, C. G. B., Barreto, M. M., Eaton, M., BaOmar, J., Zubier, K., et al. (2019). Coral bacterial community structure responds to environmental change in a host-specific manner. *Nat. Commun.* 10:3092. doi: 10.1038/s41467-019-10969-5

Ziegler, M., Roder, C., Bchel, C., and Voolstra, C. R. (2015). Niche acclimatization in Red Sea corals is dependent on flexibility of host-symbiont association. *Mar. Ecol. Progr. Ser.* 533, 163–176. doi: 10.3354/meps11365

Ziegler, M., Seneca, F. O., Yum, L. K., Palumbi, S. R., and Voolstra, C. R. (2017). Bacterial community dynamics are linked to patterns of coral heat tolerance. *Nat. Commun.* 8:14213. doi: 10.1038/ncomms14213

Conflict of Interest: The authors declare that the research was conducted in the absence of any commercial or financial relationships that could be construed as a potential conflict of interest.

frontiers in Physiology

ORIGINAL RESEARCH
published: 10 February 2022
doi: 10.3389/fphys.2022.819111

Intrinsically High Capacity of Animal Cells From a Symbiotic Cnidarian to Deal With Pro-Oxidative Conditions

Pauline Cotinat[1,2], Clara Fricano[1,2‡], Gaëlle Toullec[1†‡], Eric Röttinger[1,2], Stéphanie Barnay-Verdier[1,2,3§] and Paola Furla[1,2§]*

[1] CNRS, INSERM, Institute for Research on Cancer and Aging, Nice, Université Côte d'Azur, Nice, France, [2] Institut Fédératif de Recherche – Ressources Marines (MARRES), Université Côte d'Azur, Nice, France, [3] UFR 927, Sorbonne Université, Paris, France

OPEN ACCESS

Edited by:
Davide Seveso,
University of Milano-Bicocca, Italy

Reviewed by:
Tingting Xiang,
University of North Carolina at Charlotte, United States
John Robert Finnerty,
Boston University, United States

***Correspondence:**
Paola Furla
paola.furla@unice.fr

†Present address:
Gaëlle Toullec,
Laboratory for Biological Geochemistry, School of Architecture, Civil and Environmental Engineering, Ecole Polytechnique Fédérale de Lausanne, Lausanne, Switzerland

‡These authors have contributed equally to this work

§These authors share senior authorship

Specialty section:
This article was submitted to Aquatic Physiology, a section of the journal Frontiers in Physiology

Received: 20 November 2021
Accepted: 10 January 2022
Published: 10 February 2022

Citation:
Cotinat P, Fricano C, Toullec G, Röttinger E, Barnay-Verdier S and Furla P (2022) Intrinsically High Capacity of Animal Cells From a Symbiotic Cnidarian to Deal With Pro-Oxidative Conditions. Front. Physiol. 13:819111. doi: 10.3389/fphys.2022.819111

The cnidarian-dinoflagellate symbiosis is a mutualistic intracellular association based on the photosynthetic activity of the endosymbiont. This relationship involves significant constraints and requires co-evolution processes, such as an extensive capacity of the holobiont to counteract pro-oxidative conditions induced by hyperoxia generated during photosynthesis. In this study, we analyzed the capacity of *Anemonia viridis* cells to deal with pro-oxidative conditions by *in vivo* and *in vitro* approaches. Whole specimens and animal primary cell cultures were submitted to 200 and 500 μM of H_2O_2 during 7 days. Then, we monitored global health parameters (symbiotic state, viability, and cell growth) and stress biomarkers (global antioxidant capacity, oxidative protein damages, and protein ubiquitination). In animal primary cell cultures, the intracellular reactive oxygen species (ROS) levels were also evaluated under H_2O_2 treatments. At the whole organism scale, both H_2O_2 concentrations didn't affect the survival and animal tissues exhibited a high resistance to H_2O_2 treatments. Moreover, no bleaching has been observed, even at high H_2O_2 concentration and after long exposure (7 days). Although, the community has suggested the role of ROS as the cause of bleaching, our results indicating the absence of bleaching under high H_2O_2 concentration may exculpate this specific ROS from being involved in the molecular processes inducing bleaching. However, counterintuitively, the symbiont compartment appeared sensitive to an H_2O_2 burst as it displayed oxidative protein damages, despite an enhancement of antioxidant capacity. The *in vitro* assays allowed highlighting an intrinsic high capacity of isolated animal cells to deal with pro-oxidative conditions, although we observed differences on tolerance between H_2O_2 treatments. The 200 μM H_2O_2 concentration appeared to correspond to the tolerance threshold of animal cells. Indeed, no disequilibrium on redox state was observed and only a cell growth decrease was measured. Contrarily, the 500 μM H_2O_2 concentration induced a stress state, characterized by a cell viability decrease from 1 day and a drastic cell growth arrest after 7 days leading to an uncomplete recovery after treatment. In conclusion, this study highlights the overall high capacity of cnidarian cells to cope with H_2O_2 and opens new perspective to investigate the molecular mechanisms involved in this peculiar resistance.

Keywords: ***Anemonia viridis*, *in vitro* cell cultures, oxidative stress, hydrogen peroxide, cnidarian**

INTRODUCTION

The evolutionary success of symbiotic cnidarians is based on a mutualism with dinoflagellates of the family Symbiodiniaceae. The symbionts, living inside the gastrodermal host cells, find a protected and stable environment and benefit from inorganic compounds provided by the animal cells (e.g., nitrogen, phosphorus, and sulfate) for their photosynthetic activity. Conversely, the animal host benefits from the organic compounds produced by algal photosynthesis (e.g., glucose and subsequently amino-acids, lipids) and largely transferred from the alga to the animal cell (Davy et al., 2012). This partner cooperation allows autotrophy to the animal host, leading to the colonization of oligotrophic waters by the symbiotic holobiont.

Concomitantly with those advantages, some constraints appear, especially the photosynthetic-dependent production of oxygen in the animal tissue. Such oxygen production causes diurnal hyperoxia condition in a symbiotic cnidarian, leading to a pro-oxidant state with reactive oxygen species (ROS) overproduction (Dykens et al., 1992; Richier et al., 2003; Saragosti et al., 2010; Shaked and Armoza-Zvuloni, 2013). Both partners have the pathways for cross-regulating the intracellular redox state, especially by ROS detoxication through a full suite of antioxidant enzymes to avoid cellular damages (Shick and Dykens, 1985; Richier et al., 2003, 2005; Plantivaux et al., 2004; Furla et al., 2005; Merle et al., 2007; Pey et al., 2017).

The study of ROS sensitivity in these organisms is also of environmental interest. Environmental perturbations (especially variations in temperature and UV radiation) induce oxidative stress that may lead in extreme cases to symbiosis breakdown, a process commonly called bleaching. Thus, under stressful oxidative conditions, Symbiodiniaceae can be eliminated from or exit the host through different cellular processes, like exocytosis, cell detachment, necrosis or apoptosis (see for review Suggett and Smith, 2020). Oxidative stress is known to induce specific cellular damages such as DNA modification (DNA adducts), lipid peroxidation and protein oxidation. In symbiotic cnidarians, several biochemical biomarkers (e.g., protein carbonylation, lipid peroxidation, and protein ubiquitination) were validated in studies following imbalances between ROS overproduction and antioxidant defenses during environmental stress, resulting in the disruption of the symbiotic association (e.g., Lesser and Farrell, 2004; Richier et al., 2006; Pey et al., 2011).

Among ROS, hydrogen peroxide (H_2O_2) is a relatively stable chemical formed from O_2 and is naturally present in the aquatic systems (Ndungu et al., 2019) with concentrations ranging from 0.3 μM in the water column to 4 μM in intertidal areas (Abele-Oeschger et al., 1997). It originates from marine biota (Hansel and Diaz, 2021) or is carried by the rain (Cooper et al., 1987). In all the organisms, intracellular H_2O_2 levels can reach tens of micromolar and is generated during normal cellular metabolism (i.e., photosynthesis and respiration) playing crucial roles in the intracellular signaling such as hypoxic signal transduction, cell differentiation and proliferation as well as for immune responses (Halliwell et al., 2000; Apel and Hirt, 2004; Giorgio et al., 2007). At high production levels, the H_2O_2 effect can be mitigated by several antioxidant defenses including peroxidases, catalases, thioredoxin reductase, peroxiredoxins, and glutathione S-transferases family enzymes which can lead to rapidly decreasing intracellular H_2O_2 concentrations. However, if cellular redox homeostasis cannot be maintained, H_2O_2 leads to reversible and irreversible oxidative modifications of proteins (e.g., carbonylation), enhancing protein ubiquitination and subsequent proteasome activation. In addition, cell cycle arrest or apoptosis could also be observed (see for review Fulda et al., 2010). Although the impact of H_2O_2 has been more widely investigated in mammalian cells and particularly in tumor cells (see for review Lennicke et al., 2015), studies have shown a similar impact in marine invertebrates, such as bivalves or polychaetes (Abele-Oeschger et al., 1994; McDonagh and Sheehan, 2006, 2007; Da Rosa et al., 2008; Friedman et al., 2018; Nguyen, 2020).

In the coral symbiont, H_2O_2 has been shown to be a by-product of photosynthesis processes (Suggett et al., 2008; Armoza-Zvuloni and Shaked, 2014). Thanks to its cell-permeable properties, H_2O_2 may diffuse from algal to animal host cells. Interestingly, some studies reported a release of H_2O_2 from non-stressed corals (Armoza-Zvuloni and Shaked, 2014) and an extracellular production by the dynamics of the superoxide anion (Saragosti et al., 2010). Therefore, due to their symbiosis lifestyle, animal host cells are daily exposed to H_2O_2, raising the question of their intrinsic potential to resist a massive influx of H_2O_2. Nevertheless, in excess, ROS (including H_2O_2) cause negative impact (mostly on protein and lipids) on the symbiont, leading to photosynthesis impairment, even if no bleaching phenomenon is induced (Higuchi et al., 2009; Roberty et al., 2015, 2016).

Anemonia viridis is a temperate sea anemone deeply studied as biological model of the cnidarian-dinoflagellate symbiosis. Its enzymatic antioxidant properties, tissue distribution and regulation have been intensively investigated (Hawkridge et al., 2000; Richier et al., 2003, 2005; Plantivaux et al., 2004; Merle et al., 2007; Ganot et al., 2011; Pey et al., 2017). In addition, the sensitivity of *A. viridis* to thermal and UV stresses has been well described and some mechanisms of bleaching have been decrypted, including oxidative stress and apoptosis (Richier et al., 2006; Moya et al., 2012). Recently, we succeeded in the establishment of primary cell cultures from *A. viridis* exhibiting a gastrodermal signature (Barnay-Verdier et al., 2013; Ventura et al., 2018; Fricano et al., 2020). Thus, to test the hypothesis of an intrinsic resistance of animal cells to H_2O_2, we exposed *A. viridis* specimens and primary cell cultures at the same H_2O_2 concentrations (200 and 500 μM) during the same periods of time (24 h and 7 days), and compared the respective responses. For each treatment, we monitored global health parameters (symbiotic state, viability and cell growth) and stress biomarkers (global antioxidant capacity, oxidative protein damages, and protein ubiquitination). This allowed us to assess the cnidarian cell susceptibility to H_2O_2 exposure, highlighting the putative influence of the tissue organization or/and of the presence of symbionts.

MATERIALS AND METHODS

Biological Material

Anemonia viridis Specimens

Specimens of *A. viridis* (Forskal 1775) were collected (prefectural authorization n107; 28 February 2019) from "Plage des ondes," Antibes, France, (43°33′17″ N, 7°07′17.7″ E), and maintained in a closed-circuit aquarium with artificial seawater (ASW, Prodibio Expert Reef Salt) at 36–38‰ at 18.0 ± 0.5°C with weekly water changes. A LED bar (450 nm—Deckey LED aquarium) provided light at a constant saturating irradiance of 100 μmol $m^{-2}s^{-1}$ (measured using a special sensor QSL-100, Biospherical Instruments Inc., San Diego, CA, United States) on a 12 h:12 h (light:dark) photoperiod. Sea anemones were fed once a week with oysters.

Gastrodermal Primary Cell Cultures

Independent primary cell cultures were obtained from different *A. viridis* individuals and maintained as described in Ventura et al. (2018) and Fricano et al. (2020). Briefly, cells were cultured in the dark in a thermo-regulated incubator (POL-EKO-APARATURA, Poland) at 20.0 ± 0.5°C. The optimized culture medium was replaced weekly and consisted of 20% GMIM (Gibco, Carlsbad, CA, United States), 5% fetal bovine serum (FBS; PAA/GE Healthcare, Chicago, IL, United States), 1% kanamycin (100 μg/mL, Sigma-Aldrich), 1% amphotericin B (2.5 μg/mL; Interchim, Montluçon, France), 1% antibiotic antimycotic solution (Sigma-Aldrich), 1% L-glutamate (Sigma-Aldrich), and 71% of filtered ASW. The medium was adapted in respect to the Mediterranean Seawater characteristics (i.e., salinity 40 ppt and pH 8.1).

Hydrogen Peroxide Experimental Design

In vivo Experiments

Eight specimens of *A. viridis* were kept individually in 5 L tanks under controlled conditions. Six tentacles were cut from each specimen after 24 h and 7 days to assess the control condition. For 200 and 500 μM H_2O_2 treatments, a solution of H_2O_2 (Sigma-Aldrich) was added in each tank (200 μM for four of them and 500 μM for the four others). After 24 h and 7 days of treatment, six tentacles were cut from each specimen to assess the treatment condition. All tentacles from the different time points and conditions were longitudinally opened and the gastroderm (containing the dinoflagellates) was manually separated from the epiderm. A centrifugation at 1,000 × *g* for 5 min was used to separate the gastrodermal compartment from the dinoflagellates fraction (Richier et al., 2003).

In vitro Experiments

The cell response to H_2O_2 treatment was assessed on at least three independent primary cell cultures. Cells seeded in 12-well plates were exposed to H_2O_2 treatment (Sigma-Aldrich) starting with a dose-response experiment (between 0 and 2 mM) for 7 days. Another set of experiments was performed by incubating cells to 0 (control), 200 and 500 μM H_2O_2 for short term (1, 2, and 6 h) or long term (1 day or 7 days) exposure. We then conducted resilience experiments by reseeding the treated cells in their normal culture medium for 7 days to assess their recovery capacity. Three wells, for each condition and time point, were used for all analyses.

Symbiotic State Assessment of *A. viridis* Specimens

The density of the endosymbionts from the genus *Philozoon* sp. (LaJeunesse et al., 2021) was assessed according to Zamoum and Furla (2012). Briefly, two tentacles were cut from each animal before and after H_2O_2 treatment in each condition (0, 200, or 500 μM H_2O_2) and then put in 2 M solution of NaOH and incubated at 37°C for 1 h to dissolve all animal tissue. To determine symbiont density, three replicate samples were counted using a modified Neubauer hemocytometer (Sigma-Aldrich). The remaining extract was used to determine the protein content from which we normalized symbiont density.

Protein Extractions

Gastrodermal cells from primary cultures and the animal's epidermal and gastrodermal tissues were all separately placed in 200 μL of lysis extraction buffer (HEPES 25 mM, MgCl2 5 mM, EDTA 5 mM, DTT 5 mM, and PMSF 2 mM) and homogenized. Tissue samples were potterized, and both tissue and cell samples were sonicated and centrifuged to obtain the cytosoluble protein content. The total protein concentration of each sample was then assessed by a Bradford assay (Bradford reagent; SIGMA-ALDRICH), using 0–2 μg/ml bovine serum albumin solutions as standard curve.

Cell Viability and Growth Rate of Cultivated Cells

Cell viability was assessed by evaluating the membrane integrity using the Evans blue method. Therefore, viable cells (unstained) and dead cells (stained) were identified and counted on a Neubauer improved hemocytometer (Sigma-Aldrich) using an optic microscope (Zeiss Axio Imager Z1). The cell viability was defined as the percentage of viable cells relative to total cells (i.e., viable and dead cells). Cell growth rate was assessed every week using the cells counts with Evans blue method, as previously described in Ventura et al. (2018) and Fricano et al. (2020). The following formula was then used to calculate the weekly growth rate:

$$\text{Growth rate} = \frac{(\text{Viable cells (d} + 7) - \text{Viable cells (d)})}{\text{Viable cells (d)}}\ \text{d} = \text{day}$$

Total Oxidative Scavenging Capacity Assay

The oxygen radical scavenging activities of protein samples were determined using fluorometric assay according to Naguib (2000). Protein samples are incubated with phosphate buffer (75 mM pH 7.5), in presence of 180 nM 6-carboxyfluorescein as fluorescent probe and 36 mM AAPH [2,2′-azobis(2-amidinopropane) dihydrochloride] as the peroxyl radical generator. In the assay, Trolox [6-hydroxy-2,5,7,8-tetramethylchroman-2-carboxylic acid] is used as antioxidant calibrator. Fluorescence recordings were performed in black microplates (96-wells Greiner Bio-One),

and fluorescence decay was measured by spectrofluorometer (Safas, Monaco) every minute for a total duration of 1 h at an excitation/emission wavelength of 520/495 nm. Relative antioxidant activities of protein samples (tested in duplicate) were measured by comparison with Trolox standard. Results were expressed in Trolox equivalents and represented in the figures as a ratio to the control condition.

Protein Carbonylation Analysis

Carbonyl content of the cytosolic extractions was measured using an ELISA assay and spectrophotometry, according to Buss et al. (1997). Protein derivatization was done by adding a dinitrophenylhydrazine (DNP) solution (10 mM in 6 M guanidine hydrochloride, 0.5 M potassium phosphate buffer) to the protein samples. The ELISA assay used anti-DNP antibody produced in rabbit (1:500; Sigma-Aldrich) and anti-rabbit Ig (1:2000; Bio-Rad). 0–100% reduced bovine serum albumin (BSA) were used as standard curve. Carbonyl content of protein samples was expressed in nanomoles per milligram of protein and was then represented in the figures as a ratio to the control condition.

Ubiquitin Conjugates Dot-Blot Analysis

Ubiquitinated proteins were assayed, according to Haas and Bright (1985), by dot-blotting 3 μg of protein samples fixed to a nitrocellulose membrane, which was incubated with primary antibody (1:1000; Mono- and polyubiquitinylated conjugates recombinant monoclonal antibody; Enzo Life Sciences). The membrane was next incubated with the secondary antibody (1:5000; anti-mouse antibody; Sigma-Aldrich). After chemiluminescence revelation (ECL), levels of spot density were measured using image analysis on GeneTools (SynGene). Levels of ubiquitinated proteins were obtained after normalization by spot density measured after amido black solution staining. Results were represented in the figures as a ratio to the control condition.

Detection of Intracellular Reactive Oxygen Species

Intracellular ROS were detected in cultivated cells treated or not with H_2O_2 using a sensitive fluorescent probe that penetrates the cell and, when oxidized by intracellular free radicals, binds to DNA, emitting a more intense green fluorescence (CellROX^{TM} Green Reagent, Invitrogen). We followed the manufacturer's instructions. Briefly, 10 μL of a 500 μM solution of CellROX^{TM} Green were added to each treated well during 30 min at room temperature in the dark. After rinsing, cells were resuspended in 200 μL of PBS 0.6 M. Samples were then analyzed by flow cytometry (CytoFLEX LX, Beckman Coulter), excited at 488 nm and detected at 515–530 nm. For data analysis, we selected the green-fluorescent cells (CellROX-positive cells) within the population of interest. The population of interest corresponds to the cell population from which the analysis has been conducted after hierarchical exclusion of debris and doublets. For each experiment, controls (i.e., untreated cells) allowed to evaluate the basal intracellular ROS level in the cell cultures.

Statistical Analysis

For all cellular and biochemical markers evaluated in this study, the effect of the different treatments was analyzed with a two-way ANOVA test or Kruskal–Wallis test followed by, respectively, a Tukey's or Dunn *post hoc*, depending on the homoscedasticity of the data set. All experiments, i.e., *in vivo* and *in vitro*, were conducted on at least three independent biological replicates.

RESULTS

Hydrogen Peroxide Effects on *A. viridis* Specimens

To determine the susceptibility of *A. viridis* specimen to H_2O_2, we monitored the sign of bleaching, tissue necrosis and potential mortality during 7 days of exposure. No sign of tissue necrosis or mortality of the *A. viridis* specimens have been observed during H_2O_2 exposure. In addition, no differences in the symbiotic state have been measured since the quantity of symbionts, *Philozoon* sp. genus, per mg of protein remained the same after 7 days of treatment with both H_2O_2 concentrations (**Figure 1**). In addition, the sea anemones were also monitored several weeks after the treatment, and no signs of bleaching or disease were observed (data not shown).

Hydrogen Peroxide Effects on Stress Biomarkers of *A. viridis* Tissues Under Treatments

To analyze the impact of H_2O_2 at the tissue level, we assessed three biochemical stress markers (TOSC, carbonylation, and ubiquitination) known to be associated with oxidative stress conditions, in the three tissue compartments (epiderm, gastroderm, and symbiont) separately. In the epiderm, we only observed a slight but significant decrease of TOSC after 7 days of 200 μM H_2O_2 (**Figures 2A–C**). It is noteworthy

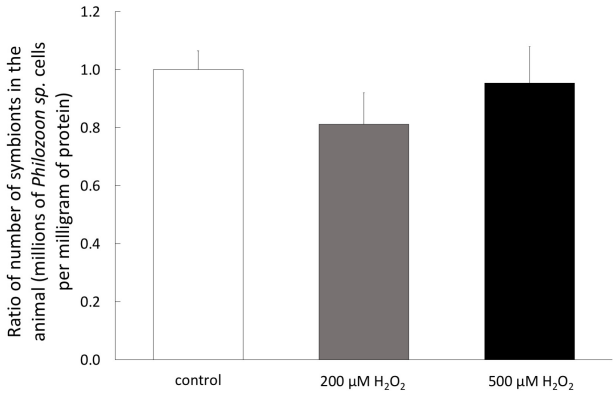

FIGURE 1 | Symbiotic state of *A. viridis* specimens under H_2O_2 treatments. Content of *Philozoon* sp. symbionts in the tentacles of *A. viridis* before and after 7 days of 0 μM (control, white bars) 200 μM (gray bars) and 500 μM (black bars). At day 0, the *A. viridis* specimens hosted 2.3×10^6 symbiont mg^{-1}. Data are represented as means with standard error bars.

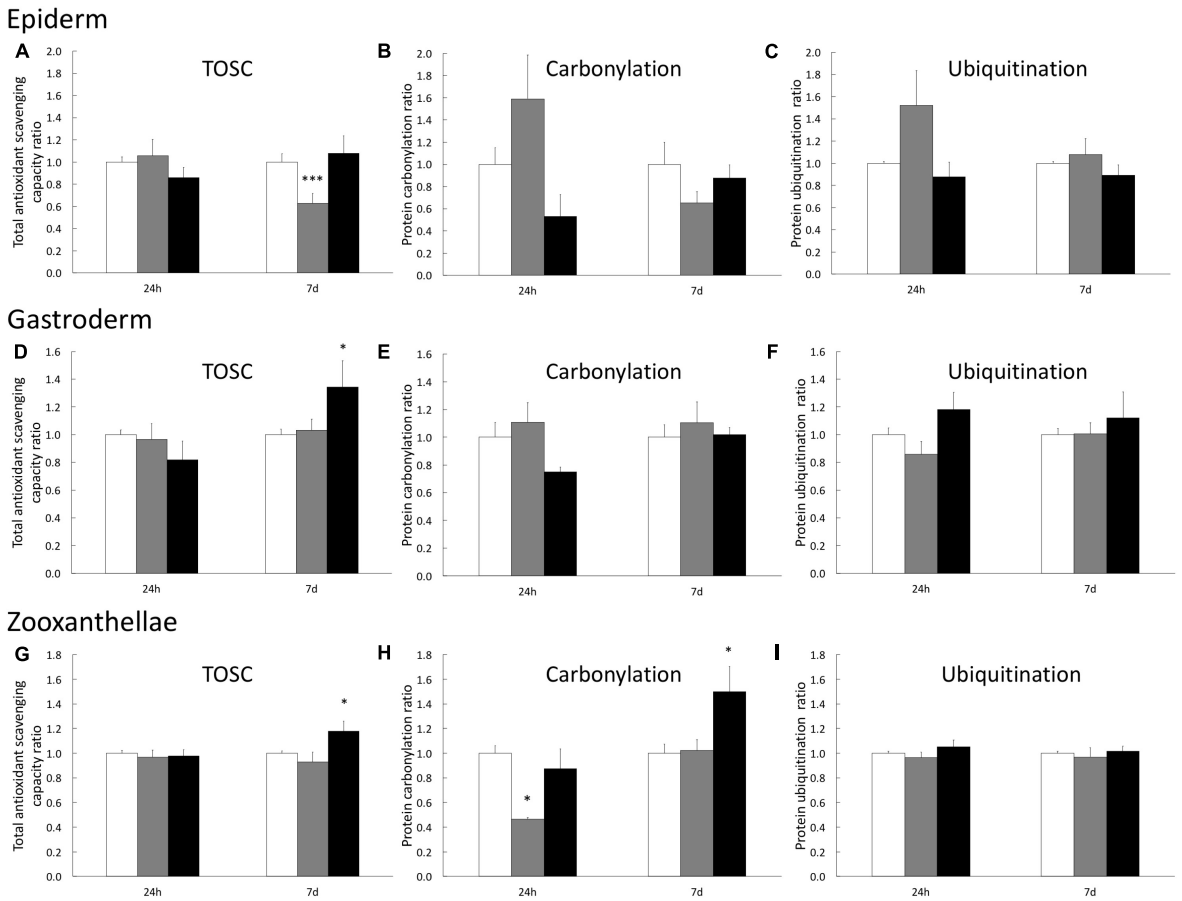

FIGURE 2 | Stress biomarkers in *A. viridis* tissues under H_2O_2 treatments. Measurements have been performed separately on animal's epiderm extracts **(A–C)**, on animal's gastroderm extract **(D–F)** and on symbiont extracts **(G–I)** from the gastroderm. Total Oxidative Scavenging Capacity **(A,D,G)**, protein carbonylation **(B,E,H)** and protein ubiquitination **(C,F,I)** were measured under 0 μM H_2O_2 (control; white bars), 200 μM H_2O_2 (gray bars) and 500 μM H_2O_2 (black bars). Data are expressed relative to the control condition (ratio of the control condition). Means values with standard error bars are presented. Significant differences between control and stress condition are expressed by $*p < 0.05$ and $***p < 0.001$.

that after 1 day of 200 μM H_2O_2, we observed a trend of increasing protein damages (carbonylation and ubiquitination), which totally disappeared after 7 days.

In the gastrodermal compartment (i.e., animal tissue), we only observed an effect of H_2O_2 treatments after 7 days of 500 μM H_2O_2, inducing a 34% increase of TOSC (**Figure 2D**) which is sufficient to avoid protein damages (**Figures 2E,F**). Finally, the analysis on the symbiont fraction showed an increase of TOSC (17% higher than the control), associated with an increase of protein carbonylation level (50% higher than the control) after 7 days at 500 μM H_2O_2 (**Figures 2G,H**). No impact on symbiont protein ubiquitination has been measured (**Figure 2I**). Taken together these data suggest a higher capacity of cnidarian animal cells to cope with H_2O_2 and prevent protein damages compared to the algal symbiont.

Dose Response of Gastrodermal Cultivated Cells to Hydrogen Peroxide

To gain more insight in the capacity of the animal gastrodermal compartment to cope with ROS we first assessed the overall toxicity of H_2O_2 using gastrodermal cell cultures from *A. viridis*. More precisely, we applied a range of H_2O_2 concentrations from 100 μM to 2 mM for 7 days and assessed cellular growth and viability (**Figure 3**). Without any treatment, the mean viability of cultivated cells was 93% ± 1.17 and the weekly growth rate was 18.7 ± 4.5. At 100 μM, no effect on viability and growth rate was observed. The first significant effects on both parameters appeared at 200 μM (10% viability and 42% growth rate decreases) and drastically exacerbated at 500 μM. With a concentration of 500 μM H_2O_2, the viability was decreased by 58% (EC_{50} = 400.8 μM) and the growth was totally arrested. These results led us to direct further experiments toward the concentrations of 200 and 500 μM H_2O_2, where the response of the cells seemed pivotal and allowing the comparison with the *in vivo* experiments.

Hydrogen Peroxide Effects on Oxidative Status of Gastrodermal Cultivated Cells

To test whether H_2O_2 treatments induced an intracellular ROS increase, we stained cultivated cells with specific fluorescent

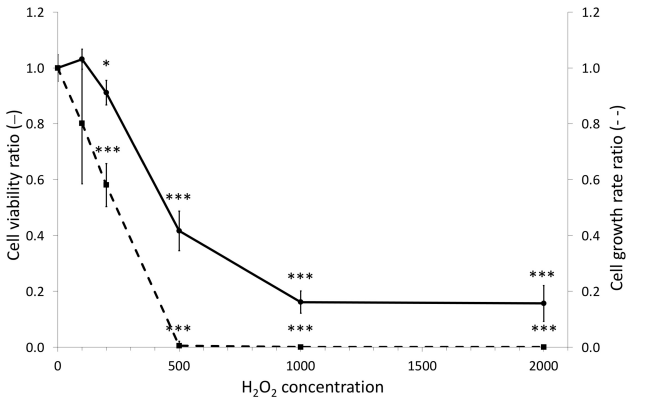

FIGURE 3 | Dose viability and growth responses of gastrodermal cultivated cells under H_2O_2 treatments. *A. viridis* gastrodermal cultivated cells were treated with H_2O_2 at different concentrations for 7 days before measuring cell viability (solid line) and cell growth rate (dashed line). Cell viability and growth rate are expressed relative to the control condition (ratio of the control condition). Means values with standard error bars are presented. Significant differences between control and stress condition are expressed by $^*p < 0.05$ and $^{***}p < 0.001$.

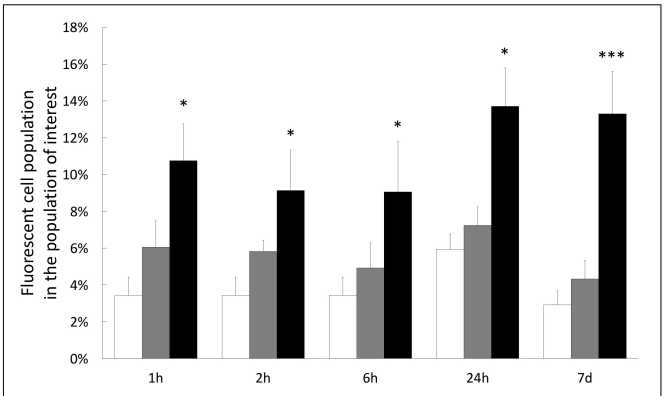

FIGURE 4 | Quantification of intracellular ROS in gastrodermal cultivated cells under H_2O_2 treatments. Intracellular content of ROS was measured by staining cells with CellROX Green Reagent after 1 h, 2 h, 6 h, 1 day, or 7 days with 0 μM H_2O_2 (control condition; white bars), 200 μM H_2O_2 (gray bars) or 500 μM H_2O_2 (black bars). Results represent the percentage of fluorescent cells (CellROX-positive cells), within the population of interest, quantified by flow cytometry. Data are represented as means with standard error bars. Significant differences between control and treatments are expressed by $^*p < 0.05$ and $^{***}p < 0.001$.

probe (CellROX^{TM} Green) allowing to quantify the positive cells for CellROX^{TM} Green. The level of intracellular ROS was thus correlated to the percentage of positive cells for CellROX^{TM} Green. Interestingly, this analysis revealed that although an increasing trend, there was no significant difference between the control (no treatment) and the cells treated with 200 μM H_2O_2, whatever the time point (**Figure 4**). However, there was a significant increase of ROS-positive cells (2.7 times higher in average, 11.2% vs. 4.1%) within the cells treated with 500 μM H_2O_2 from 1 h until 7 days of treatment.

Hydrogen Peroxide Effects on Cellular Parameters Under Treatments and Resilience Phase

We next wondered whether H_2O_2 exposures induce a stress at the cellular level by monitoring cellular parameters during treatments. In addition, we also evaluated the resilience capacity of treated cells by following the same parameters after a week-recovery phase. Firstly, the analysis of the cell viability, during 1–6 h of exposures, showed no impact of 200 or 500 μM H_2O_2 treatments (see **Supplementary Figure 1**). At 200 μM, there was only a light significant decrease in cell viability (9%) after 7 days of exposure, which was totally recovered after the resilience period (**Figure 5A**). At 500 μM, a 28% decrease was observed at 1 day that worsened after 7 days (58% of decrease, **Figure 5A**), confirming our results obtained during the dose-response assay. After a resilience period, only a partial recovery was observed (71% of the control condition), suggesting that not all the cells that survived may be able to compensate the H_2O_2–induced stress. In line with this hypothesis, the analysis of the cell population by flow-cytometry showed, after 7 days of 500 μM H_2O_2, a modification of cell-population pattern associated with a significant increase of autofluorescence (in average: 3.86% vs. 0.53% for the control condition; p-value = 0.021; **Figure 6**), which could be reflecting cell apoptosis.

The growth rate measurements showed a significant impact of both treatments, 200 and 500 μM H_2O_2, with a dose-dependent response as we observed a decrease of 38 and 97%, respectively (**Figure 5B**). This H_2O_2 dose-dependent response was maintained after the resilience period with a partial growth rate recovery for both treatments (75 and 39% of control, respectively, for 200 and 500 μM H_2O_2). Taken together these data suggested that 200 μM H_2O_2 can be considered as the tolerance threshold of cultivated cnidarian cells while 500 μM H_2O_2 can represent a critical concentration inducing deleterious cellular injuries.

Hydrogen Peroxide Effects on Stress Biomarkers Under Treatments and Resilience Phase

To determine the cellular response induced by H_2O_2 treatments on cultivated cells we analyzed biochemical stress markers (TOSC, carbonylation, and ubiquitination). After 1–6 h of treatment, we observed no significant effect on any of the three biomarkers (**Supplementary Figure 2**). However, after 24 h of treatment TOSC was impaired at both 200 and 500 μM H_2O_2. A full recovery was observed after 7 days of treatment and maintained during the resilience phase (**Figure 7A**), suggesting an acclimation of the cells to the pro-oxidant conditions. No signs of protein damage (protein carbonylation and ubiquitination) were measured after 24 h. However, the 200 μM H_2O_2 treatment induced an increase of ubiquitinated proteins after 7 days (**Figure 7C**). This effect was totally abolished after the resilience period (**Figure 7C**). These data suggest that H_2O_2 exposures, even at 500 μM and after 7 days, didn't

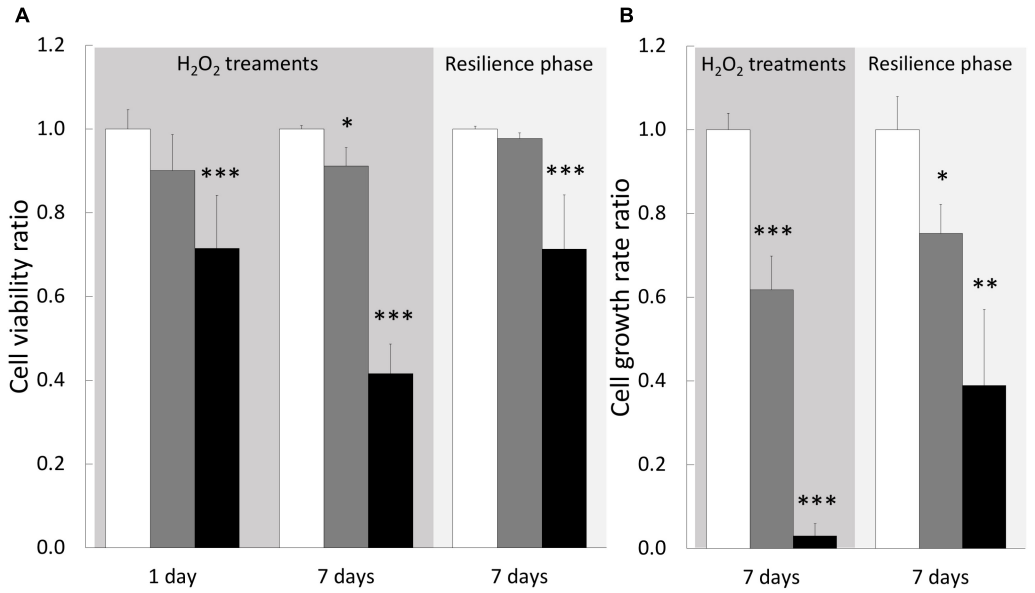

FIGURE 5 | Cellular parameters of gastrodermal cultivated cells under H_2O_2 treatments and resilience phase. Cell viability **(A)** and cell growth rate **(B)** were measured under cell treatment with H_2O_2 at 200 and 500 μM and during resilience phase (back to control condition for 7 days): 0 μM H_2O_2 (control condition; white bars), 200 μM H_2O_2 (gray bars) and 500 μM H_2O_2 (black bars). Cell viability and growth rate are expressed relative to the control condition (ratio of the control condition). Data are represented as means with standard error bars. Significant differences between control and treatments are expressed by $*p < 0.05$, $**p < 0.01$, and $***p < 0.001$.

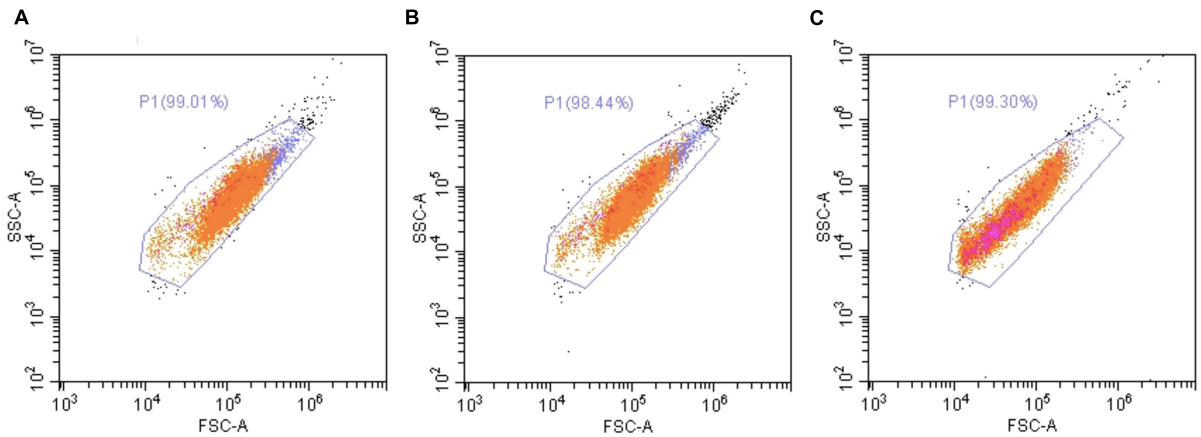

FIGURE 6 | Flow cytometry analysis of *A. viridis* cultivated cells under a 7-days treatment with H_2O_2. Flow cytometry analysis were performed on cultivated cell population by excitation at 488 nm and detection at 515–530 nm, after 7 days of incubation without H_2O_2 **(A)** or with 200 μM **(B)** or 500 μM **(C)** of H_2O_2. Representative dot plots of all experiments performed are shown. Orange dots: cells of interest; pink dots: green-autofluorescent cells.

lead to persistent oxidative damages on proteins in cnidarian cultivated cells.

DISCUSSION

Extended Tolerance of Symbiotic Cnidarians to Hydrogen Peroxide

In this study, we used H_2O_2 to induce pro-oxidative condition and to investigate the stress response in the symbiotic sea anemone *A. viridis* at both whole animal and cellular scales. The H_2O_2 concentrations used in the present study correspond to extremely high levels never measured in the seawater. However, rainwater can temporally induced increase of H_2O_2 to tens of micromolar (Ndungu et al., 2019; Jones and Lee, 2020). Benthic marine organisms from coastal areas are therefore regularly facing H_2O_2, that could lead to oxidative stress (Abele-Oeschger et al., 1997). Indeed, among ROS, H_2O_2 is the most abundant and long-lived in sea water and contrary to other ROS, H_2O_2

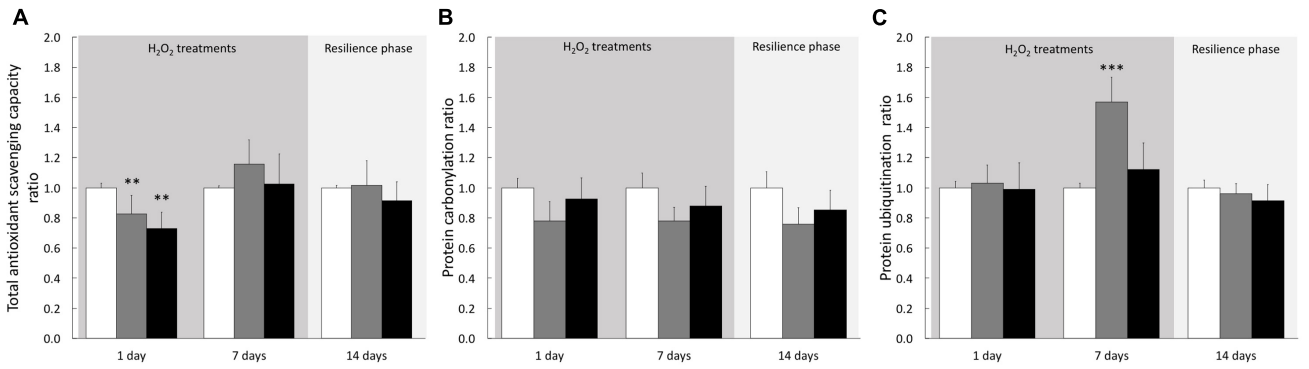

FIGURE 7 | Stress biomarkers in *A. viridis* cultivated cells under H_2O_2 treatments and resilience phase. Total Oxidative Scavenging Capacity, TOSC **(A)**, protein carbonylation **(B)** and protein ubiquitination **(C)** were measured under cell treatment with H_2O_2 at 200 and 500 μM and during resilience phase (back to control condition for 7 days): 0 μM H_2O_2 (control; white bars), 200 μM H_2O_2 (gray bars) and 500 μM H_2O_2 (black bars). Data are expressed relative to control condition (ratio of the control condition). Means values with standard error bars are presented. Significant differences between control and treatments are expressed by $^{**}p < 0.01$ and $^{***}p < 0.001$.

could rapidly diffuse across membranes (see for review Halliwell and Gutteridge, 2015).

In our study model, at both whole animal and cellular scales, 200 μM of H_2O_2 did not create a condition of stress, since very weak impact was observed in global health: no sign of mortality or bleaching on specimens (**Figure 1**), no intracellular ROS accumulation (**Figure 4**) and only very slight effect on viability after 7 days exposure in cell cultures (**Figure 5**). In addition, no effect was observed on any stress biomarkers we tested (**Figures 2**, **7**). In cell cultures, we nevertheless measured a significant cellular growth arrest (**Figure 5**), reflecting a common feature of stress response and could be interpreted as an usual resistance mechanism (see for review Davies, 1999, 2000).

H_2O_2 usually represents a threat for most organisms. Indeed, in diverse mammalian cell lines, a cytotoxic effect of H_2O_2 could be observed from 60 μM (Coyle et al., 2006) with drastic and irreversible impacts (i.e., apoptosis and necrosis) induced at 400 μM H_2O_2 (Xiang et al., 2016). Some studies performed on marine invertebrates showed that micromolar concentrations of H_2O_2, ranging from 0.5 to 20 μM, could impact the metabolism of the whole animal. For example, a 40% drop in O_2 consumption was observed in the Polychaete *Nereis diversicolor* under 5 μM of H_2O_2 (Abele-Oeschger et al., 1994), while higher level of H_2O_2 (50 μM) can cause oxidative damages (i.e., lipid peroxidation), as observed in another Polychaete species, *Laenoereis acuta* (Da Rosa et al., 2008).

Contrasting with those results, our study highlighted an extended tolerance of symbiotic cnidarian facing even greater H_2O_2 concentrations. This resistance to H_2O_2 is, however, not a general cnidarian feature as it has been shown that concentrations exceeding 163 μM H_2O_2 caused mortality of the non-symbiotic sea anemone *Nematostella vectensis* (Friedman et al., 2018). Therefore, these results reinforced the hypothesis of the adaptation of symbiotic cnidarians to pro-oxidative conditions, due to their lifestyle with a photosynthetic symbiont. Indeed, it has been already highlighted that symbiotic cnidarians exhibited a wide diversity of biochemical antioxidant actors, compared to non-symbiotic species (Furla et al., 2005). For instance, higher number of superoxide dismutase (SOD) isoforms was identified in the symbiotic cnidarian *A. viridis* compared to the non-symbiotic one *Actinia schmidti*. In complement, another comparative analysis showed that the glutathione peroxidase (GPx) isoforms were less numerous in the non-symbiotic sea anemone *N. vectensis* than in the symbiotic sea anemone *A. viridis* (Pey et al., 2017). To confirm the hypothesis of the adaptative process, it will be required to extend the comparison of the antioxidant battalion between symbiotic and non-symbiotic cnidarians at multiple scales, even by including the non-enzymatic actors.

Importance of Host Cells to Hydrogen Peroxide Defense

In the present study, H_2O_2 exposure on whole organism affected mainly the endosymbiont, *Philozoon* sp. genus (LaJeunesse et al., 2021), rather than the animal host tissues. Although antioxidant defenses were stimulated after 7 days, an increase of protein carbonylation was measured in the symbiont fraction, whereas no increase was observed in the animal compartments (**Figure 2**). The susceptibility of free-living algae to H_2O_2 is well documented and highlighted an important heterogeneity in H_2O_2 response. For example, although the cyanobacterium *Synechococcus aeruginosus* tolerated until 2 mM H_2O_2, another cyanobacterium species, *Microcystis aeruginosa,* was affected by around 20 μM (EC50) and the diatoms *Navicula seminulum* by 200 μM (Drábková et al., 2007). Few studies have been performed on Symbiodiniaceae sensitivity to ROS and again they highlighted species-specific impacts on photosynthesis (Wietheger et al., 2015; Roberty et al., 2016). For example, cultured *Symbiodinium microadriaticum* strain showed high resistance to 1 mM H_2O_2, compared to *Fugacium kawagutii* showing drastic damage to photosystem function at the same H_2O_2 concentration (Wietheger et al., 2015). In addition, light exposure increased the photosynthesis impairment of cultured

Symbiodiniaceae from 30 min of >1 mM H_2O_2 exposure (Wietheger et al., 2015).

Protected inside the gastrodermal host cell, the endosymbiont would not have shown any signs of oxidative stress under H_2O_2 exposure, but the sensitivity assessed in our study did not confirm this assumption. This sensitivity to H_2O_2 could, however, be correlated to previous studies demonstrating that Symbiodiniaceae living *in hospite* present a reduction of the antioxidant enzymatic defenses (i.e., SOD, catalases or peroxidases) compared to the free-living condition (Lesser and Shick, 1989; Richier et al., 2005; Pey et al., 2017). Nevertheless, it has been shown that *in hospite*, Symbiodiniaceae harbor a higher surface volume of thylakoid lamellae (Lesser and Shick, 1990), increasing definitely the photosystem density and consequently the source of ROS associated with electron chain transports (Saragosti et al., 2010).

These data, in addition with measurements of H_2O_2 diffusion from the symbiont (Suggett et al., 2008; Armoza-Zvuloni and Shaked, 2014), support the conclusion that, in *hospite*, the redox homeostasis of the symbiont is bolstered by the antioxidant defenses of the animal host cells. For example, in *A. viridis* it has been frequently observed that the animal compartment constitutes the major contributor to the holobiont antioxidant potential, with higher amount of antioxidant defenses compared to the symbiont fraction (Richier et al., 2003, 2005; Plantivaux et al., 2004; Merle et al., 2007; Pey et al., 2017). This agrees with studies performed on other symbiotic cnidarian species (Yakovleva et al., 2004; Levy et al., 2006; Krueger et al., 2015). By consequence, an experimental burst of H_2O_2 leads to more deleterious effects in the endosymbiont than in animal cells, illustrating their capacity to cope with H_2O_2.

No Bleaching Induction by Hydrogen Peroxide

Even at highest H_2O_2 exposure, no bleaching was observed neither during, nor after the exposure period in the treated *A. viridis* specimens (**Figure 1**). Interestingly, despite the protein damages observed in the symbiont, the equilibrium of the symbiosis was maintained. It has been largely documented in symbiotic cnidarians that stress-induced bleaching (e.g., thermal stress) is linked with the over-production of ROS by the endosymbiont, leading to significant oxidative damages in the host cells (see for review Suggett and Smith, 2020). Due to its permeable properties and its overproduction in several strains of Symbiodiniaceae exposed to thermal stress (Lesser, 1996; Suggett et al., 2008; Roberty et al., 2015), this ROS has then been suggested to be responsible of oxidative stress occurring in host cells during bleaching events. However, in this study, the absence of bleaching and of oxidative damages in host cells under H_2O_2 exposures can support the conclusion that H_2O_2 may not be the most important ROS associated with coral bleaching.

Limits of the Resistance

At cellular level, pro-oxidative condition can elicit a broad spectrum of responses from proliferation to growth arrest, or senescence and cell death, depending on the cell capacity to overcome the stress by repairing or removing damaged molecules. The observed effect reflects the balance between intracellular pathways activated in response to the oxidative injury and can vary significantly with the concentration of the oxidant agent and the treatment exposure. In our *in vitro* study model, 500 μM of H_2O_2 induced a decrease of cell viability, particularly pronounced after 7 days of treatment and associated with a drastic growth arrest (**Figure 5**).

This response could be explained by a strategy of the "sacrifice" signaling pathway set up by the cells to eliminate the most damaged cell population (Davies, 2000). Indeed, a change in the cell population pattern was highlighted after 7 days at 500 μM H_2O_2 (**Figure 6**) and no protein damages were observed in these surviving cells (**Figure 7**). Nevertheless, the increase of autofluorescence measured in surviving cells after 7 days at 500 μM H_2O_2 (**Figure 6**) might be correlated with changes in metabolic activity of mitochondria that cells undergo during apoptosis, as it has been previously observed in mammalian cells (Levitt et al., 2006). In addition, the partial recovery of cell growth after the resilience period (**Figure 5**) suggested a non-reversible impact of 500 μM H_2O_2 injury on surviving cells, whose mechanisms should be deeply addressed in the future.

Finally, comparing the *in vitro* and the *in vivo* approaches, we highlighted that the sensitivity of *A. viridis* gastrodermal cells at 500 μM of H_2O_2 exposure is less pronounced in the gastrodermal tissue than in the isolated cultivated cells (**Figures 2**, **7**). This is likely due to the contribution of the tissue organization thanks to host cell/cell communication, more efficient turnover of damaged cells and/or by a signaling pathway linked to the presence of the symbiont.

Moving forward thanks to the *in vitro* cnidarian cell culture, an ambitious perspective of this study will be to disentangle the mechanisms of H_2O_2 resistance of cnidarian cells and more specifically to assess the impact of other ROS (as the superoxide anion and the hydroxyl radical), thus contributing to decipher the adaptative tools that have evolved for a successful symbiosis stability and conversely to better understand the bleaching processes.

DATA AVAILABILITY STATEMENT

The original contributions presented in the study are included in the article/**Supplementary Material**, further inquiries can be directed to the corresponding author/s.

AUTHOR CONTRIBUTIONS

PC did all the investigations (experimental work) and statistical analyses. CF contributed to the obtaining of cell cultures and their maintenance. CF and GT initialized the H_2O_2 experiments on cell cultures. PF and SB-V designed and supervised the research. PC, ER, SB-V, and PF wrote the manuscript. All authors read and agreed to the published version of the manuscript.

FUNDING

This work was supported by a doctoral fellowship (CIFRE) from SO.F.I.A Cosmétiques company and the Association Nationale de la Recherche et de la Technologie (ANRT) to PC.

ACKNOWLEDGMENTS

The authors greatly acknowledge Ludovic Cervera of the CYTOMED facility (IRCAN's Flow Cytometry Facility that was supported by the FEDER, Ministère de l'Enseignement Supérieur, Région Provence-Alpes-Côte d'Azur, Conseil Départemental 06, ITMO Cancer Aviesan, Cancéropole PACA, INCa, CNRS, and INSERM). The authors are also grateful to Aldine Amiel from the ANTIAGE facility [IRCAN's Marine Invertebrate Facility for (Anti-)Aging Research] as well as Thamilla Zamoum, Brigitte Poderini, and Maxence Burtin, for the maintenance of the aquarium and the monitoring and feeding of *Anemonia viridis* specimens. Finally, the authors would like to thank particularly Thalassa Marine Research & Environmental Awareness (Patricia Ventura and Alexis Pey) for the sampling of the sea anemones.

SUPPLEMENTARY MATERIAL

The Supplementary Material for this article can be found online at: https://www.frontiersin.org/articles/10.3389/fphys.2022.819111/full#supplementary-material

REFERENCES

Abele-Oeschger, D., Oeschger, R., and Theede, H. (1994). Biochemical adaptations of Nereis diversicolor (Polychaeta) to temporarily increased hydrogen peroxide levels in intertidal sandflats. *Mar. Ecol. Progr. Ser.* 106, 101–110. doi: 10.3354/meps106101

Abele-Oeschger, D., Tüg, H., and Röttgers, R. (1997). Dynamics of UV-driven hydrogen peroxide formation on an intertidal sandflat. *Limnol. Oceanogr.* 42, 1406–1415. doi: 10.4319/lo.1997.42.6.1406

Apel, K., and Hirt, H. (2004). Reactive oxygen species: metabolism, oxidative stress, and signal transduction. *Annu. Rev. Plant Biol.* 55, 373–399. doi: 10.1146/annurev.arplant.55.031903.141701

Armoza-Zvuloni, R., and Shaked, Y. (2014). Release of hydrogen peroxide and antioxidants by the coral Stylophora pistillata to its external milieu. *Biogeosciences* 11, 4587–4598. doi: 10.5194/bg-11-4587-2014

Barnay-Verdier, S., Dall'Osso, D., Joli, N., Olivré, J., Priouzeau, F., Zamoum, T., et al. (2013). Establishment of primary cell culture from the temperate symbiotic cnidarian, Anemonia viridis. *Cytotechnology* 65, 697–704. doi: 10.1007/s10616-013-9566-2

Buss, H., Chan, T. P., Sluis, K. B., Domigan, N. M., and Winterbourn, C. C. (1997). Protein Carbonyl Measurement by a Sensitive ELISA Method. *Free Radic. Biol. Med.* 23, 361–366. doi: 10.1016/S0891-5849(97)00104-4

Cooper, W. J., Saltzman, E. S., and Zika, R. G. (1987). The contribution of rainwater to variability in surface ocean hydrogen peroxide. *J. Geophys. Res. Oceans* 92, 2970–2980. doi: 10.1029/JC092iC03p02970

Coyle, C. H., Martinez, L. J., Coleman, M. C., Spitz, D. R., Weintraub, N. L., and Kader, K. N. (2006). Mechanisms of H2O2-induced oxidative stress in endothelial cells. *Free Radic. Biol. Med.* 40, 2206–2213. doi: 10.1016/j.freeradbiomed.2006.02.017

Da Rosa, C. E., Bianchini, A., and Monserrat, J. M. (2008). Antioxidant responses of Laeonereis acuta (Polychaeta) after exposure to hydrogen peroxide. *Braz. J. Med. Biol. Res.* 41, 117–121. doi: 10.1590/s0100-879x2008000200007

Davies, K. J. (1999). The Broad Spectrum of Responses to Oxidants in Proliferating Cells: a New Paradigm for Oxidative Stress. *IUBMB Life* 48, 41–47. doi: 10.1080/713803463

Davies, K. J. (2000). Oxidative stress, antioxidant defenses, and damage removal, repair, and replacement systems. *IUBMB Life* 50, 279–289. doi: 10.1080/713803728

Davy, S. K., Allemand, D., and Weis, V. M. (2012). Cell Biology of Cnidarian-Dinoflagellate Symbiosis. *Microbiol. Mol. Biol. Rev.* 76, 229–261. doi: 10.1128/MMBR.05014-11

Drábková, M., Admiraal, W., and Maršálek, B. (2007). Combined Exposure to Hydrogen Peroxide and LightSelective Effects on Cyanobacteria, Green Algae, and Diatoms. *Environ. Sci. Technol.* 41, 309–314. doi: 10.1021/es060746i

Dykens, J. A., Shick, J. M., Benoit, C., Buettner, G. R., and Winston, G. W. (1992). Oxygen radical production in the sea anemone Anthopleura elegantissima and its endosymbiotic algae. *J. Exp. Biol.* 168, 219–241. doi: 10.1242/jeb.168.1.219

Fricano, C., Röttinger, E., Furla, P., and Barnay-Verdier, S. (2020). Cnidarian Cell Cryopreservation: a Powerful Tool for Cultivation and Functional Assays. *Cells* 9:2541. doi: 10.3390/cells9122541

Friedman, L. E., Gilmore, T. D., and Finnerty, J. R. (2018). Intraspecific variation in oxidative stress tolerance in a model cnidarian: differences in peroxide sensitivity between and within populations of Nematostella vectensis. *PLoS One* 13:e0188265. doi: 10.1371/journal.pone.0188265

Fulda, S., Gorman, A. M., Hori, O., and Samali, A. (2010). Cellular Stress Responses: cell Survival and Cell Death. *Int. J. Cell Biol.* 2010:214074. doi: 10.1155/2010/214074

Furla, P., Allemand, D., Shick, J. M., Ferrier-Pagès, C., Richier, S., Plantivaux, A., et al. (2005). The Symbiotic Anthozoan: a Physiological Chimera between Alga and Animal. *Integr. Comp. Biol.* 45, 595–604. doi: 10.1093/icb/45.4.595

Ganot, P., Moya, A., Magnone, V., Allemand, D., Furla, P., and Sabourault, C. (2011). Adaptations to Endosymbiosis in a Cnidarian-Dinoflagellate Association: differential Gene Expression and Specific Gene Duplications. *PLoS Genet.* 7:e1002187. doi: 10.1371/journal.pgen.1002187

Giorgio, M., Trinei, M., Migliaccio, E., and Pelicci, P. G. (2007). Hydrogen peroxide: a metabolic by-product or a common mediator of ageing signals? *Nat. Rev. Mol. Cell Biol.* 8, 722–728. doi: 10.1038/nrm2240

Haas, A. L., and Bright, P. M. (1985). The immunochemical detection and quantitation of intracellular ubiquitin-protein conjugates. *J. Biol. Chem.* 260, 12464–12473. doi: 10.1016/S0021-9258(17)38895-6

Halliwell, B., Clement, M. V., and Long, L. H. (2000). Hydrogen peroxide in the human body. *FEBS Lett.* 486, 10–13. doi: 10.1016/S0014-5793(00)02197-9

Halliwell, B., and Gutteridge, J. M. C. (2015). *Free Radicals in Biology and Medicine*, 5th Edn. Oxford: Oxford University Press.

Hansel, C. M., and Diaz, J. M. (2021). Production of Extracellular Reactive Oxygen Species by Marine Biota. *Ann. Rev. Mar. Sci.* 13, 177–200. doi: 10.1146/annurev-marine-041320-102550

Hawkridge, J. M., Pipe, R. K., and Brown, B. E. (2000). Localisation of antioxidant enzymes in the cnidarians Anemonia viridis and Goniopora stokesi. *Mar. Biol.* 137, 1–9. doi: 10.1007/s002270000324

Higuchi, T., Fujimura, H., Ikota, H., Arakaki, T., and Oomori, T. (2009). The effects of hydrogen peroxide on metabolism in the coral Goniastrea aspera. *J. Exp. Mar. Biol. Ecol.* 370, 48–55. doi: 10.1016/j.jembe.2008.11.013

Jones, M. R., and Lee, K. (2020). Precipitation of hydrogen peroxide during winter storms and summer typhoons. *Sci. Total Environ.* 733:139377. doi: 10.1016/j.scitotenv.2020.139377

Krueger, T., Hawkins, T. D., Becker, S., Pontasch, S., Dove, S., Hoegh-Guldberg, O., et al. (2015). Differential coral bleaching—Contrasting the activity and response of enzymatic antioxidants in symbiotic partners under thermal stress. *Comp. Biochem. Physiol. A Mol. Integr. Physiol.* 190, 15–25. doi: 10.1016/j.cbpa.2015.08.012

LaJeunesse, T. C., Wiedenmann, J., Casado-Amezúa, P., D'Ambra, I., Turnham, K. E., Nitschke, M. R., et al. (2021). Revival of Philozoon Geddes for host-specialized dinoflagellates, 'zooxanthellae', in animals from coastal temperate

zones of northern and southern hemispheres. *Eur. J. Phycol.* 0, 1–15. doi: 10.1080/09670262.2021.1914863

Lennicke, C., Rahn, J., Lichtenfels, R., Wessjohann, L. A., and Seliger, B. (2015). Hydrogen peroxide - production, fate and role in redox signaling of tumor cells. *Cell Commun. Signal* 13:39. doi: 10.1186/s12964-015-0118-6

Lesser, M., and Farrell, J. (2004). Exposure to solar radiation increases damage to both host tissues and algal symbionts of corals during thermal stress. *Coral Reefs* 23, 367–377. doi: 10.1007/s00338-004-0392-z

Lesser, M. P. (1996). Elevated temperatures and ultraviolet radiation cause oxidative stress and inhibit photosynthesis in ymbiotic dinoflagellates. *Limnol. Oceanogr.* 41, 271–283. doi: 10.4319/lo.1996.41.2.0271

Lesser, M. P., and Shick, J. M. (1989). Effects of irradiance and ultraviolet radiation on photoadaptation in the zooxanthellae of Aiptasia pallida: primary production, photoinhibition, and enzymic defenses against oxygen toxicity. *Mar. Biol.* 102, 243–255. doi: 10.1007/BF00428286

Lesser, M. P., and Shick, J. M. (1990). Effects of visible and ultraviolet radiation on the ultrastructure of zooxanthellae (Symbiodinium sp.) in culture and in situ. *Cell Tissue Res.* 261, 501–508. doi: 10.1007/BF00313529

Levitt, J. M., Baldwin, A., Papadakis, A., Puri, S., Xylas, J., Münger, K., et al. (2006). Intrinsic fluorescence and redox changes associated with apoptosis of primary human epithelial cells. *JBO* 11:064012. doi: 10.1117/1.2401149

Levy, O., Achituv, Y., Yacobi, Y. Z., Stambler, N., and Dubinsky, Z. (2006). The impact of spectral composition and light periodicity on the activity of two antioxidant enzymes (SOD and CAT) in the coral Favia favus. *J. Exp. Mar. Biol. Ecol.* 328, 35–46. doi: 10.1016/j.jembe.2005.06.018

McDonagh, B., and Sheehan, D. (2006). Redox proteomics in the blue mussel Mytilus edulis: carbonylation is not a pre-requisite for ubiquitination in acute free radical-mediated oxidative stress. *Aquat. Toxicol.* 79, 325–333. doi: 10.1016/j.aquatox.2006.06.020

McDonagh, B., and Sheehan, D. (2007). Effect of oxidative stress on protein thiols in the blue mussel Mytilus edulis: proteomic identification of target proteins. *Proteomics* 7, 3395–3403. doi: 10.1002/pmic.200700241

Merle, P. L., Sabourault, C., Richier, S., Allemand, D., and Furla, P. (2007). Catalase characterization and implication in bleaching of a symbiotic sea anemone. *Free Radic. Biol. Med.* 42, 236–246. doi: 10.1016/j.freeradbiomed.2006.10.038

Moya, A., Ganot, P., Furla, P., and Sabourault, C. (2012). The transcriptomic response to thermal stress is immediate, transient and potentiated by ultraviolet radiation in the sea anemone Anemonia viridis. *Mol. Ecol.* 21, 1158–1174. doi: 10.1111/j.1365-294X.2012.05458.x

Naguib, Y. M. A. (2000). A Fluorometric Method for Measurement of Oxygen Radical-Scavenging Activity of Water-Soluble Antioxidants. *Anal. Biochem.* 284, 93–98. doi: 10.1006/abio.2000.4691

Ndungu, L. K., Steele, J. H., Hancock, T. L., Bartleson, R. D., Milbrandt, E. C., Parsons, M. L., et al. (2019). Hydrogen peroxide measurements in subtropical aquatic systems and their implications for cyanobacterial blooms. *Ecol. Eng.* 138, 444–453. doi: 10.1016/j.ecoleng.2019.07.011

Nguyen, L. (2020). *The Effects of Photosymbiosis on Gene Expression in the Facultatively Symbiotic Coral Astrangia poculata, With a Focus on NF-Kappab Signaling and Antioxidant Enzymes*. Available Online at: https://open.bu.edu/handle/2144/41678 [accessed Dec 13, 2021].

Pey, A., Zamoum, T., Allemand, D., Furla, P., and Merle, P.-L. (2011). Depth-dependant thermotolerance of the symbiotic Mediterranean gorgonian Eunicella singularis: evidence from cellular stress markers. *J. Exp. Mar. Biol. Ecol.* 404, 73–78. doi: 10.1016/j.jembe.2011.05.007

Pey, A., Zamoum, T., Christen, R., Merle, P.-L., and Furla, P. (2017). Characterization of glutathione peroxidase diversity in the symbiotic sea anemone Anemonia viridis. *Biochimie* 132, 94–101. doi: 10.1016/j.biochi.2016.10.016

Plantivaux, A., Furla, P., Zoccola, D., Garello, G., Forcioli, D., Richier, S., et al. (2004). Molecular characterization of two CuZn-superoxide dismutases in a sea anemone. *Free Radic. Biol. Med.* 37, 1170–1181. doi: 10.1016/j.freeradbiomed.2004.06.043

Richier, S., Furla, P., Plantivaux, A., Merle, P.-L., and Allemand, D. (2005). Symbiosis-induced adaptation to oxidative stress. *J. Exp. Biol.* 208, 277–285. doi: 10.1242/jeb.01368

Richier, S., Merle, P.-L., Furla, P., Pigozzi, D., Sola, F., and Allemand, D. (2003). Characterization of superoxide dismutases in anoxia- and hyperoxia-tolerant symbiotic cnidarians. *Biochim. Biophys. Acta Gen. Subj.* 1621, 84–91. doi: 10.1016/S0304-4165(03)00049-7

Richier, S., Sabourault, C., Courtiade, J., Zucchini, N., Allemand, D., and Furla, P. (2006). Oxidative stress and apoptotic events during thermal stress in the symbiotic sea anemone, Anemonia viridis. *FEBS J.* 273, 4186–4198. doi: 10.1111/j.1742-4658.2006.05414.x

Roberty, S., Fransolet, D., Cardol, P., Plumier, J.-C., and Franck, F. (2015). Imbalance between oxygen photoreduction and antioxidant capacities in Symbiodinium cells exposed to combined heat and high light stress. *Coral Reefs* 34, 1063–1073. doi: 10.1007/s00338-015-1328-5

Roberty, S., Furla, P., and Plumier, J.-C. (2016). Differential antioxidant response between two Symbiodinium species from contrasting environments. *Plant Cell Environ.* 39, 2713–2724. doi: 10.1111/pce.12825

Saragosti, E., Tchernov, D., Katsir, A., and Shaked, Y. (2010). Extracellular Production and Degradation of Superoxide in the Coral Stylophora pistillata and Cultured Symbiodinium. *PLoS One* 5:e12508. doi: 10.1371/journal.pone.0012508

Shaked, Y., and Armoza-Zvuloni, R. (2013). Dynamics of hydrogen peroxide in a coral reef: sources and sinks. *J. Geophys. Res. Biogeosci.* 118, 1793–1801. doi: 10.1002/2013JG002483

Shick, J. M., and Dykens, J. A. (1985). Oxygen detoxification in algal-invertebrate symbioses from the Great Barrier Reef. *Oecologia* 66, 33–41. doi: 10.1007/BF00378549

Suggett, D. J., and Smith, D. J. (2020). Coral bleaching patterns are the outcome of complex biological and environmental networking. *Glob. Chang. Biol.* 26, 68–79. doi: 10.1111/gcb.14871

Suggett, D. J., Warner, M. E., Smith, D. J., Davey, P., Hennige, S., and Baker, N. R. (2008). Photosynthesis and Production of Hydrogen Peroxide by Symbiodinium (Pyrrhophyta) Phylotypes with Different Thermal Tolerances. *J. Phycol.* 44, 948–956. doi: 10.1111/j.1529-8817.2008.00537.x

Ventura, P., Toullec, G., Fricano, C., Chapron, L., Meunier, V., Röttinger, E., et al. (2018). Cnidarian Primary Cell Culture as a Tool to Investigate the Effect of Thermal Stress at Cellular Level. *Mar. Biotechnol.* 20, 144–154. doi: 10.1007/s10126-017-9791-3

Wietheger, A., Fisher, P. L., Gould, K. S., and Davy, S. K. (2015). Sensitivity to oxidative stress is not a definite predictor of thermal sensitivity in symbiotic dinoflagellates. *Mar. Biol.* 162, 2067–2077. doi: 10.1007/s00227-015-2736-3

Xiang, J., Wan, C., Guo, R., and Guo, D. (2016). Is Hydrogen Peroxide a Suitable Apoptosis Inducer for All Cell Types? *Biomed. Res. Int.* 2016:7343965. doi: 10.1155/2016/7343965

Yakovleva, I., Bhagooli, R., Takemura, A., and Hidaka, M. (2004). Differential susceptibility to oxidative stress of two scleractinian corals: antioxidant functioning of mycosporine-glycine. *Comp. Biochem. Physiol. B Biochem. Mol. Biol.* 139, 721–730. doi: 10.1016/j.cbpc.2004.08.016

Zamoum, T., and Furla, P. (2012). Symbiodinium isolation by NaOH treatment. *J. Exp. Biol.* 215, 3875–3880. doi: 10.1242/jeb.074955

Conflict of Interest: The authors declare that the research was conducted in the absence of any commercial or financial relationships that could be construed as a potential conflict of interest.

Publisher's Note: All claims expressed in this article are solely those of the authors and do not necessarily represent those of their affiliated organizations, or those of the publisher, the editors and the reviewers. Any product that may be evaluated in this article, or claim that may be made by its manufacturer, is not guaranteed or endorsed by the publisher.

frontiers in Marine Science

ORIGINAL RESEARCH
published: 14 February 2022
doi: 10.3389/fmars.2022.797517

Shotgun Proteomics Identifies Active Metabolic Pathways in Bleached Coral Tissue and Intraskeletal Compartments

Jeremy B. Axworthy[1], Emma Timmins-Schiffman[2], Tanya Brown[1], Lisa J. Rodrigues[3], Brook L. Nunn[2†] and Jacqueline L. Padilla-Gamiño[1†]*

[1] School of Aquatic and Fishery Sciences, University of Washington, Seattle, WA, United States, [2] Department of Genome Sciences, University of Washington, Seattle, WA, United States, [3] Department of Geography and the Environment, Villanova University, Villanova, PA, United States

OPEN ACCESS

Edited by:
Davide Seveso, University of Milano-Bicocca, Italy

Reviewed by:
Rowan H. McLachlan, Oregon State University, United States
Jeremie Vidal-Dupiol, Institut Français de Recherche pour l'Exploitation de la Mer (IFREMER), France

***Correspondence:**
Jeremy B. Axworthy
jeremyax@uw.edu

† These authors have contributed equally to this work and share last authorship

Specialty section:
This article was submitted to Aquatic Physiology, a section of the journal Frontiers in Marine Science

Received: *18 October 2021*
Accepted: *11 January 2022*
Published: *14 February 2022*

Citation:
Axworthy JB, Timmins-Schiffman E, Brown T, Rodrigues LJ, Nunn BL and Padilla-Gamiño JL (2022) Shotgun Proteomics Identifies Active Metabolic Pathways in Bleached Coral Tissue and Intraskeletal Compartments. Front. Mar. Sci. 9:797517. doi: 10.3389/fmars.2022.797517

Coral bleaching events are increasing with such frequency and intensity that many of the world's reef-building corals are in peril. Some corals appear to be more resilient after bleaching but the mechanisms underlying their ability to recover from bleaching and persist are not fully understood. We used shotgun proteomics to compare the proteomes of the outer layer (OL) tissue and inner core (IC) tissue and skeleton compartments of experimentally bleached and control (i.e., non-bleached) colonies of *Montipora capitata*, a perforate Hawaiian species noted for its resilience after bleaching. We identified 2,361 proteins in the OL and IC compartments for both bleached and non-bleached individuals. In the OL of bleached corals, 63 proteins were significantly more abundant and 28 were significantly less abundant compared to the OL of non-bleached corals. In the IC of bleached corals, 22 proteins were significantly more abundant and 17 were significantly less abundant compared to the IC of non-bleached corals. Gene ontology (GO) and pathway analyses revealed metabolic processes that were occurring in bleached corals but not in non-bleached corals. The OL of bleached corals used the glyoxylate cycle to derive carbon from internal storage compounds such as lipids, had a high protein turnover rate, and shifted reliance on nitrogen from ammonia to nitrogen produced from the breakdown of urea and betaine. The IC of bleached corals compartmentalized the shunting of glucose to the pentose phosphate pathway. Bleached corals increased abundances of several antioxidant proteins in both the OL and IC compartments compared to non-bleached corals. These results highlight contrasting strategies for responding to bleaching stress in different compartments of bleached *M. capitata* and shed light on some potential mechanisms behind bleaching resilience.

Keywords: coral bleaching, eco-physiology, metabolic pathways, calcification, glyoxylate, betaine, proteins, perforate skeleton

INTRODUCTION

Rising seawater temperatures threaten the future of coral reefs and the ecosystem services they provide. Increased temperatures can result in the breakdown of mutualistic symbiosis between corals and Symbiodiniaceae (i.e., coral bleaching), causing a severe energy deficit to the coral that impairs critical physiological functions and can lead to mortality. However, if temperature stress abates before the coral's energy stores are consumed, symbiosis can be restored, and the coral can recover. To survive and recover from bleaching, corals must rely on internal energy and nutrient stores and/or employ alternative strategies to sustain themselves until the stressor abates and their Symbiodiniaceae population can recover (Grottoli et al., 2006; Rodrigues and Grottoli, 2007). For example, some corals exploit energy from stored lipids following bleaching, and some corals increase feeding on zooplankton to make up the energy deficit (Grottoli et al., 2006; Rodrigues and Grottoli, 2007; Ferrier-Pagès et al., 2010; Hughes and Grottoli, 2013). Bleaching comes with physiological costs and important consequences for coral fitness, such as decreased fecundity and skeletal growth, shifts in metabolic activity, increased antioxidant response and susceptibility to diseases and mortality (Lesser et al., 1990; Ward et al., 2000; Rodrigues and Grottoli, 2007; Cantin et al., 2010; Muller et al., 2018). While these processes are well documented, and we are beginning to understand their underlying cellular mechanisms, many knowledge gaps remain, including how a coral's proteome responds to bleaching stress and how variable the response is in different parts of the colony. Identifying such proteins and patterns can help to develop physiological biomarkers of coral resilience and improve our mechanistic understanding of recovery from bleaching.

The coral host has two distinct compartments: the tissue, where cellular functions involved in the overall maintenance and fitness of the coral occur; and the skeleton, which provides structural foundation for individual corals and entire reef ecosystems. The coral's polyps and interconnecting tissue or coenosarc between polyps make up the tissue fraction where physiological functions such as feeding, nutrient acquisition and reproduction occur, and it is in this compartment where the majority of Symbiodiniaceae reside (Yost et al., 2013). The coral's skeleton consists of an inorganic aragonitic calcium carbonate structure deposited by the coral tissue and an intra-skeletal organic matrix, including sugars, lipids and proteins (Isa and Okazaki, 1987; Dauphin, 2001; Puverel et al., 2005). The interface between coral tissue and skeleton depends on a coral's skeletal architecture. In corals with a perforate (porous) skeleton, tissue penetrates the cavities of the skeletal matrix. In contrast, tissue does not typically penetrate imperforate coral skeletons. It has been suggested that perforate corals are more resistant to external stressors than imperforate corals because they provide refuge for coral tissue and Symbiodiniaceae (Brown et al., 1994; Santos et al., 2009; Yost et al., 2013). Furthermore, tissue that penetrates perforate coral skeletons can host Symbiodiniaceae which may enhance calcification (Pearse and Muscatine, 1971; Gladfelter, 1983; Yost et al., 2013). These benefits of having a perforate skeleton suggest that there may be differences in cellular functions and biological processes that occur between a corals outer tissue layer and intra-skeletal tissue. However, to our knowledge, no studies have attempted to uncover these potential differences. Nor has there been a comparison of how these different compartments respond to bleaching stress.

Proteomics is a powerful tool that has advantages over other "omics" technologies for exploring how an organism responds to stress. While genomics and epigenomics provide the blueprint for all potential proteins, revealing the metabolic flexibility of an organism, they do not reveal metabolic pathways that are actively responding to the environment at a time of interest. In contrast, transcriptomics reveals which genes are transcribed in response to a specific stress, yet it has been demonstrated to be a magnified response that does not often correlate to protein translation (Gygi et al., 1999; Maier et al., 2009; Mayfield et al., 2016; Mayfield, 2020). As a result, there are challenges with relating how genes and transcripts equate to biological processes occurring in cells at the time of collection. High-throughput discovery-based proteomics circumvents these challenges by directly identifying and quantifying proteins in the cells at the time of collection, which are closer to the realized function of mRNA and have been shown to be environmentally sensitive (Pandey and Mann, 2000; Tomanek, 2014; Stuhr et al., 2018). Recent advances in proteomics allow for the identification of potentially thousands of proteins by coupling liquid chromatography with tandem mass spectrometry, i.e., "shotgun" proteomics.

In this study, we used shotgun proteomics to explore how a reef-building perforate coral, *Montipora capitata*, responds at the proteomic level to experimental bleaching and to investigate whether the outer layer (OL) tissue and inner core (IC) intra-skeletal tissue and skeleton compartments respond to bleaching differently. By examining proteins from these two distinct compartments, we aimed to uncover connections between metabolic functions of the OL that support overall maintenance of the coral, and of the IC that support skeletal processes. Specifically, we aimed to address these questions: (1) Are there differential abundances of metabolic proteins in the OL and IC? and (2) Which metabolic pathways differ between these different coral compartments in response to bleaching? We hypothesized that the proteomes of coral OL and IC reflect different functions specific to these two compartments, and that the proteomes and metabolic pathways of coral's OL and IC respond differently to bleaching.

MATERIALS AND METHODS

Species and Experimental Design

Montipora capitata is locally abundant, dominant reef-building coral in Hawai'i, United States. It is a small-polyp species (ca. 0.8 mm) that grows in branching and plating forms, or it can exhibit both morphologies in a single colony. Only the branching form was collected for this study. *M. capitata* was chosen because it has a highly perforate skeleton, and because it is often noted for its resilience (Ritson-Williams and Gates, 2020) indicated by its shift from auto- to heterotrophy (Grottoli et al., 2006) and

its ability to reproduce following thermally induced bleaching (Cox, 2007).

Between August 22–25, 2017, 10 colonies of *Montipora capitata* with a diameter of ∼ 24 cm were collected from the inner lagoon of Kāneʻohe Bay, surrounding the Hawaiʻi Institute of Marine Biology (HIMB, 21.428° N, 157.792° W). Individual colonies were collected more than 3 m apart and although no genetic analyses were conducted, they were considered to be different genets. Upon collection, each colony was halved using a hammer and chisel to produce two genetically identical colonies (ramets). The two halves from each colony were randomly assigned to one of three outdoor flow-through tanks for the ambient temperature control group or one of three tanks for the bleaching treatment group. Colonies were allowed to acclimate for 7–10 days prior to temperature adjustments. The thermal stress treatment started in September during the period when coral bleaching events may occur. Maximum monthly mean temperature for the main Hawaiian Islands is 27°C and occurs between August–September (NOAA Coral Reef Watch, 2018). On September 1, the temperature in the bleaching treatment tanks was elevated (600 W Titanium Aquarium Heater, Bulk Reef Supply, United States) 0.6°C day^{-1} over 4 days, reaching a mean (±SD) temperature of 30.4 ± 0.5°C (range: 29.4–31°C). The control tanks had a temperature of 28 ± 0.9°C. On September 26, the heat in the bleaching treatment tanks was gradually decreased to ambient levels by September 29. Twenty-four hours later, two small fragments (ca. 2 cm) were sampled from each colony, one to quantify chlorophyll *a* and Symbiodiniaceae density, and one for proteomics. Samples were cut from the colonies using toe-nail clippers (Revlon Inc., United States) and were immediately frozen in liquid nitrogen. They were stored at −80°C at HIMB until they were shipped on dry ice to the University of Washington, WA, United States.

All tanks were maintained with a volume of 400 L of ambient sand-filtered seawater from Kāneʻohe Bay. Throughout the experiment, corals were randomly rotated among tanks weekly to minimize any tank effects. Water was circulated using 100 W submersible pumps (Rio® 26HF HyperFlow Water Pump 6019 LPH, TAAM, United States). Mean daytime photosynthetic active radiation (PAR) levels in the tanks were 584 μmol photons m^{-2} s^{-1}, and mean PAR at 12:00 was 1,249 μmol photons m^{-2} s^{-1}, measured using a waterproof PAR logger (Odyssey®, Dataflow Systems Limited, NZ). Corals were not given any supplemental food during the experiment.

Bleaching Status

Bleaching was measured by quantifying chlorophyll *a* and Symbiodiniaceae densities. Chlorophyll *a* was extracted by first grinding each sample in separate glass mortar and pestle. Extractions were then conducted for two consecutive 24 h-periods with fresh 100% acetone used at the start of each period. The two-part extraction allowed us to extract total chlorophyll per coral fragment. At the end of each 24-h period absorbances were measured at 630, 663, and 750 nm. Equations from Jeffrey and Humphrey (1975) were used to calculate chlorophyll concentration for each period and summed to determine total chlorophyll per sample. Symbiodiniaceae were separated from ground coral tissue by centrifugation (two times for 5 min at 4,000 rpm). Symbiodiniaceae pellets were resuspended in filtered seawater with 1% formalin and 2–3 drops of Lugol's iodine, then homogenized using a Tissue Tearer™ (Model# 985–370). Three subsamples were counted using a hemocytometer and the mean was determined. Chlorophyll *a* and Symbiodiniaceae densities were standardized to grams of ash-free dry weight (gdw) of coral tissue.

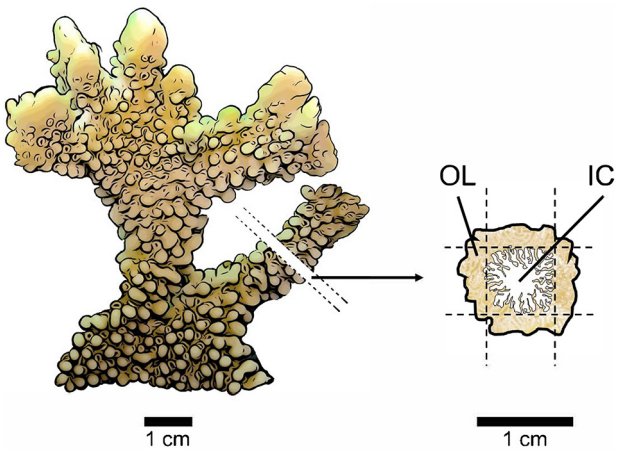

FIGURE 1 | Sampling method for protein extractions from bleached and non-bleached *Montipora capitata* colonies. A small cross-section (∼5 mm thick) was removed from one branch of each coral fragment at least 1 cm from the tip. The cross-section was laid flat, and a thin layer of tissue (∼1–2 mm) was removed from four sides using a sterilized razor blade producing an outer layer (OL) of tissue and an inner core (IC) of intra-skeletal tissue and skeleton. The cross-section diagram shows the composition of our two sample types as the tissue of *M. capitata* penetrates the perforate skeleton (coral tissue indicated in brown and skeleton indicated in white).

Proteomics

Coral branches for proteomics were sub-sectioned into two sample types: an outer layer (OL) of coral tissue and an inner core (IC) consisting of intra-skeletal tissue and skeleton (**Figure 1**). Samples were collected at least 1 cm from the tip of the fragment. A cross-section, about 5 mm thick, was cut from the fragment, then the OL and IC were separated using a razor blade. An effort was made to collect OL samples of tissue from the oral surface of the coral to the base of the polyps where tissue meets the surface of the skeleton. The remaining skeleton and intra-skeletal tissue material made up the IC samples. All samples were crushed with a metal spatula, placed in 1.5 ml microcentrifuge tubes and frozen at −80°C until proteomic analyses.

To lyse cells, coral samples were sonicated in a 100 μl solution of 50 mM sodium bicarbonate (NH_4HCO_3) with 6 M urea three times (for 15 s then placed on ice for 20–30 s each time), using a titanium micro-probe sonicator (Branson 250 Sonifier; 20 kHz), then flash frozen in a dry ice bath for 30 s and stored at −80°C. Samples were thawed on ice and centrifuged at 4°C at 5,000 rpm for 10 min to separate and remove solid skeletal material to prevent particles from

clogging the chromatography system and from disrupting pH balance during the digestion step. Protein concentrations were quantified from the supernatant in triplicate using a BCA assay (Pierce^{TM}), following the manufacturer's instructions for limited sample size (microplate procedure). Samples from one coral colony yielded extremely low protein concentration and were removed from further analyses. For each sample, 50 μg of protein were aliquoted into a new microcentrifuge tube, then brought to a total volume of 100 μl using a solution of 50 mM NH_4HCO_3 with 6 M urea. Samples were frozen at −80°C until further processing.

Enzymatic digestions of the 50 μg protein lysate aliquots were performed following Nunn et al. (2015). Briefly, samples were reduced with T tris(2-carboxyethyl)phosphine, alkylated with iodoacetamide, and diluted with a 4:1 ratio of ammonium bicarbonate to methanol prior to enzymatic digestion with Promega Trypsin (1:20; enzyme: protein) overnight at 37°C. To stop the digestion, each sample's pH was modified with 10% formic acid to a pH $\leq$ 2. Samples were evaporated to near dryness (<20 μl) in a speed vacuum (CentriVap® Refrigerated Centrifugal Concentrator Model 7310021) prior to desalting. To remove buffer salts, urea and other non-peptide molecules prior to mass spectrometry analysis, samples were desalted with MicroSpin^{TM} Columns (Nest Group) following the manufacturer's instructions. The resulting peptide samples were evaporated to near dryness, then reconstituted in 5% acetonitrile (ACN) with 0.1% formic acid to final concentration of 0.5 μg μl^{-1} and stored at −80°C prior to analysis.

Liquid chromatography tandem mass spectrometry was performed on Thermo Fisher QExactive according to Nunn et al. (2015). Liquid chromatography was performed using a 28 cm, 75 μm i.d., fused silica capillary column (Magic C18AQ, 100 Å, 5; Michrom, Bioresources, CA) with a 4 cm, 100 mm i.d., precolumn (Magic C18AQ, 100 Å, 5; Michrom). Peptide samples were randomized in the autosampler and loaded on the precolumn for 10 min with 5% ACN, followed by elution onto the analytical column using a 90 min gradient of 5–35% ACN with 0.1% formic acid. Top 20 data dependent acquisition (DDA) was used to collect tandem mass spectrometry data. MS1 data was collected on the mass range of 400–1,400 *m/z* and collision energy was set to 25. The 20 most intense ions with + 2 to + 4 charge states were selected for collision induced fragmentation and subsequent data acquisition in the MS2 using a dynamic exclusion of 10 s. The column was then washed for 10 min with 80% ACN and 0.1% formic acid and equilibrated for 10 min in 5% ACN and 0.1% formic acid prior to the next sample. Quality control standards were introduced every five runs to monitor chromatography and MS performance and visualized using Skyline (MacLean et al., 2010).

To generate a high quality protein database, the transcriptome of *M. capitata* (Frazier et al., 2017; GSE97888_Montiporacapitata_transcriptome.fasta) was translated using Transdecoder v 2.0.1 (Haas et al., 2013). Peptide tandem mass spectra were searched against the resulting protein database of *M. capitata* concatenated with 50 common contaminant proteins (Mellacheruvu et al., 2013). Spectra were searched using Comet version 2017.01 rev. 4 (Eng et al., 2013). Search parameters included a concatenated decoy search, peptide mass tolerance of 10 ppm, trypsin as the search enzyme, oxidized methionine as a variable modification (+ 15.9949 Da), alkylated cysteine (57.021464 Da), and up to three missed cleavages. PeptideProphet (Keller et al., 2002) and ProteinProphet (Nesvizhskii et al., 2003) were used to assign probabilities to peptide and protein identifications. Adjusted normalized spectral abundance factor (ADJNSAF) for each sample was determined using Abacus (Fermin et al., 2011). Abacus parameters included minimum PeptideProphet score "maxIniProbTH" = 0.99 and "miniProbTH" = 0.50, and a combined ProteinProphet score > 0.88 (FDR of 0.01) (**Supplementary File 1**). For all downstream analyses, the dataset included only proteins with at least 2 unique peptides across all samples and proteins identified at FDR < 0.01. The mass spectrometry proteomics data have been deposited to the ProteomeXchange Consortium *via* the PRIDE [1] partner repository with the dataset identifier PXD021243.

Data Analysis

To investigate the role of proteins identified by the proteomics experiments we used Gene Ontology (GO) and Kyoto Encyclopedia of Genes and Genomes (KEGG) (Kanehisa and Goto, 2000) pathway analyses. To recover GO terms for each protein, protein sequences were BLASTed against the UniProtKB Swiss-Prot non-redundant protein database (downloaded 10.15.2018). Top results are reported with cutoff *E*-value < 1E-10. Due to a low annotation rate retrieved from the UniProtKB database (∼49%), a second BLAST analysis was performed against the National Center for Biotechnology Information (NCBI) nr database on proteins that lacked detailed UniProt annotations. KEGG ID numbers were retrieved from BlastKoala (Kanehisa et al., 2016) using *M. capitata* predicted protein sequence data. GO terms and KEGG data were used to organize proteins into functional categories (e.g., carbon metabolism, response to oxidative stress, etc.; **Supplementary File 2**).

Proteomics differences among all sample types were visualized using non-metric multidimensional scaling (NMDS) plots based on log (base 10) transformed adjusted normalized spectral abundance factor (ADJNSAF) values. NMDS was performed with distance = "bray," trymax = 100 and autotransform = FALSE, using the vegan package in R (Oksanen et al., 2020). Bray-Curtis dissimilarity was used to account for a high amount of zero values in the dataset. Analysis of similarity (ANOSIM) was used to test for significant differences among all sample types and between the following comparisons: bleached outer layer (BOL) vs. non-bleached outer layer (NBOL), bleached inner core (BIC) vs. non-bleached inner core (NBIC), and NBOL vs. NBIC. Statistical differences of protein abundances between sample types were determined using Qspec, a program that computes differential protein abundance (Choi et al., 2015). Analyses were performed on (n = 9) paired samples (ramets) using the qspec-paired command (burn-in = 2,000, iterations = 10,000, normalized = 1) for the following comparisons: BOL vs. NBOL, BIC vs. NBIC, and NBOL vs. NBIC. Qspec was performed using raw spectral counts with a sum of at least two unique peptides for each protein in each

comparison. Qspec output included a protein-length corrected log-fold change analysis (base 2) and a false discovery rate (FDR)-corrected z-score based on the posterior distribution of the LFC parameter, guided by the FDR estimated by a well-known Empirical Bayes method. Differential expression was reported using a LFC $\geq |0.5|$ and z-score $\geq |2|$ (**Supplementary File 3**). Enrichment analysis of biological processes were compared between NBOL and NBIC using MetaGOmics ver. 0.1.1 (Riffle et al., 2017). MetaGOmics quantifies functional differences among treatments based on peptide, not protein, abundance using GO. The *M. capitata* proteome identified in this study was set as the background reference. Then, for each treatment group spectral counts were pooled across all samples (n = 9) and compared against the reference. GO terms were considered significant when Laplace corrected LFC > |0.5| and when Laplace corrected and Bonferroni corrected p-value < 0.01. The Laplace correction adds one to every spectral count for each GO term to account for spectral counts that equal zero when calculating log fold ratios, while the Bonferroni correction controls for type I errors due to multiple hypothesis testing (Riffle et al., 2017). As above, GO term data were used to organize proteins into functional categories.

RESULTS

Bleaching Status

Photobiological data confirmed that the bleaching treatment corals were bleached (**Figure 2**). Symbiodiniaceae density (number of cells gdw^{-1}) decreased ∼71% in bleached corals compared to non-bleached control corals (Wilcoxon rank sum test, W = 8, p-value = 0.002756). Chlorophyll *a* concentration (μg gdw^{-1}) decreased ∼78% in bleached corals compared to non-bleached corals (T-test, t = −8.0304, df = 13.91, p-value = 1.368e-06).

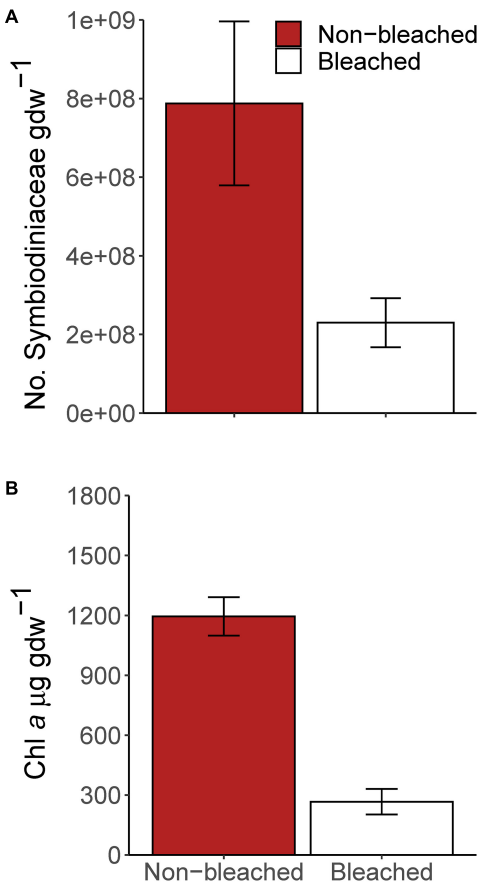

FIGURE 2 | Photobiological measurements of experimental corals. Bars indicate the mean and error bars indicate 1 standard error, for **(A)** Symbiodiniaceae density (number of cells gdw^{-1}) and **(B)** chlorophyll *a* concentration (μg gdw^{-1}).

Proteomic Results Across All Sample Types

Proteomic analyses revealed a total of 2,361 proteins that were identified across all treatments and sample types. Overall, ∼90% (2,128) of the proteins identified in this study were annotated with either National Center for Biotechnology Information (NCBI) (n = 2,082) or UniProtKB IDs (n = 1,167) and ∼81% (1,918) were associated with GO terms. Of all 2,361 proteins, ∼71% (1,687) had associated KEGG terms. This high percentage of annotated proteins allowed for more detailed analysis of active metabolic pathways utilized in each sample type across both treatments. About 70% (1,660 proteins) of all proteins were found in every sample group and the number of unique proteins per treatment or sample type ranged from 0.5–2%, with the highest number of unique proteins observed in the OL of bleached corals (**Figure 3A**). NMDS ordination of protein profiles of all sample types show a distinction between the OL and IC compartments but not between bleached and non-bleached samples for either OL or IC (**Figure 3B**). ANOSIM revealed that there was a significant difference of protein profiles among all sample types (R = 0.5701; p = 9.999e-05).

Comparison of Protein Profiles From the Outer Layer and Inner Core of Non-bleached Corals

To gain a general understanding of the overall protein differences between *M. capitata* OL and IC, we compared the proteomes of the OL and IC of non-bleached corals. Across the two sample types, we identified 2,242 proteins. ANOSIM revealed that there was a significant difference of protein profiles between the OL and IC of non-bleached samples (R = 0.5936; p = 0.001). Further analysis revealed that 187 proteins were significantly more abundant in the OL and 132 proteins were more abundant in the IC (**Supplementary File 3**). Based on enrichment analysis, the OL of non-bleached *M. capitata* was enriched in biological processes involved in anatomical development, carbohydrate metabolism, cell differentiation, endocytosis, lipid metabolism, protein metabolism, RNA processing and small molecule processing (**Figure 4A** and **Supplementary File 4**). Peroxidasin (PER2; m.25079; LFC−3.7) was detected at the highest abundance in the OL and is part of cellular response to oxidative stress. Several other proteins related to carbon and nitrogen

metabolism were also present in high abundances such as GDP-mannose 4,6 dehydratase (GMD; m.26053; LFC−1.2), pyruvate dehydrogenase (PDH; m.4559; LFC−1.1), aconitate hydratase (ACN; m.20259; LFC−0.7), and isocitrate dehydrogenase (IDH; m.11767; LFC−0.7) (**Figure 4B**). The IC was characterized by an enrichment in GO biological processes involved in cellular structure and adhesion, carbohydrate metabolism, immune response, lipid metabolism, oxidoreductase activity and response to stimulus (**Figure 4A** and **Supplementary File 4**). The protein identified in the OL to have the highest fold change difference compared to the IC was a lipase-related protein (LIP1; m.21324, LFC + 2.1) that is involved in lipid metabolism (**Figure 4B**). Von Willebrand factor type A (VWA; m.31548, LFC + 1.5), an important adhesion structural protein, was also present at significantly high concentration in the IC (**Figure 4B**).

Comparison of Bleaching Effects on the Outer Layer Proteome

In the OL of bleached and non-bleached *M. capitata*, 2,281 proteins were identified. ANOSIM did not reveal a significant difference of protein profiles between OL of bleached and non-bleached corals (R = 0.05316; p = 0.159). Qspec analysis of differential abundances between the OL of bleached and non-bleached corals revealed 63 significant proteins at higher, and 28 at lower, abundance in bleached corals compared to non-bleached corals (**Supplementary File 3**). Biological enrichment analysis of GO terms identified that the OL of bleached corals have a higher abundance of proteins involved in carbon metabolism, lipid metabolism, nitrogen metabolism, protein metabolism, response to oxidative stress, RNA processing and cellular signaling and transport than non-bleached corals (**Figures 5A**, **6**). Proteins with the highest log-fold change included calumenin (CALU; m.10914, LFC + 1.8), betaine-homocysteine S-methyltransferase (BHMT; m.1453, LFC + 1.6), peroxidasin (PER1; m.28022, LFC + 1.5), urease (URE; m.24102, LFC + 1.4), and catalase (CAT; m.4762, LFC + 1) (**Figures 5A**, **6**). Key cellular pathways that increased in the OL of bleached corals include the glyoxylate cycle, fatty acid beta oxidation, beta alanine metabolism, protein degradation and synthesis, betaine degradation and urea degradation. GO terms associated with less abundant proteins in the OL of bleached corals are associated with biological processes involved in lipid metabolism, amino acid synthesis, protein metabolism, RNA processing, cellular signaling and transport, and cellular structure (**Figures 5A**, **6**). Proteins that were significantly lower in abundance in the OL of bleached corals included cholesterol transporter (CHLT; m.15955, LFC −1.8), glutamine synthetase (GS; m.30399, LFC −1.6), phospholipase B (PLIP; m.27749, LFC −1.1), and mucin protein (MUC; m.29491, LFC −1) (**Figures 5A**, **6**).

Comparison of Bleaching Effects on the Inner Core Proteome

In the IC of bleached and non-bleached *M. capitata*, 2,181 proteins were identified. ANOSIM did not reveal a significant difference of protein profiles between the IC of bleached and non-bleached corals (R = −0.04287; p = 0.636). Qspec analysis of relative abundances of the proteins detected in the IC revealed 22 proteins at significantly higher abundance and 17 at lower abundance in the IC of bleached corals compared to non-bleached corals. Associated GO terms indicate that proteins at higher abundance in the IC of bleached corals are involved in biological functions including carbon metabolism, protein metabolism, response to oxidative stress and RNA processing (**Figures 5B**, **6**). The top 5 proteins with the highest positive log-fold change in the IC of bleached corals included peroxidasin (PER2; m.25079, LFC 1.9), ependymin (EPDR; m.10937, LFC 1), aldehyde dehydrogenase (ALDH; m.27710, LFC 1), calumenin (CALU; m.10914, LFC 0.9), and stomatin (STOM; m.21902, LFC 0.8) (**Figures 5B**, **6**). Additionally, a protein involved in the pentose phosphate pathway was also represented in this dataset with significantly increased abundance (**Figures 5B**, **6**). Biologically enriched GO terms associated with the IC of non-bleached corals were involved in nitrogen metabolism, cellular signaling and cellular structure (**Figures 5B**, **6**). The proteins that were lower in abundance in the IC of bleached corals compared to the IC of non-bleached corals included glutamine synthetase (GS; m.30399, LFC −1.9), peroxidasin (PER3; m.6107, LFC −1.2), and mucin (MUC; m.29491, LFC −0.8) (**Figures 5B**, **6**).

DISCUSSION

Proteomics has proven to be a valuable tool for uncovering active cellular processes and elucidating the response of different biological compartments of symbiotic cnidarians in response to stress (Weston et al., 2015; Ricaurte et al., 2016; Cziesielski et al., 2018; Hernández-Elizárraga et al., 2019; Mayfield, 2020; Mayfield et al., 2021; Petrou et al., 2021). Our high-throughput discovery-based proteomic analyses of the OL and IC of bleached and non-bleached corals support our hypothesis that proteomic signatures differ between *M. capitata* OL and IC, reflecting different biological functions associated with these two compartments. Additionally, comparisons of bleached and non-bleached proteomes support our hypothesis that *M. capitata* OL and IC respond in different metabolic ways to bleaching stress. We observed bleaching induced differences in carbon metabolism, response to oxidative stress, protein turnover and nitrogen metabolism between corals' OL and IC compartments. Our results corroborate several previous transcriptomics studies (DeSalvo et al., 2010, 2012; Barshis et al., 2013; Kenkel et al., 2013; Polato et al., 2013; Aguilar et al., 2019) by providing direct evidence of protein translation in response to bleaching stress. To our knowledge, our analysis was the first to compare the simultaneous bleaching proteomic response in both OL and IC. Our results highlight the differential metabolic response between OL and IC in *M. capitata* that may reflect the compartmentalization of specific physiological functions and energy acquisition and allocation in each compartment.

Biological Functions of (Non-bleached) Outer Layer and Inner Core

Among our four sample types, the most significant proteomic difference was found when comparing the OL and IC (see

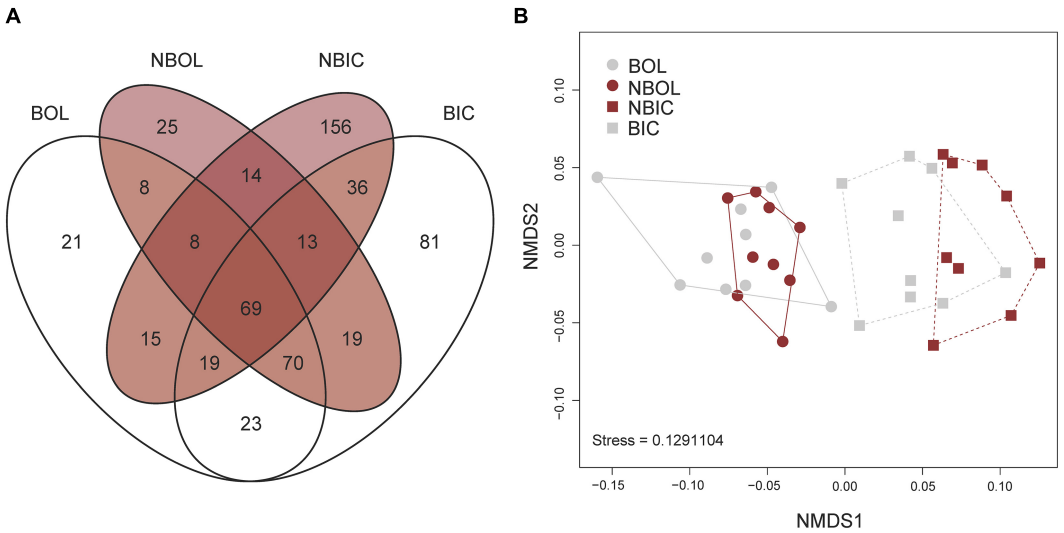

FIGURE 3 | Global results of proteomics analysis of bleached and non-bleached *Montipora capitata* outer layer (OL) tissue and inner core (IC) intra-skeletal tissue and skeleton. **(A)** Venn diagram depicts number of proteins identified in each sample type, and **(B)** non-metric dimensional scaling (NMDS) plot of all treatments. BOL, bleached outer layer; NBOL, non-bleached outer layer; NBIC, bleached inner core; BIC, bleached inner core.

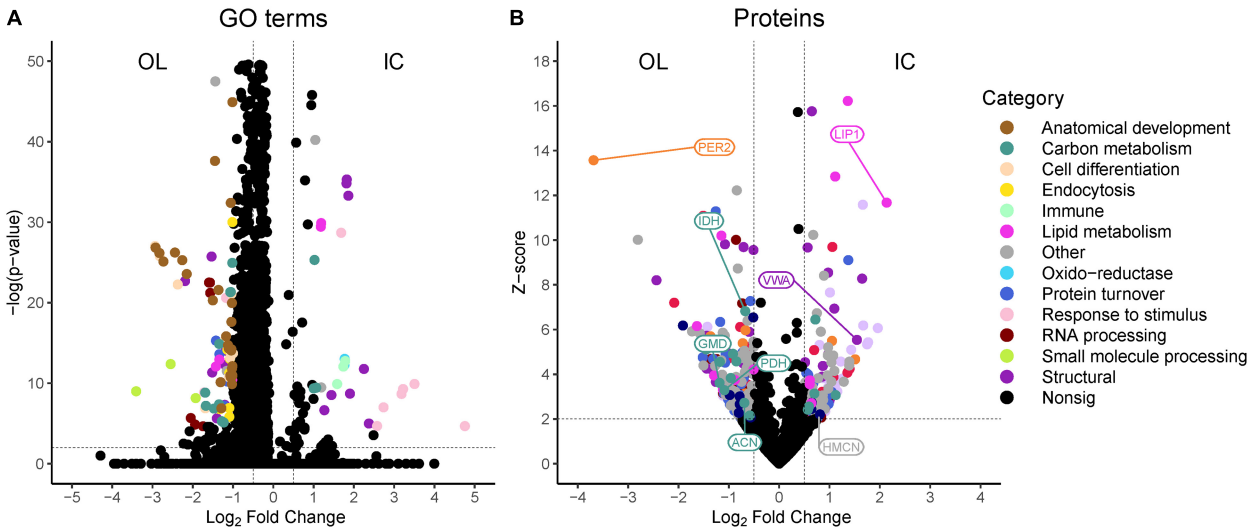

FIGURE 4 | Volcano plots of **(A)** associated gene ontology (GO) terms derived from MetaGOmics and **(B)** proteins identified in non-bleached outer layer (OL) tissue and inner core (IC) intra-skeletal tissue and skeleton of *Montipora capitata*. Points represent the magnitude of the $\log_2$ fold change and the -log(*p*-value) or z-score for each GO term or protein, respectively. Dashed lines indicate significance thresholds. Select proteins that are discussed in the text are indicated by their abbreviated protein name.

Figure 3B). Biological enrichment analysis of GO terms using MetaGOmics highlight how the coral OL is characterized by routine cellular activities such as metabolic processes, cellular maintenance, and growth, while the IC was significantly enriched in proteins related to structural maintenance, cell adhesion, immune and stimulus response, as well as carbon and lipid metabolism. These differences in biological processes suggest that there are compartmentalized pathways between the OL and IC, with IC proteins playing a larger role in skeletal formation than OL proteins. Previous proteomic studies of coral skeleton report the presence of structural and cell adhesion proteins that were also found in this study in the *M. capitata* IC compartment, including von Willebrand factor type A (VWA), hemicentin (HMCN), and collagens (COL) (Drake et al., 2013; Ramos-Silva et al., 2013). The von Willebrand factor type A containing proteins have been suggested to play a role in connecting the layer of cells at the interface of the skeleton organic matrix to the skeleton, and collagen has been suggested to serve as a site for

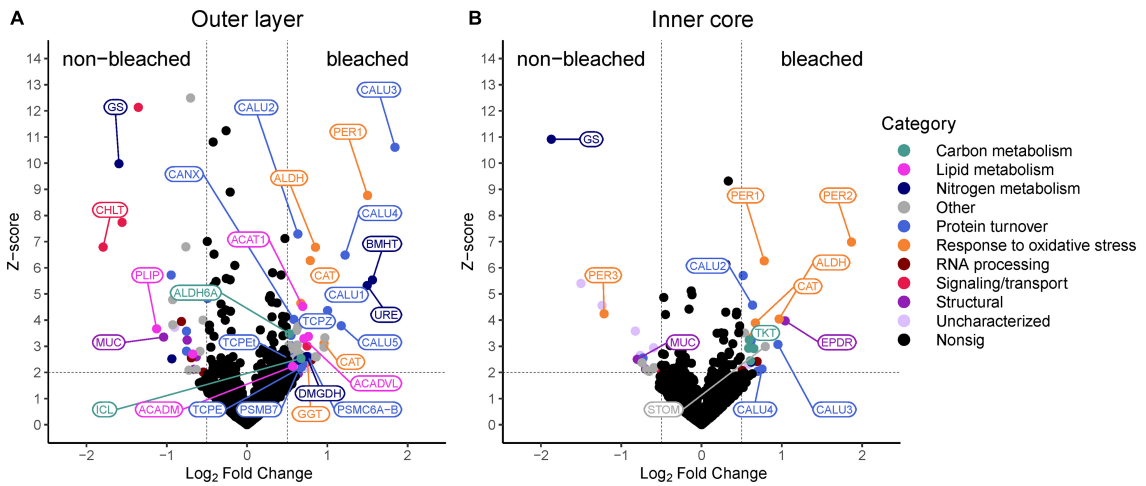

FIGURE 5 | Volcano plots of proteins identified in non-bleached and bleached **(A)** outer layer (OL) tissue and **(B)** inner core (IC) intra-skeletal tissue and skeleton of *Montipora capitata*. Points represent the magnitude of the $\log_2$ fold change and the z-score for each protein. Dashed lines indicate significance thresholds. Select proteins that are discussed in the text are indicated by their abbreviated protein name.

proteins to bind where minerals, such as calcium carbonate, can nucleate (Drake et al., 2013).

A considerable amount of redundancy was revealed between the OL and IC of *M. capitata* as ∼2,000 proteins were detected with similar abundances between the two compartments, which is likely due in part to our sampling method of a perforate coral. In corals with a perforate skeleton, tissue penetrates the complex matrix of crevices and cavities and can host Symbiodiniaceae that can drive biological activity (Pearse and Muscatine, 1971; Gladfelter, 1983; Yost et al., 2013). In contrast, the skeleton of imperforate corals is more dense and typically does not contain coral tissue. Evidence suggests that perforate corals are more robust to stressful events than imperforate corals (Krupp et al., 1992; Jokiel et al., 1993; Santos et al., 2009), which may be due to higher protein and Symbiodiniaceae densities in their deep tissue compared to imperforate corals (Schlöder and D'Croz, 2004). It has also been suggested that perforate skeletons can provide refuge for deep coral tissue and Symbiodiniaceae that reside deep in the skeleton during stressful conditions (Santos et al., 2009). Given that the IC samples collected here contain both coral tissue and skeleton, it is likely that there is some overlap in metabolic processes and pathways that occur between the OL and IC compartments, which would explain some of the similarity in proteins between them. Furthermore, proteins from tissue within the skeleton that do not play a role in calcification may have been at a higher abundance and were more likely to be sampled with our mass spectrometry methods than proteins that are directly involved in calcification, such as carbonic anhydrase, calcium ion pumps or the coral acid rich proteins identified by other studies (Drake et al., 2013; Ramos-Silva et al., 2013).

Molecular Responses to Bleaching

Carbon Metabolism

Carbon is a critical nutrient for corals that is primarily provided in the form of glucose-based photosynthate that is passed to the host from Symbiodiniaceae (Muscatine et al., 1981). As corals bleach and the association with Symbiodiniaceae is weakened and carbon-based photosynthate decreases, it has been proposed that corals maintain their energetic needs through the degradation of stored lipids (Grottoli and Rodrigues, 2011). Here, we provide direct evidence of modifications to carbon metabolic pathways through quantitative analyses of proteins that are differentially abundant in bleached corals compared to non-bleached corals. Our results reveal mitigation strategies for bleached corals to generate the required energy needed to persist after bleaching stress.

In the OL of bleached *M. capitata*, increased abundance of isocitrate lyase (ISL) suggests an increased capacity to produce glyoxylate. Typically produced in the glyoxylate cycle, glyoxylate is a two-carbon metabolite and a precursor to glucose and many other C-storage molecules. The glyoxylate cycle, a variation of the Krebs cycle, uses acetyl-CoA as a source of carbon and conserves carbon by bypassing two decarboxylation steps of the Krebs Cycle (Kornberg and Krebs, 1957). Although it was once thought to only occur in plants and bacteria, recent transcriptomics studies have shown that glyoxylate cycle enzymes also occur in corals (DeSalvo et al., 2010; Kenkel et al., 2013; Polato et al., 2013). Bleached corals may upregulate the glyoxylate cycle, or the production of glyoxylate, to metabolize energy in stored lipids, breaking down triacylglycerol into their component fatty acids for release of acetyl-CoA, when carbohydrate supply is low (Polato et al., 2013; Wright et al., 2015; Petrou et al., 2021). Malate synthetase (MS), the other key enzyme of the glyoxylate cycle that converts glyoxylate and acetyl-CoA to malate, was present in the proteomes identified in this study, but no significant difference was detected between bleached and non-bleached corals. The same trend of increased ISL abundance and no increase in MS abundance has been reported for *Porites asteroides* (Kenkel et al., 2013) and *Acropora millepora* (Petrou et al., 2021). We also detected three key enzymes involved in lipid metabolism

FIGURE 6 | Heatmap of differentially abundant proteins in non-bleached and bleached *Montipora capitata* outer layer (OL) tissue and inner core (IC) intra-skeletal tissue and skeleton. Cell shading represents the mean NSAF value for each treatment normalized by the row mean. Rows are clustered using the "correlation" method of the pheatmap function in R. The dendrogram was set to cut 5 distinct clusters. The row annotations (categories) represent broad biological function categories based on GO and KEGG terms associated with each protein. NBOL, non-bleached outer layer; BOL, bleached outer layer; NBIC, non-bleached inner core; BIC, bleached inner core.

in higher abundance in the OL of bleached corals compared to the OL of non-bleached corals: very long-chain specific acyl-CoA dehydrogenase (ACADVL), medium chain specific acyl-CoA dehydrogenase (ACADM) and acetyl-CoA acetyltransferase (ACAT1). The presence of these enzymes further supports the hypothesis that bleached corals utilize the glyoxylate cycle to extract energy from lipids when Symbiodiniaceae-derived photosynthate is decreased (**Figure 7**).

Malonate-semialdehyde dehydrogenase (ALDH) was another enzyme that was significantly increased in bleached corals and can provide an additional source of acetyl-CoA that could be used in the glyoxylate cycle. ALDH is involved in several metabolic pathways including carbon metabolism, beta-alanine metabolism and propanoate metabolism where it catalyzes the conversion of malonate semialdehyde (3-oxopropanoate) to acetyl-CoA. Enzymes associated with the glyoxylate cycle and fatty acid beta-oxidation were higher in the OL of bleached corals than the OL of non-bleached corals. However, ALDH was more abundant in both the OL and IC of bleached corals compared to these compartments in non-bleached corals (**Figure 5**).

An enzyme involved in the pentose phosphate pathway (PPP), transketolase (TKT), was lower in the IC of non-bleached corals compared to the OL of non-bleached corals, but higher in the IC of bleached corals than the IC of non-bleached corals, suggesting that this pathway is initially prioritized in the OL but becomes more essential in the IC during bleaching. The PPP helps maintain carbon homeostasis, generates precursors to nucleotides, and produces reducing molecules (e.g., NADPH) to fight oxidative stress. This pathway has been elevated in stressed cnidarians suffering from disease (Wright et al., 2015; Garcia et al., 2016) as well as thermal stress (Oakley et al., 2017; Fonseca et al., 2019). Hernández-Elizárraga et al. (2019) found proteomic evidence that bleached fire coral, *Millepora complanata*, redirected carbohydrate flux from glycolysis to the PPP, which would help the coral alleviate oxidative stress through the production of NADPH. Additionally, the generation of nucleotides could assist with multiple other cellular processes. Future research should investigate potential links between the pentose phosphate pathway and coral calcification.

Response to Oxidative Stress

Oxidative stress, due to production of excess reactive oxygen species (ROS), has been implicated as a key underlying mechanism in the breakdown of coral-algal symbiosis leading to bleaching (Lesser et al., 1990; Lesser, 1997; Downs et al., 2002). Under environments favoring physiological homeostasis, ROS produced during metabolic processes of the coral host, Symbiodiniaceae, and in the chloroplasts of Symbiodiniaceae, are kept in check by cellular antioxidants. Under environmental stress, however, this tightly regulated process can become unbalanced resulting in excess ROS, leading to cellular damage and bleaching (Lesser et al., 1990; Downs et al., 2002). One possible mechanism for a coral's resilience to bleaching may be explained by the timing, magnitude, and types of antioxidants regulated during stress (Gardner et al., 2017).

Several enzymes involved in oxidative stress response were at higher abundance in both the OL and IC of bleached *M. capitata* compared to samples from non-bleached corals. This observation is consistent with proteomics (e.g., Weston et al., 2015; Cziesielski et al., 2018; Petrou et al., 2021) and transcriptomics (e.g., DeSalvo et al., 2008, 2010; Voolstra et al., 2009) studies that have demonstrated increased antioxidant activity in response to thermal stress in cnidarians. Multiple catalases (CAT) were elevated in the OL and IC of bleached corals. This antioxidant enzyme is an efficient scavenger of hydrogen peroxide and is commonly observed in high quantities in bleached corals (Lesser et al., 1990; Seneca et al., 2010; Krueger et al., 2015; Gardner et al., 2017). Peroxidasins (PER1, PER2, PER3) that also neutralize hydrogen peroxide were detected at significantly higher abundances in both compartments from bleached corals. In coral embryos, significant upregulation of peroxidasin genes, a multi-domain peroxidase, has been observed after 48 h of thermal stress (Voolstra et al., 2009), while in adult corals it was downregulated after 11 days of thermal stress exposure (DeSalvo et al., 2008). Here we report that peroxidases are present in an adult coral following nearly 1 month of thermal stress. Peroxidasin has been proposed as a biomarker for heat stress in coral embryos and adults (Voolstra et al., 2009) and may be important for resilience to high temperatures (Barshis et al., 2013).

Another enzyme higher in the OL of bleached corals, gamma-glutamyltranspeptidase 1 (GGT1), likely plays an indirect role in oxidative stress response through its role in the glutathione cycle. Glutathione, in its reduced form, is important for various metabolic processes where it can neutralize ROS and help break down toxins (Mailloux et al., 2013; Bachhawat and Yadav, 2018). GGTs break down oxidized glutathione that has been transported out of the cell into glutamate and cysteine-glycine. Cysteine-glycine can then be transported back into the cell to produce more glutathione in its reduced form, ready to neutralize ROS (Mailloux et al., 2013; Bachhawat and Yadav, 2018).

Protein Turnover

Environmental stressors that have the potential to induce cellular damage, or significantly alter homeostatic metabolisms, drive high protein turnover rates (Downs et al., 2002; Oakley et al., 2017). Several pathways, including protein degradation, translation, and protein folding, play key roles in the turnover of proteins and maintaining proteostasis. Significantly higher abundances of proteins involved in each of those pathways were quantified in bleached corals compared to non-bleached controls, indicating a significantly higher level of protein turnover. In the OL of bleached corals, protein degradation was indicated by higher abundance of two proteins associated with proteasomes, the protein complexes responsible for degrading extraneous or damaged proteins: 26S proteasome regulatory subunit 6A-B (PSMC6A-B) and proteasome subunit beta type-7-like (PSMB7). The observed increase in proteasome components in this study is consistent with transcriptomic (Traylor-Knowles et al., 2017) and proteomic (Petrou et al., 2021) research investigating short term heat stress in corals.

Multiple chaperone subunits of the T-complex protein Ring Complex (TRiC: TCPE, TCPEt, TCPZ), as well as calnexin (CANX) were in high abundance in the OL of bleached corals,

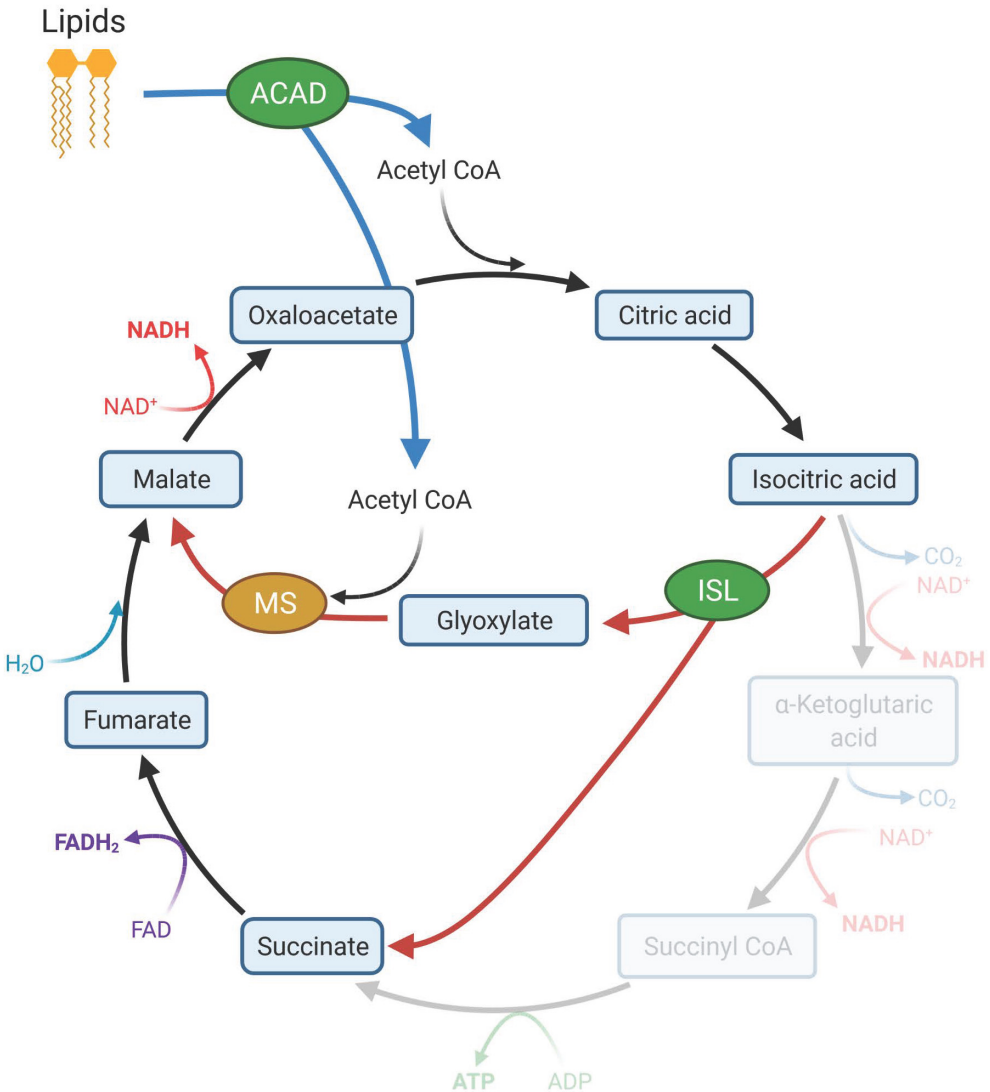

FIGURE 7 | Lipid degradation and the glyoxylate cycle. Increased abundance of acyl-CoA dehydrogenases (ACAD) in the outer layer (OL) tissue of bleached coral indicated the breakdown of lipids that produce acetyl CoA (blue arrows). Acetyl CoA is the primary source of carbon in the glyoxylate cycle (red arrows). The glyoxylate cycle, a modified version of the Kreb's cycle (black arrows), utilizes isocitrate lyase (ISL) and malate synthetase (MS) and can produce additional intermediate molecules of the Krebs cycle that can be used to generate glucose. ISL was significantly elevated in the OL of bleached corals while MS was elevated but not significantly. Created with BioRender.com.

suggesting that bleached corals were undergoing endoplasmic reticulum (ER) stress. ER stress occurs due to accumulation of unfolded or misfolded proteins and initiates the unfolded protein response which, under prolonged or severe stress, can lead to cell death (Xu et al., 2005). The TRiC assists the folding of up to 10% of eukaryotic cytosolic proteins involved in a broad range of functions (Yam et al., 2008). It is suggested to be well-equipped for folding complex, slow-folding proteins that are prone to aggregation (Yam et al., 2008; Gestaut et al., 2019), making it critical for maintaining proteostasis and reducing ER stress. Calnexin is recognized for its role in processing glycoproteins in the ER where it binds to unfolded or misfolded proteins and prohibits their release (Ou et al., 1993). Eight different calumenins (CALU) were in higher abundance in bleached corals, including five in the OL (CALU1-5) and three in the IC (CALU2, CALU3, CALU4). Although its role as a chaperone in the ER has not been directly confirmed, increased abundance of calumenin resulted in down-regulation of proteins involved in ER stress reduction, suggesting it functions similarly to chaperones (Lee et al., 2013). Chaperones, most notably heat shock proteins, are commonly detected in heat-stressed and bleached corals (Black et al., 1995; Brown et al., 2002; Barshis et al., 2013; Weston et al., 2015; Ricaurte et al., 2016; Traylor-Knowles et al., 2017; Seveso et al., 2020) because of their role in stress response. However, no heat shock proteins were identified at significant

levels in this study. Few coral bleaching studies have reported the presence of the chaperone proteins detected in the current study (Bellantuono et al., 2012; Maor-Landaw et al., 2014; Chakravarti et al., 2020).

The increased abundances of proteins related to high protein turnover in our bleached samples, one day after the heat stress was removed, may be the result of a rapid adjustment to a change in the coral's environment (e.g., a recovery phase) *via* alteration of its proteome. High rates of protein turnover have been associated with an organism's ability to acclimatize (Hawkins, 1991). For corals it has been suggested that slow growth rates and high metabolic rates correlate to high protein turnover and acclimatization potential (Gates and Edmunds, 1999). An analysis of protein turnover rates in bleached and healthy states between *M. capitata* and other species would allow more direct testing of the hypothesis that protein turnover is directly linked to thermal acclimation.

Nitrogen Metabolism

Nitrogen (N) is a critical element used for synthesizing nucleotides, amino acids, proteins and other molecules in both the coral host and Symbiodiniaceae. Living in oligotrophic, tropical waters, the coral holobiont has adapted to efficiently acquire N from the surrounding environment *via* heterotrophy, or assimilation of dissolved organic and inorganic N by the host and the Symbiodiniaceae (Grover et al., 2006, 2008; Pernice et al., 2012). Although ammonia is the primary N-based metabolite (Grover et al., 2008), corals also have the enzymatic capacity for transport and assimilation of nitrate, dissolved free amino acids and, to a much lesser degree, urea from the surrounding water, providing them with a range of mechanisms to adapt to changing nutrient conditions (Grover et al., 2008). Nitrogen is transferred between the host and Symbiodiniaceae (Rahav et al., 1989; Atkinson et al., 1994; Hoegh-Guldberg and Williamson, 1999), however, when symbiosis breaks down due to prolonged thermal stress, mutualistic N-exchange decreases, demanding the coral host independently acquire N from the environment or intracellularly recycle it. Here we show that bleached *M. capitata* switches its dominant N- acquisition strategy from ammonia uptake to the degradation of urea and betaine (**Figure 8**).

Enzymes involved in the typical pathway of ammonia assimilation decreased in bleached corals. Both the coral host and Symbiodiniaceae are able to assimilate ammonia *via* catalysis by glutamine synthetase (GS) or glutamine dehydrogenase in the host (Yellowlees et al., 1994; Wang and Douglas, 1998; Su et al., 2018) and *via* the glutamine synthetase/glutamine:2-oxoglutarate aminotransferase (GS/GOGAT) cycle in Symbiodiniaceae (D'Elia et al., 1983; Roberts et al., 2001). In bleached corals, GS was present at significantly lower abundances in both the OL and the IC compared to non-bleached corals, suggesting an alternate route for N acquisition must be utilized (**Figures 5**, **6**). This result is consistent with recent studies in corals (Petrou et al., 2021; Rädecker et al., 2021), however, increased GS activity has been reported for other cnidarians (Wang and Douglas, 1998; Lipschultz and Cook, 2002; Oakley et al., 2016). Both Petrou et al. (2021) and Rädecker et al. (2021) also observed concurrent increases in glutamate dehydrogenase (GDH) in bleached corals, which catabolizes glutamate to α-ketoglutarate, an intermediate of the Krebs Cycle. Thus, GDH indicates the degradation of amino acids for use as energy while producing ammonia as a byproduct. While we did not observe any change in GDH in bleached corals in this study, we propose two alternative nitrogen sources in bleached corals.

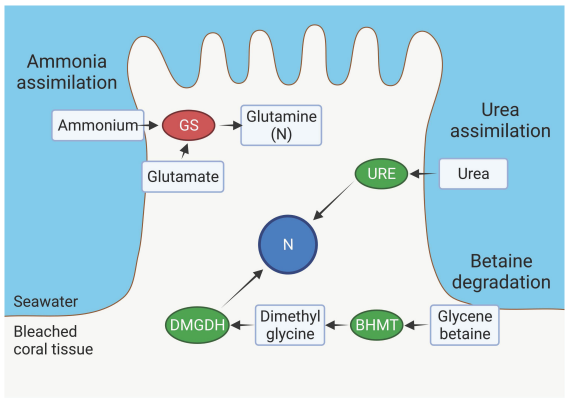

FIGURE 8 | Nitrogen (N) source pathways in the outer layer (OL) tissue of bleached *Montipora capitata*. Decreased abundance of glutamine synthetase (GS) suggests a decrease in ammonium assimilation from surrounding seawater. An increased abundance of urease (URE) suggests an increase in assimilation of urea from surrounding seawater that is broken down by URE to ammonia and carbon dioxide. Increased abundances of dimethylglycine dehydrogenase (DMGDH) and betaine–homocysteine S-methyltransferase (BHMT) indicate an increase in the betaine degradation pathway. Created with BioRender.com.

Urease (URE), an enzyme that catalyzes the conversion of urea to ammonia and carbon dioxide, provides another metabolic pathway for acquiring nitrogen and was significantly more abundant in the OL of bleached corals than non-bleached corals. Urea is thought to be an important source of nitrogen for corals (Grover et al., 2006; Crandall and Teece, 2012) because they can easily assimilate it from the surrounding environment where it accumulates from anthropogenic runoff and is a naturally produced metabolite from a variety of biological sources (Conover and Gustavson, 1999; Lomas et al., 2002; Glibert et al., 2006; McDonald et al., 2006). Grover et al. (2008), however, calculated that urea only constitutes about three percent of nitrogen uptake in *Stylophora pistillata*. Corals may also produce urea on their own, but the mechanism remains unclear because the complete enzymatic toolkit of the urea cycle has yet to be observed in corals (Streamer, 1980). Genes encoding four of the five enzymes of the urea cycle are present in the *M. capitata* genome, including: carbamoyl phosphate synthetase I (CPS1), ornithine transcarbamylase (OTC), argininosuccinate synthase (ASS) and argininosuccinate lyase (ASL), but the fifth enzyme, arginase (ARG1), has not been identified. Three of those enzymes, OTC, ASS, and ASL, were detected in the proteome identified in this study. Regardless, the elevated level of urease provides direct evidence that

bleached corals rely on urea as a source of nitrogen, which may help to counteract the effects of decreased GS activity described above.

Here, we reveal that a critical source of nitrogen in bleached corals likely comes from the intracellular degradation of glycine betaine. Two enzymes involved in betaine degradation pathway, betaine-homocysteine S-methyltransferase (BHMT) and dimethylglycine dehydrogenase (DMGDH), were significantly more abundant in the OL of bleached corals than non-bleached corals. Enzymatic components of this pathway have been observed in multiple marine organisms, including marine invertebrates and corals (DeSalvo et al., 2012; Aguilar et al., 2019; Sproles et al., 2019). Glycine betaine is an important osmolyte because of its role in counteracting osmotic and other abiotic stressors (Rathinasabapathi, 2000; Jahn et al., 2006) and may have been produced in abundance in response to bleaching (DeSalvo et al., 2012). Recently, however, betaine has been proposed as a major source of nitrogen in reef-building corals where it can account for up to 16% of total nitrogen biomass (Ngugi et al., 2020). A recent metabolomics study on the bleaching history of *M. capitata* demonstrates that betaine-lipids are depleted in bleached samples, whereas historically non-bleached *M. capitata* is enriched in this metabolite (Roach et al., 2021). These proteomic profiles on the same coral species complement the metabolomic profiles of bleached vs. non-bleached *M. capitata* and provide direct evidence of active molecular pathways utilized by bleached corals to acquire N from stored betaine-lipids, potentially leading to its long-term persistence on reefs.

CONCLUSION

Through analyzing the proteomes of the OL and IC of bleached and non-bleached *M. capitata*, we investigated: (1) whether there were differential abundances of metabolic proteins in the OL and IC compartments, and (2) if metabolic pathways differ between these two compartments in response to bleaching. We identified several metabolic pathways and biological processes that are used in specific compartments or shared across compartments following bleaching stress. These included different strategies for metabolizing carbon, lipids and nitrogen by each compartment and high oxidative stress response and protein turnover in both compartments following bleaching. Our findings suggest that some molecular responses to bleaching are compartmentalized, which may be the most efficient way to continue functions specific to each compartment following bleaching. Future research should assess whether these compartmentalized responses to bleaching are linked to compartment-specific physiological functions. For example, does energy produced from lipids *via* the glyoxylate cycle help fuel reproductive output in the coral OL compartment? Or are there links between the products of the pentose phosphate pathway, such as NADPH and nucleotide generation, and calcification? Additionally, employing these compartmentalized strategies may convey resilience to bleaching and studies targeting these pathways, such as the glyoxylate cycle, the pentose phosphate pathway, protein turnover, urea assimilation and betaine degradation, should be undertaken to better understand their influence on coral resilience. Answers to questions like these will further our understanding of how and where distinct physiological functions in corals are affected by thermal stress and bleaching. Furthermore, elucidating the precise role of these metabolic pathways and cellular responses to bleaching could provide management with molecular-based tools, such as biomarkers, for conservation and restoration.

DATA AVAILABILITY STATEMENT

Data are available *via* ProteomeXchange with identifier PXD021243.

AUTHOR CONTRIBUTIONS

JA performed the experiments, analyzed the data, and wrote the manuscript. ET-S performed the experiments, analyzed the data, and edited the manuscript. TB performed the experiments and edited the manuscript. LR and JP-G designed, performed the experiments, and edited the manuscript. BN designed, performed the experiments, and wrote the manuscript. All authors contributed to the article and approved the submitted version.

FUNDING

This work was supported in part by the University of Washington's Proteomics Resource (UWPR95794), NSF IOS-IEP 1655682 awarded to JP-G and BN, NSF IOS-IEP 1655888 to LR, and NSF GFRP DGE1762114 awarded to JA.

ACKNOWLEDGMENTS

We offer our warmest gratitude to the Gates Coral Lab for hosting and supporting us during this experiment at the Hawai'i Institute of Marine Biology. We thank Brenner Wakayama, Gavin Kreitman, Melissa Jaffe and Sean Frangos for help with collecting and culturing the experimental corals. We thank Callum Backstrom for assistance with processing Symbiodiniaceae and chlorophyll data. We also thank Hyungwon Choi for assistance with statistical software.

SUPPLEMENTARY MATERIAL

The Supplementary Material for this article can be found online at: https://www.frontiersin.org/articles/10.3389/fmars.2022.797517/full#supplementary-material

REFERENCES

Aguilar, C., Raina, J.-B., Fôret, S., Hayward, D. C., Lapeyre, B., Bourne, D. G., et al. (2019). Transcriptomic analysis reveals protein homeostasis breakdown in the coral *Acropora millepora* during hypo-saline stress. *BMC Genomics* 20:148. doi: 10.1186/s12864-019-5527-2

Atkinson, M. J., Kotler, E., and Newton, P. (1994). Effects of water velocity on respiration, calcification, and ammonium uptake of a *Porites compressa* community. *Pac. Sci.* 48, 296–303.

Bachhawat, A. K., and Yadav, S. (2018). The glutathione cycle: glutathione metabolism beyond the γ-glutamyl cycle. *IUBMB Life* 70, 585–592.

Barshis, D. J., Ladner, J. T., Oliver, T. A., Seneca, F. O., Traylor-Knowles, N., and Palumbi, S. R. (2013). Genomic basis for coral resilience to climate change. *Proc. Natl. Acad. Sci. U.S.A.* 110, 1387–1392. doi: 10.1073/pnas.1210224110

Bellantuono, A. J., Granados-Cifuentes, C., Miller, D. J., Hoegh-Guldberg, O., and Rodriguez-Lanetty, M. (2012). Coral thermal tolerance: tuning gene expression to resist thermal stress. *PLoS One* 7:e50685. doi: 10.1371/journal.pone.0050685

Black, N. A., Voellmy, R., and Szmant, A. M. (1995). Heat shock protein induction in *Montastraea faveolata* and *Aiptasia pallida* exposed to elevated temperatures. *Biol. Bull.* 188, 234–240. doi: 10.2307/1542301

Brown, B., Downs, C., Dunne, R., and Gibb, S. (2002). Exploring the basis of thermotolerance in the reef coral *Goniastrea aspera*. *Mar. Ecol. Prog. Ser.* 242, 119–129. doi: 10.3354/meps242119

Brown, B. E., Le Tissier, M. D. A., and Dunne, R. P. (1994). Tissue retraction in the scleractinian coral *Coeloseris mayeri*, its effect upon coral pigmentation, and preliminary implications for heat balance. *Mar. Ecol. Prog. Ser.* 105, 209–218.

Cantin, N. E., Cohen, A. L., Karnauskas, K. B., Tarrant, A. M., and McCorkle, D. C. (2010). Ocean warming slows coral growth in the central red sea. *Science* 329, 322–325. doi: 10.1126/science.1190182

Chakravarti, L. J., Buerger, P., Levin, R. A., and van Oppen, M. J. H. (2020). Gene regulation underpinning increased thermal tolerance in a laboratory-evolved coral photosymbiont. *Mol. Ecol.* 29, 1684–1703. doi: 10.1111/mec.15432

Choi, H., Kim, S., Fermin, D., Tsou, C.-C., and Nesvizhskii, A. I. (2015). QPROT: statistical method for testing differential expression using protein-level intensity data in label-free quantitative proteomics. *J. Proteomics* 129, 121–126. doi: 10.1016/j.jprot.2015.07.036

Conover, R., and Gustavson, K. (1999). Sources of urea in arctic seas: zooplankton metabolism. *Mar. Ecol. Prog. Ser.* 179, 41–54. doi: 10.3354/meps179041

Cox, E. F. (2007). Continuation of sexual reproduction in *Montipora capitata* following bleaching. *Coral Reefs* 26, 721–724. doi: 10.1007/s00338-007-0251-9

Crandall, J. B., and Teece, M. A. (2012). Urea is a dynamic pool of bioavailable nitrogen in coral reefs. *Coral Reefs* 31, 207–214.

Cziesielski, M. J., Liew, Y. J., Cui, G., Schmidt-Roach, S., Campana, S., Marondedze, C., et al. (2018). Multi-omics analysis of thermal stress response in a zooxanthellate cnidarian reveals the importance of associating with thermotolerant symbionts. *Proc. R. Soc. B Biol. Sci.* 285:20172654. doi: 10.1098/rspb.2017.2654

Dauphin, Y. (2001). Comparative studies of skeletal soluble matrices from some Scleractinian corals and Molluscs. *Int. J. Biol. Macromol.* 28, 293–304. doi: 10.1016/S0141-8130(01)00124-6

D'Elia, C. F., Domotor, S. L., and Webb, K. L. (1983). Nutrient uptake kinetics of freshly isolated zooxanthellae. *Mar. Biol.* 75, 157–167. doi: 10.1007/BF00405998

DeSalvo, M., Sunagawa, S., Voolstra, C., and Medina, M. (2010). Transcriptomic responses to heat stress and bleaching in the elkhorn coral *Acropora palmata*. *Mar. Ecol. Prog. Ser.* 402, 97–113. doi: 10.3354/meps08372

DeSalvo, M. K., Estrada, A., Sunagawa, S., and Medina, M. (2012). Transcriptomic responses to darkness stress point to common coral bleaching mechanisms. *Coral Reefs* 31, 215–228. doi: 10.1007/s00338-011-0833-4

DeSalvo, M. K., Voolstra, C. R., Sunagawa, S., Schwarz, J. A., Stillman, J. H., Coffroth, M. A., et al. (2008). Differential gene expression during thermal stress and bleaching in the Caribbean coral *Montastraea faveolata*. *Mol. Ecol.* 17, 3952–3971. doi: 10.1111/j.1365-294X.2008.03879.x

Downs, C. A., Fauth, J. E., Halas, J. C., Dustan, P., Bemiss, J., and Woodley, C. M. (2002). Oxidative stress and seasonal coral bleaching. *Free Radic. Biol. Med.* 33, 533–543. doi: 10.1016/S0891-5849(02)00907-3

Drake, J. L., Mass, T., Haramaty, L., Zelzion, E., Bhattacharya, D., and Falkowski, P. G. (2013). Proteomic analysis of skeletal organic matrix from the stony coral *Stylophora pistillata*. *Proc. Natl. Acad. Sci. U.S.A.* 110, 3788–3793. doi: 10.1073/pnas.1301419110

Eng, J. K., Jahan, T. A., and Hoopmann, M. R. (2013). Comet: an open-source MS/MS sequence database search tool. *Proteomics* 13, 22–24. doi: 10.1002/pmic.201200439

Fermin, D., Basrur, V., Yocum, A. K., and Nesvizhskii, A. I. (2011). Abacus: a computational tool for extracting and pre-processing spectral count data for label-free quantitative proteomic analysis. *Proteomics* 11, 1340–1345. doi: 10.1002/pmic.201000650

Ferrier-Pagès, C., Rottier, C., Beraud, E., and Levy, O. (2010). Experimental assessment of the feeding effort of three scleractinian coral species during a thermal stress: effect on the rates of photosynthesis. *J. Exp. Mar. Biol. Ecol.* 390, 118–124. doi: 10.1016/j.jembe.2010.05.007

Fonseca, S. J., Marangoni, B. L. F., Marques, J. A., and Bianchini, A. (2019). Energy metabolism enzymes inhibition by the combined effects of increasing temperature and copper exposure in the coral *Mussismilia harttii*. *Chemosphere* 236:124420. doi: 10.1016/j.chemosphere.2019.124420

Frazier, M., Helmkampf, M., Bellinger, M. R., Geib, S. M., and Takabayashi, M. (2017). De novo metatranscriptome assembly and coral gene expression profile of *Montipora capitata* with growth anomaly. *BMC Genomics* 18:710. doi: 10.1186/s12864-017-4090-y

Garcia, G. D., Santos, E. O., Sousa, G. V., Zingali, R. B., Thompson, C. C., and Thompson, F. L. (2016). Metaproteomics reveals metabolic transitions between healthy and diseased stony coral *Mussismilia braziliensis*. *Mol. Ecol.* 25, 4632–4644. doi: 10.1111/mec.13775

Gardner, S. G., Raina, J.-B., Nitschke, M. R., Nielsen, D. A., Stat, M., Motti, C. A., et al. (2017). A multi-trait systems approach reveals a response cascade to bleaching in corals. *BMC Biol.* 15:117. doi: 10.1186/s12915-017-0459-2

Gates, R. D., and Edmunds, P. J. (1999). The physiological mechanisms of acclimatization in tropical reef corals. *Am. Zool.* 39, 30–43. doi: 10.1093/icb/39.1.30

Gestaut, D., Limatola, A., Joachimiak, L., and Frydman, J. (2019). The ATP-powered gymnastics of TRiC/CCT: an asymmetric protein folding machine with a symmetric origin story. *Curr. Opin. Struct. Biol.* 55, 50–58. doi: 10.1016/j.sbi.2019.03.002

Gladfelter, E. H. (1983). Circulation of fluids in the gastrovascular system of the reef coral *Acropora cervicornis*. *Biol. Bull.* 165, 619–636. doi: 10.2307/1541469

Glibert, P. M., Harrison, J., Heil, C., and Seitzinger, S. (2006). Escalating worldwide use of Urea – a global change contributing to coastal eutrophication. *Biogeochemistry* 77, 441–463. doi: 10.1007/s10533-005-3070-5

Grottoli, A. G., and Rodrigues, L. J. (2011). Bleached *Porites compressa* and *Montipora capitata* corals catabolize δ13C-enriched lipids. *Coral Reefs* 30:687. doi: 10.1007/s00338-011-0756-0

Grottoli, A. G., Rodrigues, L. J., and Palardy, J. E. (2006). Heterotrophic plasticity and resilience in bleached corals. *Nature* 440, 1186–1189. doi: 10.1038/nature04565

Grover, R., Maguer, J.-F., Allemand, D., and Ferrier-Pagès, C. (2006). Urea uptake by the scleractinian coral *Stylophora pistillata*. *J. Exp. Mar. Biol. Ecol.* 332, 216–225. doi: 10.1016/j.jembe.2005.11.020

Grover, R., Maguer, J.-F., Allemand, D., and Ferrier-Pages, C. (2008). Uptake of dissolved free amino acids by the scleractinian coral *Stylophora pistillata*. *J. Exp. Biol.* 211, 860–865. doi: 10.1242/jeb.012807

Gygi, S. P., Rochon, Y., Franza, B. R., and Aebersold, R. (1999). Correlation between Protein and mRNA abundance in Yeast. *Mol. Cell. Biol.* 19, 1720–1730. doi: 10.1128/MCB.19.3.1720

Haas, B. J., Papanicolaou, A., Yassour, M., Grabherr, M., Blood, P. D., Bowden, J., et al. (2013). De novo transcript sequence reconstruction from RNA-Seq: reference generation and analysis with Trinity. *Nat. Protoc.* 8:10.1038/nrot.2013.084. doi: 10.1038/nprot.2013.084

Hawkins, A. J. S. (1991). Protein turnover: a functional appraisal. *Funct. Ecol.* 5:222. doi: 10.2307/2389260

Hernández-Elizárraga, V. H., Olguín-López, N., Hernández-Matehuala, R., Ocharán-Mercado, A., Cruz-Hernández, A., Guevara-González, R. G., et al. (2019). Comparative analysis of the soluble proteome and the cytolytic activity of unbleached and bleached *Millepora complanata* ("Fire Coral") from the Mexican Caribbean. *Mar. Drugs* 17:393. doi: 10.3390/md17070393

Hoegh-Guldberg, O., and Williamson, J. (1999). Availability of two forms of dissolved nitrogen to the coral *Pocillopora damicornis* and its symbiotic zooxanthellae. *Mar. Biol.* 133, 561–570. doi: 10.1007/s002270050496

Hughes, A. D., and Grottoli, A. G. (2013). Heterotrophic compensation: a possible mechanism for resilience of coral reefs to global warming or a sign of prolonged stress? *PLoS One* 8:e81172. doi: 10.1371/journal.pone.0081172

Isa, Y., and Okazaki, M. (1987). Some observations on the Ca^{2+}-binding phospholipid from scleractinian coral skeletons. *Comp. Biochem. Physiol. Part B Comp. Biochem.* 87, 507–512. doi: 10.1016/0305-0491(87)90045-9

Jahn, M. P., Cavagni, G. M., Kaiser, D., and Kucharski, L. C. (2006). Osmotic effect of choline and glycine betaine on the gills and hepatopancreas of the *Chasmagnathus granulata* crab submitted to hyperosmotic stress. *J. Exp. Mar. Biol. Ecol.* 334, 1–9. doi: 10.1016/j.jembe.2006.01.006

Jeffrey, S. W., and Humphrey, G. F. (1975). New spectrophotometric equations for determining chlorophylls *a*, *b*, *c1* and *c2* in higher plants, algae and natural phytoplankton. *Biochem. Physiol. Pflanz.* 167, 191–194. doi: 10.1016/S0015-3796(17)30778-3

Jokiel, P. L., Hunter, C. L., Taguchi, S., and Watarai, L. (1993). Ecological impact of a fresh-water "reef kill" in Kaneohe Bay, Oahu, Hawaii. *Coral Reefs* 12, 177–184. doi: 10.1007/BF00334477

Kanehisa, M., and Goto, S. (2000). KEGG: kyoto encyclopedia of genes and genomes. *Nucleic Acids Res.* 28, 27–30. doi: 10.1093/nar/28.1.27

Kanehisa, M., Sato, Y., and Morishima, K. (2016). BlastKOALA and GhostKOALA: KEGG tools for functional characterization of genome and metagenome sequences. *J. Mol. Biol.* 428, 726–731. doi: 10.1016/j.jmb.2015.11.006

Keller, A., Nesvizhskii, A. I., Kolker, E., and Aebersold, R. (2002). Empirical statistical model to estimate the accuracy of peptide identifications made by MS/MS and database search. *Anal. Chem.* 74, 5383–5392. doi: 10.1021/ac025747h

Kenkel, C. D., Meyer, E., and Matz, M. V. (2013). Gene expression under chronic heat stress in populations of the mustard hill coral (*Porites astreoides*) from different thermal environments. *Mol. Ecol.* 22, 4322–4334. doi: 10.1111/mec.12390

Kornberg, H. L., and Krebs, H. A. (1957). Synthesis of cell constituents from C_2-units by a modified tricarboxylic acid cycle. *Nature* 179, 988–991. doi: 10.1038/179988a0

Krueger, T., Hawkins, T. D., Becker, S., Pontasch, S., Dove, S., Hoegh-Guldberg, O., et al. (2015). Differential coral bleaching—Contrasting the activity and response of enzymatic antioxidants in symbiotic partners under thermal stress. *Comp. Biochem. Physiol. A. Mol. Integr. Physiol.* 190, 15–25. doi: 10.1016/j.cbpa.2015.08.012

Krupp, D. A., Jokiel, P. L., and Chartrand, T. S. (1992). "Asexual reproduction by the solitary scleractinian coral Fungia scutaria on dead parent coralla in Kaneohe Bay, Oahu, Hawaiian Islands," in *Proceeding of the 7th International. Coral Reef Symposium*, Vol. 1 (Guam University Guam Press RH Richmond), 527–534

Lee, J. H., Kwon, E. J., and Kim, D. H. (2013). Calumenin has a role in the alleviation of ER stress in neonatal rat cardiomyocytes. *Biochem. Biophys. Res. Commun.* 439, 327–332. doi: 10.1016/j.bbrc.2013.08.087

Lesser, M. P. (1997). Oxidative stress causes coral bleaching during exposure to elevated temperatures. *Coral Reefs* 16, 187–192. doi: 10.1007/s003380050073

Lesser, M. P., Stochaj, W. R., Tapley, D. W., and Shick, J. M. (1990). Bleaching in coral reef anthozoans: effects of irradiance, ultraviolet radiation, and temperature on the activities of protective enzymes against active oxygen. *Coral Reefs* 8, 225–232. doi: 10.1007/BF00265015

Lipschultz, F., and Cook, C. (2002). Uptake and assimilation of 15N-ammonium by the symbiotic sea anemones *Bartholomea annulata* and *Aiptasia pallida*: conservation versus recycling of nitrogen. *Mar. Biol.* 140, 489–502. doi: 10.1007/s00227-001-0717-1

Lomas, M. W., Mark Trice, T., Glibert, P. M., Bronk, D. A., and McCarthy, J. J. (2002). Temporal and spatial dynamics of urea uptake and regeneration rates and concentrations in Chesapeake Bay. *Estuaries* 25, 469–482. doi: 10.1007/BF02695988

MacLean, B., Tomazela, D. M., Shulman, N., Chambers, M., Finney, G. L., Frewen, B., et al. (2010). Skyline: an open source document editor for creating and analyzing targeted proteomics experiments. *Bioinform. Oxf. Engl.* 26, 966–968. doi: 10.1093/bioinformatics/btq054

Maier, T., Güell, M., and Serrano, L. (2009). Correlation of mRNA and protein in complex biological samples. *FEBS Lett.* 583, 3966–3973.

Mailloux, R. J., McBride, S. L., and Harper, M.-E. (2013). Unearthing the secrets of mitochondrial ROS and glutathione in bioenergetics. *Trends Biochem. Sci.* 38, 592–602. doi: 10.1016/j.tibs.2013.09.001

Maor-Landaw, K., Karako-Lampert, S., Ben-Asher, H. W., Goffredo, S., Falini, G., Dubinsky, Z., et al. (2014). Gene expression profiles during short-term heat stress in the red sea coral *Stylophora pistillata*. *Glob. Change Biol.* 20, 3026–3035. doi: 10.1111/gcb.12592

Mayfield, A. B. (2020). Proteomic signatures of corals from thermodynamic reefs. *Microorganisms* 8:1171. doi: 10.3390/microorganisms8081171

Mayfield, A. B., Aguilar, C., Kolodziej, G., Enochs, I. C., and Manzello, D. P. (2021). Shotgun proteomic analysis of thermally challenged reef corals. *Front. Mar. Sci.* 8:547. doi: 10.3389/fmars.2021.660153

Mayfield, A. B., Wang, Y., Chen, C., Chen, S., and Lin, C. (2016). Dual-compartmental transcriptomic + proteomic analysis of a marine endosymbiosis exposed to environmental change. *Mol. Ecol.* 25, 5944–5958.

McDonald, M. D., Smith, C. P., and Walsh, P. J. (2006). The physiology and evolution of Urea transport in fishes. *J. Membr. Biol.* 212, 93–107. doi: 10.1007/s00232-006-0869-5

Mellacheruvu, D., Wright, Z., Couzens, A. L., Lambert, J.-P., St-Denis, N. A., Li, T., et al. (2013). The CRAPome: a contaminant repository for affinity purification–mass spectrometry data. *Nat. Methods* 10, 730–736. doi: 10.1038/nmeth.2557

Muller, E. M., Bartels, E., and Baums, I. B. (2018). Bleaching causes loss of disease resistance within the threatened coral species *Acropora cervicornis*. *eLife* 7:e35066. doi: 10.7554/eLife.35066

Muscatine, L., McCloskey, L. R., and Marian, R. E. (1981). Estimating the daily contribution of carbon from zooxanthellae to coral animal respiration. *Limnol. Oceanogr.* 26, 601–611. doi: 10.4319/lo.1981.26.4.0601

Nesvizhskii, A. I., Keller, A., Kolker, E., and Aebersold, R. (2003). A statistical model for identifying proteins by Tandem mass spectrometry. *Anal. Chem.* 75, 4646–4658. doi: 10.1021/ac0341261

Ngugi, D. K., Ziegler, M., Duarte, C. M., and Voolstra, C. R. (2020). Genomic blueprint of glycine betaine metabolism in coral metaorganisms and their contribution to reef nitrogen budgets. *iScience* 23:101120. doi: 10.1016/j.isci.2020.101120

NOAA Coral Reef Watch (2018). *NOAA Coral Reef Watch Virtual Station for the Main Hawaiian Islands, Jan. 1, 2007-Dec. 31, 2017*. College Park, MD: NOAA Coral Reef Watch.

Nunn, B. L., Slattery, K. V., Cameron, K. A., Timmins-Schiffman, E., and Junge, K. (2015). Proteomics of *Colwellia psychrerythraea* at subzero temperatures - a life with limited movement, flexible membranes and vital DNA repair: proteomics of microbes at subzero temperatures. *Environ. Microbiol.* 17, 2319–2335. doi: 10.1111/1462-2920.12691

Oakley, C. A., Ameismeier, M. F., Peng, L., Weis, V. M., Grossman, A. R., and Davy, S. K. (2016). Symbiosis induces widespread changes in the proteome of the model cnidarian *Aiptasia*. *Cell. Microbiol.* 18, 1009–1023.

Oakley, C. A., Durand, E., Wilkinson, S. P., Peng, L., Weis, V. M., Grossman, A. R., et al. (2017). Thermal shock induces host proteostasis disruption and endoplasmic reticulum stress in the model symbiotic cnidarian *Aiptasia*. *J. Proteome Res.* 16, 2121–2134. doi: 10.1021/acs.jproteome.6b00797

Oksanen, J., Blanchet, F. G., Friendly, M., Kindt, R., Legendre, P., McGlinn, D., et al. (2020). *vegan: Community Ecology Package*. Available online at: https://CRAN.R-project.org/package=vegan (accessed February 11, 2021).

Ou, W.-J., Cameron, P. H., Thomas, D. Y., and Bergeron, J. J. M. (1993). Association of folding intermediates of glycoproteins with calnexin during protein maturation. *Nature* 364, 771–776. doi: 10.1038/364771a0

Pandey, A., and Mann, M. (2000). Proteomics to study genes and genomes. *Nature* 405, 837–846. doi: 10.1038/35015709

Pearse, V. B., and Muscatine, L. (1971). Role of symbiotic algae (zooxanthellae) in coral calcification. *Biol. Bull.* 141, 350–363. doi: 10.2307/1540123

Pernice, M., Meibom, A., Van Den Heuvel, A., Kopp, C., Domart-Coulon, I., Hoegh-Guldberg, O., et al. (2012). A single-cell view of ammonium assimilation in coral–dinoflagellate symbiosis. *ISME J.* 6, 1314–1324.

Petrou, K., Nunn, B. L., Padula, M. P., Miller, D. J., and Nielsen, D. A. (2021). Broad scale proteomic analysis of heat-destabilised symbiosis in the hard coral *Acropora millepora*. *Sci. Rep.* 11:19061. doi: 10.1038/s41598-021-98548-x

Polato, N. R., Altman, N. S., and Baums, I. B. (2013). Variation in the transcriptional response of threatened coral larvae to elevated temperatures. *Mol. Ecol.* 22, 1366–1382. doi: 10.1111/mec.12163

Puverel, S., Tambutté, E., Pereira-Mouriès, L., Zoccola, D., Allemand, D., and Tambutté, S. (2005). Soluble organic matrix of two Scleractinian corals: partial and comparative analysis. *Comp. Biochem. Physiol. B Biochem. Mol. Biol.* 141, 480–487. doi: 10.1016/j.cbpc.2005.05.013

Rädecker, N., Pogoreutz, C., Gegner, H. M., Cárdenas, A., Roth, F., Bougoure, J., et al. (2021). Heat stress destabilizes symbiotic nutrient cycling in corals. *Proc. Natl. Acad. Sci. U.S.A.* 118:e2022653118. doi: 10.1073/pnas.2022653118

Rahav, O., Dubinsky, Z., Achituv, Y., and Falkowski, P. G. (1989). Ammonium metabolism in the zooxanthellate coral, *Stylophora pistillata*. *Proc. R. Soc. Lond. B Biol. Sci.* 236, 325–337. doi: 10.1098/rspb.1989.0026

Ramos-Silva, P., Kaandorp, J., Huisman, L., Marie, B., Zanella-Cléon, I., Guichard, N., et al. (2013). The skeletal proteome of the coral *Acropora millepora*: the evolution of calcification by co-option and domain shuffling. *Mol. Biol. Evol.* 30, 2099–2112. doi: 10.1093/molbev/mst109

Rathinasabapathi, B. (2000). Metabolic engineering for stress tolerance: installing osmoprotectant synthesis pathways. *Ann. Bot.* 86, 709–716.

Ricaurte, M., Schizas, N. V., Ciborowski, P., and Boukli, N. M. (2016). Proteomic analysis of bleached and unbleached *Acropora palmata*, a threatened coral species of the Caribbean. *Mar. Pollut. Bull.* 107, 224–232. doi: 10.1016/j.marpolbul.2016.03.068

Riffle, M., May, D., Timmins-Schiffman, E., Mikan, M., Jaschob, D., Noble, W., et al. (2017). MetaGOmics: a web-based tool for peptide-centric functional and taxonomic analysis of metaproteomics data. *Proteomes* 6:2. doi: 10.3390/proteomes6010002

Ritson-Williams, R., and Gates, R. D. (2020). Coral community resilience to successive years of bleaching in Kāneʻohe Bay, Hawaiʻi. *Coral Reefs* 39, 757–769. doi: 10.1007/s00338-020-01944-4

Roach, T. N. F., Dilworth, J., Martin H, C., Jones, A. D., Quinn, R. A., and Drury, C. (2021). Metabolomic signatures of coral bleaching history. *Nat. Ecol. Evol.* 5, 495–503. doi: 10.1038/s41559-020-01388-7

Roberts, J. M., Fixter, L. M., and Davies, P. S. (2001). Ammonium metabolism in the symbiotic sea anemone *Anemonia viridis*. *Hydrobiologia* 461, 25–35. doi: 10.1023/A:1012752828587

Rodrigues, L. J., and Grottoli, A. G. (2007). Energy reserves and metabolism as indicators of coral recovery from bleaching. *Limnol. Oceanogr.* 52, 1874–1882. doi: 10.4319/lo.2007.52.5.1874

Santos, S. R., Toyoshima, J., and Kinzie, R. A. 3rd. (2009). Spatial and temporal dynamics of symbiotic dinoflagellates (*Symbiodinium*: dinophyta) in the perforate coral *Montipora capitata*. *Galaxea J. Coral Reef Stud.* 11, 139–147.

Schlöder, C., and D'Croz, L. (2004). Responses of massive and branching coral species to the combined effects of water temperature and nitrate enrichment. *J. Exp. Mar. Biol. Ecol.* 313, 255–268. doi: 10.1016/j.jembe.2004.08.012

Seneca, F. O., Forêt, S., Ball, E. E., Smith-Keune, C., Miller, D. J., and van Oppen, M. J. H. (2010). Patterns of gene expression in a scleractinian coral undergoing natural bleaching. *Mar. Biotechnol.* 12, 594–604.

Seveso, D., Arrigoni, R., Montano, S., Maggioni, D., Orlandi, I., Berumen, M. L., et al. (2020). Investigating the heat shock protein response involved in coral bleaching across scleractinian species in the central Red Sea. *Coral Reefs* 39, 85–98. doi: 10.1007/s00338-019-01878-6

Sproles, A. E., Oakley, C. A., Matthews, J. L., Peng, L., Owen, J. G., Grossman, A. R., et al. (2019). Proteomics quantifies protein expression changes in a model cnidarian colonised by a thermally tolerant but suboptimal symbiont. *ISME J.* 13, 2334–2345. doi: 10.1038/s41396-019-0437-5

Streamer, M. (1980). Urea and arginine metabolism in the hard coral, *Acropora acuminata*. *Comp. Biochem. Physiol. Part B Comp. Biochem.* 65, 669–674. doi: 10.1016/0305-0491(80)90177-7

Stuhr, M., Blank-Landeshammer, B., Reymond, C. E., Kollipara, L., Sickmann, A., Kucera, M., et al. (2018). Disentangling thermal stress responses in a reef-calcifier and its photosymbionts by shotgun proteomics. *Sci. Rep.* 8:3524. doi: 10.1038/s41598-018-21875-z

Su, Y., Zhou, Z., and Yu, X. (2018). Possible roles of glutamine synthetase in responding to environmental changes in a scleractinian coral. *Mol. Biol. Rep.* 45, 2115–2124. doi: 10.1007/s11033-018-4369-3

Tomanek, L. (2014). Proteomics to study adaptations in marine organisms to environmental stress. *J. Proteomics* 105, 92–106. doi: 10.1016/j.jprot.2014.04.009

Traylor-Knowles, N., Rose, N. H., Sheets, E. A., and Palumbi, S. R. (2017). Early transcriptional responses during heat stress in the coral *Acropora hyacinthus*. *Biol. Bull.* 232, 91–100. doi: 10.1086/692717

Voolstra, C. R., Schnetzer, J., Peshkin, L., Randall, C. J., Szmant, A. M., and Medina, M. (2009). Effects of temperature on gene expression in embryos of the coral *Montastraea faveolata*. *BMC Genomics* 10:627. doi: 10.1186/1471-2164-10-627

Wang, J., and Douglas, A. E. (1998). Nitrogen recycling or nitrogen conservation in an alga-invertebrate symbiosis? *J. Exp. Biol.* 201, 2445–2453.

Ward, S., Harrison, P., and Hoegh-Guldberg, O. (2000). "Coral bleaching reduces reproduction of scleractinian corals and increases susceptibility to future stress," in *Proceeding of the 9th International Coral Reef Symposium. Bali Indones. 23-27 Oct. 2000*, 7, (Bali).

Weston, A. J., Dunlap, W. C., Beltran, V. H., Starcevic, A., Hranueli, D., Ward, M., et al. (2015). Proteomics links the redox state to calcium signaling during bleaching of the scleractinian coral acropora microphthalma on exposure to high solar irradiance and thermal stress. *Mol. Cell. Proteomics* 14, 585–595. doi: 10.1074/mcp.M114.043125

Wright, R. M., Aglyamova, G. V., Meyer, E., and Matz, M. V. (2015). Gene expression associated with white syndromes in a reef building coral, *Acropora hyacinthus*. *BMC Genomics* 16:371. doi: 10.1186/s12864-015-1540-2

Xu, C., Bailly-Maitre, B., and Reed, J. C. (2005). Endoplasmic reticulum stress: cell life and death decisions. *J. Clin. Invest.* 115, 2656–2664. doi: 10.1172/JCI26373

Yam, A. Y., Xia, Y., Lin, H.-T. J., Burlingame, A., Gerstein, M., and Frydman, J. (2008). Defining the TRiC/CCT interactome links chaperonin function to stabilization of newly made proteins with complex topologies. *Nat. Struct. Mol. Biol.* 15, 1255–1262. doi: 10.1038/nsmb.1515

Yellowlees, D., Rees, T. A. V., and Fiti, W. K. (1994). Effect of ammonium-supplemented seawater on glutamine synthetase and glutamate dehydrogenase activities in host tissue and zooxanthellae of *Pocillopora damicornis* and on ammonium uptake rates of the zooxanthellae. *Pac. Sci.* 48, 291–295.

Yost, D. M., Wang, L.-H., Fan, T.-Y., Chen, C.-S., Lee, R. W., Sogin, E., et al. (2013). Diversity in skeletal architecture influences biological heterogeneity and *Symbiodinium* habitat in corals. *Zoology* 116, 262–269. doi: 10.1016/j.zool.2013.06.001

Conflict of Interest: The authors declare that the research was conducted in the absence of any commercial or financial relationships that could be construed as a potential conflict of interest.

frontiers in Physiology

ORIGINAL RESEARCH
published: 01 March 2022
doi: 10.3389/fphys.2022.801672

Does Predation Exacerbate the Risk of Endosymbiont Loss in Heat Stressed Hermatypic Corals? Molecular Cues Provide Insights Into Species-Specific Health Outcomes in a Multi-Stressor Ocean

Carolina Madeira[1,2,3†], Marta Dias[3*†], Ana Ferreira[4], Raúl Gouveia[4], Henrique Cabral[3,5], Mário S. Diniz[1,2] and Catarina Vinagre[3,6]*

[1]i4HB – Associate Laboratory Institute for Health and Bioeconomy, NOVA School of Science and Technology, NOVA University Lisbon, Caparica, Portugal, [2]UCIBIO – Applied Molecular Biosciences Unit, NOVA School of Science and Technology, NOVA University of Lisbon, Caparica, Portugal, [3]MARE – Marine and Environmental Sciences Centre, Faculty of Sciences, University of Lisbon, Lisbon, Portugal, [4]Biology Department, Oceanário de Lisboa, Lisbon, Portugal, [5]INRAE – National Research Institute for Agriculture, Food and Environment, UR EABX, Cestas, France, [6]CCMAR – Centre of Marine Sciences, University of Algarve, Faro, Portugal

OPEN ACCESS

Edited by:
Davide Seveso,
University of Milano-Bicocca, Italy

Reviewed by:
Renaud Grover,
Centre Scientifique de Monaco, Monaco
Oren Levy,
Bar-Ilan University, Israel

***Correspondence:**
Carolina Madeira
scg.madeira@fct.unl.pt
orcid.org/0000-0003-1632-634X
Marta Dias
maddias@fc.ul.pt
orcid.org/0000-0003-0447-6009

†These authors have contributed equally to this work

Specialty section:
This article was submitted to Aquatic Physiology, a section of the journal Frontiers in Physiology

Received: 25 October 2021
Accepted: 31 January 2022
Published: 01 March 2022

Citation:
Madeira C, Dias M, Ferreira A, Gouveia R, Cabral H, Diniz MS and Vinagre C (2022) Does Predation Exacerbate the Risk of Endosymbiont Loss in Heat Stressed Hermatypic Corals? Molecular Cues Provide Insights Into Species-Specific Health Outcomes in a Multi-Stressor Ocean. Front. Physiol. 13:801672. doi: 10.3389/fphys.2022.801672

Ocean warming has been a major driver of coral reef bleaching and mass mortality. Coupled to other biotic pressures, corals' ability for acclimatization and adaptation may become compromised. Here, we tested the combined effects of warming scenarios (26, 30, and 32°C) and predation (wound vs. no wound) in coral health condition (paleness, bleaching, and mortality), cellular stress responses (heat shock protein 70 kDa Hsp70, total ubiquitin Ub, and total antioxidant capacity TAC), and physiological state (integrated biomarker response index, IBR) of seven Scleractinian coral species, after being exposed for 60 days. Results show that although temperature was the main factor driving coral health condition, thermotolerant species (*Galaxea fascicularis*, *Psammocora contigua*, and *Turbinaria reniformis*) displayed increased paleness, bleaching, and mortality in predation treatments at high temperature, whereas thermosensitive species (*Acropora tenuis*, *Echinopora lamellosa*, and *Montipora capricornis* brown and green morphotypes) all died at 32°C, regardless of predation condition. At the molecular level, results show that there were significant main and interactive effects of species, temperature, and predation in the biomarkers assessed. Temperature affected Hsp70, Ub, and TAC, evidencing the role of protein folding and turnover, as well as reactive oxygen species scavenging in heat stress management. Predation increased Hsp70 and Ub, suggesting the activation of the pro-phenoloxidase system and cytokine activity, whereas the combination of both stressors mainly affected TAC during moderate stress and Ub under

severe stress, suggesting that redox balance and defense of homeostasis are crucial in tissue repair at high temperature. IBR levels showed an increasing trend at 32°C in predated coral fragments (although non-significant). We conclude that coral responses to the combination of high temperature and predation pressure display high inter-species variability, but these stressors may pose a higher risk of endosymbiont loss, depending on species physiology and stress intensity.

Keywords: coral reefs, tissue wounds, ocean warming, predation, molecular responses, biomarkers, health condition, endosymbiont loss

INTRODUCTION

Large-scale bleaching caused by climate change and extreme weather events has become a major theme of coral research in the past years (e.g., Le Nohaïc et al., 2017; Stuart-Smith et al., 2018; Sully et al., 2019; Vargas-Ángel et al., 2019; Hédouin et al., 2020). These bleaching events have caused coral mass mortality in a recent past, with impacts for biogenic reef systems (Hughes et al., 2017, 2018a,b,c), including loss of complex habitat and apex predators, and population explosions of macroalgae that lead to regime shifts (Jackson, 2008; Mumby and Van Woesik, 2014). Based on the current trends of coral reef degradation, the future seems increasingly dire for these critically endangered habitats.

Global climate modeling and satellite observations indicate that the unfavorable thermal conditions that elicit coral bleaching are becoming more prevalent in today's oceans (Hoegh-Guldberg, 2014; Heron et al., 2016; Liu et al., 2017; IPCC, 2021). Continuous warming of tropical oceans, which are already 1.0 to 1.3°C warmer than in the previous century (Deser et al., 2010), combined with more severe and frequent El Niño events (Power et al., 2013) will continue to aggravate the severity of heat stress suffered by reef corals (Frieler et al., 2013; Ainsworth et al., 2016; Hughes et al., 2018b). Particularly, regions in the Indian and Pacific Oceans where coral reefs occur have shown significant changes in heat content, reflected in the largest increases in surface area with temperatures above 29°C (Lin et al., 2011).

Moreover, warmer seas are likely to drive more intense and frequent tropical storms (Emanuel, 2005; IPCC, 2014, 2021) with an expected increase in the physical damage experienced by coral reefs (Hoegh-Guldberg, 2011). Strong wave action and currents generated during storms, particularly in shallow reefs, are expected to produce an increasing number of coral fragments, through breakage of coral sections from the edges of the colonies (Harmelin-Vivien, 1994). This coral debris can vary in size from small nubbins to fragments as large as 100 cm in length (Highsmith et al., 1980; Forsman et al., 2006), but the increasing magnitude of extreme weather events and consequent mechanical impacts to reefs will likely lead to the generation of increasingly smaller fragments in size. Coupled to evidence from several studies showing that heat stress can negatively affect corals' sexual reproductive cycles (e.g., Richmond, 1993; Negri et al., 2007; Nozawa and Harrison, 2007; Randall and Szmant, 2009; Levitan et al., 2014), the predicted increases in SSTs may lead to the failure of sexual reproductive processes, which, when coupled to more frequent storms may favor alternative asexual means of propagation, such as coral fragmentation. The detachment and re-distribution of scleractinian corals are important processes in reef systems, as fragmentation leads to colonization of otherwise inaccessible habitats, patch reef development, reef extension, and colony multiplication (Highsmith et al., 1980; Lirman, 2000; Foster et al., 2013; Roth et al., 2013). However, there is a knowledge gap on how and if these small fragments will cope in a multi-stressor environment, and whether they may become key colonizers, allowing for species persistence under climate change.

Evidence from the field and laboratory experiments show that hermatypic coral colonies are overall highly sensitive to heat stress (e.g., see Marshall and Baird, 2000; Hoegh-Guldberg et al., 2007b; Hoegh-Guldberg, 2011; Dias et al., 2018, 2019a), despite species-specific susceptibilities (Dias et al., 2020; McClanahan et al., 2020). Such interspecific variability has been related to corals intrinsic characteristics as well as extrinsic factors. Among intrinsic ones, coral morphology, tissue thickness, metabolic rates, heterotrophic feeding capacity, mucus production rates, and tissue concentration of fluorescent pigments have been shown to play relevant roles in the physiological plasticity of corals and their ability to recover and overcome temperature-induced bleaching (e.g., Salih et al., 1998; Loya et al., 2001; Wooldridge, 2009; Levas et al., 2013; Dias et al., 2018). These intrinsic characteristics can vary with coral size (e.g., full colony vs. large fragment vs. nubbin), affecting coral's ability to survive under challenging conditions (e.g., see Highsmith et al., 1980; Bowden-Kerby, 2001; Lindahl, 2003). Extrinsic factors include, for instance, the coral location in the reef (i.e., corals in marginal locations are normally exposed to harsher abiotic conditions, see Keshavmurthy et al., 2021).

Eco-physiological studies have provided insights into pathways of coral coping mechanisms through thermal challenges. Authors have highlighted in the literature the importance of Symbiodiniaceae clades to the holobiont thermotolerance (Nesa and Hidaka, 2009; Hillyer et al., 2017; Williams and Patterson, 2020), as well as the relevance of increased abundance of certain proteins (e.g., repertoire of heat shock protein homologs) and antioxidant enzymes that act as intracellular stabilizers (Lesser, 2006). These biomolecules play a role in corals' cellular stress responses, by controlling macromolecular damage that arises during physiological stress and by scavenging reactive oxygen species (Cziesielski et al., 2019). Nevertheless, the use of these biomolecules as diagnostic biomarkers was only

implemented during the early 2000s (Downs et al., 2000; Parkinson et al., 2019).

Since hermatypic corals are the base species of biogenic reef systems, they influence ecosystems' structure and function (Ellison, 2019), and provide habitats and micro-habitats to a wide range of marine organisms. The importance of predators in maintaining high habitat spatial heterogeneity as well as in structuring benthic communities and has been shown by multiple observational and manipulative studies (Dulvy et al., 2004; Clements and Hay, 2018). Damage by coral predators (i.e., corallivorous organisms), such as butterflyfish, parrotfish, pufferfish, triggerfish, filefish, wrasses, damselfish, *Drupella* snails, and starfish (especially *Acanthaster planci*), range from minor to lethal. The intensity of predation can trigger cascading effects on coral populations (Done et al., 2010; Kayal et al., 2012), as predation causes lacerations to tissues and injuries to the aragonite skeleton that require extensive energetic, molecular, and cellular resources to repair (Rice et al., 2019). Even small wounds on tissue or skeletal structures can cause growth disturbances with fitness consequences (Rotjan and Lewis, 2008), and repeated corallivory can become a source of chronic stress. In fact, outbreaks of both *Drupella* spp. snails and starfish *A. planci*, for instance, have provoked severe biological disturbance of tropical coral reefs throughout the Indo-Pacific oceans (e.g., see Cumming, 2009; Pratchett et al., 2009; Osborne et al., 2011; De'ath et al., 2012; Bruckner et al., 2017). Intense predation by corallivorous organisms has the potential to decimate hermatypic coral communities, thus modifying the physical structure of reefs (Hoeksema et al., 2013; Liu et al., 2017; Moerland et al., 2019). In addition, coral predators also feed preferentially of specific coral genera (e.g., De'ath and Moran, 1998; Pratchett, 2001; Morton et al., 2002), which may affect the composition of reef coral communities.

In this study, we aimed to investigate the combined effects of ocean warming and predation pressure in small coral fragments (mimicking recently re-attached storm-generated fragments) of seven Scleractinian coral species. We assessed corals' health, bleaching, mortality, and molecular biomarkers, through laboratory experiments. In a recent meta-analysis reviewing the methods of coral heat stress experiments in the past 30 years, although around 47% of the studies included multiple factors in the design, these were essentially abiotic factors (e.g., temperature combined with acidification, light, or nutrients), and only 12% of studies used long-term experiments (≥35 days; McLachlan et al., 2020). Therefore, we will fill the knowledge gap by using a design that combines testing three levels of temperature treatments coupled to two levels of predation pressure for 60 days in small coral fragments. We will identify the most vulnerable species in a post-storm environment under different multi-stressor scenarios, by assessing corals' physiological condition and ability to survive under the combined stressors.

MATERIALS AND METHODS

Experimental Design and Sampling

This study evaluated seven coral species: *Acropora tenuis* and *Psammocora contigua* with branching morphologies, *Montipora capricornis* brown morphotype (BM), *Turbinaria reniformis*, and *Echinopora lamellosa* with plating morphologies, *M. capricornis* green morphotype (GM) with encrusting morphology, and *Galaxea fascicularis* with massive morphology. Colony morphology designations were based on Marshall and Baird (2000) and Loya et al. (2001). The coral colonies used in the present study were obtained from a stock aquarium at Oceanário de Lisboa (Portugal), with known thermal history for the past 5 years (where they were maintained at a constant temperature of 25°C).

All experiments were also performed at Oceanário de Lisboa, Portugal.[1] A total of 60 small coral fragments (replicates) for each of the seven species were cut from each mother colony using a pair of pliers or a pincer. Fragments were about 20–40 mm in height for the branching coral colonies, and approximately 30 mm sided squares for the plating, encrusting, and massive corals. Fragment size aimed to mimic small coral fragments potentially generated during tropical storms. Each fragment was placed on the top of a nylon expansion anchor, glued with epoxy putty and properly labeled, to simulate recently re-attached small coral fragments (post-storm). Fragments from branching corals were placed in a vertical position, whereas fragments of corals from the remaining morphologies were placed in a horizontal position. The positioning of the fragments was performed with the aim of minimizing the dead tissue area that resulted from the epoxy putty application. Fragments (mounted in their respective anchors) were allowed to recover from handling for 1 day in the coral stock aquarium over egg crate panels, prior to being transferred to the experiment system.

To determine long-term responses of different coral species to the effects of increased temperatures combined with predation pressure, the coral fragments were exposed to different treatments in a $7 \times 3 \times 2$ factorial design: (a) seven coral species as previously described; (b) three temperatures, including control (26 ± 0.2°C) and elevated temperatures (30 ± 0.5 and 32 ± 0.5°C, respectively); and (c) two predation treatments including control (undamaged coral fragments) and predated corals (single predation wound in coral tissue/polyps).

The experiment design consisted of doing three sequential treatments of 60 days using different coral fragments. The experiment system used in all treatments included one aquarium (400 L), a sump (280 L) with bioballs to improve water quality through biological filtration, a Hailea 500 chiller, and two Fluval M300 heaters to control for temperature. Additionally, a Litpa Jet5 floodlight with an AquaMedic 400 W HQi lamp (13,000 K) ensured appropriate light conditions and was kept on a 12L:12D cycle. To maintain low nutrient concentrations, an AquaMedic Turboflotor 5,000 Shorty protein skimmer was also used. An AquaMedic OceanRunner 3,500 pump was used for water circulation, providing a turnover rate of 12 min. Additionally, an AquaClear 110 powerhead was used to maintain surface water motion. Air-stones were used to maintain high oxygen concentrations.

Each of the sequential treatments consisted of setting the experimental aquarium to 26°C (first treatment), 30°C (second

[1]www.oceanario.pt

treatment), and 32°C (third treatment) for 60 days. Temperature was increased in each treatment at a 1°C hour^{-1} rate, starting at the temperature of the coral stock aquarium (25°C), allowing for coral fragments to acclimate to the new temperatures for 1, 5, and 7 h, respectively, in each treatment, prior to the experiment start. The selected heating rate mimics temperature changes during spring tides in coral reef-flat communities (Berkelmans and Willis, 1999), where most of the coral species in this study inhabit (Brown and Suharsono, 1990). Within each temperature treatment, $N = 20$ small coral fragments of each species were used. Of these, $N = 10$ fragments species^{-1} were used as predation controls (undamaged), whereas the remaining $N = 10$ fragments species^{-1} were used in the predation groups. In summary, sample sizes included $N = 10$ coral fragments of each species per combination tested (26°C undamaged; 26°C predated; 30°C undamaged; 30°C predated; 32°C undamaged; and 32°C predated); $N_{species} = 60$ coral fragments; and $N_{total} = 420$ coral fragments. Corals in the predation treatments were inflicted with circular injuries (3 mm in diameter) to the tissue, designed to simulate damage caused by predators, specifically butterflyfish, which rip off the coral tissue, but do not affect the calcium carbonate skeleton. Injuries were performed with a cutting disk using a Dremel rotatory tool. To avoid edge effects, one injury was inflicted to each replicate fragment, in their middle section. Undamaged and predated coral fragments from the different species were placed over 40 × 40 cm egg crate panels in the same experimental aquarium for each treatment, to better mimic an emerging biodiverse reef and increase ecological realism, as multiple coral species usually co-exist in the wild (Clements and Hay, 2019, 2021). Nevertheless, to avoid unpredictable agonistic inter-species effects, coral fragments of the same species were grouped together, and species were randomly allocated in pairs of parallel rows positioned 2 cm apart from one another (undamaged fragments in one row vs. predated fragments in a parallel row). Egg crates were suspended 15 cm below the water surface of aquaria.

A spheric quantic sensor (LI-193SA) coupled to a data logger (1,400 model) was used to measure Photosynthetically Active Radiation (PAR) levels, which varied between 320 and 345 µE.m^{-2} s^{-1} (400–700 nm waveband). Water quality parameters including temperature, pH (kept at 8.3), and salinity (kept at 33 psu) were measured once a day. Ammonium (kept at 0 mg L^{-1}), nitrites (kept between 0.002 and 0.005 mg L^{-1}), nitrates (kept between 0 and 2 mg L^{-1}), calcium concentration (kept between 389 and 401 mg L^{-1}), alkalinity (kept at 100 mg L^{-1}), and oxygen concentration (kept between 6.5 and 8.0 mg L^{-1}) and oxygen saturation (kept at 104%) were measured once a week. Cleaning routines were performed at least three times a week to avoid algal growth, and these included cleaning the expansion anchors with a toothbrush and replacing egg crates.

Coral Health Condition Assessments

Health condition of coral fragments was assessed visually according to the following categories: normal, pale, bleached, and dead, as defined by Jokiel and Coles (1974) and Obura (2001). Whereas "normal" corals had healthy tissue and their regular coloration pattern, "pale" corals had visible decreases in their pigmentation, consistent with partial bleaching, but were not white. "Bleached" corals on the other hand had brilliant white or colorless tissue, indicating total loss of endosymbionts, and "dead" corals were devoid of tissue, and only their skeleton remained (i.e., visible corallite structure). Coral health condition was assessed on the last day of the experimental period by the same technician to avoid observer bias. The number of coral fragments fitting into each condition category was counted and transformed into percentage values (%). Afterward, five coral fragments of each species were sampled per treatment combination for biochemical analyses, by removing them from their respective anchor, and placing each fragment inside labeled sterilized tubes on ice-cold conditions. However, there were treatment combinations where no fragments could be sampled at all due to 100% mortality after 60 days of exposure (**Table 1**) (Overall sample sizes for biomarker assessments were as follows: $N = 5$ fragments species^{-1} per combination tested, when available; $N_{species} = 30$ coral fragments for each of the three species that survived at 32°C, $N_{species} = 20$ coral fragments for each of the for four species that died at 32°C; and $N_{total} = 170$ coral fragments). Samples were then stored at −80°C until further analysis.

Biomarkers

Scleractinian coral samples were briefly washed with ultrapure water to clean debris. Samples were then crushed using a mortar and pestle and the mixture of crushed tissue and aragonite were transferred to microtubes and further homogenized in 1 ml of phosphate buffer saline solution (PBS, pH 7.4) on ice. Homogenized samples were centrifuged for 15 min at 10,000 × g at 4°C. Supernatants were stored ultra-frozen at −60°C.

Total proteins were quantified using the Bradford assay (Bradford, 1976). Briefly, sample duplicates were added to microplate wells (96-well polystyrene microplates from Greiner, Austria) to which Bradford reagent (from Bio-Rad, United States) was added and absorbance was read at 595 nm in a microplate reader (Synergy HTX, BioTek, Winooski, VT, United States). Protein concentration was calculated from a calibration curve of 0.0 to 2.0 mg ml^{-1} constructed from bovine serum albumin (BSA) standards.

Stress biomarkers heat shock protein 70 kDa (Hsp70), total ubiquitin (Ub), and total antioxidant capacity (TAC) were then quantified. These biomarkers were selected due to their important roles in cellular stress responses of organisms to environmental challenges and thermal adaptation: (i) Hsp70 is a chaperone that stabilizes degrading proteins (Jolly et al., 2018); (ii) Ub signals irreversibly damaged proteins for degradation in the proteasome (Madeira et al., 2014) and TAC quantifies both enzymatic and non-enzymatic antioxidants, which indicates the ability to counteract oxidative stress-induced damage in cells (Padmini and Geetha, 2009).

Hsp70 and Ub were both quantified through indirect enzyme linked immunosorbent assays (ELISA; see Madeira et al., 2017). Briefly, for each of these biomarkers, duplicates of each sample were pipetted into microplates wells (96-well high-binding microplates from Greiner, Austria) and incubated overnight at 4°C. On the following day, microplates were washed three times with PBS 0.05% Tween-20, blocked with 1% BSA in

TABLE 1 | Summary of coral health condition [normal, pale, bleached, and dead (%)] per individual species and grouped species (thermosensitive vs. thermotolerant) and treatment tested at 60 days (N_{total} = 420 coral fragments).

					Condition (%)			
Species	**Morphology**	**Temperature (°C)**	**Predation**	***N***	**Normal**	**Pale**	**Bleached**	**Dead**
Acropora tenuis	Branching	26	no lesion	10	100.0	-	-	-
			with lesion	10	80.0	-	-	20.0
		30	no lesion	10	100.0	-	-	-
			with lesion	10	100.0	-	-	-
		32	no lesion	10	-	-	-	100.0
			with lesion	10	-	-	-	100.0
Echinopora lamellosa	Plating	26	no lesion	10	100.0	-	-	-
			with lesion	10	100.0	-	-	-
		30	no lesion	10	100.0	-	-	-
			with lesion	10	100.0	-	-	-
		32	no lesion	10	-	-	-	100.0
			with lesion	10	-	-	-	100.0
Montipora capricornis BM	Plating	26	no lesion	10	100.0	-	-	-
			with lesion	10	100.0	-	-	-
		30	no lesion	10	40.0	60.0	-	-
			with lesion	10	10.0	90.0	-	-
		32	no lesion	10	-	-	-	100.0
			with lesion	10	-	-	-	100.0
M. capricornis GM	Encrusting	26	no lesion	10	100.0	-	-	-
			with lesion	10	100.0	-	-	-
		30	no lesion	10	100.0	-	-	-
			with lesion	10	100.0	-	-	-
		32	no lesion	10	-	-	-	100.0
			with lesion	10	-	-	-	100.0
Thermosensitive species	Multiple	26	no lesion	40	100.0	-	-	-
			with lesion	40	95.0	-	-	5.0
		30	no lesion	40	85.0	15.0	-	-
			with lesion	40	78.0	23.0	-	-
		32	no lesion	40	-	-	-	100.0
			with lesion	40	-	-	-	100.0
Galaxea fascicularis	Massive	26	no lesion	10	100.0	-	-	-
			with lesion	10	100.0	-	-	-
		30	no lesion	10	100.0	-	-	-
			with lesion	10	100.0	-	-	-
		32	no lesion	10	40.0	10.0	50.0	-
			with lesion	10	10.0	20.0	70.0	-
Psammocora contigua	Branching	26	no lesion	10	100.0	-	-	-
			with lesion	10	100.0	-	-	-
		30	no lesion	10	37.5	62.5	-	-
			with lesion	10	10.0	90.0	-	-
		32	no lesion	10	-	70.0	-	30.0
			with lesion	10	-	50.0	-	50.0
Turbinaria reniformis	Plating	26	no lesion	10	100.0	-	-	-
			with lesion	10	100.0	-	-	-
		30	no lesion	10	9.1	90.9	-	-
			with lesion	10	-	100.0	-	-
		32	no lesion	10	-	100.0	-	-
			with lesion	10	-	100.0	-	-
Thermotolerant species	Multiple	26	no lesion	40	100.0	-	-	
			with lesion	40	100.0	-	-	
		30	no lesion	40	49.0	51.0	-	
			with lesion	40	37.0	63.0	-	
		32	no lesion	40	13.0	60.0	17.0	10.0
			with lesion	40	3.0	57.0	23.0	17.0

Thermosensitive species include A. tenuis, E. lamellosa, and M. capricornis BM and GM; thermotolerant species include G. fascicularis, P. contigua, and T. reniformis.

PBS, and incubated at 37°C for 90 min. After microplate washing (as described previously), primary monoclonal antibodies anti-Hsp70/Hsc70 (OriGene, Germany) and anti-Ub (Abcam, United Kingdom) were diluted to 1.0 µg ml^{-1} in 1% BSA in PBS and were added to microplates wells, respectively. Microplates were then incubated at 37°C for 90 min, followed by another washing step. The secondary antibody (anti-mouse IgG, fab specific, and alkaline phosphatase conjugate, Sigma-Aldrich, United States) was used in both Hsp70 and Ub protocols—it was diluted to 1.0 µg ml^{-1} in 1% BSA in PBS and added to each microplate well, followed by another incubation step at 37°C for 90 min. Microplates were then washed again and substrate was added (SIGMA FAST p-Nitrophenyl Phosphate Tablets, Sigma-Aldrich, United States), and incubated at room temperature for 30 min. Finally, a stop solution (3 M NaOH) was added to each well to stop the reaction and absorbance was read at 405 nm in a microplate reader (Synergy HTX, BioTek, Winooski, VT, United States). Hsp70 and Ub concentrations were then calculated using calibration curves constructed from serial dilutions of purified Hsp70 active protein (OriGene, Germany) and of purified Ub (UbpBIO, United States) standards, respectively, to give a range of 0.0 to 2.0 mg ml^{-1}.

TAC assay followed procedures developed by Miller et al. (1993) and Kambayashi et al. (2009). Duplicates of each sample were added to microplates wells (96-well polystyrene microplates from Greiner, Austria). Then, 90 µM myoglobin in phosphate buffer 50 mM pH 8.0 was added to each well, followed by 600 µM ABTS [2,2′-Azino-bis (3-ethylbenzthiazoline-6-sulfonic acid)] and 500 µM hydrogen peroxide. Microplates were incubated at room temperature for 5 min and absorbance was read at 410 nm. Trolox (6-hydroxy-2,5,7,8-tetramethylchroman-2-carboxylic acid) standards were used to produce a calibration curve from 0.0 to 0.330 mM, then used for TAC concentration calculations.

Biomarker values were normalized per total proteins in each sample (µg mg^{-1} for Hsp70 and Ub, and mM mg^{-1} for TAC).

Data Analyses

Data matrices were first tested for assumptions of normality and homoscedasticity with Shapiro's Wilk and Levene's test, respectively. When assumptions were rejected, data were log-transformed and auto-scaled (i.e., mean centered and divided by the standard deviation, SD).

Coral health condition datasets for individual species were analyzed as percentages, and a MANOVA was then employed to test for effects of (i) temperature and predation, as well as their interactive effects in overall health condition of all coral species combined; whereas Student's t-tests were used to (ii) test the effects of species thermal sensitivity (thermotolerant vs. thermosensitive) in paleness, bleaching, and mortality, using Statistica v8 (Statsoft, United States).

To explore biomarker data structure, multivariate analyses were employed. Principal component analysis (PCA) was performed based on group separation within each independent categorical variable (species, temperature, and predation), followed by heatmaps constructed based on hierarchical cluster analysis of biomarkers, using Euclidean distance and complete linkage algorithm as metrics. Metaboanalyst v5.0 online software was used to run these analyses (https://www.metaboanalyst.ca/, Chong et al., 2019).

To identify the main effects and interactions of variables (i) species, (ii) temperature, and (iii) predation in biomarkers, multi-factorial MANOVAs and ANOVAs were employed. Given that our design was incomplete due to 100% mortality of four species at 32°C, for which biomarker measurements are missing in that treatment, we performed two separate sets of tests: one for species that survived moderate stress (30°C, all seven species) and another one for species that also survived severe stress (32°C, three species).

Integrated biomarker indices were then calculated for each species and stress conditions, following the methodology described in our previous papers (Madeira et al., 2018; Dias et al., 2020). First, the overall mean (m) and the standard deviation (s) for each biomarker were calculated and standardized (Y) as $Y = (X - m)/s$, where X is the mean value for the biomarker at a given experimental condition. Afterward, Z was calculated using $Z = -Y$ or $Z = Y$, in the case of biomarker inhibitions or stimulations, respectively. The score (S) was calculated by $S = Z + |\mathrm{Min}|$, where $S \geq 0$ and $|\mathrm{Min}|$ is the absolute value for the minimum of all calculated Y for a given biomarker. Star plots were then used to display score results (S) and to calculate the IBR as:

$$IBR = \sum_{i=1}^{n} Ai$$

$$Ai = \frac{Si}{2}\sin\beta\left(Si\cos\beta + S_{i+1} + \sin\beta\right)$$

$$\beta = \tan^{-1}\frac{S_{i+1}\sin\alpha}{Si - S_{i+1}\cos\alpha}$$

where Si and Si + 1 are two consecutive scores (radius coordinates and clockwise direction) of a given star plot; Ai is the area connecting two scores; n is the number of biomarkers used for calculations; and $\alpha = 2\pi/n$. To identify temperature and predation main and interactive effects in Scleractinian corals' IBRs (joining all species), a factorial ANOVA was employed.

RESULTS

Coral health condition results are presented in **Table 1** and **Figure 1**. The most temperature-sensitive species were *A. tenuis*, *E. lamellosa*, and both morphotypes of *M. capricornis* (hereinafter defined as thermosensitive), which displayed 100% mortality after 60 days at 32°C, independently of predation conditions (**Table 1**). The effects of temperature alone were also seen in the remaining species *G. fascicularis*, *P. contigua*, and *T. reniformis*, which were able to withstand the 32°C treatment (hereinafter defined as thermotolerant); however, *P. contigua* displayed 30% mortality and *G. fascicularis* showed 50% bleaching (in undamaged, non-wounded corals), besides increased paleness. Even though all species tolerated 60 days at 30°C, *M. capricornis* BM, *T. reniformis*, and *P. contigua* also displayed increased paleness at this temperature (**Table 1**). Changes in coral condition upon predation at control temperature occurred only in *A.*

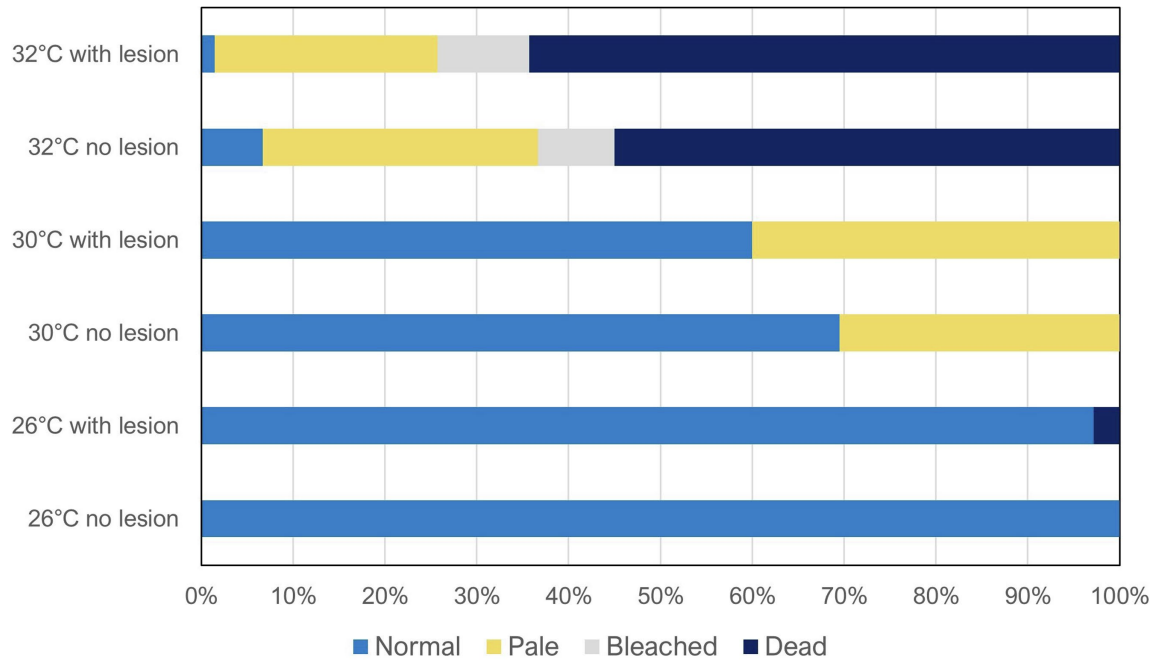

FIGURE 1 | Coral reef health condition (normal, pale, bleached, and dead) after 60 days of exposure to the different treatments (temperatures: 26 vs. 30 vs. 32°C; predation: no lesion vs. with wound lesion). The graph shows average percentage values for all species combined ($N = 60$ fragments per species, $N_{total} = 420$ coral fragments).

tenuis (20% mortality). Additionally, decreases in coral health under the combination of elevated temperature and predation only occurred in four species: (i) *M. capricornis* BM at 30°C—paleness increased from 60% in undamaged fragments to 90% in wounded fragments, (ii) *G. fascicularis* at 32°C—paleness and bleaching increased from 10 to 20% and from 50 to 70%, respectively, in undamaged and wounded fragments, (iii) *P. contigua* at 30 and 32°C—paleness increased from 62.5 to 90% (30°C) and mortality increased from 30 to 50% (32°C) in undamaged vs. wounded fragments, and finally (iv) *T. reniformis* at 30°C—paleness increased from 90.9 to 100% in undamaged vs. wounded fragments (**Table 1**). Moreover, species thermal sensitivity (thermosensitive vs. thermotolerant) was found to have an effect in coral paleness and mortality under the tested multi-stressors (Student's *t*-tests, paleness $t = -3.18$, value of $p = 0.002$, mortality $t = 2.56$, value of $p = 0.014$).

Overall, when analyzing all species combined (**Figure 1**), temperature was found to be the main factor significantly affecting coral health condition (Wilks' test, $F = 18.99$, value of $p < 0.0001$), whereas predation alone was not significant (Wilks' test, $F = 0.23$, value of $p = 0.873$). Despite the also non-significant interaction between temperature and predation in health condition of all species combined (Wilks' test, $F = 0.055$, value of $p = 0.999$), as high inter-species variability was observed, there still seems to be a trend of decreased condition with predation in some individual species, specifically at 30 and 32°C, as previously described (**Table 1**).

PCA results plotting biomarkers by independent factors showed an explained variance of 62.1% for PC1 and 31.3% for PC2, yielding a cumulative value of 93.4% for the first two components. PCA 2D scores plot for different species (**Figure 2**) showed a certain degree of overlap between them; however, there was a distinction between *E. lamellosa* and *P. contigua* clusters from the remaining species. Heatmap results further evidenced these differences, showing that *E. lamellosa* displays higher overall concentrations of TAC, whereas *P. contigua* displays higher overall concentrations of Hsp70 and Ub, when compared to the remaining species. PCA 2D scores plot for predation conditions (**Figure 3**), in turn, showed overlap between specimens with a wound lesion vs. no lesion; however, specimens with wound lesions displayed higher variance in stress responses. The heatmap showed that specimens with no lesion had higher TAC, which decreased under predation. In contrast, Hsp70 and Ub concentrations generally increased in specimens with predation wounds. Finally, PCA 2D scores plot for temperature differences (**Figure 4**) showed that specimens exposed to 26°C were grouped in a small cluster, whereas specimens exposed to both 30 and 32°C were grouped in larger clusters with higher variability in responses. Heatmap results showed that all biomarker concentrations were relatively low at 26°C, but all increased at 30°C (especially TAC and Hsp70), and then at 32°C, two different trends were observed: TAC and Hsp70 concentrations decreased, but Ub concentrations increased further, in comparison with the previous temperature conditions.

Results from multivariate factorial MANOVAs (**Table 2**) showed that all stressors (species, predation, and temperature) and their interactions had a significant effect in the tested biomarkers, both in species that survived moderate thermal stress (30°C, all species), as well as severe thermal stress (32°C, *G. fascicularis*, *P. contigua*, and *T. reniformis*). Univariate factorial ANOVAs (**Table 2**) showed

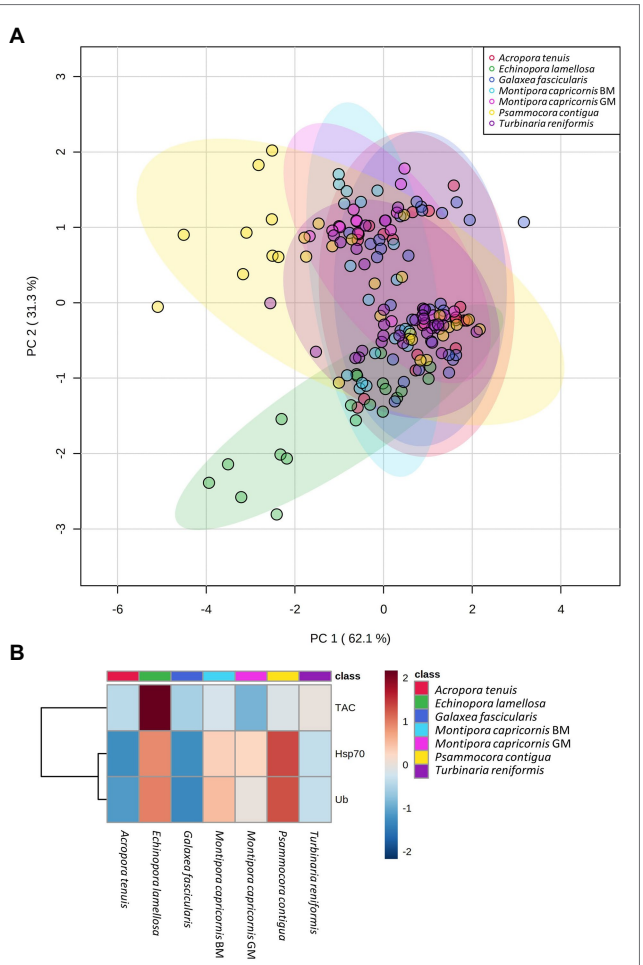

FIGURE 2 | Differences in biomarker profiles of seven Scleractinian coral species tested in this study. **(A)** PCA score plot of biomarker profiles; **(B)** heatmap of clustered biomarkers; in the color scale, red indicates higher than mean concentration, and blue indicates lower than mean concentration. Rows are biomarker concentrations and columns are group averages. Significant differences were found for biomarker profiles between species (**Table 2**).

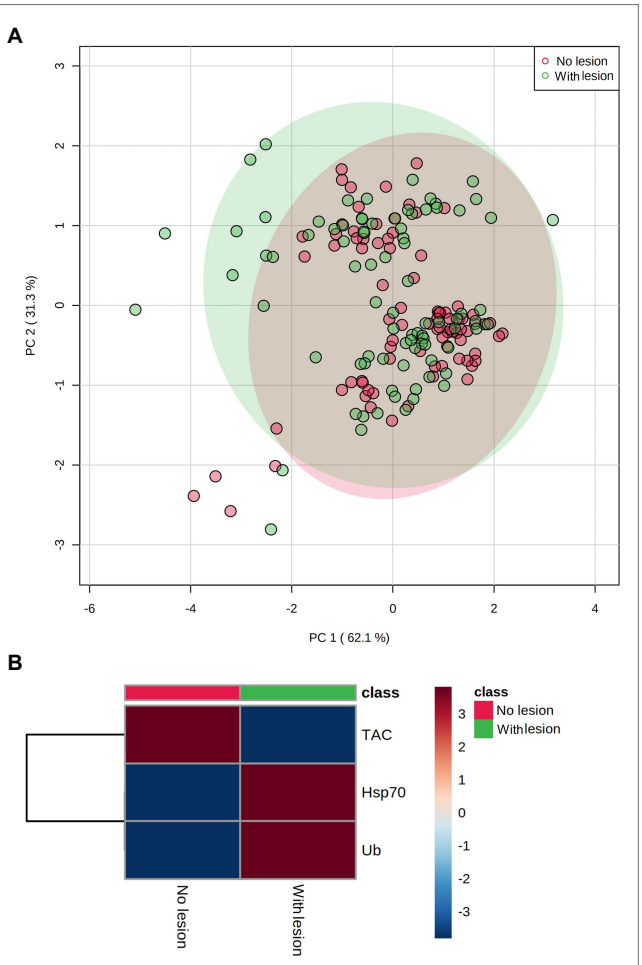

FIGURE 3 | Differences in biomarker profiles of corals with tissue wound lesions from predation vs. no tissue lesions. **(A)** PCA score plot of biomarker profiles; **(B)** heatmap of clustered biomarkers; in the color scale, red indicates higher than mean concentration, and blue indicates lower than mean concentration. Rows are biomarker concentrations and columns are group averages. Significant differences were found for biomarker profiles between predation conditions (**Table 2**).

significant differences for Hsp70 for factor "species" and "temperature" as well as interactions "species × predation" "species × temperature," and "species × predation × temperature" in corals that survived moderate stress (**Table 2A**). Moreover, corals that survived severe stress showed significant differences in Hsp70 concentration for all factors and their combinations tested, except for "predation × temperature" (**Table 2B**). Ub showed identical results to Hsp70, with the exception for "predation × temperature" for species that survived severe stress, which was also significant (**Table 2B**). Results for TAC concentrations in species that survived moderate stress showed that both "predation" and "temperature" alone did not significantly affect this biomarker; however, all factors' interactions showed significant effects (**Table 2A**). For species that survived severe stress, factors "species" and "temperature," as well as interactions "species × predation" and "species × temperature" showed significant effects in TAC concentrations (**Table 2B**). Overall, the results of this table show that all biomarkers were different between species, that predation only affected Hsp70 and Ub and that temperature affected all biomarkers. All factor interactions also affected the tested biomarkers, and the most relevant interaction in the context of this study—"predation × temperature," differentially affected species that survived moderate stress (TAC levels) and species that survived severe stress (Ub levels), respectively (**Table 2**). See also supplemental material for post-hoc Tukey HSD tests for ANOVAs (**Supplementary Tables SM1–SM9**; **Supplementary Figures SM1–SM7**).

IBR results are shown in **Figures 5–7** (and **Supplemental Material**, **Supplementary Figures SM8–SM12**). Overall, changes in IBRs with temperature and predation were highly variable between species. For coral fragments without predation lesions, increases in IBRs with temperature were observed for *A. tenuis*, *M. capricornis* BM, and *G. fascicularis* (from 26 to 30°C, **Figures 5A,C, 6A**) and for *T. reniformis* (from 30 to 32°C, **Figure 6C**), whereas decreases were observed for *M.*

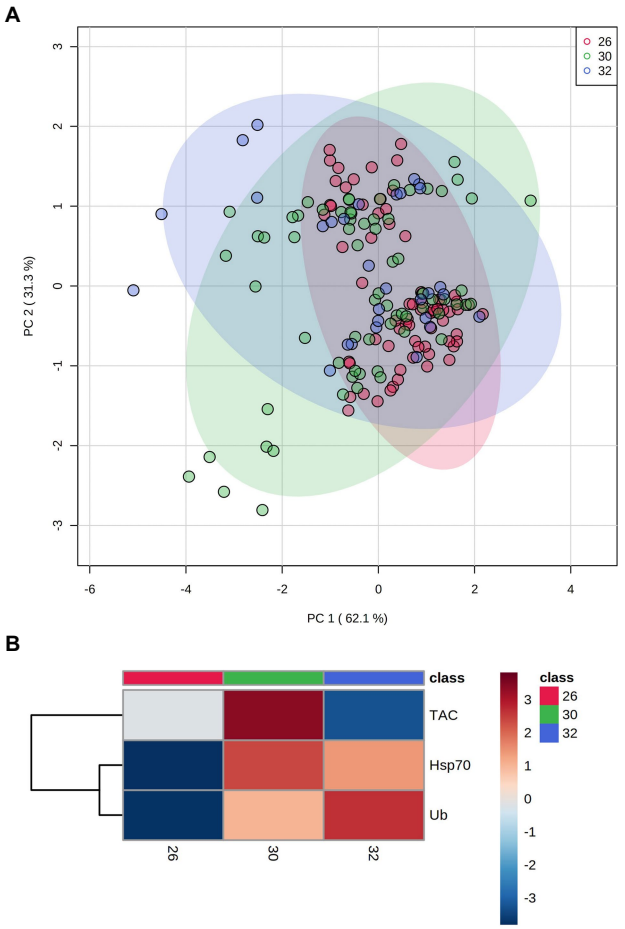

FIGURE 4 | Differences in biomarker profiles of corals exposed to three temperature conditions: 26 vs. 30 vs. 32°C. **(A)** PCA score plot of biomarker profiles; **(B)** heatmap of clustered biomarkers; in the color scale, red indicates higher than mean concentration, and blue indicates lower than mean concentration. Rows are biomarker concentrations and columns are group averages. Significant differences were found for biomarker profiles between temperature conditions (**Table 2**).

capricornis GM from 26 to 30°C (**Figure 5D**), *T. reniformis* from 26 to 30°C (**Figure 6C**), and *G. fascicularis* as well as *P. contigua* from 30 to 32°C (**Figures 6A,B**). For coral fragments with predation lesions, an increase in IBR with temperature was mostly evident for *T. reniformis* (**Figure 6C**, both at 30 and 32°C) and *P. contigua* (at 30°C, **Figure 6B**), whereas decreases were observed for *E. lamellosa* and *M. capricornis* BM (**Figures 5B,C**). Results from the factorial ANOVA testing the effects of both temperature and predation in IBR values for all coral species combined showed, however, no significant differences for any of the factors or interactions assessed (temperature, $F=0.04$, value of $p=0.957$; predation, $F=2.06$, value of $p=0.161$; and temperature × predation, $F=1.641$, value of $p=0.212$). Nevertheless, **Figure 7** shows that for corals exposed to 32°C, there was an increasing trend in IBR when comparing undamaged fragments to fragments with predation lesions. Moreover, for predated coral fragments, mean IBR at 32°C was generally trending higher than at 30 or 26°C.

DISCUSSION

In this study, we investigated how small fragments of hermatypic coral species were affected by ocean warming combined with predation wounds. Specifically, we investigated changes in overall corals' health condition, namely, paleness, bleaching, and mortality, as well as in molecular responses of Hsp70, Ub, and TAC, and assessed whether the combined stressors had additive or synergistic effects in the tested species.

First, our results showed that under favorable temperature conditions (i.e., control treatment), almost 100% of small coral fragments from the different species not only survived but maintained a healthy pigmentation throughout the experiment, even under predation conditions. This finding suggests that storm-generated fragments can contribute to species persistence in the wild, despite their reduced size, if the post-storm abiotic environment is appropriate. Additionally, low intensity predation alone also does not seem to be a determining factor in small coral fragments' health outcomes (except for *A. tenuis* that displayed 20% mortality in predated fragments at control temperature), suggesting that they can resist the pressure of agonistic biotic interactions early after re-attachment. These results contradict earlier hypothesis of coral fragment size-dependent survivorship, which proposes that the percentage of fragments surviving is a power function of fragment size (in cm; see Highsmith et al., 1980). Research from the last decades has also found opposing trends to this hypothesis. For instance, Lewis (1991) did not find size-dependent survival of *Millepora complanata* fragments along fringing reefs in Barbados, West Indies. Forsman et al. (2006) on the other hand found that the occurrence of size-specific mortality in coral nubbins of *Porites lobata* and *P. compressa* from Hawaii depends on the *ex-situ* nursery conditions.

Second, we found that small coral fragments potential contribution to species persistence may be compromised under future ocean warming conditions. Our results overall show that high temperatures decreased small coral fragments' health condition after 60 days of exposure, as corroborated by other studies with coral colonies (e.g., Weis, 2010; Fujise et al., 2014; Zinke et al., 2015). Increased coral paleness was already visible at 30°C for three species in our experiment, suggesting some degree of zooxanthellae loss and/or photosynthetic pigments degradation (Dias et al., 2018), whereas at 32°C, not only paleness increased further, but bleaching reached values as high as 50% in one species and mortality ranged from 30 to 100%, in the remaining species. The previous result shows that the magnitude of temperature effects is species-specific, but impacts can be consistently expected across the Scleractinia order under ocean warming. Previous studies have already shown that coral species (including colonies and fragments) have different susceptibilities to heat stress and tolerance to bleaching (Marshall and Baird, 2000; Weis, 2010; Pandolfi et al., 2011; Dias et al., 2018; Hughes et al., 2018c). For instance, Gates and Edmunds (1999) suggested that massive corals with high metabolic rates that constrain the quick conversion of energy into body mass and thus have low growth rates acclimatize more efficiently. Conversely, branching species that have a low maintenance metabolism and therefore high growth rates as they can allocate

TABLE 2 | Factorial MANOVAs and ANOVAs testing the main and interactive effects of (i) species, (ii) predation, and (iii) temperature in biomarkers Hsp70, Ub, and TAC concentrations: (A) for coral species that survived up to 30°C (all seven species); (B) for coral species that also survived at 32°C (thermotolerant *Galaxea fascicularis*, *Psammocora contigua,* and *Turbinaria reniformis*).

			Species	Predation	Temperature	Species × Predation	Species × Temperature	Predation × Temperature	Species × Predation × Temperature
A	Multivariate	λ	0.217	0.874	0.710	0.615	0.315	0.903	0.543
		F	12.356	5.272	14.957	3.240	8.729	3.926	4.162
		p-value	<0.001*	0.001*	<0.001*	<0.001*	<0.001*	0.010*	<0.001*
	Hsp70	MS	2.702	0.027	6.681	2.593	3.355	0.214	3.408
		F	5.986	0.060	14.801	5.745	7.431	0.473	7.550
		p-value	<0.001*	0.806	<0.001*	<0.001*	<0.001*	0.493	<0.001*
	Ub	MS	2.405	2.816	14.535	1.776	3.763	0.112	1.163
		F	7.093	8.303	42.861	5.238	11.096	0.331	3.430
		p-value	<0.001*	0.005*	<0.001*	<0.001*	<0.001*	0.566	0.004*
	TAC	MS	12.113	0.228	1.040	0.785	5.030	3.190	0.788
		F	41.801	0.787	3.590	2.710	17.360	11.009	2.721
		p-value	<0.001*	0.377	0.061	0.017*	<0.001*	0.001*	0.017*
B	Multivariate	λ	0.473	0.628	0.365	0.640	0.395	0.790	0.630
		F	10.568	13.815	15.280	5.832	6.491	2.907	2.948
		p-value	<0.001*	<0.001*	<0.001*	<0.001*	<0.001*	0.010*	<0.001*
	Hsp70	MS	9.740	4.967	5.197	4.681	2.872	1.272	3.923
		F	19.109	9.746	10.197	9.185	5.634	2.495	7.696
		p-value	<0.001*	0.003*	<0.001*	<0.001*	0.001*	0.090	<0.001*
	Ub	MS	8.626	12.638	15.074	3.170	5.658	1.924	0.922
		F	28.884	42.315	50.472	10.615	18.946	6.441	3.086
		p-value	<0.001*	<0.001*	<0.001*	<0.001*	<0.001*	0.003*	0.021*
	TAC	MS	1.512	0.000	1.919	1.717	1.121	0.874	0.639
		F	4.667	0.001	5.922	5.300	3.459	2.699	1.973
		p-value	0.012*	0.974	0.004*	0.007*	0.012*	0.074	0.108

Significant results (value of p <0.05) are presented with an asterisk (*).

more energy for production are more thermally sensitive (see also Steyermark, 2002 on the relationship between basal metabolism and growth in animals). Hongo and Yamano (2013) also showed that some branching coral colonies, such as *Acropora* spp. from clear-water reefs, cannot tolerate severe thermal stress, whereas massive coral colonies are generally more tolerant. Morikawa and Palumbi (2019) on their turn found that the massive species *Porites cylindrica* had the greatest heat tolerance when compared to acroporid corals *Acropora hyacinthus* (tabular morphology) and *Acropora gemmifera* and the branching *Pocillopora damicornis*. On the other hand, we found that coral fragments of *A. tenuis*, together with *E. lamellosa* and *M. capricornis* brown and green morphotypes (the former with branching and the two latter with plating and encrusting morphologies), were intolerant to 32°C, displaying 100% mortality after 60 days of exposure. In contrast, the massive species in our study *G. fascicularis* and one other plating species *T. reniformis* were the only ones that did not display any mortality at the highest temperature. This last observation suggests a high degree of thermotolerance and ability to sustain prolonged stress, as Marshall and Baird (2000) had also observed for these two genera (*Galaxea* and *Turbinaria*) in the Great Barrier Reef during field surveys in March 1998, after a mass bleaching event. Although coral condition was only assessed at the end of the experiment in the present study, our observations throughout the experiment suggest that small coral fragments that were dead at 60 days had suffered previous bleaching. As Matsuda et al. (2020) proposed, coral bleaching susceptibility can therefore be a good predictor of subsequent mortality within species but not between coral species. Ecologically, this likely means that future community composition of novel coral reefs emerging from storm-induced asexual fragmentation may become dominated by thermotolerant species in ocean areas with faster warming rates (Smith et al., 2013).

Third, our results failed to identify a common and/or generalizable effect of combined temperature and predation in overall Scleractinian species' health condition. This was mainly due to high interspecific variability. However, it is also possible that the use of an experimental design that mixed the seven coral species in the experiment tanks may have helped corals to perform better under the multi-stressors, especially under moderate stress (e.g., 30°C combined with predation). Indeed, multiple coral species co-exist in a biodiverse reef and mixed species assemblages have been shown to enhance growth and tissue survivorship, as stated by Clements and Hay (2019, 2021). Nevertheless, our condition assessments of individual species still suggest that some corals, when experiencing heat stress, may be disproportionately negatively affected by the additional pressure caused by fish predators, such as browsers that feed on coral mucus and tissue, as simulated in our experiment. This assertion seems to hold true for at least four species tested, namely, *M. capricornis* BM and *T. reniformis* at 30°C, *P. contigua* at 30 and 32°C, and *G. fascicularis* at 32°C. Changes in health condition in these cases were mainly reflected by an increase in the percentage of pale fragments (all four species), and to a smaller extent on the percentage of bleached and dead fragments (only observed in *G. fascicularis* and *P. contigua*,

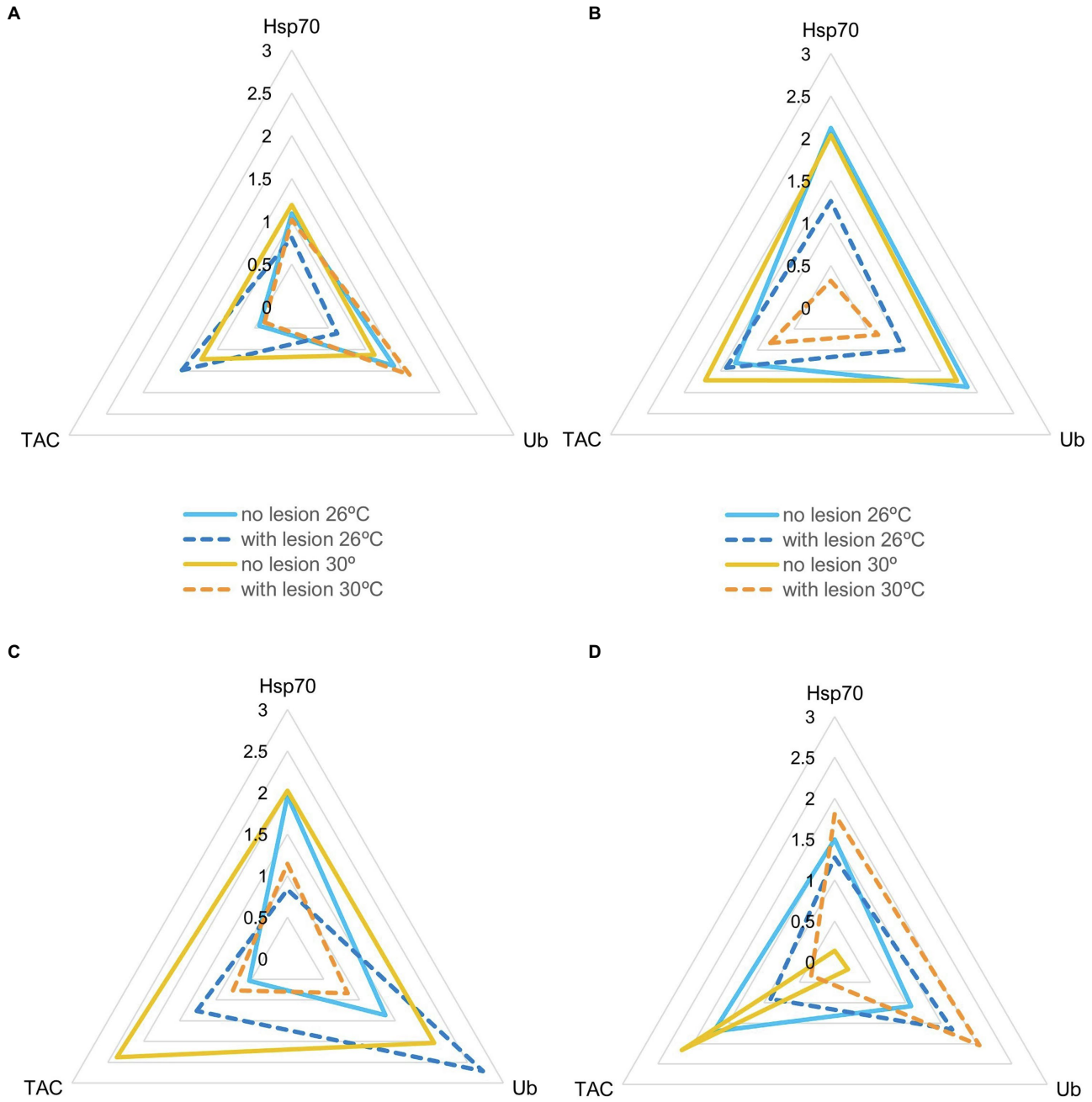

FIGURE 5 | Star plots with mean scores obtained in each experimental condition for thermosensitive coral species that only survived up to 30°C (N_{total} = 20 fragments per species, N = 5 specimens of each species per experimental condition). **(A)** *Acropora tenuis* ($IBR_{26+no\ lesion}$ = 1.29; $IBR_{26+lesion}$ = 1.30; $IBR_{30+no\ lesion}$ = 2.07; $IBR_{30+lesion}$ = 1.28); **(B)** *Echinopora lamellosa* ($IBR_{26+no\ lesion}$ = 4.58; $IBR_{26+lesion}$ = 2.22; $IBR_{30+no\ lesion}$ = 4.97; $IBR_{30+lesion}$ = 0.49); **(C)** *Montipora capricornis* BM ($IBR_{26+no\ lesion}$ = 2.21; $IBR_{26+lesion}$ = 3.37; $IBR_{30+no\ lesion}$ = 6.86; $IBR_{30+lesion}$ = 1.22); and **(D)** *M. capricornis* GM ($IBR_{26+no\ lesion}$ = 3.00; $IBR_{26+lesion}$ = 2.38; $IBR_{30+no\ lesion}$ = 0.35; $IBR_{30+lesion}$ = 2.48).

respectively). Therefore, we suggest that in these cases, an agonistic interaction with predators in a temperature-challenging environment may pose a higher risk of endosymbiont loss. Moreover, these effects seem to occur at different onset temperatures for each species, which suggests a correlation with species heat susceptibility. However, observations of decreases in coral health under elevated temperature and predation are lost once the temperature is too high and induces mass mortality, at least in thermosensitive species. Previous studies have shown relatable findings; for instance, Clements and Hay (2018) showed that coral predators may suppress the resilience of certain coral foundation species especially in stressed or degraded reefs and that selective coral mortality may occur upon high predator densities

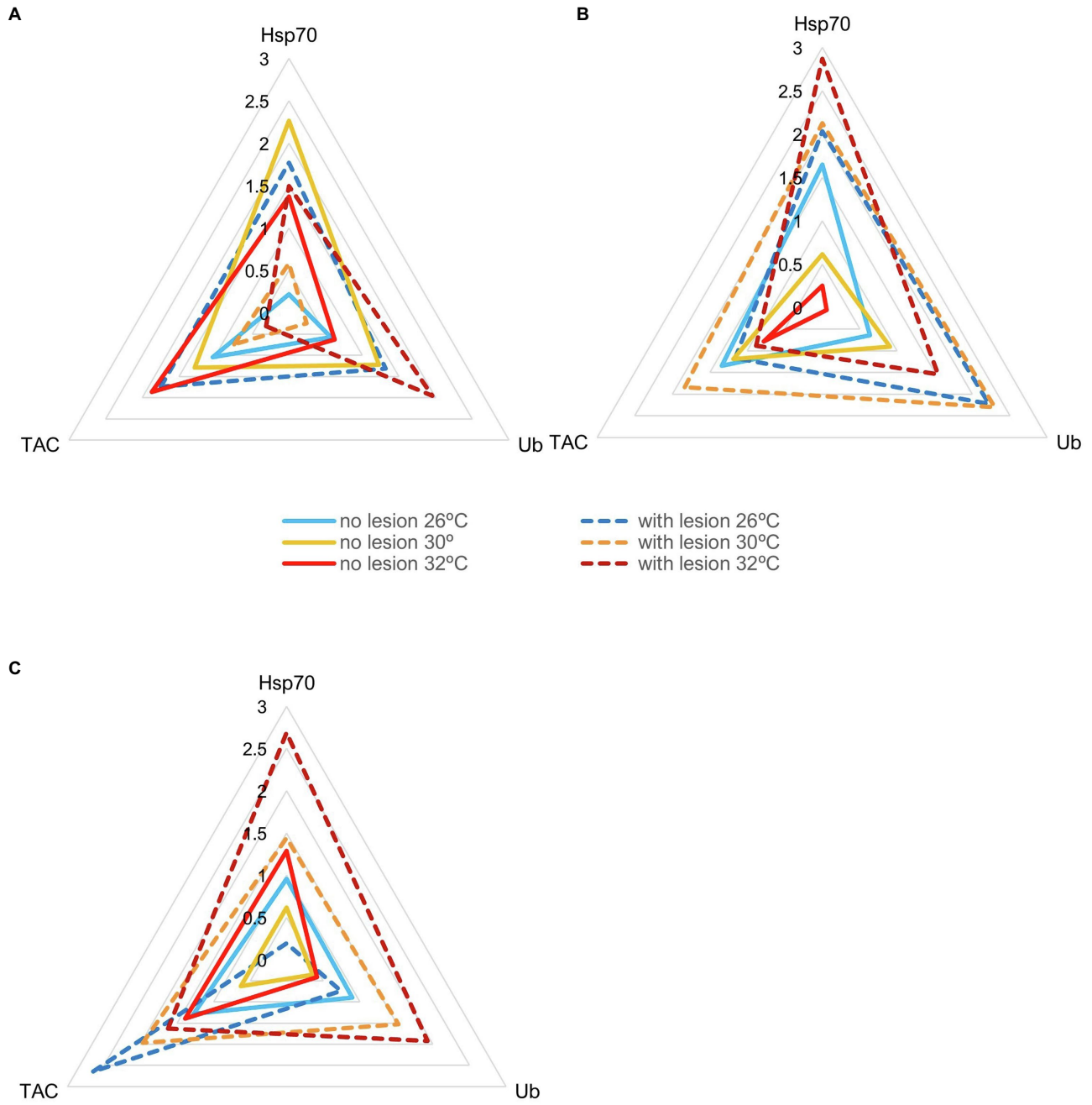

FIGURE 6 | Star plots with mean scores obtained in each experimental condition for thermotolerant coral species that survived up to 32°C (N_{total} = 30 fragments per species, N = 5 specimens of each species per experimental condition). **(A)** *Galaxea fascicularis* ($IBR_{26+no\ lesion}$ = 0.47; $IBR_{26+lesion}$ = 3.85; $IBR_{30+no\ lesion}$ = 3.63; $IBR_{30+lesion}$ = 0.37, $IBR_{32+no\ lesion}$ = 2.28; $IBR_{32+lesion}$ = 1.99); **(B)** *Psammocora contigua* ($IBR_{26+no\ lesion}$ = 2.05; $IBR_{26+lesion}$ = 4.74; $IBR_{30+no\ lesion}$ = 1.17; $IBR_{30+lesion}$ = 6.50, $IBR_{32+no\ lesion}$ = 0.13; $IBR_{32+lesion}$ = 4.16); and **(C)** *Turbinaria reniformis* ($IBR_{26+no\ lesion}$ = 1.60; $IBR_{26+lesion}$ = 1.30; $IBR_{30+no\ lesion}$ = 0.41; $IBR_{30+lesion}$ = 4.03, $IBR_{32+no\ lesion}$ = 1.44; $IBR_{32+lesion}$ = 6.34).

(Pratchett et al., 2009). Although we did not assess coral growth or fitness in this study, previous authors have also reported decreases in both parameters upon corallivory (Rotjan and Lewis, 2008; Rice et al., 2019), as well as negative population growth if the prey population size is small, even in healthy corals (Dulvy et al., 2004). Nevertheless, more experiments are needed to quantify the effects of different types of corallivore animals on reef corals, given that we did not test deeper lesions, such as the ones caused by scrapers (e.g., parrotfishes) or by excavators (e.g., pufferfishes)—in which skeleton layers/pieces are also removed, together with tissue and mucus (Rice et al., 2019). This would likely have

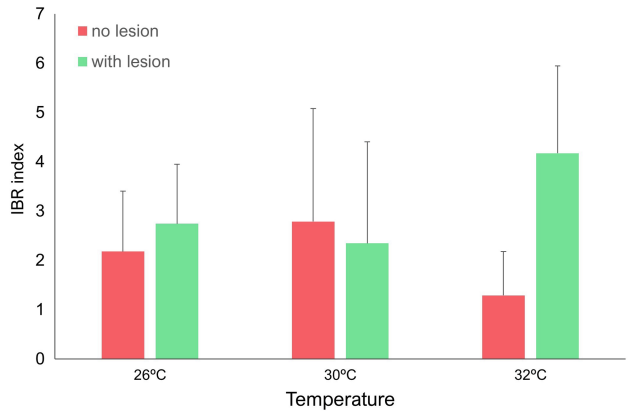

FIGURE 7 | IBR (Integrated Biomarker Response) index (mean + sd of the seven coral species) for all temperatures tested (26, 30, and 32°C) under different predation treatments (no lesion vs. with wound lesion in coral fragments).

caused higher coral mortality levels in the predation treatment groups after 60 days. Also, testing different predator abundances (e.g., testing one wound lesion vs. multiple wound lesions) would also help us understand and predict coral species trajectories upon predator outbreaks.

Fourth, even though molecular processes involved in heat stress and bleaching are similar among hermatypic corals, there are variations in mechanisms that may lead to different outcomes (Carballo-Bolaños et al., 2020). Results from molecular biomarker analyses in this study showed that temperature significantly affected all biomarkers tested, *via* changes in heat shock proteins, protein ubiquitination, and reactive oxygen species scavengers (the latter only in species that survived the 32°C treatment). These results suggest two things: (i) protein folding, metabolism, and turnover are essential acclimatization mechanisms to elevated temperatures in biogenic corals, as also stated by Gates and Edmunds (1999) and (ii) the inability of thermosensitive species to induce antioxidant responses even during moderate stress (30°C) may explain their mass mortality at 32°C, likely due to potential macromolecular damage and accumulation of cytotoxic by-products derived from oxidative stress (e.g., lipid peroxides, see studies by Lesser, 2006; Ayala et al., 2014 and Dias et al., 2019a). Moreover, Hsp70 and Ub were also key biomarkers in responses to tissue damage caused by predation. The involvement of heat shock-related proteins in the immune system of corals has been previously reported (e.g., for *Acropora millepora*, Brown et al., 2013) and is thought to be related to the activation of the pro-phenoloxidase (ProPO) system in invertebrates (Baruah et al., 2010). This system is linked to invertebrate cytokine activity (Mak and Saunders, 2006), and cytokines are known to regulate the wound-healing cascade (Ottaviani et al., 2004). Moreover, the ProPO system is responsible for the production of melanin and several intermediates which are toxic to pathogens and enhance phagocytosis, avoiding infection of wounded tissues (Brown et al., 2013).

Fifth, the combination of temperature and predation differentially affected molecular responses of corals, which may explain why at a higher biological organization level (whole fragment health condition), changes were observed in some species but not in others, and why we got an overall insignificant result for adverse health outcomes. In species that survived moderate thermal stress, the interaction of both factors resulted in a reduction in TAC levels, vs. in species that survived severe thermal stress, in which an increase in Ub levels was observed when temperature and predation were combined. This suggests that different cellular stress mechanisms are involved in responses to multi-stressors depending on species inherent physiologies and stress intensity. A reduction in TAC levels during exposure to the combined stressors could indicate, in thermosensitive species, the exhaustion of molecular defensive systems and could explain an increase in percentage of paleness in predated fragments at 30°C (e.g., as observed in *M. capricornis* BM). This would occur due to an increase in oxidative stress caused by less effective ROS scavenging, which leads to photosynthetic dysfunction of endosymbionts and damage to their cell compartments (Curran and Barnard, 2021). In consequence, coral hosts probably digested and/or expelled damaged *Symbiodinium* (see Fujise et al., 2014) at higher rates, leading to changes in corals' pigmentation levels. Similarly, an increase in total ubiquitin levels in thermotolerant corals during exposure to severe thermal stress and predation combined would be expected given that apoptosis regulatory components (including ubiquitin) function primarily as coordinators of tissue repair and remodeling, to regulate the defense of homeostasis, and only secondarily function as cell death inducers, when everything else fails (see Meier et al., 2015). Nevertheless, tissue regeneration is an energetically expensive process (Henry and Hart, 2005), as multiple wound-healing mechanisms are activated, such as TOLL-like pathways to fight pathogens, melanin synthesis for tissue regeneration, apoptosis of damaged cells, and re-distribution of amoebocytes to the wound site (Meszaros and Bigger, 1999; Kramarsky-Winter and Loya, 2000; DuBuc et al., 2014; Rice et al., 2019). This usually requires the transfer of resources between coral polyps, from healthy tissues to wound sites for healing (Rice et al., 2019). Given that skeleton porosity and polyp connection may vary between species, and available resources are limited in small coral fragments, this may explain why thermotolerant species like *G. fascicularis*, *P. contigua*, and *T. reniformis* still displayed variable increases in percentage of paleness, bleaching, and mortality after 60 days of exposure to temperature and predation. Alternatively, Palmer et al. (2011) also found that *Symbiodinium* density was significantly lower in freshly injured tissues when compared to coral healthy tissue, which could trigger molecular and physiological cascades in corals that are already loosing symbionts and becoming pale or bleached due to thermal stress, such as in our experiment. As Meesters and Rolf (1993) pointed out, bleached corals indeed present reduced tissue regeneration potential, increasing colony vulnerability. This may be a determinant factor in coral survival, as healing rates will differ between species, according to their physiology, thermotolerance, and phenotypes (Traylor-Knowles, 2016).

Sixth, previous studies from our team had also found that the combination of elevated temperature (30 and 32°C) with other stressors (e.g., low salinity) induced molecular changes in Scleractinian corals, indirectly revealing oxidative stress, measured by an increase in antioxidant enzymes' activities, and macromolecular damage, namely, lipid peroxidation (see Dias et al., 2019a,b). Cellular stress responses are fairly conserved among organisms, and similar changes have also been reported for corals exposed to multiple global change stressors in the Mediterranean Sea (Franzellitti et al., 2018), the Red Sea (Seveso et al., 2020), the Maldives (Seveso et al., 2018), the Great Barrier Reef (Hoegh-Guldberg et al., 2007a), the Caribbean (Robbart et al., 2004; Desalvo et al., 2008; Dimos et al., 2019), and altogether, from all tropical latitudes (e.g., see Downs et al., 2000; Edge et al., 2013; Olsen et al., 2013; Seveso et al., 2014; Tisthammer et al., 2021).

Seventh, we found that different coral species employ specific physiological strategies to deal with environmental stress. *E. lamellosa* and *P. contigua* employed a similar molecular strategy: both displayed highly inducible cellular stress responses (CSR) upon stress exposure. However, *P. contigua* had higher overall concentrations of Hsp70 and Ub, when compared to *E. lamellosa*, which had, in contrast, higher overall TAC concentrations. Given that *E. lamellosa* did not tolerate temperatures above 30°C, whereas *P. contigua* did (despite decreased condition in some coral fragments, especially when combined with predation), this suggests that (i) antioxidants *per se* were not enough to prevent mortality induced by extreme oxidative stress and that (ii) molecular chaperones, ubiquitin, and protein regulation may be key to increase survival under unfavorable conditions. These latter biomarkers are, for instance, crucial to prevent the occurrence of cytotoxic protein aggregations in cells (Iwama et al., 1999; Tomanek and Somero, 1999; Sørensen et al., 2003). Notwithstanding, this cannot be raised as a general mechanism, given that it was only observed in these two species. On the other hand, other species, namely, *M. capricornis* (both morphotypes) employed a different molecular strategy, by having high basal/constitutive biomarker expression levels, even in control conditions, which facilitate a faster reaction to mild and moderate stress (e.g., 30°C and/or occasional predation) but were not enough to cope with extreme stress (e.g., 32°C), because their responses were overall less inducible, which is probably explained by energetic trade-offs that exhaust the available defense mechanisms or that prevent an increase in synthesis of protective enzymes and proteins to save energy and molecular resources, as metabolic costs accelerate with high temperatures in ectotherms (Angilletta et al., 2003; Van Der Meer, 2006; Huey and Kingsolver, 2019). This strategy of constitutively expressing a set of protective proteins and enzymes has also been proposed for other corals (*A. hyacinthus*, Barshis et al., 2013) and has been observed in other marine sessile cnidarians, such as sea anemones (Madeira et al., 2019), and invertebrates from environments with low thermal inertia, such as tidal pools (e.g., limpet *Cellana toreuma* Dong and Williams, 2011; *Palaemon longirostris*, *P. elegans*, and *Carcinus maenas*, Madeira et al., 2012). The most stress-tolerant species like *G. fascicularis* and *T. reniformis*, however, showed more oscillation in molecular responses, including bi-phasical responses (i.e., several increases followed by decreases in biomarker levels or *vice-versa*). This suggests that these organisms display considerable molecular flexibility and can quickly acclimatize to changing conditions, which explains their overall tolerance to stress. In future studies, histological analysis of coral samples would be useful to anchor molecular results at higher biological complexity levels and identify tissue changes and pathological processes contributing to thermosensitivity (for a detailed review of histological methods in aquatic organisms, see Costa, 2017; for coral sampling techniques for histological analysis, see Greene et al., 2020).

Eighth, we highlight here that interspecific differences in physiological strategies and molecular responses found in this study are not a product of different recent thermal histories, as this potential source of variability was minimized by using mother coral colonies raised under controlled aquarium temperature in the previous 5 years of the experiment (25°C). This ensured that coral fragments used in this study were not pre-conditioned to neither short- nor long-term thermal stress, which could have caused corals to shift their thermal thresholds and increase tolerance (Brown et al., 2002; Heron et al., 2016; Keshavmurthy et al., 2021).

Lastly, albeit overall IBRs showed non-significant differences under the tested stressors, both separately as well as their interactions, there was a noteworthy trend evidencing that IBR still displayed increasing values for combined effects of high temperature with predation wounds, suggesting higher stress levels. In fact, our previous studies on reef corals indicate that IBRs are generally responsive to increasing temperatures and depend on the coral species (Dias et al., 2020). This is not exclusive of corals, as similar results have been found for other tropical organisms, from fish to crustaceans and gastropods (Madeira et al., 2018). Therefore, the trend found for IBR values under combined stressors is unsurprising. If we transpose these results into a real-word, multi-stressor scenario, in which there are repeated events of thermal stress as well as corallivory, recurrent bleaching, variable wound sizes (in-depth, perimeter, and location), and multiple wounds occurring simultaneously which need longer healing times (Cróquer et al., 2002); then, coral condition and organism ability to respond to multiple interacting stressors may be significantly affected, to the point of becoming compromised (Henry and Hart, 2005). Moreover, coral wounds can be the starting point for disease, especially in thermally stressful environments, during which disease outbreaks increase (Tracy et al., 2019), such as black-band disease or white-band disease (Mayer and Donnelly, 2013; Contardi et al., 2020). Therefore, the combination of these stressors could facilitate the spread of disease vectors (Porter and Tougas, 2001). Altogether, the combination of temperature and predation showed that stressor interaction effects in corals are highly variable among the Scleractinia order, and impacts may be detected only at the molecular level in some species, whereas in a few others, stressors will synergistically interact to decrease coral heath condition. Whether this will ultimately affect reef structure, composition and dynamics remains to be tested.

CONCLUSION

Altogether, we consider the main take-home messages from this study to be: (i) the majority of the tested coral species was already suffering from heat stress at 30°C; (ii) thermosensitive species (*A. tenuis*, *E. lamellosa*, and *M. capricornis* BM and GM) displayed mass mortality at 32°C; (iii) under control temperature conditions, most species tolerated predation quite well, maintaining healthy coloration; (iv) predation, when combined with high temperature, increased the risk of endosymbiont loss and/or pigment degradation, mainly in thermotolerant species (*G. fascicularis*, *P. contigua*, and *T. reniformis*); (v) thermotolerant corals presented different morphologies but similar molecular flexibilities which allowed them to acclimate and increase survival odds under stress; and (vi) despite physiological plasticity of thermotolerant corals during stress exposure, this may not always mean that coral resilience will be re-defined by acclimatization, especially if multi-stressors are at play. We can therefore conclude that delving into the inherent variability underlying organisms' physiology and survival, and "exploring life in context," as pertinently posed by Heard (2022) seems crucial to understand the dimensions of climate change impacts on biodiversity.

DATA AVAILABILITY STATEMENT

The datasets presented in this study can be found in online repositories. The names of the repository/repositories and accession number(s) can be found at: doi: 10.5281/zenodo.5831999.

AUTHOR CONTRIBUTIONS

CV, HC, and MSD designed the study and supervised the work. AF and RG supervised the experiments. MSD supervised the lab work and MD did the experiments. CM did the lab work and the statistical analyses. CM and MD drafted the paper. All authors critically revised the paper, agreed to the author order, approved the final manuscript version, and agreed to be accountable for the work and take responsibility for accuracy and integrity of the research conducted.

FUNDING

Fundação para a Ciência e Tecnologia (FCT, I.P.) funded this study through the project WarmingWebs PTDC/MAR-EST/2141/2012 and strategic projects UIDB/04292/2020 awarded to MARE, UIDB/04326/2020 awarded to CCMAR, and UIDB/04378/2020 and UIDP/04378/2020 awarded to UCIBIO, as well as LA/P/0140/2020 awarded to i4HB. CM was supported by a researcher grant CEECIND/01526/2018, and MD was supported by a PhD grant SFRH/BD/103047/2014, both awarded by FCT. This publication was also funded by the European Union's Horizon 2020 Research and Innovation Programme under grant agreement N810139: Project Portugal Twinning for Innovation and Excellence in Marine Science and Earth Observation—PORTWIMS.

ACKNOWLEDGMENTS

The authors thank P. Napier for help in maintenance of the experimental system and N. Jogee for help with sample homogenization.

SUPPLEMENTARY MATERIAL

The Supplementary Material for this article can be found online at: https://www.frontiersin.org/articles/10.3389/fphys.2022.801672/full#supplementary-material

REFERENCES

Ainsworth, T. D., Heron, S. F., Ortiz, J. C., Mumby, P. J., Grech, A., Ogawa, D., et al. (2016). Climate change disables coral bleaching protection on the great barrier reef. *Science* 352, 338–342. doi: 10.1126/science.aac7125

Angilletta, M. J., Wilson, R. S., Navas, C. A., and James, R. S. (2003). Tradeoffs and the evolution of thermal reaction norms. *Trends Ecol. Evol.* 18, 234–240. doi: 10.1016/S0169-5347(03)00087-9

Ayala, A., Muñoz, M. F., and Argüelles, S. (2014). Lipid peroxidation: production, metabolism and signaling mechanisms of malondialdehyde and 4-hydroxy-2-nonenal. *Oxidative Med. Cell. Longev.* 20, 253–262. doi: 10.1093/europace/eux022

Barshis, D. J., Ladner, J. T., Oliver, T. A., Seneca, F. O., Traylor-Knowles, N., and Palumbi, S. R. (2013). Genomic basis for coral resilience to climate change. *Proc. Natl. Acad. Sci. U. S. A.* 110, 1387–1392. doi: 10.1073/pnas.1210224110

Baruah, K., Ranjan, J., Sorgeloos, P., and Bossier, P. (2010). Efficacy of heterologous and homologous heat shock protein 70s as protective agents to Artemia franciscana challenged with *Vibrio campbellii*. *Fish Shellf. Immunol.* 29, 733–739. doi: 10.1016/j.fsi.2010.07.011

Berkelmans, R., and Willis, B. L. (1999). Seasonal and local spatial patterns in the upper thermal limits of corals on the inshore central great barrier reef. *Coral Reefs* 18, 219–228. doi: 10.1007/s003380050186

Bowden-Kerby, A. (2001). Low-tech coral reef restoration methods modeled after natural fragmentation processes. *Bull. Mar. Sci.* 69, 915–931.

Bradford, M. M. (1976). A rapid and sensitive method for the quantitation of microgram quantities of protein utilizing the principle of protein-dye binding. *Anal. Biochem.* 72, 248–254. doi: 10.1016/0003-2697(76)90527-3

Brown, T., Bourne, D., and Rodriguez-Lanetty, M. (2013). Transcriptional activation of C3 and HSP70 as part of the immune response of *Acropora millepora* to bacterial challenges. *PLoS One* 8:e67246. doi: 10.1371/journal.pone.0067246

Brown, B. E., Downs, C. A., Dunne, R. P., and Gibb, S. W. (2002). Exploring the basis of thermotolerance in the reef coral *Goniastrea aspera*. *Mar. Ecol. Prog. Ser.* 242, 119–129. doi: 10.3354/meps242119

Brown, B. E., and Suharsono, (1990). Damage and recovery of coral reefs affected by El Niño related seawater warming in the Thousand Islands, Indonesia. *Coral Reefs* 8, 163–170. doi: 10.1007/BF00265007

Bruckner, A. W., Coward, G., Bimson, K., and Rattanawongwan, T. (2017). Predation by feeding aggregations of *Drupella* spp. inhibits the recovery of reefs damaged by a mass bleaching event. *Coral Reefs* 36, 1181–1187. doi: 10.1007/s00338-017-1609-2

Carballo-Bolaños, R., Soto, D., and Chen, C. A. (2020). Thermal stress and resilience of corals in a climate-changing world. *J. Mar. Sci. Eng.* 8:15. doi: 10.3390/jmse8010015

Chong, J., Wishart, D. S., and Xia, J. (2019). Using MetaboAnalyst 4.0 for comprehensive and integrative Metabolomics data analysis. *Curr. Protoc. Bioinformatics* 68, e86–e128. doi: 10.1002/cpbi.86

Clements, C. S., and Hay, M. E. (2018). Overlooked coral predators suppress foundation species as reefs degrade. *Ecol. Appl.* 28, 1673–1682. doi: 10.1002/eap.1765

Clements, C. S., and Hay, M. E. (2019). Biodiversity enhances coral growth, tissue survivorship and suppression of macroalgae. *Nat. Ecol. Evol.* 3, 178–182. doi: 10.1038/s41559-018-0752-7

Clements, C. S., and Hay, M. E. (2021). Biodiversity has a positive but saturating effect on imperiled coral reefs. *Sci. Adv.* 7:eabi8592. doi: 10.1126/sciadv.abi8592

Contardi, M., Montano, S., Liguori, G., Heredia-Guerrero, J. A., Galli, P., Athanassiou, A., et al. (2020). Treatment of coral wounds by combining an antiseptic bilayer film and an Injectable antioxidant biopolymer. *Sci. Rep.* 10, 988–910. doi: 10.1038/s41598-020-57980-1

Costa, P. M. (2017). *The Handbook of Histopathological Practices in Aquatic Environments: Guide to Histology for Environmental Toxicology. 1st Edn.* Elsevier: Academic Press, 292.

Cróquer, A., Villamizar, E., and Noriega, N. (2002). Environmental factors affecting tissue regeneration of the reef - building coral *Montastraea annularis* (Faviidae) at Los Roques National Park, Venezuela. *Rev. Biol. Trop.* 50, 1055–1065.

Cumming, R. L. (2009). Population outbreaks and large aggregations of *Drupella* on the great barrier reef. *Rep. Gt. Barrier Reef Mar. Park Authority, Townsville, Aust.* 96, 1–44.

Curran, A., and Barnard, S. (2021). What is the role of zooxanthellae during coral bleaching? Review of zooxanthellae and their response to environmental stress. *S. Afr. J. Sci.* 117:8369. doi: 10.17159/sajs.2021/8369

Cziesielski, M. J., Schmidt-Roach, S., and Aranda, M. (2019). The past, present, and future of coral heat stress studies. *Ecol. Evol.* 9, 10055–10066. doi: 10.1002/ece3.5576

De'ath, G., Fabricius, K. E., Sweatman, H., and Puotinen, M. (2012). The 27-year decline of coral cover on the great barrier reef and its causes. *Proc. Natl. Acad. Sci. U. S. A.* 109, 17995–17999. doi: 10.1073/pnas.1208909109

De'ath, G., and Moran, P. J. (1998). Factors affecting the behaviour of crown-of-thorns starfish (*Acanthaster planci* L.) on the great barrier reef: 2: feeding preferences. *J. Exp. Mar. Biol. Ecol.* 220, 107–126. doi: 10.1016/S0022-0981(97)00100-7

Desalvo, M. K., Voolstra, C. R., Sunagawa, S., Schwarz, J. A., Stillman, J. H., Coffroth, M. A., et al. (2008). Differential gene expression during thermal stress and bleaching in the Caribbean coral *Montastraea faveolata*. *Mol. Ecol.* 17, 3952–3971. doi: 10.1111/j.1365-294X.2008.03879.x

Deser, C., Phillips, A. S., and Alexander, M. A. (2010). Twentieth century tropical sea surface temperature trends revisited. *Geophys. Res. Lett.* 37, 1–6. doi: 10.1029/2010GL043321

Dias, M., Ferreira, A., Gouveia, R., Cereja, R., and Vinagre, C. (2018). Mortality, growth and regeneration following fragmentation of reef-forming corals under thermal stress. *J. Sea Res.* 141, 71–82. doi: 10.1016/j.seares.2018.08.008

Dias, M., Ferreira, A., Gouveia, R., Madeira, C., Jogee, N., Cabral, H., et al. (2019a). Long-term exposure to increasing temperatures on scleractinian coral fragments reveals oxidative stress. *Mar. Environ. Res.* 150:104758. doi: 10.1016/j.marenvres.2019.104758

Dias, M., Madeira, C., Jogee, N., Ferreira, A., Gouveia, R., Cabral, H., et al. (2019b). Oxidative stress on scleractinian coral fragments following exposure to high temperature and low salinity. *Ecol. Indic.* 107:105586. doi: 10.1016/j.ecolind.2019.105586

Dias, M., Madeira, C., Jogee, N., Ferreira, A., Gouveia, R., Cabral, H., et al. (2020). Integrative indices for health assessment in reef corals under thermal stress. *Ecol. Indic.* 113:106230. doi: 10.1016/j.ecolind.2020.106230

Dimos, B. A., Mahmud, S. A., Fuess, L. E., Mydlarz, L. D., and Pellegrino, M. W. (2019). Uncovering a mitochondrial unfolded protein response in corals and its role in adapting to a changing world. *Proc. R. Soc. B Biol. Sci.* 286:20190470. doi: 10.1098/rspb.2019.0470

Done, T. J., DeVantier, L. M., Turak, E., Fisk, D. A., Wakeford, M., and van Woesik, R. (2010). Coral growth on three reefs: development of recovery benchmarks using a space for time approach. *Coral Reefs* 29, 815–833. doi: 10.1007/s00338-010-0637-y

Dong, Y., and Williams, G. A. (2011). Variations in cardiac performance and heat shock protein expression to thermal stress in two differently zoned limpets on a tropical rocky shore. *Mar. Biol.* 158, 1223–1231. doi: 10.1007/s00227-011-1642-6

Downs, C. A., Mueller, E., Phillips, S., Fauth, J. E., and Woodley, C. M. (2000). A molecular biomarker system for assessing the health of coral (*Montastraea faveolata*) during heat stress. *Mar. Biotechnol.* 2, 533–544. doi: 10.1007/s101260000038

DuBuc, T. Q., Traylor-Knowles, N., and Martindale, M. Q. (2014). Initiating a regenerative response; cellular and molecular features of wound healing in the cnidarian *Nematostella vectensis*. *BMC Biol.* 12:24. doi: 10.1186/1741-7007-12-24

Dulvy, N. K., Freckleton, R. P., and Polunin, N. V. C. (2004). Coral reef cascades and the indirect effects of predator removal by exploitation. *Ecol. Lett.* 7, 410–416. doi: 10.1111/j.1461-0248.2004.00593.x

Edge, S. E., Shearer, T. L., Morgan, M. B., and Snell, T. W. (2013). Sub-lethal coral stress: detecting molecular responses of coral populations to environmental conditions over space and time. *Aquat. Toxicol.* 128-129, 135–146. doi: 10.1016/j.aquatox.2012.11.014

Ellison, A. M. (2019). Foundation Species, Non-trophic Interactions, and the Value of Being Common. *iScience* 13, 254–268. doi: 10.1016/j.isci.2019.02.020

Emanuel, K. (2005). Increasing destructiveness of tropical cyclones over the past 30 years. *Nature* 436, 686–688. doi: 10.1038/nature03906

Forsman, Z. H., Rinkevich, B., and Hunter, C. L. (2006). Investigating fragment size for culturing reef-building corals (*Porites lobata* and *P. compressa*) in ex situ nurseries. *Aquaculture* 261, 89–97. doi: 10.1016/j.auaculture.2006.06.040

Foster, N. L., Baums, I. B., Sanchez, J. A., Paris, C. B., Chollett, I., Agudelo, C. L., et al. (2013). Hurricane-driven patterns of clonality in an ecosystem engineer: the Caribbean coral *Montastraea annularis*. *PLoS One* 8:e53283. doi: 10.1371/journal.pone.0053283

Franzellitti, S., Airi, V., Calbucci, D., Caroselli, E., Prada, F., Voolstra, C. R., et al. (2018). Transcriptional response of the heat shock gene hsp70 aligns with differences in stress susceptibility of shallow-water corals from the Mediterranean Sea. *Mar. Environ. Res.* 140, 444–454. doi: 10.1016/j.marenvres.2018.07.006

Frieler, K., Meinshausen, M., Golly, A., Mengel, M., Lebek, K., Donner, S. D., et al. (2013). Limiting global warming to 2°C is unlikely to save most coral reefs. *Nat. Clim. Chang.* 3, 165–170. doi: 10.1038/nclimate1674

Fujise, L., Yamashita, H., Suzuki, G., Sasaki, K., Liao, L. M., and Koike, K. (2014). Moderate thermal stress causes active and immediate expulsion of photosynthetically damaged zooxanthellae (*Symbiodinium*) from corals. *PLoS One* 9:e114321. doi: 10.1371/journal.pone.0114321

Gates, R. D., and Edmunds, P. J. (1999). The physiological mechanisms of acclimatization in tropical reef corals. *Am. Zool.* 39, 30–43. doi: 10.1093/icb/39.1.30

Greene, A., Leggat, W., Donahue, M. J., Raymundo, L. J., and Moriarty, T., …, Ainsworth, T. D. (2020) Complementary sampling methods for coral histology, metabolomics, and microbiome. *Methods Ecol. Evol.* 11, 1012-1020. doi: 10.1111/2041-210X.13431.

Harmelin-Vivien, M. L. (1994). The effects of storms and cyclones on coral reefs: a review. *J. Coast. Res.* 12, 211–231.

Heard, E. (2022). Molecular biologists: let's reconnect with nature. *Nature* 601:9. doi: 10.1038/d41586-021-03818-3

Hédouin, L., Rouzé, H., Berthe, C., Perez-Rosales, G., Martinez, E., Chancerelle, Y., et al. (2020). Contrasting patterns of mortality in Polynesian coral reefs following the third global coral bleaching event in 2016. *Coral Reefs* 39, 939–952. doi: 10.1007/s00338-020-01914-w

Henry, L. A., and Hart, M. (2005). Regeneration from injury and resource allocation in sponges and corals - A review. *Int. Rev. Hydrobiol.* 90, 125–158. doi: 10.1002/iroh.200410759

Heron, S. F., Maynard, J. A., Van Hooidonk, R., and Eakin, C. M. (2016). Warming trends and bleaching stress of the World's coral reefs 1985-2012. *Sci. Rep.* 6, 1–14. doi: 10.1038/srep38402

Highsmith, R. C., Riggs, A. C., and D'Antonio, C. M. (1980). Survival of hurricane-generated coral fragments (*Acropora palmata*) and a disturbance model of reef-calcification/growth rates. *Oecologia* 46, 322–329. doi: 10.1007/BF00346259

Hillyer, K. E., Dias, D. A., Lutz, A., Wilkinson, S. P., Roessner, U., and Davy, S. K. (2017). Metabolite profiling of symbiont and host during thermal stress and bleaching in the coral *Acropora aspera*. *Coral Reefs* 36, 105–118. doi: 10.1007/s00338-016-1508-y

Hoegh-Guldberg, O. (2011). Coral reef ecosystems and anthropogenic climate change. *Reg. Environ. Chang.* 11, 215–227. doi: 10.1007/s10113-010-0189-2

Hoegh-Guldberg, O. (2014). Coral reef sustainability through adaptation: glimmer of hope or persistent mirage? *Curr. Opin. Environ. Sustain.* 7, 127–133. doi: 10.1016/j.cosust.2014.01.005

Hoegh-Guldberg, O., Anthony, K., Berkelmans, R., Dove, S., Fabricus, K., Lough, J., et al. (2007a). "Chapter 10 Vulnerability of reef-Building Corals on the Great Barrier Reef to Climate change," in *Climate Change and the Great Barrier Reef: a Vulnerability Assessment*. eds. J. E. Johnson and P. A. Marshall (Australia: Great Barrier Reef Marine Park Authority and the Australian Greenhouse Office).

Hoegh-Guldberg, O., Mumby, P. J., Hooten, A. J., Steneck, R. S., Greenfield, P., Gomez, E., et al. (2007b). Coral reefs Under rapid climate change and ocean acidification. *Science* 318, 1737–1742. doi: 10.1126/science.1152509

Hoeksema, B. W., Scott, C., and True, J. D. (2013). Dietary shift in corallivorous *Drupella* snails following a major bleaching event at Koh Tao, Gulf of Thailand. *Coral Reefs* 32, 423–428. doi: 10.1007/s00338-012-1005-x

Hongo, C., and Yamano, H. (2013). Species-specific responses of corals to bleaching events on anthropogenically turbid reefs on Okinawa Island, Japan, over a 15-year period (1995-2009). *PLoS One* 8:e60952. doi: 10.1371/journal.pone.0060952

Huey, R., and Kingsolver, J. (2019). Climate warming, resource availability, and the metabolic meltdown of ectotherms. *Am. Nat.* 194, E140–E150. doi: 10.1086/705679

Hughes, T. P., Anderson, K. D., Connolly, S. R., Heron, S. F., Kerry, J. T., Lough, J. M., et al. (2018a). Spatial and temporal patterns of mass bleaching of corals in the Anthropocene. *Science* 359, 80–83. doi: 10.1126/science.aan8048

Hughes, T. P., Kerry, J. T., Álvarez-Noriega, M., Álvarez-Romero, J. G., Anderson, K. D., Baird, A. H., et al. (2017). Global warming and recurrent mass bleaching of corals. *Nature* 543, 373–377. doi: 10.1038/nature21707

Hughes, T. P., Kerry, J. T., Baird, A. H., Connolly, S. R., Dietzel, A., Eakin, C. M., et al. (2018b). Global warming transforms coral reef assemblages. *Nature* 556, 492–496. doi: 10.1038/s41586-018-0041-2

Hughes, T. P., Kerry, J. T., and Simpson, T. (2018c). Large-scale bleaching of corals on the great barrier reef. *Ecology* 99:501. doi: 10.1002/ecy.2092

IPCC (2014). *Climate Change 2014: Synthesis Report. Contribution of Working Groups I, II and III to the Fifth Assessment Report of the Intergovernmental Panel on Climate Change*. eds. Core Writing Team, R. K. Pachauri and L. A. Meyer (Geneva, Switzerland: IPCC), 151.

IPCC (2021). *Climate Change 2021: The physical science basis. Contribution of Working Group I to the Sixth Assessment Report of the Intergovernmental Panel on Climate Change*. eds. V. Masson-Delmotte, P. Zhai, A. Pirani, S. L. Connors, C. Péan, S. Berger et al., (UK: Cambridge University Press) (in press).

Iwama, G. K., Vijayan, M. M., Forsyth, R. O. B. B., and Ackerman, P. A. (1999). Heat shock proteins and physiological stress in fish. *Am. Zool.* 39, 901–909. doi: 10.1093/icb/39.6.901

Jackson, J. B. C. (2008). Ecological extinction and evolution in the brave new ocean. *Proc. Natl. Acad. Sci.* 105, 11458–11465. doi: 10.1073/pnas.0802812105

Jokiel, P., and Coles, S. (1974). Effects of heated effluent on Hermatypic corals at Kahe point, Oahu. *Pac. Sci.* 28, 1–18.

Jolly, E., Liang, S., Yu, X., and Wood, D. (2018). HSP70, HSP90A, and HSP90B are differentially regulated in response to thermal, osmotic and hypoxic stressors. *Ann. Exp. Mol. Biol.* 1:000101.

Kambayashi, Y., Binh, N. T., Asakura, H. W., Hibino, Y., Hitomi, Y., Nakamura, H., et al. (2009). Efficient assay for total antioxidant capacity in human plasma using a 96-well microplte. *J. Clin. Biochem. Nutr.* 44, 46–51. doi: 10.3164/jcbn.08-162

Kayal, M., Vercelloni, J., Lison de Loma, T., Bosserelle, P., Chancerelle, Y., Geoffroy, S., et al. (2012). Predator crown-of-thorns starfish (*Acanthaster planci*) outbreak, mass mortality of corals, and cascading effects on reef fish and benthic communities. *PLoS One* 7:e47363. doi: 10.1371/journal.pone.0047363

Keshavmurthy, S., Beals, M., Hsieh, H. J., Choi, K. S., and Chen, C. A. (2021). Physiological plasticity of corals to temperature stress in marginal coral communities. *Sci. Total Environ.* 758:143628. doi: 10.1016/j.scitotenv.2020.143628

Kramarsky-Winter, E., and Loya, Y. (2000). Tissue regeneration in the coral *Fungia granulosa*: The effect of extrinsic and intrinsic factors. *Mar. Biol.* 137, 867–873. doi: 10.1007/s002270000416

Le Nohaïc, M., Ross, C. L., Cornwall, C. E., Comeau, S., Lowe, R., McCulloch, M. T., et al. (2017). Marine heatwave causes unprecedented regional mass bleaching of thermally resistant corals in northwestern Australia. *Sci. Rep.* 7, 14999–14911. doi: 10.1038/s41598-017-14794-y

Lesser, M. P. (2006). Oxidative stress in marine environments: biochemistry and physiological ecology. *Annu. Rev. Physiol.* 68, 253–278. doi: 10.1146/annurev.physiol.68.040104.110001

Levas, S. J., Grottoli, A. G., Hughes, A., Osburn, C. L., and Matsui, Y. (2013). Physiological and biogeochemical traits of bleaching and recovery in the mounding species of coral *Porites lobata*: implications for resilience in mounding corals. *PLoS One* 8:e63267. doi: 10.1371/journal.pone.0063267

Levitan, D. R., Boudreau, W., Jara, J., and Knowlton, N. (2014). Long-term reduced spawning in Orbicella coral species due to temperature stress. *Mar. Ecol. Prog. Ser.* 515, 1–10. doi: 10.3354/meps11063

Lewis, J. B. (1991). Testing the coral fragment size-dependent survivorship hypothesis for the calcareous hydrozoan *Millepora complanata*. *Mar. Ecol. Prog. Ser.* 70, 101–104. doi: 10.3354/meps070101

Lin, C. Y., Ho, C. R., Zheng, Q., Kuo, N. J., and Chang, P. (2011). Warm pool variability and heat flux change in the global oceans. *Glob. Planet. Chang.* 77, 26–33. doi: 10.1016/j.gloplacha.2011.02.006

Lindahl, U. (2003). Coral reef rehabilitation through transplantation of staghorn corals: effects of artificial stabilization and mechanical damages. *Coral Reefs* 22, 217–223. doi: 10.1007/s00338-003-0305-6

Lirman, D. (2000). Fragmentation in the branching coral *Acropora palmata* (Lamarck): growth, survivorship, and reproduction of colonies and fragments. *J. Exp. Mar. Biol. Ecol.* 251, 41–57. doi: 10.1016/S0022-0981(00)00205-7

Liu, G., Skirving, W. J., Geiger, E. F., De, J. L., Cour, L., Marsh, B. L., et al. (2017). NOAA coral reef Watch's 5km satellite coral bleaching heat stress monitoring product suite version 3 and four-month outlook version 4. *Reef Encount. News. J. Int. Soc. Reef Stud.* 32, 39–45.

Loya, Y., Sakai, K., Yamazato, K., Nakano, Y., Sambali, H., and Van Woesik, R. (2001). Coral bleaching: The winners and the losers. *Ecol. Lett.* 4, 122–131. doi: 10.1046/j.1461-0248.2001.00203.x

Madeira, C., Madeira, D., Diniz, M. S., Cabral, H. N., and Vinagre, C. (2017). Comparing biomarker responses during thermal acclimation: A lethal vs non-lethal approach in a tropical reef clownfish. Comp. *Biochem. Physiol. Part A Mol. Integr. Physiol.* 204, 104–112. doi: 10.1016/j.cbpa.2016.11.018

Madeira, C., Mendonça, V., Leal, M. C., Flores, A. A. V., Cabral, H. N., Diniz, M. S., et al. (2018). Environmental health assessment of warming coastal ecosystems in the tropics – application of integrative physiological indices. *Sci. Total Environ.* 643, 28–39. doi: 10.1016/j.scitotenv.2018.06.152

Madeira, D., Mendonça, V., Madeira, C., Gaiteiro, C., Vinagre, C., and Diniz, M. S. (2019). Molecular assessment of wild populations in the marine realm: importance of taxonomic, seasonal and habitat patterns in environmental monitoring. *Sci. Total Environ.* 654, 250–263. doi: 10.1016/j.scitotenv.2018.11.064

Madeira, D., Narciso, L., Cabral, H. N., Vinagre, C., and Diniz, M. S. (2012). HSP70 production patterns in coastal and estuarine organisms facing increasing temperatures. *J. Sea Res.* 73, 137–147. doi: 10.1016/j.seares.2012.07.003

Madeira, D., Vinagre, C., Costa, P. M., and Diniz, M. S. (2014). Histopathological alterations, physiological limits, and molecular changes of juvenile *Sparus aurata* in response to thermal stress. *Mar. Ecol. Prog. Ser.* 505, 253–266. doi: 10.3354/meps10794

Mak, T. W., and Saunders, M. E. (eds.) (2006). "Chapter 21 - comparative immunology," in *The Immune Response: Basic and Clinical Principles*. (Oxford, UK: Elsevier Academic Press), 611–637.

Marshall, P. A., and Baird, A. H. (2000). Bleaching of corals on the great barrier reef: differential susceptibilities among taxa. *Coral Reefs* 19, 155–163. doi: 10.1007/s003380000086

Matsuda, S. B., Huffmyer, A. S., Lenz, E. A., Davidson, J. M., Hancock, J. R., Przybylowski, A., et al. (2020). Coral bleaching susceptibility is predictive

of subsequent mortality within but not Between coral species. *Front. Ecol. Evol.* 8:178. doi: 10.3389/fevo.2020.00178

Mayer, J., and Donnelly, T. (eds.) (2013). "Infectious diseases of acroporid corals," in *Clinical Veterinary Advisor-Birds and Exotic Pets* (USA: Elsevier), 9–10.

McClanahan, T. R., Darling, E. S., Maina, J. M., Muthiga, N. A., D'Agata, S., Leblond, J., et al. (2020). Highly variable taxa-specific coral bleaching responses to thermal stresses. *Mar. Ecol. Prog. Ser.* 648, 135–151. doi: 10.3354/meps13402

McLachlan, R. H., Price, J. T., Solomon, S. L., and Grottoli, A. G. (2020). Thirty years of coral heat-stress experiments: a review of methods. *Coral Reefs* 39, 885–902. doi: 10.1007/s00338-020-01931-9

Meesters, E. H., and Rolf, P. M. (1993). Effects of coral bleaching on tissue regeneration potential and colony survival. *Mar. Ecol. Prog. Ser.* 96, 189–198. doi: 10.3354/meps096189

Meier, P., Morris, O., and Broemer, M. (2015). Ubiquitin-mediated regulation of cell death, inflammation, and defense of homeostasis. *Curr. Top. Dev. Biol.* 114, 209–239. doi: 10.1016/bs.ctdb.2015.07.015

Meszaros, A., and Bigger, C. (1999). Qualitative and quantitative study of wound healing processes in the coelenterata, *Plexaurella fusifera*; spatial, temporal and environmental influences. *J. Invertebr. Pathol.* 73, 321–331. doi: 10.1006/jipa.1999.4851

Miller, N. J., Rice-Evans, C., Davies, M. J., Gopinathan, V., and Milner, A. (1993). A novel method for measuring antioxidant capacity and its application to monitoring the antioxidant status in premature neonates. *Clin. Sci.* 84, 407–412. doi: 10.1042/cs0840407

Moerland, M. S., Scott, C. M., and Hoeksema, B. W. (2019). Prey selection of corallivorous muricids at Koh Tao (Gulf of Thailand) four years after a major coral bleaching event. *Contrib. Zool.* 85, 291–309. doi: 10.1163/18759866-08503003

Morikawa, M. K., and Palumbi, S. R. (2019). Using naturally occurring climate resilient corals to construct bleaching-resistant nurseries. *Proc. Natl. Acad. Sci. U. S. A.* 116, 10586–10591. doi: 10.1073/pnas.1721415116

Morton, B., Blackmore, G., and Kwok, C. T. (2002). Corallivory and prey choice by *Drupella* rugosa (Gastropoda: Muricidae) in Hong Kong. *J. Molluscan Stud.* 68, 217–223. doi: 10.1093/mollus/68.3.217

Mumby, P. J., and Van Woesik, R. (2014). Consequences of ecological, evolutionary and biogeochemical uncertainty for coral reef responses to climatic stress. *Curr. Biol.* 24, R413–R423. doi: 10.1016/j.cub.2014.04.029

Negri, A. P., Marshall, P. A., and Heyward, A. J. (2007). Differing effects of thermal stress on coral fertilization and early embryogenesis in four Indo Pacific species. *Coral Reefs* 26, 759–763. doi: 10.1007/s00338-007-0258-2

Nesa, B., and Hidaka, M. (2009). High zooxanthella density shortens the survival time of coral cell aggregates under thermal stress. *J. Exp. Mar. Biol. Ecol.* 368, 81–87. doi: 10.1016/j.jembe.2008.10.018

Nozawa, Y., and Harrison, P. L. (2007). Effects of elevated temperature on larval settlement and post-settlement survival in scleractinian corals, *Acropora solitaryensis* and *Favites chinensis*. *Mar. Biol.* 152, 1181–1185. doi: 10.1007/s00227-007-0765-2

Obura, D. (2001). Can differential bleaching and mortality among coral species offer useful indicators for assessment and management of reefs under stress? *Bull. Mar. Sci.* 69, 421–442.

Olsen, K., Ritson-Williams, R., Ochrietor, J. D., Paul, V. J., and Ross, C. (2013). Detecting hyperthermal stress in larvae of the hermatypic coral *Porites astreoides*: The suitability of using biomarkers of oxidative stress versus heat-shock protein transcriptional expression. *Mar. Biol.* 160, 2609–2618. doi: 10.1007/s00227-013-2255-z

Osborne, K., Dolman, A. M., Burgess, S. C., and Johns, K. A. (2011). Disturbance and the dynamics of coral cover on the great barrier reef (1995-2009). *PLoS One* 6:e17516. doi: 10.1371/journal.pone.0017516

Ottaviani, E., Malagoli, D., and Franchini, A. (2004). Invertebrate humoral factors: cytokines as mediators of cell survival. *Prog. Mol. Subcell. Biol.* 34, 1–25. doi: 10.1007/978-3-642-18670-7_1

Padmini, E., and Geetha, B. V. (2009). Modulation of ASK1 expression during overexpression of Trx and HSP70 in stressed fish liver mitochondria. *Cell Stress Chaperones* 14, 459–467. doi: 10.1007/s12192-009-0099-8

Palmer, C. V., Traylor-Knowles, N. G., Willis, B. L., and Bythell, J. C. (2011). Corals use similar immune cells and wound-healing processes as those of higher organisms. *PLoS One* 6:e23992. doi: 10.1371/journal.pone.0023992

Pandolfi, J. M., Connolly, S. R., Marshall, D. J., and Cohen, A. L. (2011). Projecting coral reef futures under global warming and ocean acidification. *Science* 333, 418–422. doi: 10.1126/science.1204794

Parkinson, J. E., Davies, S. W., Matz, M. V., Baker, A. C., Baums, I. B., Kitchen, S. A., et al. (2019). Molecular tools for coral reef restoration: Beyond biomarker discovery. *Conserv. Lett.* 13, 1–12. doi: 10.1111/conl.12687

Porter, J. W., and Tougas, J. I. (2001). Reef ecosystems: threats to their biodiversity. *Encycl. Biodivers.* 5, 73–95. doi: 10.1016/b0-12-226865-2/00229-7

Power, S., Delage, F., Chung, C., Kociuba, G., and Keay, K. (2013). Robust twenty-first-century projections of El Niño and related precipitation variability. *Nature* 502, 541–545. doi: 10.1038/nature12580

Pratchett, M. S. (2001). Influence of coral symbionts on feeding preferences of crown-of-thorns starfish *Acanthaster planci* in the Western Pacific. *Mar. Ecol. Prog. Ser.* 214, 111–119. doi: 10.3354/meps214111

Pratchett, M. S., Schenk, T. J., Baine, M., Syms, C., and Baird, A. H. (2009). Selective coral mortality associated with outbreaks of *Acanthaster planci* L. in Bootless Bay, Papua New Guinea. *Mar. Environ. Res.* 67, 230–236. doi: 10.1016/j.marenvres.2009.03.001

Randall, C. J., and Szmant, A. M. (2009). Elevated temperature reduces survivorship and settlement of the larvae of the *Caribbean scleractinian* coral, *Favia fragum* (Esper). *Coral Reefs* 28, 537–545. doi: 10.1007/s00338-009-0482-z

Rice, M. M., Ezzat, L., and Burkepile, D. E. (2019). Corallivory in the anthropocene: interactive effects of anthropogenic stressors and corallivory on coral reefs. *Front. Mar. Sci.* 5:525. doi: 10.3389/fmars.2018.00525

Richmond, R. H. (1993). Coral reefs: present problems and future concerns resulting from anthropogenic disturbance. *Am. Zool.* 33, 524–536. doi: 10.1093/icb/33.6.524

Robbart, M. L., Peckol, P., Scordilis, S. P., Curran, H. A., and Brown-Saracino, J. (2004). Population recovery and differential heat shock protein expression for the corals *Agaricia agaricites* and *A. tenuifolia* in Belize. *Mar. Ecol. Prog. Ser.* 283, 151–160. doi: 10.3354/meps283151

Roth, L., Muller, E. M., and Van Woesik, R. (2013). Tracking *Acropora* fragmentation and population structure through thermal-stress events. *Ecol. Model.* 263, 223–232. doi: 10.1016/j.ecolmodel.2013.05.002

Rotjan, R. D., and Lewis, S. M. (2008). Impact of coral predators on tropical reefs. *Mar. Ecol. Prog. Ser.* 367, 73–91. doi: 10.3354/meps07531

Salih, A., Hoegh-Guldberg, O., and Cox, G. (1998). Photoprotection of symbiotic dinoflagellates by fluorescent pigments in reef corals. Proc. Aust. Coral Reef Soc. 75th Anniv. Conf. Heron Isl. Oct. 1997, 217–230. Available at: https://citeseerx.ist.psu.edu/viewdoc/download?doi=10.1.1.474.4650&rep=rep1&type=pdf (Accessed October 20, 2021).

Seveso, D., Arrigoni, R., Montano, S., Maggioni, D., Orlandi, I., Berumen, M. L., et al. (2020). Investigating the heat shock protein response involved in coral bleaching across scleractinian species in the Central Red Sea. *Coral Reefs* 39, 85–98. doi: 10.1007/s00338-019-01878-6

Seveso, D., Montano, S., Maggioni, D., Pedretti, F., Orlandi, I., Galli, P., et al. (2018). Diel modulation of Hsp70 and Hsp60 in corals living in a shallow reef. *Coral Reefs* 37, 801–806. doi: 10.1007/s00338-018-1703-0

Seveso, D., Montano, S., Strona, G., Orlandi, I., Galli, P., and Vai, M. (2014). The susceptibility of corals to thermal stress by analyzing Hsp60 expression. *Mar. Environ. Res.* 99, 69–75. doi: 10.1016/j.marenvres.2014.06.008

Smith, T. B., Brandt, M. E., Calnan, J. M., Nemeth, R. S., Blondeau, J., Kadison, E., et al. (2013). Convergent mortality responses of Caribbean coral species to seawater warming. *Ecosphere* 4, art87–art40. doi: 10.1890/ES13-00107.1

Sørensen, J. G., Kristensen, T. N., and Loeschcke, V. (2003). The evolutionary and ecological role of heat shock proteins. *Ecol. Lett.* 6, 1025–1037. doi: 10.1046/j.1461-0248.2003.00528.x

Steyermark, A. C. (2002). A high standard metabolic rate contrains juvenile growth. *Zoology* 105, 147–151. doi: 10.1078/0944-2006-00055

Stuart-Smith, R. D., Brown, C. J., Ceccarelli, D. M., and Edgar, G. J. (2018). Ecosystem restructuring along the great barrier reef following mass coral bleaching. *Nature* 560, 92–96. doi: 10.1038/s41586-018-0359-9

Sully, S., Burkepile, D. E., Donovan, M. K., Hodgson, G., and van Woesik, R. (2019). A global analysis of coral bleaching over the past two decades. *Nat. Commun.* 10, 1264–1265. doi: 10.1038/s41467-019-09238-2

Tisthammer, K. H., Timmins-Schiffman, E., Seneca, F. O., Nunn, B. L., and Richmond, R. H. (2021). Physiological and molecular responses of lobe coral indicate nearshore adaptations to anthropogenic stressors. *Sci. Rep.* 11, 3423–3411. doi: 10.1038/s41598-021-82569-7

Tomanek, L., and Somero, G. N. (1999). Evolutionary and acclimation-induced variation in the heat-shock responses of congeneric marine snails (genus *Tegula*) from different thermal habitats: implications for limits of thermotolerance and biogeography. *J. Exp. Biol.* 202, 2925–2936. doi: 10.1016/S1095-6433(99)90421-X

Tracy, A. M., Pielmeier, M. L., Yoshioka, R. M., Heron, S. F., and Harvell, C. D. (2019). Increases and decreases in marine disease reports in an era of global change. *Proc. R. Soc. B* 2:E120. doi: 10.1371/journal.pbio.0020120

Traylor-Knowles, N. (2016). Distinctive wound-healing characteristics in the corals *Pocillopora damicornis* and *Acropora hyacinthus* found in two different temperature regimes. *Mar. Biol.* 163, 231–236. doi: 10.1007/s00227-016-3011-y

Van Der Meer, J. (2006). Metabolic theories in ecology. *Trends Ecol. Evol.* 21, 136–140. doi: 10.1016/j.tree.2005.11.004

Vargas-Ángel, B., Huntington, B., Brainard, R. E., Venegas, R., Oliver, T., Barkley, H., et al. (2019). El Niño-associated catastrophic coral mortality at Jarvis Island, central equatorial Pacific. *Coral Reefs* 38, 731–741. doi: 10.1007/s00338-019-01838-0

Weis, V. M. (2010). The susceptibility and resilience of corals to thermal stress: adaptation, acclimatization or both?: NEWS and VIEWS. *Mol. Ecol.* 19, 1515–1517. doi: 10.1111/j.1365-294X.2010.04575.x

Williams, S. D., and Patterson, M. R. (2020). Resistance and robustness of the global coral–symbiont network. *Ecology* 101, e02990–e02913. doi: 10.1002/ecy.2990

Wooldridge, S. A. (2009). A new conceptual model for the enhanced release of mucus in symbiotic reef corals during "bleaching" conditions. *Mar. Ecol. Prog. Ser.* 396, 145–152. doi: 10.3354/meps08310

Zinke, J., Hoell, A., Lough, J. M., Feng, M., Kuret, A. J., Clarke, H., et al. (2015). Coral record of Southeast Indian Ocean marine heatwaves with intensified Western Pacific temperature gradient. *Nat. Commun.* 6:8562. doi: 10.1038/ncomms9562

Conflict of Interest: The authors declare that the research was conducted in the absence of any commercial or financial relationships that could be construed as a potential conflict of interest.

Publisher's Note: All claims expressed in this article are solely those of the authors and do not necessarily represent those of their affiliated organizations, or those of the publisher, the editors and the reviewers. Any product that may be evaluated in this article, or claim that may be made by its manufacturer, is not guaranteed or endorsed by the publisher.

frontiers in Marine Science

ORIGINAL RESEARCH
published: 04 March 2022
doi: 10.3389/fmars.2022.748308

An Acute Permethrin Exposure Causes Significant Microbial Shifts in *Montastraea cavernosa*

*Nicholas J. MacKnight[1,2], Lindsay Arick[1], Amelia C. Crawford[1], Michael Henry[1], Richard Pierce[1] and Erinn M. Muller[1]**

[1] Mote Marine Laboratory, Sarasota, FL, United States, [2] The University of Texas at Arlington, Arlington, TX, United States

Insecticide use is common in developed tropical regions where it may enter coastal reef ecosystems through land-based sources. This local introduction of contaminants could affect ecosystem health as corals can better withstand global stressors more readily if local pressures are reduced. The present study investigated the microbial community and photochemical efficiency of the reef building coral, *Montastraea cavernosa*, when exposed to the commercially applied insecticide, permethrin. *Montastraea cavernosa* was exposed to an acute concentration of permethrin for 24 h in a controlled laboratory setting. Fourteen fragments were integrated across four treatments (2 or 0.325 μg/l of permethrin, acetone control, and saltwater control) with three to four replicates per treatment. Photosynthetic efficiency was measured by quantifying the maximum photochemical yield and maximum electron transport rate (ETR), which were recorded for each fragment before exposure and 24 h after exposure to permethrin. The microbial communities of *M. cavernosa* tissue was measured using 16S rRNA sequencing for each fragment. Permethrin exposure at the tested concentrations suggested no significant effect on the *M. cavernosa*'s photochemical parameters measured during the 24-h permethrin exposure. Microbial communities were significantly different between permethrin treated (2 and 0.325 μg/l) and non-treated conditions (acetone and saltwater controls). In permethrin treated coral, this study documented a significant increase in *Burkholderia pyroccinnia* and *Bacillus* sp., bacteria groups known to bioremediate insecticides. Exposure of permethrin also decreased the relative abundance of *Mesorhizobium* sp., *Sediminibacterium* sp., *Sphingorhabdus* sp., and *Chondromyces* sp., which are known to inhibit pathogen colonization and provide essential macromolecules. Therefore, although the symbiotic relationship between the host and the intracellular algae remained intact after the corals were exposed to permethrin, the significant shift in the microbiome indicate permethrin may destabilize the microbial composition of the holobiont.

Keywords: permethrin, *Montastraea cavernosa*, PAM, microbiome, coral, dysbiosis, bioremediation, microbial shift

OPEN ACCESS

Edited by:
Ranjeet Bhagooli,
University of Mauritius, Mauritius

Reviewed by:
Josef Velišek,
University of South Bohemia, Czechia
Neviaty Zamani,
Bogor Agricultural University, Indonesia

***Correspondence:**
Erinn M. Muller
emuller@mote.org

Specialty section:
This article was submitted to Aquatic Physiology, a section of the journal Frontiers in Marine Science

Received: *27 July 2021*
Accepted: *28 January 2022*
Published: *04 March 2022*

Citation:
MacKnight NJ, Arick L, Crawford AC, Henry M, Pierce R and Muller EM (2022) An Acute Permethrin Exposure Causes Significant Microbial Shifts in Montastraea cavernosa. Front. Mar. Sci. 9:748308. doi: 10.3389/fmars.2022.748308

INTRODUCTION

Corals are frequently threatened by both global and local stressors that are causing significant mortality worldwide (Bruno et al., 2007; Eakin et al., 2010; Kennedy et al., 2013). Considerable research has focused on global issues such as high water temperatures from climate change, ocean acidification, and disease (Hoegh-Guldberg et al., 2007; Hughes et al., 2016). However, it is imperative to investigate other existing anthropogenic and natural influences affecting reefs on the local scale, especially because those threats could be alleviated through local management action. Previous research suggest that corals may be able to withstand some global pressures more readily if local threats are reduced (Carilli et al., 2009; Kennedy et al., 2013; Donovan et al., 2021). One potential local threat that has had little attention includes the applications of pesticides within nearshore environments. Permethrin [(3-phenoxyphenyl)methyl(+)*cis*,*trans*-3-(2,2-dichloroethenyl)-2,2-dimethylcyclopropane-carboxylate] is a mix of synthetically produced *cis* and *trans* isomer pyrethroids, which functions to paralyze the nervous system of insects (Pierce, 1998). Often, permethrin is sprayed from a mounted sprayer attached to the back of a moving vehicle, typically applied in the summer rainy season (May–October) to target when adult mosquitos hatch after a rainfall (Monroe County Mosquito Control) (Ross et al., 2015). Permethrin has been detected in surface water canal systems throughout the Florida Keys (5.1–9.4 μg/l) and within the Florida Keys National Marine Sanctuary ranging from 0.5 to 50.1 $\mu g/m^2$ due to aerial drift and runoff (Pierce, 2005). Permethrin is highly toxic to aquatic invertebrates, with reported 96-h LC-50 to be 0.02 μg/l for mysid shrimp, 0.2 μg/l for penaeid shrimp, and 2.2 μg/l for silverside minnows (Clark et al., 1989; Tietze et al., 1995). Permethrin typically has a half-life of 14 days in water and sediment (Lee et al., 2004).

Very few investigations have studied the effects of insecticides on corals. However, one study showed that the mosquito pesticide naled, which is typically sprayed intermittently with permethrin, has a negative effect to larval settlement in *Porites astreoides* by reducing survivorship (Ross et al., 2015). Permethrin, however, did not affect larval settlement success under ambient conditions nor was there a negative response when corals were exposed to permethrin in concert with increased water temperatures. Low concentrations of permethrin (0.3–1.0 μg/l), however, showed reduced settlement and metamorphosis on the larvae of *Acropora millepora* (Markey et al., 2007), suggesting species and life-stage specific responses. *Acropora cervicornis* corals also showed specific transcription of stress-associated genes after being exposed to low doses of permethrin (Morgan et al., 2001). To date, studies have focused on the effects of insecticides on the coral host and its associated algal symbiont although a suite of microbes exist to create the coral holobiont (Morgan et al., 2001; Ritchie, 2006). The effects of the widely commercialized insecticides on the microbiome of corals are generally unknown.

A healthy coral microbiome can exhibit antibiotic properties to defend the coral from invasive bacteria (Ritchie, 2006). However, as the health of reef ecosystems have shifted from fully functioning to disturbed, microbial shifts within corals often occur with these environmental stressors that result in the introduction of opportunistic bacteria (Sunagawa et al., 2009). Known stressors that elicit a bacterial shift include high water temperatures, excessive nutrients, coastal development, and overfishing, which all influence coral health (Bruno et al., 2003, 2007; Brandt and Mcmanus, 2009) as well as others. The present study aimed to further investigate the effects of anthropogenic effects on corals by characterizing the microbial community within corals as well as a suite of photochemical efficiency parameters after exposure to two different concentrations of permethrin within a controlled setting. We hypothesized that exposure to permethrin would reduce photochemical efficiency within the coral holobiont, which would suggest a disruption in the coral-algal symbiosis. Additionally, we hypothesized that permethrin exposure would result in a dysbiosis of the microbial community through identifiable shifts in bacterial members. Quantifying the response of the holobiont physiology and the microbiome community characterized the effects of this short-term contaminant exposure on a major reef building coral of Florida's Coral Reef.

MATERIALS AND METHODS

Coral Collection

Montastraea cavernosa, the great star coral, was originally collected from the National Oceanic and Atmospheric Administration (NOAA) Rescue Nursery located off of Key West, Florida using permit FKNMS-2015-082 and transferred to Mote Marine Laboratory's research facility in Sarasota, Florida. Ten parent colonies of *M. cavernosa* were cut into fourteen 1.5″ × 1.5″ fragments and allowed to recover for 14 days within a flow-through raceway prior to random fragment assignment in the subsequent exposure experiment. The raceway was equipped with a scheduled 12-h activated T5 light (Wave Point). The temperature-regulated raceway provided consistent water parameters by circulating water with additional water jets. To conduct the exposure experiment, 14 glass beakers (1 L) were distributed within the water bath of the raceway. A randomly selected single fragment of coral was placed within each beaker and allowed to further acclimate to the controlled system for 7 days. Treatments were then assigned to beakers as controls or permethrin treatments (**Supplementary Figure 1**). Each glass beaker was assigned a water hose for flow through water exchange during acclimation and an air stone to provide additional aeration and to eventually aid in the mixing of permethrin. Water quality parameters, including temperature, pH, dissolved oxygen, and salinity were recorded daily. Temperatures were maintained at 27°C (±0.006), pH averaged 7.94 [±0.001; National Bureau of Standards (NBS)], salinity averaged 36.35 ppt (±0.005), and dissolved oxygen averaged 5.98 mg/L (±0.003).

Permethrin Exposure

Permethrin (Chem Service Inc., West Chester, PA, United States, 99.25% purity) concentrations for exposure to *M. cavernosa* were 2 (high) and 0.325 ug/L (low), plus acetone and seawater controls,

for a total of four treatments. Acetone (5 μl/L) was utilized to increase the solubility of the permethrin treatments. The target doses of permethrin were selected due to the limited solubility of permethrin in acetone, which precipitates in excess of 10 μg/L (Ross et al., 2015). Low permethrin and acetone treatments had four replicate aquaria each and high and saltwater controls both had three replicate aquaria. The high permethrin treatment and saltwater control had one less replicate due to sample processing error at the end of the exposure and subsequent contamination, which warranted their removal from the analysis.

The corals were dosed with treatment conditions on October 12, 2016, a week after the fragments were placed into the 1-L beakers for acclimation. Water samples (500 ml) were collected for analysis of permethrin concentration 30 mins and 24-h after dosing occurred. Permethrin was recovered from water samples by liquid-liquid extraction into dichloromethane (DCM). The DCM was replaced with MeOH by rotary evaporation for DCM solvent recovery. The MeOH containing permethrin extract was reduced to 1 ml volume for HPLC-MS/MS analysis of both the *cis*- and *trans*-permethrin isomers.

Permethrin analysis was conducted using a Thermo Electron Quantum Access HPLC system, interfaced with a Quantum Access triple quadrupole MS/MS. A Phenomenex Kinetex 2.6 μm particle size, 100 mm × 2.1 mm analytical column was used with mobile phase gradient of 10 mM Ammonium Formate in Methanol, 10 mM Ammonium Formate in HPLC water, initial ratio 20:80 for 5 min, then to 99:1 for 8 min, back to 20:80 for 2 min, total sample run time 15 min at a flow rate of 200 μl/min. Analytical standards, *Trans*- and *Cis*-Permethrin solutions were purchased from Chem Service.

Pulse Amplitude Modulation Fluorometer

To determine the state of the coral-algal symbiosis the photochemical efficiency on each colony was measured using a Walz Imaging Pulse Amplitude Modulator (PAM) Fluorometer. The imaging PAM measures the spatial distribution of chlorophyll fluorescence of photosystem II. *Montastraea cavernosa* colonies were dark acclimated (30 min) prior to conducting light curves. Light curves provided information on photochemical yield (F_v/F_m) and electron transport rate (ETR). The photochemical yield (F_v/F_m) is a normalizing ratio created by dividing the variable fluorescence (F_v) by the maximum fluorescence (F_m). By dark acclimating the colony, this relaxes the photosystem II reaction centers. When the colony was exposed to a pulse of light, the calculated yield represented the maximum potential quantum efficiency of photosystem II if all capable reaction centers were open. The maximum ETR represents the photosynthetic capacity of an organism after which photoinhibition occurs where the organism cannot process additional photosynthetic active radiation (PAR) that is being emitted by the PAM. The ETR represents photosynthetic capacity because it is informative of the number of electrons passing through photosystem II where four electrons pass through photosystem II for every O_2 produced during photosynthesis (Ritchie and Bunthawin, 2010). The PAM measurements were taken prior to permethrin exposure and 24 h after exposure. After passing the assumptions for normality using the Shapiro-Wilk test and homoscedasticity, tested using the Levene's test, a paired *t*-test, and the multiple comparison's false discovery rate (FDR) test compared replicates within treatments before exposure and 24 h after exposure to permethrin in R v1.2.5033 (R Core Team, 2019).

Microbial Community

After 24 h of exposure, tissue samples were collected from each of the *M. cavernosa* fragments for DNA isolation by scraping off a single polyp using a sterile scalpel. DNA extraction was performed on the coral tissue using a Powersoil DNA isolation kit (Qiagen, Germantown, MD, United States). The extracted DNA was sent to MR DNA for sequencing of the 16S rRNA gene V1–V3 region using PCR primers 27 F and 519 R. Polymerase chain reaction protocol required a 28 cycle PCR using HotStarTaq Plus Master Mix Kit (Qiagen, United States) under the following conditions: 94°C for 3 min, followed by 28 cycles of 94°C for 30 s, 53°C for 40 s, and 72°C for 1 min, after which a final elongation step at 72°C for 5 min. Samples were purified using Ampure XP beads and then sequenced at MR DNA[1] (Shallowater, TX, United States) on a Miseq following the manufacturer's standard guidelines. Sequence data was processed using MR DNA analysis pipeline. In summary, sequences were stitched together to assemble contigs, and sequences <150 bp or with ambiguous nucleotide identification were removed. Operational taxonomic units (OTUs) were categorized by clustering at 97% sequence similarity (**Supplementary Table 1**). Using the 16S barcoding region, 3,311 of the final OTUs were taxonomically classified using the nucleotide basic local alignment search tool (BLASTn) against a database derived from the Ribosomal Database Project (RDPII)[2] and the National Center for Biotechnology Information (NCBI)[3] and organized into each taxonomic level.

A permutational analysis of variance (PERMANOVA) tested for differences in the bacterial community between water samples and coral tissue samples. A PERMANOVA was also used to test for differences in the bacterial community within the coral fragments among treatments. Dominant bacterial classes were identified as those with greater than 3% average relative abundance in any treatment condition. Classes were compared among treatments using a Kruskal Wallis test. A similarity percentage (SIMPER) analysis was used to determine the dissimilarity between treatments and provided the percent dissimilarity caused by each bacterial OTUs. The top six OTUs that contributed to dissimilarity were tested for differences among treatments using the Kruskal Wallis test and *post-hoc* analysis was performed using a Dunnett's test. Bacterial OTUs for each sample were processed through a non-metric multidimensional scaling (NMDS) plot, which provided a visual representation of the bacterial community in multidimensional space in a two-dimension visual plot. The relative abundance of bacterial classes and genera of coral tissue and water samples were also graphed for visualization.

[1] www.mrdnalab.com

[2] http://rdp.cme.msu.edu

[3] www.ncbi.nlm.nih.gov

Simpson diversity, Pielou's richness, and beta diversity of the bacterial community was calculated at the bacterial species level for each sample (**Supplementary Figure 2** and **Supplementary Table 2**). Using an analysis of variance (ANOVA) test, the differences in diversity and richness among treatments for each sample was applied after passing assumptions of normality using the Shapiro-Wilk test and homoscedasticity using the Levene Test.

RESULTS

Permethrin Adsorption

The high treatment dose of permethrin (n = 3) ranged between 1.60 and 2.20 μg/L with an average of 2.0 μg/l (±0.122 μg/l SE) (**Supplementary Figure 3**). The low permethrin treatments (n = 4) received a dosing concentration between 0.20 and 0.40 μg/L with an average of 0.325 μg/l (±0.046 μg/l SE). No permethrin was found in the saltwater control (n = 3) or acetone controls (n = 4). Measurements after 24 h showed an absence of permethrin for all but one sample within low concentration treatment, which generated an average of 0.0125 μg/l (±0.0125 μg/l SE). The loss of permethrin from exposure solutions was most likely a result of the hydrophobic nature of permethrin causing it to adsorb to surfaces when dispersed in seawater or potentially the biological accumulation of permethrin within the coral tissue itself. However, identifying where the permethrin adsorbed to during the depuration process was outside of the scope of the present project.

Photochemical Parameters of the Algal Symbiont

Within each treatment, there were no significant differences between the initial and post photochemical yields ($p > 0.1$ for all comparisons; **Supplementary Figure 4**). The photochemical yield decreased for corals exposed to permethrin in high and low treatments, but this was not significant (t = 1.0182, df = 6, p-value = 0.3479, FDR padj = 0.80; **Supplementary Figure 4**). The ETR had a significant increase in post permethrin exposure relative to before permethrin exposure in only coral exposed to permethrin, however the *post-hoc* FDR test showed no significant differences (t = −3.2609, df = 6, p-value = 0.01723, FDR padj = 0.075; **Supplementary Figure 5**).

Microbial Community

The 16S rDNA sequencing resulted in an average of 47,993 (±5,633 SE) reads per coral tissue sample and the water samples had an average of 108,899 (±7,453 SE) reads. There were a total number of 1,350 distinct OTUs within the coral tissue samples, whereas there was a total of 2,771 distinct OTUs within the water samples. A permutational ANOVA showed a significant difference between the bacterial community within the water compared to the bacterial community of the *M. cavernosa* tissue, suggesting the tissue samples indeed represent the community associated with the living coral tissue (F = 9.5354, df = 1, p-value < 0.001; **Supplementary Table 3** and **Supplementary Figures 6, 7**). There was also a significant difference in the bacterial community of *M. cavernosa* among treatments (F = 5.272, df = 3, p-value = 0.0028; **Figure 1**). However, pairwise PERMANOVAs detected no significance between treatment pairs (**Supplementary Table 4**) due to the conservative approach of the test.

The coral tissue bacterial community of the seawater control treatment was dominated by two classes: Alphaproteobacteria (41.7%) and Sphingobacteria (33.9%). The acetone control tissue samples were dominated by three bacterial classes, Alphaproteobacteria (24%), Betaproteobacteria (34.5%), and Sphingobacteria (22.5%). In seawater controls, Alphaproteobacteria (41.7%) was primarily composed of *Sphingopyxis* sp. (16%), *Mesorhizobium* sp. (11.4%), and *Bradyrhizobium* sp. (6.8%) (**Figure 2C**). Alphaproteobacteria (24%) abundance was lower in acetone control corals but was still primarily composed of *Sphingopyxis* sp. (3.6%), *Mesorhizobium* sp. (8.6%), and *Bradyrhizobium* sp. (5%) (**Figures 2B,C**). Betaproteobacteria was dominated by *Burkholderia pyrrocinia* (**Figure 2D**), and Sphingobacteria was dominated by *Sediminibacterium* sp. (**Figure 2E**) within the acetone and saltwater control colonies.

In low permethrin treatment coral, Betaproteobacteria contributed to 67% of the coral's microbiome, nearly exclusively composed of *B. pyrrocinia* (66.4%) (**Figure 2D**). Betaproteobacteria was higher in abundance in low-dosed coral compared with the other treatments and the bacterial community of this treatment also showed significantly lower (p = 0.006) abundances of the bacterial classes that were dominant in the control coral tissue. Alphaproteobacteria (14%) and Sphingobacteria (0.9%) were lower in the low dose treated corals compared with controls (**Figure 2A**). Alphaproteobacteria was dominated by *Sphingopyxis* sp., *Mesorhizobium* sp., and *Bradyrhizobium* sp. in the controls, but these genera were nearly absent in the low-dosed tissue. Rather, this class was composed primarily of *Novosphingobium* sp. (3.6%) and *Acidocella* sp. (3.3%) (**Figure 2C**). The relative abundance of Sphingobacteria (0.9%) remained dominated by *Sediminibacterium* sp. (0.9%) in low-dosed coral (**Figure 2E**).

In the high-dosed coral bacterial community, Betaproteobacteria (64.8%), dominated by *B. pyrrocinia* (62.7%), comprised most of the microbiome. Alphaproteobacteria (5.6%) abundance in the high-dosed treatment was less than in the controls and low-dosed coral. *Sphingopyxis* sp. and *Mesorhizobium* sp. were significantly reduced (df = 3, p-value < 0.05; df = 3, p-value < 0.05; **Figure 3**) in permethrin treated microbiomes and the Alphaproteobacteria was represented by different bacterial genera and primarily composed of *Acidocella* sp. and *Novosphingobium* sp. (**Figure 2C**). Sphingobacteria was relatively less abundant in high-dosed tissue (1.2%) than in the controls (24%) and was similar in abundance compared with the low-dosed tissue (0.9%) (**Figure 2E**). Bacilli (13.8%), dominated by *Bacillus* sp., increased in abundance in high-dosed tissue (**Figure 2F**). In comparison, Bacilli was observed at decreased abundance in low-dosed (2.3%), acetone control (0.8%), and seawater controls (0.14%).

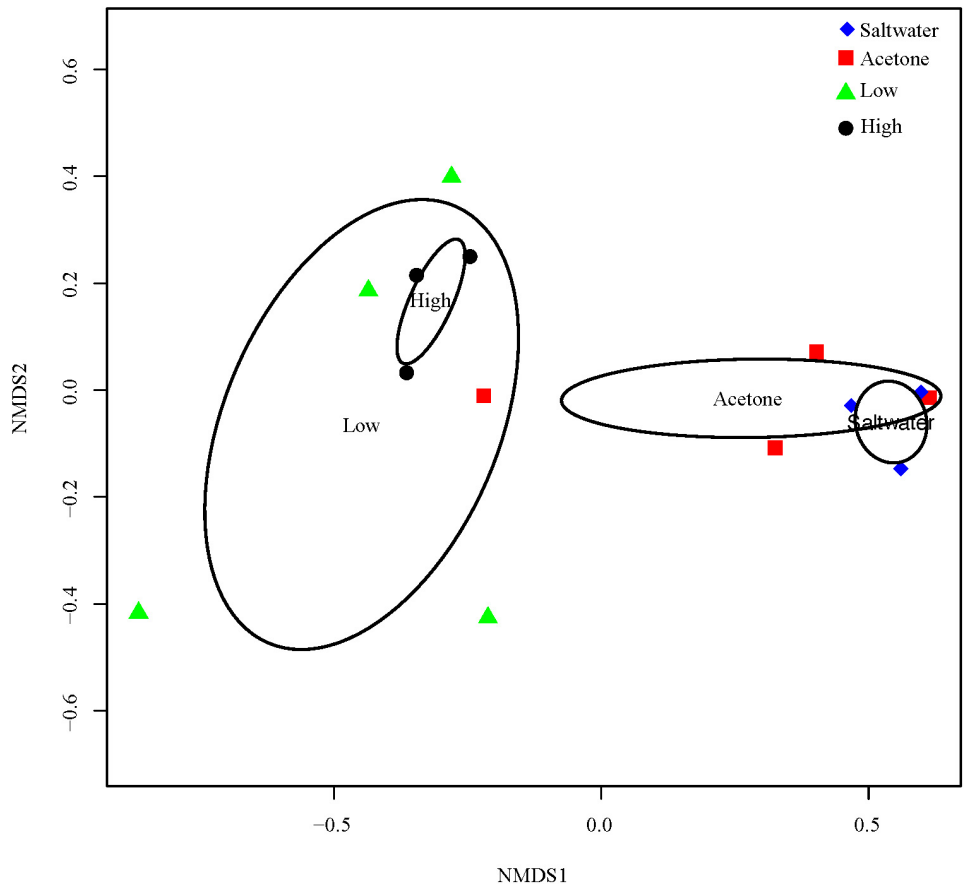

FIGURE 1 | Nonmetric dimensional scaling (NMDS) of microbiome reads from *M. cavernosa* tissue samples. "High" indicates samples that were dosed with a concentration of 1.93 mg/l of permethrin 24 h prior to sampling. "Low" indicates samples that were dosed with a concentration of 0.33 mg/l of permethrin. "Acetone" represents the coral that was dosed with 5 ml/l of acetone to match the acetone concentration used to dilute the permethrin in permethrin-treated aquaria. "Seawater" controls were dosed with seawater from the controlled flow-through system to account for a control treatment.

Dissimilarity Among Treatments

The SIMPER analysis showed that the six OTU's were responsible for the greatest dissimilarity among treatments included: (1) *B. pyrrocinia* (homology identified at 99%; **Figure 3**), (2) *Sediminibacterium* sp. (homology identified at 96%; **Figure 3**), (3) *Sphingopyxis* sp. (homology identified at 99%; **Figure 3**), (4) *Chondromyces* sp. (homology identified at 97%; **Figure 3**), (5) *Bacillus* sp. (homology identified as 99%; **Figure 3**), and (6) *Mesorhizobium* sp. (homology identified as 98%; **Figure 3**). Comparisons of these genera among treatments using non-parametric Kruskal-Wallis tests presented significant differences in the relative abundance (**Supplementary Table 5**) for *B. pyrrocinia* (x^2 = 8.3476, df = 3, p = 0.039; **Figure 3**), *Sediminibacterium* sp. (x^2 = 8.7238, df = 3, p = 0.033; **Figure 3**), *Mesorhizobium* sp. (x^2 = 10.799, df = 3, p = 0.012; **Figure 3**), *Sphyngopyxis* sp. (x^2 = 9.8762, df = 3, p = 0.02; **Figure 3**), and *Chondromyces* sp. (x^2 = 10.933, df = 3, p = 0.012; **Figure 3**). The multiple comparison *post-hoc* Dunnett's test showed that *B. pyrrocinia* was significantly higher in the high permethrin treatment compared to the saltwater control (t = 3.957, p = 0.007). This conservative *post-hoc* test did not detect any difference in *Bacillus* sp. among treatments. *Sediminibacterium* sp., *Mesorhizobium* sp., *Sphingopyxis* sp., and *Chondromyces* sp. were significantly more abundant in seawater control corals compared to low permethrin exposure conditions ($p < 0.037$ for all comparisons). *Sediminibacterium* sp., *Mesorhizbium* sp., and *Sphingopyxis* sp., were also significantly more abundant in seawater control corals compared with the high permethrin exposure conditions ($p < 0.005$ for all comparisons).

Microbial Diversity and Richness

Statistical analyses showed no significant differences in the alpha diversity of the bacterial community among treatments (**Supplementary Figures 2A–C** and **Supplementary Table 2**). Interestingly, both the Simpson's diversity and the Pielou's Evenness metrics showed a trending linear decrease among treatments from controls to the high treatment exposure (**Supplementary Figure 2C**). Beta diversity of the microbial community was not significantly different among treatments (**Supplementary Figure 2B**) with no apparent trends visible.

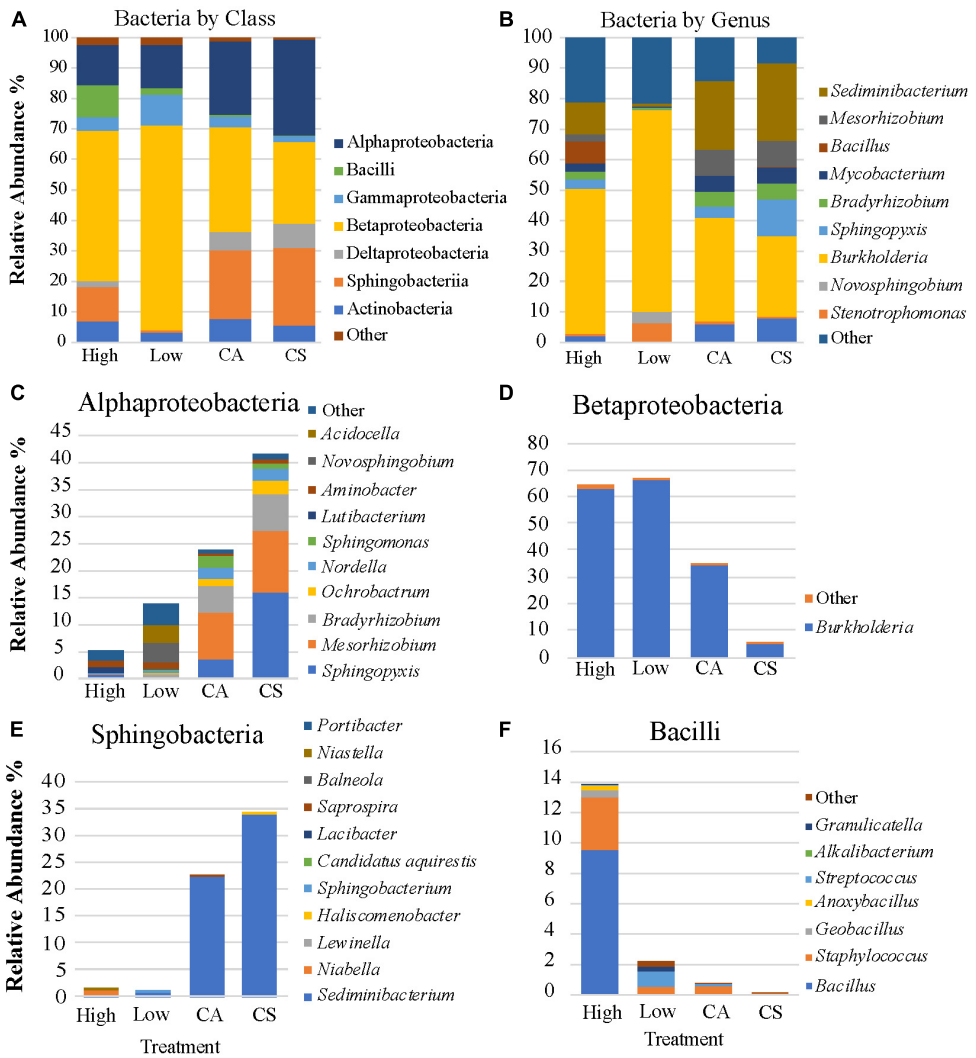

FIGURE 2 | The average relative abundance of the bacterial community members by class **(A)**, genus **(B)**, and the genera that comprise the four dominant classes **(C–F)**.

DISCUSSION

Stable Photochemical Efficiency

Previous investigations on the effects of pesticide exposure on coral have documented a decline in settlement, survivorship, stunted metamorphosis, and transcriptional stress response in the larvae of *Acropora* sp. (Morgan et al., 2001; Markey et al., 2007; Ross et al., 2015). However, Ross et al. (2015) showed no significant effects of permethrin exposure on *Porites astreoides* larvae settlement and survival. The present study measured the photochemical and microbial community response in adult *M. cavernosa* to an acute permethrin exposure. The maintenance of similar maximum ETR and maximum photochemical yield suggests the algal-coral symbiosis of adult *M. cavernosa* exposed to an acute permethrin dose over 24 h was not negatively affected. The lack of an effect on the coral-algal symbiosis suggests that the dose may have been too low to elicit a response, the exposure may have been too short, or the corals tested may be resistant to permethrin exposure. Further studies that incorporate repeated or long-term exposure, increased levels of dosing, and additional species are needed to quantify the level of resistance corals may have to this commonly used insecticide.

Microbiome Shifts May Mediate Insecticide Resistance

Burkholderia pyrrocinia, a nitrogen fixing bacteria, was the most abundant bacteria within the bacterial community of the fragments exposed to permethrin, consisting of approximately 60% of the bacterial community. On the other hand, the presence of *Burkholderia* contributed to less than 10% of the bacterial community within the control corals. *Burkholderia* has been identified as an insecticide resistant bacterium found in the soybean bug *Riptortus pedestris*, which allowed the bean bug to survive fenitrothion spraying (Kikuchi et al., 2012). *Burkholderia*

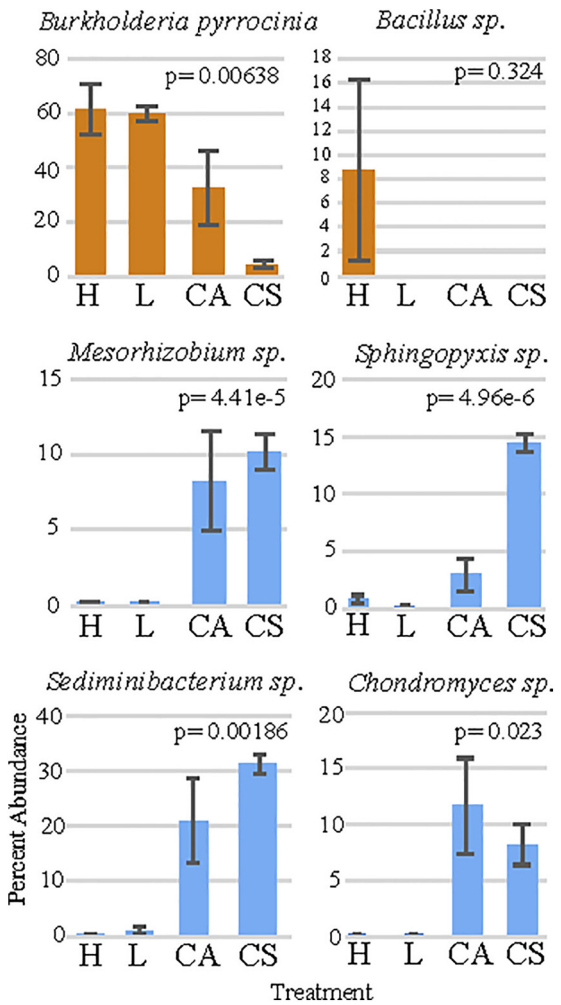

FIGURE 3 | The percent abundance of the six bacteria that are responsible for the largest dissimilarity between treatments. "H" = high permethrin concentration treatment, "L" = low permethrin concentration treatment, "CA" = acetone control, and "CS" = seawater control. Error bars represent standard error.

hydrolyzes fenitrothion, an organophosphorous insecticide, into 3-methyl 4-nitrophenol and metabolizes the degradation product as a carbon source for *Burkholderia*'s growth. *Burkholderia* has also been identified with insecticide degradation properties toward bifenthrin, a pyrethroid that includes permethrin (Lee et al., 2004). The increased relative abundance of this particular bacteria within corals exposed to permethrin suggests it may function in a similar way within corals. However, further study is needed to target the function of the bacterial group that becomes dominant within the microbiome of *M. cavernosa* exposed to acute levels of permethrin.

Bacillus sp., which was also abundant within permethrin exposed corals, has the ability to hydrolyze pyrethroids, particularly even permethrin into non-insecticidal compounds (Maloney et al., 1992, 1993; Chen et al., 2014). *Bacillus* shifted to an 8.76% abundance in the high dosage of permethrin treatment compared to the near 0% of *Bacillus* in other treatments. These results may suggest bioremediation, or a breakdown of permethrin is occurring by the microbiome to mitigate the insecticide presence. However, *Bacillus* is a large genus with hundreds of species with different functional roles. Further exploring how the increase of this bacterial genera may affect the coral holobiont could be an important research topic for follow-up studies. Alternatively, the exposure could have simply resulted in a selection for insecticide resistant bacteria, thus changing the community to have more representation of bacteria that can survive and even break down the compounds within insecticides.

Permethrin Reduced Potentially Stabilizing Bacteria

The exposure of corals to permethrin caused a significant shift in the bacterial community, perhaps reducing beneficial bacterial found within healthy corals. For example, *Sediminibacterium* sp. was highest in abundance in control corals (up to 32%) and completely lost in permethrin exposed coral. This bacteria has been identified in healthy coral tissues in previous studies (Lesser and Jarett, 2014). Similarly, *Chondromyces* sp. was approximately 10% of the bacterial community in acetone and seawater control coral tissues. However, permethrin treated coral had close to 0% relative abundance of *Chondromyces* sp. This bacteria species has been identified in sponges and produce the bacterial metabolite Apicularen A isolates, which have strong inhibition of angiogenesis, or blood vessel development associated with tumor growth (Kwon, 2002). While *Sediminibacterium* sp.'s function in coral is unknown in corals, it is a well-recognized plant growth promoting rhizobacteria and reported to be responsible for subduing soil borne pathogens, suggesting at least some species within this genus may have probiotic properties (Han et al., 2019). Additionally, the reduced abundance of *Chondromyces* sp.'s to nearly absent as a consequence of permethrin exposure implicates a functional loss in opportunity for this bacteria species when corals interact with this contaminant.

The loss of *Sphingopyxis* sp. bacterium in the permethrin exposed fragments may also have negative effects to the host. *Sphingorhabdus litoris* (previously *Sphingopyxis litoris*) is the closest phylogenetically related bacterium within *Sphingopyxis* sp. that has been observed in coral and isolated from the gorgonian *Eunicella labiate*. Genome annotation of *S. litoris* presented genes coding for polyphosphate kinase and exopolyphosphatase, which mitigates the synthesis of energetic polyphoshatases (Silva et al., 2018). This likely provides phosphorous for the host, an important requirement for stony corals, soft corals, and sponges. Further annotation of the *S. litoris* genome presents genes that are associated with homeostasis with metals, and even resistance to antibiotics. Some strains (EL 138) of *S. litoris* contain genes with homology to astaxanthin, which has anti-inflammatory properties (Silva et al., 2018). Finally, *Sphingopyxis* sp. in general can extrude porphyrin-like growth factors that promote the growth of other bacteria that otherwise grew poorly (Bhuiyan et al., 2015). The beneficial properties of this bacteria within other similar marine organisms

suggest that the loss of this genus within corals exposed to permethrin could have larger implications on coral health by the insecticide exposure resulting in the loss of beneficial microbes within the holobiont.

Finally, *Mesorhizobium* sp. showed a similar result as *Sediminibacterium* sp., *Chrondromyces* sp., and *Sphingopyxis* sp. *Mesorhizobium* composed approximately 8.6% of the relative abundance in controls only to decline to 2.25% in high permethrin treatment and 0.1% in low permethrin treated coral tissues. The nitrogen fixing *Mesorhizobium* sp. have been identified in previous coral studies (Kaneko et al., 2000; Carlos et al., 2013), but little is known about this bacterial group. However, a bacterial isolate completed Koch's postulate to induce white plague type II had the highest homology to *Mesorhizobium mediterraneum* with 92% similarity, and so this isolate was given a new genus and species name to become the more well-known, *Aurantimonas coralicida* (Denner et al., 2003). While *Aurantimonas coralicida* and *Mesorhizobium* sp. possess phylogenic proximity, their homologous functional contributions to the host are unknown. They are still both Rhizobiales bacteria, and likely have a meaningful prokaryotic-eukaryotic relationship suggesting that the reduced abundance of *Mesorhizobium* sp. functional proclivity to fix nitrogen in permethrin exposed coral may have negative impacts to the health of the coral holobiont.

CONCLUSION

The present 24-h study, designed to mimic an acute permethrin exposure that a coral may experience under natural circumstances, suggests the algal-coral symbiosis and particularly the photochemical parameters of the algal symbionts within the coral host are not significantly impaired under this scenario. Rather, it appears the microbiome of the host significantly shifts after just a single acute exposure to permethrin. While the observed shift in the microbiome toward the potential for insecticide bioremediating bacteria may be beneficial for the coral to mitigate the immediate permethrin exposure, it is unclear if these bacteria indeed bioremediate and if this microbial shift is optimal for the stability of the microbiome to mitigate other stressors. Shifts in the microbiome may be detrimental to the health of the coral as opportunistic bacteria colonize the host during times of microbial dysbiosis. The increased abundance of *Burkholderia* and *Bacillus* along with the reduced abundance in *Sediminibacterium* sp., *Chondromyces*, *Sphingopyxis* sp., and *Mesorhizobium* sp., in permethrin exposed coral suggest significant shifts in the bacterial community are occurring, which could leave the host more vulnerable to secondary threats such as infectious disease. However, the functional changes in the coral holobiont associated with this microbiome shift are largely unknown. Further investigations would benefit from determining the functional role of these shifting bacteria within the coral holobiont and conducting chronic insecticide exposures to determine if these microbial shifts return to pre-exposure communities or settle into a community dominated by opportunistic bacteria.

DATA AVAILABILITY STATEMENT

The datasets presented in this study can be found in online repositories. The names of the repository/repositories and accession number(s) can be found below: NCBI (accession: PRJNA747979).

AUTHOR CONTRIBUTIONS

EM and RP were responsible for compiling the intellectual merit behind the research objectives, design, and acquiring funding for this original research. NM, LA, and AC recorded pulse amplitude modulator measurements and extracted DNA. MH prepared permethrin concentrations and recorded actual permethrin results. EM designed the statistical analysis and implemented by NM created all the figures. NM wrote the manuscript with considerable editorial input from EM with additional revisions from all authors. All authors contributed to the experimental permethrin exposure and submitted the approved version.

FUNDING

This work was supported by the Environmental Protection Agency award number 00D51817 to RP.

ACKNOWLEDGMENTS

We thank the members of the ecotoxicology and coral nursery staff at Mote Marine laboratory.

SUPPLEMENTARY MATERIAL

The Supplementary Material for this article can be found online at: https://www.frontiersin.org/articles/10.3389/fmars.2022.748308/full#supplementary-material

REFERENCES

Bhuiyan, T., Mitsuhashi, S., Shigetomi, K., Tanaka, Y., Kamagata, Y., and Ubukata, M. (2015). *Zincmethylphyrins and Coproporphyrins, Novel Growth Factors Released by Sphingopyxis Sp., Enable Laboratory Cultivation of Previously Uncultured Leucobacter Sp. Through Interspecies Mutualism*. Tokyo: The Journal of Antibiotics.

Brandt, M. E., and Mcmanus, J. W. (2009). Disease incidence is related to bleaching extent in reef-building corals. *Ecology* 90, 2859–2867. doi: 10.1890/08-0445.1

Bruno, J. F., Selig, E. R., Casey, K. S., Page, C. A., Willis, B. L., Drew Harvell, C., et al. (2007). Thermal stress and coral cover as drivers of coral disease outbreaks. *PLoS Biol.* 5:e124. doi: 10.1371/journal.pbio.0050124

Bruno, J. F., Stachowicz, J. J., and Bertness, M. D. (2003). Inclusion of facilitation into ecological theory. *Trends Ecol. Evol.* 18, 119–125. doi: 10.1016/S0169-5347(02)00045-9

Carilli, J. E., Norris, R. D., Black, B. A., Walsh, S. M., and McField, M. (2009). Local stressors reduce coral resilience to bleaching. *PLoS One* 4:e6324. doi: 10.1371/journal.pone.0006324

Carlos, C., Torres, T. T., and Ottoboni, L. M. M. (2013). Bacterial communities and species-specific associations with the mucus of Brazilian coral species. *Sci. Rep.* 3:1634. doi: 10.1038/srep01624

Chen, S., Chang, C., Deng, Y., An, S., Dong, Y. H., Zhou, J., et al. (2014). Fenpropathrin biodegradation pathway in *Bacillus* Sp. DG-02 and its potential for bioremediation of pyrethroid-contaminated soils. *J. Agric. Food Chem.* 62, 2147–2157. doi: 10.1021/jf404908j

Clark, L. R. Jr., Goodman, P. W., Borthwick, J. M., Patrick, G. M., Cripe, P. M., Moody, J. C., et al. (1989). Toxicity of pyrethroids to marine invertebrates and fish: a literature review and test results with sediment-sorbed chemicals. *Environ. Toxicol. Chem.* 8, 393–401. doi: 10.1002/etc.5620080505

Denner, E. B. M., Smith, G. W., Busse, H. J., Schumann, P., Narzt, T., Polson, S. W., et al. (2003). *Aurantimonas coralicida* gen. nov., sp. nov., the causative agent of white plague type II on Caribbean scleractinian corals. *Int. J. Syst. Evol. Microbiol.* 53, 1115–1122. doi: 10.1099/ijs.0.02359-0

Donovan, M. K., Burkepile, D. E., Kratochwill, C., Shlesinger, T., Sully, S., Oliver, T. A., et al. (2021). Local conditions magnify coral loss following marine heatwaves. *Science* 980, 977–980. doi: 10.1126/science.abd9464

Eakin, C. M., Morgan, J. A., Heron, S. F., Smith, T. B., Liu, G., Alvarez-Filip, L., et al. (2010). Caribbean corals in crisis: record thermal stress, bleaching, and mortality in 2005. *PLoS One* 5:e13969. doi: 10.1371/journal.pone.0013969

Han, L., Wang, Z., Li, N., Wang, Y., Feng, J., and Zhang, X. (2019). *Bacillus amyloliquefaciens* B1408 suppresses *Fusarium wilt* in cucumber by regulating the rhizosphere microbial community. *Appl. Soil Ecol.* 136, 55–66. doi: 10.1016/j.apsoil.2018.12.011

Hoegh-Guldberg, O., Mumby, P. J., Hooten, A. J., Steneck, R. S., Greenfield, P., Gomez, E., et al. (2007). Coral reefs under rapid climate change and ocean acidification. *Science* 318, 1737–1742. doi: 10.1126/science.1152509

Hughes, T. P., Baird, A. H., Bellwood, D. R., Card, M., Connolly, S. R., Folke, C., et al. (2016). Climate change, human impacts, and the resilience of coral reefs. *Science* 301, 929–933. doi: 10.1126/science.1085046

Kaneko, T., Nakamura, Y., Sato, S., Asamizu, E., Kato, T., Sasamoto, S., et al. (2000). Complete genome structure of the nitrogen-fixing symbiotic bacterium *Mesorhizobium loti*. *DNA Res.* 7, 331–338. doi: 10.1093/dnares/7.6.331

Kennedy, E. V., Perry, C. T., Halloran, P. R., Iglesias-Prieto, R., Schönberg, C. H. L., Wisshak, M., et al. (2013). Avoiding coral reef functional collapse requires local and global action. *Curr. Biol.* 23, 912–918. doi: 10.1016/j.cub.2013.04.020

Kikuchi, Y., Hayatsu, M., Hosokawa, T., Nagayama, A., and Tago, K. (2012). Symbiont-mediated insecticide resistance. *Proc. Natl. Acad. Sci. U.S.A.* 109, 8618–8622. doi: 10.1073/pnas.1200231109

Kwon, H. J. (2002). Apicularen A, a macrolide from *Chondromyces* Sp., inhibits growth factor induced *in vitro* angiogenesis. *J. Microbiol. Biotechnol.* 12, 702–705.

Lee, S., Gan, J., Kim, J. S., Kabashima, J. N., and Crowley, D. E. (2004). Microbial transformation of pyrethroid insecticides in aqueous and sediment phases. *Environ. Toxicol. Chem.* 23, 1–6. doi: 10.1897/03-114

Lesser, M. P., and Jarett, J. K. (2014). Culture-dependent and culture-independent analyses reveal no prokaryotic community shifts or recovery of *Serratia Marcescens* in *Acropora palmata* with White pox disease. *FEMS Microbiol. Ecol.* 88, 457–467. doi: 10.1111/1574-6941.12311

Maloney, S. E., Maule, A., and Smith, A. R. (1993). Purification and preliminary characterization of permethrinase from a pyrethroid-transforming strain of *Bacillus cereus*. *Appl. Environ. Microbiol.* 59, 2007–2013. doi: 10.1128/aem.59.7.2007-2013.1993

Maloney, S. E., Maule, A., and Smith, A. R. W. (1992). Transformation of synthetic pyrethroid insecticides by a thermophilic *Bacillus* Sp. *Arch. Microbiol.* 158, 282–286. doi: 10.1007/BF00245246

Markey, K. L., Baird, A. H., Humphrey, C., and Negri, A. P. (2007). Insecticides and a fungicide affect multiple coral life stages. *Mar. Ecol. Prog. Ser.* 330, 127–137. doi: 10.3354/meps330127

Morgan, M. B., Vogelien, D. L., and Snell, T. W. (2001). Assessing coral stress responses using molecular biomarkers of gene transcription. *Environ. Toxicol. Chem.* 20, 537–543. doi: 10.1002/etc.5620200312

Pierce, R. H. (1998). *Effects of Mosquito Control Measures on Non-Targeted Organisms in the Florida Keys National Marine Sanctuary Draft Final, No. 609*. Sarasota, FL: Mote Marine Laboratory.

Pierce, R. H. (2005). Aerial and tidal transport of mosquito control pesticides into the Florida keys national marine sanctuary. *Rev. Biol. Trop.* 53, 117–125.

R Core Team (2019). *R: A Language and Environment for Statistical Computing*. Vienna: R Foundation for Statistical Computing.

Ritchie, K. B. (2006). Regulation of microbial populations by coral surface mucus and mucus-associated bacteria. *Mar. Ecol. Prog. Ser.* 322, 1–14. doi: 10.3354/meps322001

Ritchie, R. J., and Bunthawin, S. (2010). The use of pulse amplitude modulation (PAM) fluorometry to measure photosynthesis in a CAM orchid, *Dendrobium* Spp. (D. CV. Viravuth Pink). *Int. J. Plant Sci.* 171, 575–585. doi: 10.1086/653131

Ross, C., Olsen, K., Henry, M., and Pierce, R. (2015). Mosquito control pesticides and sea surface temperatures have differential effects on the survival and oxidative stress response of coral larvae. *Ecotoxicology* 24, 540–552. doi: 10.1007/s10646-014-1402-8

Silva, S. G., Lago-lestón, A., Costa, R., and Keller-Costa, T. (2018). *Crossm*. Tokyo: The Journal of Antibiotics, 1–2.

Sunagawa, S., Desantis, T. Z., Piceno, Y. M., Brodie, E. L., Desalvo, M. K., Voolstra, C. R., et al. (2009). Bacterial diversity and White Plague disease-associated community changes in the Caribbean coral *Montastraea faveolata*. *ISME J.* 3, 512–521. doi: 10.1038/ismej.2008.131

Tietze, N. S., Hester, P. G., and Shaffer, K. R. (1995). Acute effects of permanone 31-66 (Permethrin-Piperonyl Butoxide) on nontarget minnows and grass shrimp. *J. Am. Mosq. Control Assoc.* 11, 476–479.

Conflict of Interest: The authors declare that the research was conducted in the absence of any commercial or financial relationships that could be construed as a potential conflict of interest.

Publisher's Note: All claims expressed in this article are solely those of the authors and do not necessarily represent those of their affiliated organizations, or those of the publisher, the editors and the reviewers. Any product that may be evaluated in this article, or claim that may be made by its manufacturer, is not guaranteed or endorsed by the publisher.

frontiers in Marine Science

PERSPECTIVE
published: 16 March 2022
doi: 10.3389/fmars.2022.806491

A Road Map for the Development of the Bleached Coral Phenotype

Kelly Gómez-Campo[1], Susana Enríquez[2] and Roberto Iglesias-Prieto[1]**

[1] Department of Biology, The Pennsylvania State University, University Park, PA, United States, [2] Unidad Académica de Sistemas Arrecifales Puerto Morelos, Instituto de Ciencias del Mar y Limnología, Universidad Nacional Autónoma de México, Puerto Morelos, Mexico

Mass coral bleaching compromises the long-term persistence of coral reefs, yet our current understanding of the different cellular mechanisms leading to the development of a bleached coral is still limited. In this perspective, we mapped the cascade of cellular events and physiological responses of symbiotic corals triggered by thermal stress. Based on existing knowledge, we created an integrated model that describes phenotypic changes induced by sensing mechanisms. Cellular responses are mapped in the context of reactive oxygen species (ROS) production in the algal symbiont chloroplast, followed by signaling to the nucleus and subsequent "leak" to the coral host cell. The starting point is set by ROS production and signaling, which is a day-to-day mechanism by which symbiotic corals maintain homeostasis and acclimate to environmental variation. As stress and acclimation are intimately linked, our model maps coral responses from the initial stimulus in the chloroplast to the complex cascade of events leading to seasonal phenotypic changes (*i.e.,* seasonal acclimation), and if stress progresses, to the downstream coral bleached phenotype (*i.e.,* when the coral's capacity to acclimate is overwhelmed by heat stress). Placing acclimation, heat stress and bleaching responses in a common ground is a critical step to reduce the source of uncertainty in understanding the coral response to climate change, fundamental for the development of predictive climate models.

Keywords: oxidative stress, seasonal phenotype, coral bleaching, ROS, bleached coral phenotype

OPEN ACCESS

Edited by:
Davide Seveso, University of Milano-Bicocca, Italy

Reviewed by:
Joshua Patterson, University of Florida, United States
Gretchen Goodbody-Gringley, Central Caribbean Marine Institute, Cayman Islands

****Correspondence:***
Kelly Gómez-Campo
kjg27@psu.edu
Roberto Iglesias-Prieto
rzi3@psu.edu

Specialty section:
This article was submitted to Aquatic Physiology, a section of the journal Frontiers in Marine Science

Received: *31 October 2021*
Accepted: *25 January 2022*
Published: *16 March 2022*

Citation:
Gómez-Campo K, Enríquez S and Iglesias-Prieto R (2022) A Road Map for the Development of the Bleached Coral Phenotype. Front. Mar. Sci. 9:806491. doi: 10.3389/fmars.2022.806491

INTRODUCTION

Mass coral bleaching is a widespread and conspicuous aspect of climate change in coral reefs. Thermal anomalies (+ 1.5–2°C above the long-term average of the warmest month) impose heat stress levels above the limits of tolerance of the symbiotic relationship, inducing the collapse of the algal and coral functional association (Hoegh-Guldberg, 1999). As a result, coral reefs are projected to decline by a further 70–90% (> 99% at 2°C) (Hoegh-Guldberg, 1999; IPCC, 2019). Driven by the association between coral bleaching and coral reef persistence, intense research efforts have been directed to understand coral responses to heat-stress, with a large body of evidence directing to the impairment of algal symbiont photosynthesis and subsequent host programmed cell death (PCD) [reviewed in Weis (2008)]. However, understanding the cascade of events that leads to the development of the bleached coral phenotype is still very limited.

Advances in our understanding of the inter-partner communication during thermal stress responses place reactive oxygen species (ROS) at the center of the physiological disturbance (Weis, 2008; Baird et al., 2009). In homeostasis, chloroplasts, peroxisomes, and mitochondria are continuously producing ROS, maintaining radicals at relatively low

levels (Chan et al., 2010). When thermal stress is under the limits of tolerance for the symbiosis, increased ROS levels are non-deleterious, and corals adjust to alternative homeostatic states depending on the overall cellular quantity of ROS. When thermal stress is outside the limits of tolerance, deleterious oxidative stress triggers coral bleaching, suggested by the strong correlation between induction of ROS and the accumulation of oxidative damage products in both the algal symbiont and host (Brown et al., 2002; Downs et al., 2002; Dias et al., 2019). Long-standing attributions of "oxidative-damage" associated with ROS are challenged by the realization that they are secondary intracellular messengers, essential for the homeostasis of organisms (Chan et al., 2010; Acín-Pérez et al., 2014). This results in the difficult task of separating coral light acclimation and thermal acclimation with the development of the bleached phenotype.

Homeostasis is accomplished through a complex network of interacting genes and biochemical pathways, where different stressors can affect common sets of genes or gene families, which is consistent with the observation that certain overlapped pathways are involved in coral physiological responses to various stressors. Although key phenotypic descriptions may solve this limitation, there no agreement on the definition of the bleached coral phenotype. Large losses of pigments and/or symbionts are insufficient in identifying the bleached condition, and alternative descriptors such as the cessation of photosynthetic activity and large alterations to optical traits have been found to be robust proxies (Scheufen et al., 2017a,b). In this perspective, we used the optical trait a^*_{Chla} (holobiont light absorption efficiency) to quantify the seasonal variability of the acclimatory coral condition and to identify the bleached phenotype (Scheufen et al., 2017b). We conceptually delineate the possible sequence of events linking early sensing of thermal stress in the algal symbiont chloroplast, with host cascade responses leading to the bleached phenotype.

LIMITS OF SEASONAL ACCLIMATION

Solar radiation is the main source of energy for all photosynthetic primary producers, as well as for symbiotic corals, an evolutionary consequence of a mutualistic association with intracellular photosynthetic algae. Translocation of algal photosynthates satisfies the majority of the carbon metabolic requirements of the coral host and is also responsible for the high rates of calcification that allow for the creation of tropical coral reefs. A prominent emergent property of this mutualism is the optimization of light absorption with a minimum investment of resources, making symbiotic corals one of the most efficient light collectors currently known (Enríquez et al., 2005, 2017; Terán et al., 2010). Given the metabolic integration of host and symbiont, acclimation to light or photoacclimation is a time-dependent process that occur in all cellular compartments. At the symbiont chloroplast level, adjustments in the photosynthetic apparatus (Iglesias-Prieto and Trench, 1997; Gorbunov et al., 2001) operate on the scale of seconds to days. At the coral colony level, changes in tissue pigmentation (Fitt et al., 2000; Scheufen et al., 2017a), relative abundance of different algal symbiont species (Rowan and Knowlton, 1995; Kemp et al., 2015; Hoadley et al., 2019) and morphological and skeletal changes (Gladfelter, 1984; Todd, 2008; Malik et al., 2021) operate over periods of weeks to months. Overall, responses involve changes in host metabolism (Lohr et al., 2019) and gene expression (Malik et al., 2021). Distinctly, a main feature of symbiotic coral photoacclimation to light is to ensure optimal photosynthetic activity that guarantees enough translocation of photosynthates to the host. This places the photosynthetic activity of symbionts *in hospite* at the center of cellular processes that regulate coral phenotypes (Scheufen et al., 2017a).

Seasonal changes in photosynthetic active radiation (PAR) and sea surface temperature (SST) drive seasonal acclimation in symbiotic corals, resulting in winter and summer phenotypes (Brown et al., 1999; Fagoonee et al., 1999; Carricart-Ganivet et al., 2000; Fitt et al., 2000; Warner et al., 2002; Scheufen et al., 2017a). Winter phenotypes are generally characterized by higher pigmentation and quantum yield of Chlorophyll *a* (Chl*a*) fluorescence *in hospite* (*Fv/Fm*). In contrast, summer phenotypes are more efficient light collectors (**Figure 1A**), characterized by decreased symbiont densities, Chl*a*, *Fv/Fm*, and increased photosynthetic and calcification rates. With the overall decrease of Chl*a* density in the tissue, corals increase exponentially the absorption efficiency of their pigments (a^*_{Chla}) due to multiple scattering processes in the coral skeleton (Enríquez et al., 2005). This results in a distinguishable winter-to-summer shift of the light absorption efficiency of the holobiont (a^*_{Chla}) (**Figure 1A**). Multiple scattering of light on the coral skeleton produces diffuse light in the tissue, reducing pigment self-shading and increasing the probability of light absorption for the symbionts *in hospite* (Enríquez et al., 2005). In summer phenotypes, these processes allow significant enhancements of the local irradiance within the tissue for a smaller symbiont population, setting the limits of the seasonal variation with this reduction (Enríquez et al., 2005) (**Figure 1A**).

The well-balanced winter-to-summer oscillation is disrupted during thermal anomalies (Hoegh-Guldberg, 1999). Under these conditions, the symbiosis falls into a positive feed-back loop, with the loss of symbiont cells enhancing the local irradiance within the tissue, inducing further losses of symbiont cells. Increase in magnitude of the environmental stress accelerates this symbiont loss and bleaching (Swain et al., 2016), which is evident in an a^*_{Chla} inflection point (**Figure 1A**). This pushes the symbiosis outside the limits of tolerance, compromising homeostasis, and crosses the "tipping point" toward the bleached phenotype. The severe loss of the symbiont population results in a no longer functional symbiosis. If the deleterious stress is removed in time, the symbiosis may be functionally re-established, but if the stress persists, a further "tipping point" will lead to mass mortality accompanied with an ecosystem collapse.

CASCADE OF CELLULAR EVENTS

Homeostasis establishment associated with a new acclimatory state is not the result of a single physiological process, but rather the result of many biological processes that the coral

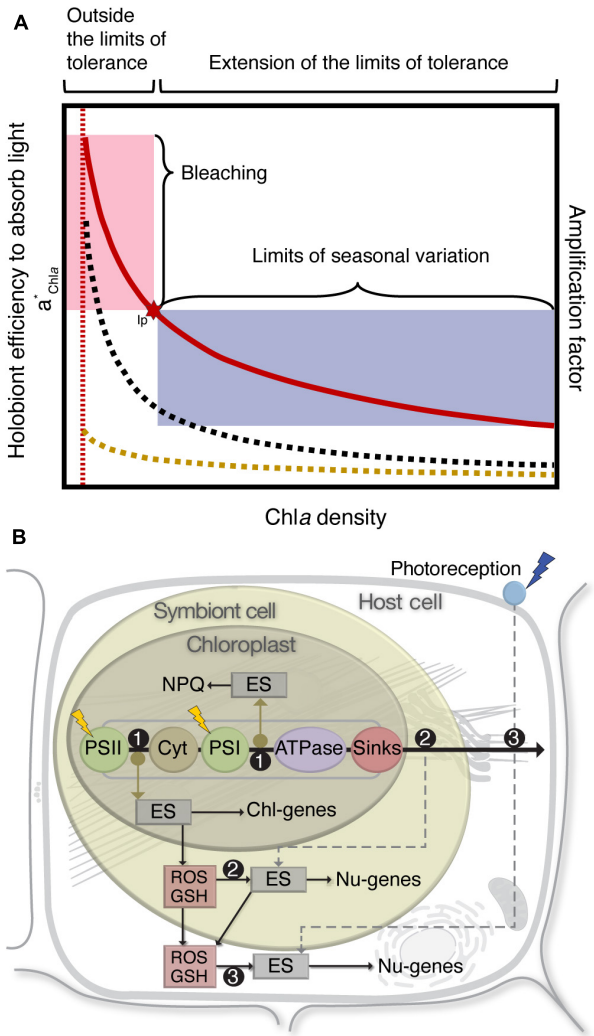

FIGURE 1 | Seasonal phenotypic variation and cellular communication in symbiotic corals. **(A)** Seasonal changes in holobiont light absorption efficiency (quantified by means of the specific absorption coefficient of Chlorophyll *a*, a^*_{Chla}) as a function of pigment (Chl*a*) density in corals. Lines show the comparative increase in light absorption efficiency of freshly isolated symbiont cells (yellow dashed line), absorption by intact coral laminae (black dashed line), and the estimated enhanced factor of light absorption resulting from the comparison of both optical measurements (red line). This amplification or "enhancement factor" is the consequence of the capacity of the coral skeleton to induce multiple scattering of light. Inflection point (*Ip*) of a^*_{Chla} sets a limit for the variation of the coral photoacclimatory response (shaded blue area) and the development of the bleached phenotype (shaded red area) [modified from Enríquez et al. (2005)]. **(B)** Responses in the different cellular compartments of the holosymbiont: (1) Chloroplasts perceive the environmental change as "light stress," the increase in electron transfer produces over-reduction in the PQ-pool and a ΔpH + (with associated NPQ) across the thylakoid membrane; the net result is the decrease in *Fv/Fm* and the generation of an alternative homeostatic state. (2) Symbiont cells perceive the change as "oxidative stress," energy sensors (ES) activate changes in gene expression; the net result is the decrease in symbiont pigmentation and an alternative homeostatic state. (3) Host cells perceive the change as "thermal stress," energy sensors activate changes in gene expression, and immune responses facilitate symbiont trafficking to adjust symbiont cell density in the host tissue; the net result is an alternative homeostatic state that sets the limits of acclimation. (Chl-genes) Chloroplast genes, (Nu-genes) Nuclear genes, (GSH) Glutathione.

integrates over time. Compartmentalization of the eukaryotic cell into different organelles presents paradigms in the regulation of homeostasis compared to prokaryotes, where all the main cellular processes happen within the same compartment (Chan et al., 2010). Compartmentalization is especially relevant for symbiotic corals, where additional cellular compartments are present (chloroplasts, algal symbiont cells). Descriptions of changes in coral metabolic activity over the past few decades has led to the general agreement that crosstalk between the chloroplast, the symbiont cell and the host occur to coordinate holosymbiont homeostasis [reviewed in Davy et al. (2012)]. In this context, ROS is the key player as a secondary intracellular messenger among the different cellular compartments and its production is required for cellular signaling to induce different cellular adjustments (Cruz De Carvalho, 2008). Reactive oxygen species levels are kept under control by an orchestrated enzymatic and antioxidant efficient system that sets the redox-status of the cell. Its signaling to the nucleus turns on such defense mechanisms to minimize its deleterious effects (Erickson et al., 2015). Moreover, extra-mitochondrial source of ROS can trigger metabolic cellular adjustments in the mitochondria (Acín-Pérez et al., 2014), fundamental in any acclimatory response to temperature variation.

The starting point for the transition to a summer phenotype is in the chloroplast (**Figure 1B**). The documented coral response suggests that this environmental change is perceived as "light stress" resulting in increased light absorption and decreased *Fv/Fm*. The increased electron transport via a series of electron carriers produces an over reduction of the plastoquinone pool (PQ-pool) and expands the pH gradient (ΔpH +) across the membrane, producing more adenosine triphosphate (ATP). ΔpH + influences thermal dissipation via non-photochemical quenching (NPQ), which provides a mechanism that protects the photosynthetic apparatus from excess excitation energy (EEE), and has been shown to be associated with the conversion of diadinoxanthin to diatoxanthin (xanthophyll cycling) (Brown, 1997). With the change in electron transfer, ROS can fluctuate in specific concentrations due to phase transitions of thylakoid membrane lipids (Iglesias-Prieto et al., 1992; Tchernov et al., 2004), thermal inactivation of both photosystem II (PSII) (Iglesias-Prieto, 1996; Warner et al., 1996, 1999; Iglesias-Prieto and Trench, 1997) and Ribulose-1,5-bisphosphate carboxylase-oxygenase (RuBisCO) (Jones et al., 1998), damage of repair mechanisms in PSII (Warner et al., 1999; Takahashi et al., 2004), and changes in inorganic carbon concentrations (sink limitation) (Buxton et al., 2009). This alters chloroplast gene expression and ROS "leak" to the symbiont cytoplasm, functioning as components of environmental-signaling pathways (Chan et al., 2010). The modulation of this response can be considered as the signal for corals to establish a new homeostatic state, which is reversible upon removal of the external stress.

As SST and PAR continue to increase toward the summer, symbiont cells perceive *in hospite* the environmental change as increasing levels of "oxidative stress" and increases in excitation pressure in their photosynthetic apparatus. Under these conditions, an energy sensor from the cytochrome b6f

(Cytb6f) activates changes in nuclear gene expression to modify light-harvesting antenna size (**Figure 1B**) (Gierz et al., 2016, 2017). Light and thermal stress are associated with the loss and inhibition of *de novo* synthesis of the major light-harvesting complexes (Dove et al., 2006; Takahashi et al., 2008). Moreover, NPQ-associated xanthophyll cycling decreases photon flux to PSII reaction centers, thus preventing over reduction of the PQ-pool by reducing the functional absorption cross-section of PSII reaction centers (σPSII). This new homeostatic state with decreased symbiont pigmentation is reversible upon removal of the external stress.

Later in the summer, with continuation of the environmental change, levels of oxidative stress continue to increase, and ROS can activate changes in nuclear gene expression to induce PCD in the host cell (and/or symbiont cell), reducing the number of symbionts in the host tissue (**Figure 1B**). Although the exact mechanism by which symbiont cell numbers are controlled is not known, immune responses play a key role in symbiont trafficking (Davy et al., 2012). Moreover, it is recognized that cellular mechanisms of symbiont loss involve symbiont degradation, exocytosis, host cell detachment (with the intact symbiont), host cell apoptosis, autophagy, and/or necrosis (Gates et al., 1992; Dunn et al., 2002, 2007; Weis, 2008; Downs et al., 2009; Paxton et al., 2013). The decrease of overall Chl*a* density in the host tissue, via reduction in Chl*a* per symbiont cell as well as symbiont cell loss, results in the development of the summer phenotype at the end of the warmest period. This new homeostatic state with decreased *Fv/Fm*, symbiont densities, and host tissue pigmentation is the result of ROS-mediated changes in the different cellular compartments of a mechanism tightly controlled by oxidant scavengers providing the flexibility to acclimate to PAR and SST. The fact that the summer phenotype presents higher coral performance (photosynthesis and calcification rates) (Scheufen et al., 2017a), demonstrates a successful acclimation through a cascade of cellular events previously described. This state is reversible when environmental conditions change, and the coral returns to the previous homeostatic state. If temperature continues to increase into a prolonged thermal anomaly over the symbiosis limits of tolerance, all these homeostatic mechanisms can be overwhelmed, and a bleached coral phenotype is developed.

THE BLEACHED CORAL PHENOTYPE

Prolonged thermal anomalies (+ 1.5–2°C above the long-term average of the warmest month) drive the symbiosis outside its limits of tolerance. The thermal stress is exacerbated by the enhanced local illumination of the symbionts within the tissue, a physical change that explains the severe loss of symbionts during thermal stress. The extreme environmental condition accelerates the production of ROS, eventually overwhelming antioxidant responses. This extremely high reactivity facilitates extensive cellular damage, including cellular membrane lipid peroxidation (LPO), DNA degradation, and protein denaturation (Weis, 2008; Roth, 2014). Although carbon fixation may continue via the Calvin cycle, net translocation is significantly reduced (Hillyer et al., 2017).

In this view, a plausible mechanistic road map recognizes acclimatory states before the development of a bleached coral phenotype. When exposed to thermal anomalies above the limits of tolerance, several attempts to acclimate will take place within the chloroplast, the symbiont cell (by oxidative stress), and the host cell (with PCD), with subsequent failure to maintain a functional symbiosis. With the accumulation of deleterious oxidative damage, most symbiotic corals will eventually develop a bleached phenotype through the same acclimatory attempts. However, differences in coral susceptibility arise when we disentangle the acclimatory state prior to the exposure to stress and the susceptibility of the resident symbiont species. Understanding these differences will allow for the determination of a starting point in the road map that will determine the steps involved in developing the bleached phenotype.

The last few decades have seen many new and exciting findings paving the way to a better understanding of coral stress responses [reviewed in Putnam (2021)]. Some of the major areas of focus include genomics, symbiont responses in cultured conditions, acclimation in depth gradients, and coral bleaching. These conditions are associated with the need to partition coral light acclimation, thermal acclimation, and the definition of a bleached coral phenotype. However, there are scarce approaches to delineate these differences, even when environmental stress is a major factor changing homeostatic states and coral acclimation. ROS are produced during normal cell metabolism and their regulation is a common cellular event accompanied with oxidative damage (Dat et al., 2000). This mechanism triggers different homeostatic states in the coral

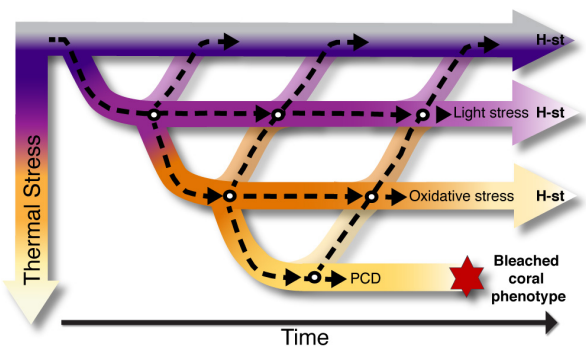

FIGURE 2 | Road map of homeostatic states leading to the bleached coral phenotype. Light and thermal responses triggered by ROS as a secondary cellular messenger, are considered as the signal for corals to initiate processes required for the establishment of new homeostatic states (H-st). Within the road map, several phenotypic steps take place (white circles) to achieve the new H-st. These states are time dependent and take place in the different compartments of the cell: in the chloroplast (light stress), symbiont cell (oxidative stress) and host cell (oxidative stress and Program Cell Death). All H-st are reversible when environmental conditions change, and the coral may return to previous homeostatic states. When thermal stress increases above the limits of tolerance of the symbiosis, the net accumulation of oxidative damage is deleterious and corals are unable to adjust by establishing a new homeostatic state, developing the bleached phenotype.

(**Figure 2**), with initial stimuli in the chloroplast, evident in the variation of excitation pressure and *Fv/Fm* of symbionts *in hospite*. If acclimation is not successful, the next step may be controlled by ROS levels regulating expression of the light-harvesting complexes (Gierz et al., 2016, 2017). If acclimation is still not successful and the production of ROS continues, it may trigger the regulation of symbiont cell densities in the host tissue, similar to seasonal variation (**Figure 2**). In this context, a continuous reduction in symbiont cell numbers may lead to the development of the bleached coral phenotype.

The different roles of ROS, both in acclimation and in the development of a bleached phenotype, results in a duality that drives distinct processes in the symbiosis. Ecological studies may track seasonal and bleaching dynamics at the ecosystem level with non-invasive techniques. However, to disentangle bleaching mechanisms, experimental approaches are more suitable. In this case, commonly used parameters to quantify coral bleaching such as, decrease in *Fv/Fm*, decrease in pigmentation (merely chl*a* density and color charts), increase in ROS abundance, are insufficient to identify a bleached phenotype and fully describe the physiological condition of the coral. It is imperative to account for the loss of symbiont cells in the host tissue, to distinguish between acclimatory conditions (limits of acclimation) and bleached coral conditions. This, to reduce the source of uncertainties in the understanding of coral responses to climate change, fundamental for the development of predictive climate models.

DATA AVAILABILITY STATEMENT

The original contributions presented in the study are included in the article/supplementary material, further inquiries can be directed to the corresponding authors.

AUTHOR CONTRIBUTIONS

KG-C and RI-P wrote the manuscript. SE critical conceptual inputs. All authors contributed to manuscript revision, read, and approved the submitted version.

FUNDING

Projects to complement gaps in knowledge has received funding from The Pennsylvania State University Start-up awarded to RI-P.

REFERENCES

Acín-Pérez, R., Carrascoso, I., Baixauli, F., Roche-Molina, M., Latorre-Pellicer, A., Fernández-Silva, P., et al. (2014). ROS-triggered phosphorylation of complex II by Fgr kinase regulates cellular adaptation to fuel use. *Cell Metab.* 19, 1020–1033. doi: 10.1016/j.cmet.2014.04.015

Baird, A. H., Bhagooli, R., Ralph, P. J., and Takahashi, S. (2009). Coral bleaching: the role of the host. *Trends Ecol. Evol.* 24, 16–20.

Brown, B. E. (1997). Coral bleaching: causes and consequences. *Coral Reefs*. 16, 129–138.

Brown, B. E., Downs, C. A., Dunne, R. P., and Gibb, S. W. (2002). Exploring the basis of thermotolerance in the reef coral Goniastrea aspera. *Mar. Ecol. Prog. Ser.* 242, 119–129.

Brown, B. E., Dunne, R. P., Ambarsari, I., Tissier, M. D. A. Le, and Satapoomin, U. (1999). Seasonal fluctuations in environmental factors and variations in symbiotic algae and chlorophyll pigments in four Indo-Pacific coral species. *Mar. Ecol. Prog. Ser.* 191, 53–69. doi: 10.3354/meps191053

Buxton, L., Badger, M., and Ralph, P. (2009). Effects of moderate heat stress and dissolved inorganic carbon concentration on photosynthesis and respiration of symbiodinium sp. (dinophyceae) in culture and in symbiosis. *J. Phycol.* 45, 357–365. doi: 10.1111/j.1529-8817.2009.00659.x

Carricart-Ganivet, J. P., Beltrán-Torres, A. U., Merino, M., and Ruiz-Zárate, M. A. (2000). Skeletal extension, density and calcification rate of the reef building coral Montastraea annularis (Ellis and Solander) in the Mexican Caribbean. *Bull. Mar. Sci.* 66, 215–224.

Chan, K. X., Crisp, P. A., Estavillo, G. M., and Pogson, B. J. (2010). Chloroplast-to-nucleus communication: Current knowledge, experimental strategies and relationship to drought stress signaling. *Plant Signal. Behav.* 5, 1575–1582. doi: 10.4161/psb.5.12.13758

Cruz De Carvalho, M. H. (2008). Drought stress and reactive oxygen species: Production, scavenging and signaling. *Plant Signal. Behav.* 3, 156–165. doi: 10.4161/psb.3.3.5536

Dat, J., Vandenabeele, S., Vranová, E., Van Montagu, M., Inzé, D., and Van Breusegem, F. (2000). Dual action of the active oxygen species during plant stress responses. Cell. Mol. Life Sci. 57, 779–795. doi: 10.1007/s000180050041

Davy, S. K., Allemand, D., and Weis, V. M. (2012). Cell Biology of Cnidarian-Dinoflagellate Symbiosis. *Microbiol. Mol. Biol. Rev.* 76, 229–261. doi: 10.1128/MMBR.05014-11

Dias, M., Ferreira, A., Gouveia, R., Madeira, C., Jogee, N., Cabral, H., et al. (2019). Long-term exposure to increasing temperatures on scleractinian coral fragments reveals oxidative stress. *Mar. Environ. Res.* 150:104758. doi: 10.1016/j.marenvres.2019.104758

Dove, S., Ortiz, J. C., Enríquez, S., Fine, M., Fisher, P., Iglesias-Prieto, R., et al. (2006). Response of holosymbiont pigments from the scleractinian coral Montipora monasteriata to short-term heat stress. *Limnol. Oceanogr.* 51, 1149–1158.

Downs, C. A., Fauth, J. E., Halas, J. C., Dustan, P., Bemiss, J., and Woodley, C. M. (2002). Oxidative stress and seasonal coral bleaching. *Free Radic. Biol. Med.* 33, 533–543. doi: 10.1016/s0891-5849(02)00907-3

Downs, C. A., Kramarsky-Winter, E., Martinez, J., Kushmaro, A., Woodley, C. M., Loya, Y., et al. (2009). Symbiophagy as a cellular mechanism for coral bleaching. *Autophagy*. 5, 211–216. doi: 10.4161/auto.5.2.7405

Dunn, S. R., Bythell, J. C., Le Tissier, M. D. A., Burnett, W. J., and Thomason, J. C. (2002). Programmed cell death and cell necrosis activity during hyperthermic stress-induced bleaching of the symbiotic sea anemone Aiptasia sp. *J. Exp. Mar. Bio. Ecol.* 272, 29–53. doi: 10.1016/s0022-0981(02)00036-9

Dunn, S. R., Schnitzler, C. E., and Weis, V. M. (2007). Apoptosis and autophagy as mechanisms of dinoflagellate symbiont release during cnidarian bleaching: Every which way you lose. *Proc. R. Soc. B Biol. Sci.* 274, 3079–3085. doi: 10.1098/rspb.2007.0711

Enríquez, S., Méndez, E. R., Hoegh-Guldberg, O., and Iglesias-Prieto, R. (2017). Key functional role of the optical properties of coral skeletons in coral ecology and evolution. *Proc. R. Soc. B Biol. Sci.* 284:20161667. doi: 10.1098/rspb.2016.1667

Enríquez, S., Méndez, E. R., and Iglesias-Prieto, R. (2005). Multiple scattering on coral skeletons enhances light absorption by symbiotic algae. *Limnol. Oceanogr.* 50, 1025–1032. doi: 10.1364/AO.49.005032

Erickson, E., Wakao, S., and Niyogi, K. K. (2015). Light stress and photoprotection in Chlamydomonas reinhardtii. *Plant J.* 82, 449–465. doi: 10.1111/tpj.12825

Fagoonee, I., Wilson, H. B., Hassell, M. P., and Turner, J. R. (1999). The Dynamics of Zooxanthellae Populations: A Long-Term Study in the Field. *New Ser.* 283, 843–845. doi: 10.1126/science.283.5403.843

Fitt, W. K., McFarland, F. K., Warner, M. E., and Chilcoat, G. C. (2000). Seasonal patterns of tissue biomass and densities of symbiotic dinoflagellates in reef corals and relation to coral bleaching. *Limnol. Oceanogr.* 45, 677–685. doi: 10.1371/journal.pone.0029535

Gates, R. D., Baghdasarian, G., and Muscatine, L. (1992). Temperature stress causes host cell detachment in symbiotic cnidarians: implications for coral bleaching. *Biol. Bull.* 182, 324–332. doi: 10.2307/1542252

Gierz, S. L., Forêt, S., and Leggat, W. (2017). Transcriptomic analysis of thermally stressed Symbiodinium reveals differential expression of stress and metabolism genes. *Front. Plant Sci* 8:271. doi: 10.3389/fpls.2017.00271

Gierz, S. L., Gordon, B. R., and Leggat, W. (2016). Integral Light-Harvesting Complex Expression in Symbiodinium Within the Coral Acropora aspera under Thermal Stress. *Sci. Rep.* 6:25081. doi: 10.1038/srep25081

Gladfelter, E. H. (1984). Skeletal development in Acropora cervicornis - III. A comparison of monthly rates of linear extension and calcium carbonate accretion measured over a year. *Coral Reefs.* 3, 51–57. doi: 10.1007/bf00306140

Gorbunov, M. Y., Kolber, Z. S., and Lesser, M. P. (2001). Photosynthesis and photoprotection in symbiotic corals. *Limnol. Oceanogr.* 46, 75–85. doi: 10.4319/lo.2001.46.1.0075

Hillyer, K. E., Dias, D. A., Lutz, A., Roessner, U., and Davy, S. K. (2017). Mapping carbon fate during bleaching in a model cnidarian symbiosis: the application of 13C metabolomics. *New Phytol.* 214, 1551–1562. doi: 10.1111/nph.14515

Hoadley, K. D., Lewis, A. M., Wham, D. C., Pettay, D. T., Grasso, C., Smith, R., et al. (2019). Host–symbiont combinations dictate the photo-physiological response of reef-building corals to thermal stress. *Sci. Rep.* 9, 1–15. doi: 10.1038/s41598-019-46412-4

Hoegh-Guldberg, O. (1999). Climate change, coral bleaching and the future of the world's coral reefs. *Mar. Freshw. Res.* 50, 839–866.

Iglesias-Prieto, R. (1996). Temperature-dependent inactivation of photosystem II in symbiotic dinoflagellates. *Proc 8th Int Coral Reef Symp. Panama* 2, 1313–1318.

Iglesias-Prieto, R., Matta, J. L., Robins, W. A., and Trench, R. K. (1992). Photosynthetic response to elevated temperature in the symbiotic dinoflagellate Symbiodinium microadriaticum in culture. *Proc. Natl. Acad. Sci. U.S.A.* 89, 10302–10305. doi: 10.1073/pnas.89.21.10302

Iglesias-Prieto, R., and Trench, R. K. (1997). Acclimation and adaptation to irradiance in symbiotic dinoflagellates. II. Response of chlorophyll-protein complexes to different photon-flux densities. *Mar. Biol.* 130, 23–33. doi: 10.1007/s002270050221

IPCC. (2019). "Summary for Policymakers," in *IPCC Special Report on the Ocean and Cryosphere in a Changing Climate*, eds H.-O. Pörtner, D. C. Roberts, and V. Masson (Switzerland: IPCC).

Jones, R. J., Hoegh-Guldberg, O., Larkum, A. W. D., and Schreiber, U. (1998). Temperature-induced bleaching of corals begins with impairment of the CO2 fixation mechanism in zooxanthellae. *Plant Cell Environ.* 21, 1219–1230. doi: 10.1046/j.1365-3040.1998.00345.x

Kemp, D. W., Thornhill, D. J., Rotjan, R. D., Iglesias-Prieto, R., Fitt, W. K., and Schmidt, G. W. (2015). Spatially distinct and regionally endemic Symbiodinium assemblages in the threatened Caribbean reef-building coral Orbicella faveolata. *Coral Reefs.* 34, 535–547. doi: 10.1007/s00338-015-1277-z

Lohr, K. E., Camp, E. F., Kuzhiumparambil, U., Lutz, A., Leggat, W., Patterson, J. T., et al. (2019). Resolving coral photoacclimation dynamics through coupled photophysiological and metabolomic profiling. *J. Exp. Biol.* 222:jeb195982. doi: 10.1242/jeb.195982

Malik, A., Einbinder, S., Martinez, S., Tchernov, D., Haviv, S., Almuly, R., et al. (2021). Molecular and skeletal fingerprints of scleractinian coral biomineralization: From the sea surface to mesophotic depths. *Acta Biomater.* 120, 263–276. doi: 10.1016/j.actbio.2020.01.010

Paxton, C. W., Davy, S. K., and Weis, V. M. (2013). Stress and death of cnidarian host cells play a role in cnidarian bleaching. *J. Exp. Biol.* 216, 2813–2820. doi: 10.1242/jeb.087858

Putnam, H. M. (2021). Avenues of reef-building coral acclimatization in response to rapid environmental change. *J. Exp. Biol.* 224:jeb239319. doi: 10.1242/jeb.239319

Roth, M. S. (2014). The engine of the reef: Photobiology of the coral-algal symbiosis. *Front. Microbiol.* 5:422. doi: 10.3389/fmicb.2014.00422

Rowan, B., and Knowlton, N. (1995). Intraspecific diversity and ecological zonation in coral-algal symbiosis. *Proc. Natl. Acad. Sci.U.S.A.* 92, 2850–2853. doi: 10.1073/pnas.92.7.2850

Scheufen, T., Iglesias-prieto, R., and Enríquez, S. (2017a). Changes in the Number of Symbionts and Symbiodinium Cell Pigmentation Modulate Differentially Coral Light Absorption and Photosynthetic Performance. *Front. Mar. Sci.* 4:309. doi: 10.3389/fmars.2017.00309/full

Scheufen, T., Kraemer, W. E., Iglesias-Prieto, R., and Enriquez, S. (2017b). Seasonal variation modulates coral sensibility to heat-stress and explains annual changes in coral productivity. *Sci. Rep* 7:4937. doi: 10.1038/s41598-017-04927-8

Swain, T. D., DuBois, E., Gomes, A., Stoyneva, V. P., Radosevich, A. J., Henss, J., et al. (2016). Skeletal light-scattering accelerates bleaching response in reef-building corals. *BMC Ecol* 16:10. doi: 10.1186/s12898-016-0061-4

Takahashi, S., Nakamura, T., Sakamizu, M., Van Woesik, R., and Yamasaki, H. (2004). Repair Machinery of Symbiotic Photosynthesis as the Primary Target of Heat Stress for Reef-Building Corals. *Plant Cell Physiol.* 45, 251–255. doi: 10.1093/pcp/pch028

Takahashi, S., Whitney, S., Itoh, S., Maruyama, T., and Badger, M. (2008). Heat stress causes inhibition of the de novo synthesis of antenna proteins and photobleaching in cultured Symbiodinium. *Proc. Natl. Acad. Sci.U.S.A.* 105, 4203–4208. doi: 10.1073/pnas.0708554105

Tchernov, D., Gorbunov, M. Y., Vargas, C. De, Yadav, S. N., Milligant, A. J., Häggblom, M., et al. (2004). Membrane lipids of symbiotic algae are diagnostic of sensitivity to thermal bleaching in corals. *Proc. Natl. Acad. Sci.U.S.A.* 101, 13531–13535. doi: 10.1073/pnas.0402907101

Terán, E., Méndez, E. R., Enríquez, S., and Iglesias-Prieto, R. (2010). Multiple light scattering and absorption in reef-building corals. *Appl. Opt.* 49, 5032–5042.

Todd, P. A. (2008). Morphological plasticity in scleractinian corals. *Biol. Rev.* 83, 315–337.

Warner, M. E., Chilcoat, G. C., McFarland, F. K., and Fitt, W. K. (2002). Seasonal fluctuations in the photosynthetic capacity of photosystem II in symbiotic dinoflagellates in the Caribbean reef-building coral Montastraea. *Mar. Biol.* 141, 31–38. doi: 10.1007/s00227-002-0807-8

Warner, M. E., Fitt, W. K., and Schmidt, G. W. (1999). Damage to photosystem II in symbiotic dinoflagellates: a determinant of coral bleaching. *Proc. Natl. Acad. Sci.U.S.A.* 96, 8007–8012. doi: 10.1073/pnas.96.14.8007

Warner, W. K., Fitt, W. K., and Schmidt, G. W. (1996). The effects of elevated temperature on the photosynthetic efficiency of zooxantheliae in hospiteUom four different species of reef coral: a novel approach. *Plant Cell Environ.* 19, 291–299.

Weis, V. M. (2008). Cellular mechanisms of Cnidarian bleaching: Stress causes the collapse of symbiosis. *J. Exp. Biol.* 211, 3059–3066. doi: 10.1242/jeb.009597

Conflict of Interest: The authors declare that the research was conducted in the absence of any commercial or financial relationships that could be construed as a potential conflict of interest.

frontiers | Frontiers in Physiology

ORIGINAL RESEARCH
published: 11 April 2022
doi: 10.3389/fphys.2022.806171

Metatranscriptomic Analysis of Corals Inoculated With Tolerant and Non-Tolerant Symbiont Exposed to High Temperature and Light Stress

Ikuko Yuyama[1], Tomihiko Higuchi[2], Takuma Mezaki[3], Hisako Tashiro[4] and Kazuho Ikeo[4]*

[1] Graduate School of Science and Technology for Innovation, Yamaguchi University, Yamaguchi, Japan, [2] Atmosphere and Ocean Research Institute, The University of Tokyo, Kashiwa, Japan, [3] Kuroshio Biological Research Foundation, Otsuki, Japan, [4] Department of Genomics and Evolutionary Biology, National Institute of Genetics, Mishima, Japan

OPEN ACCESS

Edited by:
Davide Seveso, University of Milano-Bicocca, Italy

Reviewed by:
Javier Antonio Rodriguez-Casariego, Florida International University, United States
Jitendra Kumar Sundaray, Indian Council of Agricultural Research, India
Josef Velíšek, University of South Bohemia, Czechia

***Correspondence:**
Ikuko Yuyama
yuyamai@gmail.com

Specialty section:
This article was submitted to Aquatic Physiology, a section of the journal Frontiers in Physiology

Received: *31 October 2021*
Accepted: *17 February 2022*
Published: *11 April 2022*

Citation:
Yuyama I, Higuchi T, Mezaki T, Tashiro H and Ikeo K (2022) Metatranscriptomic Analysis of Corals Inoculated With Tolerant and Non-Tolerant Symbiont Exposed to High Temperature and Light Stress. Front. Physiol. 13:806171. doi: 10.3389/fphys.2022.806171

Algal symbionts of corals can influence host stress resistance; for example, in the Pacific Ocean, whereas *Cladocopium* (C-type) is generally dominant in corals, *Durusdinium* (D-type) is found in more heat-resistant corals. Thus, the presence of D-type symbiont likely increases coral heat tolerance, and this symbiotic relationship potentially provides a hint to increase the stress tolerance of coral–algal symbioses. In this study, transcriptome profiles of *Cladocopium*- and *Durusdinium*-harboring *Acropora solitaryensis* (C-coral and D-coral, respectively) and algal photosystem functioning (F_v/F_m) under bleaching conditions (high temperature and light stress) were compared. Stress treatment caused algal photoinhibition that the F_v/F_m value of Symbiodiniaceae was immediately reduced. The transcriptome analysis of corals revealed that genes involved in the following processes were detected: endoplasmic reticulum (ER) stress, mitophagy, apoptosis, endocytosis, metabolic processes (acetyl-CoA, chitin metabolic processes, etc.), and the PI3K-AKT pathway were upregulated, while DNA replication and the calcium signaling pathway were downregulated in both C- and D-corals. These results suggest that unrepaired DNA and protein damages were accumulated in corals under high temperature and light stress. Additionally, some differentially expressed genes (DEGs) were specific to C- or D-corals, which includes genes involved in transient receptor potential (TRP) channels and vitamin B metabolic processes. Algal transcriptome analysis showed the increased expression of gene encoding photosystem and molecular chaperone especially in D-type symbiont. The transcriptome data imply a possible difference in the stress reactions on C-type and D-type symbionts. The results reveal the basic process of coral heat/light stress response and symbiont-type-specific coral transcriptional responses, which provides a perspective on the mechanisms that cause differences in coral stress tolerance.

Keywords: coral bleaching, endosymbiosis, *Cladocopium*, *Durusdinium*, *Acropora solitaryensis*, RNA-seq

INTRODUCTION

Mass coral bleaching, which mainly occurs due to elevated sea surface temperatures, is a state in which algal symbionts (family Symbiodiniaceae, hereinafter referred to as "symbionts") are decreased in host corals over a wide area. Bleaching phenomena cause fatal impact in the most cases to host corals because the loss of alga does not provide the expected amount of energy source to the host (Baker et al., 2008; Baird et al., 2017). Coral bleaching, caused by high temperatures and strong irradiance, is accompanied by photoinhibition of Symbiodiniaceae (Lesser and Shick, 1989; Warner et al., 1999; Gorbunov et al., 2001; Lesser, 2011). Photoinhibition refers to light-induced reduction of the photosynthetic rate as a result of the generation of reactive oxygen species (ROS) from the excess light energy over the limits of the CO_2 fixation process (Murata et al., 2007). ROS damage the reaction center of photosystem II (PSII), and high temperatures inhibit the repair of this damage, which results in a decline of the photosynthetic rate of symbiont algae (Takahashi et al., 2009). Symbiont-produced ROS can also damage lipids, proteins, and DNA of host corals and increase expression and/or activity of the antioxidant enzymes superoxide dismutase and catalase in corals (Lesser, 1997; Higuchi et al., 2009). In addition, the generation of nitric oxide (NO) has also been reported as a key factor of bleaching phenomena (Trapido-Rosenthal et al., 2005; Perez and Weis, 2006; Bouchard and Yamasaki, 2008; Hawkins et al., 2013).

The underlying process of coral bleaching has been studied at the molecular level and the expression changes of heat shock proteins (Hsp, DnaJ) (Császár et al., 2009; Meyer et al., 2011; Yuyama et al., 2012; Maor-Landaw and Levy, 2016), antioxidant enzymes (catalase, thioredoxin, MnSOD) (Edge et al., 2005; Császár et al., 2009; Seneca et al., 2010; Maor-Landaw and Levy, 2016), immune system-related genes (TNF receptors, TNF receptor-associated factors) (Voolstra et al., 2009; Barshis et al., 2013), and metabolic process-related genes (carbonic anhydrase, adenine transporter, and calcium channels) (Edge et al., 2005; Meyer et al., 2011) have been reported. Furthermore, the involvement of apoptosis and autophagy-related proteins, such as Bcl-2 and caspase, in the bleaching response was also revealed by the studies using inhibitors and by investigating their gene expression patterns (Dunn et al., 2007; Kvitt et al., 2016). The recent large-scale transcriptome analyses using *Exaiptasia* and *Acropora hyacinthus* have highlighted ER stress as an associated pathway involved in bleaching phenomena (Oakley et al., 2017; Ruiz-Jones and Palumbi, 2017). With the development of next-generation sequencing analysis, the number of reports on the molecular response to bleaching is increasing. Transcriptome analysis *in hospite* Symbiodiniaceae has also been carried out, and light-harvesting complex (LHC), heat-shock, and photosystem-constitutional proteins have been reported as the heat stress-responsive transcripts (Rosic et al., 2011; Gierz et al., 2017).

Although symbiont type has a large effect on the bleaching sensitivity of corals, less is known about how different symbiont types contribute to coral stress tolerance. There are seven genera in Symbiodiniaceae, among which *Cladocopium* is ubiquitous genus associated with corals, while *Durusdinium* is associated with high-temperature stress tolerance in corals. It has been reported that during a bleaching event, the dominant symbiont type in the coral shifts from the general symbiont *Cladocopium* (previously classified as *Symbiodinium* clade C, hereafter referred to as C-type) to a stress-resistant type, *Durusdinium* (previously *Symbiodinium* clade D, hereafter referred to as D-type) (Baker, 2003; Baker et al., 2004; Berkelmans and van Oppen, 2006; LaJeunesse et al., 2018). The influence of each symbiont on the stress sensitivity of corals has been revealed by genotyping the symbionts of corals that survive a bleaching event (Baker, 2003; Berkelmans and van Oppen, 2006) and by the physiological studies using corals associated with each symbiont type (Rowan, 2004; Abrego et al., 2008; Mieog et al., 2009; Yuyama and Higuchi, 2014; Yuyama et al., 2016). D-type colonized corals (hereafter referred to as D-corals) have a higher survival ratio under temperature stress than C-type-colonized corals (hereafter referred to as D-corals). At higher temperatures, the C-type shows a more pronounced photoinhibitory response, which negatively impacts coral viability (Mieog et al., 2009; Yuyama et al., 2016). The C-type has a higher carbon fixation rate than does the D-type, and it promotes coral growth to a greater extent (Cantin et al., 2009). The efficiency of nitrogen acquisition also differs between C- and D-types; the C-type has a higher acquisition rate at normal temperatures, but a lower rate than that of the D-type at higher temperatures (Baker et al., 2013). Thus, the contributions of the D-type and C-type to coral growth and nutrient sources vary with the temperature (Cunning et al., 2015).

However, there are knowledge gaps in the difference in bleaching sensitivity derived from each symbiont due to the difficulty of preparing corals associated with symbionts, although there are a few molecular studies recently reported (Cunning and Baker, 2020; Rodriguez-Casariego et al., 2022). To address this gap, we first attempted to prepare a model symbiosis system suitable for gene expression analysis, namely, juvenile corals harboring cultured monoclonal C-type or D-type Symbiodiniaceae (Yuyama and Higuchi, 2014; Yuyama et al., 2018). The advantages of using such juvenile corals are as follows: (1) the prevention of contamination by other organisms, because juvenile corals can be kept in filtered seawater or artificial seawater, (2) selected alga can be introduced, and (3) a more homogenous response can be detected (Yuyama et al., 2005) (adult colonies have large variations in physiological responses). To clarify the different influences of C- and D-type symbionts on coral bleaching as well as a common molecular mechanism of coral bleaching, we exposed the coral associated with each symbiont to high temperature and light stress. Then, the maximum quantum yield of PSII (F_v/F_m) of symbiont was measured by pulse amplitude-modulated (PAM) fluorometry and performed large-scale gene expression analysis of coral–algal associations.

MATERIALS AND METHODS

Symbiodiniaceae and Coral Samples

Symbiodiniaceae strains CCMP 2556 (D-type, genus *Durusdinium*) and CCMP 2466 (C-type, genus *Cladocopium*) were purchased from the Bigelow Laboratory for Ocean Sciences (West Boothbay Harbor, ME, USA; https://ccmp.bigelow.org).

Acropora solitaryensis larvae were generated from ∼5 different colonies located in the area of 32°48′16.5″ N 132°39′11.1″ E (permit number 106, Kochi Prefecture) as described by Omori and Iwao (Omori and Iwao, 2014). Planula larvae were induced to metamorphose into polyps with neuropeptide Hym248 (Iwao et al., 2002) and infected with the two Symbiodiniaceae alga as described by Yuyama et al. (2016, 2018). Each Symbiodiniaceae strain (∼1,000 cells per polyp) was introduced to corals 1 week after metamorphosis; polyps were grown in petri dishes (55 mm) at 26–27°C with a 12-h light–dark cycle at 80 μmol m^{-2} s^{-1}. As C-type algae take ∼3 months to colonize corals, corals maintained for 3 months were used in the stress experiments (Yuyama and Higuchi, 2014; Yuyama et al., 2016) (**Figure 1**, **Supplementary Figure S1**). To verify the genotypes of Symbiodiniaceae colonizing corals, Restriction Fragment Length Polymorphism (RFLP) analysis was performed with five corals, each, as described in Yuyama and Higuchi (2014) (**Supplementary Figure S3**). Corals were maintained without feeding. During this 3-month incubation period, the corals associated with D-type (D-corals) tended to be larger than those associated with C-type (C-corals) (data not shown), as previously reported in *Acropora tenuis* (Yuyama and Higuchi, 2014).

Stress (High Temperature and Strong Light) Exposure Experiments

A number of two separate experiments were performed using the same conditions to avoid the effects of photography and FvFm measurements on RNA-seq samples (**Supplementary Figure S2**). First, each five C- and D-corals were incubated under bleaching conditions (high temperature and strong light) to monitor the coral bleaching states including photosynthetic responses of the endosymbiotic algae. The corals were incubated under a 12-h light–dark cycle at high irradiance (1,500 μmol m^{-2} s^{-1}) and the water temperature was increased gradually from 27 to 31°C over 21 h. The temperature was controlled by a thermo-controller (TC-101; Eaton, Tokyo, Japan). We confirmed that the temperature accuracy was within ± 0.5°C by thermometer under digital microscope (VHX2000; Keyence, Osaka, Japan). This bleaching condition was determined in the preliminary experiments conducted with juvenile *A. solitaryensis* corals. Coral polyps were photographed with a stereomicroscope (LZ; Kenis, Osaka, Japan) mounted on a CMOS camera (Tucsen Photonics, Fuzhou, China). These photographs enabled us to confirm the symbiont cell densities in the coral tissue, and to visualize the decrease therein (**Supplementary Figure S1**). A number of two containers for the experimental control population (each with five corals associated with C-type or D-type) were maintained at 27°C under a 12-h light/dark cycle at 80–100 μmol m^{-2} s^{-1} (**Figure 1**).

Second, other corals were exposed to the same stress conditions described above and fixed after 6 (29°C) or 30 h (31°C) to prepare the samples for transcriptome analysis. Approximately 90 colonies each were prepared for C- and D-type corals as the samples for RNA-seq. Among them, 30 corals each were used for the control, stress day 1 and stress day 2 treatments. These 30 corals were divided into two containers and prepared as the two biological replicates. For the control condition for RNA-seq analysis, corals were maintained at 27°C and 80 μmol m^{-2} s^{-1} for ∼2 months and then fixed at the same time as the stress day 2 corals. Due to the limited number of samples, the

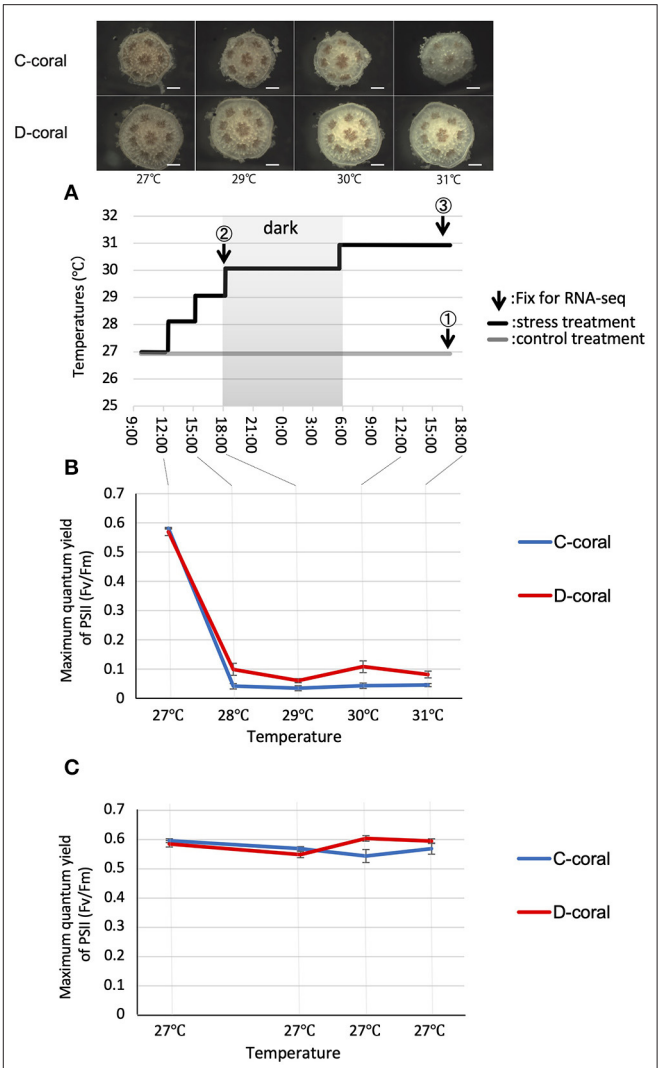

FIGURE 1 | (A) Experimental design for stress experiments and stereoscopic microscope images of *Acropora solitaryensis* during temperature increase from 27 to 31°C. The upper pictures show *A. solitaryensis* colonized by C-type algae (C-coral); lower pictures show *A. solitaryensis* colonized by D-type algae (D-coral). The graph shows the transition of the temperature setting during the experiment. Arrows indicate the time of fixation for RNA-seq analysis. The samples derived from each time point are referred to as day 1 (at 29°C, collected before setting 30°C), day 2 (at 31°C), and control. For RNA-seq analysis, we prepared two replicates (each replicate with 15 pooled colonies) for each treatment (stress conditions and control conditions) (**Supplementary Figure S2**). Scale bars = 0.5 mm. **(B,C)** Maximum quantum yield (*Fv/Fm*) of C-type (*Cladocopium*) and D-type (*Durusdinium*) Symbiodiniaceae associated with corals in stress **(B)** and control treatments **(C)**. No significant difference was found between C-type and D-type in same treatment; however, there were significant differences between control and stress treatments in both C-type and D-type (Turkey–Kramer HSD, $p < 0.05$). Values are means ± SE.

control coral for the second day of stress (stress day 2) treatment was also used as the control for the first day of stress (stress day 1) treatment. Here, it was assumed that the expression pattern would not change even if the fixation time for RNA-seq was shifted by 1 day, since the condition is stable after 2 months of culture. Corals were fixed on day 1 (after 6 h, at 29°C) and on day 2 (after 30 h at 31°C) in RNAlater (Ambion, Austin, TX, USA) and stored at −80°C. The control population was maintained at 27°C and 80 μmol m^{-2} s^{-1} (12-h light–dark cycle) and fixed after 30 h.

Measurement of Photosynthetic Parameter (F_v/F_m)

The photosynthetic parameter (F_v/F_m) of endosymbiotic algae was monitored by PAM fluorometry (MiniPAM; Walz GmbH, Effeltrich, Germany) (Yuyama et al., 2016). All F_v/F_m measurements were taken after a 15-min dark adaptation period. In the measurement, PAM probes were fixed near the coral body wall. F_v/F_m values for the symbiotic C-type and D-type were compared for the different treatments. *Post-hoc* differences were assessed using the Tukey–Kramer honestly significant difference test (Anaconda 3-5.2.0, Python version 3.6.5; Continuum Analytics, Austin, TX, USA).

Counting Algal Symbiont (Estimating Symbiont Density)

After the end of the stress experiment, corals were fixed in 3% formaldehyde to count symbiont cells inside corals (corals from the control and stress day 2 treatments were fixed to investigate the symbiont density). The fixed corals were decalcified in solution containing 0.5 M EDTA and homogenized in 0.01% Triton X using the method described by Yuyama and Higuchi (2014). Then, symbiont cells in the coral homogenate were counted using a hemocytometer (Thomas Scientific, Swedesboro, NJ, USA) under a digital microscope (VHX2000; Keyence, Osaka, Japan). To estimate symbiont density (cells/ mm^2), the surface area of photographed corals was calculated using ImageJ software. These corals do not differ in height; thus, only the surface area was estimated. To clarify that a bleaching response was occurring, algal cell density ratios of "stress day 2" / "control" were calculated.

Transcriptome Analysis

Each treatment was performed in two replicates, and a total of 12 RNA libraries were prepared. Total RNAs were extracted from each replicate using the PureLink RNA Mini Kit, and *Poly(A) RNA isolation* from total *RNA* was performed with a protocol of Next Poly(A) mRNA Magnetic Isolation Module (New England Biolabs, Ipswich, MA, USA). The RNA quality of each sample was checked using an Agilent 2100 Bioanalyzer (Agilent Technologies, Santa Clara, CA, USA) before producing the libraries. The sequencing libraries were generated from poly(A) mRNA using the NEBNext Ultra RNA Library Prep Kit (New England Biolabs). All libraries were sequenced on the HiSeq 4000 platform (Illumina, San Diego, CA, USA) by Macrogen Japan. The resulting 101-bp paired-end reads were first pre-processed [trimming of low-quality bases using a Phred quality score (Qv) <20 from the 5′ and 3′ ends of each read, and removing short reads (<25 bp) and low-quality reads (30% of bases with Qv ≤15)] using the DNA Data Bank of Japan (DDBJ) Read Annotation Pipeline (Nagasaki et al., 2013).

Transcriptome Analysis of Host Corals

Trimmed reads from all samples were assembled *de novo* using trinity in the DNA Data Bank of Japan (DDBJ) Read Annotation Pipeline (Nagasaki et al., 2013). Assembled contigs were translated using TransDecoder (Haas et al., 2013) to isolate likely coding sequences. The peptide sequences were filtered for redundancy using CD-Hit (v4.6.1; Fu et al., 2012) specifying a 95% similarity threshold and then obtained 168,491 contigs. To detect contig sequences originating from the host coral, we built custom coral and Symbiodiniaceae databases. The contigs derived from *A. solitaryensis* were isolated by the alignment to coral databases, and symbiont sequences were removed, as previously described (Yuyama et al., 2018). Reads were mapped to the *A. solitaryensis* contigs using the Bowtie2—very-sensitive algorithm (run with options: -D 20 -R 3 -N 0 -L 20 -i S,1,0.50) (Langmead and Salzberg, 2012). The eXpress was used to quantify the transcript abundances. To identify differentially expressed genes (DEGs) between the control and stress conditions (days 1 and 2), the edgeR method in the TCC package of R (Sun et al., 2013) was used (**Supplementary Figure S2**). Genes were determined to be significantly differentially expressed based on a false-discovery rate < 0.05. All *A. solitaryensis* contigs were annotated using the public Swiss-Prot database and the non-redundant protein database (NCBI-nr) by BLASTx search with an e-value cutoff of 1e-4. Gene Ontology (GO) enrichment analyses were performed on the annotated dataset of DEGs using the Database for Annotation, Visualization, and Integrated Discovery (Huang et al., 2009b) (https://david.ncifcrf.gov/). In the analysis, annotated DEGs were compared with the annotation of the whole transcriptome, and GO terms enriched among the DEGs were identified. To summarize the major pathways involved in corals exposed to high-temperature/light, Kyoto Encyclopedia of Genes and Genomes (KEGG) pathway analyses (Kanehisa and Goto, 2000) of the DEGs detected in both C- and D-type corals were also performed. As the background for the GO enrichment analysis, the Swiss-Prot annotation results of all *A. solitaryensis* contigs were used.

Transcriptome Analysis of Algal Symbiont

Transcriptome analyses of Cladocopium and Durudsinium was performed using same RNA-seq short reads with the coral analysis. *De novo* assembly of C-type and D-type was performed, respectively, using FASTQ data of C- and D-type corals, obtained in this study. To detect coding sequences of the assembled contigs, TransDecoder (v. 2.0.1) was used (Haas et al., 2013). In total, 157,584 and 156,284 contigs were obtained from the C- and D-type coral datasets. Subsequently, contigs with more than 95% nucleotide sequence identity were removed using CD-HIT (v. 4.7; Fu et al., 2012). The contigs derived from C-type and D-type were isolated by alignment to coral databases and symbiont sequences were removed, as previously described (Yuyama et al., 2018). As a result, 98,707 and 97,948 contigs (clusters) were obtained

from the C- and D-type corals (**Supplementary Figure S3**). The contigs derived from *Cladocopium and Durusdinium* were isolated by the alignment to custom Symbiodiniaceae databases and coral sequences using BLASTn (v. 2.2.30; NCBI, Bethesda, MD, USA). The Symbiodiniaceae database included the genomes of *Symbiodinium minutum* (Shoguchi et al., 2013), *Symbiodinium kawagutii* (Lin et al., 2015), *Symbiodinium tridacnidorum* and *Cladocopium* sp. (Shoguchi et al., 2018), and the transcriptomes of *Cladocopium* sp. and *Durusdinium* sp. (Ladner et al., 2012). The coral database included the *Acropora digitifera* genome (Shinzato et al., 2011) and transcriptomes of non-symbiotic *Acropora hyacinthus* (https://matzlab.weebly.com/data--code.html) and *A. tenuis* (Yuyama et al., 2018). Reads were mapped to *Cladocopium*- or *Durusdinium*-derived contigs with the Bowtie2 (v. 2.2.4) very-sensitive algorithm. Then, the quantification of transcript abundances and identification of DEGs were performed by the same method used for the identification of coral transcripts. The eXpress (v. 1.5.1) program was used to quantify transcript abundances and estimate fragments per kilobase of transcript per million mapped reads (FPKM) values (Roberts and Pachter, 2013). To identify transcripts expressed differentially between the control and stress conditions, analysis using iDEGES/edgeR in the TCC package (Sun et al., 2013) was performed. The differentially expressed transcriptome was annotated using Swiss-Prot and the non-redundant protein database. GO enrichment was also performed on the DAVID website (https://david.ncifcrf.gov/) (Huang et al., 2009a). In the analysis, all *Cladocopium* or *Durusdinium* transcripts annotated with GO terms were used as the background.

RESULTS

Stress Response

During the increase in temperature, the appearances of both corals (C-coral and D-coral) remained largely unchanged until 6 h, and the color of the body gradually became white over the following 24 h (**Figure 1**, **Supplementary Figure S4**). To investigate the responses of endosymbiotic algae under high temperature and light stress, their photosynthetic efficiencies were measured (**Figure 1**). The photosynthetic ratios (F_v/F_m) of the C- and D-types were 0.582 ± 0.002 and 0.57 ± 0.013 (average $\pm$ standard error [SE]), at the beginning of the experiment; these values decreased to 0.042 ± 0.009 and 0.099 ± 0.002 (average $\pm$ SE), in the first 3 h. After this point, the photosynthetic activity of algae remained low until the end of the experiment. At 3 h, when the temperature was increased to 28°C under strong light, the D-type tended to show more photosynthetic activity than did the C-type. In the control treatment (27°C, 80 μmol m^{-2} s^{-1}), no significant fluctuation of F_v/F_m was observed in either type; the F_v/F_m values were ∼0.6. F_v/F_m values were significantly decreased under stress compared with control conditions, in both C- and D-types ($p < 0.05$), although no significant difference was observed between the two types. At the end of the experiment, the corals were fixed and decalcified to measure the symbiont densities. Cell density tended to decrease during the experimental period, with a 51% decrease in C-type and a 28% decrease in D-type compared to control conditions (**Supplementary Figure S4**).

Transcriptomic Change in Corals

For RNA-seq analysis, samples were fixed at 6 h (day 1, at 29°C) and 30 h (day 2, at 31°C) after the start of the experiment. We sequenced cDNA libraries derived from each sample, and ∼40 million reads were obtained from each. Sequence data were deposited in the DDBJ Read Archive (DRA008078). As a result of the *de novo* assembly using reads from all samples, 663,795 contigs were generated. Subsequently, the protein-coding regions were estimated, and redundant sequences were removed, which resulted in 168,491 sequences. Among them, 40,036 contigs (DDBJ/ENA/GenBank accession codes ICPH01000001-ICPH01040036) assigned to the coral database by BLASTN search were used as a reference gene set of corals for subsequent analyses (**Supplementary Tables S1, S2**). All of the reads from each population were aligned to the reference using Bowtie2; we then attempted to detect DEGs in the two biological replicates. In the Bowtie2 analysis, ∼14–16 million reads were mapped to reference contigs. The expression levels in the control population were compared with those in the stress day 1 or day 2 treatment in each coral, and DEGs under the stress conditions, as compared to controls, were detected. Of these DEGs, 9,537 were annotated by BLASTX searches against the UniProt/Swiss-Prot database. In the stress day 1 treatment, 1,685 and 1,081 DEGs were detected in C- and D-type corals, and in stress day 2, 2,954 DEGs and 3,516 DEGs were detected (**Supplementary Figure S5**).

Next, the UniProt accession IDs assigned to each DEG were used for GO enrichment analysis. DEGs from stress days 1 and 2 were subjected to GO enrichment analysis, and the top enriched GO terms with low *p*-values were selected and shown in **Figure 2**. GO terms related to the organs not found in cnidarians and GO terms with duplicate meanings were deleted. GO analysis revealed that the up-regulated genes are significantly enriched in protein folding, oxidation-reduction process, and immune response, whereas the down-regulated genes are highly involved in skeletal system development, DNA replication, and telomere maintenance *via* recombination (**Figure 2**). Their expression patterns indicated that the gene expression response of D-coral was slower than that of C-coral. Some metabolic systems, such as glucose, metabolic processes, and ammonium ion metabolic processes, were upregulated at 29°C (day 1) in C-corals, while they were hardly changed in D-corals; similar cases were also detected among downregulated genes.

Kyoto Encyclopedia of Genes and Genomes pathway analysis was also performed to identify the major molecular processes among the DEGs. Transcriptome data at 31°C (day 2) were mainly used for KEGG pathway analysis. **Figure 3** shows several upregulated genes, which include those involved in endocytosis, lysosome organization, acetyl-CoA, NO, chitin metabolic process, and the PI3K-AKT pathway, and downregulated genes, which include those involved in DNA replication and the calcium signaling pathway. In addition, specific DEGs for C- and D-type corals were detected from DEG gene list (**Figure 4**). As a result, inflammatory mediator

regulation of transient receptor potential (TRP) channels was identified as a pathway specifically upregulated in D-type corals. Additionally, different types of vitamin B metabolic pathways were identified as downregulated under stress conditions in the two corals: riboflavin in C-coral, and folate and thiamine in D-coral.

Transcriptomic Change in Algal Symbiont

De novo assembly of C- and D-type symbionts was performed, respectively, using FASTQ data of C-and D-corals, which resulted in the identification of 44,446 contigs (DDBJ/ENA/GenBank accession codes ICPI01000001–ICPI01003338) from C-type and 20,368 contigs (DDBJ/ENA/GenBank accession codes ICPJ01000001–ICPJ01004504) from D-type (**Supplementary Tables S1, S2**). FASTQ reads of C- and D-corals were aligned to candidate each symbiont (C-type and D-type) derived contigs, respectively. Then, the expression levels of each contig were estimated from FPKM values. The expression pattern of each contig was then compared between the control and stress conditions (day 1 or 2) using edgeR and the TCC program (false discovery rate < 0.05). In total, 117 and 56 algal DEGs were detected in C- and D-type in stress day 1, and in stress day 2, 109 DEGs and 296 DEGs were detected (**Supplementary Figure S6**). Of them, 204 C-type and 321 D-type DEGs had protein functional annotations (BLASTX e-value $<$ 10e-4). GO enrichment analysis was performed based on the DEG annotations detected for each treatment and algae type. The 29 enriched GO terms (p-value < 0.05, Fisher's exact test) are shown in **Figure 5**. **Figure 6** shows typical GO terms of C-type and D-type symbionts and their related genes (since the same contigs were shared by GO terms with similar names, representative GOs with high originality were summarized in **Figure 6**). The stress response of the C-type was characterized by GO terms related to "regulation of translation" and "proteolysis." For the D-type, GO terms associated with "photosynthesis" were upregulated, while those associated with "ion transport" and "protein folding" were downregulated. The DEGs indicated that several types of transcripts coding chaperon proteins were downregulated in both C-type and D-type. In addition, D-type had many DEGs related to photosynthesis that were upregulated under stress conditions.

DISCUSSION

In this study, corals associated with C-type or D-type symbionts were incubated under coral bleaching conditions (increasing temperature and strong light conditions), and their stress response patterns and transcriptomic changes were investigated. By the stress treatment, a decrease in symbiotic cell density, which is a typical coral bleaching phenomenon, was observed. Photosynthetic activity (F_v/F_m) of both Symbiodiniaceae immediately decreased, and the D-type

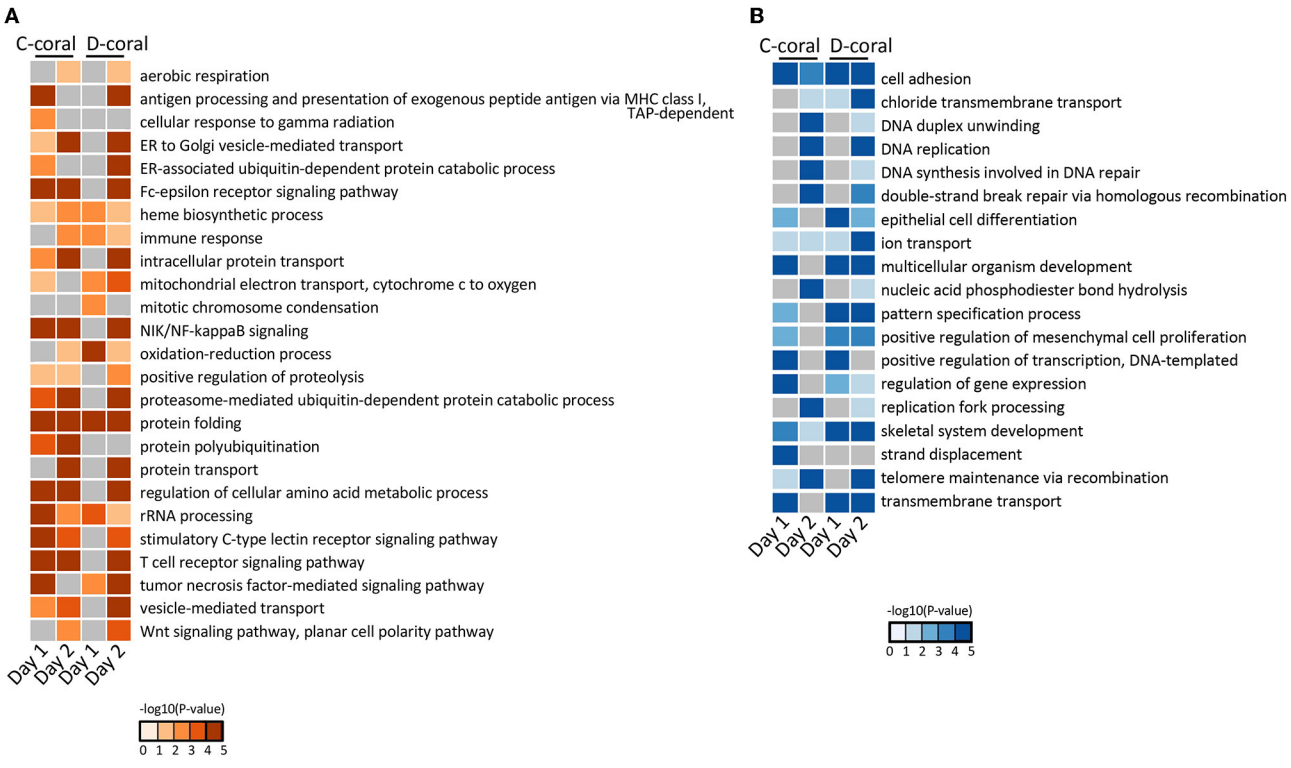

FIGURE 2 | Heatmap of enrichment scores [–log10 (p-value)] from GO enrichment analysis using upregulated coral DEGs **(A)** and using downregulated coral DEGs **(B)**. The detected significantly ($p < 0.05$) enriched GO terms in biological process are shown.

maintaining a slightly higher F_v/F_m than the C-type under stress conditions. This is similar to the reports that the degree of F_v/F_m decline in the D-type was smaller than in the C-type under strong light conditions (Yuyama et al., 2016). These results were suggested that D-corals have slightly more stress-resistant properties than C-corals. To examine the difference in stress response between C- and D-corals, we performed transcriptome analyses and investigated DEGs between stress treatments and non-stressed control. As a result, we identified 9,884 annotated DEGs derived from corals and 204 and 321 annotated DEGs derived from Cladocopium and Durusdinium. First, we focus on coral genes and discuss the major pathways commonly detected in C- and D-type coral (**Figure 3**), and then, we focused on the unique gene expression changes of each coral (**Figure 4**). Our RNA-seq results were limited by insufficient replication (two replicates, each containing ∼15 corals). For that reason, rather than focusing on the response of a single gene, we mainly focused on the phenomena detected by GO enrichment analysis of the DEGs. Algal DEGs detected from RNA-seq analyses were lower than the number of host corals, but typical stress-responsive genes, such as genes coding molecular chaperon proteins, were detected. The final section of the discussion focused on the response of symbiotic algae. Transcriptome data on day 2 were mainly used for discussion, because the data on day 1 are in the process of temperature increasing and a lesser number of DEGs were detected.

Common Transcriptomic Reactions of Corals Between C- and D-Type Corals

ER Stress, Apoptosis, and Mitophagy

A total of 107 DEGs involved in "Protein processing in endoplasmic reticulum" were detected in the corals exposed to stresses. These genes have been reported in the previous studies and are considered to be a major molecular response associated with the bleaching response (Oakley et al., 2017; Ruiz-Jones and Palumbi, 2017). These enormous changes in

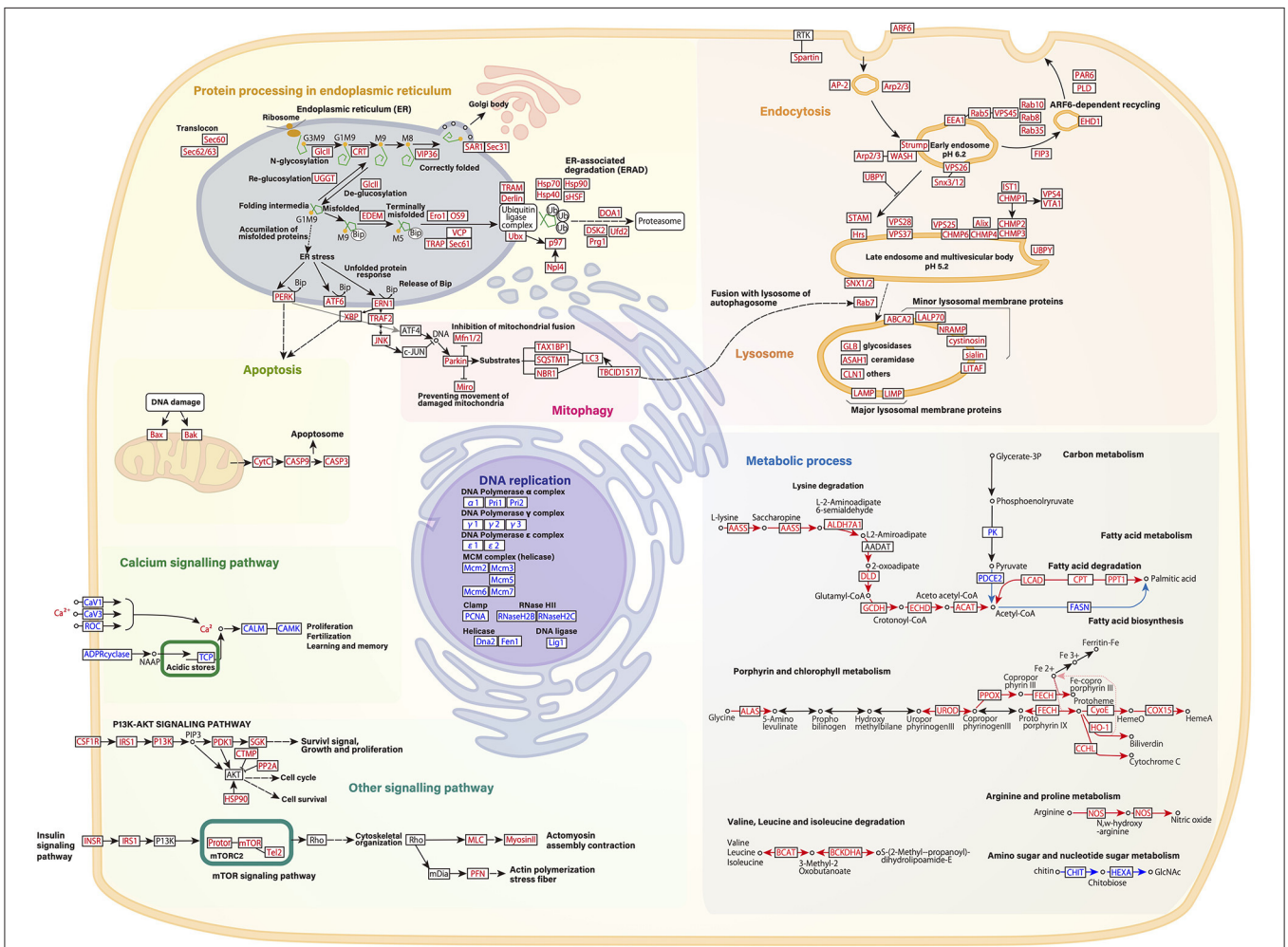

FIGURE 3 | Schematic presentation of several gene pathways involved in high temperature and strong light stress based on RNA-seq data of host corals. Common changes in gene expression between C-coral and D-corals at 31 °C are indicated. Each pathway is described based on the KEGG pathway database (Kanehisa and Goto, 2000). Upregulated transcripts during high temperature and/light stress are shown in red; downregulated transcripts are indicated in blue. Each gene expression pattern is also shown in **Supplementary Figure S1**.

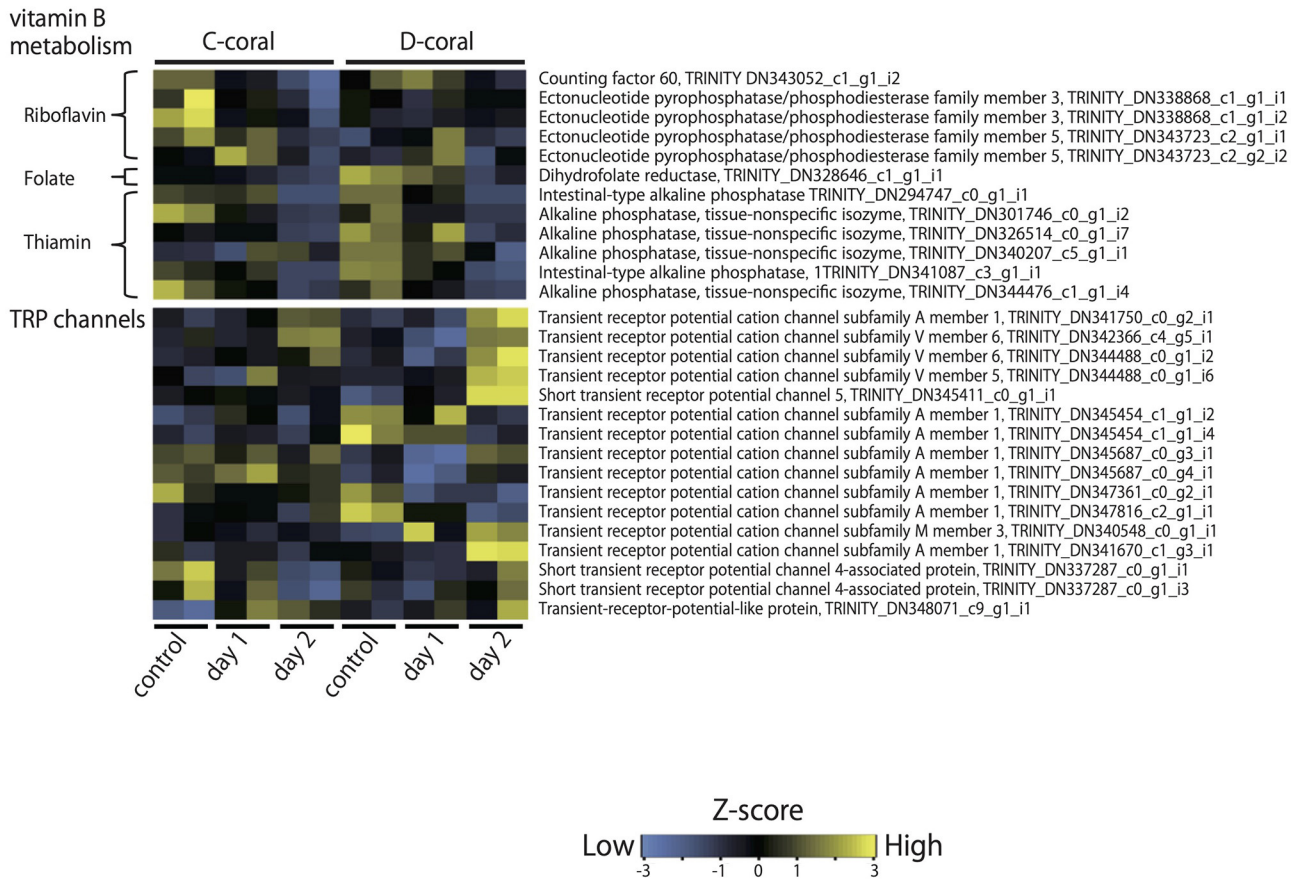

FIGURE 4 | Heatmap displaying the relative expression values (*z*-score of TMM-normalized FPKM values) of contigs, which shows the different expression patterns of C- and D-corals during treatment with high temperature and strong light. As representative examples, the expression patterns of contigs encoding TRP channels and genes involved in vitamin B metabolism are shown. Expression values were converted into z-scores and plotted by heatmap.2 in R.

gene expression associated with the unfolded protein response (ER-stress) indicate that corals suffer from increased protein denaturation during the bleaching process. In addition, other processes related to ER stress, such as mitophagy and apoptosis-like responses, were also detected by GO enrichment and KEGG pathway analyses. Mitophagy is a response in which damaged mitochondria are degraded by autophagy and a similar response has been observed in *Exaiptasia* (a model animal of coral–algal endosymbiosis) under high temperature conditions (Dunn et al., 2012). The caspase-mediated apoptosis has also been reported to be involved in bleaching phenomena (Tchernov et al., 2011). This series of responses, such as ER stress, mitophagy, and apoptosis, is likely caused by ROS generated from the photoinhibition of endosymbiotic alga under high temperature and strong light conditions (Lesser, 2011). These ROS attack protein in corals, and this might increase the expression of genes involved in ER stress, mitophagy, and apoptosis, which leads to the coral bleaching.

Endocytosis

Expression of genes related to ER stress or mitophagy could also link to the upregulation of Rab 7 protein, which is responsible for the fusion of lysosomes and endosomes (**Figure 3**). In *Aiptasia*, a Rab 7 homolog is located in putative late endocytic and phagocytic compartments containing either heat-killed or photosynthesis-impaired symbionts (Chen et al., 2003). The Rab 7 homolog may be involved in the digestion of denatured alga; our results that show the upregulation of Rab 7 might be a sign of the bleaching process. In addition to Rab 7, various endocytosis-related DEGs were identified. The expression of Rab proteins, charged multivesicular body proteins (CHMPs), and vacuolar protein sorting (VPS) proteins, which are involved in endocytic trafficking and endosomal sorting, increased under the stress conditions. Less is known about the functions of endocytosis-related genes involved in coral bleaching except for the fact that Rab protein is localized in the symbiosome membrane (Chen et al., 2003, 2005; Song et al., 2015). In plant–microbe symbioses, however, the regulation of the expression of membrane trafficking proteins, such as VPS, causes shrinkage of vacuoles and, in turn, is involved in maturation of the symbiosome membrane (Gavrin et al., 2014). In the case of corals, these fluctuations in endocytosis-related genes such as VPS, Rab, and CHMP will be also important for understanding the status of symbiosome membranes during coral bleaching.

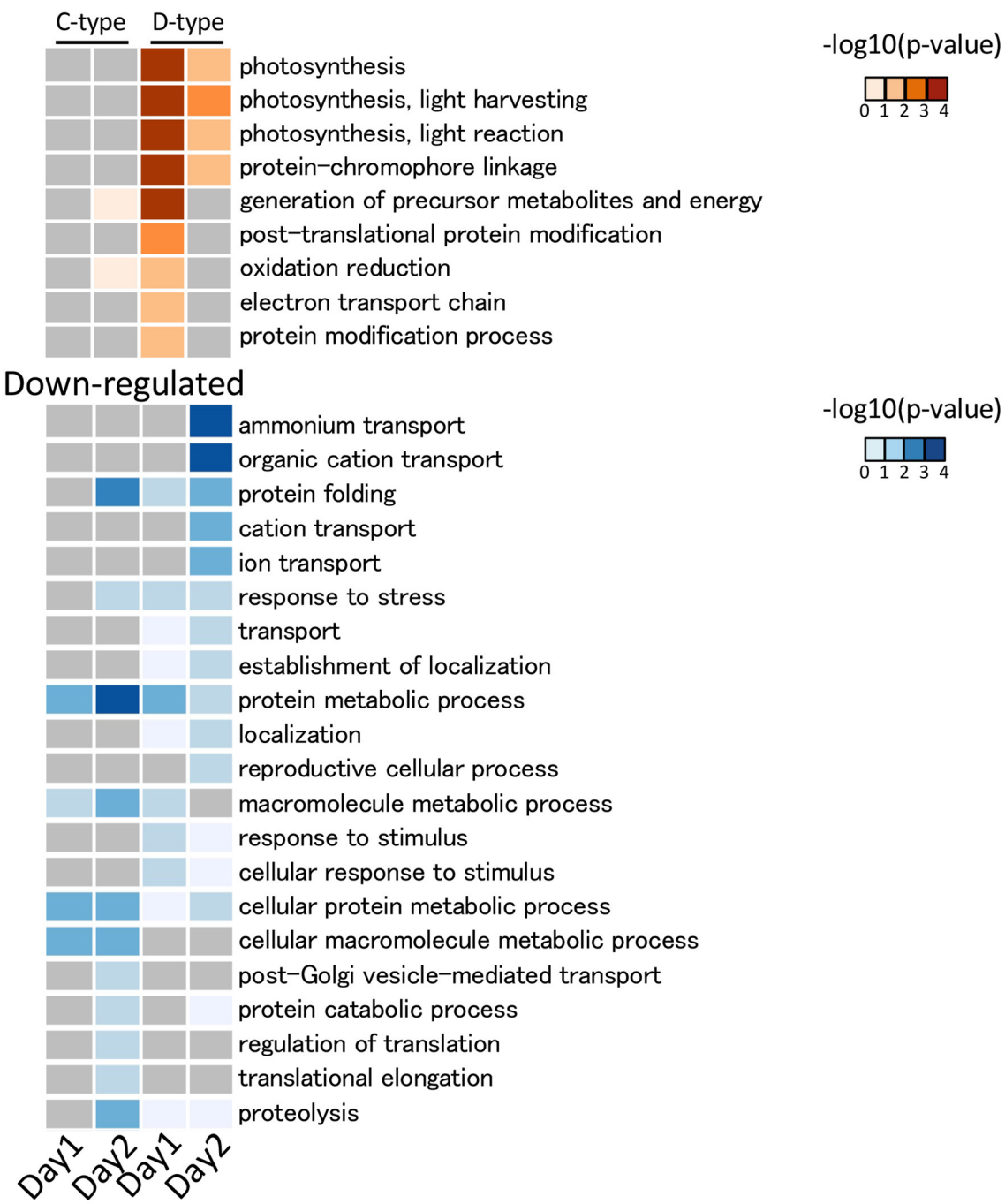

FIGURE 5 | GO functional analysis of Symbiodiniaceae DEGs detected using DAVID. The detected significantly ($p < 0.05$) enriched GO terms in biological process are shown. The legend shows the color scaling with negative log10 *p*-value. In the C-type (*Cladocopium*), no significantly enriched GO term was detected in the upregulated DEG, while in D-type (*Durusdinium*), some photosynthesis-related GO terms were detected as upregulated DEGs. Among the downregulated DEGs, a GO term related to protein folding was enriched in both Symbiodiniaceae.

Metabolic Processes

Stress exposure reduces the expression of genes involved in the generation of acetyl-CoA from glycolysis (**Figure 3**). It also reduces the expression of the fatty acid biosynthetic pathway that consumes acetyl-CoA; by contrast, it increases the expression of L-lysine and fatty acid metabolism pathways that generate

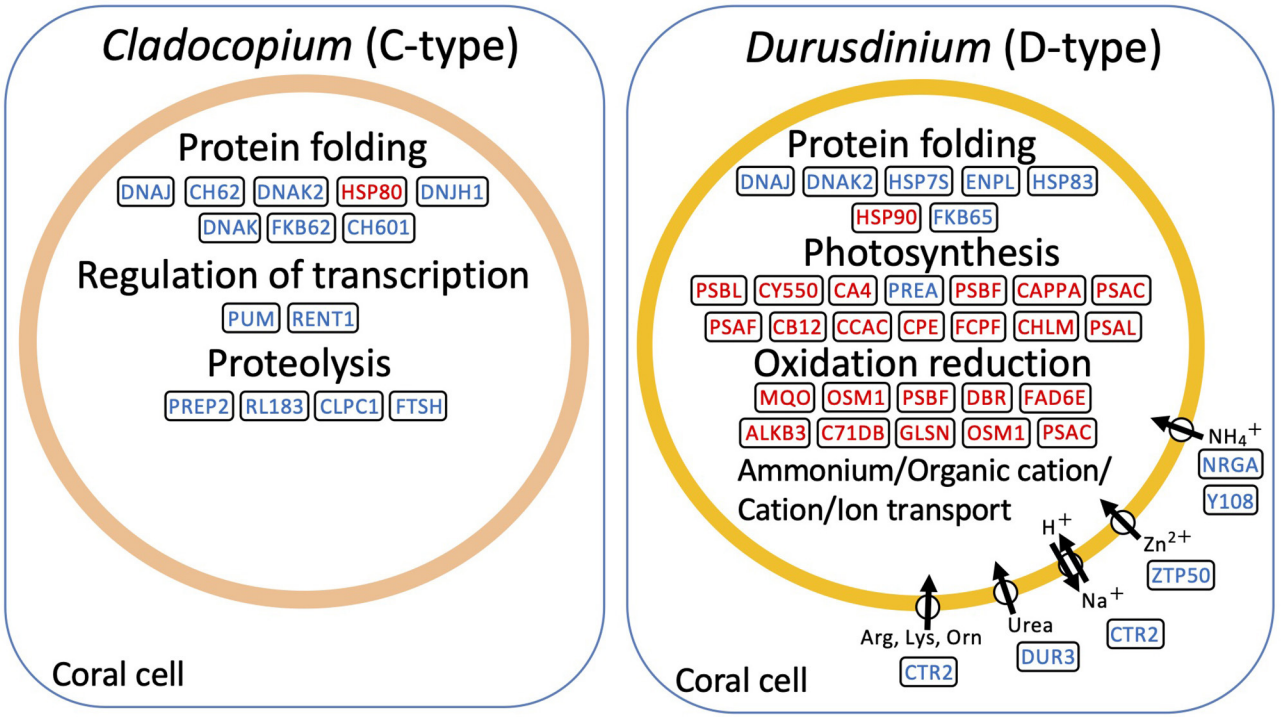

FIGURE 6 | Schematic presentation of representative genes involved in high temperature and strong light stress based on RNA-seq data of symbiont, Cladpcopium (C-type) and Durusdinium (D-type). The representative enriched GO and their related genes were shown. Upregulated transcripts during bleaching are shown in red; downregulated transcripts are indicated in blue.

acetyl-CoA. In other words, the expression levels of L-lysine and fatty acid metabolism-related genes increase to enhance the production of acetyl-CoA under stressed conditions in which less acetyl-CoA is generated through glycolysis. These findings suggest that during bleaching, corals maintain their energy-producing pathway, in which acetyl-CoA enters the TCA cycle, by supplementing acetyl-CoA production using metabolic pathways other than glycolysis. In addition to those mentioned above, other stress response processes, which include cytochrome c release, the heme biosynthetic pathway, arginine and proline metabolism, valine isoleucine, and the chitin metabolic pathway degradation, were also detected. Our results suggest that these metabolic processes are susceptible to coral bleaching or symbiotic state with algae.

DNA Replication

The expression of genes involved in DNA replication decreased under stress conditions; that is, genes encoding enzymes such as DNA polymerase, helicase, RNase, and ligase were drastically decreased. The downregulation of DNA replication-related genes can be associated with the "DNA-damage response" induced by heat stress or oxidative stress reported as shown in the study of Kantidze et al. (2016). Corals reportedly suffer DNA damage under oxidative stress caused by photoinhibition of symbionts at high temperatures (Nesa and Hidaka, 2009; Nesa et al., 2012). Our results indicate that, during coral bleaching, DNA damage becomes more serious due to the reduced ability to repair DNA (**Supplementary Figure S7**).

Signaling Pathways

The calcium signaling pathway is a typical gene set known to change in corals at high temperatures (Desalvo et al., 2008; Rosic et al., 2015; Weston et al., 2015). Our RNA-seq data showed decreased expression of genes involved in the calcium signaling pathway, which indicated that under high temperature and strong light conditions, the expression levels of molecules that sense calcium were deceased, and expression levels of calmodulin kinase, which involved in modification of cell functions, also decreased. In addition, signaling systems that control cell proliferation that includes PI3K-AKT, insulin signaling, and mTOR pathways were upregulated under the stress conditions. The PI3K-AKT and mTOR pathways are known to relieve the stress induced by ROS (Yu and Cui, 2016). The upregulation of these gene sets in bleached corals may be attributable to the corals' response to damage caused by ROS stress. The expression of similar pathways has been reported to increase in corals under the influence of light pollution (Rosenberg et al., 2019), and therefore, the upregulation of these pathways could be an indicator of coral stress.

Unique Gene Expression Changes in C-Corals and D-Corals

Vitamin B Biosynthesis

Various genes involved in vitamin B metabolism were specifically downregulated in each of the two corals; DEGs related to riboflavin metabolism were detected in C-corals, while DEGs

related to folate and thiamine metabolism were detected in D-corals. Vitamin B is an essential supplement for growing alga (Croft et al., 2005; Agostini et al., 2009; Helliwell et al., 2016), which includes Symbiodiniaceae. These unique DEGs involved in vitamin B metabolism, whose expression levels were decreased with decreasing symbiont density on day 2 (although changes in symbiont density are not statistically significant), imply that each symbiont requires different B vitamins. The present results support the connection between symbiont alga and host vitamin B metabolism and revealed symbiote specificity for various B vitamins.

TRP Channels

The expression change of TRP channels is noteworthy because the channels have been extensively characterized as thermosensors (Schepers and Ringkamp, 2009; Samanta et al., 2018). The coral TRP channel, homologous to TRPA1, TRPV5/6, and TRPM3, increased in stress-tolerant D-corals under high temperature and strong light conditions, while C-corals showed few changes regarding these proteins. In general, these channels are known to control the entry of calcium that causes an internal signal to regulate cell activities (Schepers and Ringkamp, 2009; Samanta et al., 2018). The symbiont-associated altered expression levels of TRP and their function in corals are the interesting issues to be addressed in the future and may help us to understand the connection between symbiont type and temperature resistance of the host.

Transcriptomic Changes of Symbiont

The different stress responsiveness between C- and D-type Symbiodiniaceae in corals was also detected by RNA-seq analysis. The photosynthesis-related GO term was enriched in upregulated DEGs in the D-type (**Figure 5**). By contrast, in the C-type, only a few photosynthesis-related were differentially expressed (**Figure 6**). The altered expression of transcripts related to the photosynthetic reaction center suggested that algae are affected by photoinhibition, which damages the photosynthetic system under strong light conditions (Constant et al., 1997). In addition, several genes involved in ion transport were downregulated in the D-type (**Figures 5**, **6**). These gene expression changes are likely to reflect an increase or decrease in the amount of substances transported from corals, and downregulation of ammonia transport proteins may reflect a decrease in the transport of ammonia received by symbiotic algae from the host (Pernice et al., 2012). Other transporter that includes zinc transporter and cationic amino acid transporter is also downregulated in D-type, which suggested that D-type cells usually utilize these substances, but their utilization is reduced under stress conditions.

The RNA-seq analysis that focusses on the *in hospite* Symbiodiniaceae detected protein-folding-related transcripts as DEGs in both the C- and D-types, most of which were downregulated by stress exposure (**Figure 6**). The expression pattern of these transcripts was previously reported in the symbiont of *Acropora millepora* and is considered to be a general symbiont response (Gierz et al., 2017). Interestingly, our results showed that a few protein-folding-related transcripts were upregulated. The upregulation of these heat shock proteins might be associated with increased stress tolerance of Symbiodiniaceae (Mayer and Bukau, 2005; ul Haq et al., 2019). In the bleaching situation, these upregulated chaperone transcripts are thought to be involved in maintaining the functional stability of C- and D-type symbionts.

In summary, the differential expression of many bleaching stress-related genes in corals was detected, and representative changes included upregulation of genes associated with ER stress, apoptosis, mitophagy, endocytosis, PI3K/AKT/mTOR signaling, and metabolic processes related to acetyl-CoA, as well as decreased DNA replication. In addition, the use of corals colonized with two different types of symbionts revealed differences in the expression patterns of TRP channel genes and vitamin B metabolic genes, which shows the influence of symbiont algal type on the coral host. In the algal DEGs, typical stress response genes, such as gene related to molecular chaperon proteins and gene related to photosystem, were detected. Some of those DEGs were frequently detected in the D-type, which has relatively stress-resistant properties. To reveal how the above-mentioned genes are involved in coral bleaching, further examination of the localization of the proteins encoded by each gene and the confirmation of their functions by gene knockdown will be needed. We have summarized typical pathways, but the published transcriptomic data include more information than discussed here. It is expected that these data will help to reveal the underlying mechanisms of coral bleaching in the future studies.

DATA AVAILABILITY STATEMENT

The raw fastq files for the RNA-seq libraries were deposited in the DDBJ Sequence Read Archive (DRA) under the accession number DRA008078 under DDBJ bioproject PRJDB6866. All nucleotide sequences assembled in this study have been deposited in the DDBJ/ENA/GenBank: A. solitaryensis assembly (accession codes ICPH01000001-ICPH01040036), Cladocopium assembly (accession codes ICPI01000001–ICPI01003338), and Durusdinium assembly (accession codes ICPJ01000001–ICPJ01004504; https://www.ddbj.nig.ac.jp/news/en/190927_2-e.html).

AUTHOR CONTRIBUTIONS

IY: study conception, design, data collection, and draft manuscript preparation. TH: statistical analysis, drafting, and writing. HT and TM: sample preparation. KI: drafting and writing. All authors contributed to the article and approved the submitted version.

FUNDING

This work was supported by research grants from the Japan Society for the Promotion of Science

(IY, No. 14J40135 and No. 19H03026) and the Environment Research and Technology Development Fund (No. 4–1806) from the Ministry of the Environment, Japan.

ACKNOWLEDGMENTS

We are grateful to the members of the Laboratory for DNA Data Analysis at the National Institute of Genetics (NIG). RNA-seq data analysis was partially performed on the NIG supercomputer.

SUPPLEMENTARY MATERIAL

The Supplementary Material for this article can be found online at: https://www.frontiersin.org/articles/10.3389/fphys.2022.806171/full#supplementary-material

Supplementary Material: Lists of all contigs identified as *Acropora solitaryensis* (Data sheet 1.csv) -, *Cladocopium* (Data sheet 2.csv) -and *Durusdinium* (Data sheet 3.csv) -derived contigs. Annotation results of all contigs in the Swiss-Prot and non-redundant protein databases; normalized transcript expression levels of each contig are also shown.

REFERENCES

Abrego, D., Ulstrup, K. E., Willis, B. L., and van Oppen, M. J. H. (2008). Species-specific interactions between algal endosymbionts and coral hosts define their bleaching response to heat and light stress. *Proc. Biol. Sci.* 275, 2273–2282. doi: 10.1098/rspb.2008.0180

Agostini, S., Suzuki, Y., Casareto, B. E., Nakano, Y., Hidaka, M., and Badrun, N. (2009). Coral symbiotic complex: hypothesis through vitamin B12 for a new evaluation. *Galaxea J. Coral Reef Stud.* 11, 1–11. doi: 10.3755/galaxea.11.1

Baird, A. H., Keith, S. A., Woolsey, E., Yoshida, R., and Naruse, T. (2017). Rapid coral mortality following unusually calm and hot conditions on Iriomote, Japan. *F1000Research* 6, 1728. doi: 10.12688/f1000research.12660.2

Baker, A. C. (2003). Flexibility and specificity in coral-algal symbiosis: diversity, ecology, and biogeography of *Symbiodinium*. *Annu. Rev. Ecol. Evol. Syst.* 34, 661–689. doi: 10.1146/annurev.ecolsys.34.011802.132417

Baker, A. C., Glynn, P. W., and Riegl, B. (2008). Climate change and coral reef bleaching: an ecological assessment of long-term impacts, recovery trends and future outlook. *Estuar. Coast. Shelf Sci.* 80, 435–471. doi: 10.1016/j.ecss.2008.09.003

Baker, A. C., Starger, C. J., McClanahan, T. R., and Glynn, P. W. (2004). Corals' adaptive response to climate change. *Nature.* 430, 741. doi: 10.1038/430741a

Baker, D. M., Andras, J. P., Jordán-Garza, A. G., and Fogel, M. L. (2013). Nitrate competition in a coral symbiosis varies with temperature among *Symbiodinium* clades. *ISME J.* 7, 1248–1251. doi: 10.1038/ismej.2013.12

Barshis, D. J., Ladner, J. T., Oliver, T. A., Seneca, F. O., Traylor-Knowles, N., and Palumbi, S. R. (2013). Genomic basis for coral resilience to climate change. *Proc. Natl. Acad. Sci. U. S. A.* 110, 1387–1392. doi: 10.1073/pnas.1210224110

Berkelmans, R., and van Oppen, M. J. H. (2006). The role of zooxanthellae in the thermal tolerance of corals: a "nugget of hope" for coral reefs in an era of climate change. *Proc. Biol. Sci.* 273, 2305–2312. doi: 10.1098/rspb.2006.3567

Bouchard, J. N., and Yamasaki, H. (2008). Heat stress stimulates nitric oxide production in *Symbiodinium microadriaticum*: a possible linkage between nitric oxide and the coral bleaching phenomenon. *Plant Cell Physiol.* 49, 641–652. doi: 10.1093/pcp/pcn037

Cantin, N. E., van Oppen, M. J. H., Willis, B. L., Mieog, J. C., and Negri, A. P. (2009). Juvenile corals can acquire more carbon from high-performance algal symbionts. *Coral Reefs* 28, 405. doi: 10.1007/s00338-009-0478-8

Chen, C. A., Wang, J., Fang, L., and Yang, Y.-W. (2005). Fluctuating algal symbiont communities in *Acropora palifera* (Scleractinia: Acroporidae) from Taiwan. *Mar. Ecol. Prog. Ser.* 295, 113–121. doi: 10.3354/meps295113

Chen, M.-C., Cheng, Y.-M., Sung, P.-J., Kuo, C.-E., and Fang, L.-S. (2003). Molecular identification of Rab7 (ApRab7) in Aiptasia pulchella and its exclusion from phagosomes harboring zooxanthellae. *Biochem. Biophys. Res. Commun.* 308, 586–595. doi: 10.1016/S0006-291X(03)01428-1

Constant, S., Perewoska, I., Alfonso, M., and Kirilovsky, D. (1997). Expression of the psbA gene during photoinhibition and recovery in Synechocystis PCC 6714: inhibition and damage of transcriptional and translational machinery prevent the restoration of photosystem II activity. *Plant Mol. Biol.* 34, 1–13. doi: 10.1023/A:1005754823218

Croft, M. T., Lawrence, A. D., Raux-Deery, E., Warren, M. J., and Smith, A. G. (2005). Algae acquire vitamin B12 through a symbiotic relationship with bacteria. *Nature* 438, 90–93. doi: 10.1038/nature04056

Császár, N., Seneca, F., and van Oppen, M. (2009). Variation in antioxidant gene expression in the scleractinian coral *Acropora millepora* under laboratory thermal stress. *Mar. Ecol. Prog. Ser.* 392, 93–102. doi: 10.3354/meps08194

Cunning, R., and Baker, A. C. (2020). Thermotolerant coral symbionts modulate heat stress-responsive genes in their hosts. *Mol. Ecol.* 29, 2940–2950. doi: 10.1111/mec.15526

Cunning, R., Gillette, P., Capo, T., Galvez, K., and Baker, A. C. (2015). Growth tradeoffs associated with thermotolerant symbionts in the coral *Pocillopora damicornis* are lost in warmer oceans. *Coral Reefs* 34, 155–160. doi: 10.1007/s00338-014-1216-4

Desalvo, M. K., Voolstra, C. R., Sunagawa, S., Schwarz, J. A., Stillman, J. H., Coffroth, M. A., et al. (2008). Differential gene expression during thermal stress and bleaching in the Caribbean coral *Montastraea faveolata*. *Mol. Ecol.* 17, 3952–3971. doi: 10.1111/j.1365-294X.2008.03879.x

Dunn, S. R., Pernice, M., Green, K., Hoegh-Guldberg, O., and Dove, S. G. (2012). Thermal stress promotes host mitochondrial degradation in symbiotic cnidarians: are the batteries of the reef going to run out? *PLoS ONE* 7, e39024. doi: 10.1371/journal.pone.0039024

Dunn, S. R., Schnitzler, C. E., and Weis, V. M. (2007). Apoptosis and autophagy as mechanisms of dinoflagellate symbiont release during cnidarian bleaching: every which way you lose. *Proc. R. Soc. B Biol. Sci.* 274, 3079–3085. doi: 10.1098/rspb.2007.0711

Edge, S. E., Morgan, M. B., Gleason, D. F., and Snell, T. W. (2005). Development of a coral cDNA array to examine gene expression profiles in *Montastraea faveolata* exposed to environmental stress. *Mar. Pollut. Bull.* 51, 507–523. doi: 10.1016/j.marpolbul.2005.07.007

Fu, L., Niu, B., Zhu, Z., Wu, S., and Li, W. (2012). CD-HIT: accelerated for clustering the next-generation sequencing data. *Bioinforma. Oxf. Engl.* 28, 3150–3152. doi: 10.1093/bioinformatics/bts565

Gavrin, A., Kaiser, B. N., Geiger, D., Tyerman, S. D., Wen, Z., Bisseling, T., et al. (2014). Adjustment of host cells for accommodation of symbiotic bacteria: vacuole defunctionalization, HOPS suppression, and TIP1g retargeting in medicago. *Plant Cell* 26, 3809–3822. doi: 10.1105/tpc.114.128736

Gierz, S. L., Forêt, S., and Leggat, W. (2017). Transcriptomic analysis of thermally stressed *Symbiodinium* reveals differential expression of stress and metabolism genes. *Front. Plant Sci.* 8, 271. doi: 10.3389/fpls.2017.00271

Gorbunov, M. Y., Kolber, Z. S., Lesser, M. P., and Falkowski, P. G. (2001). Photosynthesis and photoprotection in symbiotic corals. *Limnol. Oceanogr.* 46, 75–85. doi: 10.4319/lo.2001.46.1.0075

Haas, B. J., Papanicolaou, A., Yassour, M., Grabherr, M., Blood, P. D., Bowden, J., et al. (2013). De novo transcript sequence reconstruction from RNA-Seq: reference generation and analysis with Trinity. *Nat. Protoc.* 8, 1494–512. doi: 10.1038/nprot.2013.084

Hawkins, T. D., Bradley, B. J., and Davy, S. K. (2013). Nitric oxide mediates coral bleaching through an apoptotic-like cell death pathway: evidence from a model sea anemone-dinoflagellate symbiosis. *FASEB J. Off. Publ. Fed. Am. Soc. Exp. Biol.* 27, 4790–4798. doi: 10.1096/fj.13-235051

Helliwell, K. E., Lawrence, A. D., Holzer, A., Kudahl, U. J., Sasso, S., Kräutler, B., et al. (2016). Cyanobacteria and eukaryotic algae use different chemical variants of vitamin B12. *Curr. Biol. CB* 26, 999–1008. doi: 10.1016/j.cub.2016.02.041

Higuchi, T., Fujimura, H., Arakaki, T., and Oomori, T. (2009). Activities of antioxidant enzymes (SOD and CAT) in the coral *Galaxea fascicularis* against increased hydrogen peroxide concentrations in seawater. *Proc. 11th Int. Coral Reef Symp.* 926–930.

Huang, D. W., Sherman, B. T., and Lempicki, R. A. (2009a). Systematic and integrative analysis of large gene lists using DAVID bioinformatics resources. *Nat. Protoc.* 4, 44–57. doi: 10.1038/nprot.2008.211

Huang, D. W., Sherman, B. T., Zheng, X., Yang, J., Imamichi, T., Stephens, R., et al. (2009b). Extracting biological meaning from large gene lists with DAVID. *Curr. Protoc. Bioinforma. Chapter* 13, 13. doi: 10.1002/0471250953.bi1311s27

Iwao, K., Fujisawa, T., and Hatta, M. (2002). A cnidarian neuropeptide of the GLWamide family induces metamorphosis of reef-building corals in the genus Acropora. *Coral Reefs* 21, 127–129. doi: 10.1007/s00338-002-0219-8

Kanehisa, M., and Goto, S. (2000). KEGG: kyoto encyclopedia of genes and genomes. *Nucleic Acids Res.* 28, 27–30. doi: 10.1093/nar/28.1.27

Kantidze, O. L., Velichko, A. K., Luzhin, A. V., and Razin, S. V. (2016). Heat stress-induced DNA damage. *Acta Nat.* 8, 75–78. doi: 10.32607/20758251-2016-8-2-75-78

Kvitt, H., Rosenfeld, H., and Tchernov, D. (2016). The regulation of thermal stress induced apoptosis in corals reveals high similarities in gene expression and function to higher animals. *Sci. Rep.* 6, 30359. doi: 10.1038/srep30359

Ladner, J. T., Barshis, D. J., and Palumbi, S. R. (2012). Protein evolution in two co-occurring types of *Symbiodinium*: an exploration into the genetic basis of thermal tolerance in *Symbiodinium* clade D. *BMC Evol. Biol.* 12, 217. doi: 10.1186/1471-2148-12-217

LaJeunesse, T. C., Parkinson, J. E., Gabrielson, P. W., Jeong, H. J., Reimer, J. D., Voolstra, C. R., et al. (2018). Systematic revision of Symbiodiniaceae highlights the antiquity and diversity of coral endosymbionts. *Curr. Biol.* 28, 2570–2580.e6. doi: 10.1016/j.cub.2018.07.008

Langmead, B., and Salzberg, S. L. (2012). Fast gapped-read alignment with Bowtie 2. *Nat. Methods* 9, 357–359. doi: 10.1038/nmeth.1923

Lesser, M. P. (1997). Oxidative stress causes coral bleaching during exposure to elevated temperatures. *Coral Reefs* 16, 187–192. doi: 10.1007/s003380050073

Lesser, M. P. (2011). "Coral bleaching: causes andmechanisms," in *Coral Reefs: An Ecosystem in Transition*, eds Z. Dubinsky and N. Stambler (Dordrecht: Springer Netherlands), 405–419. doi: 10.1007/978-94-007-0114-4_23

Lesser, M. P., and Shick, J. M. (1989). Effects of irradiance and ultraviolet radiation on photoadaptation in the zooxanthellae of *Aiptasia pallida*: primary production, photoinhibition, and enzymic defenses against oxygen toxicity. *Mar. Biol.* 102, 243–255. doi: 10.1007/BF00428286

Lin, S., Cheng, S., Song, B., Zhong, X., Lin, X., Li, W., et al. (2015). The *Symbiodinium kawagutii* genome illuminates dinoflagellate gene expression and coral symbiosis. *Science* 350, 691–694. doi: 10.1126/science.aad0408

Maor-Landaw, K., and Levy, O. (2016). Gene expression profiles during short-term heat stress; branching vs. massive Scleractinian corals of the Red Sea. *PeerJ* 4, e1814. doi: 10.7717/peerj.1814

Mayer, M. P., and Bukau, B. (2005). Hsp70 chaperones: cellular functions and molecular mechanism. *Cell. Mol. Life Sci. CMLS* 62, 670–684. doi: 10.1007/s00018-004-4464-6

Meyer, E., Aglyamova, G. V., and Matz, M. V. (2011). Profiling gene expression responses of coral larvae (Acropora millepora) to elevated temperature and settlement inducers using a novel RNA-Seq procedure. *Mol. Ecol.* 20, 3599–3616. doi: 10.1111/j.1365-294X.2011.05205.x

Mieog, J. C., Olsen, J. L., Berkelmans, R., Bleuler-Martinez, S. A., Willis, B. L., and van Oppen, M. J. H. (2009). The roles and interactions of symbiont, host and environment in defining coral fitness. *PLoS ONE* 4, e6364. doi: 10.1371/annotation/e06b31ef-6b29-44ae-aec1-1740daa93f4b

Murata, N., Takahashi, S., Nishiyama, Y., and Allakhverdiev, S. I. (2007). Photoinhibition of photosystem II under environmental stress. *Biochim. Biophys. Acta* 1767, 414–421. doi: 10.1016/j.bbabio.2006.11.019

Nagasaki, H., Mochizuki, T., Kodama, Y., Saruhashi, S., Morizaki, S., Sugawara, H., et al. (2013). DDBJ read annotation pipeline: a cloud computing-based pipeline for high-throughput analysis of next-generation sequencing data. *DNA Res. Int. J. Rapid Publ. Rep. Genes Genomes* 20, 383–390. doi: 10.1093/dnares/dst017

Nesa, B., Baird, A. H., Harii, S., Yakovleva, I., and Hidaka, M. (2012). Algal symbionts increase DNA damage in coral planulae exposed to sunlight. *Zool. Stud.* 51, 12–17.

Nesa, B., and Hidaka, M. (2009). Thermal stress increases oxidative DNA damage in coral cell aggregates. *J. Exp. Mar. Biol. Ecol.* 15, 81–87. doi: 10.1016/j.jembe.2008.10.018

Oakley, C. A., Durand, E., Wilkinson, S. P., Peng, L., Weis, V. M., Grossman, A. R., et al. (2017). Thermal Shock Induces Host proteostasis disruption and endoplasmic reticulum stress in the model symbiotic cnidarian *Aiptasia*. *J. Proteome Res.* 16, 2121–2134. doi: 10.1021/acs.jproteome.6b00797

Omori, M., and Iwao, K. (2014). *Methods of Farming Sexually Propagated Corals and Out Planting for Coral Reef Rehabilitation; With List of References for Coral Reef Rehabilitation Through Active Restoration Measure*. Okinawa: Akajima Marine Science Laboratory.

Perez, S., and Weis, V. (2006). Nitric oxide and cnidarian bleaching: an eviction notice mediates breakdown of a symbiosis. *J. Exp. Biol.* 209, 2804–2810. doi: 10.1242/jeb.02309

Pernice, M., Meibom, A., Van Den Heuvel, A., Kopp, C., Domart-Coulon, I., Hoegh-Guldberg, O., et al. (2012). A single-cell view of ammonium assimilation in coral–dinoflagellate symbiosis. *ISME J.* 6, 1314–1324. doi: 10.1038/ismej.2011.196

Roberts, A., and Pachter, L. (2013). Streaming fragment assignment for real-time analysis of sequencing experiments. *Nat. Methods* 10, 71–73. doi: 10.1038/nmeth.2251

Rodriguez-Casariego, J. A., Cunning, R., Baker, A. C., and Eirin-Lopez, J. M. (2022). Symbiont shuffling induces differential DNA methylation responses to thermal stress in the coral *Montastraea cavernosa*. *Mol. Ecol.* 31, 588–602. doi: 10.1111/mec.16246

Rosenberg, Y., Doniger, T., and Levy, O. (2019). Sustainability of coral reefs are affected by ecological light pollution in the gulf of Aqaba/Eilat. *Commun. Biol.* 2, 1–9. doi: 10.1038/s42003-019-0548-6

Rosic, N., Ling, E. Y. S., Chan, C.-K. K., Lee, H. C., Kaniewska, P., Edwards, D., et al. (2015). Unfolding the secrets of coral–algal symbiosis. *ISME J.* 9, 844–856. doi: 10.1038/ismej.2014.182

Rosic, N. N., Pernice, M., Dove, S., Dunn, S., and Hoegh-Guldberg, O. (2011). Gene expression profiles of cytosolic heat shock proteins Hsp70 and Hsp90 from symbiotic dinoflagellates in response to thermal stress: possible implications for coral bleaching. *Cell Stress Chaperones* 16, 69–80. doi: 10.1007/s12192-010-0222-x

Rowan, R. (2004). Coral bleaching: thermal adaptation in reef coral symbionts. *Nature* 430, 742. doi: 10.1038/430742a

Ruiz-Jones, L. J., and Palumbi, S. R. (2017). Tidal heat pulses on a reef trigger a fine-tuned transcriptional response in corals to maintain homeostasis. *Sci. Adv.* 3, e1601298. doi: 10.1126/sciadv.1601298

Samanta, A., Hughes, T. E. T., and Moiseenkova-Bell, V. Y. (2018). Transient receptor potential (TRP) channels. *Subcell. Biochem.* 87, 141–165. doi: 10.1007/978-981-10-7757-9_6

Schepers, R. J., and Ringkamp, M. (2009). Thermoreceptors and thermosensitive afferents. *Neurosci. Biobehav. Rev.* 33, 205–212. doi: 10.1016/j.neubiorev.2008.07.009

Seneca, F. O., Forêt, S., Ball, E. E., Smith-Keune, C., Miller, D. J., and van Oppen, M. J. H. (2010). Patterns of gene expression in a scleractinian coral undergoing natural bleaching. *Mar. Biotechnol. N. Y. N* 12, 594–604. doi: 10.1007/s10126-009-9247-5

Shinzato, C., Shoguchi, E., Kawashima, T., Hamada, M., Hisata, K., Tanaka, M., et al. (2011). Using the *Acropora digitifera* genome to understand coral responses to environmental change. *Nature* 476, 320–323. doi: 10.1038/nature10249

Shoguchi, E., Beedessee, G., Tada, I., Hisata, K., Kawashima, T., Takeuchi, T., et al. (2018). Two divergent *Symbiodinium* genomes reveal conservation of a gene cluster for sunscreen biosynthesis and recently lost genes. *BMC Genomics* 19, 458. doi: 10.1186/s12864-018-4857-9

Shoguchi, E., Shinzato, C., Kawashima, T., Gyoja, F., Mungpakdee, S., Koyanagi, R., et al. (2013). Draft assembly of the *Symbiodinium minutum* nuclear genome reveals dinoflagellate gene structure. *Curr. Biol.* 23, 1399–1408. doi: 10.1016/j.cub.2013.05.062

Song, P.-C., Wu, T.-M., Hong, M.-C., and Chen, M.-C. (2015). Elevated temperature inhibits recruitment of transferrin-positive vesicles and induces

iron-deficiency genes expression in *Aiptasia pulchella* host-harbored *Symbiodinium*. *Comp. Biochem. Physiol. B Biochem. Mol. Biol.* 188, 1–7. doi: 10.1016/j.cbpb.2015.05.005

Sun, J., Nishiyama, T., Shimizu, K., and Kadota, K. (2013). TCC: an R package for comparing tag count data with robust normalization strategies. *BMC Bioinformatics* 14, 219. doi: 10.1186/1471-2105-14-219

Takahashi, S., Whitney, S. M., and Badger, M. R. (2009). Different thermal sensitivity of the repair of photodamaged photosynthetic machinery in cultured *Symbiodinium* species. *Proc. Natl. Acad. Sci. U. S. A.* 106, 3237–3242. doi: 10.1073/pnas.0808363106

Tchernov, D., Kvitt, H., Haramaty, L., Bibby, T. S., Gorbunov, M. Y., Rosenfeld, H., et al. (2011). Apoptosis and the selective survival of host animals following thermal bleaching in zooxanthellate corals. *Proc. Natl. Acad. Sci. U. S. A.* 108, 9905–9909. doi: 10.1073/pnas.1106924108

Trapido-Rosenthal, H., Zielke, S., Owen, R., Buxton, L., Boeing, B., Bhagooli, R., et al. (2005). Increased zooxanthellae nitric oxide synthase activity is associated with coral bleaching. *Biol. Bull.* 208, 3–6. doi: 10.2307/3593094

ul Haq, S., Khan, A., Ali, M., Khattak, A. M., Gai, W.-X., Zhang, H.-X., et al. (2019). Heat shock proteins: dynamic biomolecules to counter plant biotic and abiotic stresses. *Int. J. Mol. Sci.* 20, 5321. doi: 10.3390/ijms20215321

Voolstra, C. R., Schnetzer, J., Peshkin, L., Randall, C. J., Szmant, A. M., and Medina, M. (2009). Effects of temperature on gene expression in embryos of the coral *Montastraea faveolata*. *BMC Genomics* 10, 627. doi: 10.1186/1471-2164-10-627

Warner, M. E., Fitt, W. K., and Schmidt, G. W. (1999). Damage to photosystem II in symbiotic dinoflagellates: a determinant of coral bleaching. *Proc. Natl. Acad. Sci.* 96, 8007–8012. doi: 10.1073/pnas.96.14.8007

Weston, A. J., Dunlap, W. C., Beltran, V. H., Starcevic, A., Hranueli, D., Ward, M., et al. (2015). Proteomics links the redox state to calcium signaling during bleaching of the scleractinian coral *Acropora microphthalma* on exposure to high solar irradiance and thermal stress. *Mol. Cell. Proteomics* 14, 585–595. doi: 10.1074/mcp.M114.043125

Yu, J. S. L., and Cui, W. (2016). Proliferation, survival and metabolism: the role of PI3K/AKT/mTOR signalling in pluripotency and cell fate determination. *Dev. Camb. Engl.* 143, 3050–3060. doi: 10.1242/dev.137075

Yuyama, I., Hayakawa, H., Endo, H., Iwao, K., Takeyama, H., Maruyama, T., et al. (2005). Identification of symbiotically expressed coral mRNAs using a model infection system. *Biochem. Biophys. Res. Commun.* 336, 793–798. doi: 10.1016/j.bbrc.2005.08.174

Yuyama, I., and Higuchi, T. (2014). Comparing the effects of symbiotic algae (*Symbiodinium*) clades C1 and D on early growth stages of *Acropora tenuis*. *PLoS ONE* 9, e98999. doi: 10.1371/journal.pone.0098999

Yuyama, I., Ishikawa, M., Nozawa, M., Yoshida, M., and Ikeo, K. (2018). Transcriptomic changes with increasing algal symbiont reveal the detailed process underlying establishment of coral-algal symbiosis. *Sci. Rep.* 8, 16802. doi: 10.1038/s41598-018-34575-5

Yuyama, I., Ito, Y., Watanabe, T., Hidaka, M., Suzuki, Y., and Nishida, M. (2012). Differential gene expression in juvenile polyps of the coral Acropora tenuis exposed to thermal and chemical stresses. *J. Exp. Mar. Biol. Ecol.* 430–431, 17–24. doi: 10.1016/j.jembe.2012.06.020

Yuyama, I., Nakamura, T., Higuchi, T., and Hidaka, M. (2016). Different stress tolerances of juveniles of the coral *Acropora tenuis* associated with clades C1 and D *Symbiodinium*. *Zool. Stud.* 55, e9. doi: 10.6620/ZS.2016.55-19

Conflict of Interest: The authors declare that the research was conducted in the absence of any commercial or financial relationships that could be construed as a potential conflict of interest.

Publisher's Note: All claims expressed in this article are solely those of the authors and do not necessarily represent those of their affiliated organizations, or those of the publisher, the editors and the reviewers. Any product that may be evaluated in this article, or claim that may be made by its manufacturer, is not guaranteed or endorsed by the publisher.

frontiers | Frontiers in Marine Science

REVIEW
published: 12 May 2022
doi: 10.3389/fmars.2022.805113

Coral Reef Electrotherapy: Field Observations

Thomas J. F. Goreau *

Global Coral Reef Alliance, Cambridge, MA, United States

Coral reefs are the fastest collapsing ecosystems from accelerating global warming, sea level, disease, and pollution. Urgent steps are essential to regenerate them, and their biodiversity and environmental services, if there is to be a sustainable "Blue Economy". Methods that greatly increase settlement, growth, survival and resistance to extremely high temperature and pollutant stress are critically needed to regenerate coral reef and coastal ecosystems now and in the future. Safe Extremely Low Voltage (SELV) electrical fields generated by the Biorock electrolytic reef process have been documented for more than 35 years to greatly increase settlement, growth, healing, and survival of marine organisms in general under extreme stress conditions. The visibly observable benefits of electrical stress relief on marine organisms are summarized, and testable hypotheses are proposed to determine mechanisms and improve applications. Although these field observations strongly imply that electricity in the proper range improves stress resistance and health, the mechanisms have never been studied at cellular, biophysical, biochemical, molecular, or genetic levels. Electrical stimulation is the only method known to reverse the impacts of extreme stresses on corals and other marine organisms. Widespread regeneration of coral reef ecosystems by electrotherapy is urgently needed before they become functionally extinct.

Keywords: coral reefs, electricity, healing, growth, stimulation, regeneration

OPEN ACCESS

Edited by:
Ranjeet Bhagooli,
University of Mauritius, Mauritius

Reviewed by:
Ricardo Tapilatu,
Ricardo F. Tapilatu, Indonesia
Munasik Munasik,
Diponegoro University, Indonesia

***Correspondence:**
Thomas J. F. Goreau
goreau@globalcoral.org

Specialty section:
This article was submitted to Aquatic Physiology, a section of the journal Frontiers in Marine Science

Received: *29 October 2021*
Accepted: *31 March 2022*
Published: *12 May 2022*

Citation:
Goreau TJF (2022) Coral Reef Electrotherapy: Field Observations. Front. Mar. Sci. 9:805113. doi: 10.3389/fmars.2022.805113

INTRODUCTION

Coral stresses from pollution, climate change, and pathogens were negligible before the 1980s (Goreau et al., 1979; Hayes and Goreau, 1998) but have since then killed most corals in the world. Global warming passed the tipping point for mass coral bleaching in the 1980s (Hayes and Goreau, 1991; Goreau and Hayes, 1994; Goreau and Hayes, 2021), but governments failed to respond to the data with effective measures to save coral reefs.

Most studies of coral stress measure negative impacts of high levels of imposed stressors on coral health. This volume contains many state-of-the-art applications of recent advances in biological instrumentation and methods to quantify negative stress impacts. This chapter takes an alternative approach, using natural history observations under beneficial growth conditions instead of harmful ones. The effects of stress are only too well known; they are visible almost everywhere; dead and dying corals are now regarded as "normal" by most reef researchers with less than 50 years of experience. The Goreau coral reef photograph archive, the world's largest from the 1940s, 1950s,

and 1960s, which will be posted on line by the Global Coral Reef Alliance, shows no diseased or dying corals except those being smothered by dredging sediments.

Observations of Biorock electric reefs showed that all visible measures of good coral health are improved by the method (Goreau and Hilbertz, 2005). Nearly 35 years of field observations are systematically summarized here for the first time. The effects of Safe Extremely Low Voltage (SELV) direct current electrical stimulation of corals and all other marine organisms include significantly increased settlement, biodiversity, growth, healing, reproduction, survival, and resistance to lethal extreme environmental stresses. No adverse impacts have been seen. Testable hypotheses are proposed for research to elucidate the biophysical and biochemical mechanisms. The work of authors of other chapters of this volume will prove essential for testing these hypotheses and improving applications for coral reef regeneration.

The Biorock technique of ecosystem regeneration greatly increases coral growth under adverse water quality conditions and protects corals from severe bleaching mortality (Goreau and Hilbertz, 2005; Goreau and Trench, 2012), providing our most powerful tool to save coral reef ecosystems from functional extinction by global warming. Its discovery came from unexpected empirical field observations.

The use of electricity to grow solid limestone structures of any size or shape in the oceans was invented by architect Wolf Hilbertz in 1976 (Hilbertz, 1979), building on Michael Faraday's original work on electrolysis of sea water (Goreau, 2012a). In 1987 I invited Wolf to Jamaica to collaborate applying the method to coral reef regeneration, and we worked around the globe until his death 20 years later (https://en.wikipedia.org/wiki/Wolf_Hilbertz). Jamaican corals were being overgrown by harmful algae blooms caused by sewage (Goreau, 1992), so our first goal was to grow structures to revive dying coral populations above the slime smothering them. We quickly found that previously unsuspected biological benefits far outweighed purely physical ones. This chapter summarizes field observations from perhaps around a thousand Biorock reefs built by our students and us in 45 countries over more than four decades in a wide range of sizes, shapes, environments, and purposes. The process works over a wide range of electrical voltages and currents (Hilbertz, 1979) in the Safe Extremely Low Voltage (SELV) range that are insensible to humans, and a very wide range of power sources are used, including solar, wind, wave, ocean current, and conventional sources that span a wide range of conditions. As the electrical current depends on type of power source and size of the reef, most are probably run under sub-optimal conditions.

Low voltage direct current electrical stimulation of marine life is widely misunderstood due to fear of the well-known deadly effects of high voltage alternating currents. Demonstrated benefits of low voltage direct current are widely ridiculed by those who have never seen them and are unwilling to look for themselves. Nevertheless, a wide range of electro-therapy methods have been applied medically to wound healing and nervous system, bone, and muscle regeneration (Tai et al., 2018). These generally use alternating current at much higher voltages than the work described in this chapter, which deals only with Safe Extremely Low Voltage (SELV) direct current electrical fields.

All living organisms, from bacteria and archaea throughout the evolutionary tree of life, use proteins inherited from the last universal common ancestor, perhaps around 4 billion years ago (Weiss et al., 2018). These enzymes transform electrical currents flowing down electrical potential (voltage) differences across biological membranes of around a tenth of a volt to synthesize the universal biochemical energy currencies, ATP and NADP (O'Rourke et al., 2005).

All organisms lose a major part of their energy pumping ions, protons, and electrons back across the membrane to maintain the voltage gradient across it because if this collapses, they quickly run out of energy and die. Very low direct current electrical fields increase ATP, NADP, and protein synthesis in cell cultures up to an optimal voltage, with benefits then decreasing and turning negative at very high currents (Cheng et al., 1982).

Ambient electrical fields used in the Biorock process appear to reduce the energy organisms waste maintaining membrane voltage gradients, providing increased energy for growth, healing, reproduction, and general good health. We hypothesize that the Biorock process directly stimulates biochemical energy availability *via* increased end-use energy efficiency, providing all marine organisms with energy for superior health and stress resistance (Goreau, 2012b; Goreau, 2014). Despite overwhelming field evidence for its benefits, no studies of the biophysics and biochemistry of the process have yet been done. This chapter summarizes around 35 years of field observations on biological effects of electrical currents, and proposes many testable hypotheses for such future research studies relevant to field applications. A separate chapter by the author on the ecological effects of Biorock reef structures, Biorock electric reefs greatly enhance coral reef structure and function for climate change adaptation, has been submitted to a separate book, Corals - Habitat Formers From the Shallow to the Deep, Dr. Giovanni Chimienti, Editor.

RESULTS: VISIBLE BIOLOGICAL HEALTH BENEFITS OF BIOROCK

Growth Rates

Greatly accelerated coral growth rates were the first effect noted. On the first Biorock structure we built in Discovery Bay in the 1980s, I attached a few small loose fragments of *Porites porites*. This species had previously been very abundant but been almost entirely overgrown and killed by weedy algae overgrowth over-fertilized by sewage nutrients (Goreau, 1992). The first small pale fragments, a few centimeters across, grew astonishingly fast and tripled in size in three months, growing onto and over the Biorock structure, with polyp tentacles vigorously feeding and branching (**Figures 1A, B**). Thus we grew most Jamaican corals

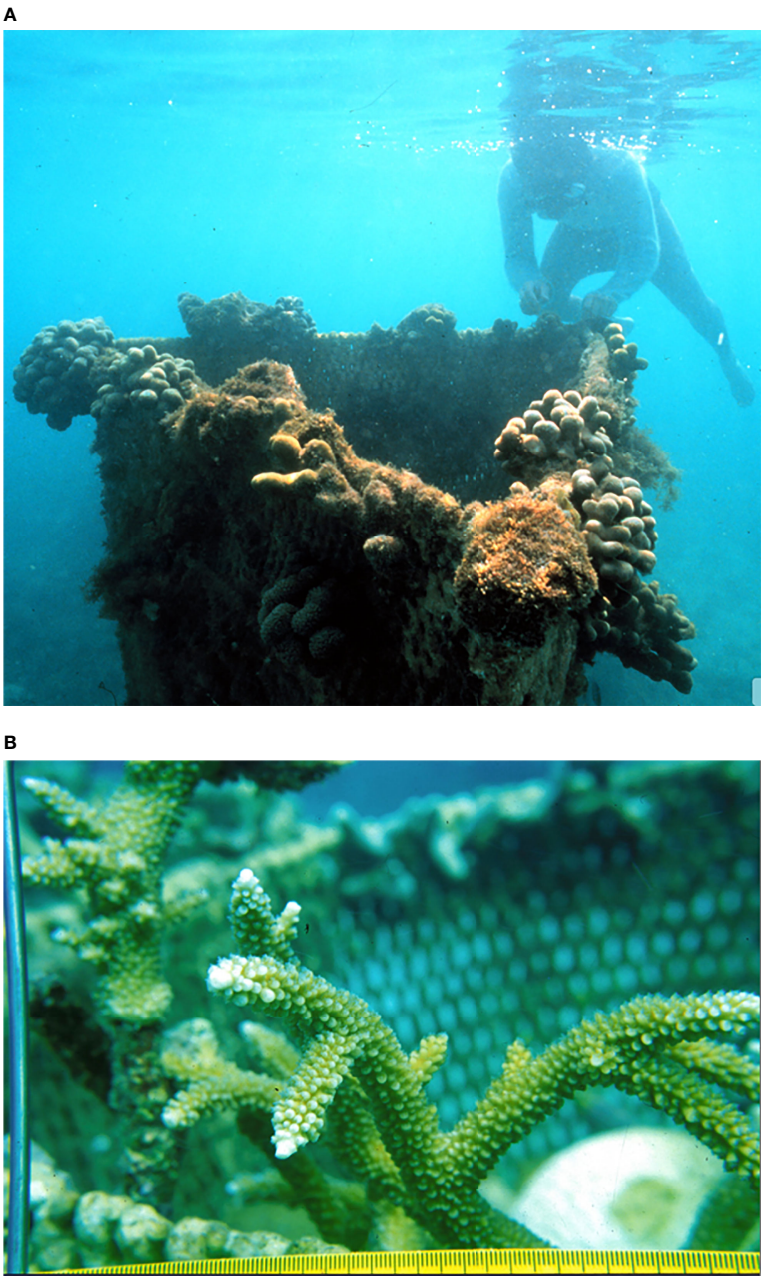

FIGURE 1 | **(A)** The prolific growth of *Porites porites* on Biorock. Densely branching *Porites porites* colonies are interspersed with sand-producing red coralline algae that grew spontaneously (front corner of Biorock reef). Discovery Bay, Jamaica, 1989 photograph by Dr. Peter Goreau. **(B)** *Acropora cervicornis* grew 0.8 cm per week in an area of poor water quality. Negril, Jamaica, 1991 photograph by Wolf Hilbertz.

several times faster than documented record rates for those species in clean water, but in poor water quality where corals were dying (see photographs in Goreau and Hilbertz, 2012).

We first thought coral calcification was accelerated by high pH produced by water electrolysis. Although only coral fragments were placed on Biorock structures, all forms of marine life spontaneously settled on and around the Biorock structures, both with and without limestone skeletons. Greatly accelerated growth was seen in hard coral, soft corals, sponges, tunicates, oysters, mussels, giant clams, seagrasses, salt marsh grass, calcareous algae, and every marine animal and plant examined (See chapters in Goreau and Trench, 2012; reviewed in Goreau, 2014).

The growth rate increase compared to controls depends on precise electrical conditions and species. In general, most organisms measured grew 3-5 times faster than controls

(**Figure 2**), but some cases were much higher, up to 6-20 times faster than controls (**Figures 3A, B**) (Bakti et al., 2012; Goreau, 2012b; Jompa et al., 2012; Munandar et al., 2018; Natasasmita et al., 2016; https://www.globalcoral.org/biorock-corals-grow-faster-longer-and-wider-depending-on-species-and-depth/). All organisms have been seen to benefit, but some proliferate faster than others. The effect is similar to throwing fertilizer on an empty field: the fastest growing weeds quickly dominate unless the lot is carefully weeded to produce roses or tomatoes.

The effects of applied electrical currents on rapid settlement and growth of corals and all other forms of sessile reef organisms have long been familiar to commercial divers, who spend most of their time smashing living corals and other prolific growth off oil and gas rigs and other marine structures that are electrically protected from corrosion (Gabriel Despaigne & Paul Sammarco, personal communications). Unfortunately, no scientific papers have ever been written on this, nor a systematic comparison of settlement and growth on electrically-protected structures versus controls.

Healing From Physical Damage

Healing of damaged coral tissues by Biorock electrical fields was immediately noted. Coral fragments transplanted onto Biorock structures had been naturally broken and were almost all in poor condition when rescued. Many corals had been badly damaged from rolling on the bottom or been partially buried in sand and mud, with most tissue dead or rotting. These injured corals were releasing prolific mucus when collected and transported, which continues until they fully heal, typically days or weeks later, but corals recovered fully overnight after being placed in the electrical field and stopped releasing mucus.

The corals shown in the following photographs had been collected as damaged naturally broken fragments late afternoon the previous day in Gili Trawangan, Lombok, Indonesia. They looked terrible when they were placed lying loosely, not attached, on top of a Biorock mesh overnight, prior to transplantation onto Biorock reefs the next morning. Normally broken corals collected from the field like this release mucus from injured tissue for days afterward, a sign of stress (Hayes and Goreau, 1998), and most were slimy with mucus when put on the mesh, but they had no mucus the next morning. **Figures 4A, B** were taken early the next morning, after one night of exposure to Biorock electrical fields. All the corals that looked so sorry the day before regained vibrant colors overnight and their polyps were fully extended and actively feeding. In addition, orange fan tube worms in coral skeletons were fully expanded (lower right, **Figure 4A**). The transformation was so incredible we were astonished!

The large Jamaican head coral shown in **Figures 4C, D** was broken off by hurricane waves in November 2020, and rolled

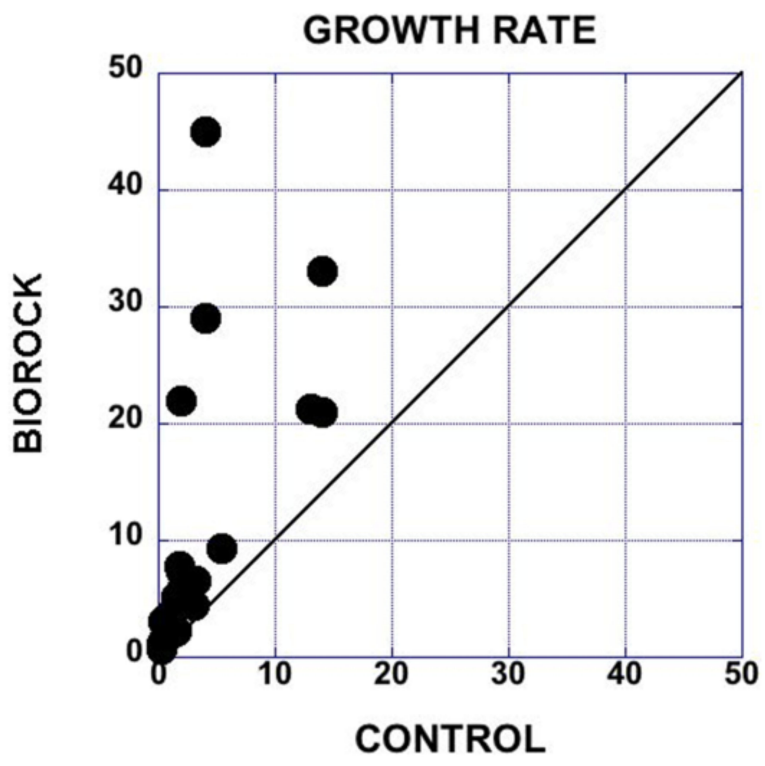

FIGURE 2 | Comparisons in growth rates between various species on Biorock versus controls. Each dot is a different species on a different Biorock reef under different conditions, from Goreau (2014).

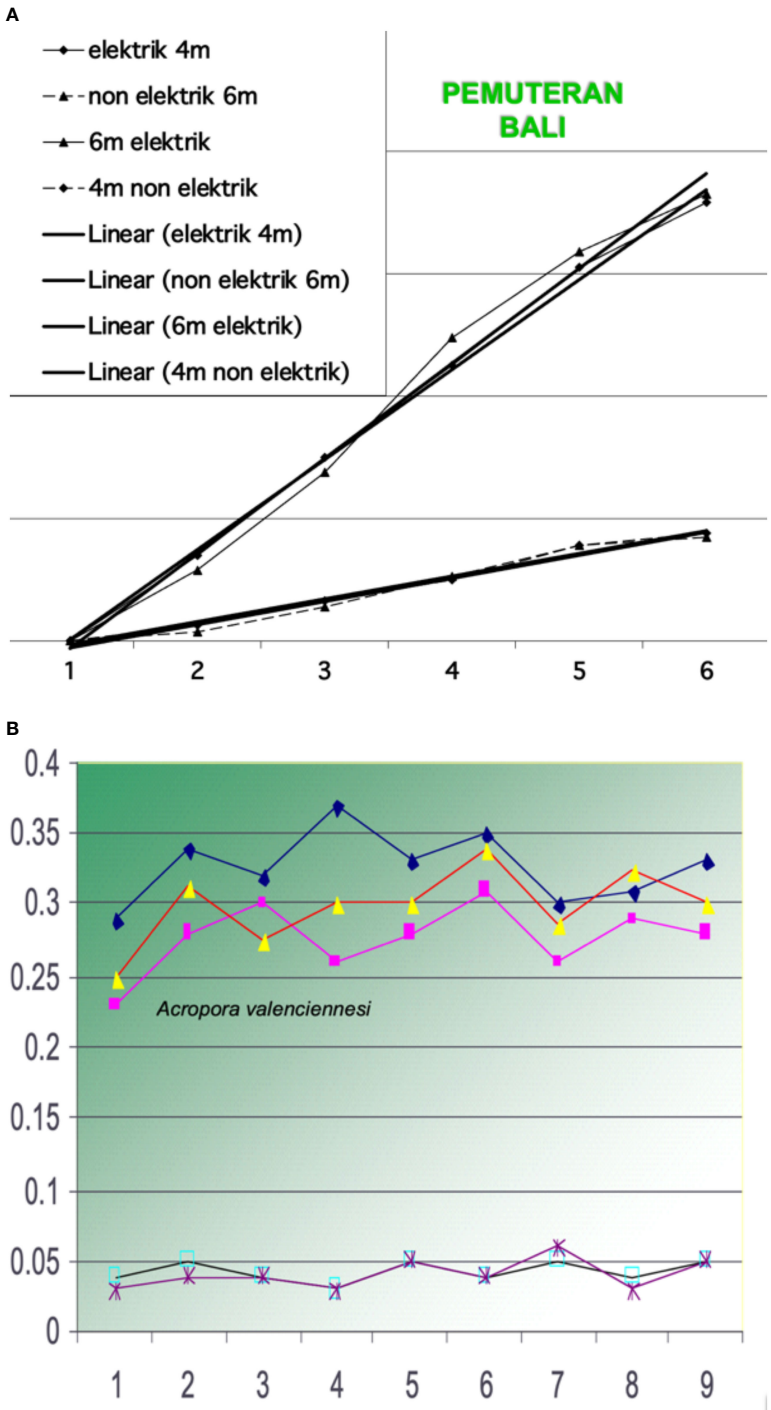

FIGURE 3 | **(A)** The first measurements of coral growth in Pemuteran, Bali found Biorock corals (top two curves) grew 4.01 times faster than controls (bottom two curves, overlapping). However, it was later realized that this increase was an underestimate because the controls were also in the electrical field even though they were not directly connected to it. Their growth had also been stimulated more than if they had been farther away. The vertical axis is the coral length in centimeters, the horizontal axis is weeks, each data point is the average of 8 corals. Data by Putra Nyoman Dwija, Udayana University, from Jompa et al., 2012. **(B)** Enhanced growth rate with Biorock (Jompa et al., 2012). Colored symbols on the top three lines are Biorock, x symbols at the bottom are controls. Vertical axis growth rate in centimeters per week, horizontal axis weeks, from Bakti et al., 2012.

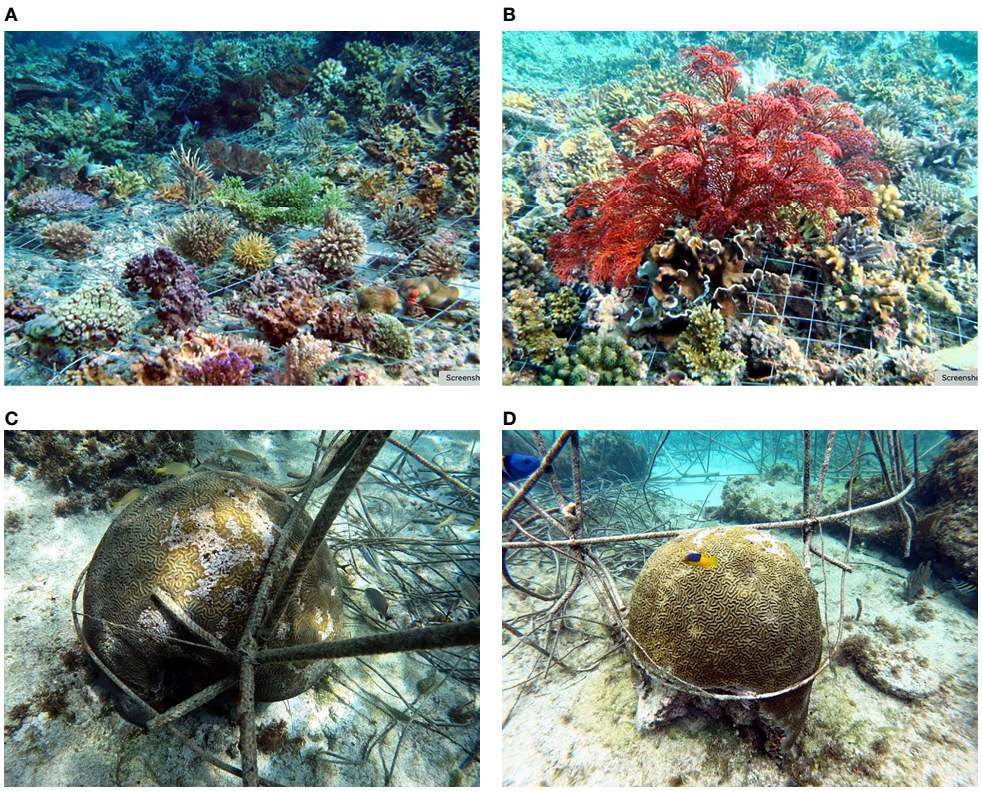

FIGURE 4 | **(A)** Loose broken hard and soft corals, with bright colors and with polyps fully expanded, after one night of electrical stimulation. Gili Trawangan, Lombok, Indonesia. **(B)** The red soft coral had been broken across the base by a storm and had been completely limp when placed on the mesh. The next morning it had not only healed the broken stalk; it was fully expanded and feeding. Gili Trawangan, Lombok, Indonesia. **(C)** February 23 2021, after three months in the electrical field, the damaged areas have healed and are growing back as with dark rims of proliferating new tissue growing over the dead coral skeleton. Before being placed in the electrical field, the tissue next to them had been necrotic and dying back. **(D)** After eight months, on June 4 2021 this old coral was nearly completely healed from severe injuries. It had not been expected to survive before it was placed in the electrical field. Negril, Jamaica, photographs by Sharren Robinson.

around upside down on rocks and sand in heavy waves for nearly a month before we could rescue it and place it in the Biorock electrical field. By that time most living tissue on top had been scraped off, and the skeleton surface was abraded and damaged. Within months healthy dark yellow-brown new coral tissue grew back over dead areas, and nearly completely healed over the damaged areas (**Figures 4C, D**). Such healing is now exceptional in Jamaica; severely damaged corals rarely recover like they used to in the old days unless they are in extremely clean water. Now we usually observe damaged coral tissues to be slimy, develop infectious diseases, and die, with tissue necrosis often expanding from damaged areas to kill the entire coral (Goreau et al., 1998).

Settlement

Rapid spontaneous settlement of larval corals and other species was quickly noticed on Biorock reefs (**Figure 5**). Tiny newly settled juvenile corals, about a millimeter across, were seen on Biorock at densities near one per square centimeter, orders of magnitudes higher than reported in natural coral reefs (Goreau, 2014).

After Hurricane Gilbert in 1989 I found rusty chicken wire fencing scraps in the bushes, wired them to a Biorock reef, and two years later found hundreds of young *Favia fragum* and *Agaricia agaricites* corals had settled all over the biorock coated wire mesh and grown several centimeters across (**Figures 6A, B**). Unfortunately, this reef had little or no natural coral recruitment for years since dead coral was smothered by weedy fleshy algae (Goreau and Hilbertz, 2012).

We have since seen many Biorock structures around the world spontaneously overgrown by corals and other marine organisms such as sponges, tunicates, oysters, mussels, and barnacles, and entire reefs spring up spontaneously all around them (**Figures 7**, **8**), and see video from Indonesia at https://www.globalcoral.org).

Biodiversity

Rapid Biodiversity increase on Biorock structures was noted, giving them the name "Biorock Coral Reef Arks". Only small, loose, naturally broken coral fragments found on the bottom below the reef were transplanted onto Biorock reefs, but all other components of coral reef biodiversity spontaneously followed. A year old Jamaican Biorock reef about 1.5 square meters in the area had more than a hundred species living on it (Goreau and

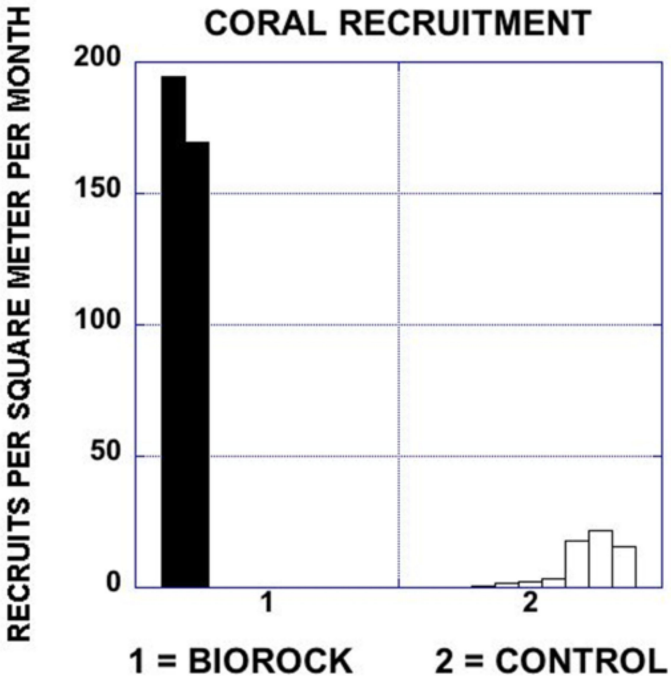

FIGURE 5 | Coral recruitment, from Goreau, 2014.

Hilbertz, 2012). A wide range of sessile organisms, such as corals, settled spontaneously onto the structure as larvae, and mobile marine organisms, such as juvenile reef fishes, crabs, sea urchins, and others migrated to it.

An astonishing local increase in biodiversity has been observed on Biorock reefs on sandy eutrophic rubble devoid of corals and fishes worldwide. In many places the biodiversity of the Biorock reefs is now considerably more remarkable than the reefs had been before, for example the corals and fishes in Pemuteran, Bali (**Figures 9A, B**). Fish densities and diversities are visibly higher on Biorock than surrounding areas, often by astonishing amounts, but few measurements have been made.

Different shaped Biorock structures side by side are dominated by different species of fish. The abundance of juvenile reef fish around Biorock reefs also corresponds to electrical currents, decreasing when power is turned off and rapidly increasing when restored. Biorock lobster habitats in Jamaica and Mexico had dozens to hundreds of lobsters crowded into around 2 square meters. This opens the possibilities of sustainable mariculture of entire ecosystems that grow their own food without external input and designed to the specific needs of desired species (Goreau, 2018).

Biodiversity increase in Biorock reefs needs to be measured by environmental DNA (eDNA). This method reveals nearly complete biodiversity of the habitat sampled, not just that which is visible. eDNA measurements reveals large amounts of cryptic biodiversity, identifying species playing a role in the ecosystem that are not observed by short term observers. The new species identified are especially noticeable in Indonesia, the center of marine biodiversity (Gelis et al., 2021; Maduppa et al., 2021). Therefore, Biorock reefs should be compared for eDNA of all taxa in comparison to reefs on either side.

Fluorescence

Biorock corals were noted to have more fluorescence than controls. The corals became brighter while under electrical power, but when power was turned off, they became notably paler over several days, and when power was restored, they visibly brightened within hours (**Figure 10A**). Observations first made in Jamaica were later confirmed in Maldives, Seychelles, Antigua, and Indonesia. Coral fluorescence is thought to be a measure of coral health, but there is little data.

Budding and Branching

Coral budding on Biorock showed very high polyp densities and dense formation of new growing tips (**Figure 10B**). Branching patterns were denser and better developed for all coral forms, including branching corals, foliose corals, head corals, and encrusting corals. Corals growing on Biorock show exceptional perfection in shape, with dense branching and bright colors compared to genetically identical corals growing away from the electrical field. This strongly suggests the Biorock process stimulates tissue growth more than calcification, with increased skeletal growth a secondary consequence of improved tissue health.

Survival

Survival of all organisms on Biorock, hard corals, soft corals, oysters, seagrass, salt marsh, etc. has been found to be higher on Biorock than nearby controls in the same habitat, typically 3-5

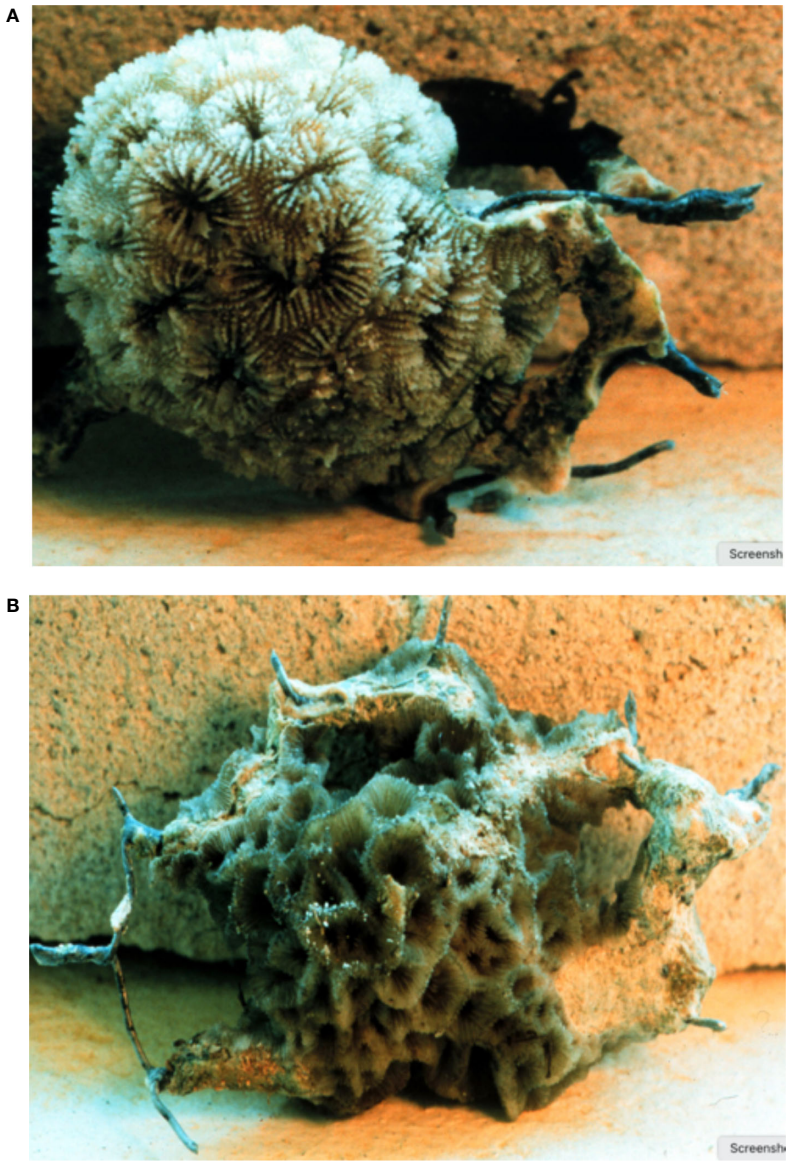

FIGURE 6 | **(A, B)** *Favia fragum* (above) and *Agaricia agaricites* (below) spontaneously settle on one inch chicken wire mesh, about 1-2 years old. Photographs by T. J. F. Goreau, 1990, Discovery Bay, Jamaica.

times greater, but often infinitely higher after extreme stress events when all the controls die and most growing on Biorock survive (**Figure 11**, from Goreau, 2014).

Resistance to Mud and Nutrient Stress

Resistance of corals on Biorock reefs to extremely high mud and nutrient stress was seen in Jamaica, Panama, Dominican Republic, Thailand, Indonesia, the Philippines, Dubai, and India. We have been able to grow mud-intolerant species, such as *Acropora cervicornis* and *Acropora palmata*, in places with poor water quality where they normally could not survive. We grew dense coralline sand-producing algae around Biorock reefs, replacing weedy algae that smother hard bottoms and prevent natural regeneration. We grew beautiful, healthy Acropora at the Jumeirah Palm in Dubai in the Persian Gulf. The Biorock corals survived near-opaque turbidity from dredging, but we could not photograph them because the visibility of the water was only 1-2 cm, less than the minimum focusing distance of the camera.

Recovery From Coral Bleaching

Biorock is the only method known to greatly increase coral survival from extreme bleaching events that imminently threaten to wipe out the world's remaining coral reefs (Goreau and Hayes, 1994; Goreau and Hayes, 2021). Survival of Biorock corals from severe bleaching was first observed during the 1998 Maldives mass bleaching event. I had been filming natural reefs as controls to

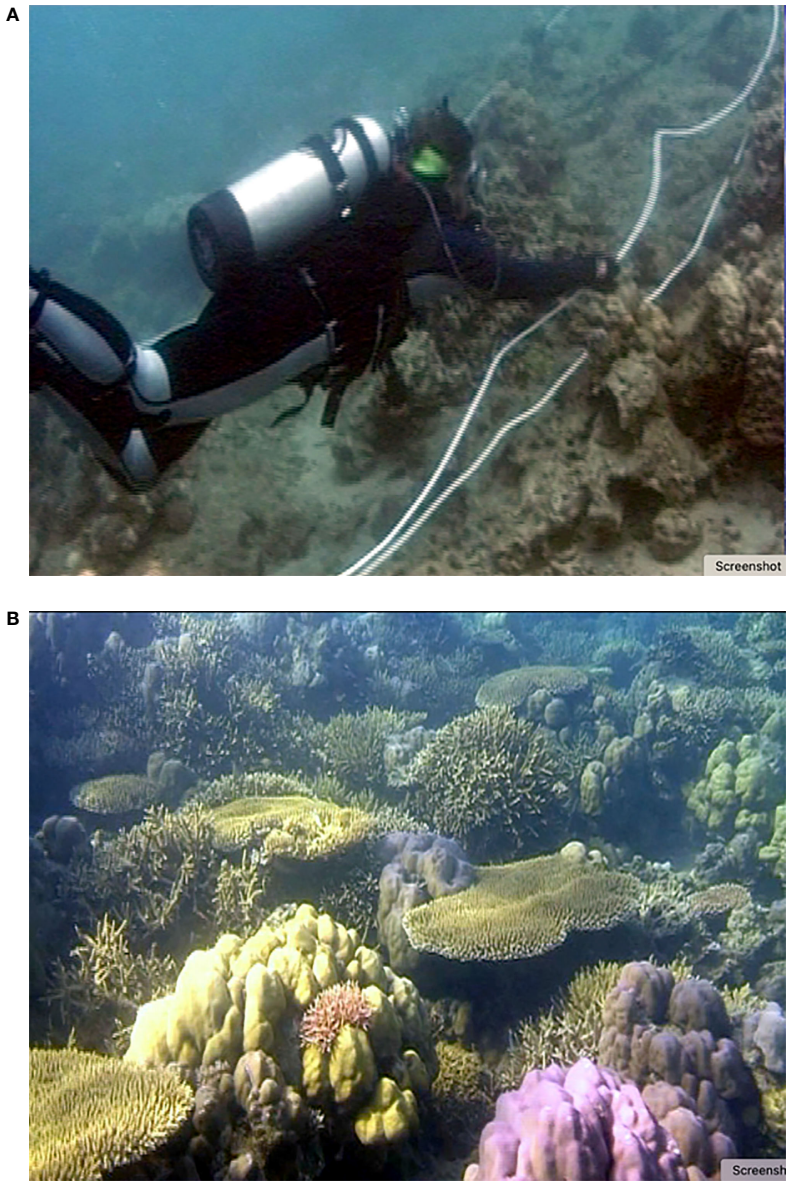

FIGURE 7 | **(A)** Before Biorock the site looked like a barren moonscape. The project started two years after almost all the corals had bleached and died in 1998. Pemuteran, Bali, Photograph by Rani Morrow-Wuigk. **(B)** Same site ten years later. Seemingly dead Porites heads recovered, and large amounts of spontaneous Acropora recruitment took place on top of the dead reef corals. The cable is invisible because it was buried under up to a meter of coral growth. Photograph by Rani Morrow-Wuigk.

compare their coral growth to Biorock corals, as well as thousands of coral fragments that had been previously cemented onto concrete and coral blocks by Azeez Hakeem, which had grown well for years. Around 95-99% of the corals on the natural reef died in a few weeks, along with every single one (100%) of the thousands of previously transplanted control corals, while most corals on Biorock survived the extremely high temperatures (Goreau and Hilbertz, 2005). Many surviving corals had been killed on their tops by high temperature and light, but portions of surviving tissue underneath then overgrew the dead coral areas above. These surviving corals may have been a Noah's Ark that helped reseed Maldivian reefs, which lost most of their reproducing corals so reef recovery had to wait for new recruits from Indonesia during the East monsoon to reach reproductive age (Goreau, 2022). Biorock kept reefs alive with very little coral mortality and complete recovery of fully bleached corals following repeated severe bleaching events that killed 90-99% of corals on nearby reefs in the Maldives, Thailand, and Indonesia. Less bleaching and much faster recovery were noted (Goreau, 2012b, See **Figure 12**). Photographs and video of Biorock reefs recovered from severe bleaching in Indonesia can be seen at: https://www.globalcoral.org.

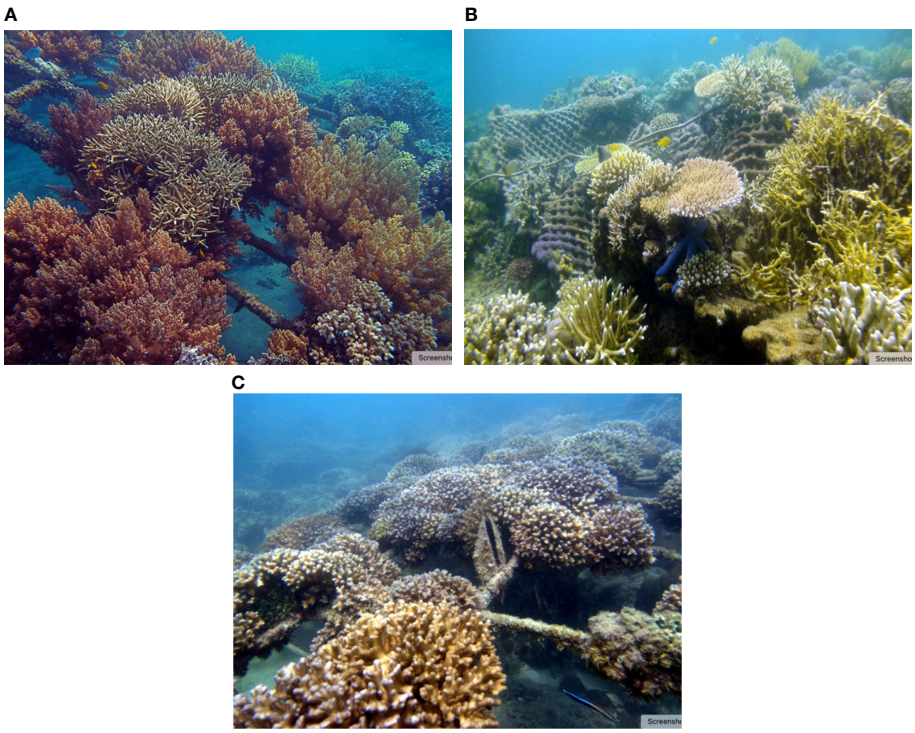

FIGURE 8 | **(A)** Most hard corals seen here were started from small fragments, but soft corals spontaneously settled over this Biorock reef in Pemuteran, Bali. Photograph by Rani Morrow Wuigk. **(B)** Corals quickly overgrow Biorock mesh that stabilizes dead coral rubble. Pemuteran, Bali. Many corals settled on the underside of the mesh and grew up through it. Photograph by Wolf Hilbertz. **(C)** Spontaneous settlement of corals and oysters on a two year old Biorock reef, Ko Samui, Thailand, photograph by Thomas Sarkisian.

Symbiosis

Six different genera of corals were found to have higher symbiotic algae densities on Biorock than controls, along with higher division rates of these algae, but had generally lower chlorophyll per algal cell (Goreau et al., 2004). Reminiscent of light shock adaptation of corals exposed to sudden light increases suppressing algae photosynthesis. This suggests Biorock methods may help experimentally decouple symbiotic interactions and provide insight into their regulation under stress (Goreau, 2021).

Increased Electro-taxis and Cellular Development

At the Woods Hole Marine Biological Laboratory course on marine algae physiology in the 1970s I learned larvae of algae and all marine organisms are electrically polarized. The examples demonstrated were the green alga *Ulva*, but were claimed to be general for marine organisms. One end of the larva is positively charged, the other negative, and they migrate toward the negative terminal along an imposed electrical field like Biorock electrolysis (electro-taxis). A calcium ion current flows down the central axis of marine larvae, cueing cellular differentiation of the embryo into the head-tail axis. Then a diffuse return electrical current flows back through the water to complete the electrical circuit.

The axial electrical current cues tissue development, segmentation, cell differentiation, and organism development (Whited and Levin, 2019). Responses of cells to mechanical forces are mediated by ATP generated by calcium electrical currents (Fukui et al., 2021). Electro-taxis is known to be important in wound healing; electrical currents in one direction can close wounds, while those in the opposite direction open them. Although electro-taxis is long known to be a universal feature of all marine larvae, both animals and plants, no research appears to have been done for a generation on marine organisms larval electro-taxis. Although Biorock negative terminals show dense settlement of all types of marine organisms, none are attracted to the other terminal, creating a small barren area that is vastly smaller in size. Ecological implications of electro-taxis and Biorock are discussed below.

High densities of zooplankton were noted at night in the electrical field, but were not present further away (Dr. Nathalie Ledee, personal communication), indicating that electro-taxis could also be providing increased food supplies for Biorock filter-feeding organisms. Further studies are needed on the response of zooplankton and marine larvae to electrical fields.

Growth Throughout Dormant Periods

Oysters grown at the New York City Superfund toxic waste site grew about 7.67 times faster in length on Biorock than controls (Shorr et al., 2012); and also in width and height, so 451 times greater in volume, over the summer growth season (**Figure 13A**). Biorock oysters grew all winter continuously with zero mortality and without any normal winter dormant period. At the same

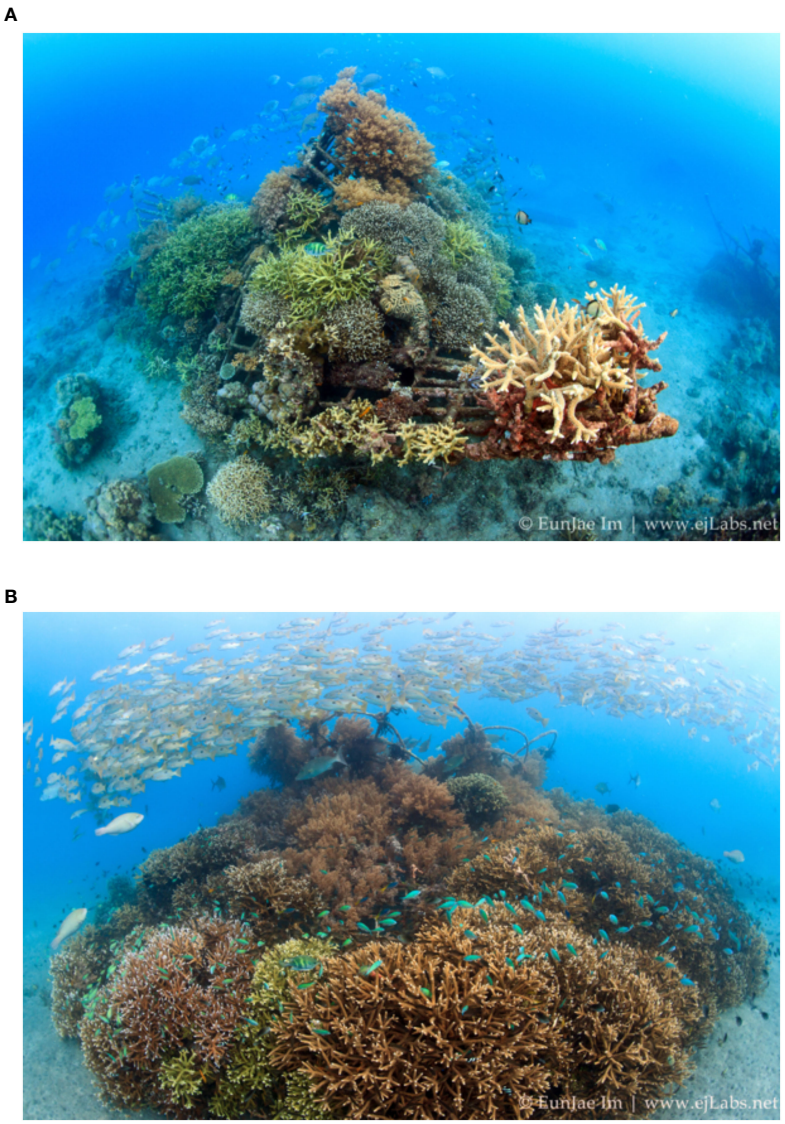

FIGURE 9 | **(A)** 4 Year old Biorock reef in Pemuteran, Bali. Photograph by Eun Jae Im. **(B)** High fish diversities and densities are found in four year-old Biorock reefs over sand and rubble previously barren of corals and fishes. Photograph Pemuteran, Bali, by Eun Jae Im.

time, 93% of control oysters died over winter, and the 7% surviving control oysters shrank in size due to shell dissolution during winter dormancy (**Figure 13B**, after data in Shorr et al., 2012). Biorock oyster shells were growing, shiny, and bright instead of chalky and crumbling like control oysters.

Underground Plant Growth

All species of seagrass have been seen to proliferate around Biorock reefs in Indonesia, Panama, and the Bahamas, as well as sand-producing coralline algae. In Italy, we grew the seagrass *Posidonia oceanica* on Biorock placed on bare limestone rock. This had been thought impossible because seagrass roots usually require 5-10 centimeters of sand or mud to grow in. However, Biorock sea grass roots grew so prolifically that they anchored themselves to bedrock and were quickly overgrown by mussels and oysters, with rich crab, shrimp, and juvenile fish populations (**Figures 14A–C** and **15A**) (Vaccarella and Goreau, 2012). The controls without electricity all died.

The salt marsh grass *Spartina alterniflora* grown with Biorock in construction debris at a New York City Superfund toxic waste site, grew twice as fast in height as controls, and was also darker green, had many more stems per clump (**Figure 15B**), flowered earlier and more, and attracted denser mussel populations around the roots that raised the height of the bottom by 5-10 centimeters around the plants. Saltmarsh grass was grown with Biorock in water normally too deep to grow without the roots being washed out. As a result the Biorock plants proliferated from only five root clumps to hundreds of plants, springing back more abundantly each spring after winter die-back. Control

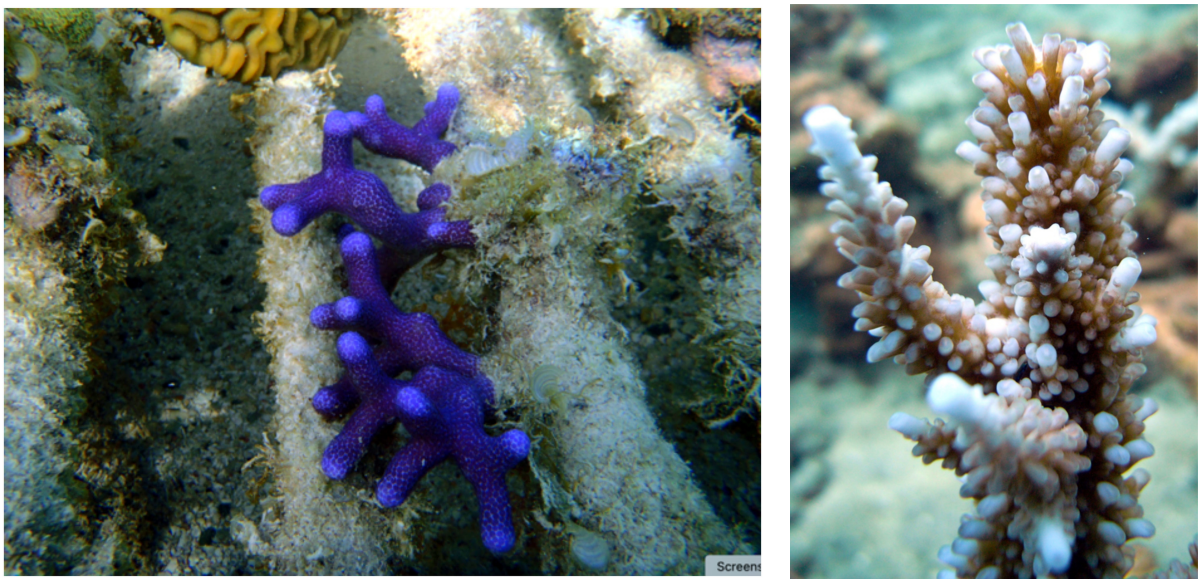

FIGURE 10 | **(A)** The intense glowing purple color of these Biorock corals fades when power is off for a few days and darkens in hours when power is restored. Antigua, photograph by Martha Watkins Gilkes. **(B)** Biorock corals have more densely packed and more brightly colored polyp tips than controls. Pemuteran, Bali. Closeup photograph by Wolf Hilbertz.

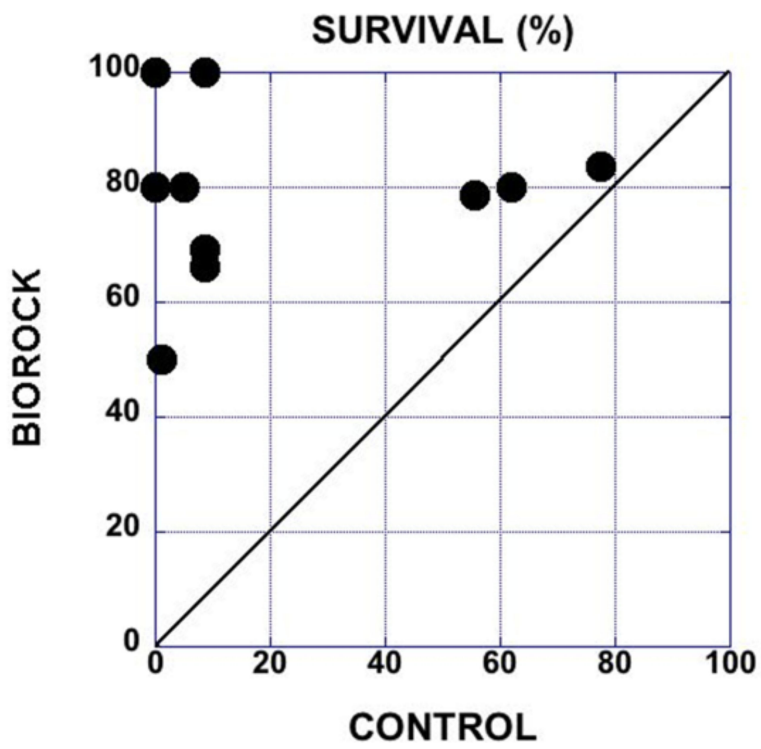

FIGURE 11 | Survival on Biorock versus controls for hard corals, soft corals, oysters, and other marine organisms. Each dot represents comparisons of Biorock versus controls for a different species on a different project under different conditions, from Goreau (2014).

FIGURE 12 | Twenty year-old Biorock reef in Bali, Indonesia that has survived two severe bleaching events. Photographed August 5 2021 by Komang Astika.

plantings had poor summer growth, died in winter, and failed to grow back in the spring (Cervino et al., 2012).

Shore Regeneration and Adaptation to Sea-Level Rise

Most large planting projects of seagrass, salt marsh, and mangroves fail because waves washed away plants before their roots can grow. Biorock greatly increases below-ground and above-ground productivity. It is the best hope of extending wave protecting marine plant ecosystems seaward along shores where they are now retreating landward due to global sea-level rise.

Biorock structures and their associated coral, oyster, mussel, and seagrass ecosystems greatly reduce wave energy at the shoreline, regenerating severely eroded beaches at record rates (Goreau and Prong, 2017). Furthermore, applied to seagrass, salt

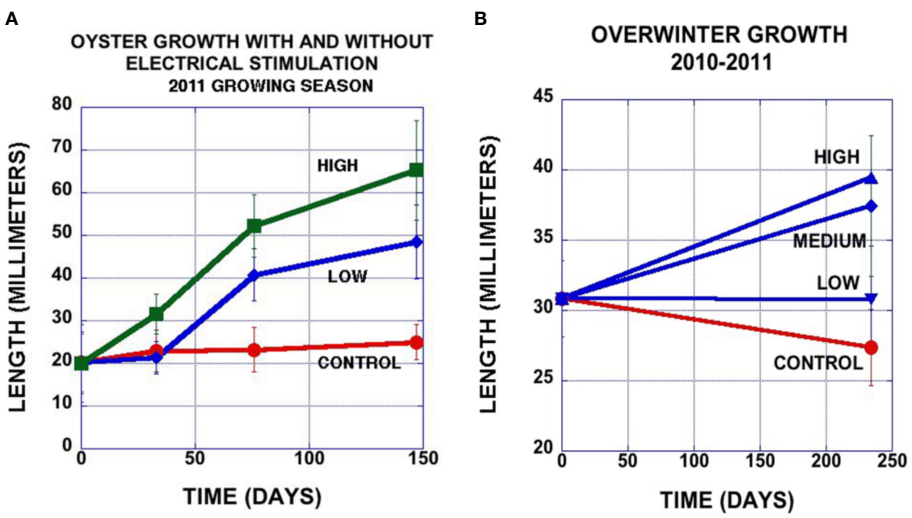

FIGURE 13 | **(A)** Summer growth of oysters with high, low, and no electricity. Data from Shorr et al., 2012. **(B)** Growth of oysters over winter with high, medium, low, and no electrical current. All high current Biorock oysters survived and kept growing all winter long. 93% of control oysters died, and the survivors all went dormant and shrank in size as their shells dissolved in cold acidic water. Data from Shorr et al., 2012.

FIGURE 14 | **(A–C)** Rapid growth of seagrass roots attached to limestone rock and produced dense and diverse sea grass communities. Photographs Torre de Guaceto, Puglia, Italy, Raffaele Vaccarella.

marsh, and mangrove regeneration, they can greatly increase underground root biomass and peat carbon production. The Biorock process itself also creates geochemical conditions leading to increased carbon preservation and storage (see below).

Naturally High Electrical Environments

Biorock electrical signals attract larvae at high levels. Because seawater is an electrical conductor, electrical currents are induced whenever water flows through the Earth's magnetic field (Xu et al., 2018; Dommermuth, 2020). These natural electrical currents are strongest where waves break on hard reef surfaces. Reef-building organisms seek high wave energy environments. Marine larvae are hypothesized here to use electro-taxis to the electrical fields naturally generated by breaking waves to find high-energy conditions they need. Corals in high wave energy sites are also seen grow faster and are more brightly colored, as if they can tap the electrical field to produce more biochemical energy more than corals in low wave energy sites, another hypothesis needing testing. It is hypothesized that organisms living in very low energy muddy environments, like benthic deposit feeders, might exhibit negative electro-taxis. Experimental tests are required.

Settlement of hard corals, soft corals, tunicates, sponges, and all other reef fauna, including fishes, are very prominent around

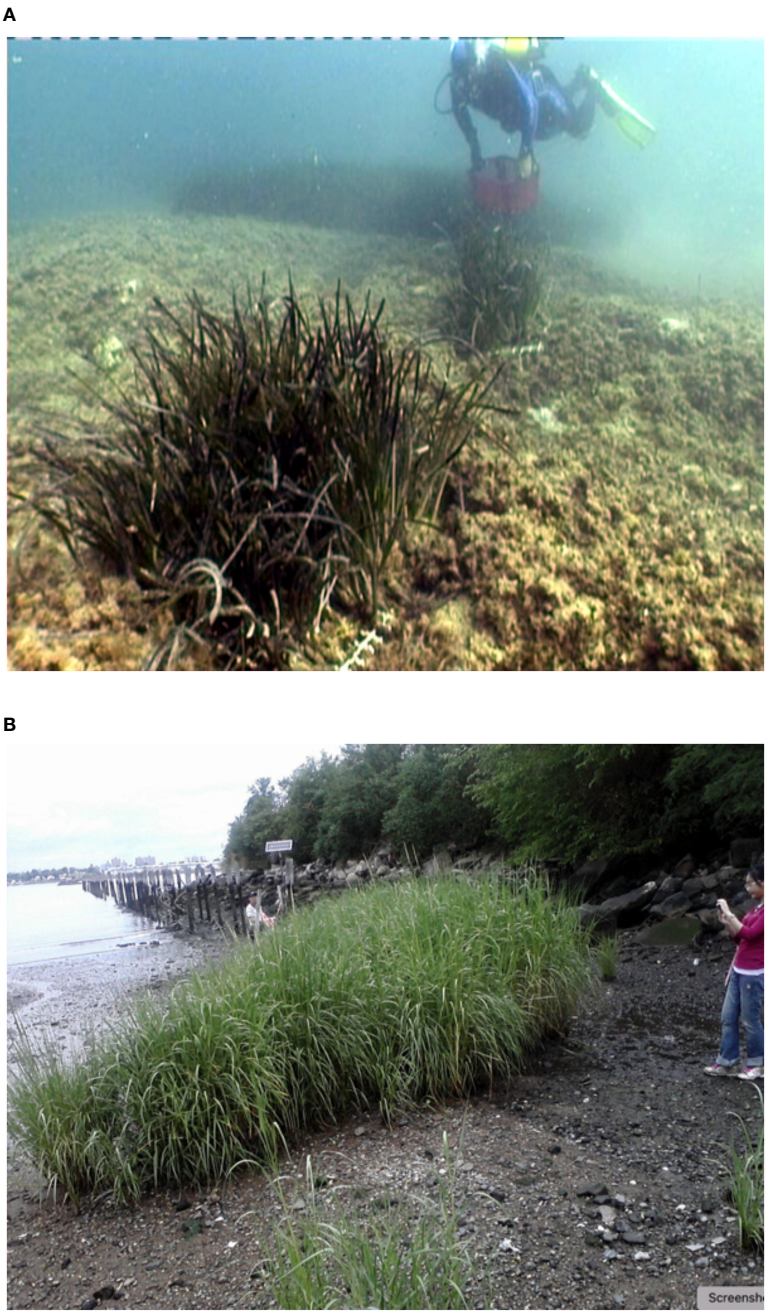

FIGURE 15 | **(A)** Two patches of Biorock seagrass growth on limestone bedrock in the Adriatic Sea, Italy. Controls all died. Photograph by Raffaele Vaccarella. **(B)** Saltmarsh grass grows higher and spreads underground, powered by a solar panel. Biorock salt marsh grass at right, controls at left and in front. Biorock salt marsh survives winters and expands seaward, while controls die and wash away. College Point, New York City, photograph by James Cervino.

Biorock structures, typically orders of magnitude higher than further away, creating lush oases of life (video of spectacular settlement and growth on these reefs can be seen at https://www.globalcoral.org). Much more field and laboratory research on electro-taxis and their ecological effects is needed to understand how to use them to most rapidly regenerate biodiversity. However, it is already clear that the largest variety of structural shapes and interior passages give the fastest results.

Reproduction

Several observations suggest the profound effects of Biorock on reproduction of corals and other species although systematic studies

on the impact remain to be done. *Porites porites* on the first Biorock projects in Jamaica in the 1980s quickly showed pink polyp colors associated with coral egg and sperm reproduction on a lunar calendar cycle. Branches of *Acropora cervicornis* on Biorock projects in Curaçao were observed to release coral planulae by Michael Duss of Biorock Curaçao. There is strong reason to hypothesize that Biorock corals will have much higher reproductive output due to their generally healthier conditions. Still no studies of reproduction of corals on Biorock have yet been made. If corals are found to be more fecund in electrical fields, Biorock Coral Arks will become essential to efforts to maintain reproducing populations and coral genetic diversity despite the extinction emergency from global warming and global sea level rise. Experimental work on coral fecundity on Biorock is badly needed.

Disease

Corals in several Biorock projects in the Caribbean and Indonesia have been affected by deadly coral diseases at times when waves of disease pass through local reefs, so it appears that Biorock does not prevent attack by pathogens that land on corals. However, in several cases, we have noticed virulent coral diseases on Biorock corals that would normally kill the entire colony, suddenly stop spreading, recover, and new coral tissue from the surviving areas to eventually regrow the dead areas, something we now rarely see in the reef. This included White Plague on table Acroporas in Indonesia and the deadly White Plague variant now widely mis-named Stony Coral Tissue Loss Disease on *Acropora palmata* in Saint Barthelemy (Nathalie Ledee, personal communication). Experimental work is needed to see if Biorock corals are more resistant to disease.

Hurricanes

The first Biorock reefs built in Jamaica in the 1980s have had no power for more than 30 years and have survived every hurricane that has hit since. Biorock reefs survived direct wave impacts on reef crests from Category 5 hurricanes that destroyed almost all the buildings on the land in the Turks and Caicos Islands with little or no coral damage (Wells et al., 2010), and Saint Barthelemy (Nathalie Ledee, personal communication, see images in https://www.youtube.com/watch?v=cv2h8Uv-MEs).

Algae

A fine surface fuzz of brownish-green micro-filamentous algae coating the structures is avidly grazed by fishes, whose bite marks down to limestone indicate the entire crop is harvested and converted into fish biomass. No measurements have yet been made of the importance of this food source. Still the sizes of the herbivorous fish populations indicate it is ecologically and energetically significant for local fisheries' food chains, and studies are badly needed. If protected from herbivores, Biorock might be able to increase the growth of algae in mariculture (Goreau, 2018).

Weedy fleshy algae have never been a problem on Biorock reefs, even when local benthic harmful algae blooms are caused by seasonal nutrient inputs or eutrophication. This is because of intense grazing by herbivorous fish that move into Biorock reefs. Structures defended from herbivores by damselfish develop fleshy algae populations not seen on Biorock reefs free of damselfish. The vast majority of Biorock reefs have few weedy algae, and damselfish have established themselves in only around 4 or 5 out of more than 150 Biorock structures at Pemuteran. These may be structures too small to build up resident grouper populations to control damselfish.

Instead of weedy fleshy algae, what proliferates around Biorock reefs are sand-producing coralline algae like *Halimeda* and *Amphiroa*. Their limestone skeletons noticeably whiten the sediment under and around the structures and have piled up to regenerate an entire beach in Pemuteran (Goreau and Prong, 2017).

Microbiology

The Biorock process creates intensely localized sources of alkalinity and hydrogen at some sites and acidity and oxygen (plus a bit of chlorine) at others, stimulating the growth of microbes with extreme requirements, in particular hydrogen-oxidizing bacteria and nitrogen-fixing bacteria that consume hydrogen and make fixed nitrogen. Microbial nitrogen fixation is the only new source of ecosystem nitrogen from external sources (other than that internally recycled) and plays a key role limiting productivity and biodiversity. The Biorock reefs are hypothesized to be a significant source of new nitrogen driving the food chain. This can be measured using stable isotopes. No isotopic studies have yet been made, nor have any of the Biorock microbial community. Still it is hypothesized that environmental DNA measurements will reveal essential and unexpected components of the microbial flora.

Higher Vertebrate Attractant

Fish of all kinds swarm around Biorock reefs, and higher vertebrates appear to seek them out too. A friendly turtle has been sleeping blissfully on the same Biorock reef in Indonesia every night for around ten years, and really seems to get a charge from it! We have done no Biorock projects in places with marine mammals, so we have no information on their responses.

Humans snorkeling on Biorock reefs are observed smiling blissfully on exiting because of the numbers and diversity of fishes and corals (**Figures 12**). Entire Indonesian villages and islands live from tourists who come to snorkel in the Biorock reef gardens. Local people are smiling and happy because Biorock charges their economy too: people come from all over the world to their villages to see the underwater beauty they nourish (see figures above).

Shark Attack Preventer

All marine animals seen seem to be attracted except predatory sharks, which seem to avoid Biorock as we never see them! They are inhibited from biting by Biorock because the Biorock electrical field confuses the electrical sense organs used in the final bite: they avoid biting fish they know are in front of their mouth and want to eat (Uchoa et al., 2017). Biorock's ability to reduce shark-human interaction is a positive benefit for both sharks and humans, making Biorock reefs exceptionally safe for ecotourism. On the other hand, nurse sharks (Panama) and sting rays (Maldives) have freely chosen to sleep in Biorock reefs at

night, but they are bottom feeders who don't use electrical senses like predatory sharks do and are minor threat to humans except through acts of stupidity.

NEGATIVE IMPACTS OF BIOROCK

In contrast to more than 22 different visible biological benefits described above, no adverse biological effects of Biorock have been observed. Negative effects of acidity and chlorine at the positive electrode are limited by design and conditions and are very limited in range: fish swim past it without avoidance, and if the positive electrode is placed directly on living coral, tissue growth is inhibited in the immediate contact zone only but has no effect on coral tissue beyond 1-2 millimeters distance.

CONCLUSIONS: CORAL REEF ELECTROTHERAPY RESEARCH AND DEVELOPMENT NEEDS

By directly stimulating the health of marine organisms, Biorock provides unique advantages for marine ecosystem service preservation, regeneration, and adaptation to extreme stress events, which will be increasingly needed as global warming, pollution, and storm strength increase. Biorock methods are ideally suited for keeping marine ecosystems alive during lethal stress events from excessive temperatures, mud and nutrient pollution, and hurricanes and for rapidly regenerating entire complex ecosystems in places where there has been no natural recovery.

The work in this paper is based purely on observational natural history, as we had no funding for laboratories or research equipment. Our results were entirely unexpected. Testing the hypotheses raised in this paper with modern research methods will provide valuable insights for marine biology and marine resource management.

Since there has never been funding for Biorock scientific research, laboratories, and equipment from any funding agency we worked for decades in the field with local groups in developing countries to build more than a thousand Biorock reef structures in some 45 countries, each different. There is a tremendous need for systematic experimental research to measure the degree of stimulation of different species to determine their optimal values, which may be different for each species, and how varying power levels can affect competitive outcomes.

Why does Biorock work so well by every single visually observable biological measure of good health? The Biorock process appears to directly stimulate natural membrane electrical potentials and the fundamental mechanism of biochemical energy formation for all forms of marine life, fortifying natural health promoting mechanisms. Unlike conventional mariculture of mono-specific populations, Biorock significantly increases all components of biodiversity, growing complete ecosystems that generate their own food without additional external feeds (Goreau, 2018). Yet despite the profound effects observed for 35 years, there has been no funding for systematic work on how the biophysical effects of low voltage electricity affect biochemical energy and the health of marine organisms. Specific tests of these hypotheses are mentioned here, but the process involves all aspects of science. To build local research capacity where it is most needed, most of this work should be done by students from coral reef countries.

With coral reef ecosystems threatened by extinction from global warming, it is critically urgent that work be done to understand the mechanisms by which Biorock works and how to manage Biorock marine ecosystem regeneration to maximize the natural healing power of electrotherapy. The electricity needed to grow back a hundred meters of severely eroded beach in front of a hotel might be one or two air conditioner's worth of electricity, a small amount compared to the benefits of a beach, with a living coral reef and healthy fisheries, and could save the hotel itself from hurricanes and sea level rise, and fishing villages from starving.

Electrotherapy is no shocking execution; it accentuates natural energy production with a life-giving, healing electro-trickle charge that organisms respond to visibly as if electro-tickled orgasmically! This book chapter is the first to document 35 years of systematic observations of remarkable large-scale healing properties of low-voltage direct current on marine organisms. Suppose these findings are acted on the scale and urgency needed, in that case they can help rescue dying marine ecosystems and fisheries, reverse the worst impacts of global warming and sea level rise, and create sustainable Blue Economies in now collapsing coastal ecosystems. Governments of rich countries have ignored inconvenient warnings about their energy use impacts and knowingly let corals die for more than 30 years. For poor countries, regenerating reefs is a matter of survival until global warming and global sea-level rise are reversed. Coral reef countries have been the first and worst victims of climate change, sacrificed by fossil fuel-addicted countries' politically-motivated inaction on global warming. An immediate crash Biorock Coral Ark program is needed if coral reefs are to survive coming years. At time of submission of this chapter a prolonged La Niña is ending and the next El Niño is just starting, which will cause severe bleaching in many places. Coral reef countries urgently need to be prepared to regenerate all the coastal reefs they can by recharging their reefs with Biorock Coral Arks to save their biodiversity, biomass, and ecosystem services.

We strongly urge island nations to make their own decisions to take full advantage of breakthrough endogenous island technologies like Biorock instead of funding mass coral breaking and killing methods of coral reef "restoration" used as foreign scientific tourism and volunteers in place of developing endogenous management capacity of coastal populations. The standard fragmentation methods greatly increase coral tissue stress instead of healing it as Biorock does. Their corals grow only until the first extreme high temperature, mud, pollution, hurricane, or disease event kills them (Foo and Asner, 2020), conditions Biorock reefs can survive. They mean well, but in the

long run, they are just killing corals. Biorock is the only method of reef regeneration with a hope of working until CO_2 is reduced to safe pre-industrial levels for coral reefs (Goreau, 2014). The fundamental limitation of Biorock is being able to provide direct current at the site, so it can only protect sites where that is cost effective, which will not be the case for remote sites. But if we don't save all that we can, what will we have left?

DEDICATION

This paper is dedicated to Wolf Hilbertz, inventor of Biorock, my inspired collaborator for 20 years, and my wise coral teachers: Maurice Yonge, Thomas F. Goreau, Nora I. Goreau, and Robert K. Trench.

AUTHOR CONTRIBUTIONS

All authors listed have made a substantial, direct, and intellectual contribution to the work and approved it for publication.

ACKNOWLEDGMENTS

I thank all of the hundreds of great people who have worked with us on all the Biorock projects over the decades around the world. You know who you are, and you will be all be listed as partners when we write the chronicle of the projects. Thanks go to constructive suggestions by a reviewer. Special thanks go to all those who preserved these projects with the beautiful images shown, they are individually identified in the captions with their photographs.

REFERENCES

Bakti, L. A. A., Virgota, A., Damayanti, L. P. A., Radiman, T. H. U., Retnowulan, A., Sabil, A., et al. (2012). "Biorock Reef Restoration in Gili Trawangan, North Lombok, Indonesia," in *Innovative Methods of Marine Ecosystem Restoration*. Eds. T. J. Goreau and R. K. Trench (Boca Raton: CRC Press), 59–80. doi: 10.1201/b14314-7

Cervino, J., Gjoza, D., Lin, C., Weeks, R., and Goreau, T. J. (2012). "Electrical Fields Increase Salt Marsh Survival and Growth and Speed Restoration in Adverse Conditions," in *Innovative Technologies for Marine Ecosystem Restoration*. Eds. T. J. Goreau and R. K. Trench (Boca Raton: CRC Press).

Cheng, N., Van Hoof, H., Bockx, E., Hoogmartens, M. J., Mulier, J. C., De Ducker, F. J., et al. (1982). The Effects of Electric Currents on ATP Generation, Protein Synthesis, and Membrane Transport in Rat Skin. *Clin. Orthopaedics Related Res.* 171, 264–272. doi: 10.1097/00003086-198211000-00045

Dommermuth, D. G. (2020). "Magnetic Induction Due to the Effects of Breaking Ocean Waves," in *Breaking Wave Analysis Technical Report*. (San Diego) vol. 11, 1–7.

Foo, S. A., and Asner, G. P. (2020). Sea Surface Temperature in Coral Reef Restoration Outcomes. *Environ. Res. Lett.* 15, 074045. doi: 10.1088/1748-9326/ab7dfa

Fukui, H., Chow, R. W. Y., Xie, J., Foo, Y., Yap, C. H., Minc, N., et al. (2021). Bioelectric Signaling, and the Control of Cardiac Cell Identity in Response to Mechanical Forces. *Science* 374, 351–354. doi: 10.1126/science.abc6229

Gelis, E. R. E., Kamal, M. M., Subhan, B., Bachtiar, I., Sani, L. M. I., and Madduppa, H. (2021). Environmental Biomonitoring of Reef Fish Community Structure With eDNA Metabarcoding in the Coral Triangle. *Environ. Biol. Fish* 104, 887–903. doi: 10.1007/s10641-021-01118-3

Goreau, T. J. (1992). Bleaching and Reef Community Change in Jamaica: 1951-1991. In Symposium On Long Term Dynamics Of Coral Reefs. *Am. Zoologist* 32, 683–695. doi: 10.1093/icb/32.6.683

Goreau, T. J. (2012a). "Marine Electrolysis for Building Materials and Environmental Restoration," in *Electrolysis*. Eds. J. Kleperis and V. Linkov (Rijeka, Croatia: InTech Publishing), 273–290.

Goreau, T. J. (2012b). "Marine Ecosystem Electrotherapy: Practice and Theory," in *Innovative Technologies for Marine Ecosystem Restoration*. Eds. T. J. Goreau and R. K. Trench (Boca Raton: CRC Press).

Goreau, T. J. (2014). Electrical Stimulation Greatly Increases Settlement, Growth, Survival, and Stress Resistance of Marine Organisms. *Natural Resources* 5, 527–537. doi: 10.4236/nr.2014.510048

Goreau, T. (2014). "Global Biogeochemical Restoration to Stabilize CO2 at Safe Levels in Time to Avoid Severe Climate Change Impacts to Earth's Life Support Systems: Implications for the United Nations Framework Convention on Climate Change," in *Geotherapy: Innovative Technologies for Soil Fertility Restoration, Carbon Sequestration, and Reversing Atmospheric CO2 Increase*. Eds. T. J. Goreau, R. G. Larson and J. A. Campe (Boca Raton: CRC Press).

Goreau, T. J. F. (2018). "Biorock Technology: A Novel Tool for Large-Scale Whole-Ecosystem Sustainable Mariculture Using Direct Biophysical Stimulation of Marine Organism's Biochemical Energy Metabolism," in *Proceedings of the International Summit on Fisheries and Aquaculture* (Amsterdam: Scientific Federation), 24.

Goreau, T. J. F. (2021). "Robert Kent Trench: In Memoriam," in *Global Coral Reef Alliance* (Cambridge, MA). Available at: https://www.globalcoral.org/robert-kent-trench-in-memoriam-2/.

Goreau, T. J. F. (2022). "Maldives Biorock: Past Results and Future Applications," in *Global Coral Reef Alliance White Paper* (Cambridge, MA). Available at: https://www.globalcoral.org/maldives-biorock-past-results-future-applications/.

Goreau, T. J., Cervino, J., Goreau, M., Hayes, R., Hayes, M., Richardson, L., et al. (1998). Rapid Spread of Diseases in Caribbean Coral Reefs. *Rev. Biol. Tropical* 46 Supl5, 157–171.

Goreau, T., Cervino, J., and Polina, R. (2004). Increased Zooxanthellae Numbers and Mitotic Index in Electrically Stimulated Corals. *Symbiosis* 37, 107–120.

Goreau, T. F., Goreau, N. I., and Goreau, T. J. (1979). Corals and Coral Reefs. *Sci. American* 241, 124–136. doi: 10.1038/scientificamerican0879-124

Goreau, T. J., and Hayes, R. L. (1994). Coral Bleaching and Ocean "Hot Spots". *Ambio* 23, 176–180.

Goreau, T. J. F., and Hayes, R. L. (2021). Global Warming Triggers Coral Reef Bleaching Tipping Point. *Ambio* 50, 1137–1140. doi: 10.1007/s13280-021-01512-2

Goreau, T. J., and Hilbertz, W. (2005). Marine Ecosystem Restoration: Costs and Benefits for Coral Reefs. *World Resource Rev.* 17, 375–409.

Goreau, T. J., and Hilbertz, W. (2012). "Reef Restoration Using Seawater Electrolysis in Jamaica," in *Innovative Technologies for Marine Ecosystem Restoration*. Eds. T. J. Goreau and R. K. Trench (Boca Raton: CRC Press).

Goreau, T. J. F., and Prong, P. (2017). Biorock Reefs Grow Back Severely Eroded Beaches in Months. In T. Wahl, J. E. O. Nilsen, I. Haigh, & S. Brown (Eds.). P. 243-263 Coastal Sea Levels, Impacts, and Adaptation. *J. Mar. Sci. Eng.* 5 (4), 48. doi: 10.3390/jmse5040048

T. J. Goreau and R. K. Trench (Eds.) (2012). *Innovative Technologies for Marine Ecosystem Restoration* (Boca Raton: CRC Press).

Hayes, R. L., and Goreau, T. J. (1991). The Tropical Coral Reef Ecosystem as a Harbinger of Global Warming. Proc 2nd International Conference on Global Warming. *World Resour. Rev.* 3, 306–322.

Hayes, R. L., and Goreau, N. I. (1998). The Significance of Emerging Diseases in the Tropical Coral Reef Ecosystem. *Rev. Biol. Trop.* 46 Supp5, 173–185.

Hilbertz, W. H. (1979). Electrodeposition of Minerals in Sea Water: Experiments and Applications. *IEEE J. Oceanic Eng.* OE4, 94–113. doi: 10.1109/JOE.1979.1145428

Jompa, J., Suharto, J., Anpusyahnur, E. M., Dwija, P. N., Subagio, J., Alimin, I., et al. (2012). "Electrically Stimulated Corals in Indonesia Reef Restoration Projects Show Greatly Accelerated Growth Rates," in *Innovative Methods of Marine Ecosystem Restoration*. Eds. T. J. Goreau and R. K. Trench (Boca Raton: CRC Press), 47–58. doi: 10.1201/b14314-6

Maduppa, H., Cahyani, N. K. D., Anggoro, A. W., Subhan, B., Jefri, E., Sani, L. M. I., et al. (2021). eDNA Metabarcoding Illuminates Species Diversity and Composition of Three Phyla (Chordata, Mollusca and Echinodermata) Across Indonesian Coral Reefs. *Biodiversity Conserv.* 30, 3087–3114. doi: 10.1007/s10531-021-02237-0

Munandar, M., Rizal, M., Rani, C., and Faizal, A. (2018). The Escalation of Coral Growth by Biorock Technology Applied in Sabang Marine Ecotourism. *AACL Bioflux* 11 (5), 1633–1647.

Natasasmita, D., Wijayanti, D. P., and Suryono, C. A. (2016). The Effects of Electrical Voltage Differences and Initial Fragment Size on Growth Performance and Survival

Rate of Coral *Acropora Cerealis* in Biorock Method. *J. Aquaculture Marine Biol.* 4 (4), 00086. doi: 10.15406/jamb.2016.04.00086

O'Rourke, B., Cortassa, S., and Aon, M. A. (2005). Mitochondrial Ion Channels: Gatekeepers of Life and Death. *Physiology* 20, 303–315. doi: 10.1152/physiol.00020.2005

Shorr, J., Cervino, J., Lin, C., Weeks, R., and Goreau, T. J. (2012). "Electrical Stimulation Increases Oyster Growth and Survival in Restoration ProjectsIn," in *Innovative Technologies for Marine Ecosystem Restoration*. Eds. T. J. Goreau and R. K. Trench (Boca Raton: CRC Press).

Tai, G., Tai, M., and Zhao, M. (2018). Electrically Stimulated Cell Migration and its Contribution to Wound Healing. *Burns Trauma* 6, 20. doi: 10.1186/s41038-018-0123-2

Uchoa, M. P., O'Connell, C. C., and Goreau, T. J. (2017). The Effects of Biorock-Associated Electric Fields on the Caribbean Reef Shark (*Carcharhinus Perezi*) and the Bull Shark (*Carcharhinus Leucas*). *Anim. Biol.* 67, 191–208. doi: 10.1163/15707563-00002531

Vaccarella, R., and Goreau, T. J. (2012). "Restoration of Seagrass Mats (Posidonia Oceanica) With Electrical Stimulation," in *Innovative Technologies for Marine Ecosystem Restoration*. Eds. T. J. Goreau and R. K. Trench (Boca Raton: CRC Press).

Weiss, M. C., Preiner, M., Xavier, J. C., Zimorski, V., and Martin, W. F. (2018). The Last Universal Common Ancestor Between Ancient Earth Chemistry and the Onset of Genetics. *PloS Genet.* 14, e1007518. doi: 10.1371/journal.pgen.1007518

Wells, L., Perez, F., Hibbert, M., Clervaux, L., Johnson, J., and Goreau, T. (2010). Effect of Severe Hurricanes on Biorock Coral Reef Restoration Projects in Grand Turk, Turks and Caicos Islands. *Rev. Biol. Tropical* 58, 141–149.

Whited, J. L., and Levin, M. (2019). Bioelectrical Controls on Morphogenesis: From Ancient Mechanisms of Cell Coordination to Biomedical Opportunities. *Curr. Opin. Genet. Dev.* 57, 61–69. doi: 10.1016/j.gde.2019.06.014

Xu, Z. H., Du, C. P., and Xia, M. Y. (2018). Electromagnetic Fields Due to the Wake of a Slender Moving Body in a Finite Depth Ocean With Density Stratification. *Nat. Sci. Rep.* 8, 14647. doi: 10.1038/s41598-018-32789-1

Conflict of Interest: The author invented the word Biorock in the 1980s as a better synonym for what had previously been called Mineral Accretion, Seacrete, and Seament. Biorock technology is open source and the copyright on Biorock® is held by Blue Regeneration, a company for which the author is Chief Scientist. As President of the Global Coral Reef Alliance, a non-profitable organization, he received no financial benefit from 35 years of work described in this paper, but wishes he had, because he and the late Wolf Hilbertz exhausted their personal resources (and their families'). Only occasional small donations from kind individuals kept them marching onward through the fog.

Publisher's Note: All claims expressed in this article are solely those of the authors and do not necessarily represent those of their affiliated organizations, or those of the publisher, the editors and the reviewers. Any product that may be evaluated in this article, or claim that may be made by its manufacturer, is not guaranteed or endorsed by the publisher.

frontiers | Frontiers in Physiology

ORIGINAL RESEARCH
published: 19 May 2022
doi: 10.3389/fphys.2022.804193

Bleaching Susceptibility and Resistance of Octocorals and Anemones at the World's Southern-Most Coral Reef

Rosemary K Steinberg[1,2]*, *Tracy D Ainsworth*[1], *Tess Moriarty*[3], *Teresa Bednarek*[1,4], *Katherine A Dafforn*[5] *and Emma L Johnston*[1]

[1]Evolution and Ecology Research Centre and Centre for Marine Science and Innovation, School of Biological, Earth, and Environmental Sciences, Faculty of Science, University of New South Wales, Sydney, NSW, Australia, [2]Sydney Institute of Marine Science, Mosman, NSW, Australia, [3]School of Environmental and Life Sciences, The University of Newcastle, Ourimbah, NSW, Australia, [4]RUHR Universtad Bouchum, Bouchum, Germany, [5]School of Natural Sciences, Macquarie University, Sydney, NSW, Australia

OPEN ACCESS

Edited by:
Ranjeet Bhagooli,
University of Mauritius, Mauritius

Reviewed by:
Tamar Goulet,
University of Mississippi, United States
Sylvain Agostini,
University of Tsukuba, Japan
Mark E Warner,
University of Delaware, United States

***Correspondence:**
Rosemary K Steinberg
rosiekstein@gmail.com

Specialty section:
This article was submitted to Aquatic Physiology, a section of the journal Frontiers in Physiology

Received: *29 October 2021*
Accepted: *29 March 2022*
Published: *19 May 2022*

Citation:
Steinberg RK, Ainsworth TD, Moriarty T, Bednarek T, Dafforn KA and Johnston EL (2022) Bleaching Susceptibility and Resistance of Octocorals and Anemones at the World's Southern-Most Coral Reef. Front. Physiol. 13:804193. doi: 10.3389/fphys.2022.804193

Coral reefs are amongst the most biodiverse ecosystems on earth, and while stony corals create the foundational complexity of these ecosystems, octocorals and anemones contribute significantly to their biodiversity and function. Like stony corals, many octocorals contain Symbiodiniaceae endosymbionts and can bleach when temperatures exceed the species' upper thermal limit. Here, we report octocoral bleaching susceptibility and resistance within the subtropical Lord Howe Island coral reef ecosystem during and after marine heatwaves in 2019. Octocoral and anemone surveys were conducted at multiple reef locations within the Lord Howe Island lagoon during, immediately after, and 7 months after the heatwaves. One octocoral species, *Cladiella* sp. 1, experienced bleaching and mortality, with some bleached colonies detaching from the reef structure during the heatwave (presumed dead). Those that remained attached to the benthos survived the event and recovered endosymbionts within 7 months of bleaching. *Cladiella* sp. 1 Symbiodiniaceae density (in cells per µg protein), chlorophyll *a* and c_2 per µg protein, and photosynthetic efficiency were significantly lower in bleached colonies compared to unbleached colonies, while chlorophyll *a* and c_2 per symbiont were higher. Interestingly, no other symbiotic octocoral species of the Lord Howe Island lagoonal reef bleached. Unbleached *Xenia* cf *crassa* colonies had higher Symbiodiniaceae and chlorophyll densities during the marine heatwave compared to other monitoring intervals, while *Cladiella* sp. 2 densities did not change substantially through time. Previous work on octocoral bleaching has focused primarily on gorgonian octocorals, while this study provides insight into bleaching variability in other octocoral groups. The study also provides further evidence that octocorals may be generally more resistant to bleaching than stony corals in many, but not all, reef ecosystems. Responses to marine heating events vary and should be assessed on a species by species basis.

Keywords: soft coral, alcyonacea, chlorophyll, coral bleaching, symbiodiniaceae, marine heatwave

1 INTRODUCTION

Tropical and subtropical coral reefs are under increasing threat due to human induced climate change as they bleach in response to a variety of stressors, notably thermal stress (Harrison et al., 2011; Hughes et al., 2017; Suggett and Smith, 2020). Coral bleaching is the breakdown of the partnership between endosymbiotic dinoflagellates of the family Symbiodiniaceae and their cnidarian coral host. Bleaching is often measured as a loss in endosymbiont density within the coral or loss of chlorophyll from the Symbiodiniaceae themselves (Coles and Jokiel, 1978; Kleppel et al., 1989; Gates et al., 1992; Brown, 1997; Hoegh-Guldberg, 1999). The consequences of coral bleaching on coral reefs include extensive coral mortality, reduced fecundity and recruitment rates, and loss of associated function and biodiversity (Michalek-Wagner and Willis, 2001a; Loya et al., 2001; Pratchett et al., 2008; Stuart-Smith et al., 2018; Hughes et al., 2019; Donovan et al., 2021; González-barrios and Cabral-tena, 2021). The consequences of bleaching can be affected by local stressors, with turbidity, wave exposure, macroalgae cover, and urchin abundance all significantly affecting changes in coral cover in the year after heat-induced bleaching (Donovan et al., 2021). The frequency of coral bleaching has increased in recent years, with annual bleaching events predicted by 2055 and periods of annual bleaching already occurring on some reefs (Van Hooidonk et al., 2014; Hughes et al., 2017; Slattery et al., 2019). Bleaching susceptibility differs between cnidarian groups (anemone, octocoral, stony coral, etc.) and between stony coral species, where growth forms and even size classes within species are reported to have differential bleaching susceptibilities (Loya et al., 2001; Brandt, 2009; Fabricius et al., 2011; Grottoli et al., 2014).

While stony corals are generally the focus of bleaching studies across coral reef ecosystems, other cnidarians supporting photoendosymbionts, such as octocorals and anemones, are also susceptible (Loya et al., 2001; Saenz-Agudelo et al., 2011; Hill et al., 2014; Maucieri and Baum, 2021). In fact, while some species of massive stony corals, such as Poritid corals, are sometimes considered "winners" under increased sea surface temperatures, branching stony corals and octocorals have previously been considered "losers" during bleaching events (Loya et al., 2001). The consequences of coral bleaching on individual octocoral colonies include loss of photoendosymbionts and chlorophyll, changes in Symbiodiniaceae community structure, increase in production of nitric oxide and heat shock proteins by Symbiodiniaceae, changes to lipid, protein, and metabolite content and composition, and more (Michalek-Wagner and Willis, 2001a; Ross, 2014; Panithanarak, 2015; Farag et al., 2018; Sikorskaya et al., 2020; Maucieri and Baum, 2021). Thus, to truly understand the impacts of climate change on coral reef systems and individual colonies, it is necessary to include a range of cnidarians in bleaching studies.

Although octocorals and anemones are not typically considered "reef builders", they do share a role as soft benthic habitat formers. Both are important members of benthic communities in reef and non-reef environments, including artificial habitats (Perkol-Finkel and Benayahu, 2004; Baillon et al., 2012; Ng et al., 2015; Epstein and Kingsford, 2019). Octocorals and anemones are attractive habitat for mobile vertebrate and invertebrate species, including generalists and obligate mutualists (Elliott and Mariscal, 2001; Lourie and Randall, 2003; Valdivia and Stotz, 2006; Huebner et al., 2012; Poulos et al., 2013). In fact, fish species diversity at two reefs in the GBR increased with increasing octocoral, but not stony coral, cover (Epstein and Kingsford, 2019). Both are also important food sources for many species and are especially popular with butterflyfishes (Pratchett, 2007; Slattery and Gochfeld, 2016; Epstein and Kingsford, 2019). However, many studies of coral reef community structure and bleaching do not consider octocorals (exceptions are reviewed in Steinberg et al. (2020) and below), leading to a critical knowledge gap of how they might respond to global stressors. Both stony corals and anemones have previously been recorded as bleaching at Lord Howe Island (Harrison et al., 2011; Boulotte et al., 2016); however, octocoral response to and recovery from thermal bleaching in subtropical reef systems in Australia, such as Lord Howe Island, are unknown.

Of the global studies that have considered octocorals, most report a link between ocean warming and bleaching and mass mortality and many describe variability by site and taxa (Loya et al., 2001; Goulet et al., 2008a; Prada et al., 2010; Dias and Gondim, 2016; Maucieri and Baum, 2021). In Japan, Loya et al. (2001) reported declines of the two dominant octocoral species on the reefs of Sesoko Island, Japan, and Maucieri and Baum. (2021) found that octocorals were lost completely from all surveyed sites at Kiritimati atoll during the 2015/2016 El Niño heatwave. In contrast, in the Caribbean octocorals are generally more resistant to bleaching than stony corals, but responses are variable between species and extreme heat can cause octocoral bleaching and mortality (Lasker, 2003, 2005; Drohan et al., 2005; Prada et al., 2010; Dias and Gondim, 2016; Goulet et al., 2017; Mccauley et al., 2018; Cerpovicz and Lasker, 2021). Octocorals on Puerto Rico and Brazil's reefs varied greatly in bleaching susceptibility by genus (Prada et al., 2010; Dias and Gondim, 2016). On the reefs of the Paraíba coast, Brazil, a gorgonian octocoral bleached along with four stony species and one hydrocoral, but only the gorgonian exhibited mortality during the study period (Dias and Gondim, 2016). In reefs of southwest Puerto Rico, octocoral response to elevated water temperatures was also taxa dependent, and only one species experienced mortality (Prada et al., 2010). Heat-induced mortality of octocorals can also occur without prior visual signs of bleaching (Lasker, 2005). Overall, there is considerable variability in bleaching response across octocoral taxa, including mortality.

In the Caribbean, studies of octocoral bleaching have focused on gorgonian octocorals, while in other parts of the world studies focus on Alcyonaceans, which may affect geographic bleaching patterns. Additionally, octocorals show biogeographical patterns of Symbiodiniaceae clade distribution, which may affect bleaching susceptibility and resistance (Goulet et al., 2008b). On Australia's Great Barrier Reef, extensive bleaching of stony coral species was recorded in 1998, 2004, 2016, 2017 and 2020,

which has resulted in loss of stony coral cover across the ecosystem (Thompson and Dolman, 2010; Hughes et al., 2017, 2018a, 2018b; Stuart-Smith et al., 2018; Thiault et al., 2021). Octocorals were also affected, with 43% of inshore octocoral colonies bleached during the 1998 bleaching event and significant taxonomic variability observed (Goulet et al., 2008a). Similarly, bleaching events were recorded in the Austral summers of 2010/2011 and 2015/2016 for coral reef ecosystems of the Indian ocean along Australia's west coast coral reefs, though the majority of studies did not quantify octocoral bleaching (Moore et al., 2012; Le Nohaïc et al., 2017). Octocoral bleaching was quantified at the isolated Scotts Reef of North-western Australia, where bleaching resulted in a decline of up to 80% in total coral cover, and 6 years after bleaching stony corals had begun recovering while octocorals cover had barely changed (Smith et al., 2008). As such, there is limited information currently available on the bleaching susceptibility for octocorals across the extent of Australia's coral reef ecosystems.

Previously stony corals and anemones were reported to undergo bleaching within the Lord Howe Island coral reefs, but octocoral bleaching has not been recorded in this UNESCO world-heritage listed marine park (Harrison et al., 2011; Boulotte et al., 2016). A major difficulty when studying octocorals and anemones is that they often leave little or no traces of existence following a mortality event. The consequences of bleaching can therefore be difficult–if not impossible–to detect if the immediate impact of high sea surface temperature (SST) is not quantified and no prior population data exist. The lack of prior data is often the case for the understudied octocoral populations on coral reefs (Steinberg et al., 2020). The consequences of increased sea surface temperature to the coral reef ecosystem of Lord Howe Island may also extend beyond the immediate impacts of coral bleaching and coral mortality on reefs. Increased SST reduces the ability of coral colonies to heal from fragmentation or damage, increases susceptibility to infectious disease, has been linked to Symbiodiniaceae-coral relationship shifting to parasitism by the endosymbiotic dinoflagellate, and decreases fecundity and reproduction in the year following bleaching events (Michalek-Wagner and Willis, 2001a, 2001b; Ruiz-Moreno et al., 2012; Bonesso et al., 2017; Baker et al., 2018).

The reefs of the Lord Howe Island lagoon marine park are ecologically and socially important to the ecosystem and people of Lord Howe Island. The waters around Lord Howe Island rank fifth in the Indo-Pacific for endemism, with 7.2% endemic fish species, many of which are supported by the reef structure (Randall, 1998). In addition, the local marine environment is important for the 350 permanent residents of the island, with local businesses providing tourism accommodation, boating, fishing, snorkelling, and diving both in and out of the lagoon (Lord Howe Island Tourism Association, 2021). Residents and tourists are attracted to the unique and pristine natural environment and the island's commitment to sustainability (Lord Howe Island Tourism Association, 2021), both of which may be negatively impacted by reef degradation. To better predict the impact of climate change and increasing sea surface temperatures within high latitude reefs it is important to understand how different species within the remote Lord Howe Island reef system are impacted by marine heatwaves. Here, we provide the first report of octocoral bleaching susceptibility and resilience in the world's southernmost coral reef ecosystem, Lord Howe Island. In doing so, we provide insight into the impact of climate driven increasing SSTs and marine heatwave events to these remote, valuable, and understudied coral reef ecosystems.

2 METHODS

2.1 Study Locations

Benthic cover was surveyed at five reef sites within Lord Howe Island marine park lagoon—Sylphs Hole, North Bay, Coral Gardens, Erscotts Reef, and Comets Hole (**Figure 1A**). Three of the five sites, Sylphs Hole, North Bay, and Coral Gardens were further surveyed using 20 m belt surveys and three species of octocorals were sampled (**Figure 1A**). This sub-sample of sites were chosen for further surveys and sample collections due to variable bleaching prevalence within the hard coral population. While Sylphs Hole experienced the most severe bleaching with 83% of hard corals bleached, North Bay experienced more moderate bleaching with 46% of hard coral cover undergoing bleaching, and Coral Garden's had the lowest observable bleaching at 16% of hard coral cover bleached (Moriarty et al., in review). These three sites differ in their environmental conditions, with Sylphs Hole highly sheltered and close to shore, North Bay sheltered but near the lagoon edge, and Coral Gardens unsheltered and exposed to wave action (Moriarty et al., in review). CoralWatch bleaching status and degree heating weeks (DHWs) were assessed via the satellite derived ocean temperature monitoring of NOAA Coral Reef Watch and marine heatwave status was assessed using the Marine Heatwave Tracker (NOAA, 2020; Schlegel, 2020) (**Figure 2**).

2.2 Monitoring

Monitoring of coral bleaching was first undertaken during March 13th to 29th, 2019 coinciding with peak summertime sea surface temperatures (**Figure 2A**), the sites were also re-surveyed 1 month after when bleaching alerts had subsided (April 26th–May 2nd, 2019, **Figure 2B**), and again in the southern hemisphere's spring from October 16th to 31st, 2019. All species of soft cnidarians including *Anthelia* sp., *Xenia* cf *crassa, Xenia* sp., *Cladiella* sp. 1, *Cladiella* sp. 2 sp., *Entacmaea quadricolor,* and *Palythoa* sp. were quantified in photo quadrat and belt surveys. Octocoral cover was assessed in 1 × 1 m quadrat photos at intervals 4, 12, and 16 m along each transect (Nikon Coolpix and an Olympus TG5 in underwater mode). The fixed intervals 4, 12, and 16 m were randomly chosen from a number sheet. All quadrats were photographed on the same side of the transect tape for each transect. Photo quadrats were annotated using CoralNet using 20 fixed points per quadrat (Beijbom et al., 2012). Anemones could not be seen on photo quadrats as they reside within crevices. At Coral Gardens, North Bay, and Sylphs Hole, species composition and colony numbers (abundance) were recorded within 20 × 1 m belt transects (snorkel based transect

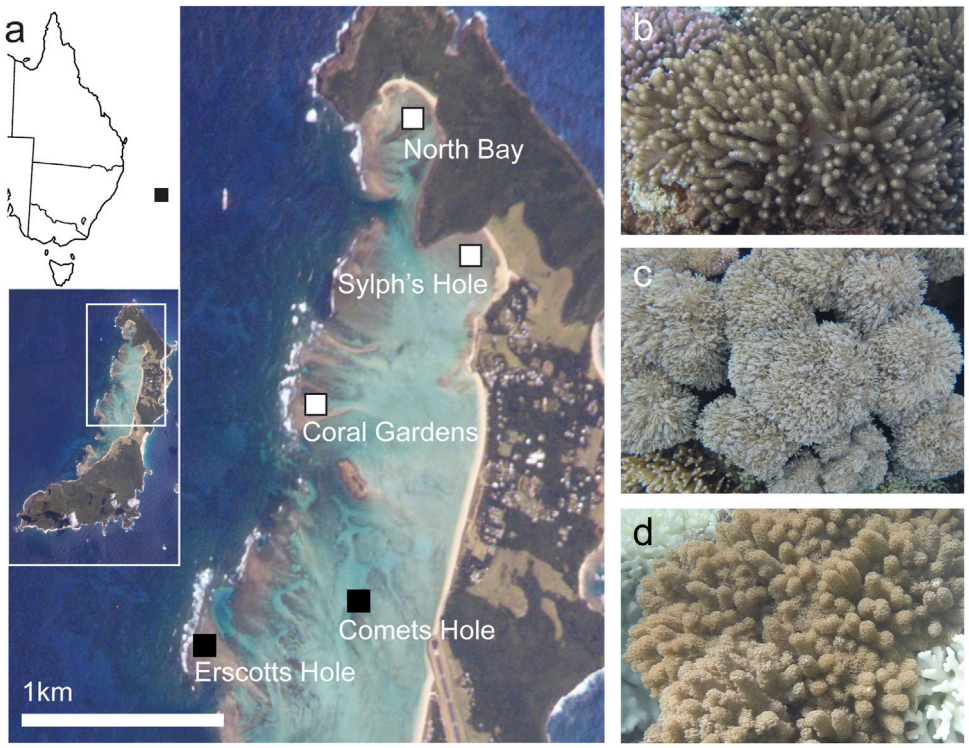

FIGURE 1 | Study sites and species. **(A)** Closeup map of Lord Howe Island, with map of the east coast of Australia and full island map inset. Sites where both surveys and collection were conducted–North Bay, Sylphs Hole, and Coral Gardens–are marked in white with black border, sites where only surveys were conducted–Comets Hole and Erscotts Hole–are marked in black. Lord Howe Island image courtesy of the Image Science and Analysis Laboratory, NASA Johnson Space Center; line map of Australia modified from "Australia states blank. png" by Golbez on Wikimedia Commons. **(B)** *Cladiella* sp. 1, **(C)** *Xenia* cf *crassa*, **(D)** *Cladiella* sp. 2. All coral photos by Rosemary K. Steinberg.

swims), wherein crevices and overhangs were extensively checked for anemones and octocoral colonies. Visual health status (visually bleached or unbleached) was noted for each surveyed cnidarian. Species not found on transects but seen during travel to and from survey sites or while collecting samples were recorded as off-transect observations.

2.3 Collection Methods

Three species of octocorals were sampled and bleaching quantified - *Cladiella* sp. 1, *Xenia* cf *crassa,* and *Cladiella* sp. 2 (**Figure 1C**.). Octocorals were identified to genus using Fabricius and Alderslade (2001) and *Cladiella* sp. 1 and sp. 2 were identified as different species based on external and spicule morphology (**Table 1**). *Xenia* cf *crassa* and *Cladiella* sp. 2 were chosen as they were common at all sampling sites and Xeniids have previously been more bleaching susceptible than Alcyoniids (Strychar et al., 2005; Sammarco and Strychar, 2013), while *Cladiella* sp. 1 (**Figure 1D**) was chosen because bleaching was first observed in this species at Sylphs Hole on 26 March 2019 (*Cladiella* sp. 1 was collected at all sites and monitoring intervals excluding North Bay in March due to logistical constraints).

Octocoral fragments were collected using Australian Entomological Supplies PTY LTD 12.5 cm blunt-tipped surgical scissors and placed in individual zip-top bags. Ten samples per species of unbleached and ten samples per species of bleached corals were collected at each coral reef site, with all samples collected from different colonies. Where no bleached samples of a species were found within a reef site only unbleached colonies were collected. Samples were minimally handled after collection, kept in individual zip-top bags in a cooler during transport, and handled and transported for as little time as possible to minimize handling, thermal, and light stress. Each sample was split into two portions–one was immediately fixed in a sterile solution of 4% formalin in 3× phosphate buffered saline (PBS) in nuclease free water and kept at 4°C for later DNA extraction. Samples were transferred to a sterile solution of 3× PBS after 10–14 h in fixative and stored at 4°C. The other portion were kept in aquaria on the day of collection within the laboratory at the Lord Howe Island research station (March), at the Lord Howe Island Marine Park Authority boat shed (April/May), or at the facility provided by Blue Lagoon Lodge (October) with aeration until 30 min after sundown to measure maximum quantum yield of photosystem II (PSII) on live colonies, after which they were frozen. Aquaria consisted of 54 L plastic tubs filled partially with unfiltered seawater and kept aerated with use of a bubbler and no source of artificial light. Soft coral fragments were kept separated by keeping them in small, submerged collection jars weighed down with stones.

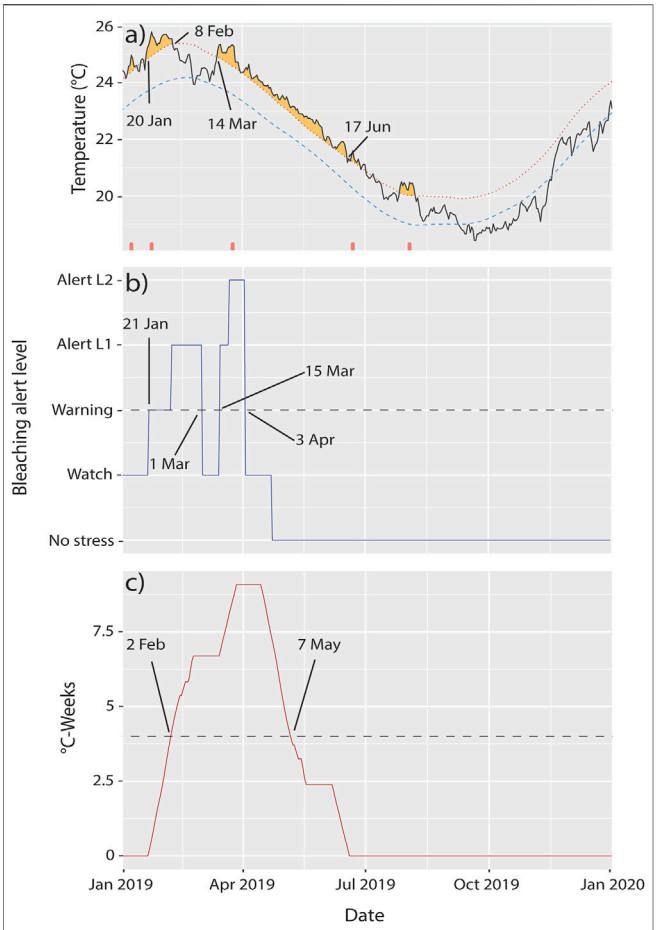

FIGURE 2 | Extreme temperatures at Lord Howe Island in 2019. **(A)** Heatwaves [plot downloaded from the Marine Heatwave Tracker (Schlegel, 2020)], **(B)** Coral Reef Watch bleaching alert levels, and **(C)** degree heating weeks at Lord Howe Island in 2019. The dashed lines in **(B,C)** represent minimum conditions at which bleaching is expected to occur.

2.4 DNA Extraction, PCR, and Sequencing

A subset of five samples each of healthy *Cladiella* sp.1, sp. 2, and *Xenia* cf *crassa* at Coral Gardens and Sylphs hole during March and October were processed to determine Symbiodiniaceae type profiles using the ITS2 gene. DNA was extracted using a Qiagen QIAamp DNA Mini Kit following the manufacturers tissue protocol (Qiagen, 2016) with the following modifications: tissue was bead-beaten in 180 µl of buffer ATL, and 20 µl of proteinase K was added, after which the tissue was digested at 56°C overnight. Following digestion and washing, DNA was eluted in the provided buffer AE and the buffer was left on the membrane for 10 minutes before centrifugation; the same aliquot of buffer was returned to the membrane for a second time for another 10 minutes and centrifuged. Cladiella sp. 1 DNA was eluted in 200 µl, Xenia cf crassa DNA was eluted in 50 µl, and Cladiella sp. 2 DNA was eluted in 100 µl buffer AE. ITS2 PCR was performed following the protocol from Hume et al. (2018) using SYM_VAR_5.8S2 - SYM_VAR_REV primers. Sequencing was performed by the Ramaciotti Centre for Genomics, UNSW (Sydney, NSW, Australia).

2.5 Pulse Amplitude Modulated Fluorimetry

Maximum quantum yield of PSII (F_v/F_m) was measured using PAM fluorimetry. Measurements were taken at least 30 min after sunset in full darkness. Point yield measurements were taken using a Walz Diving-PAM fluorimeter (Heinz Walz GmbH, Effeltrich, Germany, March 2019) and a Maxi Imaging-PAM M-series fluorimeter (Heinz Walz GmbH, Effeltrich, Germany, April/May and October 2019). PAM settings were as follows: Diving-PAM for unbleached coral colonies, MI: 8, SI: 8, Sat-width: 0.85, Gain: 2, Damp: 2. Diving-PAM for bleached colonies: MI: 8, SI: 8, Sat-width: 0.85, Gain: 10, Damp: 2. For the Imaging-PAM, settings for all colonies were MI: 8, SI: 8, Sat-width: 0.8, Gain: 12, Damp: 2. Three replicate readings per coral fragment were recorded. When using the Diving-PAM, replicates on individual fragments were achieved by waiting half an hour between runs to allow fragments to become dark-adapted again, and readings were taken from different sections of the sample (Ralph, 2005). With the Imaging-PAM, all replicates were measured at once as multiple readings can be taken together by defining separate areas of interest within the PAM image (Heinz Walz GmbH, 2019). After PAM fluorimetry, all samples were placed in −4°C freezer for up to 2 weeks in the field and transferred to a −20°C freezer in the laboratory in Sydney and kept frozen until processing for protein, Symbiodiniaceae, and chlorophyll concentrations.

2.6 Determination of Coral Protein Content, Symbiodiniaceae Concentrations, and Chlorophyll a and c2 Concentrations

Samples were processed as per Steinberg et al. (2021). In summary, octocoral samples were homogenised with reverse osmosis water using an Omni TH Tissue Homogeniser. The resulting slurry was centrifuged and supernatant removed and saved, and this step was repeated. Supernatant protein was quantified against a bovine albumin standard using the Thermo Scientific Coomasie Plus (Bradford) kit and protocol. Symbiodiniaceae were counted using a Neubauer Improved haemocytometer with three haemocytometer fills, two grids per haemocytometer, and five counts per grid, which were averaged, for a total of 6 replicate counts (Steinberg et al., 2021). Chlorophyll was extracted in 100% acetone for 48 h and measured on a VWR UV-6300PC Double Beam Spectrophotometer (see Steinberg et al. (2021) for more information).

2.7 Statistical Analysis

All graphs and analyses were completed in R version 3.4.1 (R Core Team, 2013). Plots were created with the package ggplot2 (Wickham, 2011). Differences in percent benthic cover were compared among benthic groups (octocoral, stony coral, algae, seagrass, and abiotic) and sites (Sylphs Hole, North Bay, Coral Gardens, Erscotts Reef, and Comets Hole) using a generalised linear mixed model (GLMM) in the packaged glmmTMB (Brooks et al., 2017). Differences in community composition among sites (Sylphs Hole, North Bay, and Coral Gardens) and monitoring intervals were tested using permutational multivariate analysis of

TABLE 1 | Summaries of study species morphological features and habitat preferences.

Species	Colony morphology	Polyp morphology	Body retraction	Spicule morphology	Habitat preference
Cladiella sp. 1	Lobate. Lobes short and stiff. Brown colour with some reddish or orange tints	Short (<1 mm), retractable polyps. Classic rosette tentacle formation. Polyps are darker than body	Highly retractile. Retracted colonies are the colour of the body (light brown) with small, dark pin-pricks where the polyps are retracted	Spiky, nearly rod-like dumbbell shaped spicules. The central "handle" is small and the "heads" are narrow	Near the bottom of shallow reef on rock edges. Form large, dense aggregations
Cladiella sp. 2	Lobate. Lobes long and flexible. Deep brown colour	Short (<1 mm), retractable polyps. Rosette tentacle formation with twisted, curly tentacles	Highly retractile. Stark change in colour to grey when retracted. Retracted polyps are difficult to see, can be made out as dents in the colony surface	Spiky dumbbell shaped spicules. Centre "handle" much larger than *Cladiella* sp. 1 and "heads" are large compared to the "handle"	Near the bottom of shallow reef on rock edges and in reef crevices. Form small aggregations
Xenia cf crassa	Pom-pom. Flexible, tube-shaped bodies with long (>3 cm) polyp stalks on the top side only. Tube is light brown, polyp stalks are dark brown, and tentacles are dark brown with reflective blue on the top sides, which can make colonies appear blue or silver from above	Very long polyp stalks (>3 cm) and tentacles (>5 mm). Polyp stalks are thin and densely packed, polyps have feathery tentacles with reflective blue or silver surface	Moderately retractile. Polyp stalks shrink down towards the body and polyps close	Small, flat, disk-shaped spicules	At the top of reef outcrops and on top of dead coral. Form large and expansive mats

variances (PERMANOVA) with the 'adonis' function in the R package Vegan (Oksanen et al., 2019). All zero-only transects were removed, and dispersion was tested using permutest before running the PERMANOVA. Square-root transformation of count data was performed to ensure non-significant differences in dispersion. Pairwise comparisons were performed using the package pairwiseAdonis (Marinez Arbizu, 2020).

Differences in soft coral abundance, Symbiodiniaceae counts, and chlorophyll concentrations per μg protein among sites, monitoring intervals, and visual health status were tested using a GLMM. For abundance, transect number was included as a random variable. For Symbiodiniaceae and chlorophyll the individual that the sample was taken from was included as a random factor, and either protein content or Symbiodiniaceae density was included as an offset (depending on which factor was used for standardisation). Additional offsets for particular models are outlined in the supplemental methods. For specifics on which distribution was used, see the table associated with each analysis (**Supplementary Tables S1–S7**). Differences in protein content and mean chlorophyll *a* and c_2 per Symbiodiniaceae cell among sites, monitoring intervals, and visual health status were tested using two-way ANOVAs as these datasets contained no random factors. As ANOVA requires data to be normal, datapoints that fell outside the theoretical quantiles of the QQ-plot plotted using the car package were removed (Fox and Weisberg, 2019). Differences in photosynthetic yield among monitoring intervals and visual health status was tested using a linear mixed effects model (lmer) from the package lme4 (Bates et al., 2015). Further model details and example models are included in the supplemental methods. All pairwise comparisons on significant GLMM, lmer, and ANOVA analyses were performed using the emmeans package (Lenth et al., 2018).

3 RESULTS

3.1 Temperatures in the Lord Howe Island Lagoon

During early 2019, Lord Howe Island was affected by three marine heatwaves (**Figure 2A**). Heat wave properties reported here are duration, intensity (degrees Celsius above the expected time-of-year mean, reported as mean and max intensity), and cumulative intensity (the integral of intensity over the event). The first heatwave began on 31 Dec 2018 and lasted 14 days to 13 Jan 2019, with a mean intensity of 1.3°C, max intensity of 1.67°C, and a cumulative intensity of 18.2°C. The second heatwave began on 20 Jan 2019 and lasted 20 days until 8 Feb 2019, with a mean intensity of 1.61°C, a max intensity of 2.01°C, and a cumulative intensity of 32.15°C. The third began on 14 Mar 2019 and lasted 96 days until 17 June 2019, with a mean intensity of 1.17°C, max intensity of 1.76°C, and a cumulative intensity of 112.48°C (Schlegel, 2020). Cyclone Oma made landfall on the island between the second and third marine heat waves in late February 2019 (**Figure 2A**). Coinciding with the heatwaves, NOAA Coral Reef Watch bleaching alert levels met or exceeded "Warning" during two time periods, from 21 Jan to 1 Mar 2019 with alerts reaching level 1, and 15 Mar to 3 Apr 2019 with alert levels reaching level 2. In addition, degree heating weeks (DHWs) met or exceeded 4°C-weeks from 2 Feb 2019 to 7 May 2019. Symbiodiniaceae begin to experience stress when DHWs exceed 2 DHWs, bleaching is expected at 4 DHWs, and significant mortality at 8 DHWs (Gierz et al., 2020; Hughes et al., 2018a; Kayanne, 2017, **Figure 2C**).

3.2 Octocoral Morphological Observations

The three species of octocoral chosen for further analysis (*Cladiella* sp. 1, *Xenia* cf *crassa,* and *Cladiella* sp. 2) differ in

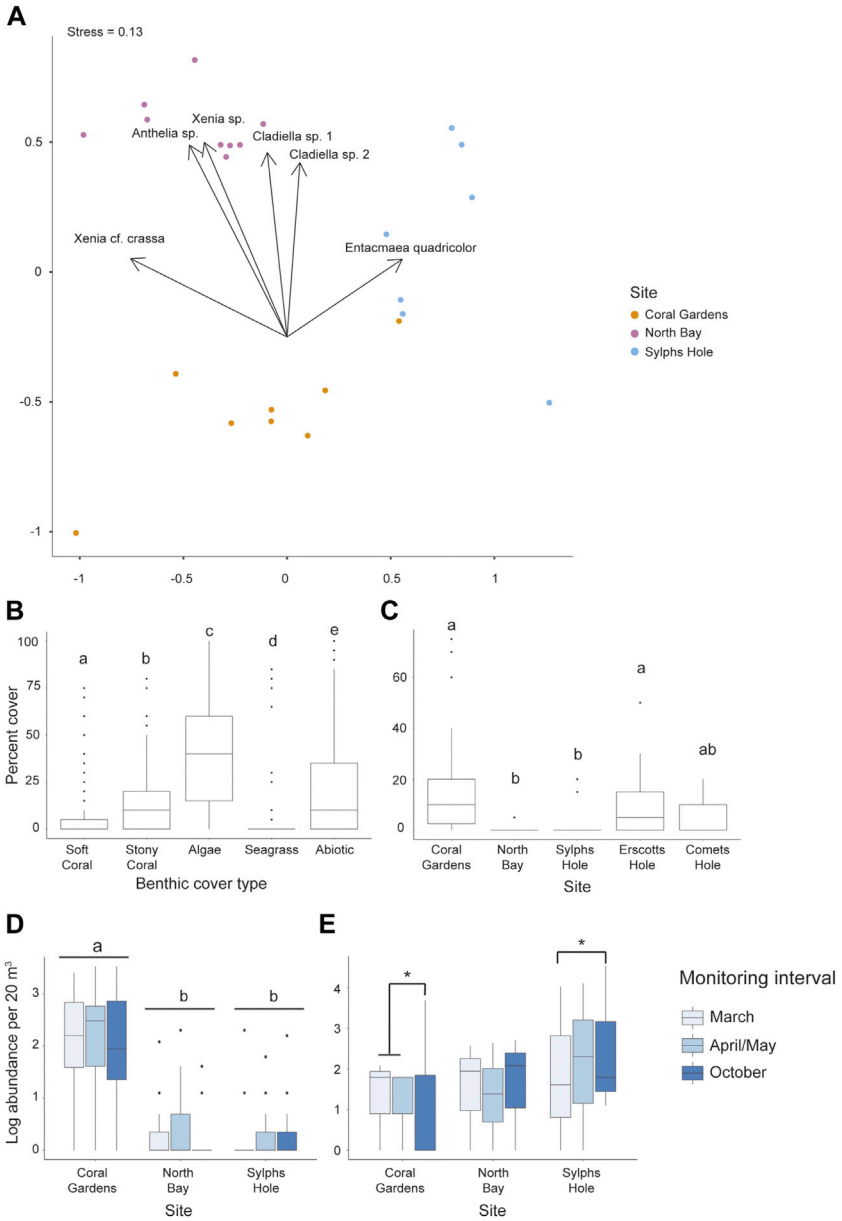

FIGURE 3 | Differences in the percent cover and abundance of octocorals and anemone among benthic groups, sites, and monitoring intervals in the Lord Howe Island lagoon. **(A)** NMDS ordination plot of species composition at each of the sites belt surveyed, Coral Gardens, North Bay, and Sylph's Hole, **(B)** percent cover from photo quadrats of each benthic group (octocoral, stony coral, algae, seagrass, and abiotic factors) across the lagoon, **(C)** percent octocoral cover from photo quadrats across 5 sites in the lagoon, **(D)** abundance (log) from belt transects of six species of octocoral across three sites in the lagoon, and **(E)** abundance (log) from belt transects of *Entacmaea quadricolor* anemones across three sites and three monitoring intervals in the lagoon. Significance is designated either by different letter group or by a bar. *p*-values are represented as follows—* for $p < 0.05$, ** for $p < 0.005$, and *** for $p < 0.0005$. Where more than one plot is grouped together, the highest *p*-value is reported.

their morphology, and as morphological differences are known to influence bleaching susceptibility and resilience in stony corals, morphology is detailed in **Table 1**. Tissue regions with high Symbiodiniaceae density were visually distinguished in all three species by noting their relative colour as they were considerably darker than surrounding non-symbiotic tissues. In the lobed species, Symbiodiniaceae were concentrated on the outer layer of flesh and in the polyps, with the centre of the lobes nearly perfectly white. In *Xenia crassa*, the polyps and polyp stalks appeared to have higher densities of Symbiodiniaceae than the body, with a dark brown colour concentrated in the polyps and a light brown colour in the coral body. Differences in spicule size and density were also evident. Both lobed species had large, densely packed spicules in the centre of the lobes. This was observed by eye and confirmed by the difficulty in cutting through the centre of large lobes, and by spicule masses

becoming lodged in the homogenisation mechanism if they were not cut down small enough. Dumbbell shaped spicules were also occasionally found while counting Symbiodiniaceae and were 2–5 × larger than Symbiodiniaceae cells. *Xenia crassa* had much smaller spicules and were extremely easy to cut and homogenise. A few small (1.5 × Symbiodiniaceae size), flat, disk-shaped spicules were observed while counting Symbiodiniaceae (**Table 1**).

3.3 Octocoral and Anemone Cover, Abundance, and Species Composition

Five species of octocoral (*Cladiella* sp. 1, *Xenia* cf *crassa, Cladiella* sp. 2, *Xenia* sp., *Anthelia* sp.), one anemone species (*Entacmaea quadricolor*), and one zoanthid species (*Palythoa* sp.) were documented within the survey locations at all five reef sites of the Lord Howe Island lagoonal reef system. One additional species of octocoral, *Sarcophyton* sp., was observed at North Bay outside of transects. From the CoralNet quantification of quadrat photos, octocoral cover in the Lord Howe Island lagoon was on average 7 ± 1% SE cover, but was heterogenous between the reef sites within the lagoon (GLMM $p < 0.0001$, min 0%, max 75%, **Figure 3B**, **Supplementary Table S1**). Anemone cover was not recorded as anemones occurred primarily in rock and coral crevices and were not visible in photo quadrats. Within the lagoon, octocoral cover (7 ± 1% SE) was significantly different from cover of other benthic groups, with significantly less cover than stony coral (15 ± 2% SE, $p < 0.0001$), algae (39 ± 2% SE, $p < 0.0001$), and abiotic factors (e.g., bare rock or sand, 21 ± 2% SE, $p < 0.0001$), and significantly more cover than seagrass (3 ± 1% SE, $p < 0.0001$, **Supplementary Table S1**). When examining octocoral cover only across the different sites in the lagoon, there was a significant effect of site, but not of monitoring interval on overall octocoral cover (GLMM $p < 0.0001$, **Supplementary Table S1**). Octocoral cover was highest at Coral Gardens (17 ± 4% SE) and lowest at North Bay (0.4 ± 0.3% SE; **Figure 3C**, **Supplementary Table S1**). Octocoral cover was also significantly higher at Coral Gardens and Erscotts Reef than North Bay or Sylphs Hole, but other site comparisons did not differ ($p < 0.05$, **Figure 3C**, **Supplementary Table S1**).

The abundance of octocorals from the belt transects differed significantly among sites (GLMM $p < 0.0001$ **Figure 3D**), but neither monitoring interval nor the interaction between monitoring interval and site were significant (**Supplementary Table S2**). Across the lagoon, abundance of all octocoral species was significantly higher at Coral Gardens than North Bay or Sylphs Hole ($p < 0.0001$), but not significantly different between North Bay and Sylphs Hole (**Figure 3C**, **Supplementary Table S2**). *Entacmaea quadricolor* abundance differed significantly between monitoring intervals at different sites (GLMM $p < 0.05$, **Figure 3A**, **Supplementary Table S2**). At Coral Gardens, octocoral abundance was significantly lower in October than March or April/May ($p < 0.05$). At Sylphs Hole, mean *E. quadricolor* abundance was significantly higher during October compared to abundance recorded during the bleaching event in March ($p < 0.05$). At North Bay abundance did not vary across monitoring intervals. There were no differences in *E. quadricolor* abundances across sites within monitoring intervals.

Sylphs Hole, Coral Gardens, and North Bay had significantly different compositions of octocorals and anemones species (PERMANOVA $p = 0.001$ **Figure 3A**). *Entacmaea quadricolor, Anthelia* sp., *Cladiella* sp. 1, *Cladiella* sp. 2, and *Xenia* sp. were all abundant at Coral Gardens, while Sylphs Hole was dominated by *Entacmaea quadricolor*, and North Bay had little octocoral or anemone cover, with *E. quadricolor* and *Xenia elongata* being most abundant (**Figure 3A**, **Supplementary Table S2**). *Anthelia* sp. and *Xenia* sp. were observed at Coral Gardens, Comets Hole, and Erscotts Reef but not at Sylphs Hole or North Bay.

3.4 Symbiodiniaceae Type Profiles

Two Symbiodiniaceae type profiles were identified based on ITS2 sequences, with both *Cladiella* species sharing the type profile C1-C1cy-C42.2-C3-C1cz-C1b and *Xenia* cf *crassa* exhibiting the type profile C1/C42.2-C1b-C1by-C3.

3.5 Response of Bleaching Susceptible Species to Heatwaves in the Lord Howe Island Lagoon

3.5.1 Entacmaea Quadricolor Bleaching Response

Bleaching or reduced pigmentation (paling) was recorded on transects for the anemone *E. quadricolor* at Sylphs Hole during March and April/May. During March, all anemones recorded were pale or bleached, while during early April we found approximately 60% of anemones were pale and none were observed to be fully bleached (**Figure 4A**). One bleached *E. quadricolor* anemone was recorded off-transect at North Bay on March 16, 2019, and observed to have partially recovered on 26 March and 29 April 2019 and appeared fully recovered by October 19, 2019 (**Figure 4B**).

3.5.2 Cladiella Sp. 1 Endosymbiont Bleaching Responses

No bleached *Cladiella* sp. 1 were recorded within the reef surveys but bleached individuals were recorded off-transect at Sylphs Hole during both March and April 2019, with the first bleached colony recorded on 22 March 2019. Bleached colonies were found near, and often mixed within, clusters of unbleached colonies (**Figure 4C**). Furthermore, seven bleached colonies of *Cladiella* sp. were observed to have detached from the hard substrate and several more colonies were observed to have partially detached (**Figure 4C**, **Supplementary Video S1**).

Symbiodiniaceae, chlorophyll *a*, and chlorophyll c_2 per μg protein were significantly lower, while chlorophyll *a* and c_2 per Symbiodiniaceae were significantly higher, in bleached than unbleached colonies (GLMM $p < 0.05$, **Figure 5**, **Supplementary Table S3**). PSII photochemistry was significantly lower during the peak SST temperature of March compared to 1 month after bleaching onset (April/May) in bleached coral colonies of *Cladiella* sp. 1 ($p < 0.0001$). PSII photochemistry was also significantly higher in unbleached than bleached colonies for *Cladiella* sp. 1 during March, though not significantly different in April/May ($p < 0.0001$, **Figure 5C**, **Supplementary Table S3**). In March, protein content was significantly lower in bleached coral colonies of

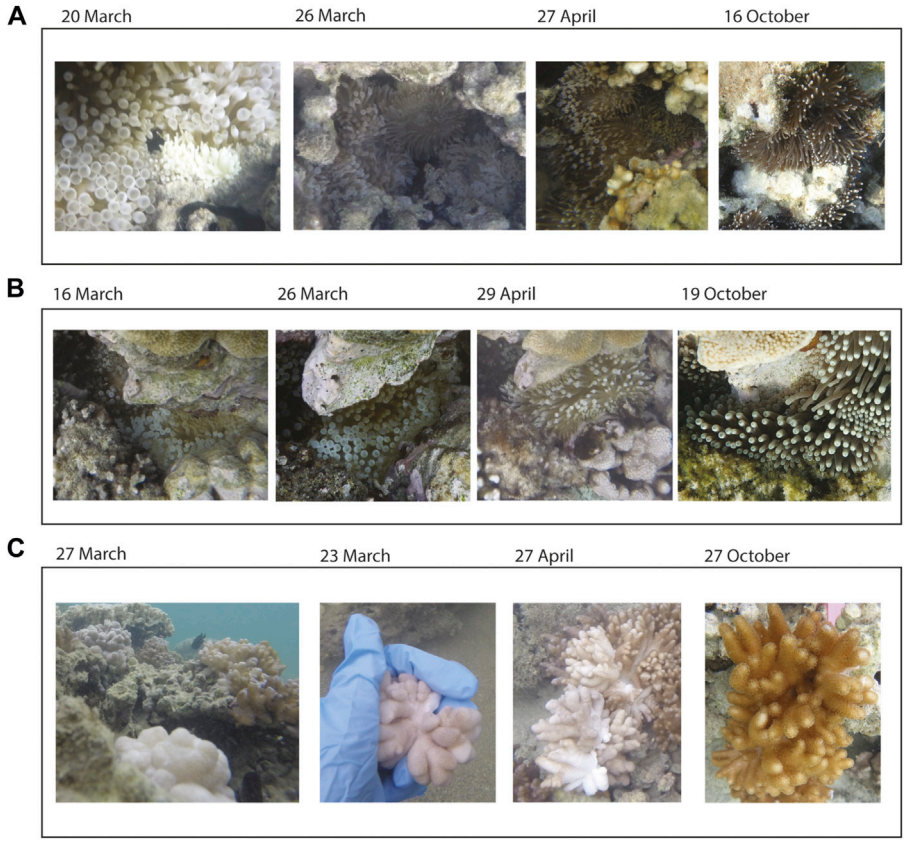

FIGURE 4 | Timelapse photos of *Entacmaea quadricolor* anemones and *Cladiella* sp. 1 octocorals. **(A)** Paled and bleached *E. quadricolor* anemones at Sylphs Hole, **(B)** a single bleached *E. quadricolor* anemone at North Bay, and **(C)** bleached, detached, and semi-detached *Cladiella* sp. 1 at Sylphs Hole. All photos by Rosemary K. Steinberg.

Cladiella sp. 1 compared to those colonies not found to undergo bleaching ($p < 0.0001$), but in April/May there was no significant difference in protein content between bleached and unbleached colonies (**Figure 5D**, **Supplementary Table S3**, two outliers from a total of 118 observations were removed prior to analysis).

3.5.3 Response of Unbleached Cladiella Sp. 1 Colonies

In unbleached *Cladiella* sp. 1 colonies, all measures are reported within site and monitoring interval, as the interaction term in the GLMM was significant (GLMM $p < 0.05$, **Figure 6**, **Supplementary Table S4**, two outliers of 271 were removed before protein analysis). In *Cladiella* sp. 1 at Coral Gardens, chlorophyll c_2 per Symbiodiniaceae was significantly higher in April/May than October, while protein per wet weight was significantly lower during March than either April/May or October ($p < 0.05$). No other measured variables were significant in *Cladiella* sp. 1 at Coral Gardens (**Figure 6**, **Supplementary Table S4**). However, at North Bay, we found both chlorophyll c_2 per µg protein and per Symbiodiniaceae in *Cladiella* sp. 1 were significantly higher during March than April ($p < 0.005$, **Figure 6**, **Supplementary Table S4**). At Sylphs Hole, concentrations of all measured factors except PSII photochemistry and protein per wet weight were significantly lower in March compared to October ($p < 0.05$, **Figure 6**, **Supplementary Table S4**), whereas protein per wet weight was significantly higher at Sylphs Hole during March compared to October ($p = 0.01$, **Figure 6E**, **Supplementary Table S4**). Additionally, there were significantly lower concentrations of chlorophyll c_2 per µg protein and per Symbiodiniaceae at Sylphs Hole in March compared to April/May ($p < 0.05$), but no differences in other factors (**Figure 6**, **Supplementary Table S4**). There were also significantly lower concentrations of all chlorophyll measures at Sylphs Hole than Coral Gardens or North Bay during March, and significantly lower concentrations of all chlorophyll measures and of Symbiodiniaceae per µg protein at Sylphs Hole than Coral Gardens or North Bay during April/May ($p < 0.001$, **Figure 6**, **Supplementary Table S4**).

3.6 Response of Bleaching Resistant Species to Heatwaves in the Lord Howe Island Lagoon

3.6.1 Response of Unbleached Xenia cf Crassa Colonies

Symbiodiniaceae per µg protein was significantly higher during the bleaching event in March compared to April/May or October ($p <$

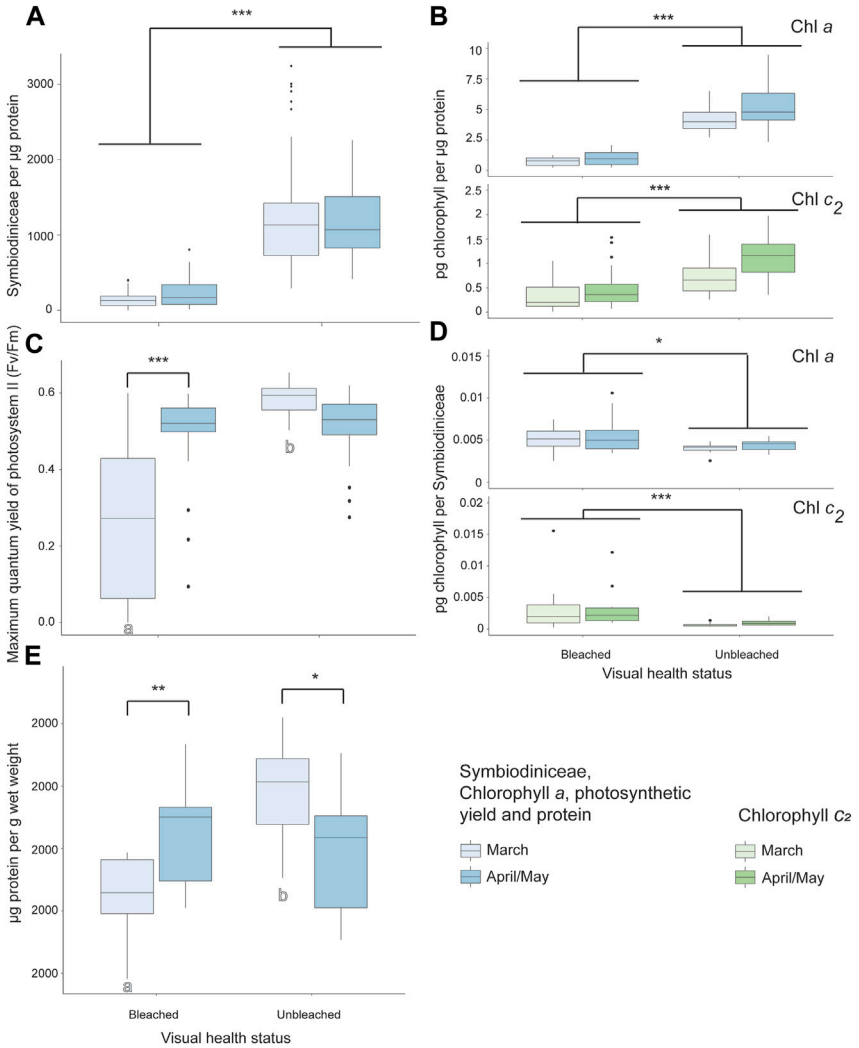

FIGURE 5 | Bleaching responses to a marine heat wave in *Cladiella* sp. 1 at Sylphs Hole Reef in Lord Howe Island lagoon. **(A)** Symbiodiniaceae density per µg protein in visually bleached and healthy *Cladiella* sp. 1 colonies during March and April/May. **(B)** Chlorophyll *a* (above) and c_2 (below) densities per µg protein in visually bleached and healthy Cladiella sp. 1 colonies during March and April/May. **(C)** PSII photochemistry of visually bleached and healthy *Cladiella* sp. 1 colonies during March and April/May. **(D)** Chlorophyll *a* (above) and c_2 (below) per Symbiodiniaceae cell in visually bleached and healthy *Cladiella* sp. 1 colonies during March and April/May. **(E)** µg protein per g wet weight in visually bleached and healthy *Cladiella* sp. 1 colonies during March and April/May. Significance is designated either by different letter group or by a bar. *p*-values are represented as follows—* for $p < 0.05$, ** for $p < 0.005$, and *** for $p < 0.0005$. Where more than one plot is grouped together, the highest *p*-value is reported. Bars above the boxplots represent monitoring interval differences within health state, and letters below the boxplots represent health state differences within monitoring intervals.

0.05, **Figure 7A**, **Supplementary Table S5**). For *Xenia sp.* collected at Coral Gardens, there was significantly higher chlorophyll *a* per µg protein during March compared to April ($p = 0.04$) and no difference in other measured factors. In colonies collected at North Bay, there was significantly higher chlorophyll *a* per µg protein in March compared to October, significantly more chlorophyll a per Symbiodiniaceae in April/May compared to March or October, and more chlorophyll c_2 per Symbiodiniaceae during April/May compared to October ($p < 0.05$, **Figure 7**, **Supplementary Table S5**). For *Xenia* collected at Sylphs Hole chlorophyll *a* per µg protein was significantly higher during March than April/May or October, and all other chlorophyll measures were significantly higher during March and April/May than October ($p < 0.05$, **Figure 7**, **Supplementary Table S5**). During March chlorophyll *a* per Symbiodiniaceae was significantly higher at Sylphs Hole than Coral Gardens, and chlorophyll c_2 per µg protein and per Symbiodiniaceae were significantly higher at Sylphs than the other two sites ($p < 0.05$, **Figure 7**, **Supplementary Table S5**). During April, chlorophyll *a* per Symbiodiniaceae was significantly lower at Coral Gardens than North Bay ($p = 0.002$, **Figure 7C**, **Supplementary Table S5**). During October chlorophyll *a* per µg protein was significantly higher at Coral Gardens than Sylphs ($p = 0.008$, **Figure 7B**, **Supplementary Table S5**). Results for PSII photochemistry and protein per wet weight are presented in

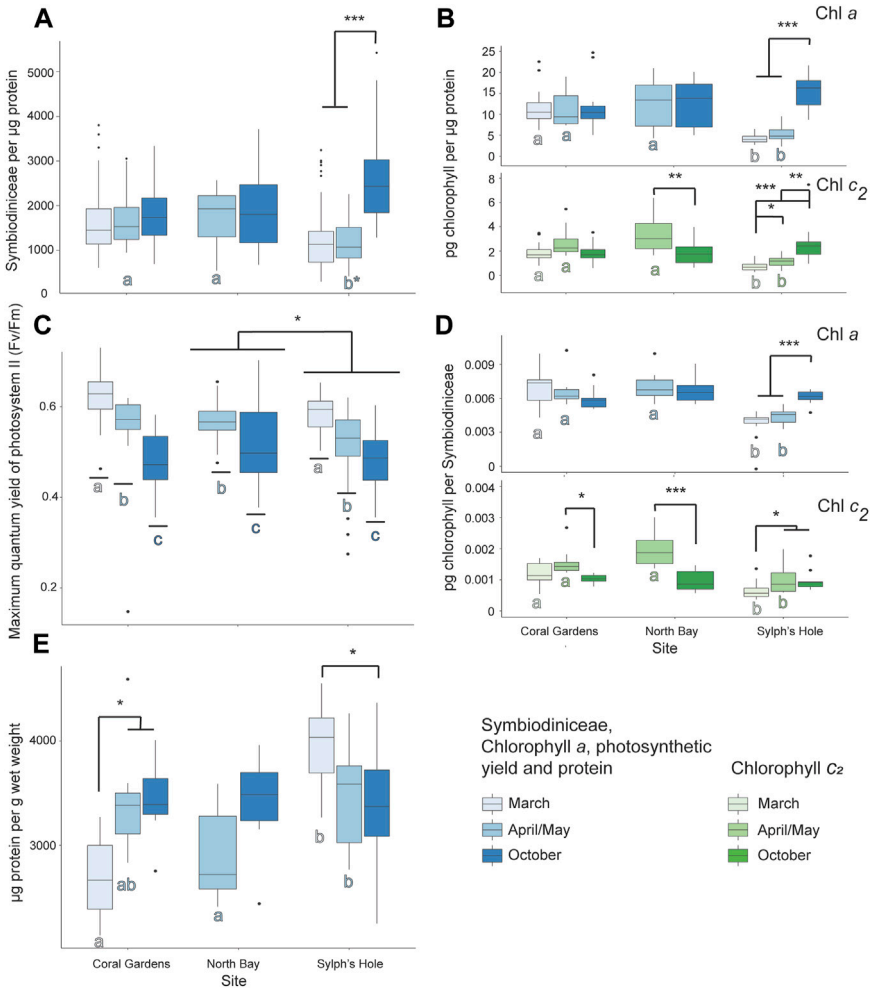

FIGURE 6 | Marine heatwave effects on unbleached *Cladiella* sp. 1 across three reefs in the Lord Howe Island lagoon. **(A)** Symbiodiniaceae density per µg protein in unbleached *Cladiella* sp. 1 colonies during March, April/May, and October. **(B)** Chlorophyll *a* (above) and c_2 (below) densities per µg protein in unbleached *Cladiella* sp. 1 colonies during March, April/May, and October. **(C)** PSII photochemistry in visually healthy *Cladiella* sp. 1 colonies during March, April/May, and October. **(D)** Chlorophyll *a* (above) and c_2 (below) per Symbiodiniaceae cell in visually healthy *Cladiella* sp. 1 colonies during March, April/May, and October. **(E)** µg protein per g wet weight in visually healthy *Cladiella* sp. 1 colonies during March, April/May, and October. Significance is designated either by different letter group or by a bar. *p*-values are represented as follows—* for $p < 0.05$, ** for $p < 0.005$, and *** for $p < 0.0005$. Where more than one plot is grouped together, the highest *p*-value is reported. Bars above the boxplots represent monitoring interval differences within site, and letters below the boxplots represent site differences within monitoring intervals.

Supplementary Table S7 and **Supplementary Figure S2** but are not discussed further here.

3.6.2 Response of Unbleached Cladiella Sp. 2 Colonies

Symbiodiniaceae density was significantly lower at Coral Gardens than the other two sites, while chlorophyll c_2 was significantly lower at Sylphs Hole than Coral Gardens ($p < 0.05$, **Figure 8**, **Supplementary Table S6**). Additionally, chlorophyll c_2 density was significantly lower during October than the other two monitoring intervals ($p < 0.05$, **Figure 8**, **Supplementary Table S6**). At Coral Gardens, Symbiodiniaceae and chlorophyll densities were not significantly different between monitoring intervals. At North Bay, corals had significantly less chlorophyll *a* per Symbiodiniaceae during April/May compared to March and October ($p < 0.0001$, **Figure 8C**, **Supplementary Table S6**). Conversely, there was significantly more chlorophyll c_2 per Symbiodiniaceae during April/May compared to October ($p = 0.001$, **Figure 8**, **Supplementary Table S6**). At Sylphs Hole, *Cladiella* sp. 2 had significantly less chlorophyll c_2 per Symbiodiniaceae during October than March or April/May ($p < 0.05$, **Figure 8**, **Supplementary Table S6**). During March chlorophyll c_2 per Symbiodiniaceae was significantly higher at Sylphs Hole than either Coral Gardens or North Bay ($p < 0.0005$, **Figure 8**, **Supplementary Table S6**), while during April chlorophyll c_2 was significantly higher at Sylphs Hole than North Bay only ($p = 0.004$, **Figure 8**, **Supplementary Table S6**). Results for PSII photochemistry and protein per wet weight are

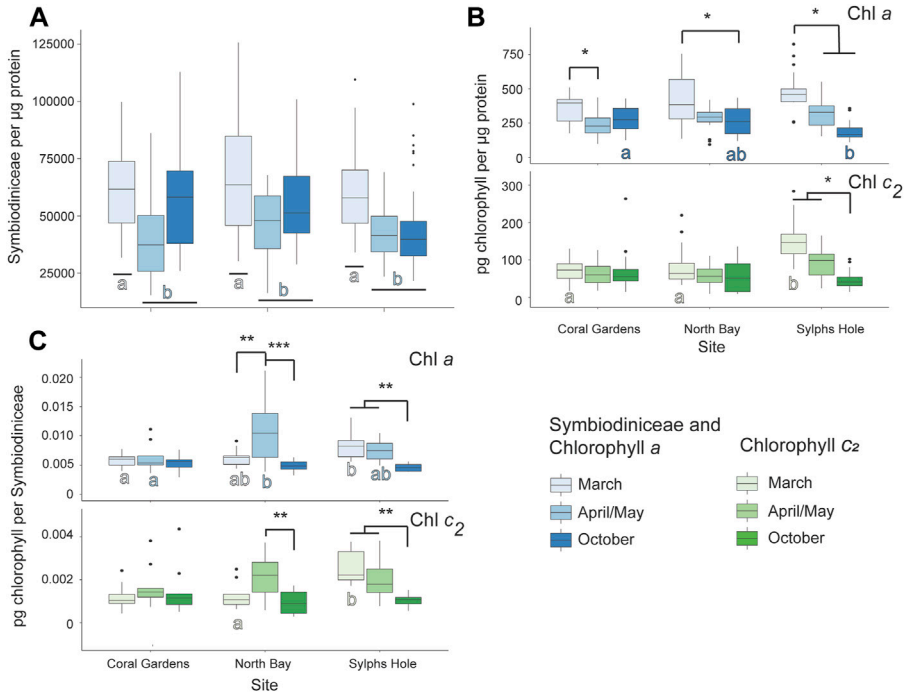

FIGURE 7 | Marine heatwave effects on unbleached *Xenia cf crassa* across three reefs in the Lord Howe Island lagoon. **(A)** Symbiodiniaceae density per µg protein in unbleached *Xenia* cf *crassa* colonies during March, April/May, and October. **(B)** Chlorophyll a (above) and c_2 (below) densities per µg protein in unbleached *Xenia* cf *crassa* colonies during March, April/May, and October. **(C)** Chlorophyll *a* (above) and c_2 (below) densities per Symbiodiniaceae cell in visually healthy *Xenia* cf *crassa* colonies during March, April/May, and October. Significance is designated either by different letter group or by a bar. *p*-values are represented as follows—* for $p < 0.05$, ** for $p < 0.005$, and *** for $p < 0.0005$. Where more than one plot is grouped together, the highest *p*-value is reported. Bars above the boxplots represent monitoring interval differences within site, and letters below the boxplots represent site differences within monitoring intervals.

presented in **Supplementary Table S8** and **Supplementary Figure S2** but are not discussed further here.

4 DISCUSSION

On Lord Howe Island marine park lagoonal reefs, species-specific octocoral bleaching responses were evident during the 2019 heatwaves. Here, we surveyed five octocoral species and one anemone species within the Lord Howe Island lagoon and found only two of the examined species bleached. While *Cladiella* sp. 1 and *Entacmaea quadricolor* both bleached, only *Cladiella* detached from the substrate and likely underwent mortality. Though other studies have recorded bleaching and mortality of octocorals, none have reported this type of behaviour. The other four octocoral species surveyed, including a congeneric *Cladiella* species, appeared resistant to the heatwaves and were not observed to undergo bleaching or mortality, during or after, the marine heatwave event. In this study we provide extensive evidence for differential bleaching thresholds of the octocoral species within the Lord Howe Island lagoonal reef system, with species in the same genus exhibiting differential susceptibilities. Previous studies of octocorals in the Great Barrier Reef revealed similar variability in bleaching responses within and among taxa, and this study provides the southernmost recording of bleaching variability in Australian octocorals (Goulet et al., 2008a).

4.1 Coral Cover, Abundance, and Species Composition at Lord Howe Island Lagoonal Reefs

Octocorals are important members of tropical and subtropical reefs worldwide. Across the Lord Howe Island lagoon, octocorals are the fourth most abundant biotic benthic group, with mean octocoral cover up to 17% on individual reefs and five species commonly found across sites. Octocoral cover and abundance was highest at the reef edge sites, Coral Gardens and Erscotts Hole, which also had two species (*Anthelia* sp. and *Xenia* sp.) not recorded at the near-shore study sites, North Bay and Sylphs Hole. This is equivalent to cover found in shallow water of the Great Barrier Reef, the Philippines, and Indonesia, higher than reported on shallow water coral reef ecosystems of the Kimberly, Hong Kong, and the lagoons of the Chagos Archipelago, and lower than reported in Guam and southern Taiwan (Dai, 1993; Fabricius and De'ath, 2001; Sheppard et al., 2008; Slattery et al., 2008; Yeung et al., 2014; Baum et al., 2016; Bryce et al., 2018; Lalas et al., 2021). On the Great Barrier Reef, inner-shelf shallow reef (0–5 m) species richness ranged from 5–8 species and octocoral cover ranged from 15 to 20%, consistent with the

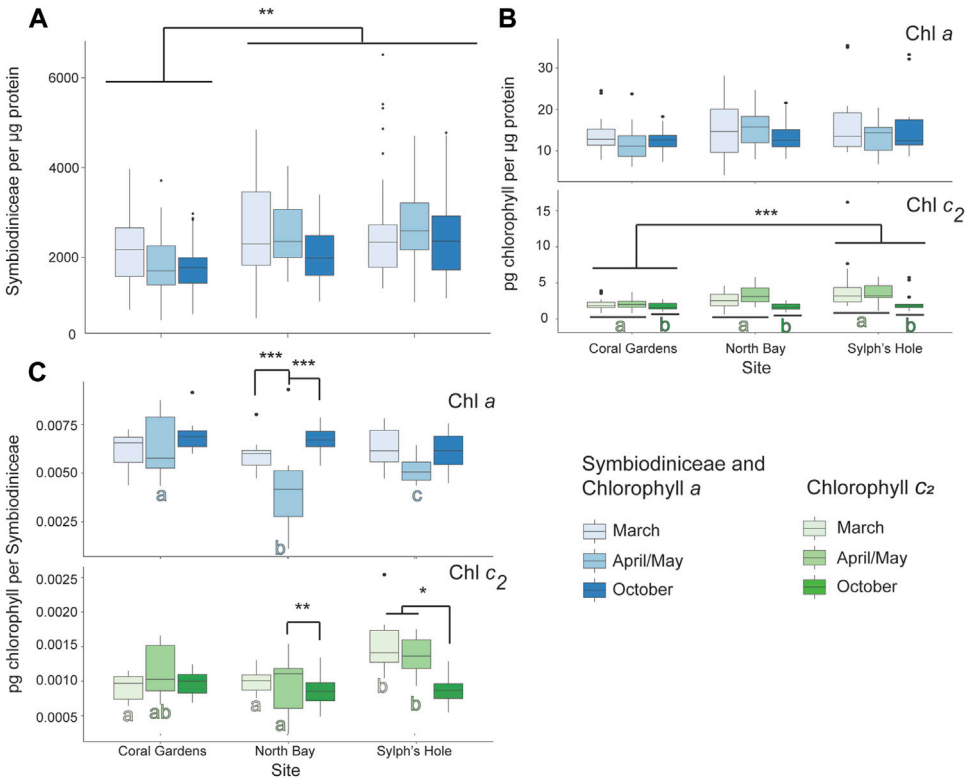

FIGURE 8 | Marine heatwave effects on unbleached *Cladiella* sp. 2 across three reefs in the Lord Howe Island lagoon. **(A)** Symbiodiniaceae density per µg protein in unbleached *Cladiella* sp. 2 colonies during March, April/May, and October. **(B)** Chlorophyll a (above) and c_2 (below) densities per µg protein in unbleached *Cladiella* sp. 2 colonies during March, April/May, and October. **(C)** Chlorophyll *a* (above) and c_2 (below) densities per µg protein in visually healthy *Cladiella* sp. 2 colonies during March, April/May, and October. Significance is designated either by different letter group or by a bar. *p*-values are represented as follows—* for $p < 0.05$, ** for $p < 0.005$, and *** for $p < 0.0005$. Where more than one plot is grouped together, the highest *p*-value is reported. Bars above the boxplots represent monitoring interval differences within site, and letters below the boxplots represent site differences within monitoring intervals.

highest cover we found at Lord Howe Island, and much higher than cover at our near-shore sites (Fabricius and De'ath, 2001). In the same vein, Philippine species richness ranged from one to eight species, while cover ranged from 0–19% (Lalas et al., 2021). In Jakarta Bay, Indonesia, octocoral cover increased with human-induced eutrophication, with cover averaging 13 ± 6% in near-city waters (Baum et al., 2016). For coral reefs in the shallow Kimberly region of Western Australia, intertidal octocoral cover ranged from 0 to 7%; In the Chagos Archipelago, lagoonal octocoral cover was only 2.65 ± 0.72% (Sheppard et al., 2013); and in the turbid and wave exposed waters of Hong Kong, octocorals were totally absent from very shallow waters (0–1 m) (Yeung et al., 2014; Bryce et al., 2018). Though Lord Howe Island octocoral cover did reach as high as 17% on some reefs, this is still lower than found on several Western Pacific reefs, with cover of individual species of *Sarcophyton, Lobophyton,* and *Sinularia* reaching up to 10% cover on shallow reefs of Taiwan, and mean soft coral cover in the shallows of Western Guam as high as 75% (Dai, 1993; Slattery et al., 2008). As such, octocorals are relatively abundant on eastern Australian reefs, and make up an important component of the benthic community of the Lord Howe Island marine park lagoon.

4.2 Response of Bleaching Susceptible Species to Heatwaves in the Lord Howe Island Lagoon

Our study of octocoral bleaching was complemented by a study of stony corals at the same sites and times (Moriarty et al., in review)[1]. While we observed bleaching in only one soft coral and in the only observed anemone species, the parallel study recorded severe bleaching in the four most abundant stony coral species, minimal bleaching recorded in one other common species, and occasional bleaching in several rare species, with up to 83% of stony coral colonies bleaching at the most affected site (Moriarty et al., in review). At nearshore reefs in the Great Barrier Reef (within 20 km of shore), octocorals were less susceptible than stony corals, with only 30% of octocoral cover lost compared to 59% of stony coral cover lost post-bleaching (Thompson and Dolman, 2010). As such, octocorals appear to be less susceptible to bleaching than stony corals in eastern Australian waters. Similar patterns were found

[1]Moriarty, T., Leggat, W., Heron, S., Steinberg, R. K., Gudge, S., and Ainsworth, T. D. Bleaching, Mortality and Lengthy Recovery on the Coral Reefs of Lord Howe Island. The 2019 marine Heatwave Suggests an Uncertain Future for High-Latitude Ecosystems. PLOS Climate.

across the Caribbean (Lasker, 2003; Dias and Gondim, 2016; Goulet et al., 2017; Mccauley et al., 2018; Cerpovicz and Lasker, 2021). On the other hand, octocorals in Sesoko Island, Japan were more susceptible to bleaching than stony corals, with overall octocoral cover dropping from 34.4 to 0.2% (Loya et al., 2001). Similarly, octocorals were more susceptible than stony corals in Sodwana Bay, South Africa, though the bleaching event was relatively mild (Floros et al., 2004). This suggests that there are differences in species' susceptibility or environmental conditions between these sites driving the range of stony and octocoral responses observed. Our study from eastern Australia, together with the majority of previous findings from Australia and the Caribbean, suggests that octocorals may be generally more resistant than stony corals to bleaching, but further research is needed over a greater area of the globe (Lasker, 2003, 2005; Drohan et al., 2005; Goulet et al., 2008a, Goulet et al., 2008b, 2017; Baker et al., 2015; Mccauley et al., 2018, 2020; Ramsby and Goulet, 2019; Cerpovicz and Lasker, 2021).

Though stony corals have relatively clear taxonomic and morphological patterns in bleaching susceptibility, octocoral studies provide little evidence for such patterns. In stony corals, branching morphologies are generally considered "losers" while massive or boulder morphologies are considered "winners" in regards to coral bleaching event outcomes (Hueerkamp et al., 2001; Loya et al., 2001; Sebastián et al., 2009). In Caribbean gorgonian octocorals, biogeochemical composition and morphology likely affect bleaching susceptibility and may confer some protection from heat-induced bleaching compared to stony corals inhabiting the same reefs, but we know little of patterns of susceptibility in Alcyonacean octocorals (Baker et al., 2015; Goulet et al., 2017; Mccauley et al., 2018). In this study, congeneric octocorals with similar morphologies displayed variable bleaching responses, as has also been found in bleaching events across the globe (Loya et al., 2001; Goulet et al., 2008a; Slattery et al., 2008; Prada et al., 2010). For example, in Sesoko Island, Japan, two lobate species of octocoral in the same family, Alcyoniidae, were a major contributor to overall reef cover, *Lobophyton* sp. and *Sinularia* sp. (Fabricius and Alderslade, 2001; Loya et al., 2001). Though both species were significantly affected by bleaching, *Sinularia* sp. was more resistant and replaced *Lobophyton* sp. as the dominant octocoral on the impacted reefs (Loya et al., 2001). Similarly, in four reefs across southern Puerto Rico, heat induced bleaching ranged from 0 to 90%, with three species resistant to bleaching pressure (Prada et al., 2010). Of those species, one unbleached (*Eunicea* sp.) and the most highly impacted (*Muricea* sp.) are both in the family Plexauridae and share similar branching morphologies (Prada et al., 2010). Even within species bleaching susceptibility can be variable, with bleached octocorals on the Great Barrier Reef found adjacent to unbleached conspecifics (Goulet et al., 2008a), which was also observed in the present study. Interestingly, the Caribbean octocoral *Briarium asbestinum* has two distinct growth forms, encrusting and branching, which exhibited differential responses to experimental heating, suggesting that the impacts of morphology on octocoral stress response needs to be investigated further (Ramsby and Goulet, 2019). Symbiodiniaceae types hosted by each coral species may also affect bleaching susceptibility as sensitivity to thermal stress can vary between Symbiodiniaceae genera and species (Rowan et al., 1997; Goulet et al., 2005, 2017), but we found that both *Cladiella* sp. 1 and sp. 2 share a type profile and all three species were dominated by Cladocopium C1. This is similar to what was found previously in the Great Barrier reef, where the dominant resident symbiont type did not explain bleaching susceptibility in octocorals (Goulet et al., 2008a; Goulet et al., 2008b). Taken together, it appears that bleaching susceptibility of octocorals cannot be predicted simply by family, genera, growth form, or symbiont type profile; and may instead be influenced by species- and environment-specific factors.

Entacmaea quadricolor anemones are important habitat for many species of anemonefish, but are susceptible to bleaching across their range, impacting both anemones and their mutualists (Chadwick and Arvedlund, 2005; Hill and Scott, 2012; Huebner et al., 2012; Thomas et al., 2015; Scott and Dixson, 2016; Frisch et al., 2019). We observed bleaching of the *E. quadricolor* anemone in the Lord Howe Island lagoon, with fairly rapid visual recovery of ~40% of anemones within a month of the end of the bleaching warnings/alerts. Previous laboratory bleaching studies found that *E. quadricolor* anemones bleached when exposed to as little as 1°C above the average summer temperature, 27°C, with bleaching apparent as little as 3 days post exposure (Hill and Scott, 2012). A second study found that *E. quadricolor* lost 90% of their endosymbiotic algae under increased irradiance at 28.5°C, but began to recover within 25 days of the end of experimental heating (Hill et al., 2014). *In-situ*, one individual *E. quadricolor* anemone took from 3 to 5 months to recover from bleaching, with recovery time increasing in the second year of bleaching (Hayashi and Reimer, 2020). Interestingly, anemone density at the most impacted site at Lord Howe Island increased over the monitoring intervals. It is unlikely the anemones had reproduced over the duration of our study, however, it is possible they became more visible following the end of the heatwave. Anemones retract when bleached (Hill et al., 2014), and it is possible that bleached anemones were retracted and so overlooked during belt surveys in March and April/May. Because bleaching can cause mortality in anemones and can have severe consequences for mutualistic anemonefish, continued monitoring of this population is warranted (Jones et al., 2008; Thomas et al., 2015; Howell et al., 2016; Scott and Dixson, 2016; Scott and Hoey, 2017; Frisch et al., 2019).

Reduction in maximum quantum yield of PSII, protein content, Symbiodiniaceae, and chlorophyll are all consequences of bleaching, and they do not all recover at the same rate. Previous work in anemones found that PSII photochemistry recovered relatively quickly post-bleaching, with incomplete recovery only 4 days after temperatures were returned to normal (Hill and Scott, 2012). This result is consistent with rapid recovery of PSII photochemistry observed in the current study. We also found that protein content recovered quickly, in contrast to protein content in bleached *Lobophytum compactum*, which was reduced during and after bleaching for at least 8 months (Michalek-Wagner and Willis, 2001b). A study on Mexican stony corals found that recovery time for

Symbiodiniaceae density differed greatly between species, with some recovering fully in as little as 6 weeks (Grottoli et al., 2014). As in the current study, bleached *Montastrea annularis* also had significantly lower protein content and significantly higher chlorophyll *a* per symbiont than their unbleached counterparts (Fitt et al., 1993). In *Acropora aspera* colonies that had not experienced protective pre-bleaching stress (sub-bleaching heat stress that induces thermal tolerance), there were similar patterns to what was found in *Cladiella* sp. 1 (Ainsworth et al., 2016; Bonesso et al., 2017). After 16 days of heat stress, there was a marked reduction in maximum quantum yield of PSII, a steady decrease in Symbiodiniaceae concentrations, and a decrease followed by an increase in chlorophyll *a* per Symbiodiniaceae (Bonesso et al., 2017). This increase in chlorophyll content may be due to decreased competition between Symbiodiniaceae for nutrients in bleached tissue, as chlorophyll concentration is an indicator of nutrient status (Rees, 1991; Fitt et al., 1993), though an increase in available nitrogen in the water could also increase chlorophyll concentrations (Grover et al., 2002). Bleaching can have long-reaching effects on octocoral population health, including reduced growth, fecundity, sperm motility, and recruitment for years after a bleaching event (Michalek-Wagner and Willis, 2001a). As such, recovery of this species may be hindered by the long-term effects of elevated lagoon temperatures.

Heat stress can also impact corals without causing visual bleaching. Often, bleaching is defined as reduction in Symbiodiniaceae density or chlorophyll (Fitt and Warner, 2001), but this is not always clear in the field as is the case at Lord Howe Island. In the lagoon, visually unbleached *Cladiella* sp. 1 colonies at the warmest and most sheltered site (Sylphs Hole; Moriarty et al., in review) had lower Symbiodiniaceae and chlorophyll concentrations during the heatwave and may have been impacted even though they did not appear bleached to the naked eye. During a bleaching event at Magnetic Island, QLD, Australia in 1994, unbleached *Acropora formosa* had lower concentrations of Symbiodiniaceae and chlorophyll during peak temperatures than during recovery, suggesting that colonies were stressed even though bleaching was not visible (Jones, 1997). Additionally, heat stress that does not result in bleaching can still lead to other adverse health effects. Colonies of *Acropora aspera* exposed to heat stress 2°C below the bleaching threshold had significantly reduced green fluorescent protein fluorescence, reduced skeletal calcification, and reduced healing ability after injury, and nearshore colonies of the Caribbean corals *Siderastrea siderea* and *Pseudodiploria strigosa* have experienced reduction in growth rates across bleaching and non-bleaching time periods (Bonesso et al., 2017; Baumann et al., 2019). As such, understanding whether unbleached corals were impacted by heat stress can help us predict recovery time of reefs after marine heatwaves.

4.3 Response of Bleaching Tolerant Species to Heatwaves in the Lord Howe Island Lagoon

Xeniids are fast growing shallow reef species that are highly successful colonisers and occasional invaders, but have previously been found to be susceptible to bleaching (Benayahu and Loya, 1985; Strychar et al., 2005; Goulet et al., 2008a; Wood and Dipper, 2008; Sammarco and Strychar, 2013; Ruiz Allais et al., 2014; Checoli et al., 2018). Interestingly, at Lord Howe Island, *Xenia* cf *crassa* appears resistant to heat induced bleaching pressure in the lagoon. This is in stark contrast to patterns observed in Xeniid corals from the Great Barrier Reef during the 1998 bleaching event, where Xeniid colonies bleached and died within a few days of the onset of bleaching, while Alcyoniids survived for long periods (Goulet et al., 2008a). In laboratory studies, *Xenia* sp. released Symbiodiniaceae cells and experienced host apoptosis at lower temperatures than either *Sarcophyton ehrenbergi* or *Sinularia* sp., both Alcyoniids (Strychar et al., 2005; Sammarco and Strychar, 2013). Additionally, *X. crassa* host cells became apoptotic at lower temperatures than Symbiodiniaceae, suggesting that host cells of *Xenia* sp. are more susceptible to bleaching stress than the Symbiodiniaceae cells (Sammarco and Strychar, 2013). As host cell responses were not measured during the present study, examination of host tissues during natural heatwaves would be beneficial to our understanding of *Xenia* spp. bleaching responses. Interestingly, the control temperature for both studies (28°C) was equal to the bleaching temperature during the Lord Howe Island bleaching event, suggesting that although *Xenia* sp. may be highly susceptible to bleaching once temperatures exceed their bleaching threshold, this was not exceeded at Lord Howe Island. Additionally, repeated heat stress can cause resistant octocoral species to experience bleaching, as reported in *Sinularia polydactyla* in Guam, which started as a "winner" during early bleaching events, but became a "loser" after experiencing six consecutive years of increased ocean summer temperatures (Slattery et al., 2019). As such, although *Xenia* cf *crassa* had increased Symbiodiniaceae and chlorophyll concentrations during the increased lagoon temperatures in this study, if future bleaching events are warmer these corals may be negatively affected.

Corals can be affected by cold stress as well as heat stress. As Lord Howe Island is subtropical, winter temperatures can reach as low as 17.5°C, which may be stressful for some species. Unlike either *Cladiella* sp. 1 or *Xenia* cf *crassa*, there were no strong effects of increased lagoon temperatures on *Cladiella* sp. 2. Instead, only chlorophyll c_2 content was reduced in October, when temperatures were lowest. This is opposite to what was previously found in manipulative non-bleaching heat stress of Caribbean gorgonian octocorals, where heat stress did not reduce Symbiodiniaceae density, but did reduce chlorophyll concentrations (Goulet et al., 2017), and where chlorophyll *a* and c_2 per Symbiodiniaceae cell were higher in winter compared to summer temperatures (Mccauley et al., 2018). Previous work in stony corals found that in cold water, *Acropora aspera* and *Montipora digitata* chlorophyll *a* concentrations were increased, and *Acropora yongei* chlorophyll content was not affected by temperature (Saxby et al., 2003; Roth et al., 2012; Nielsen et al., 2020). *Cladiella* sp. 1 may reduce chlorophyll c_2 in cold water as they are acclimated to the cool winter temperatures of the subtropical island and are not experiencing stress. Unfortunately, little is known about the heat or cold tolerance of this genus. As *Cladiella* sp. 1 was the only octocoral species to bleach during the 2019 heatwaves at Lord Howe

Island, it is evident that there is variation in susceptibility within this genus. *Cladiella* spp. are widespread throughout the world, with populations in Australia, Asia, the Pacific Islands, Africa and the Red Sea, and are moderately common in coastal waters, and as such a greater understanding of the variation in susceptibility to bleaching in this genus would have worldwide implications (Fabricius and Alderslade, 2001).

4.4 Conclusion

We found that across octocoral and anemone species the impacts of marine heatwaves in the Lord Howe Island lagoon are quite variable, with evidence of a range of thermal susceptibility and resistance in these members of the reef ecosystem. Morphological traits are recognised as important determinants of bleaching resistance in hard corals, but no such patterns have yet become evident in studies of non-gorgonian octocorals (Conti-Jerpe et al., 2020). Within soft cnidarians of the Lord Howe Island lagoon, *Xenia* cf *crassa* and *Cladiella* sp. 2 were resistant to bleaching, while *Cladiella* sp. 1 and *Entacmaea quadricolor* were susceptible during this particular series of marine heatwaves. As marine heatwaves increase in their duration, intensity and frequency (Oliver et al., 2018), it may be that octocorals become a more abundant component of the world's southern-most coral reef ecosystems (Van Hooidonk et al., 2016). Repeated bleaching events can turn octocoral winners into losers, as such, if marine heatwaves continue to affect the Lord Howe Island lagoon, current resistant species may become susceptible. In order to minimise ecological and social impacts of warming events, it is necessary to have a better understanding of susceptibility, resistance, and resilience across this delicate ecosystem. If heatwaves continue to affect the Lord Howe Island lagoon, shifts in community structure may occur as abundant yet sensitive species bleach and die, and the less common yet tolerant species, such as *Xenia* cf *crassa* and *Cladiella* sp. 2, remain unaffected, as has previously been recorded in other reefs (Norström et al., 2009; Cerpovicz and Lasker, 2021). As such, understanding the possible future of Lord Howe Island reefs under increasingly frequent bleaching events should include assessment of both soft and stony corals, and should avoid generalisation. Effective assessment requires understanding of the susceptibility of individual species.

DATA AVAILABILITY STATEMENT

The datasets presented in this study can be found in online repositories. The names of the repository/repositories and accession number(s) can be found below: Mendeley Data, DOI: 10.17632/wvcs8h8yfg.2.

ETHICS STATEMENT

All collections were undertaken under permit number LHIMP/R/19005/11032019 issued by NSW Department of Primary Industries.

AUTHOR CONTRIBUTIONS

RS was responsible for data curation, formal analysis, data visualization, and writing the initial draft. RS, TA, KD and EJ conceptualized the project. RS, TM and TB all contributed to development of the methodology and conducting field and laboratory work. TA, KD and EJ all supervised laboratory and fieldwork, TA and EJ provided resources and project administration. All authors undertook extensive review and editing of the manuscript.

FUNDING

This study was financially supported by an Australian Government Research Training Program fellowship and the University of New South Wales.

ACKNOWLEDGMENTS

The authors would like to extend our respects to the Borogegal and Bedegal people, who are the traditional owners of the land on which the laboratory component of this research was conducted. The authors would like to thank the reviewers for their time and effort in improving this manuscript. We would also like to thank Sallyann Gudge, Britt Anderson, and Caitlin Woods from NSW DPI, Dean Hiscox from Lord Howe Island Environmental Tours, Aaron and Lisa Ralph at ProDive Lord Howe Island, and Charlotte Page and Jesse Bergman from UNSW for their invaluable support and assistance in the field. We would like to thank the Thompson family at Blue Lagoon for providing accommodation and field laboratory space. We extend our thanks to Tom Bridge, Yehuda Benayahu, and Cathy McFadden for their consultation on octocoral species identification. We would like to thank Andrew Niccum, Amanda Scholes, and Nigel Coombs at the Sydney Institute of Marine Science for their help with laboratory provisions, and Eve Slavich and Ben Maslen from Stats Central at UNSW for their assistance and consultations regarding statistical analyses. We thank John Turnbull and Talia Stelling-Wood for their editorial help with this manuscript. This study was financially supported by an Australian Government Research Training Program fellowship and the University of New South Wales.

SUPPLEMENTARY MATERIAL

The Supplementary Material for this article can be found online at: https://www.frontiersin.org/articles/10.3389/fphys.2022.804193/full#supplementary-material

REFERENCES

Ainsworth, T. D., Heron, S. F., Ortiz, J. C., Mumby, P. J., Grech, A., Ogawa, D., et al. (2016). Climate Change Disables Coral Bleaching protection on the Great Barrier Reef. *Science* 352, 338–342. doi:10.1126/science.aac7125

Baillon, S., Hamel, J.-F., Wareham, V. E., and Mercier, A. (2012). Deep Cold-Water Corals as Nurseries for Fish Larvae. *Front. Ecol. Environ.* 10, 351–356. Available at: http://www.jstor.org/stable/41811419. doi:10.1890/120022

Baker, D. M., Freeman, C. J., Knowlton, N., Thacker, R. W., Kim, K., and Fogel, M. L. (2015). Productivity Links Morphology, Symbiont Specificity and Bleaching in the Evolution of Caribbean Octocoral Symbioses. *ISME J.* 9, 2620–2629. doi:10.1038/ismej.2015.71

Baker, D. M., Freeman, C. J., Wong, J. C. Y., Fogel, M. L., and Knowlton, N. (2018). Climate Change Promotes Parasitism in a Coral Symbiosis. *ISME J.* 12, 921–930. doi:10.1038/s41396-018-0046-8

Bates, D., Mächler, M., Bolker, B., and Walker, S. (2015). Fitting Linear Mixed-Effects Models Usinglme4. *J. Stat. Soft.* 67, 1–48. doi:10.18637/jss.v067.i01

Baum, G., Januar, I., Ferse, S. C. A., Wild, C., and Kunzmann, A. (2016). Abundance and Physiology of Dominant Soft Corals Linked to Water Quality in Jakarta Bay, Indonesia. *PeerJ* 4, e2625–29. doi:10.7717/peerj.2625

Baumann, J. H., Ries, J. B., Rippe, J. P., Courtney, T. A., Aichelman, H. E., Westfield, I., et al. (2019). Nearshore Coral Growth Declining on the Mesoamerican Barrier Reef System. *Glob. Change Biol.* 25, 3932–3945. doi:10.1111/gcb.14784

Beijbom, O., Edmunds, P. J., Kline, D. I., Mitchell, B. G., and Kriegman, D. (2012). "Automated Annotation of Coral Reef Survey Images," in 2012 IEEE conference on computer vision and pattern recognition, 1170–1177. doi:10.1109/cvpr.2012.6247798

Benayahu, Y., and Loya, Y. (1985). Settlement and Recruitment of a Soft Coral: Why Is Xenia Macrospiculata a Successful Colonizer? *Bull. Mar. Sci.* 36, 177–188.

Bonesso, J. L., Leggat, W., and Ainsworth, T. D. (2017). Exposure to Elevated Sea-Surface Temperatures below the Bleaching Threshold Impairs Coral Recovery and Regeneration Following Injury. *PeerJ* 5, e3719–21. doi:10.7717/peerj.3719

Boulotte, N. M., Dalton, S. J., Carroll, A. G., Harrison, P. L., Putnam, H. M., Peplow, L. M., et al. (2016). Exploring the Symbiodinium Rare Biosphere Provides Evidence for Symbiont Switching in Reef-Building Corals. *ISME J.* 10, 2693–2701. doi:10.1038/ismej.2016.54

Brandt, M. E. (2009). The Effect of Species and colony Size on the Bleaching Response of Reef-Building Corals in the Florida Keys during the 2005 Mass Bleaching Event. *Coral Reefs* 28, 911–924. doi:10.1007/s00338-009-0548-y

Brooks, M. E., Kristensen, K., Benthem, K. J. v., Magnusson, A., Berg, C. W., Nielsen, A., et al. (2017). glmmTMB Balances Speed and Flexibility Among Packages for Zero-Inflated Generalized Linear Mixed Modeling. *R. J.* 9, 378–400. doi:10.32614/rj-2017-066

Brown, B. E. (1997). Coral Bleaching: Causes and Consequences. *Coral Reefs* 16, S129–S138. doi:10.1007/s003380050249

Bryce, M., Radford, B., and Fabricius, K. (2018). Soft Coral and Sea Fan (Octocorallia) Biodiversity and Distribution from a Multitaxon Survey (2009-2014) of the Shallow Tropical Kimberley, Western Australia. *Rec. West. Aust. Mus. Sup.* 85, 45. doi:10.18195/issn.0313-122x.85.2018.045-073

Cerpovicz, A. F., and Lasker, H. R. (2021). Canopy Effects of Octocoral Communities on Sedimentation: Modern Baffles on the Shallow-Water Reefs of St. John, USVI. *Coral Reefs* 40, 295–303. doi:10.1007/s00338-021-02053-6

Chadwick, N. E., and Arvedlund, M. (2005). Abundance of Giant Sea Anemones and Patterns of Association with Anemonefishin the Northern Red Sea. *J. Mar. Biol. Ass.* 85, 1287–1292. doi:10.1017/S0025315405012440

Checoli, M., Guilherme, A., Louzada, S., Mcfadden, C. S., and Christopher, J. (2018). Invasion of Aquarium Origin Soft Corals on a Tropical Rocky Reef in the Southwest Atlantic, Brazil. *Mar. Pollut. Bull.* 130, 84–94. doi:10.1016/j.marpolbul.2018.03.014

Coles, S. L., and Jokiel, P. L. (1978). Synergistic Effects of Temperature, Salinity and Light on the Hermatypic Coral Montipora Verrucosa. *Mar. Biol.* 49, 187–195. doi:10.1007/BF00391130

Conti-Jerpe, I. E., Thompson, P. D., Wong, C. W. M., Oliveira, N. L., Duprey, N. N., Moynihan, M. A., et al. (2020). Trophic Strategy and Bleaching Resistance in Reef-Building Corals. *Sci. Adv.* 6, eaaz5443. doi:10.1126/sciadv.aaz5443

Dai, C.-F. (1993). Patterns of Coral Distribution and Benthic Space Partitioning on the Fringing Reefs of Southern Taiwan. *Mar. Ecol.* 14, 185–204. doi:10.1111/j.1439-0485.1993.tb00479.x

Dias, T. L. P., and Gondim, A. I. (2016). Bleaching in Scleractinians, Hydrocorals, and Octocorals during thermal Stress in a Northeastern Brazilian Reef. *Mar. Biodiv.* 46, 303–307. doi:10.1007/s12526-015-0342-8

Donovan, M. K., Burkepile, D. E., Kratochwill, C., Shlesinger, T., Sully, S., Oliver, T. A., et al. (2021). Local Conditions Magnify Coral Loss after marine Heatwaves. *Science* 372, 977–980. doi:10.1126/science.abd9464

Drohan, A. F., Thoney, D. A., and Baker, A. C. (2005). Synergistic Effect of High Temperature and Ultraviolet-B Radiation on the Gorgonian Eunicea Tourneforti (Octocorallia: Alcyonaceae: Plexauridae). *Bull. Mar. Sci.* 77, 257–266.

Elliott, J. K., and Mariscal, R. N. (2001). Coexistence of Nine Anemonefish Species: Differential Host and Habitat Utilization, Size and Recruitment. *Mar. Biol.* 138, 23–36. doi:10.1007/s002270000441

Epstein, H. E., and Kingsford, M. J. (2019). Are Soft Coral Habitats Unfavourable? A Closer Look at the Association between Reef Fishes and Their Habitat. *Environ. Biol. Fish.* 102, 479–497. doi:10.1007/s10641-019-0845-4

Fabricius, K. E., and Alderslade, P. (2001). *Soft Corals and Sea Fans: A Comprehensive Guide to the Tropical Shallow Water Genera of the central-west Pacific, the Indian Ocean and the Red Sea*. Townsville, QLD: Australian Institute of Marine Science.

Fabricius, K. E., and De'ath, G. (2001). "Biodiversity on the Great Barrier Reef: Large-Scale Patterns and Turbidity-Related Local Loss of Soft Coral Taxa," in *Oceanographic Processes of Coral Reefs: Physical and Biological Links in the Great Barrier Reef*. Editor E. Wolanski (London: CRC Press), 127–144. doi:10.1201/9781420041675

Fabricius, K. E., Langdon, C., Uthicke, S., Humphrey, C., Noonan, S., De'ath, G., et al. (2011). Losers and Winners in Coral Reefs Acclimatized to Elevated Carbon Dioxide Concentrations. *Nat. Clim Change* 1, 165–169. doi:10.1038/nclimate1122

Farag, M. A., Meyer, A., Ali, S. E., Salem, M. A., Giavalisco, P., Westphal, H., et al. (2018). Comparative Metabolomics Approach Detects Stress-Specific Responses during Coral Bleaching in Soft Corals. *J. Proteome Res.* 17, 2060–2071. doi:10.1021/acs.jproteome.7b00929

Fitt, W., Brown, B., Warner, M., and Dunne, R. (2001). Coral Bleaching: Interpretation of thermal Tolerance Limits and thermal Thresholds in Tropical Corals. *Coral Reefs* 20, 51–65. doi:10.1007/s003380100146

Fitt, W. K., Spero, H. J., Halas, J., White, M. W., and Porter, J. W. (1993). Recovery of the Coral Montastrea Annularis in the Florida Keys after the 1987 Caribbean ?bleaching Event? *Coral Reefs* 12, 57–64. doi:10.1007/bf00302102

Floros, C. D., Samways, M. J., and Armstrong, B. (2004). Taxonomic Patterns of Bleaching within a South African Coral Assemblage. *Biodiv. Conserv.* 13, 1175–1194. doi:10.1023/B:BIOC.0000018151.67412.c7

Fox, J., and Weisberg, S. (2019). *An {R} Companion to Applied Regression*. Third. Thousand Oaks {CA}: Sage. Available at: https://socialsciences.mcmaster.ca/jfox/Books/Companion/.

Frisch, A. J., Hobbs, J.-P. A., Hansen, S. T., Williamson, D. H., Bonin, M. C., Jones, G. P., et al. (2019). Recovery Potential of Mutualistic Anemone and Anemonefish Populations. *Fish. Res.* 218, 1–9. doi:10.1016/j.fishres.2019.04.018

Gates, R. D., Baghdasarian, G., and Muscatine, L. (1992). Temperature Stress Causes Host Cell Detachment in Symbiotic Cnidarians: Implications for Coral Bleaching. *Biol. Bull.* 182, 324–332. doi:10.2307/1542252

Gierz, S., Ainsworth, T. D., and Leggat, W. (2020). Diverse Symbiont Bleaching Responses Are Evident from 2-degree Heating Week Bleaching Conditions as thermal Stress Intensifies in Coral. *Mar. Freshw. Res.* 71, 1149–1160. doi:10.1071/MF19220

González-Barrios, F. J., Cabral-Tena, R. A., and Alvarez-Filip, L. (2021). Recovery Disparity between Coral Cover and the Physical Functionality of Reefs with Impaired Coral Assemblages. *Glob. Change Biol.* 27, 640–651. doi:10.1111/gcb.15431

Goulet, T. L., Cook, C. B., and Goulet, D. (2005). Effect of Short-Term Exposure to Elevated Temperatures and Light Levels on Photosynthesis of Different Host-Symbiont Combinations in the Aiptasia pallida/Symbiodinium Symbiosis. *Limnol. Oceanogr.* 50, 1490–1498. doi:10.4319/lo.2005.50.5.1490

Goulet, T. L., LaJeunesse, T. C., and Fabricius, K. E. (2008a). Symbiont Specificity and Bleaching Susceptibility Among Soft Corals in the 1998 Great Barrier Reef

Mass Coral Bleaching Event. *Mar. Biol.* 154, 795–804. doi:10.1007/s00227-008-0972-5

Goulet, T. L., Simmons, C., and Goulet, D. (2008b). Worldwide Biogeography of Symbiodinium in Tropical Octocorals. *Mar. Ecol. Prog. Ser.* 355, 45–58. doi:10.3354/meps07214

Goulet, T. L., Shirur, K. P., Ramsby, B. D., and Iglesias-prieto, R. (2017). The Effects of Elevated Seawater Temperatures on Caribbean Gorgonian Corals and Their Algal Symbionts, Symbiodinium Spp. *PLoS One* 12, e0171032. doi:10.1371/journal.pone.0171032

Grottoli, A. G., Warner, M. E., Levas, S. J., Aschaffenburg, M. D., Schoepf, V., Mcginley, M., et al. (2014). The Cumulative Impact of Annual Coral Bleaching Can Turn Some Coral Species Winners into Losers. *Glob. Change Biol.* 20, 3823–3833. doi:10.1111/gcb.12658

Grover, R., Maguer, J.-F., Reynaud-Vaganay, S., and Ferrier-Pagès, C. (2002). Uptake of Ammonium by the Scleractinian Coral Stylophora Pistillata : Effect of Feeding, Light, and Ammonium Concentrations. *Limnol. Oceanogr.* 47, 782–790. doi:10.4319/lo.2002.47.3.0782

Harrison, P. L., Dalton, S. J., and Carroll, A. G. (2011). Extensive Coral Bleaching on the World's Southernmost Coral Reef at Lord Howe Island, Australia. *Coral Reefs* 30, 775. doi:10.1007/s00338-011-0778-7

Hayashi, K., and Reimer, J. D. (2020). Five-year Study on the Bleaching of Anemonefish-Hosting Anemones (Cnidaria: Anthozoa: Actiniaria) in Subtropical Okinawajima Island. *Reg. Stud. Mar. Sci.* 35, 101240. doi:10.1016/j.rsma.2020.101240

Heinz Walz GmbH (2019). *IMAGING-PAM M-Series Chlorophyll Fluorometer Instrument Description and Information for Users*.

Hill, R., and Scott, A. (2012). The Influence of Irradiance on the Severity of thermal Bleaching in Sea Anemones that Host Anemonefish. *Coral Reefs* 31, 273–284. doi:10.1007/s00338-011-0848-x

Hill, R., Fernance, C., Wilkinson, S. P., Davy, S. K., and Scott, A. (2014). Symbiont Shuffling during thermal Bleaching and Recovery in the Sea Anemone Entacmaea Quadricolor. *Mar. Biol.* 161, 2931–2937. doi:10.1007/s00227-014-2557-9

Hoegh-Guldberg, O. (1999). Climate Change, Coral Bleaching and the Future of the World's Coral Reefs. *Mar. Freshw. Res.* 50, 839–866. doi:10.1071/MF99078

Howell, J., Goulet, T. L., and Goulet, D. (2016). Anemonefish Musical Chairs and the Plight of the Two-Band Anemonefish, Amphiprion Bicinctus. *Environ. Biol. Fish.* 99, 873–886. doi:10.1007/s10641-016-0530-9

Huebner, L., Dailey, B., Titus, B., Khalaf, M., and Chadwick, N. (2012). Host Preference and Habitat Segregation Among Red Sea Anemonefish: Effects of Sea Anemone Traits and Fish Life Stages. *Mar. Ecol. Prog. Ser.* 464, 1–15. doi:10.3354/meps09964

Hueerkamp, C., Glynn, P. W., D'Croz, L., Maté, J. L., and Colley, S. B. (2001). Bleaching and Recovery of Five Eastern pacific Corals in an El Niño-Related Temperature Experiment. *Bull. Mar. Sci.* 69, 215–236.

Hughes, T. P., Kerry, J. T., Álvarez-Noriega, M., Álvarez-Romero, J. G., Anderson, K. D., Baird, A. H., et al. (2017). Global Warming and Recurrent Mass Bleaching of Corals. *Nature* 543, 373–377. doi:10.1038/nature21707

Hughes, T. P., Kerry, J. T., Baird, A. H., Connolly, S. R., Dietzel, A., Eakin, C. M., et al. (2018a). Global Warming Transforms Coral Reef Assemblages. *Nature* 556, 492–496. doi:10.1038/s41586-018-0041-2

Hughes, T. P., Kerry, J. T., and Simpson, T. (2018b). Large-scale Bleaching of Corals on the Great Barrier Reef. *Ecology* 99, 501. doi:10.1002/ecy.2092

Hughes, T. P., Kerry, J. T., Baird, A. H., Connolly, S. R., Chase, T. J., Dietzel, A., et al. (2019). Global Warming Impairs Stock-Recruitment Dynamics of Corals. *Nature* 568, 387–390. doi:10.1038/s41586-019-1081-y

Hume, B. C. C., Ziegler, M., Poulain, J., Pochon, X., Romac, S., Boissin, E., et al. (2018). An improved primer set and amplification protocol with increased specificity and sensitivity targeting the Symbiodinium ITS2 region. *Peer J* 6: e4816.

Jones, A. M., Gardner, S., and Sinclair, W. (2008). Losing 'Nemo': Bleaching and Collection Appear to Reduce Inshore Populations of Anemonefishes. *J. Fish. Biol.* 73, 753–761. doi:10.1111/j.1095-8649.2008.01969.x

Jones, R. (1997). Changes in Zooxanthellar Densities and Chlorophyll Concentrations in Corals during and after a Bleaching Event. *Mar. Ecol. Prog. Ser.* 158, 51–59. doi:10.3354/meps158051

Kayanne, H. (2017). Validation of Degree Heating Weeks as a Coral Bleaching index in the Northwestern Pacific. *Coral Reefs* 36, 63–70. doi:10.1007/s00338-016-1524-y

Kleppel, G. S., Dodge, R. E., and Reese, C. J. (1989). Changes in Pigmentation Associated with the Bleaching of Stony Corals. *Limnol. Oceanogr.* 34, 1331–1335. doi:10.4319/lo.1989.34.7.1331

Lalas, J. A. A., Benayahu, Y., and Baria-Rodriguez, M. V. (2021). Community Structure and Size-Frequency Distribution of Soft Corals in a Heavily Disturbed Reef System in Northwestern Philippines. *Mar. Pollut. Bull.* 162, 111871. doi:10.1016/j.marpolbul.2020.111871

Lasker, H. R. (2003). Zooxanthella Densities within a Caribbean Octocoral during Bleaching and Non-Bleaching Years. *Coral Reefs* 22, 23–26. doi:10.1007/s00338-003-0276-7

Lasker, H. R. (2005). Gorgonian Mortality during a thermal Event in the Bahamas. *Bull. Mar. Sci.* 76, 155–162.

Le Nohaïc, M., Ross, C. L., Cornwall, C. E., Comeau, S., Lowe, R., McCulloch, M. T., et al. (2017). Marine Heatwave Causes Unprecedented Regional Mass Bleaching of Thermally Resistant Corals in Northwestern Australia. *Sci. Rep.* 7, 1–11. doi:10.1038/s41598-017-14794-y

Lenth, R. V. (2022). *emmeans: Estimated Marginal Means, aka Least-Squares Means.*

Lord Howe Island Tourism Association (2021). Lord Howe Island - Just paradise. Available at: https://lordhoweisland.info/ (Accessed September 13, 2021).

Lourie, S. A., and Randall, J. E. (2003). A New Pygmy Seahorse, Hippocampus Denise (Teleostei: Sygnathidae), from the Indo-Pacific. *Zool. Stud.* 42, 284–291.

Loya, Y., Sakai, K., Yamazato, K., Nakano, Y., Sambali, H., and van Woesik, R. (2001). Coral Bleaching: the Winners and the Losers. *Ecol. Lett.* 4, 122–131. doi:10.1046/j.1461-0248.2001.00203.x

Marinez Arbizu, P. (2020). *PairwiseAdonis: Pairwise Multilevel Coparisons Using Adonis*.

Maucieri, D. G., and Baum, J. K. (2021). Impacts of Heat Stress on Soft Corals, an Overlooked and Highly Vulnerable Component of Coral Reef Ecosystems, at a central Equatorial Pacific Atoll. *Biol. Conserv.* 262, 109328. doi:10.1016/j.biocon.2021.109328

Mccauley, M., Banaszak, A. T., and Goulet, T. L. (2018). Species Traits Dictate Seasonal-dependent Responses of Octocoral-Algal Symbioses to Elevated Temperature and Ultraviolet Radiation. *Coral Reefs* 37, 901–917. doi:10.1007/s00338-018-1716-8

Mccauley, M., Jackson, C. R., and Goulet, T. L. (2020). Microbiomes of Caribbean Octocorals Vary over Time but Are Resistant to Environmental Change. *Front. Microbiol.* 11, 1–16. doi:10.3389/fmicb.2020.01272

Michalek-Wagner, K., and Willis, B. L. (2001a). Impacts of Bleaching on the Soft Coral Lobophytum Compactum . I. Fecundity, Fertilization and Offspring Viability. *Coral Reefs* 19, 231–239. doi:10.1007/s003380170003

Michalek-Wagner, K., and Willis, B. L. (2001b). Impacts of Bleaching on the Soft Coral Lobophytum Compactum. Ii. Biochemical Changes in Adults and Their Eggs. *Coral Reefs* 19, 240–246. doi:10.1007/PL00006959

Moore, J. A. Y., Bellchambers, L. M., Depczynski, M. R., Evans, R. D., Evans, S. N., Field, S. N., et al. (2012). Unprecedented Mass Bleaching and Loss of Coral across 12° of Latitude in Western Australia in 2010-11. *PLoS One* 7, e51807. doi:10.1371/journal.pone.0051807

Ng, C. S. L., Lim, S. C., Ong, J. Y., Teo, L. M. S., Chou, L. M., Chua, K. E., et al. (2015). Enhancing the Biodiversity of Coastal Defence Structures: Transplantation of nursery-reared Reef Biota onto Intertidal Seawalls. *Ecol. Eng.* 82, 480–486. doi:10.1016/j.ecoleng.2015.05.016

Nielsen, J. J. V., Kenkel, C. D., Bourne, D. G., Despringhere, L., Mocellin, V. J. L., and Bay, L. K. (2020). Physiological Effects of Heat and Cold Exposure in the Common Reef Coral Acropora Millepora. *Coral Reefs* 39, 259–269. doi:10.1007/s00338-019-01881-x

NOAA (2020). NOAA Coral Reef Watch. Available at: https://coralreefwatch.noaa.gov/ (Accessed May 17, 2021).

Norström, A., Nyström, M., Lokrantz, J., and Folke, C. (2009). Alternative States on Coral Reefs: Beyond Coral-Macroalgal Phase Shifts. *Mar. Ecol. Prog. Ser.* 376, 295–306. doi:10.3354/meps07815

Oksanen, J., Blanchet, F. G., Friendly, M., Kindt, R., Legendre, P., McGlinn, D., et al. (2019). Vegan: Community Ecology Package. Available at: https://cran.r-project.org/package=vegan.

Oliver, E. C. J., Donat, M. G., Burrows, M. T., Moore, P. J., Smale, D. A., Alexander, L. V., et al. (2018). Longer and More Frequent marine Heatwaves over the Past century. *Nat. Commun.* 9, 1–12. doi:10.1038/s41467-018-03732-9

Panithanarak, T. (2015). Effects of the 2010 Coral Bleaching on Phylogenetic Clades and Diversity of Zooxanthellae (Symbiodinium spp.) in Soft Corals of the Genus Sinularia. *Plankton Benthos Res.* 10, 11–17. doi:10.3800/pbr.10.11

Perkol-Finkel, S., and Benayahu, Y. (2004). Community Structure of Stony and Soft Corals on Vertical Unplanned Artificial Reefs in Eilat (Red Sea): Comparison to Natural Reefs. *Coral Reefs* 23, 195–205. doi:10.1007/s00338-004-0384-z

Poulos, D. E., Harasti, D., Gallen, C., and Booth, D. J. (2013). Biodiversity Value of a Geographically Restricted Soft Coral Species within a Temperate Estuary. *Aquat. Conserv: Mar. Freshw. Ecosyst.* 23, 838–849. doi:10.1002/aqc.2362

Prada, C., Weil, E., and Yoshioka, P. M. (2010). Octocoral Bleaching during Unusual thermal Stress. *Coral Reefs* 29, 41–45. doi:10.1007/s00338-009-0547-z

Pratchett, M., Munday, P., Wilson, S., Graham, N., Cinner, J., Bellwood, D., et al. (2008). Effects of Climate-Induced Coral Bleaching on Coral-Reef Fishes 'Äî Ecological and Economic Consequences. *Oceanogr. Mar. Biol. Annu. Rev.* 46, 251–296. doi:10.1201/9781420065756.ch6

Pratchett, M. S. (2007). Dietary Selection by Coral-Feeding Butterflyfishes (Chaetodontidae) on the Great Barrier Reef, Australia. *Raffles Bull. Zool.* 14, 171–176.

Qiagen (2006). QIAamp DNA Mini and Blood Mini Handbook. 5th Edn.

R Core Team (2013). *R: A Language and Environment for Statistical Computing*.

Ralph, P. (2005). "Introduction to PAM Fluorometry," in Proceedings of the Bleaching Working Group Inaugural Workshop, Puerto Morelos, 8–9. *Understanding the Stress Response of Corals and Symbiodinium in a Rapidly Changing Environment*

Ramsby, B. D., and Goulet, T. L. (2019). Symbiosis and Host Morphological Variation: Symbiodiniaceae Photosynthesis in the Octocoral Briareum Asbestinum at Ambient and Elevated Temperatures. *Coral Reefs* 38, 359–371. doi:10.1007/s00338-019-01782-z

Randall, J. (1998). Zoogeography of Shore Fishes of the Indo-Pacific Region. *Zool. Stud.* 37, 227–268.

Rees, T. A. V. (1991). Are Symbiotic Algae Nutrient Deficient? *Proc. R. Soc. Lond. B* 243, 227–233. doi:10.1098/rspb.1991.0036

Ross, C. (2014). Nitric Oxide and Heat Shock Protein 90 Co-regulate Temperature-Induced Bleaching in the Soft Coral Eunicea Fusca. *Coral Reefs* 33, 513–522. doi:10.1007/s00338-014-1142-5

Roth, M. S., Goericke, R., and Deheyn, D. D. (2012). Cold Induces Acute Stress but Heat Is Ultimately More Deleterious for the Reef-Building Coral Acropora Yongei. *Sci. Rep.* 2, 240. doi:10.1038/srep00240

Rowan, R., Knowlton, N., Baker, A., and Jara, J. (1997). Landscape Ecology of Algal Symbionts Creates Variation in Episodes of Coral Bleaching. *Nature* 388, 265–269. doi:10.1038/40843

Ruiz Allais, J. P., Amaro, M. E., McFadden, C. S., Halász, A., and Benayahu, Y. (2014). The First Incidence of an Alien Soft Coral of the Family Xeniidae in the Caribbean, an Invasion in Eastern Venezuelan Coral Communities. *Coral Reefs* 33, 287. doi:10.1007/s00338-013-1122-1

Ruiz-Moreno, D., Willis, B., Page, A., Weil, E., Cróquer, A., Vargas-Angel, B., et al. (2012). Global Coral Disease Prevalence Associated with Sea Temperature Anomalies and Local Factors. *Dis. Aquat. Org.* 100, 249–261. doi:10.3354/dao02488

Ruiz Sebastián, C., Sink, K. J., McClanahan, T. R., and Cowan, D. A. (2009). Bleaching Response of Corals and Their Symbiodinium Communities in Southern Africa. *Mar. Biol.* 156, 2049–2062. doi:10.1007/s00227-009-1236-8

Saenz-Agudelo, P., Jones, G. P., Thorrold, S. R., and Planes, S. (2011). Detrimental Effects of Host Anemone Bleaching on Anemonefish Populations. *Coral Reefs* 30, 497–506. doi:10.1007/s00338-010-0716-0

Sammarco, P. W., and Strychar, K. B. (2013). Responses to High Seawater Temperatures in Zooxanthellate Octocorals. *PLoS One* 8, e54989. doi:10.1371/journal.pone.0054989

Saxby, T., Dennison, W., and Hoegh-Guldberg, O. (2003). Photosynthetic Responses of the Coral Montipora Digitata to Cold Temperature Stress. *Mar. Ecol. Prog. Ser.* 248, 85–97. doi:10.3354/meps248085

Schlegel, R. W. (2020). *Marine Heatwave Tracker*. doi:10.5281/zenodo.3787872

Scott, A., and Dixson, D. L. (2016). Reef Fishes Can Recognize Bleached Habitat during Settlement: Sea Anemone Bleaching Alters Anemonefish Host Selection. *Proc. R. Soc. B.* 283, 20152694. doi:10.1098/rspb.2015.2694

Scott, A., and Hoey, A. S. (2017). Severe Consequences for Anemonefishes and Their Host Sea Anemones during the 2016 Bleaching Event at Lizard Island, Great Barrier Reef. *Coral Reefs* 36, 873. doi:10.1007/s00338-017-1577-6

Sheppard, C., Harris, A., and Sheppard, A. (2008). Archipelago-wide Coral Recovery Patterns since 1998 in the Chagos Archipelago, central Indian Ocean. *Mar. Ecol. Prog. Ser.* 362, 109–117. doi:10.3354/meps07436

Sheppard, C. R. C., Ateweberhan, M., Chen, A. C., Harris, A., Jones, R., Keshavmurthy, S., et al. (2013). "Coral Reefs of the Chagos Archipelago, Indian Ocean," in *Coral Reefs of the United Kingdom Overseas Territories* (Springer), 241–252. doi:10.1007/978-94-007-5965-7_18

Sikorskaya, T. V., Ermolenko, E. V., and Imbs, A. B. (2020). Effect of Experimental thermal Stress on Lipidomes of the Soft Coral Sinularia Sp. And its Symbiotic Dinoflagellates. *J. Exp. Mar. Biol. Ecol.* 524, 151295. doi:10.1016/j.jembe.2019.151295

Slattery, M., and Gochfeld, D. J. (2016). Butterflyfishes Exhibit Species-specific Responses to Changes in Pacific Coral Reef Benthic Communities. *Mar. Biol.* 163, 1–13. doi:10.1007/s00227-016-3025-5

Slattery, M., Kamel, H. N., Ankisetty, S., Gochfeld, D. J., Hoover, C. A., and Thacker, R. W. (2008). Hybrid Vigor in a Tropical pacific Soft-Coral Community. *Ecol. Monogr.* 78, 423–443. doi:10.1890/07-1339.1

Slattery, M., Pankey, M. S., and Lesser, M. P. (2019). Annual Thermal Stress Increases a Soft Coral's Susceptibility to Bleaching. *Sci. Rep.* 9, 8064. doi:10.1038/s41598-019-44566-9

Smith, L. D., Gilmour, J. P., and Heyward, A. J. (2008). Resilience of Coral Communities on an Isolated System of Reefs Following Catastrophic Mass-Bleaching. *Coral Reefs* 27, 197–205. doi:10.1007/s00338-007-0311-1

Steinberg, R. K., Dafforn, K. A., Ainsworth, T., and Johnston, E. L. (2020). Know Thy Anemone: A Review of Threats to Octocorals and Anemones and Opportunities for Their Restoration. *Front. Mar. Sci.* 7, 1–18. doi:10.3389/fmars.2020.00590

Steinberg, R. K., Johnston, E. L., Bednarek, T., Dafforn, K. A., and Ainsworth, T. D. (2021). Its What's on the inside that Counts: An Effective, Efficient, and Streamlined Method for Quantification of Octocoral Symbiodiniaceae and Chlorophyll. *Front. Mar. Sci.* 8, 1–11. doi:10.3389/fmars.2021.710730

Strychar, K. B., Coates, M., Sammarco, P. W., Piva, T. J., and Scott, P. T. (2005). Loss of Symbiodinium from Bleached Soft Corals Sarcophyton Ehrenbergi, Sinularia Sp. And Xenia Sp. *J. Exp. Mar. Biol. Ecol.* 320, 159–177. doi:10.1016/j.jembe.2004.12.039

Stuart-Smith, R. D., Brown, C. J., Ceccarelli, D. M., and Edgar, G. J. (2018). Ecosystem Restructuring along the Great Barrier Reef Following Mass Coral Bleaching. *Nature* 560, 92–96. doi:10.1038/s41586-018-0359-9

Suggett, D. J., and Smith, D. J. (2020). Coral Bleaching Patterns Are the Outcome of Complex Biological and Environmental Networking. *Glob. Change Biol.* 26, 68–79. doi:10.1111/gcb.14871

Thiault, L., Curnock, M. I., Gurney, G. G., Heron, S. F., Marshall, N. A., Bohensky, E., et al. (2021). Convergence of Stakeholders' Environmental Threat Perceptions Following Mass Coral Bleaching of the Great Barrier Reef. *Conserv. Biol.* 35, 598–609. doi:10.1111/cobi.13591

Thomas, L., Stat, M., Kendrick, G. A., and Hobbs, J.-P. A. (2015). Severe Loss of Anemones and Anemonefishes from a Premier Tourist Attraction at the Houtman Abrolhos Islands, Western Australia. *Mar. Biodiv.* 45, 143–144. doi:10.1007/s12526-014-0242-3

Thompson, A. A., and Dolman, A. M. (2010). Coral Bleaching: One Disturbance Too many for Near-Shore Reefs of the Great Barrier Reef. *Coral Reefs* 29, 637–648. doi:10.1007/s00338-009-0562-0

Valdivia, N., and Stotz, W. (2006). Feeding Behavior of the Porcellanid Crab Allopetrolisthes Spinifrons, Symbiont of the Sea Anemone Phymactis Papillosa. *J. Crustac. Biol.* 26, 308–315. doi:10.1651/c-2607.1

Van Hooidonk, R., Maynard, J. A., Manzello, D., and Planes, S. (2014). Opposite Latitudinal Gradients in Projected Ocean Acidification and Bleaching Impacts on Coral Reefs. *Glob. Change Biol.* 20, 103–112. doi:10.1111/gcb.12394

Van Hooidonk, R., Maynard, J., Tamelander, J., Gove, J., Ahmadia, G., Raymundo, L., et al. (2016). Local-scale Projections of Coral Reef Futures and Implications of the Paris Agreement. *Sci. Rep.* 6, 1–8. doi:10.1038/srep39666

Wickham, H. (2011). ggplot2. *Wires Comp. Stat.* 3, 180–185. doi:10.1002/wics.147

Wood, E., and Dipper, F. (2008). "What Is the Future for Extensive Areas of Reef Impacted by Fish Blasting and Coral Bleaching and Now Dominated by Soft Corals ? A Case Study from Malaysia," in Proceedings of the 11th International Coral Reef Symposium (Lauderdale, Florida: Ft), 403–407.

Yeung, C. W., Cheang, C. C., Lee, M. W., Fung, H. L., Chow, W. K., and Ang, P. (2014). Environmental Variabilities and the Distribution of Octocorals and Black Corals in Hong Kong. *Mar. Pollut. Bull.* 85, 774–782. doi:10.1016/j.marpolbul.2013.12.043

Conflict of Interest: The authors declare that the research was conducted in the absence of any commercial or financial relationships that could be construed as a potential conflict of interest.

Publisher's Note: All claims expressed in this article are solely those of the authors and do not necessarily represent those of their affiliated organizations, or those of the publisher, the editors and the reviewers. Any product that may be evaluated in this article, or claim that may be made by its manufacturer, is not guaranteed or endorsed by the publisher.

Advantages of publishing in Frontiers

OPEN ACCESS
Articles are free to read for greatest visibility and readership

FAST PUBLICATION
Around 90 days from submission to decision

HIGH QUALITY PEER-REVIEW
Rigorous, collaborative, and constructive peer-review

TRANSPARENT PEER-REVIEW
Editors and reviewers acknowledged by name on published articles

Frontiers
Avenue du Tribunal-Fédéral 34
1005 Lausanne | Switzerland

Visit us: www.frontiersin.org
Contact us: frontiersin.org/about/contact

REPRODUCIBILITY OF RESEARCH
Support open data and methods to enhance research reproducibility

DIGITAL PUBLISHING
Articles designed for optimal readership across devices

FOLLOW US
@frontiersin

IMPACT METRICS
Advanced article metrics track visibility across digital media

EXTENSIVE PROMOTION
Marketing and promotion of impactful research

LOOP RESEARCH NETWORK
Our network increases your article's readership